R-04-25

Preliminary site description

Simpevarp area – version 1.1

Svensk Kärnbränslehantering AB

August 2004

Svensk Kärnbränslehantering AB
Swedish Nuclear Fuel
and Waste Management Co
Box 5864
SE-102 40 Stockholm Sweden
Tel 08-459 84 00
+46 8 459 84 00
Fax 08-661 57 19
+46 8 661 57 19

ISSN 1402-3091
SKB Rapport R-04-25

Preliminary site description
Simpevarp area – version 1.1

Svensk Kärnbränslehantering AB

August 2004

Preface

SKB started site investigations for a deep repository for spent nuclear fuel in 2002 at two different sites in Sweden, Forsmark and Oskarshamn. The investigations should provide necessary information for a license application aimed at starting underground exploration. For this reason, the site investigation data need to be interpreted and assessed into site descriptive models, which in turn are used for exploring repository design options, for safety assessment studies and for environmental impact assessment. Site descriptions are also needed for further planning of the site investigations.

A site description is an integrated description of the site and its regional setting, covering the current state of the geosphere and the biosphere as well as those ongoing natural processes which affect their long-term evolution. Development of site descriptions is an important activity during both the initial site investigation phase and the complete site investigation phase. Before the start of the initial phase in Oskarshamn, version 0 of the site descriptive model was developed /SKB, 2002b/. The results of the initial site investigation phase will be compiled into a preliminary site description (version 1.2). Late in 2002, SKB launched a project with the purpose of developing a preliminary site description for the Oskarshamn area. A parallel project was set up for the Forsmark area. The present report documents the first step in this work for the Simpevarp subarea in Oskarshamn – the development of an interim version (model version Simpevarp 1.1) of the preliminary Site Descriptive Model for the Simpevarp subarea.

The basis for this interim version is quality-assured, geoscientific and ecological field data from the Simpevarp subarea (and in part from the Laxemar area) available in the SKB SICADA and GIS data bases as of July 1, 2003 as well as version 0 of the Site Descriptive Model. A special condition applies to geology where the bedrock map and lineament interpretation available early December 2003 were included in the modelling.

The specific objectives of model version 1.1 were to:

- demonstrate the application of the site descriptive methodology,
- find and establish a structure for the modelling work, and
- give recommendations on continued investigations.

The work has been conducted by a project group and other discipline-specific working groups or persons engaged by members of the project group. The members of the project group represent the disciplines geology, rock mechanics, thermal properties, hydrogeology, hydrogeochemistry, transport properties and surface ecosystems. In addition, some group members have specific qualifications of importance in this type of project e.g. expertise in RVS modelling, GIS modelling and in statistical data analysis. During the work, experts on Quaternary geology and near-surface hydrology were included in the project group.

The overall strategy to achieve a site description is to develop discipline-specific models by interpretation and analyses of the primary data. The different discipline-specific models are then integrated into a site description. Methodologies for developing the discipline-specific models are documented in methodology reports or strategy reports. A forum for technical coordination between the sites/projects is active and also sees to that the methodology is applied as intended and developed if necessary. The group consists of specialists in each field as well as the project leaders of both modelling projects. The following individuals and expert groups contributed to the project and/or to the report:

- Anders Winberg – project leader and editor,
- Karl-Erik Almén, Roy Stanfors – investigation data,
- Carl-Henric Wahlgren, Jan Hermanson, Philip Curtis, Ola Forssberg, Paul La Pointe, Eva-Lena Tullborg – geology,
- Gustav Sohlenius – overburden including Quaternary deposits,
- Eva Hakami, Flavio Lanaro, Jan Sundberg – rock mechanics, thermal properties,

- Ingvar Rhén, Sven Follin, Lee Hartley and the HydroNET Group – hydrogeology,
- Marcus Laaksoharju and the HAG group – hydrogeochemistry,
- Sten Berglund, Johan Byegård – transport properties,
- Tobias Lindborg and Björn Söderbäck – ecosystems,
- Johan Andersson – confidence assessment,
- Martin Stigsson – rock visualisation systems, database management, and finally
- Fredrik Hartz and Anders Lindblom – production of maps and figures.

The report has been reviewed by the following members of SKB's international Site Investigation Expert Review Group (SIERG): Per-Eric Ahlström (Chairman); Jordi Bruno (Enviros, Spain); John Hudson (Rock Engineering Consultants, UK); Ivars Neretnieks (Royal Institute of Technology, Sweden); Lars Söderberg (SKB); Mike Thorne (Mike Thorne and Associates Ltd, UK). The group provided many valuable comments and suggestions for this work and also for future work, and are not to be held responsible for any remaining shortcomings of the report. Additional review comments were also provided by Raymond Munier (SKB).

Anders Ström
Site Investigations – Analysis

Summary

Site characterisation in the Oskarshamn area is currently conducted at two adjoining localities, the Simpevarp and Laxemar subareas. This report presents the interim version (model version Simpevarp 1.1 of S1.1 for short) of the preliminary Site Descriptive Model for the Simpevarp subarea. The basis for this interim version is quality-assured, geoscientific and ecological field data from the Simpevarp subarea (and in part from the Laxemar area) available in the SKB SICADA and GIS data bases as of July 1, 2003 as well as version 0 of the Site Descriptive Model. A special condition applies to geology where the bedrock map and lineament interpretation available early December 2003 were included in the modelling.

The new data collected during the initial site investigation phase up till the date of data freeze S1.1 constitute the basis for the update of version 0 to version S1.1. These data include results from surface investigations in the subarea with its regional environment and from drillings and investigations in boreholes. The surface-based data sets were, in a relative sense, extensive compared with data sets from boreholes, were the information largely was limited to information from one c. 1,000 m deep cored borehole (KSH01A), two existing cored boreholes (KLX01 and KLX02, in the Laxemar subarea) and three c. 200 m deep percussion-drilled boreholes in the Simpevarp subarea.

Discipline-specific models are developed for the selected regional and local model volumes and these models are subsequently integrated into a unified site description. The current methodologies for developing discipline-specific models and their integration are documented in methodology/strategy reports. In the present work, the procedures and guidelines given in those reports were followed to the extent possible given the data and information available at the time of data freeze for model version S1.1.

Compared with version 0 there are considerable additional features in the version S1.1, especially in the geological description and in the description of the near surface. The geological models of lithology and deformation zones are based on borehole information and surface data of much higher resolution. The lithology model includes four interpreted rock domains. The deformation zone model includes 14 zones of interpreted high confidence (of existence). A discrete fracture network (DFN) model has also been developed where attempts are made to assess effects on fracturing imposed by interpreted deformation zones. Furthermore, the validity of extrapolating surface fracture statistics to larger depths was explored. The rock mechanics strength model is based on information from the Äspö Hard Rock Laboratory and an empirical, mechanical classification of data from KSH01A and at outcrops. A first model of thermal properties of the rock has been developed largely based on data from Äspö Hard Rock Laboratory, and projections based on density and mineral content. Overall the rock at Simpevarp is characterised by a low thermal conductivity.

A consequence of the planned delay in parts of the geological model is that the hydrogeological description is based solely on the version 0 regional structural model. The regional flow pattern is found to be governed by the geometry of the interpreted deformation zones in relation to the acting hydraulic gradient. Hydrogeological simulations of the groundwater evolution since the last glaciation were compared with the developed hydrogeochemical conceptual model. The conceptual model of the development of post-glacial hydrogeochemistry was updated. Also, the salinity distribution, mixing processes and the major reactions altering the groundwater composition were described down to a depth of 300 m. A first model of the transport properties of the rock was presented, although still rather immature due to lack of site-specific data in support of the model. For the near-surface, the Simpevarp subarea is characterised by a large portion of outcrop rock (38% of the area). There is information regarding the distribution of Quaternary deposits, and some information about the stratigraphy of the till, the latter found to be of small thickness, generally l–3 m.

There is much uncertainty in the version 1.1 of the Simpevarp site descriptive model, but the main uncertainties have been identified, some have been quantified and others have been left as input to alternative hypotheses. However, since a main reason for uncertainty in S1.1 is lack of data and poor data density, and as much more data are expected in future data freezes, it was not judged meaningful to carry the uncertainty quantification or the alternative model generation too far.

Advances were made on some of the important site specific questions that were formulated in planning the execution programme for the Simpevarp area. With regards to *size and locations of rock volumes with suitable properties* possible volume-delineating deformation zones have been interpreted, although with uncertainty and only limited new information is available on material properties of the rock mass at depth. The *thermal conductance* is found to be low, accounted for by density logs and mineralogical content. Rock mechanical properties of rock mass have at this early stage been inferred indirectly through the use of empirical relationships.

Recommendations on continued field investigations during the initial site investigation are provided based on results and experience gained during the work with the development of the site descriptive model version Simpevarp 1.1. During the course of the modelling work, information exchange with the site investigation has taken place, e.g. concerning the siting of new boreholes, not only in the Simpevarp subarea, but also concerning the Laxemar subarea. Recommendations on field investigations in order to reduce uncertainties in the model version S1.1 are also given, although it is recognised that a main reason for these uncertainties is lack of data and poor data density and that much more data are expected in coming data freezes from already planned investigations.

Contents

1 Introduction

1.1 Background

The Swedish Nuclear Fuel and Waste Management Company (SKB) is undertaking site characterisation at two different locations, the Forsmark and Simpevarp areas, with the objective of siting a geological repository for spent nuclear fuel. The characterisation work is divided into an initial site investigation phase and a complete site investigation phase, /SKB, 2001a/. The results of the initial investigation phase will be used as a basis for deciding on a subsequent complete investigation phase. On the basis of the complete site investigations, a decision will be made as to whether detailed characterisation will be performed (including sinking of a shaft).

An integrated component in the characterisation work is the development of site a descriptive model that constitutes an integrated description of the site and its regional setting, covering the current state of the geosphere and the biosphere as well as those ongoing natural processes that affect their long-term evolution. The site description includes two main components:

- a written synthesis of the site summarising the current state of knowledge as well as describing ongoing natural processes which affect their long-term evolution, and
- one or several site descriptive models, in which the collected information is interpreted and presented in a form which can be used in numerical models for rock engineering, environmental impact and long-term safety assessments.

More about the general principles for site descriptive modelling and its role in the site investigation programme can be found in the general execution programme for the site investigations /SKB, 2001a/.

Central in the modelling work is the geological model which i.a. provides the geometrical context in terms of the characteristics of deformation zones and the rock mass between the zones. Using the geological and geometrical description as a basis, descriptive models for other geodiciplines (hydrogeology, hydrogeochemistry, rock mechanics, thermal properties and transport properties) are developed /SKB, 2000b/. In addition, a description is provided of the surface ecological system which is part of the interface between the geosphere and the biosphere.

Great care is taken to arrive at a general consistency in the description of the various models. In addition a comprehensive assessment of uncertainty is undertaken and possible needs for alternative models are identified /Andersson, 2003/. A test of the developed methodology for site descriptive modelling has been performed for the Laxemar subarea /Andersson et al, 2002b/, in which all disciplines except surface ecosystems and transport properties were included.

Models are developed at a regional scale (hundreds of square kilometres) and on a local scale (tens of square kilometres). The model on the regional scale model i.a. serves to provide boundary conditions for the local scale models. Unlike the Forsmark area, two local scale models are developed in the Simpevarp area, one for the Simpevarp subarea and one for the Laxemar subarea, cf. Section 1.3 and Figure 1-1. Descriptive model versions are produced at specified times that are adapted to the needs of the primary users, i.e. repository design and safety assessment. These specified times define a “data freeze” which singles out the database which should inform the model version in question. The results of the descriptive modelling also serve to produce feedback to, and set the priorities for the ongoing site characterisation.

1.2 Objectives and scope

The development of an interim version of the preliminary site description (this report) was set up to be a learning exercise with the same main objectives as the overall project (see below), i.e. to produce a site description and to provide recommendations on continued field investigations. The specific objectives of the interim version are:

- To demonstrate application of the site descriptive methodology.
- To define and establish a structure for the modelling work within the project and in relation to other main activities (field investigation, design and safety assessment).

The main objectives of the overall project are:

- To develop and present a preliminary site description of the Simpevarp subarea based on field data collected during the initial site investigation phase using version 0 of the site description for the Simpevarp area as a starting point. The result is presented in the form of a site descriptive model on a local and a regional scale with an accompanying synthesis of the current understanding of the site.
- To give recommendations on continued field investigations during the initial site investigation and in preparation for the complete site investigation, based on results and experiences gained during the work with the development of site descriptive model versions.

The preliminary site description should be sufficiently detailed to provide a basis for a decision to continue with complete site investigation. The site description shall also allow for provision of responses to site-specific questions raised in FUD-K /SKB, 2001b/.

The basis for both the interim version (model version Simpevarp 1.1) and the preliminary site description (model version Simpevarp 1.2 and the subsequent Laxemar 1.2) are quality-assured, geoscientific and ecological field data from the Simpevarp area that are available in the SKB databases SICADA and GIS at pre-defined dates. These dates for "data freeze" are 1 July 2003 for the interim version (model version Simpevarp 1.1) and 1 April 2004 for the preliminary site description (model version Simpevarp 1.2). The correspoinding data freeze for Laxemar 1.2 is 1 November 2004. All new information that becomes available up to these dates will be used to re-evaluate the pre-existing knowledge built into the version 0 and version 1.1 of the site description, respectively, in order to re-asses the validity of the previous model version.

It needs to be emphasised that this report is a first draft version of the preliminary site description. There are large uncertainties in the model description and in many aspects the confidence is low. The reason for this is two-fold; lack of primary data and too little time to carry out supporting exploratory analyses and modelling exercises.

1.3 Setting

The Simpevarp area is located in the province of Småland, within the municipality of Oskarshamn, cf. Figure 1-1, and immediately adjacent to the Oskarshamn nuclear power plant (OI-OIII) and the Central interim storage facility for spent fuel (CLAB I and CLAB II), cf. Figure 2-1. The Simpevarp area (including the Simpevarp and Laxemar subareas) is located close to the shoreline of the Baltic Sea. The easternmost part (Simpevarp subarea) includes the Simpevarp peninsula (which hosts the power plants and the interim storage facility for spent fuel (CLAB)) and the islands Hålö and Ävrö. The island of Äspö, under which the Äspö Hard Rock Laboratory (Äspö HRL) is developed, is located some two kilometres north of the Simpevarp peninsula. The areal size of the Simevarp subarea is approximately 6.6 km^2, whereas the Laxemar subarea covers some 12.5 km^2. A detailed description of underlying data for the site-descriptive model, including geographical information and definition of modelling areas is provided in Chapter 2.

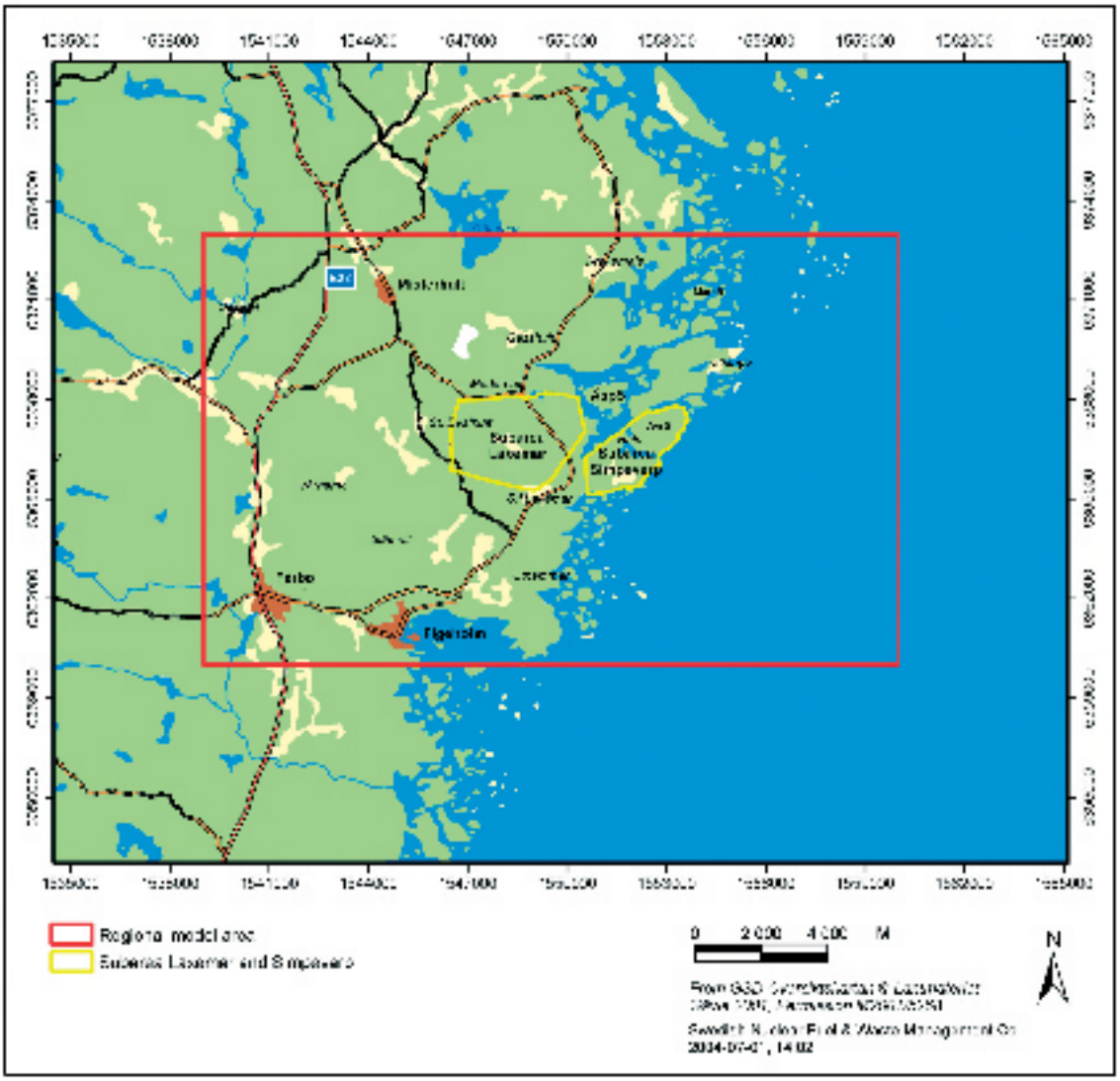

Figure 1-1. *Overview of the Simpevarp area and identification of subareas Simpevarp and Laxemar.*

1.4 Methodology and organisation of work

1.4.1 Methodology

The project is multi-disciplinary in that it should cover all potential properties of the site that are of importance for the overall understanding of the site, for the design of the deep repository, for safety assessment and for the environmental impact assessment. The overall strategy to achieve this (illustrated in Figure 1-2) is to develop discipline-specific models by interpretation and analyses of the quality-assured primary data that are stored in the two SKB databases, SICADA and GIS. The different discipline-specific models are then integrated into a site description.

The site descriptive modelling comprises the iterative steps of primary data evaluation, of descriptive and quantitative modelling in 3D and of overall confidence evaluation. A strategy for achieving sufficient integration between disciplines in producing site descriptive models is documented in a separate strategy document for integrated evaluation /Andersson, 2003/, but has *been* developed further during the work with model version Simepvarp 1.1.

Data are first evaluated within each discipline and then the evaluations are checked between the disciplines. Three-dimensional modelling, with the purpose of estimating the distribution of parameter values in space as well as their uncertainties, follows. The geometrical framework is taken from the geological model and is in turn used by the rock mechanics, thermal and

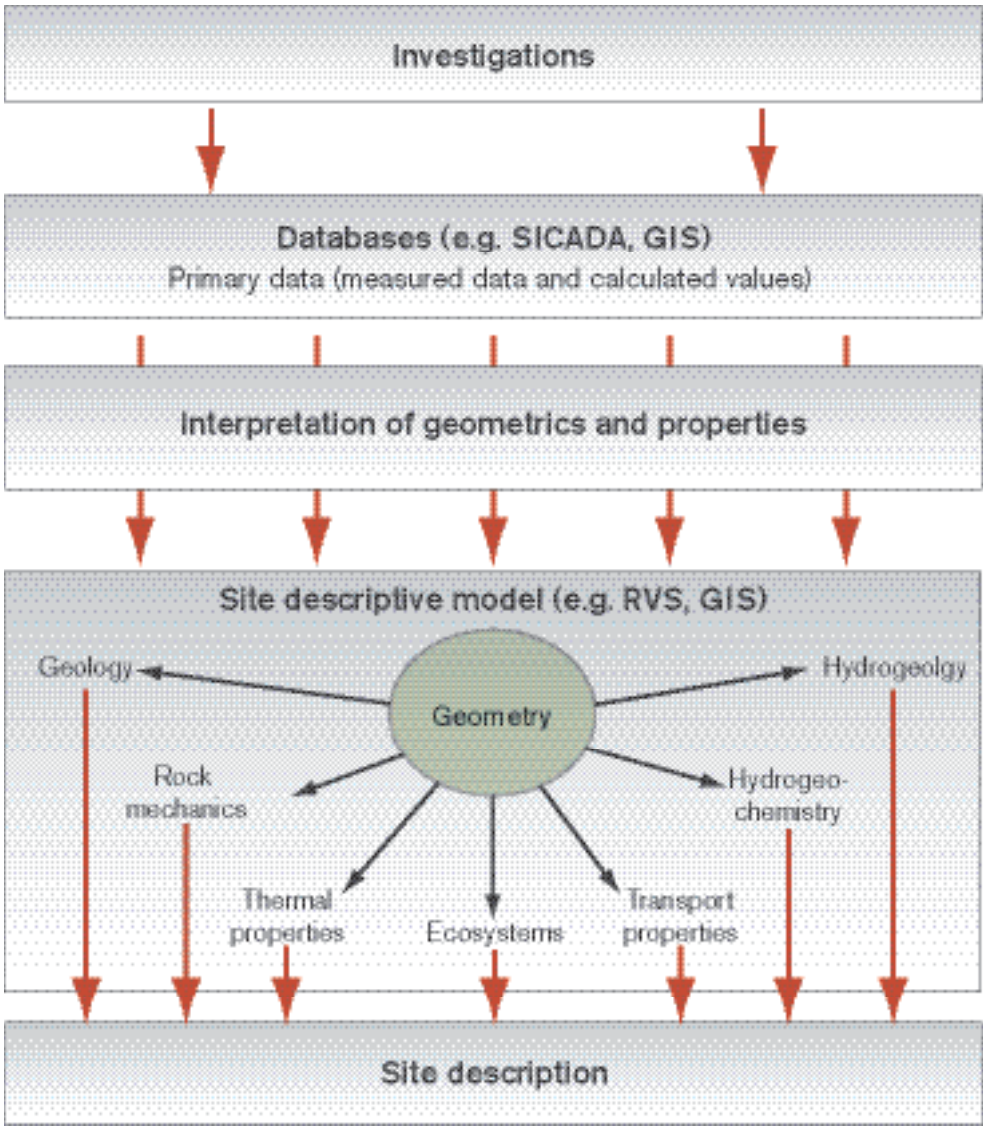

Figure 1-2. *From site investigations to site description. Primary data from site investigations are collected in databases. Data are interpreted and presented in a site descriptive model, which consists of a description of the geometry of different units in the model and the corresponding properties of the site /from SKB, 2001a/.*

hydrogeological modelling etc (see Figure 1-3). The three-dimensional description should present the parameters with their spatial variability over a relevant and specified scale, with the uncertainty included in this description. If required, different alternative descriptions should be provided.

Methodologies for developing site descriptive models are based on experiences from earlier SKB projects, e.g. the Äspö and the Laxemar modelling test projects. Before the underground laboratory at Äspö was built, forecasts of the geosphere properties and conditions were made based on pre-investigations carried out around Äspö. Comparisons of these forecasts with observations and measurements in tunnels and boreholes under ground and evaluation of the results showed that it is possible to reliably describe geological properties and conditions with the aid of analyses and modelling /Rhén et al, 1997a,b; Stanfors et al, 1997/. The Laxemar modelling test project /Andersson et al, 2002b/ was set up with the intention to explore the adequacy of available methodology for site descriptive modelling based on surface and borehole data and to identify potential needs for the development and improvements in methodology. The project was a methodology test using available data from the Laxemar area.

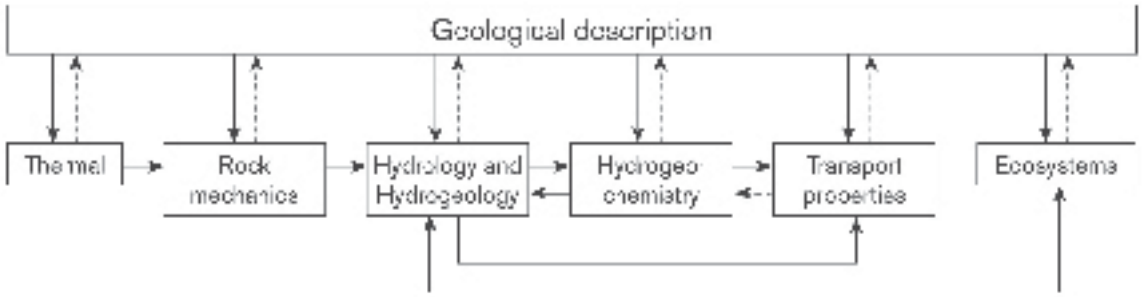

Figure 1-3. Interrelations and feedback loops between the different disciplines in site descriptive modelling where geology provides the geometrical framework /from Andersson, 2003/.

The current methodologies for developing the discipline-specific models are documented in methodology reports or strategy reports. In the present work, the guidelines given in those reports have been followed to the extent possible with the data and information available at the time for data freeze for model version Simpevarp 1.1. How the work was carried out is described further in Chapters 4 and 5 and for more detailed information on the methodologies the reader is referred to the methodology reports. These are:

- Geological Site Descriptive Modelling /Munier et al, 2003/.
- Rock Mechanical Site Descriptive Modelling /Andersson et al, 2002a/.
- Thermal Site Descriptive Modelling /Sundberg, 2003a/.
- Hydrogeological Site Descriptive Modelling /Rhén et al, 2003/.
- Hydrogeochemical Site Descriptive Modelling /Smellie et al, 2002/.
- Transport Properties Site Descriptive Modelling /Berglund and Selroos, 2003/.
- Ecosystem Descriptive Modelling /Löfgren and Lindborg, 2003/.

According to /Andersson, 2003/, the overall confidence evaluation should be based on the results of the individual discipline modelling and involve the different modelling teams. The confidence is assessed by carrying out checks concerning e.g. the status and use of primary data, uncertainties in derived models, and various consistency checks such as between models and with previous model versions. This strategy has been followed when assessing the overall confidence of model version Simepvarp 1.1. The core members of the project and the activity leaders from the Simpevarp site investigation group together accomplished protocols addressing uncertainties and biases in primary data, uncertainty in models and potential for alternative interpretations, consistency and interfaces between disciplines, consistency with understanding of past evolution and consistency with previous model versions. The results are described in Chapter 6.

1.4.2 Organisation of work

The work has been conducted by a project group and other discipline-specific working groups or persons engaged by members of the project group. The members of the project group represent the disciplines of geology, rock mechanics, thermal properties, hydrogeology, hydrogeochemistry, transport properties and surface ecosystems. In addition, some group members have specific qualifications of importance in this type of project e.g. expertise in RVS (Rock Visualisation System) modelling, GIS-modelling and in statistical data analysis. During the work, an expert in Quaternary geology was included in the project group, as it became more and more evident that the project would benefit from such an extension of the coverage of the near-surface system.

Each discipline representative in the project group has taken the responsibility for the assessment and evaluation of primary data and for the modelling work. This has been done either by the representatives themselves or together with other experts or groups of experts outside the project group. Supporting reports have been produced for some of the discipline-specific work carried out within the framework of model version Simpevarp 1.1. References to these supporting reports are given at the appropriate places in the following chapters of this report.

The project group has met at regular intervals to discuss the progress of the work and specific questions that have emerged during the modelling work. In addition, the project group has had a workshop together with activity leaders from the Simpevarp site investigation team addressing uncertainties and overall confidence in the data gathered and in the models produced. The information exchange between the modelling project and the site investigation team is an important component of the project, which is facilitated by the fact that some of the project members are also engaged as experts in the site investigation team. In addition, the investigation leader at Simpevarp has participated in most of the modelling project meetings.

1.5 This report

The disposition of this report follows a general outline for descriptive modelling reports defined for the initial investigation phase. Chapter 2 summarises available primary data and provide an overview of their usage. Chapter 3 accounts for the development of the geosphere and the surface systems in an evolutionary perspective. Chapter 4 accounts for the evaluation of the primary data and borehole-wise intercomparison of results from disciplines. Chapter 5 presents the three-dimensional modelling and also discusses identified uncertainties associated with the developed models. Chapter 6 discusses overall consistency between the various disciplines and outlines possible alternative interpretations in light of observed uncertainties. Chapter 7 encapsulates the resulting descriptive model of the Simpevarp subarea in a condensed form. Chapter 8 provides the overall conclusions of the work performed and i.a. discusses implications for the continued site investigation work and the modelling process.

It is noted that the work on the version 1.1 descriptive model of the Simpevarp subarea in essence constitutes a continued test and application of the overall methodologies defined in the above mentioned documents.

2 Available investigations and other prerequisites for the modelling

The database used for the site-descriptive modelling is evolving, successively adding more data, as more boreholes are completed. Each defined model version is associated with a "data freeze" defined at a discrete point in time. This chapter sets out to define the database used for the Simpevarp 1.1 modelling, and other associated premises and prerequisites for the modelling work. The account given here is provided primarily for future reference and for traceability. Real data are not provided, nor discussed. References are however given to the data sources. Details of the data are to be found in other reports relating to the Site Investigation. Discussions on specific data and how they have been used can be found under the different subheadings in Chapter 4. Chapter 6 discusses what data were available, but not used, and explains why those data were not used.

2.1 Overview

From about March 2002, investigations have been in process at subarea Simpevarp. The data freeze for the Simpevarp 1.1 model version was set at July 1, 2003. At that time the database associated with geology was considered too meagre to allow meaningful descriptive modelling for Simpevarp 1.1. Among the components lacking were a lithological map and an integrated lineament interpretation (based on both topography and airborne geophysics) on a local scale. As a result, the data freeze for geology was partially postponed for these two defined components with a delivery time set for December 1, 2003. These two components excluded, the database at July 1, 2003 comprised both surface and borehole investigations, the latter primarily focused on one cored borehole and three percussion-drilled boreholes. The surface investigations included work primarily focused on the Simpevarp subarea (investigations of the overburden (both the outcrop solid geology and Quaternary deposits) and review of old geological data from the construction of the nuclear power plants and the CLAB facility). The database for Simpevarp 1.1 consequently comprises:

- Primary data used in model version 0 /SKB, 2002b/.
- Data previously not considered in model version 0 (i.e. primarily the new primary data obtained from the first stage of the site investigations and data from additional review of old geological data).

2.1.1 Primary data collected before the start of the site investigation

The major data sources for the version 0 model of the Simpevarp area, developed before the beginning of the site investigations in the Simpevarp area are:

- Information from the feasibility study /SKB, 2000a/.
- Selected sources of "old data".
- Additional data collected and compiled during the preparatory work for the site investigations, especially relating to the discipline "Surface Ecosystems".

The version 0 descriptive model of the Simpevarp area was based on data available before the beginning of the site investigations, for the most part not collected for reasons directly related to deep disposal of spent nuclear fuel. An important component of the work was the compilation of a data inventory, in which the location and scope of all potential sources of relevant data were detailed and evaluated with respect to potential usefulness in future descriptive modelling. This included a general description of exiting geographically based data, most of which are stored in the SKB GIS, a survey of data already stored in the SICADA database, and an inventory of other sources of data, whose information content had not yet been assessed and/or input into SICADA or the SKB GIS.

Data sources relevant to the site descriptive modelling of the Simpevarp area which remained to be evaluated/converted/inserted into existing official databases included data related to the construction

of the Simpevarp nuclear power plants (OI–OIII) and associated tunnels and storage caverns. The y also included data related to the interim storage facility for spent nuclear fuel (CLAB) and data related to the siting, pre-investigation, predictive modelling, construction and operative phases of the Äspö Hard Rock Laboratory (Äspö HRL) . In addition, other data sources related e.g. to earlier site investigations at Bussvik, Laxemar, Kråkemåla, Simpevarp and Ävrö were only partially included in SICADA at the time of the version 0 modelling.

It was identified that the version 0 model of the Simpevarp area was, above all, regional in character. As the data identified as lacking in the official databases mainly were considered as local, this circumstance was not considered to have influenced the version 0 modelling work to any significant degree. The data inventory established in the version 0 modelling work served as a platform for prioritising analyses for the present Simpevarp 1.1 modelling.

2.1.2 Investigations performed and data colleted during the site investigations up until the data freeze for Simpevarp 1.1

The site investigations that began in March 2002 have comprised the following major components:

1) Establishment of a coordinate system including fixed points and defined grid corner points distributed across the Simpevarp area.
2) Surface investigations.
3) Drilling, including investigations during drilling.
4) Borehole investigations performed following completion of each individual borehole.

The major component of the new characterisation data were aquired from the start of the site investigation through to June 30. However, the bedrock map and the integrated map of lineaments of the Simpevarp subarea constituted two important exceptions, as they were delivered in mid December 2003. Below, those investigations that provided data for the Simpevarp 1.1 data freeze are identified and outlined.

The surface investigations undertaken in the Simpevarp subarea comprised the following :

- Airborne photography (performed in 2001).
- Airborne and surface geophysical investigationsm.
- Lithological mapping of the rock surface.
- Mapping of structural characteristics.
- Mapping of Quaternary deposits and soils.
- Marine geological investigations.
- Hydrogeochemical sampling and analysis of surface waters.
- Various surface ecological inventory compilations and investigations.

The drilling activities comprised drilling of:

- two approximately 1,000 m deep cored boreholes and one 100 m cored borehole in the immediate vicinity of one of the deep holes,
- three percussion drilled boreholes with lengths ranging up to 200 m and reaching vertical depths of 185–200 m,
- four environmental monitoring boreholes (henceforth denoted soil boreholes) that were established in the overburden.

The borehole investigations performed following the drilling of the boreholes can broadly be divided into the following:

- Logging of the bedrock parts of the core-drilled and percussion-drilled boreholes using; BIPS colour TV-camera, borehole radar with a directional antenna and a conventional suite of geophysical logs (employing electric, magnetic and radioactive methods).

- Detailed mapping of the core-drilled boreholes using the drill core and BIPS-images (so-called Boremap-mapping) and geophysical logging data from the borehole.
- Rock stress measurements using the overcoring technique.
- Mapping of percussion-drilled boreholes in solid rock using BIPS images. As no drill core exists, the mapping is here supported by samples of drill cuttings and geophysical logging data.
- Hydraulic measurements in bedrock parts of core-drilled boreholes and percussion-drilled boreholes, and in soil boreholes (full depth).
- Groundwater sampling in the bedrock parts of core-drilled boreholes, percussion-drilled boreholes, and in soil boreholes.

All data are stored in the SKB databases SICADA and SKB GIS. The basic primary data are described also in various SKB reports, c.f. tables cataloguing data available and actually used by the individual disciplines in Section 2.7.

2.2 Previous model versions

The version 0 model of the Simpevarp area /SKB, 2002b/ constitutes the point of departure for all future versions of descriptive models in the Simpevarp area. The database on which is it based is the data available at the onset of the site investigation, which is essentially identical to the data compiled for the Oskarshamn feasibility study, /SKB, 2000a/. This database is mainly 2D (surface data) with the exception of data from the Äspö HRL and is general and regional, rather than site-specific. Consequently, the version 0 model was developed at a regional scale. The principle components of the report are:

- An overview of the contents of the available data bases at the time (SICADA and GIS) and, more importantly, an inventory and assessment of relevant data in other “external” databases.
- A systematic overview of data needs and data availability for developing a site descriptive model for the Surface Eco systems (biosphere).
- A more detailed treatment of the existing data base and construction of descriptive model version 0 of the geosphere at the regional scale.

The geoscientific disciplines represented in the descriptive modelling are Geology, Rock mechanics, Hydrogeology and Hydrogeochemistry. Within each discipline identified uncertainties and alternative models are discussed with variable levels of detail.

Models preceding the version 0 model of the Simpevarp area include models developed on the basis of characterisation data produced for the siting and construction of the Äspö HRL. In this process, descriptive models have been developed for the Äspö island and its immediate environs /Rhén et al, 1997a/. As part of the operational phase of the Äspö HRL descriptive models, including conceptual models of fractures and fracture systems have been developed as part of the TRUE Programme /Winberg et al, 2000; Andersson et al, 2002c/, the Fracture Classification and Characterisation Project (FCC) /Mazurek et al, 1997; Bossart et al, 2001/, Äspö Task Force work /Dershowitz et al, 2003/ and the Repository Project /Rhén and Forsmark, 2001/. More recently, an effort has been made within the so-called GEOMOD project to revisit the 1997 site-scale descriptive models of Äspö, also attempting to incorporate the new information from the experimental work undertaken during the operational phase on a larger scale /Berglund et al, 2003/.

In preparation for the SKB site investigation programme, the Rock Visualization System (RVS) was tested out using information from the island of Ävrö /Markström et al, 2001/. A series of models of deformation zones and lithology were developed incorporating successively more information starting from using surface information only, adding surface geophysics (reflection seismics), and finally incorporating data from existing core-drilled and percussion-drilled boreholes. Important feedbacks to the modelling process using RVS were also provided.

A more full-fledged test of the developed methodology for site descriptive modelling was made on the Laxemar area /Andersson et al, 2002b/. The intent was to explore whether the available

methodology for site descriptive modelling using surface and borehole data was adequate, and further to identify needs for new developments and improvements. With limitations in scope – thermal properties and transport properties and surface ecology were not included – a descriptive model equivalent to a version 1.2 descriptive model on a local scale was developed. The underlying data consisted of various types of surface data and data from two deep core-drilled boreholes. Controls of internal consistency and processing of the primary data for use in 3D modelling were undertaken.

In order to promote cross-discipline interpretation and check for consistency, the evaluation/modelling was performed individually for each discipline followed by cross-checking. The geological modelling provides the geometric framework for the other disciplines in terms of geometry and properties of deformation zones down to a size corresponding to local minor fracture zones (length of 1–10 km) and the geometry and properties of the rock mass domains. In the hydrogeological evaluation, the developed geological model was tested using a developed numerical model and available hydraulic test data. The resulting hydrogeological description comprises hydraulic properties for defined geometrical units and pressure and flow boundary conditions applicable to present day conditions. The hydrogeochemical evaluation which i.a. included assessments of origin, turnover times and lateral/vertical distribution of groundwater included consistency checks with the hydrogeological model which enhanced the confidence in the overall model. The hydrogeochemical model also includes a conceptual model of the post-glacial development of the geochemical system. The rock mechanics description comprised the virgin rock stress field and the distribution of deformation and strength properties of the intact rock, fractures and deformation zones, and the fractured rock mass. In conclusion, despite of its limited scope, the resulting description can be viewed as an illustration of the type of product which will emerge at the end of the initial site investigation stage. This indicated that the type of descriptive modelling outlined in the general execution programme modelling is achievable. Hence, the Laxemar application serves as a preliminary and provisional model for the ongoing site-descriptive modelling in the Forsmark and Simpevarp areas.

2.3 Geographical data

The Simpevarp area is located close to the shoreline of the Baltic Sea and actually extends out into the sea. The eastern-most land masses in the area include the Simpevarp peninsula and the Ävrö island and associated smaller islets. The western limit is located immediately west of the main highway (Route E22) that runs essentially north-south. The geographical data available for the Simpevarp version 0 site descriptive model are presented in /SKB, 2002b, Section 2.1/. This report includes the applicable coordinate system, available maps (general map, topographic map, cadastral index map), digital orthophotography and elevation data.

The applicable coordinate system used for lateral spatial coordinates for the Simpevarp 1.1 modelling are:

- X/Y (N/E) : The national 2.5 gon V 0:–15, RT90 system (“RAK”).
- Z (elevation) : The national RH 70 levelling system /Wiklund, 2002/.

2.4 Surface investigations

Because of the problems associated with access to Laxemar subarea, surface investigations were primarily constrained to the Simpevarp subarea (including the islands of Ävrö and Hålö), c.f. Figure 2-3. An exception was Surface ecology for which the collected data are primarily relate to the regional model area. The investigations covered the following disciplines:

1. Bedrock geology.
2. Quaternary geology.
3. Geophysics.

4. Hydrogeochemistry.
5. Surface ecology.

In the following the investigations that have provided data for the data freeze S1.1 are summarised according to discipline. Bedrock geology and geophysical information are treated as one group, given their close interrelation.

2.4.1 Bedrock geology and geophysics

Bedrock mapping of the Simpevarp area started early 2003 and continued through the year. For the bedrock geological map and the integrated lineament interpretation, a postponed data freeze S1.1 was set to Dec 1 2003. For all other items, the following data were available at the original date of data freeze S1.1 (July 1st 2003):

- Geological outcrop database from SGU (Geological Survey of Sweden) field work.
- Bedrock map.
- Data from petrochemical and geochemical analyses made on surface samples collected from outcrops.
- Detailed fracture mapping of outcrops (Bedrock map).
- Ground-surface geophysical measurements.
- Interpretation of topographic data on land (from airborne photography).
- Interpretation of airborne geophysical data (Magnetic, EM, VLF, gamma-ray spectrometric data).
- Lineament map over the Simpevarp subarea.

2.4.2 Overburden

Overburden here refers to all surficial deposits irrespective of their origin. Mapping of Quaternary deposits in the Simpevarp subarea was initiated early in 2003 and was concluded in early fall of the same year.

Surface data

The surface data available for data freeze S1.1 comprised:

- Field data from mapping of Quaternary deposits.
- Map of Quaternary deposits of the (terrestrial parts of the) Simpevarp subarea.

Stratigraphical data

- Results from 17 augered boreholes.

2.4.3 Hydrogeochemistry

The hydrogeochemical surface investigations included in data freeze S1.1 comprised:

- Sampling and analyses of precipitation.
- Sampling and analyses of surface waters.

2.4.4 Surface ecology

The surface investigations made exclusively as part of the surface ecological programme, and producing data for data freeze S1.1 comprised:

Terrestrial (biotic)

- Bird population survey.
- Mammal population survey.
- Vegetation mapping.

Surface waters (biotic)

- Compilation of information existing in 2002.
- Benthic fauna in sediments.
- Interpretation of dominat species.
- Macrophyte communities.

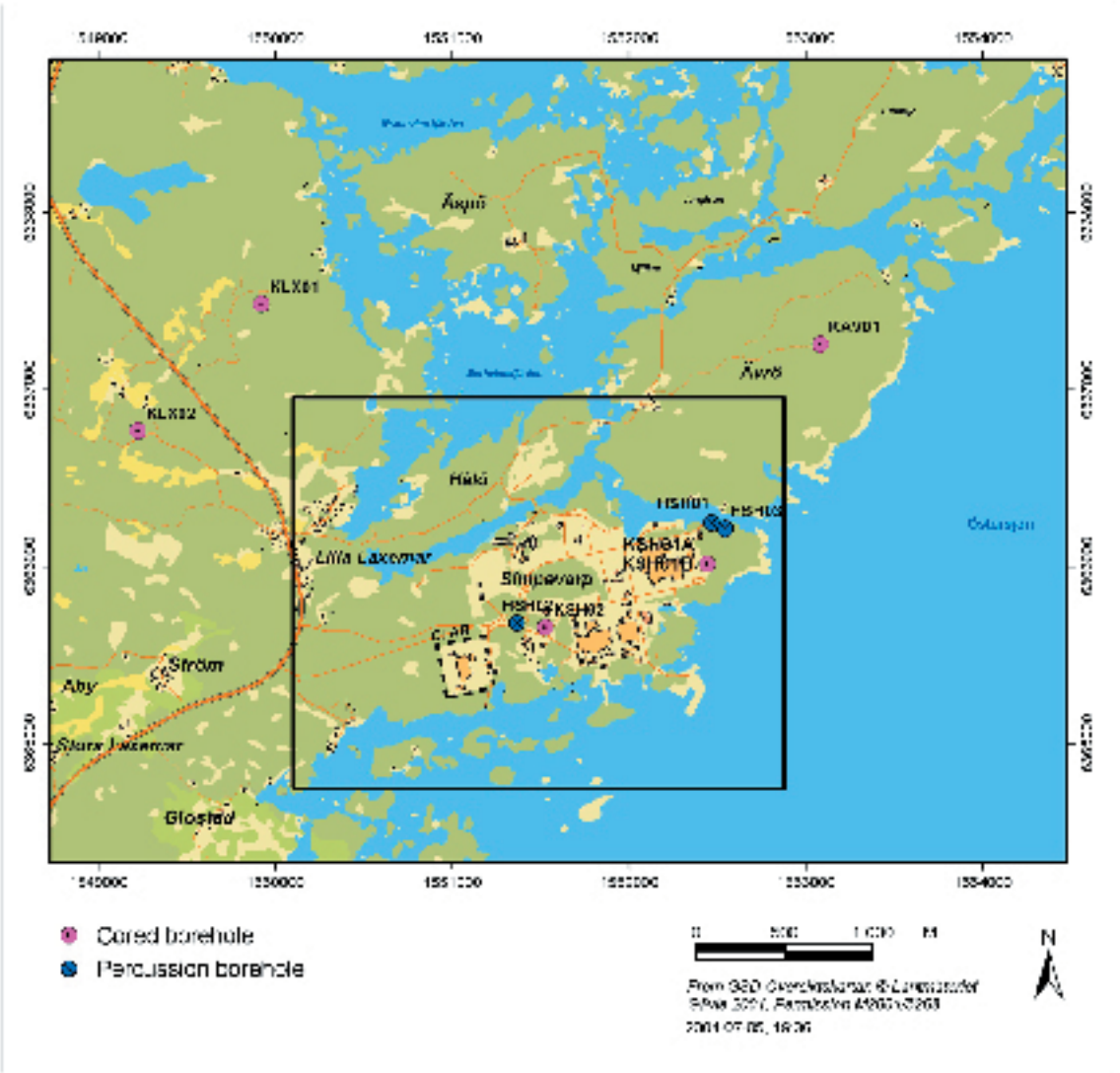

Figure 2-1. *Overview map of new core-drilled and percussion-drilled boreholes in the Simpevarp subarea. Detailed map corresponding to the area bounded by a solid black line is shown in Figure 2-2.*

2.5 Borehole investigations

The borehole investigations generating new data for the S1.1 data freeze were performed in the following cored and percussion-drilled boreholes, c.f. Figure 2-1:

- KSH01A/B and KSH02 (cored).
- HSH01, HSH02 and HSH03 (percussion).

In addition, data from four soil boreholes were available c.f. Figure 2-2. The investigations performed in the boreholes can be divided into two distinct groups:

- Measurements conducted during the drilling processes (either on a continuous basis or at discrete depth intervals in the borehole).
- Measurements conducted once the borehole was completed (usually various types of continuous logs).

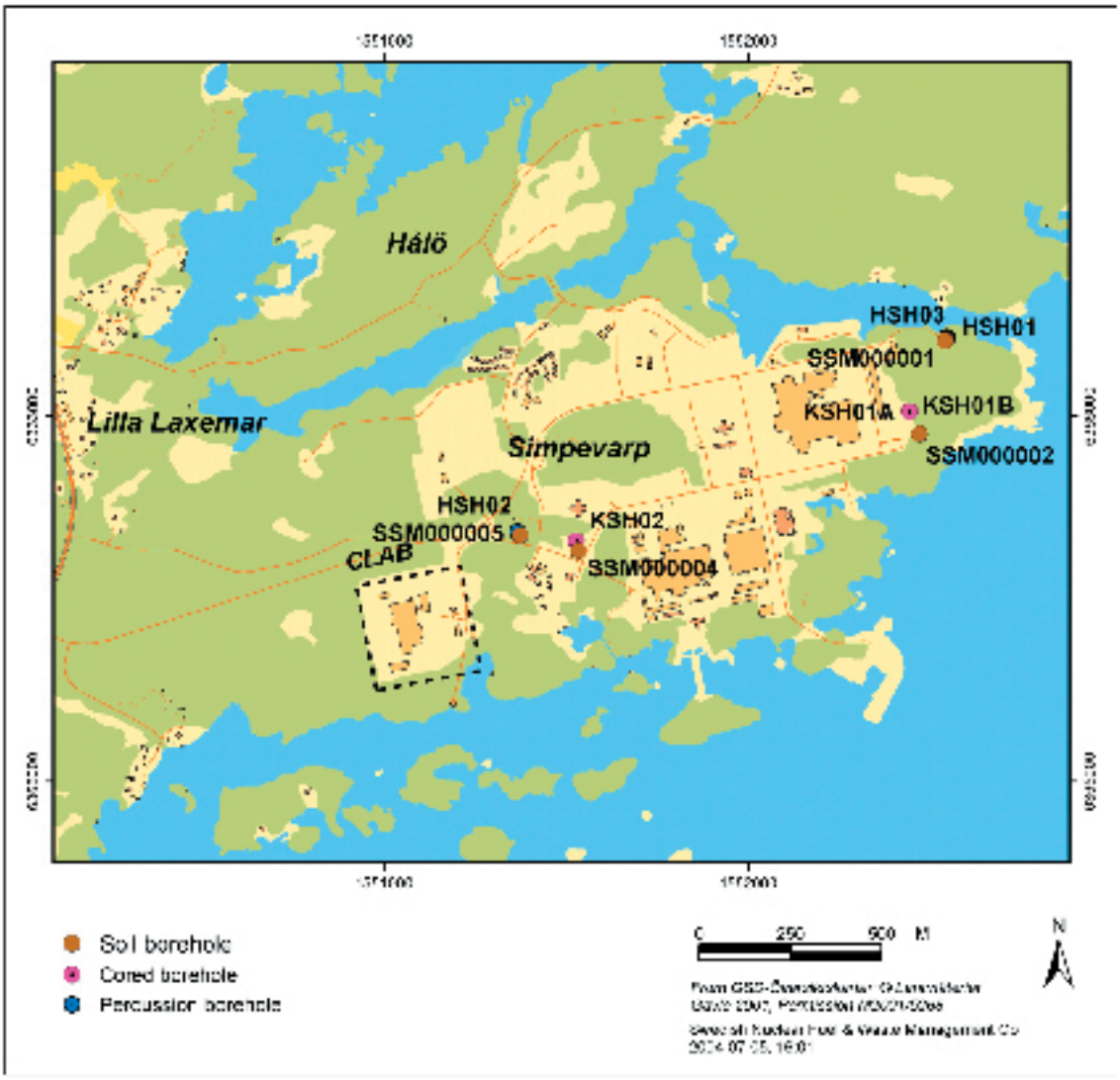

Figure 2-2. *Detailed map showing boreholes located on the Simpevarp peninsula.*

Each of the three borehole types (cored, percussion, soil) were, in various ways, and to a variable degree, associated with the two groups of investigation modes outlined above. The investigation methods associated with the two modes are presented in Sections 2.5.1 and 2.5.2, respectively, followed by a comment on the specific outcome in terms of the borehole data included in data freeze S1.1.

To the data collected in new boreholes of various types should also be added information from old existing exploration boreholes, principally from the cored boreholes KLX01 and KLX02 located in the Laxemar subarea.

2.5.1 Borehole investigations during and immediately after drilling

Cored boreholes

Borehole investigations during and immediately subsequent to core drilling should normally include /SKB, 2001a/:

- Monitoring of drilling parameters (rate of penetration, together with flushing and return water parameters : flow rates, pressure, electric conductivity and concentration of dye tracer additive, etc).
- Overview mapping of the drill core.
- Hydraulic tests employing a special test tool (the wireline probe).
- Measurements of absolute pressure using the wireline probe.
- Water sampling using the wireline probe.
- Borehole deviation measurements.
- Weighing of drill cuttings (and fine material).

If the borehole is one prioritised for rock mechanical investigations, rock stress measurements using the overcoring technique are normally conducted during the drilling process.

Specific comments regarding cored borehole KSH01A

Borehole KSH01A is a chemistry prioritised borehole, which means that a complete hydrochemical characterisation programme is to be performed. The complete sampling is made after drilling. However, during the drilling water samples are also taken and the cleaning of drilling equipment was to a higher level than standard. Drilling of KSH01A followed the general disposition employed for most deep boreholes completed during the site investigations /Ask et al, 2004/. The borehole has a varying diameter, with the upper 100.24 m of the borehole was percussion drilled with a large diameter (ϕ=200 mm). The remainder of the borehole, 100.24–1,003 metres, was core drilled using the triple-tube technique and a diameter of 76 mm (50.2 mm core). The use of both percussion- and core-drilling techniques implies that the methodologies applicable to both types of ongoing drilling process, as outlined above, were applied.

The wireline tests performed included five tests for absolute pressure and nine pumping tests for hydrogeological characterisation which were conducted at different length intervals (of which six resulted in useful transmissivity data). Three water samples were collected in three intervals of variable length between 197 and 620 m and analysed according to SKB Class 3 requirements. After drilling was completed, an airlift pumping and recovery test of the entire borehole was conducted.

The drilling of KSH01A and measurements during drilling were performed according to specified routines. As it was the first cored borehole in the site investigation of the Simpevarp subarea the technical system and routines were not fully established in the beginning of the process. However, this did not negatively affect the result of the drilling. One specified measurement was however not performed, namely the weighing of drilling cuttings as accumulated it sedimentation containers for pumped out drilling water.

Specific comments regarding cored borehole KSH01B

KSH01B is a 100 m cored borehole drilled at the same drill site as KSH01A /Ask et al, 2004/. The purpose of KSH01B was to produce drillcore from ground surface to 100 m depth, as KSH01A was percussion-drilled for the first 100 m. KSH01B was conventionally core drilled, ie not using a variable diameter as at KSH01A. The core drilling was made with the same drill rig and downhole equipment as used for borehole KSH01A, hence resulting in the same type of core as for KSH01A.

Specific comments regarding cored borehole KSH02

The drilling of KSH02 was slightly different from that of KSH01 /Ask et al, 2004./. First, there were no A and B holes. The upper 100 m was first core drilled and then reamed up to the wider diameter required. As the borehole wall was somewhat unstable it was decided to install a casing. However, the casing installation was stopped at 66 m depth and the borehole was plugged with cement. The plugged interval was re-drilled before the drilling was continued to 1,000 m depth. The resulting borehole design therefore is casing of 200 mm inner diameter down to 66 m, whereas the rest of the hole has a diameter of 76 mm.

The drilling was made with the same drilling machine and down-hole equipment as used in the KSH01 A and B holes and employing the same procedures as for the KSH01. In KSH02, the following tests and water sampling during drilling were performed:

- eleven pumping tests, of which nine gave acceptable transmissivity values,
- nine pressure measurements,
- acquisition of four water samples.

KSH02 is a borehole specifically allocated for rock stress measurements. The overcoring technique was used during the core drilling at the three intervals, 250–300 m and around 450 m level. Due to a relatively high frequency of sealed factures only one measurement resulted in useful data /Sjöberg, 2004/.

Percussion-drilled boreholes in bedrock

Borehole investigations during (and immediately after) percussion drilling followed general guidelines for the site investigations /SKB, 2001a/. For the percussion-drilled boreholes HSH01, HSH02 and HSH03 the following procedures were applied /Ask and Samuelsson, 2004/:

- Sampling of the soil during drilling through the overburden (Very thin soil cover resulted in one sample from each of boreholes HSH01 and HSH02).
- Sampling of drill cuttings (and fine material) with a frequency of one sample every third metre (preliminary inspection on location).
- Manual measurement of penetration rate.
- Registration of notable changes in the flow rate of the return drilling water with . intermediate measurements in case of an observed increase in flow.
- Recording of the colour of the return water.
- Measurement of borehole deviation after completion of the borehole.

Boreholes in soil

Four soil boreholes were drilled, all of them for the purpose of environmental control at the KSH01, KSH02, HSH01 and HSH02 drill sites /Ask, 2003/.

2.5.2 Borehole investigations after drilling

Following completion of drilling, a base programme of characterisation was carried out in all core-drilled and percussion-drilled boreholes. Depending on the assigned priority (rock mechanics or hydrochemistry) the supplementary data to the base programme may differ amongst the cored boreholes /SKB, 2000b/.

Data from base programme of characterisation were only available from core-drilled borehole KSH01A/B, as only drilling of KSH02 was completed at the time of data freeze S 1.1.

Percussion-drilled section of KSH01A, L=0–100.24 m

The following investigations were made and reported as part of data freeze S1.1:

- BIPS borehole imaging.
- Borehole radar (dipole antenna).
- Conventional suite of geophysical well logs.

Core-drilled section KSH01A and KSH01B, L=100.24–1,003 m

The following investigations were made and reported as part of data freeze S1.1:

- BIPS borehole imaging, in both the A and B holes.
- Borehole radar (dipole antenna), in both the A and B holes.
- Boremap logging (using BIPS and drill core), in both the A and B holes.
- Hydrochemical logging, in the A hole.
- Difference flow logging, in the A hole.
- Complete hydrogeochemical characterisation, in the A hole only.
- Sampling of the drill core for geological, rock mechanical, geochemical and transport analysis, from the A hole only. However, analysis data for transport properties are not included in data freeze Simpevarp S 1.1.

Percussion-drilled boreholes

The investigation methods listed below were employed in the three percussion-drilled boreholes. The resulting data formed part of data freeze S1.1.

- BIPS borehole imaging.
- Borehole radar (dipole antenna).
- Conventional suite of geophysical well logs.
- Hydraulic teste (pump tests and flow logging), in HSH01 and HSH03.

Soil boreholes

No measurements have been made in the soil boreholes.

2.6 Other data sources

Other relevant data sources are “old” data taht are either already stored in relevant official SKB databases, or are listed in the version 0 report /SKB, 2002b/ and remain to be input into the databases. One obvious extensive source of information is that provided by the characterisation data and associated descriptive models available from the Äspö HRL. The position taken by the site descriptive modelling project is to make use of selective information important for, and filling voids in the data needs of the modelling process. The ambition is by no means to integrate the huge Äspö HRL database in full, see below. Examples of data of interest are various generations of geological and structural models and compilations of transport properties relevant to Äspö HRL conditions (and the associated geology/mineralogy). Additional old data include surface and borehole information from investigations performed on the islands of Ävrö and Hålö. Old data are also available from the construction of the three nuclear power reactors on the Simpevarp

peninsula (and associated tunnels and storage caverns). A third source of old data is related to the site characterisation and construction of the central storage facility for spent nuclear fuel (CLAB I and CLAB II). The old data used as input to the descriptive modelling for Simpevarp 1.1 are summarised in Section 2.7.

Relationship to data from Äspö HRL

As indicated in the previous section, the designated Local Model area for the Simpevarp subarea partially includes the Äspö island and the Äspö HRL. There consequently exists a need to define a relationship to the wealth of data available from Äspö and the Äspö to be employed in the site descriptive modelling. A full inclusion and integration of the Äspö data set would be prohibitive for the realisation of the site modelling project and would introduce a significant bias and inbalance in the density of data. Instead, the project has adapted a flexible relationship to Äspö data and associated descriptive and conceptual models.

The site modelling project does not have to address the Äspö data base in its entirety, rather the ground rule is that Äspö data primarily are used for qualitative comparisons with data collected elsewhere in the model area(-s). However, initial lack of data, primarily in the local model area, can be compensated by selected data from Äspö. Thus, in the case when relevant data or statistics are absent in the site-specific database, such information could be imported from Äspö. This could e.g. be rock mechanics, thermal or transport-related information. However, in all cases, such import should be motivated and constrained on the basis of appropriate geological analogies and relationships.

Studies performed during the characterisation, construction and operational (experimental) phases of the Äspö HRL have resulted in various kinds of conceptual models which could be of potential use for the site modelling project. Examples of such models are; mechanistic models of geological structure evolution, mechanical stability, hydraulic anisotropy, hydrogeochemical evolution and microbial processes. Experiments focused on the natural barriers have produced conceptual micro-structural models of fractures and their immediate environs (including infillings) and conceptual models for transport and retention in fractured rock, including dominant processes and immobile zones involved. Similarly to the import of data, import/use of conceptual models developed at Äspö has to be motivated and justified by geological, petrophysical and geochemical similarities.

2.7 Databases

This section summarises the data that were available at the time of the data freeze for S1.1 and distinguishes data used and data not used in the site descriptive modelling. The basis for the presentation is a series of tables developed for each discipline. In each table, the first two columns set out the data available, columns 3 and 4 identify the data that were used, whereas column 5 identifies for data not used, and presents arguments in support of their not being used.

Table 2-1. Available bedrock geological and geophysical data and their handling in Simpevarp 1.1.

Available primary data Data specification	Ref.	Usage in S1.1 Analysis/Modelling	c.f Section	Not utilised in S1.1 Arguments/Comments
Surface-based data				
Bedrock mapping – outcrop data (rock type, ductile and some brittle structures at 353 observation points. Frequency and orientation of fractures at 16 outcrops)	Preliminary report used	Rock type, ductile deformation in the bedrock, fracture statistics and identification of possible fracture zones at the surface	4.2.2 4.2.4 5.1.3 7.3.1	
Detailed fracture mapping at four sites	P-04-35	Fracture orientation, tracelength and other geologcical parameters (mineral infilling, alteration etc)	4.2.4	
Modal analyses and geochemical analyses	Preliminary report used	Mineralogical and geochemical properties of the bedrock Assessment of thermal properties	4.2.2 7.3.1	
Petrophysical rock parameters and in situ gamma-ray spectrometric data	P-03-97	Physical properties of the bedrock	4.2.4 7.3.1	
Airborne geophysical data (magnetic, EM, VLF and gamma-ray spectrometric data)	P-03-25 P-03-63	Identification of lineaments/ deformation zones and lithological boundaries	4.2.3	
Detailed topographic data from airborne photography	P-02-02	Identification of lineaments/ deformation zones	4.2.3	
High resolution reflection seismics	P-03-71 P-03-72 TR-97-06 TR-02-19 R-01-06	Identification of inhomogeneities in the bedrock that may correspond to boundaries between different types of bedrock or to deformation zones. Supportive information used from previous models (Laxemar, Ävrö and Äspö 96)	5.1.5	
Surface geophysical data (magnetic and EM data)	P-03-66	Identification of of lineaments/ deformation zones	4.2.5 5.1.5	
Regional gravity data				Not utilised in 1.1. Too few and scattered measurements
Interpretation of airborne geophysical and topographical data (linked lineament map)	P-03-100 P-03-99 P-04-37	Deterministic structural model	4.2.3 5.1.5	
Simevarp site descriptive model v.0	R-02-35	Lithological model and deterministic structural model	5.1.3 5.1.5 5.1.6	
Cored borehole data				
Geophysical, radar and BIPS logging in KSH01A	P-03-15 P-03-16 P-03-73	Fracture statistics (including mineralogical analyses), single hole interpretation, rock type distribution down to borehole depth 1,000 m in DFN (Discrete Fracture Network), lithological and deformation zone models	5.1.3 5.1.5 5.1.6	

Table 2-2. Available rock mechanics data and their handling in Simpevarp 1.1.

Available primary data Data specification	Ref.	Usage in S1.1 Analysis/Modelling	c.f Section	Not utilised in S1.1 Arguments/Comments
Cored borehole data				
Single measurement of stress with overcoring, KSH02	P-04-32	Estimation of in-situ stress field and uncertainty in data	4.6.1	
Boremap logging of KSH01A	P-03-73	Calculation of empirical rock mass quality indices and estimation of rock mass properties	4.6.4 and 5.2.2	
Geological single hole interpretation, KSH01A	P-03-32 P-03-93	Division into geologically simlar units used for grouping of data	4.6 and 5.2.2	
Supplementary mapping of KSH01A for Q-classifications	P-03-74	Estimation of rock mechanical properties and uncertainty assessment	4.6.4 and 5.2.2	
Tilt tests and Schmidthammer tests, KSH01A	P-03-107	Estimation of rock and fracture mechanical properties	4.6.2 and 5.2.2	
P-wave velocity, transverse borehole core, KSH01A	P-03-106			Not used
Surface-based data				
Field mapping for Q-classification at ten locations		Estimations of rock mechanical properties	4.6.5 and 5.2.2	
Other borehole, construction, tunnel data and models				
Stress measurements from boreholes in the region	PR-25-89-17 PR U-97-27 IPR-02-01 IPR-02-02 IPR-02-03 IPR-02-18 R-02-26	Estimation of in-situ stress field	4.6.1 and 5.2.1	
Laboratory strength test data. Core samples from Äspö and CLAB	SICADA	Estimation of intact rock strength properties	4.6.2, 4.7.3 and 5.2.2	
Compilation of existing structural geological data covering the Simpevarp peninsula, Ävrö and Hålö	P-03-07	Estimation of the homogeneity of rock mechanical properties	5.2.2	

Table 2-3. Available data on thermal properties and their handling in Simpevarp 1.1.

Available primary data Data specification	Ref.	Usage in S1.1 Analysis/Modelling	c.f Section	Not utilised in S1.1 Arguments/Comments
Cored borehole data				
Laboratory thermal test on cores from older boreholes at Äspö	R-03-10	Estimation of thermal conductivity and specific heat capacity	4.7.1 and 5.3.2	
Density log KSH01A		Estimation of thermal conductivity	4.7.3 and 5.3.2	
Laboratory test of thermal expansion. Made on cores from Äspö HRL	/Åkesson, 2003/	Estimation of the thermal expansion coefficient	4.7.4 and 5.3.4	
Surface based data				
Modal analyses	Preliminary report used	Estimation of thermal conductivity	4.7.2 and 5.3.2	

Table 2-4. Available meteorological, hydrological and hydrogeological data and their handling in Simpevarp 1.1.

Available primary data Data specification	Ref.	Usage in S1.1 Analysis/Modelling	c.f Section	Not utilised in S1.1 Arguments/Comments
Meteorological data				
Summary of precipitation, temperature, wind, humidity and global radiation up to 2000	TR-02-03 R-99-70	Basis for general description and modelling of surface runoff and groundwater recharge	4.3	
Surface-based data				
Exploration of water courses for suitable point of measuring the run-off	P-03-04		4.3	Not used explictly. Document only used for planning of modelling work.
Ground elevation and bathymetry of the Baltic Sea	SKB GIS-data base	Topography and bathymetry	4.1	
Bathymetry of lakes				No data are available.
Hydrological data				
Inventory of private wells 2002	P-03-05		4.3	Not used explicitly. Document only used for planning of environmental impact follow-up
Topographical information for delineation of run-off areas	SKB GIS-data base	Definition of run-off areas	4.3	
Regional run-off data	TR-02-03 R-99-70	Characteristics of run-off areas	4.3	
Regional oceaographic data	TR-02-03 R-99-70	Characteristics of oceanographic conditions	4.3	
Cored borehole data				
Difference flow logging in KSH01A	P-03-70	Conductive parts of the borehole, Statistics of conductive fracture	4.5	
Wireline tests in KSH01A	P-03-113	Conductive parts of the borehole. Mean hydraulic conductivity in 100 m scale	4.3	
Hydraulic tests in HSH01, HSH02, HSH03	P-03-114	Conductive parts of the borehole. Mean hydraulic conductivity in 100 m scale	4.3	
Percussion hole data				
Hydraulic tests and water sampling in HSH03	P-03-56	Conductive parts of the borehole	4.3	
Monitoring of water levels in rock holes	SICADA database			Not used for version S1.1. Ongoing measurements. Not considered important for S1.1.
Other borehole, construction, tunnel data and models				
Hydraulic tests in the Äspö, Ävrö, Hålö, Simpevarp, Mjälen and Laxemar areas	TR-97-06, TR-02-19, R-98-55, SICADA database	Previous evaluations compared to new data	4.3	Not used in detail.

Table 2-5. Available hydrogeochemical data and their handling in Simpevarp 1.1.

Available primary data Data specification	Ref.	Usage in S1.1 Analysis/Modelling	c.f Section	Not utilised in S1.1 Arguments/Comments
Surface based data				
Preciptation	P-04-14	All hydrochemical modelling and visualisation	3.8 and 5.5	
Cored borehole data				
Complete chemical characterization KSH01A	P-04-12	All hydrochemical modelling and visualisation	3.8 and 5.5	
Hydrochemical logging of of KSH01A	P-03-87	All hydrochemical modelling and visualisation	3.8 and 5.5	
Sampling during drilling of KSH02	P-03-88	DIS (Drilling impact study)	3.8 and 5.5	
Sampling during drilling of KSH01A	P-03-113	DIS (Drilling impact study)	3.8 and 5.5	
Percussion hole data				
Samples from HSH02 and 03	P-03-113	All hydrochemical modelling and visualisation	3.8 and 5.5	

Table 2-6. Available data on transport properties and their handling in Simpevarp 1.1.

Available primary data Data specification	Ref.	Usage in S1.1 Analysis/Modelling	cf. Section	Not utilised in S1.1 Arguments/Comments
Cored hole data				
Not available				
Data and results from other diciplines				
Results from geological descriptive modelling	Prel. report used	Identification of site-specific rock types	5.6	
Petrophysical data from rock samples	P-03-97	Porosity data for site-specific rock types	5.6	
Results from hydro-geological descriptive modelling	Prel. report used	Flow paths and flow-related transport parameters	5.6	
Results from hydrogeo-chemical descriptive modelling	R-04-16	Identification of site-specific water types and water-rock interactions	5.6	
Other borehole, construction, tunnel data and models				
Old/generic data on diffusion and sorption parameters (SR 97 databases)	R-97-13 TR-97-20	Parametrisation of rock domains (general)	5.6	
Old/generic data on diffusion and sorption parameters (laboratory data from Äspö)	TR-98-18 ICR-01-04 IPR-03-13	Parametrisation of site-specific rock types (comparative purposes)	5.6	
Old/generic data on diffusion and sorption parameters (laboratory and *in situ* data from Äspö)	SKI 98:41 Research papers	First assessment of spatial variability	5.6	

Table 2-7. Available data on overburden (including Quaternary deposits) and their handling in Simpevarp 1.1.

Available primary data Data specification	Ref.	Utilised in S1.1 Analysis/Modelling	c.f Section	Not utilised in S1.1 Arguments/Comments
Surfaced based data				
Map of Quaternary deposits	P-04-22	Surface distribution of Quaternary deposits in the Simpevarp subarea		
Electric soundings	P-03-17	Depth and stratigraphy of overburden		
Stratigraphical data				
Stratigraphy of Quaternary deposits	P-04-22	Description of the stratigraphical distribution of Quaternary deposits		
Other borehole, construction, tunnel data and models				
Old maps of Quaternary deposits	SGU Ac 5 (1904)			Old map with low geographical accuracy
Stratigraphy of water laid Quaternary deposits from the sea bottom	R-02-47	Description of the stratigraphical distribution of Quaternary deposits from the sea bottom		

Table 2-8. Available surface ecological data and their handling in Simpevarp 1.1

Available site data Data specification	Ref.	Utilized in model version 1.1 Analysis/Modelling	c.f. Section	Not utilized in model version 1.1 Motivation
Terrestrial – abiotic				
Covered by other disciplines, c.f. corresponding tables: • Hydrologi • Regolith • Climate • Geology (topography/geometry)				
Terrestrial – biotic				
Bird population survey	P-03-31	Description	4.11.2, 5.7.2, 7.1.5	
Mammal population survey	P-04-04	Description	4.11.2, 5.7.2, 7.1.5	
Vegetation mapping	P-03-83	Description/modelling	4.11.1, 5.7.2, 7.1.5	
Humans and land use	R-04-11	Description/modelling	4.11.3, 5.7.3, 7.1.6	
Compilation of existing information 2002	R-02-10	Description	Chapter 4, 5 and 7	
Surface waters – abiotic				
c.f tables of other diosciplines				
Surface waters – biotic				
Compilation of existing information 2002	R-02-10	Description	Chapter 4, 5 and 7	
Bentic fauna in sediment	P-03-67	Description	4.11.2, 5.7.2, 7.1.5	
Interpretation of dominating speaces	P-03-68	Description	4.11.1, 5.7.2, 7.1.5	
Macrophyte communities	P-03-69	Description/modelling	4.11.1, 5.7.2, 7.1.5	

Table 2-9. Reports in the SKB P, IPR, ICR, R, and TR-series referenced in Tables 2-1 through 2-8.

P-02-02	**Wiklund S.** Digitala ortofoton och höjdmodeller. Redovisning av metodik för platsundersökningsområdena Oskarshamn och Forsmark samt förstudieområdet Tierp Norra (in Swedish).
P-03-04	**Lärke A, Hillgren R.** Rekognoscering av mätplatser för ythydrologiska mätningar i Simpevarpsområdet (in Swedish).
P-03-05	**Morosini M, Hultgren H.** Inventering av privata brunnar i Simpevarpsområdet, 2001–2002 (in Swedish).
P-03-07	**Curtis P, Elfström M, Stanfors R.** Oskarshamn site investigation Compilation of structural geological data covering the Simpevarp peninsula, Ävrö and Hålö
P-03-15	**Nilsson P, Gustafsson C.** Simpevarp site investigation. Geophysical, radar and BIPS logging in borehole KSH01A, HSH01, HSH02 and HSH03.
P-03-16	**Nielsen U T, Ringgaard J.** Simpevarp site investigation. Geophysical borehole logging in borehole KSH01A, KSH01B and part of KSH02.
P-03-17	**Thunehed H, Pitkänen T.** Simpevarp site investigation. Electrical soundings supporting inversion of helicopterborne EM-data. Primary data and interpretation report.
P-03-25	**Rønning H J, Kihle O, Mogaard J O, Walker P.** Simpevarp site investigation. Helicopter borne geophysics at Simpevarp, Oskarshamn, Sweden.
P-03-31	**Green M.** Platsundersökning Simpevarp. Fågelundersökningar inom SKB:s platsundersökningar 2002 (in Swedish).
P-03-56	**Ludvigson J-E, Levén J, Jönsson S.** Oskarshamn site investigation. Hydraulic tests and flow logging in borehole HSH03.
P-03-63	**Byström S, Hagthorpe P, Thunehed H.** Oskarshamn site investigation. QC-report concerning helicopter borne geophysics at Simpevarp, Oskarshamn, Sweden.
P-03-66	**Triumf C-A.** Oskarshamn site investigation. Geophysical measurements for the siting of a deep borehole at Ävrö and for investigations west of CLAB.
P-03-67	**Borgiel M.** Makroskopiska organismers förekomst i sedimentprov. En översiktlig artbestämning av makroskopiska organismer (in Swedish).
P-03-68	**Tobiasson S.** Tolkning av undervattensfilm från Forsmark och Simpevarp (in Swedish).
P-03-69	**Fredriksson R, Tobiasson S.** Simpevarp site investigation. Inventory of macrophyte communities at Simpevarp nuclear power plant. Area of distribution and biomass determination.
P-03-70	**Rouhiainen P, Pöllänen J.** Oskarshamn site investigation. Difference flow measurements in borehole KSH01A at Simpevarp.
P-03-71	**Vangkilde-Pedersen T.** Oskarshamn site investigation. Reflection seismic surveys on Simpevarpshalvön 2003 using the vibroseismic method.
P-03-72	**Juhlin C.** Oskarshamn site investigation. Evaluation of RAMBØLL reflection seismic surveys on Simpevarpshalvön 2003 using the vibroseismic.
P-03-73	**Aaltonen J, Gustafsson C, Nilsson P.** Oskarshamn site investigation. RAMAC and BIPS logging and deviation measurements in boreholes KSH01A, KSH01B and the upper part o KSH02.
P-03-74	**Barton N.** Oskarshamn site investigation. Q-logging of KSH 01A and 01B core.
P-03-83	**Boresjö Bronge L, Wester K.** Vegetation mapping with satellite data of the Forsmark, Tierp and Oskarshamn regions.
P-03-87	**Wacker P.** Oskarshamn site investigation. Hydrochemical logging in KSH01A.
P-03-88	**Berg C.** Hydrochemical logging in KSH02. Oskarshamn site investigation.
P-03-93	**Lindqvist L, Thunehed H.** Oskarshamn site investigation. Calculation of Fracture Zone Index (FZI) for KSH01A.
P-03-97	**Mattsson H, Thunehed H, Triumf, C-A.** Oskarshamn site investigation. Compilation of petrophysical data from rock samples and in situ gamma-ray spectrometry measurements.

P-03-99 **Triumf, C-A.** Oskarshamn site investigation. Identification of lineaments in the Simpevarp area by the interpretation of topographical data.

P-03-100 **Triumf C-A, Thunehed H, Kero L, Persson L.** Interpretation of airborne geophysical survey data. Helicopter borne survey data of gamma ray spectrometry, magnetics and EM from 2002 and fixed wing airborne survey data of the VLF-field from 1986. Oskarshamn site investigation.

P-03-106 **Chryssanthakis P, Tunbridge L.** Borehole: KSH01A. Determination of P-wave velocity, transverse borehole core. Oskarshamn site investigation.

P-03-107 **Chryssanthakis P.** Borehole: KSH01A. Results of tilt testing. Oskarshamn site investigation.

P-03-113 **Ask H, Morosini M,Samuelsson L-E, Stridsman H 2003.** Oskarshamn site investigation – Drilling of cored borehole KSH01. SKB P-03-113. Svensk Kärnbränslehantering AB.

P-03-114 **Ask H, Samuelsson L-E 2003.** Oskarshamn site investigation – Drilling of three flushing water wells, HSH01, HSH02 and HSH03. SKB P-03-113. Svensk Kärnbränslehantering AB.

P-04-04 **Cederlund G, Hammarström A, Wallin K.** Surveys of mammal populations in the areas adjacent to Forsmark and Oskarshamn. Results from 2003.

P-04-12 **Wacker P.** Complete hydrochemical characterization in KSH01A.

P-04-14 **Ericsson U.** Sampling of precipitation at Äspö 2002-2003.

P-04-22 **Rudmark L.** Investigation of Quaternary deposits at Simpevarp peninsula and the islands of Ävrö and Hålö. Oskarshamn site investigation.

P-04-32 **Mattsson H, Stanfors R, Wahlgren C-H, Stenberg L, Hultgren P.** Geological single-hole interpretation of KSH01A, KSH01B, HSH01, HSH02 and HSH03. Oskarshamn site investigation.

P-04-35 **Hermanson J, Hansen L, Wikholm M, Cronquist T, Leiner P, Vestgård J, Sandah K-A.** Detailed fracture mapping of four outgrops at the Simpevarp peninsula and Ävrö. Oskarshamn site investigation.

P-04-37 **Triumf C-A.** Joint interpretation of lineaments in the eastern part of the site descriptive model area. Oskarshamn site investigation.

PR-25-89-17 **Bjarnason B, Klasson H, Leijon, B, Strindell L, Öhman T 1989.** Rock stress measurements in boreholes KAS02, KAS03 and KAS05 on Äspö.

PR U-97-27 **Ljunggren C, H Klasson, 1997.** Drilling KLX02 – Phase 2 Lilla Laxemar Oskarshamn – Deep hydraulic fracturing Rock stress measurements in Borehole KLX02, Laxemar.

IPR-02-01 **Rummel F, Klee G, Weber U.** Äspö Hard Rock Laboratory. Rock Stress measurements in Oskarshamn. Hydraulic fracturing and core testing in borehole KOV01.

IPR-02-02 **Klee G, Rummel F.** Äspö Hard Rock Laboratory. Rock Stress measurements at the Äspö HRL. Hydraulic fracturing in boreholes KA2599G01 and KF0093A01.

IPR-02-03 **Collin M, Börgesson L.** Äspö Hard Rock Laboratory. Prototype Repository. Instrumentation of buffer and backfill for measuring THM processes.

IPR-02-18 **Klasson H, Lindblad K, Lindfors U, Andersson S.** Äspö Hard Rock Laboratory. Overcoring rock stress measurements in borehole KOV01, Oskarshamn.

IPR-03-13 **Dershowitz W, Winberg A, Hermanson J, Byegård J, Tullborg, E-L, Andersson P, Mazurek M.** Äspö Hard Rock Laboratory. Äspö Task Force on modelling of groundwater flow and transport of solutes. Task 6c. A semi-synthetic model of block scale conductive strctures at the Äspö HRL.

ICR-01-04 **Byegård J, Widestrand H, Skålberg M, Tullborg E-L, Siitari-Kauppi M.** First TRUE Stage. Complementary investigations of diffusivity, porosity and sorbtivity of Feature A-site specific geologic material.

R-97-13 **Carbol P, Engkvist I.** Compilation of radionuclide sorption coefficients for performance assessment.

R-98-55 **Follin S, Årebäck M, Axelsson C-L, Stigsson M, Jacks G.** Förstudie Oskarshamn. Grundvattnets rörelse, kemi och långsiktiga förändringar (in Swedish).

R-99-70 **Lindell S, Ambjörn C, Juhlin B, Larsson-McCann S, Lindquist K.** Available climatological and oceanographical data for site investigation program.

R-01-06 **Markström I, Stanfors R, Juhlin C.** Äspölaboratoriet RVS-modellering, Ävrö Slutrapport (in Swedish).

R-02-10	**Berggren J, Kyläkorpi L.** Ekosystemen i Simpevarpsområdet Sammanställning av befintlig information (in Swedish).
R-02-26	**Janson T, Stigsson M.** Test with different stress measurement methods in two orthogonal bore holes in Äspö HRL.
R-02-35	**SKB.** Simpevarp – site descriptive model version O.
R-02-47	**Risberg J.** Holocene sediment accumulation in the Äspö area. A study of a sediment core.
R-03-10	**Sundberg J.** Thermal Site Descriptive Model. A strategy for the model development during site investigations. Version 1.0.
R-04-11	**Miliander S, Punakivi M, Kyläkorpi L, Rydgren B. Human population and activities at Simpevarp.**
R-04-16	**Laaksoharju M, Smellie J, Gimeno M, Auqué L, Gómez J, Tullborg E-L, Gurban I.** Hydrogeochemical evaluation of the Simpevarp area, model version 1.1.
TR-97-06	**Rhén I (ed.) 1), Gustafson G, Stanfors R, Wikberg P.** Äspö HRL – Geoscientific evaluation 1997/5. Models based on site characterization 1986–1995.
TR-97-20	**Ohlsson Y, Neretnieks I.** Diffusion data in granite. Recommended values.
TR-98-18	**Byegård J, Johansson H, Skålberg M, Tullborg E-L.** The interaction of sorbing and non-sorbing tracers with different Äspö rock types. Sorption and diffusion experiments in the laboratory scale.
TR-02-03	**Larsson-McCann S, Karlsson A, Nord M, Sjögren J, Johansson L, Ivarsson M, Kindell S.** Meteorological, hydrological and oceanographical information and data for the site investigation program in the community of Oskarshamn.
TR-02-19	**Andersson J, Berglund J, Follin S, Hakami E, Halvarson J, Hermanson J, Laaksoharju M, Rhén I, Wahlgren C-H.** Testing the methodology for site descriptive modelling. Application for the Laxemar area.
SKI 98:41	**Xu S, Wörman A.** Statistical Patterns of Geochemistry in Crystalline Rock and Effect of Sorption Kinetics on Radionuclide Migration.

2.8 Model volumes

The site descriptive modelling is performed using two different model volumes of different scales, the regional and the local model volumes. Generally, the local model should cover the volume within which the repository is expected to be positioned, including accesses and the immediate environs. In addition to the description on the local scale, a description is also devised for a much larger volume, the regional model. The latter model provides boundary conditions and puts the local model in a larger context.

This section presents and justifies the model volumes selected for the Simpevarp area, including the Laxemar and Simpevarp subareas.

2.8.1 General

The difference between the regional and local model volumes is primarily a matter of resolution. The local volume description should be detailed enough to satisfy the needs of repository design and safety assessment. It is primarily the end users of the descriptions who can judge whether the designated local model volume is sufficiently large. The site modelling group may subsequently choose to enlarge this minimum volume in order to find more natural boundaries within the regional model volume. The regional scale description should allow a justifiable interface with the local description. In some applications, a sharp boundary between the two modelling scales is not that obvious and the transition in the description is essentially continuous However, the existence of very detailed data outside the "required" local volume is not itself a reason to expand the size of the local volume.

The need for pre-defined model volumes also stems from demands of the integrated representation in the SKB Rock Visualisation System (RVS). As discussed and explained by /Munier and Hermanson, 2001/, assignment (or prediction) of material properties should cover the entire model volume and be of the same resolution (scale) throughout. However, since the density of information varies, the confidence in the description will generally also vary within a given model volume. Furthermore, the verbal descriptions of the site need not be restricted to the bounds defined by the RVS-representation. Furthermore, boundaries of numerical models used in subsequent analyses do not necessarily have to coincide with the boundary of the RVS-representation. Selection of boundaries and boundary conditions is left at the discretion of the individual numerical modeller and should be decided on the basis of the purpose of the modelling. Naturally, it is an advantage if the boundaries coincide. In addition, the following rules of thumb apply /Andersson, 2003/:

- The local site descriptive model should cover an area of about 5–10 km^2, i.e. large enough to include the potential repository and its immediate surroundings. This also means that the location of the model area needs to be agreed upon by both the design and site descriptive modelling groups.
- The regional descriptive model should be large enough to provide boundary conditions and site understanding to the local model.
- If possible, model domains selected in previous versions should be retained. Deviations, if any, should be fully justified.
- The models should include the main sources of new information (e.g. from boreholes and areas of detailed surface geophysics).
- The local model domain should be large enough to allow meaningful hydrogeological flow simulations within the domain, even if information for boundary conditions needs to be taken from an encompassing regional scale hydrogeological model – or even beyond.
- Potentially important features, e.g. lineaments, interpreted deformation zones, rock type boundaries etc, should be considered when selecting the size of the model volumes.

However, practical considerations demand that the model domains should not be too large in relation to the selected resolution (scale) of the description.

2.8.2 Regional model volumes

Generally, the geographic scope of the regional models depends on the local premises and requirements and is controlled by the basic need to achieve understanding of the conditions and processes that determine the conditions at the site /SKB, 2001a/. The regional model volume should encompass a sufficiently large area that the geoscientific conditions that can directly or indirectly influence the local conditions, or help in understanding the geoscientific processes in the repository area, are included. In practical terms, this may entail a surface area of "a few hundred square kilometres."

Figure 2-3 shows the regional model area selected for Simpevarp 1.1. It is the same model area used in the version-0 report /SKB, 2002b/. The depth of the model volume is set to 2.2 km (from 100 m above sea level and extending down to 2,100 m).

The regional model volume has been selected on the basis of the following considerations:

- It includes the prioritised area for site investigations in the Simpevarp area /SKB, 2001b/ and it is not prohibitively large, with an approximate surface area of 273 km^2.
- It captures the extensive regional deformation zones, which strike in northnortheasterly and near east-west directions, and surround the prioritised area for site investigations. Any expansion of the regional model area to the east or west would not provide any significant changes in the regional geological picture.

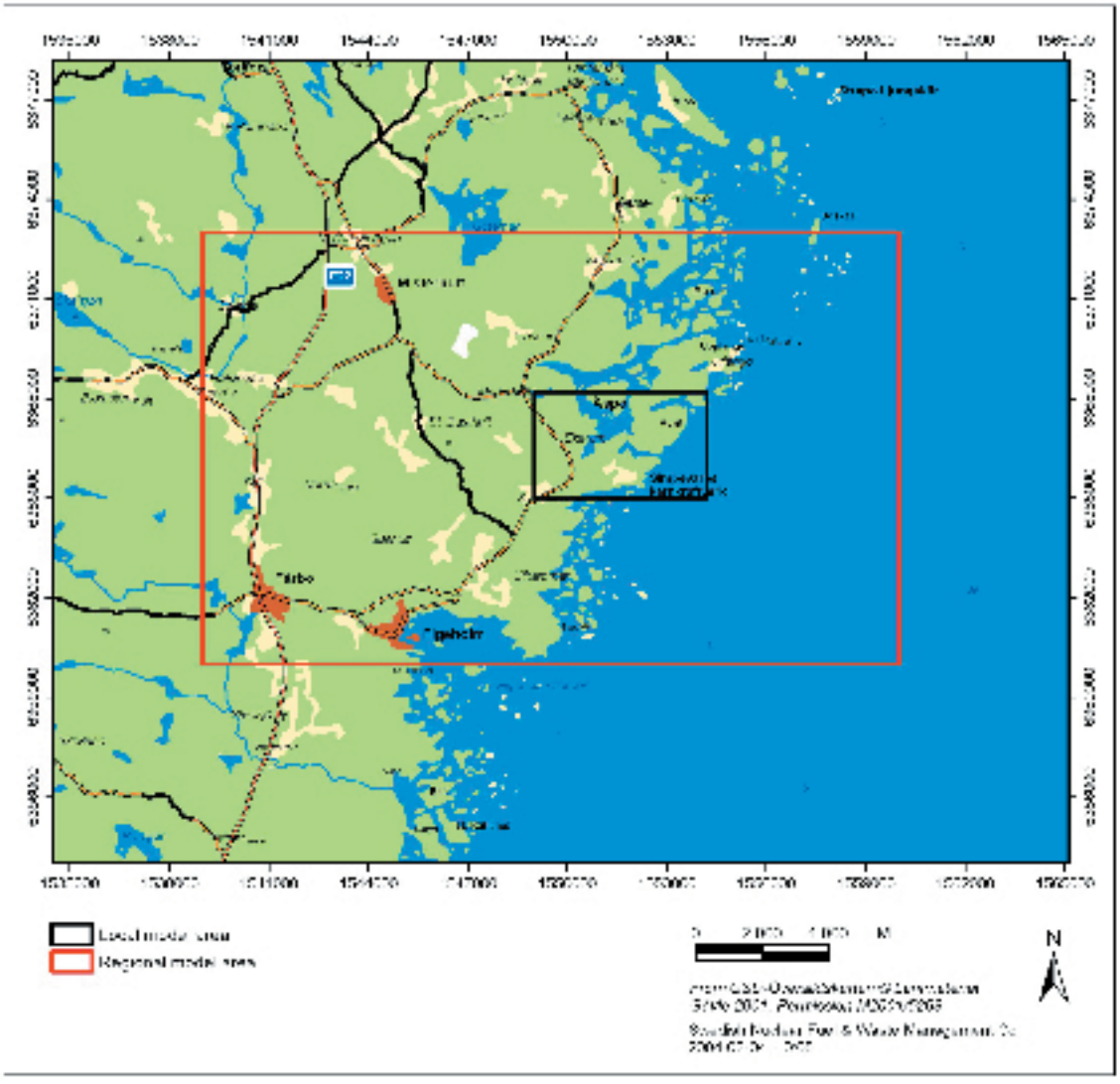

Figure 2-3. *Regional and local model areas used for Simpevarp version 1.1. The areal coverage of the regional model is the same as that used in version 0 /SKB, 2002b/.*

- It adequately covers the variations in rock type in the candidate area and its immediate surroundings.
- It captures the main features in the region interpreted to be of hydrogeological importance as the east-west boundaries are judged to be sufficiently well separated in space not to influence the groundwater flow in the region. Furthermore, the western boundary lies on the western side of a local topographic divide and the boundary to the east lies in the Kalmar Sund strait (between the mainland and the island of Öland). The area includes potential discharge areas for groundwater resulting from future shoreline displacement (see Figure 2-4 and Figure 2-5). Due to the very steep topographic relief close to the shoreline, a reduction of the extent of the regional model towards the east in the Kalmar Sund strait was considered for the Simpevarp 1.1 description. However, for convenience and easy back reference if was decided to retain the regional model boundaries used for the v0 modelling.
- A depth of 2.2 km (of which 100 m is above sea level) is considered to provide a reasonable context for the local description. Furthermore, this depth is considered the maximum down to which any meaningful extrapolations of deformation zones can be made.

The coordinates outlining the surface area of the Regional model for Simpevarp 1.1, c.f. Figure 2-3, are (in metres):

(X, Y):
(1539000, 6373000), (1560000, 6373000), (1539000, 6360000), (1560000, 6360000).

Z: (+100 m), –2,100 m.

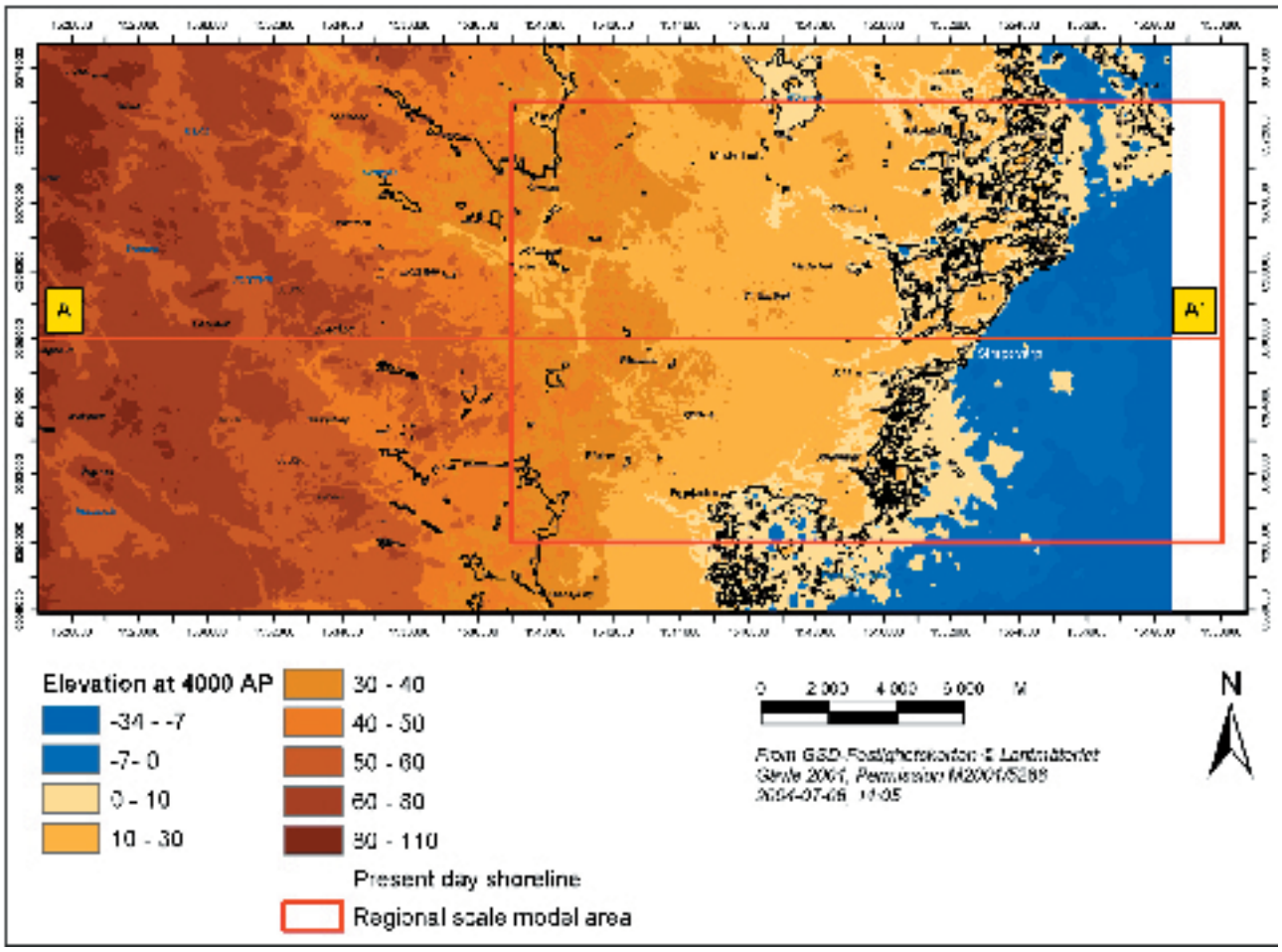

Figure 2-4. *Regional model of the Simpevarp area showing present day topography, projected shoreline and low points in the terrain (potential discharge areas) at 6,000 AD.*

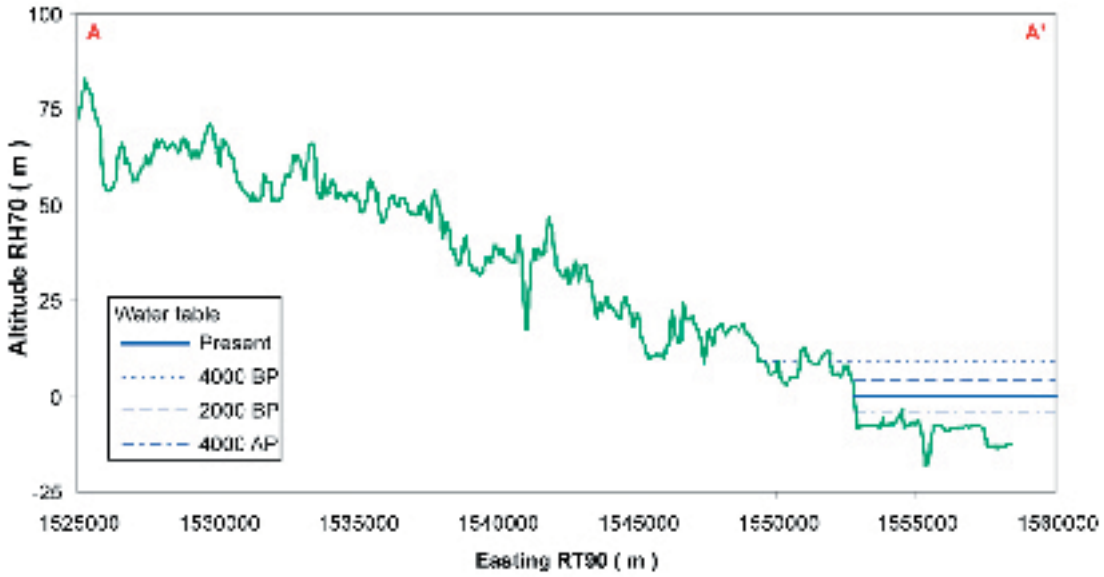

Figure 2-5. *Topographic relief along an east-west section The horizontal blue lines indicate the projected sea level at c. 4,000 before present (BP), 2,000 BP, present, and 4,000 after present (AP). The location of the section is given in Figure 2-4.*

2.8.3 Local model volume

The area covered by the deep repository (at repository depth) should ideally not be more than about 2 km^2. This assumes a fully constructed repository with approximately 4,000 canisters, a 90% utilisation of possible canister positions and centrally located space for the required infrastructure. The surface facility and the access to the deep repository are not included in this area, as their areal needs depend on whether a straight ramp, a spiral ramp or a shaft access will be employed. A geometrically ideal case will not be achieved in reality, since the layout of the deep repository will be adapted to conditions in the bedrock (deformation zones, etc). The more deposition subareas the deep repository is made up of, and the more irregular these are, the greater the total repository area that will be required, since intervening unutilised "corridors" must also be included in the total "encompassing" area. The local (investigation and) model area should be considerably larger than the repository area, above all because it is not otherwise possible to try out alternative repository layouts and gradually arrive at the optimal placement and adaptation to the rock conditions. The local model volume should therefore encompass a surface area of 5–10 km^2 /SKB, 2001a/.

In the version 0 report /SKB, 2002b/ a near circular-shaped "candidate area" with a size of some 50 km^2 was presented. The ambition of subsequent characterisation and analysis has been to reduce the candidate area to a "prioritised area for site investigation". In the case of the Simevarp area the prioritised area for site investigations is made up of two separate subareas. The first area, where drilling commenced during the summer of 2002, is denoted the "Simpevarp subarea" and is made up of major portions of the Simpevarp peninsula, together with the islands of Ävrö, Hålö and Bockholmen. The second, the "Laxemar subarea" was selected early in 2003 /SKB, 2003b/ following complementary regional investigations and subsequent evaluation /Wahlgren et al, 2003/, cf. Figure 1-1. The two areas are in essence neighbouring one another. This suggests that including the two "subareas" in one single local model would provide synergy and facilitate co-interpretation of data which will emerge from the two sites over time. Characterisation of the Laxemar subarea commenced in late 2003 and in this context comes second in time to the Simepvarp subarea. Also, the area of Hålö/Bockholmen, positioned inbetween the two subareas, is a natural candidate area for the surface installations associated with a future deep repository. By including the two subareas in one local model volume, satisfactory coverage is also provided for any type of access tunnel and/or tunnel connection from a shaft access to either of the two.

One drawback with incorporation of both subareas (Simpevarp and Laxemar) in one single local scale model for the purpose of Simepvarp 1.1, is that essentially no new information at present is available for the Laxemar subarea. This implies that, if enforced, a local model as outlined above would entail a large difference in data density and detail between the two embedded subareas. No bedrock map or integrated interpretation of lineaments is available for the Laxemar subarea. To work around this situation, a decision was taken to reduce the local model area for the purpose of the Simpevarp 1.1 model to cover basically only the area east of the northeast trending Äspö shear zone. A local adaptation of the interpretation and description of the geology and integrated lineaments is made in the area west of the Äspö shear zone.

The coordinates (X,Y,Z) outlining the surface area of the local model for Simpevarp 1.1, c.f. Figure 2-3, are (in metres):

1549000.000, 6368200.000, 100.000

1554200.000, 6368200.000, 100.000

1554200.000, 6365000.0000, 100.000

1549000.000, 6365000.000, 100.000

Figure 2-3 shows the local model area for the Simpevarp subarea as embedded in the Regional Model. The vertical extent of the local model is set to 1,200 m, 1,100 m below sea level and 100 m above sea level. It is noted that the southern parts of the Äspö island is included in the model, c.f. Section 2.6.

The local model volume has been selected on the basis of the following considerations:

- It provides a volume that includes the Simpevarp subarea and the area for potential surface facilities, access ramps and tunnels connecting from the islands of Hålö and Bockholmen.
- For future model versions it can relatively easily be expanded in size to the west to allow inclusion of the Laxemar subarea in full. This would allow co-interpretation of data emerging from the two subareas in an efficient and flexible manner. Similarly, as the site investigation progresses, it will be equally possible to diminish the size of the local model accordingly.
- The east-west boundaries are positioned along one interpreted v.0 fracture zone (ZSM0002A0), c.f. Table 5-6 and associated Figure 5-3, and a topograhically/geophysically identified lineament, respectively. The north-south boundaries of the model are not associated with any particular geographical feature.
- A depth of 1,100 m below sea level will permit inclusion of all information from the deep boreholes that will be completed at the site.
- The area has a surface area of approximately 17 (5.2x3.2) km^2 (see Figure 2-3).

3 Evolutionary aspects

3.1 Crystalline bedrock

3.1.1 Introduction

The following brief outline of the geological evolution in the Oskarshamn region is a slightly modified version of that presented in /Andersson et al, 2002b/. It is mainly based on results published in reports in various SKB series as well as in research papers in scientific journals. The Oskarshamn region is put into a regional geological context but the description is focussed on the geological evolution of rock types and structural elements that characterize the bedrock in the Oskarshamn municipality and its immediate surroundings.

The geological evolution of cratonic (stabilised) bedrock regions is generally the result of consecutive large-scale processes, e.g. orogenies, that have operated over a considerable period of time. In order to try to understand the geological development of the bedrock in southeastern Sweden, it is necessary to take into account also post-cratonization (after c. 1,750–1,700 Ma Before Present (BP)), i.e. large-scale processes more or less remote from the Oskarshamn region th at might have had a far-field effect in the already cratonised crust.

The geological development in the Oskarshamn region, including the formation of existing rocks, as well as structural and tectonic overprinting, is complex and spans a period of c. 1,900 Ma. The following text gives a brief summary and for further information of the geological evolution and processes that might have affected the bedrock in the Oskarshamn region and the rest of the southern part of the Fennoscandian Shield, the reader is referred to e.g. /Larson and Tullborg, 1993/ and /Milnes et al, 1998/.

As a reference for the following text, the geological time units and nomenclature used are displayed in Figure 3-1.

In order to put the Oskarshamn region in a large-scale geological evolutionary perspective, the successive growth of the Fennoscandian Shield and subsequent formation of Phanerozoic cover sequences from c. 1,910 Ma until the Quaternary period is displayed in Figure 3-2 through Figure 3-6. In each figure, previously formed rocks are marked in grey. The following abbreviations are used:

GP = granite-pegmatite.

GDG = granitoid-dioritoid-gabbroid.

GSDG = granite-syenitoid-dioritoid-gabbroid.

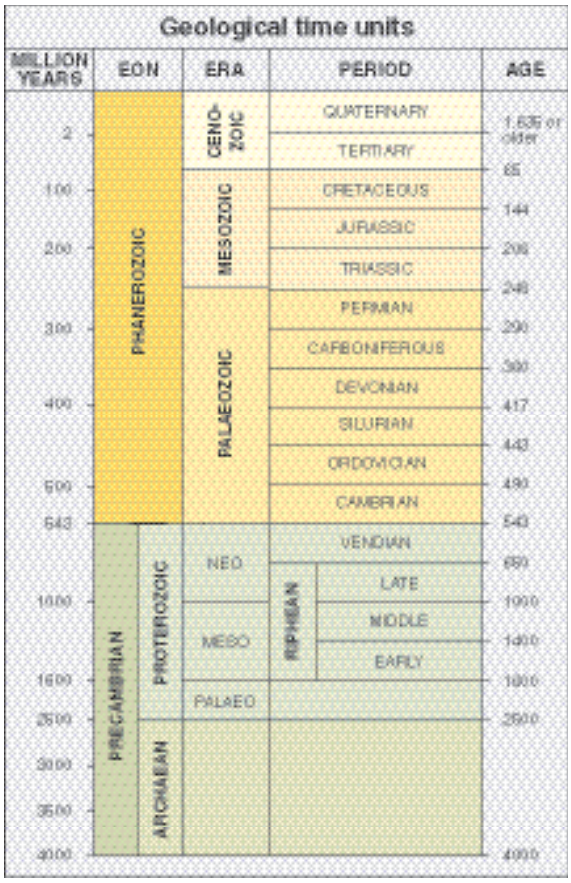

Figure 3-1. *Geological time scale. Modified after /Koistinen et al, 2001/.*

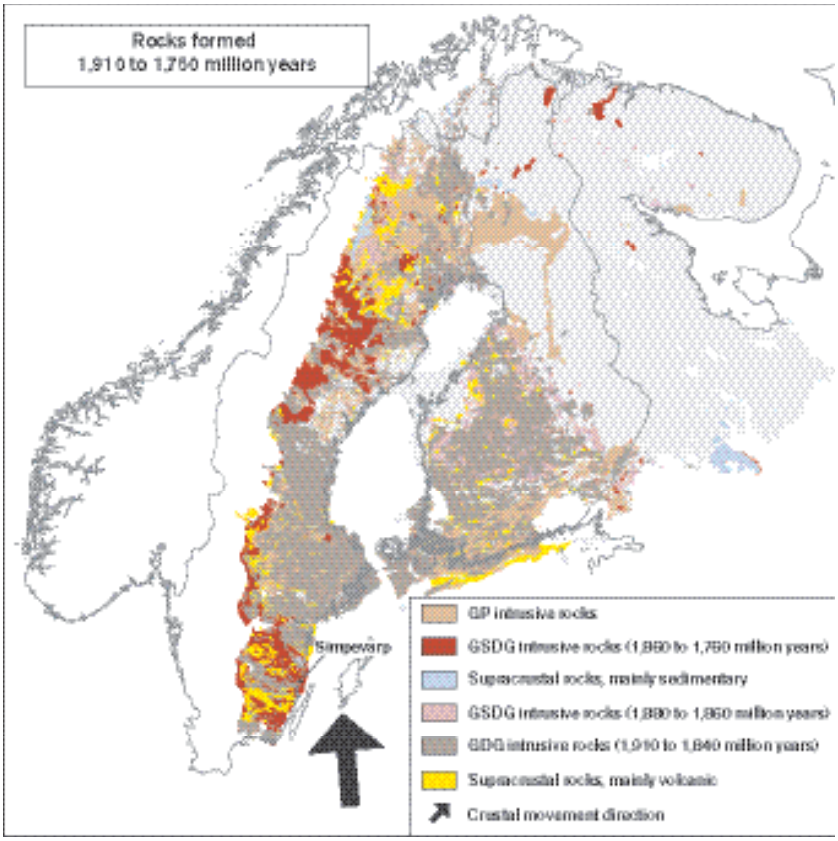

Figure 3-2. *Rocks formed in the time interval 1,910–1,750 Ma BP. The figure is based on the database presented by /Koistinen et al, 2001/.*

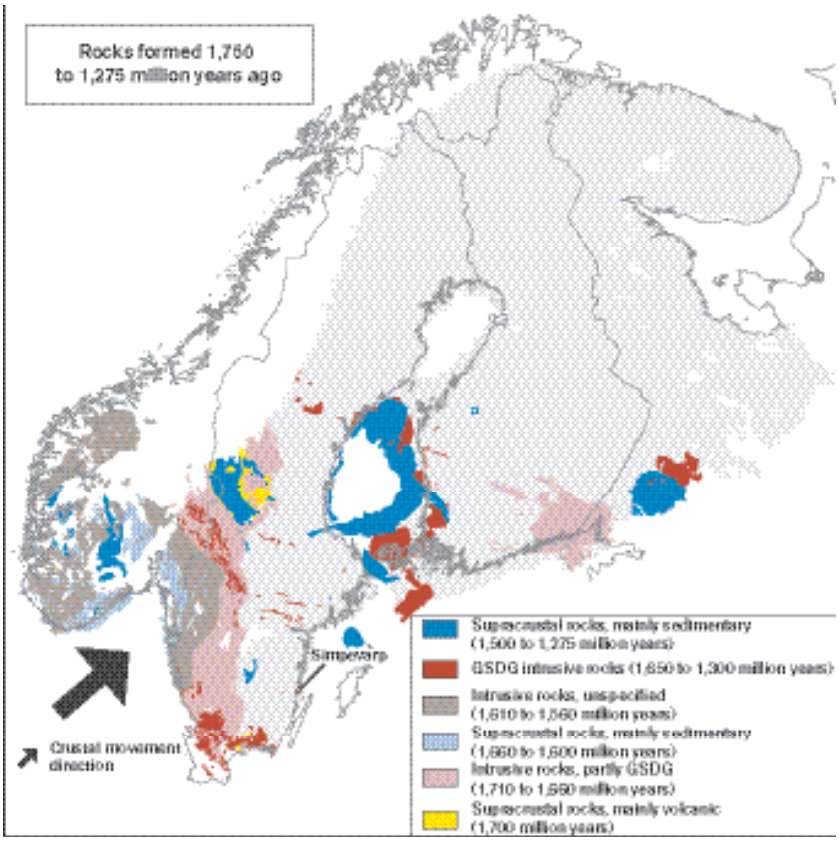

Figure 3-3. *Rocks formed in the time interval 1,750–1,275 Ma BP. The figure is based on the database presented by /Koistinen et al, 2001/.*

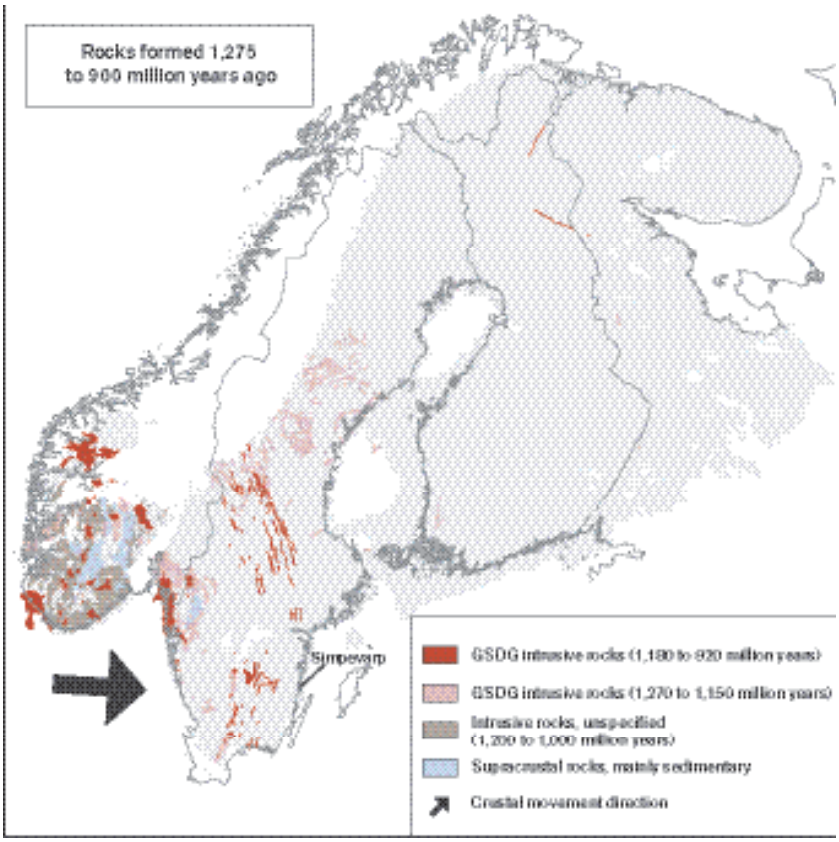

Figure 3-4. *Rocks formed in the time interval 1,275–900 Ma BP. The figure is based on the database presented by /Koistinen et al, 2001/.*

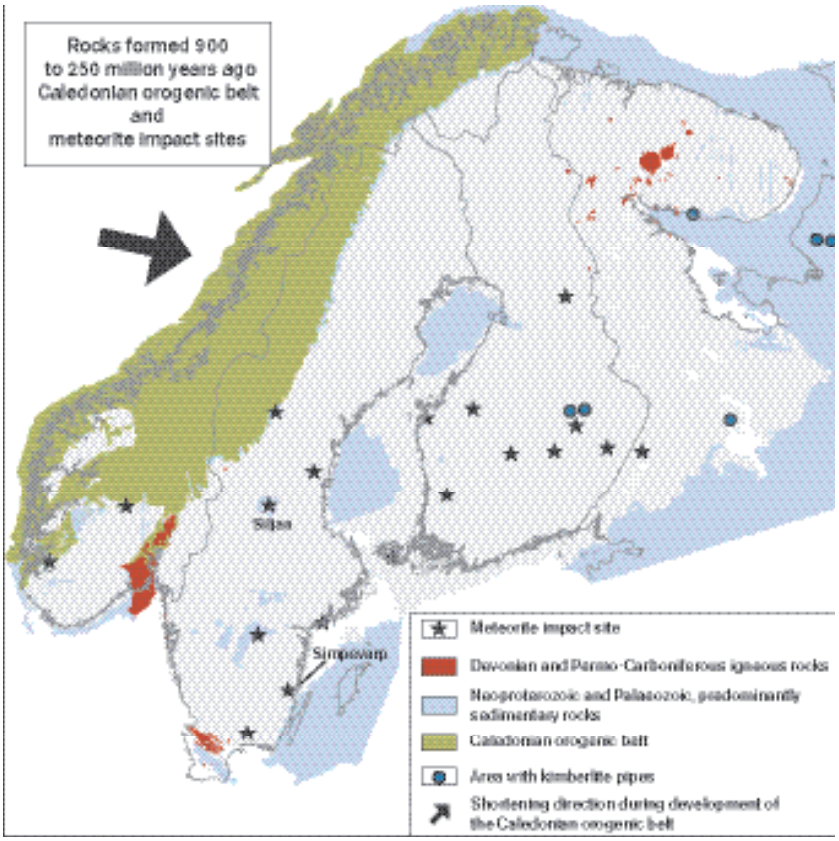

Figure 3-5. *Rocks formed in the time interval 900–250 Ma BP. The figure is based on the database presented by /Koistinen et al, 2001/.*

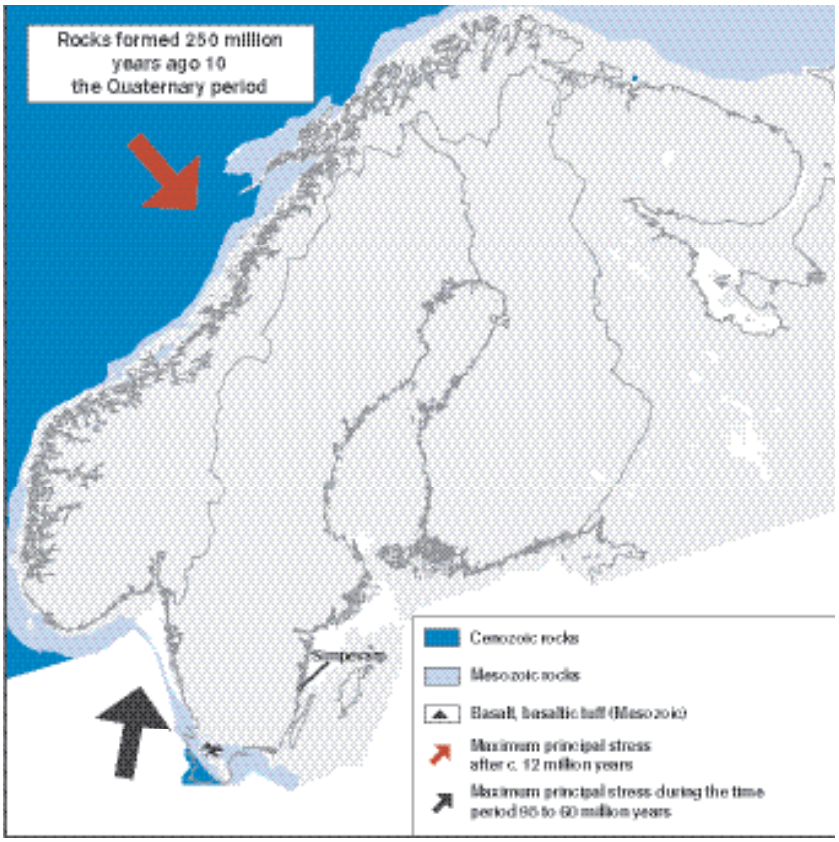

Figure 3-6. *Rocks formed in the time interval 250 Ma BP to the Quaternary period. The figure is based on the database presented by /Koistinen et al, 2001/.*

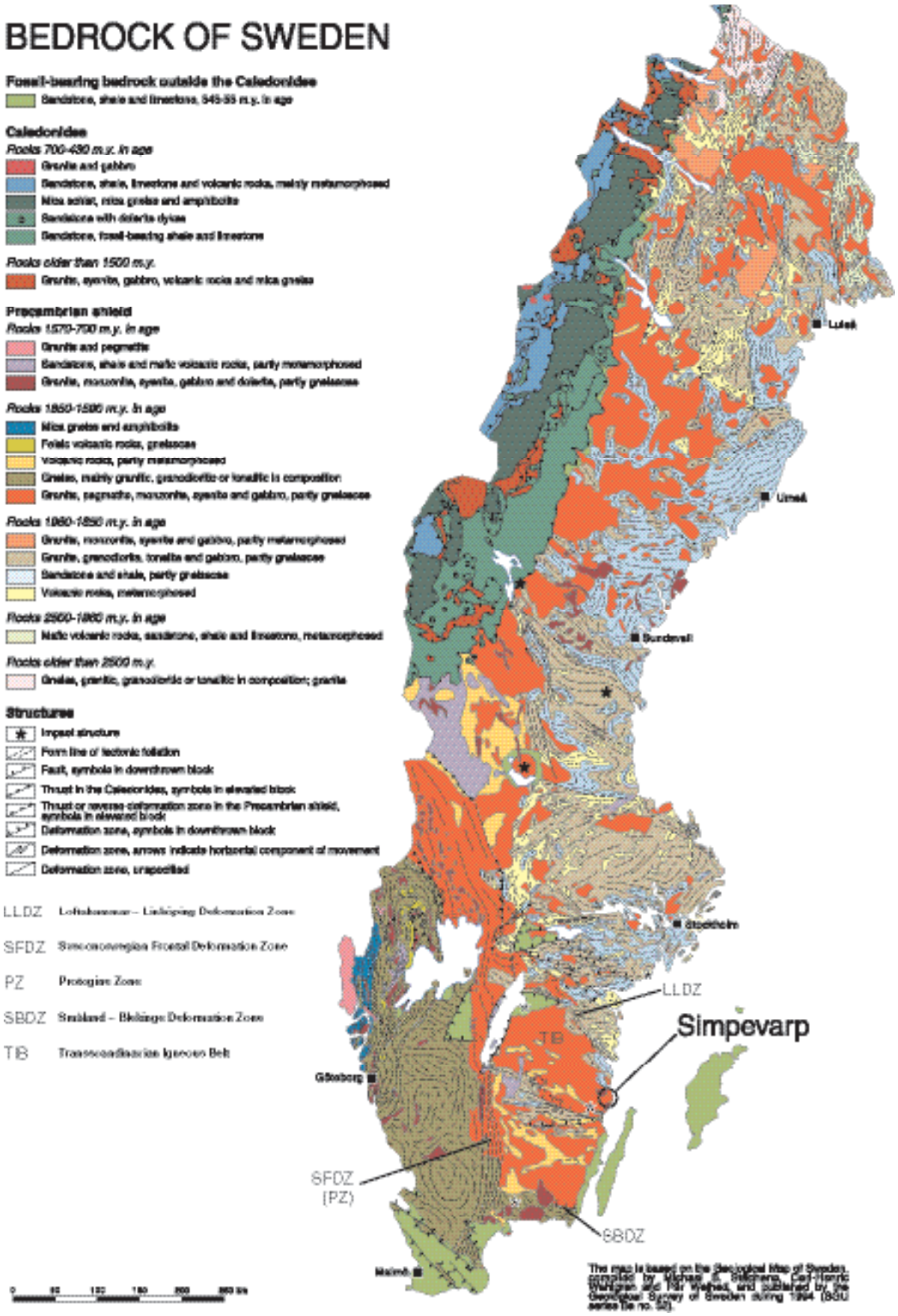

Figure 3-7. *Simplified bedrock map of Sweden. The geological province in which the Simpevarp area lies is bounded by major deformation zones along its northern /LLDZ/, southern /SBDZ/ and western /SFDZ/ boundaries. Modified after /Stephens et al, 1994/.*

3.1.2 Lithological development

The position of the Oskarshamn region in a regional geological-evolutionary perspective can be seen in Figure 3-2 through Figure 3-7. The oldest rocks in the Oskarshamn region, though subordinate, comprise more or less strongly deformed and metamorphosed supracrustal rocks of predominantly sedimentary but also of volcanic origin. The formation of the metasedimentary rocks is constrained to the time interval c. 1,870–1,860 Ma BP /Sultan et al, 2004/, and the rocks have their main expression in the Blankaholm-Västervik area, c.f. Figure 3-8 /Bergman et al, 1998, 1999, 2000/.

In the area immediately north of Oskarshamn and westwards, metagranitoids belonging to the E-W to WNW-ESE trending so-called Oskarshamn-Jönköping belt /Mansfeld, 1996/ constitute an important lithological component. These rocks were formed c. 1,834–1,823 Ma ago /Mansfeld, 1996; Åhäll et al, 2002/ and display a varying degree of tectonometamorphic overprinting and in many places they are relatively well-preserved.

The majority of the rocks at the present day erosional level in southeastern Sweden were formed during a period of intense igneous activity c. 1,810–1,760 Ma ago /e.g. Wikman and Kornfält, 1995; Kornfält et al, 1997/, during the waning stages of the Svecokarelian orogeny. The dominant rocks comprise granites, syenitoids, dioritoids and gabbroids, as well as spatially and compositionally related volcanic rocks. The granites and syenitoids, as well as some of the dioritoids are by tradition collectively referred to as Småland “granites”. Both equigranular, unequigranular and porphyritic varieties occur, and the compositional variation is displayed in Figure 3-9. Hence, the Småland “granites” comprise a variety of rock types regarding texture, mineralogical and chemical composition.

This generation of igneous rocks belongs to the so-called Transscandinavian Igneous Belt (TIB), which has a NNW extension from southeastern Sweden through Värmland and Dalarna into Norway where it finally disappears beneath the Scandinavian Caledonides (Figure 3-7). It is characterised by repeated alkalicalcic-dominant magmatism during the period c. 1,860–1,650 Ma ago. Magma-mingling and -mixing processes, exemplified by the occurrence of enclaves, hybridization and diffuse transitions etc between different TIB rocks indicate a close time-wise and genetic relationship between the different rock types. At mesoscopic scale, these processes often resulted in a more or less inhomogeneous bedrock regarding texture, mineralogical and chemical composition. However, if larger rock volumes are considered these may be regarded as being more or less homogeneous, despite some internal variations.

Locally, fine- to medium-grained granite dykes and minor massifs and also pegmatite occur frequently. Though volumetrically subordinate, these rocks constitute essential lithological inhomogeneities in parts of the bedrock in the Oskarshamn region, e.g. in the Simpevarp area. They are roughly coeval with the TIB host rock /Wikman and Kornfält, 1995; Kornfält et al, 1997/, but have been intruded at a late stage in the magmatic evolution. Furthermore, TIB-related mafic and composite dykes occur locally.

After the formation of the TIB rocks, the next rock-forming period in the Oskarshamn region, including southeastern Sweden, did not take place until c. 1,450 Ma ago. It was characterised by the local emplacement of granitic magmas in a cratonized crust. However, this granitic magmatism was presumably a far-field effect of ongoing orogenic processes elsewhere, presumably farther to the southwest of present Scandinavia. In the Oskarshamn region, the c. 1,450 Ma BP magmatism is exemplified by the occurrence of the Götemar, Uthammar and Jungfrun granites, c.f. Figure 3-8 /Kresten and Chyssler, 1976; Åhäll, 2001/. Fine- to medium-grained granitic dykes and pegmatites that are related to the c. 1,450 Ma granites occur as well, e.g. in the Götemar granite. However, these dykes are inferred to occur only within the granite and in its immediate surroundings.

The youngest magmatic rocks in the region are scattered dolerite dykes that presumably are related to the regional system of N-S trending, c. 1,000–900 Ma old dolerites that can be followed from Blekinge in the south to Dalarna in the north /Johansson and Johansson, 1990; Söderlund et al, 2004/. The dykes are emplaced in and to the east of the frontal part of the Sveconorwegian orogen. Due to the generally high content of magnetite, they usually constitute linear, positive magnetic anomalies, and their occurrence and extension may, thus, be identified on the magnetic anomaly maps. Time-wise they are related to the c. 1,100–900 Ma Sveconorwegian orogeny which is responsible for the more or less strong reworking and present structural geometry in the bedrock of southwestern Sweden.

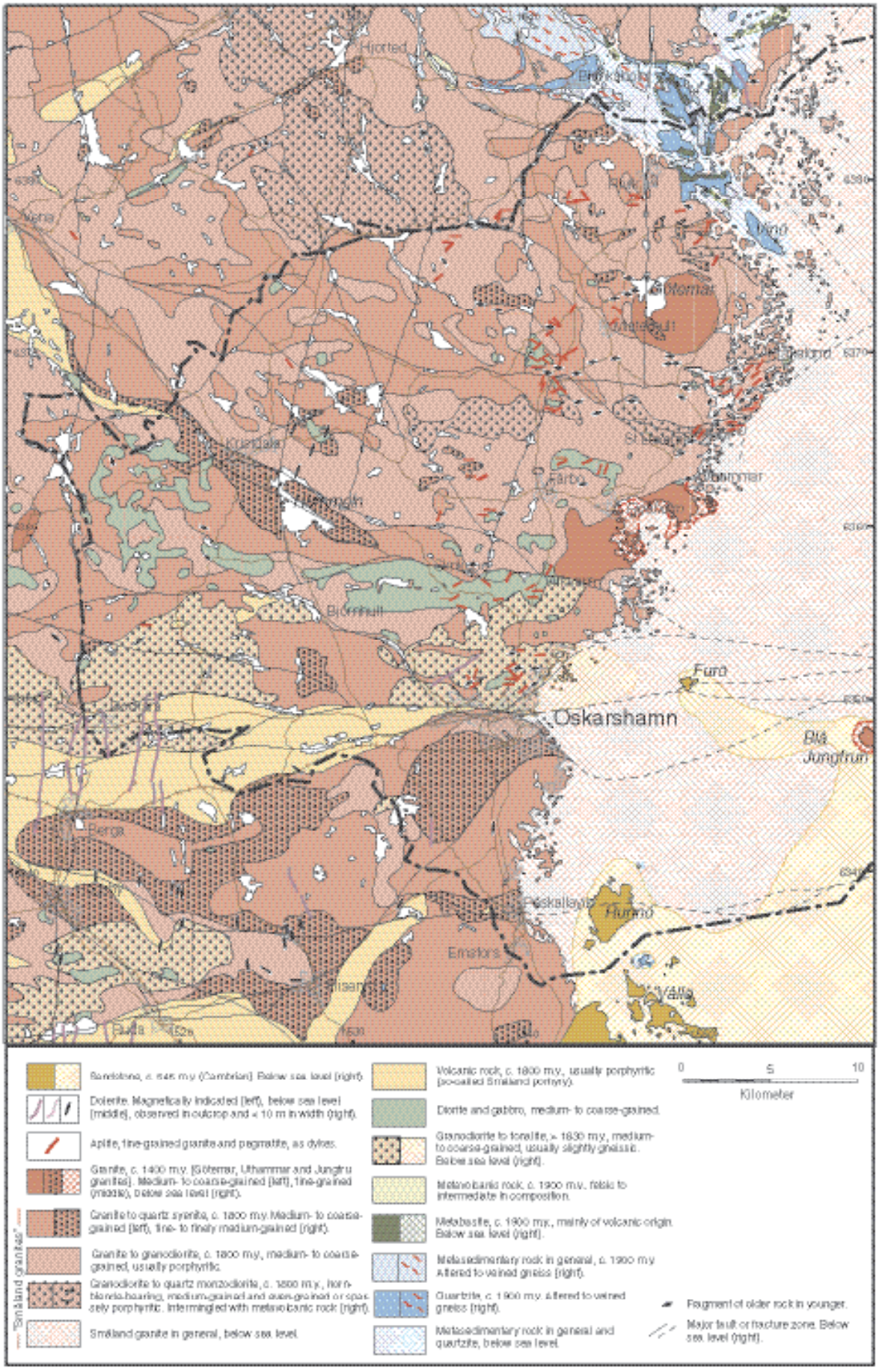

Figure 3-8. *Bedrock map of the Oskarshamn municipality and the surrounding area. Slightly modified after /Bergman et al, 1998/.*

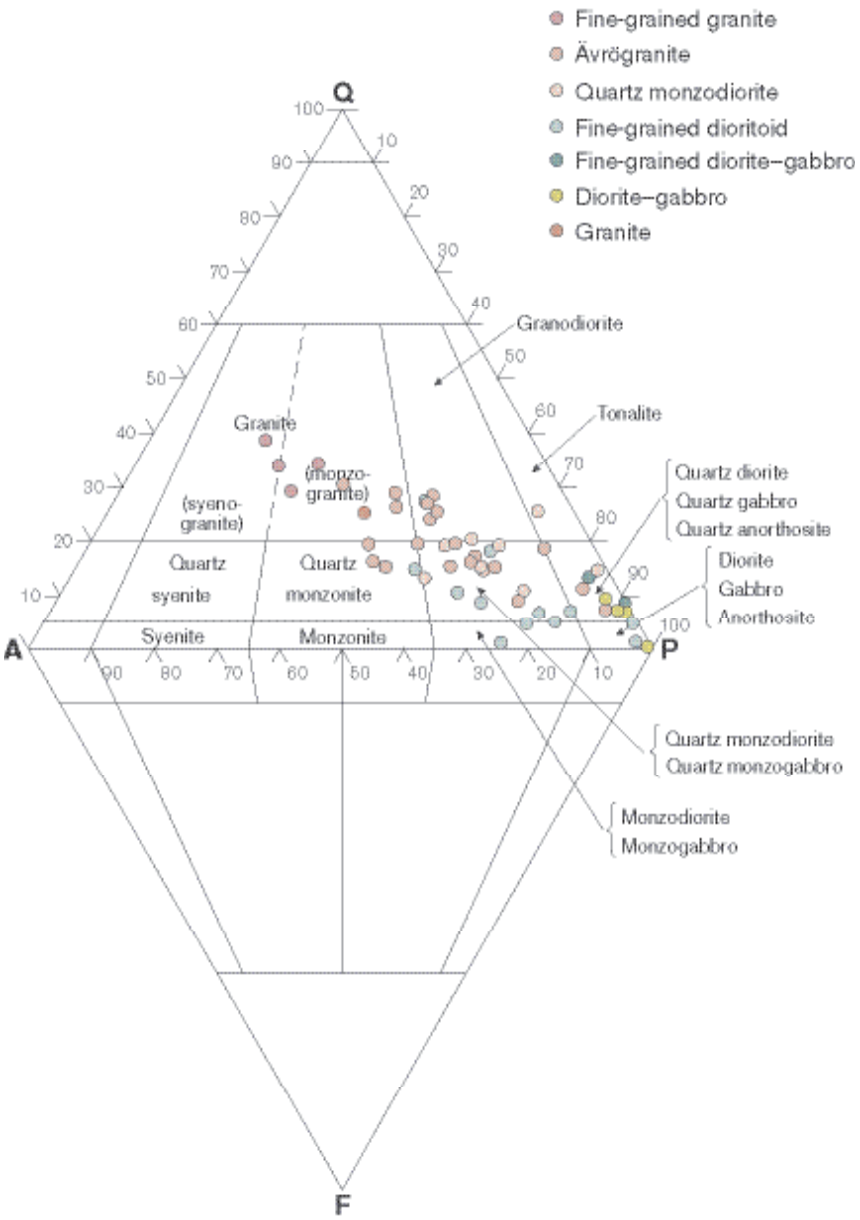

Figure 3-9. *QAPF-diagram displaying the compositional variation of magmatic rocks, examplified with modal analyses of rocks from the Simpevarp subarea.*

In late Precambrian and/or early Cambrian time, i.e. c. 600–550 Ma ago, arenitic sediments were deposited on a levelled bedrock surface, the so-called sub-Cambrian peneplain. The sediments were subsequently transformed to sandstones, which constitute the youngest rocks in the region, c.f. Figure 3-7 and Figure 3-8. The remainder of these former extensively occurring sedimentary rocks covers the Precambrian crystalline rocks along the coast of the Baltic Sea from the area south of Oskarshamn in the north to northeastern Blekinge in the south. Furthermore, fractures filled with sandstone are documented in the Oskarshamn region in e.g. the Götemar granite, east of the N-S trending fault (c.f. Figure 3-8) that transects the granite /Kresten and Chyssler, 1976/ and at Enudden, c. 4 km northeast of Simpevarp /Talbot and Ramberg, 1990; see also Röshoff and Cosgrove, 2002/. In general, the sandstone infilling has been intruded by force downward into the basement /Röshoff and Cosgrove, 2002/. A close spatial relationship between the sandstone dykes, the sub-Cambrian peneplain and Cambrian cover rocks indicates that the sandstone dykes are Cambrian in age. A characteristic feature is the local occurrence of fluorite (+/– calcite and galena) mineralisations within the pores of the sandstone dykes and along the dyke/country rock interface. The timing of formation of the mineralisations is uncertain, but they post-date the formation of the

sandstone dykes. /Alm and Sundblad, 2002/ claimed that the mineralisations are post-Cambrian and pre-Silurian in age, whereas /Röshoff and Cosgrove, 2002/ suggested that they are pre-Permian in age.

3.1.3 Structural development

Ductile deformation

The bedrock of southeastern Sweden has gone through a long and complex structural development, including both ductile and brittle deformation, since the formation of the oldest c. 1,890–1,850 Ma supracrustal rocks. The oldest deformation, which was developed under medium- to high-grade metmorphic conditions, is of regional, penetrative character, and is recorded in the supracrustal rocks in the Blankaholm-Västervik area. It pre-dates the intrusion of the c. 1,860–1,850 Ma generation of TIB rocks which, however, are deformed themselves. At variance from the more or less penetrative pre-1,860 Ma deformation in the supracrustal rocks, the deformation that has affected the 1,860–1,850 Ma generation of TIB rocks, as well as the older supracrustal rocks, was heterogeneous in character. It was caused by dextral transpression under medium-grade metamorphic conditions in response to c. N-S to NNW-SSE regional compression (see Figure 3-2), is constrained to the time-interval c. 1,850–1,800 Ma BP, and is exemplified by the dextral, strike-slip dominated Loftahammar-Linköping deformation zone, c.f. Figure 3-7 /Stephens and Wahlgren, 1996; Beunk and Page, 2001/. However, the folding of the foliation in the pre-1,850 Ma rocks was also supposedly developed in response to the same stress field /Stephens and Wahlgren, 1996; Beunk and Page, 2001/.

The 1,810–1,760 Ma BP generation of TIB rocks, that dominates the bedrock in the Oskarshamn region, is post-tectonic in relation to the regional, penetrative deformation related to the peak of the Svecokarelian orogeny. However, they are characterised by a system of ductile deformation zones of the same character as the Loftahammar-Linköping deformation zone, though developed during more low-grade conditions, i.e. at shallower levels in the crust, than the initial phase of shearing in the Loftahammar-Linköping deformation zone. However, the latter zone displays ductile reactivation during low-grade conditions, which presumably is contemporaneous with the shearing in the 1,810–1,760 Ma TIB rocks. In the Oskarshamn region, these low-grade, ductile deformation zones are exemplified by the E-W trending Oskarshamn-Bockara and NE-SW trending Oskarshamn-Fliseryd deformation zones /Bergman et al, 1998/. Presumably, also the NE-SW trending Äspö shear zone /Gustafsson et al, 1989; Bergman et al, 2000/, which is characterized by a sinistral strike-slip component, belongs to this system of ductile deformation zones.

Independent of the syn-deformational metamorphic grade, the dextral and sinistral strike-slip component in the WNW-ESE to NW-SE and NE-SW trending ductile deformation zones, respectively, indicate that a regional, c. N-S to NNW-SSE compression prevailed during their formation and subsequent ductile reactivation. Consequently, this regional stress field is inferred to have prevailed for a considerable period, at least from the time of the intrusion of the 1,850 Ma TIB generation, or possibly earlier, until c. 1,750 Ma ago. Most of the lithological contacts in the region, and also in the whole of southeastern Sweden, are more or less concordant with the orientation of the ductile deformation zones, which indicates that the emplacement of the TIB magmas was facilitated by ongoing shear zone activity. Together with the subsequent deformation of the TIB rocks, this testifies to the influence of the deformation zones in the present structural and lithological frame-work in the bedrock of southeastern Sweden.

The structural and metamorphic overprinting in rocks in the Oskarshamn region in relation to their age of formation is summarised in Table 3-1.

Apart from the mylonitic foliation in the ductile deformation zones, the 1,810–1,760 Ma TIB rocks locally display a more or less well-developed foliation /Kornfält and Wikman, 1987/, e.g. preferred orientation of feldspar phenocrysts, mafic enclaves, biotite etc. However, it is often difficult to decide whether the foliation is syn-intrusive or caused by a subsequent tectonic overprinting. Independent of origin, the orientation of the foliation suggests that there is a genetic relationship between foliation development outside the ductile deformation zones and the shear zone activity.

Table 3-1. The relation between age of rock types and the structural and metamorphic overprinting.

Age (Ma BP)	Structural and metamorphic overprinting
1,880–1,870	Penetrative, ductile deformation under medium- to high-grade metamorphic conditions.
1,860–1,850	Inhomogeneous ductile deformation under medium-grade metamorphic conditions.
1,834–1,823	Inhomogeneous ductile deformation under low- to medium-grade metamorphic conditions.
1,810–1,760	Spaced ductile shear zones developed under low-grade metamorphic conditions. Although the majority of the rocks are structurally more or less well-preserved, a low- to very low-grade metamorphic alteration occurs.
1,450	Brittle deformation. The rocks are well-preserved.
1,100–900	Brittle deformation. The rocks are well-preserved.
540	Brittle deformation. The rocks are well-preserved.

Brittle deformation

Since no ductile deformation has been observed in the c. 1,450 Ma granites /e.g. Talbot and Ramberg, 1990; Munier, 1995/ or younger rocks, it is evident that only deformations under brittle conditions have affected the bedrock in the Oskarshamn region during at least the last c. 1,450 Ma. However, the transition from ductile to brittle deformation presumably took place during the time interval c.1,750–1,700 Ma, i.e. during uplift and stabilization of the crust after the Svecokarelian orogeny.

To unravel the brittle tectonic history in the bedrock in southeastern Sweden during the last c. 1,450 Ma is difficult. It is plausible that tectonic activities that are related to more or less remote large-scale processes, such as e.g. the Gothian, Hallandian, Sveconorwegian and Caledonian orogenies, the opening of the Iapetus Ocean, the Late Palaeozoic Variscan and the Late Mesozoic to Early Cenozoic Alpine orogenies, as well as the opening of the present Atlantic Ocean, have had a far-field effect within the shield area, c.f. Table 3-1. In a global tectonic perspective, the Sveconorwegian orogeny, which corresponds to the Grenville orogeny in North-America and elsewhere, ultimately resulted in the assembly of the supercontinent Rodinia c. 900 Ma ago. Likewise the Caledonian orogeny (collision between the Laurentian and Fennoscandian Shields) was the first step in the formation of the supercontinent Pangaea, the latter part of which was finally assembled in connection with the Hercynian-Variscan orogeny in central Europe c. 250 Ma ago.

To what degree these large-scale processes have affected the bedrock in the Oskarshamn region and the rest of southeastern Sweden, and especially which brittle structure belongs to which process is difficult to decipher. The main reason for this uncertainty is the great lack of time markers for relative dating, except for the sub-Cambrian peneplain and the Cambro-Ordovician cover rocks, and the difficulties in dating brittle structures radiometrically.

The first brittle faults in the region probably developed in connection with the emplacement of younger, c. 1,450 Ma granites. During the subsequent geological evolution, faults and older ductile deformation zones have been reactivated repeatedly, due to the increasingly brittle behaviour of the bedrock. Brittle reactivation of ductile deformation zones is a general phenomenon. The Oskarshamn-Bockara, Oskarshamn-Fliseryd and Äspö shear zones display clear evidence of being reactivated in the brittle régime /see also e.g. Munier, 1995/. An inversion of the strike-slip component in the Äspö shear zone from sinistral during the older ductile deformation, to dextral during the younger brittle reactivation has been proposed by /Talbot and Munier, 1989/ and /Munier, 1989/.

K-Ar dating of biotites from the “Småland granites” /Åberg, 1978/ has yielded ages of c. 1,500–1,400 Ma. According to /Åberg, 1978/, the obtained ages are caused by the c. 1,500–1,400 Ma BP magmatic activity in southern Sweden. However, /Tullborg et al, 1996/ considered the closure of the K-Ar system in this time interval to be the result of an uplift scenario. Independent of the explanation, there is no information about any explicit tectonic features that can be related to this time period.

The occurrence of c. 1,000–900 Ma BP dolerites in southeastern Sweden testifies to a Sveco-norwegian tectonic influence, as the intrusion of the parent magmas was tectonically controlled. However, whether individual faults or fracture zones, which were not injected by mafic magma, were formed or reactivated during the Sveconorwegian orogeny, and if so which of them, is uncertain.

On the basis of titanite and zircon fission track studies in the Oskarshamn region, it has been suggested that sediments that were derived from the uplifted Sveconorwegian orogenic belt and deposited in a Sveconorwegian foreland basin reached a thickness of c. 8 km in southeastern Sweden at around 850 Ma BP /Tullborg et al, 1996; Larson et al, 1999/. Subsequent exhumation of southeastern Sweden and erosion of the sedimentary pile were completed by the establishment of the sub-Cambrian peneplain at the end of the Neoproterozoic. Remnants of this sedimentary pile are found in the Almesåkra Group in the vicinity of Nässjö /Rodhe, 1987a/. Furthermore, apatite fission track ages in the Oskarshamn region indicate that Upper Silurian to Devonian sediments, which were derived from the uplift of the Caledonian orogenic belt and deposited in a Caledonian foreland basin, covered most of Sweden and reached a thickness exceeding 2.5 km /Tullborg et al, 1995, 1996; Larson et al, 1999/. Exhumation and subsequent erosion during the Early Mesozoic removed the sedimentary cover almost completely /Tullborg et al, 1995, 1996; Larson et al, 1999/. During the Cretaceous, a transgression occurred which resulted in a thin cover of marine sediments. In the Oskarshamn region the sedimentary cover was not completely removed until the Tertiary /Lidmar-Bergström, 1991/.

The above-mentioned repeated large-scale events of subsidence, deposition of sediments, and subsequent exhumation and erosion, reasonably must have been accompanied by tectonic activity, i.e. movements along faults. However, there is no information that helps to decipher which fracture zones (faults) formed or were reactivated during these periods.

A recent (U-Th)/He geochronological study on apatites from rocks sampled in the access tunnel to the Äspö Hard Rock Laboratory and the cored boreholes KLX01 and 02 in the Laxemar area, yields decreasing ages with increasing depth (c. 270 Ma at the surface and c. 120 Ma at 1,700 m). This indicates that exhumation took place primarily during Late Palaeozoic to Mid Mesozoic /Söderlund et al, in prep./. Crustal movements younger than 120 Ma is plausible in the area although not possible to constrain until deeper borehole samples are available. The data also suggests that movement occurred during Late Palaeozoic to Mid Mesozoic time along fault zones between Äspö and the Laxemar area, e.g. reactivation in the Äspö shear zone. In future studies, this method will be used to try to estimate offset of some of the faults in the area.

According to /Milnes and Gee, 1992/ and /Munier, 1995/, the Ordovician cover rocks along the northwestern coast of Öland are tectonically undisturbed, except for displacements at the centimetre scale. This suggests that the E-W trending fracture zones/faults in the Oskarshamn-Bockara deformation zone, which can be seen in the magnetic anomaly maps to continue eastwards under Öland, have not affected the Cambro-Ordovician cover sequences on Öland. Thus, this indicates that these brittle deformation zones of regional character were not active in post-Cambrian time, but are related to the Precambrian tectonic evolution. However, post-Cambrian fracture zones/faults do occur in the Oskarshamn region. On the northwestern part of Furö, c.f. see Figure 3-8, a small island c. 10 km east of Oskarshamn, a fault contact between a brecciated Cambrian sandstone and a brecciated red granite is recorded /Bergman et al, 1998/. Furthermore, the occurrence of joints filled with sandstone east of, but not west of, the N-S trending fault in the western part of the Götemar granite, indicates that the eastern block has been down-faulted in relation to the western block in post-Cambrian time /Kresten and Chyssler, 1976; Bergman et al, 1998/.

As mentioned above, the sub-Cambrian peneplain is a potential marker to demonstrate post-Cambrian brittle tectonics. In general, all pronounced depressions and distinct differences of topographic level in the sub-Cambrian peneplain constitute potential fracture zones or faults. /Tirén et al, 1987/ studied the relative movements of regional blocks in southeastern Sweden which were bounded by fracture zones and ranged in size between 25 km^2 and 100 km^2. Differential movements were interpreted to have occurred along existing faults both during periods of uplift and subsidence.

A general problem is to decipher the relation between the formation and subsequent reactivation of faults and fracture zones. Especially the mutual age relationship between fracture zones with different orientation is difficult to determine, mainly due to the complex relationship between age of formation and age of (latest?) reactivation. Another, and perhaps the most important and complicating, factor is that brittle deformation zones are very poorly exposed, since they mostly constitute topographical depressions filled with glacial cover, rivers, swamps etc.

The brittle deformation history of a region can be regarded as the combined effect of generation of new fractures or faults and reactivation of old fractures or faults. The ratio between generation of new structures and reactivation of older structures is presumed to decrease with time, since the orientation spectrum of pre-existing structures increased with every new event of brittle deformation /Munier, 1995/. Relative age determinations of fractures, based on orientation and a succession of mineral filling with decreasing age, have been recorded on Äspö /e.g. Munier, 1995/, and it is reasonable to assume that these findings can be extrapolated to the surrounding parts of the Oskarshamn region. The oldest fractures are epidote- and quartz-bearing, and with decreasing age chlorite, zeolite and calcite appear as fracture fillings. Since the mineralogy in individual fractures within fracture zones is essentially similar to fractures in the intervening blocks /Munier, 1995/, the fracture filling is a tool for relative age determination of movement (reactivation) of the former. Consequently, the calcite-bearing fracture zones/faults represent the youngest reactivation, but its absolute age is uncertain.

Based on data from Äspö, the orientation of the maximum compressive stress during the formation of the epidote- and quartz-bearing fracture zones was N-S/subhorizontal /Munier, 1989/, but had changed orientation to NE-SW when the chlorite-filled fracture zones/faults formed /Talbot and Munier, 1989/. The maximum horizontal compression was still NE-SW when the fractures formed which are filled with Cambrian sandstone /Talbot and Munier, 1989/. The orientation of the maximum horizontal compressive stress during the subsequent tectonic evolution is presumed to have been NW-SE, i.e. the same as the present stress régime. Consequently, a roughly NW-SE maximum compressive stress is inferred to have prevailed for a considerable period of time, i.e. possibly for hundreds of million of years.

Attempts have been made to use palaeomagnetic, electron spin resonance (ESR) and isotopic dating (K-Ar, Rb-Sr) techniques on some brittle structures at the Äspö site /Maddock et al, 1993/, in order to constrain the minimum age of the most recent movements. Characterization of the sampled fault gouge material demonstrated that many fracture zones contain sequentially developed fault rocks and verifies that reactivation has occurred.

The ages given by the various dating methods reflect both inherent differences in the techniques and differences in the phase or phenomenon being dated. The interpretation of the ESR dating which was limited by the resolution of the method, yielded minimum ages of movements in the order of several hundred thousand to one million years. The results of the palaeomagnetic and K-Ar analyses strongly suggest that growth of the fracture infilling minerals took place at least 250 million years ago. The most recent fault movements are interpreted to have preceded this mineral growth. /Maddock et al, 1993/ concluded that any Quaternary and Holocene activity had little effect on the fracture zones.

According to /Mörner, 1989/, a great number of supposed post-glacial faults occur on Äspö. However, none of the faults reported showed any positive evidence of kinematics /SKB, 1990/. Some of the reported faults did not display any disturbance of Precambrian markers, others had their bases exposed by excavation and ice plucking could be positively demonstrated. /Talbot and Munier, 1989/ discussed post-glacial faults in connection with studied fault scarps, i.e. abrupt steps in the glacially polished bedrock surface on Äspö. According to /Munier, 1995/, post-glacial reactivation of individual fractures has most likely occurred, but despite searches no evidence of such features has been found on outcrops.

Ongoing tectonic activity is manifested in seismic events and aseismic slip /Larson and Tullborg, 1993/. According to /Slunga et al, 1984/, the so-called Protogine Zone of southern Sweden, c.f. Figure 3-7, has been shown to be the border between a more seismic western Sweden and the more

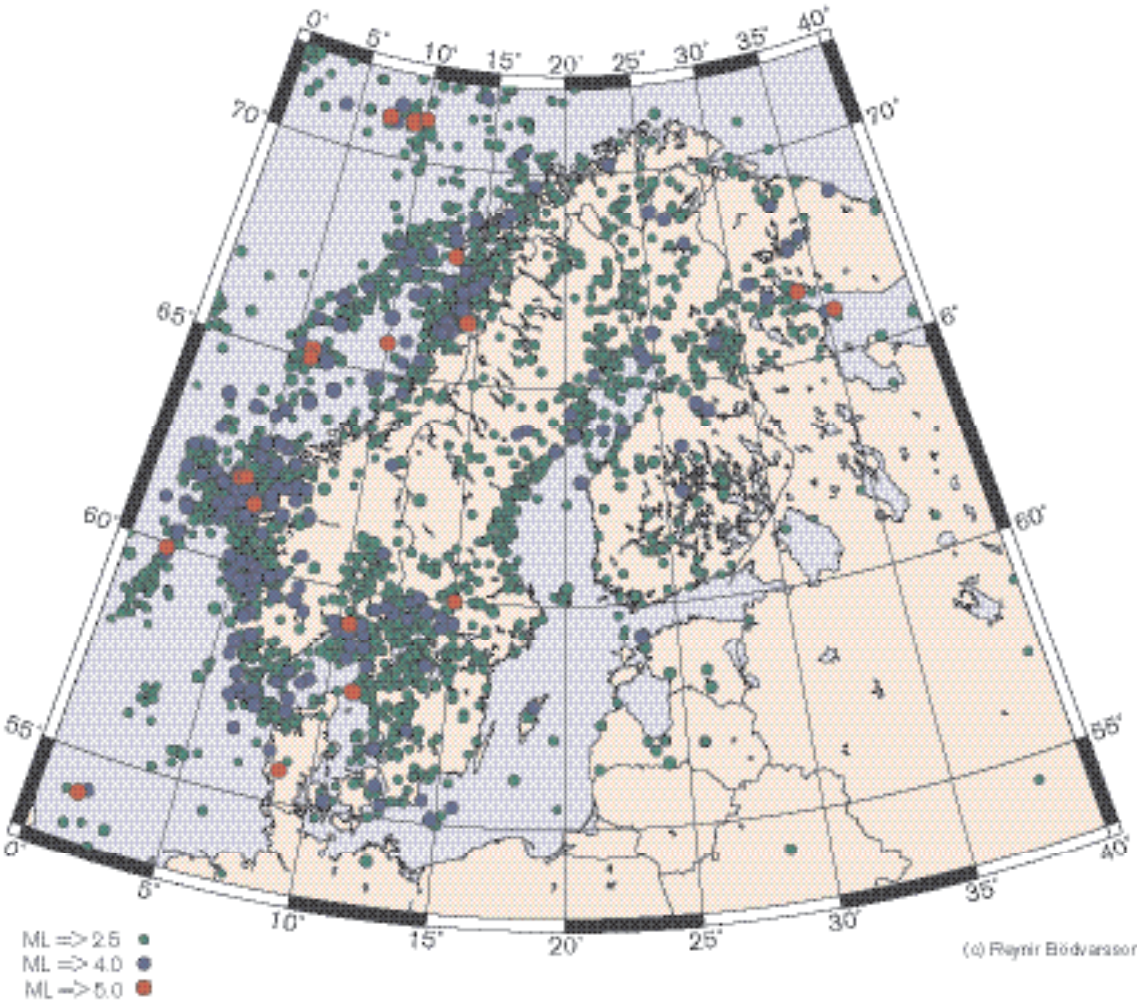

Figure 3-10. *Earthquake epicentra in Scandinavia and Finland 1375–2003. Data from the University of Uppsala.*

aseismic southeastern Sweden. Even though southeastern Sweden is a seismically very quiet area (Figure 3-10), an earthquake of magnitude 3.3 and a focal depth of 5.0 kilometres was recorded c. 100 kilometres south of Gotland in December 2002 /Bödvarsson, 2003/. In addition, an earthquake of magnitude 1.0 and focal depth of c. 16 kilometres was recorded c. 30 kilometres south of Oskarshamn in September 1988 /Slunga and Nordgren, 1990/. The orientation of the maximum horizontal principal stress relaxed by this earthquake, as well as other seismic events in Sweden, was c. NW-SE /Slunga et al, 1984; Slunga and Nordgren, 1990/. This is in agreement with the results from rock stress measurements at depths of more than 300 metres /Stephansson et al, 1987/, and also with the stress field generated by the plate movements in the North Atlantic Ocean /cf. Slunga, 1989; Gregersen et al, 1991; Gregersen, 1992/. According to /Slunga and Nordgren, 1990/, recent seismic activity in southeastern Sweden is related to plate-tectonic forces and not directly to land upheaval subsequent to and consequent on the last glaciation. /Gregersen et al, 1991/ and /Gregersen, 1992/ came to the same conclusion based on focal mechanisms for present-day earthquakes in Fennoscandia. However, /Muir-Wood, 1993/ and /Wu et al, 1999/ suggested that post-glacial rebound appears to be the cause of the post-glacial seismic activity in Fennoscandia.

The geological evolution in southeastern Sweden, with focus on the Oskarshamn region, is tentatively summarized in Table 3-2 .

Table 3-2. Tentative synopsis of the geological evolution in southeastern Sweden with a focus on the Oskarshamn region.

Age (Ma)	Geological event
0.115-0	Glaciation; syn- to post-glacial fault movements?; NW-SE to WNW-ESE maximum horizontal principal stress
95-0	**Alpine orogeny** (central Europe); Final break-up of the supercontinent Pangaea; opening and spreading of the North Atlantic Ocean; ***brittle deformation in the cratonic Oskarshamn region as a far-field effect?***
> 250	*Latest fault movements at Äspö?* (K-Ar dating of gouge material)
295-60	Tectonic activity in the Tornquist Zone (Fennoscandian border zone); ***brittle deformation in the cratonic Oskarshamn region as a far-field effect?***
360-295	**Hercynian-Variscan orogeny** (central Europe). Final assembly of the supercontinent Pangaea; *Brittle deformation in the cratonic Oskarshamn region as a far-field effect?*
420-220	Subsidence related to the development of a Caledonian foreland basin, sedimentation followed by exhumation and erosion; *brittle deformation in the cratonic Oskarshamn region?*
510-400	**Caledonian orogeny**; closure of the Iapetus Ocean; formation of the Scandinavian Caledonides; WNW-ESE shortening (regional compression?) followed by extensional collapse; ***brittle deformation in the cratonic Oskarshamn region as a far-field effect of orogenic deformation in western Baltica?***
600-550	Peneplanation; Sub-Cambrian peneplain; Marine transgression and extensive sedimentation
700-600	Final break-up of the supercontinent Rodinia and opening of the Iapetus Ocean; *far-field effect in the cratonic Oskarshamn region?*
900-700	Subsidence related to the development of a Sveconorwegian foreland basin, sedimentation followed by exhumation and erosion; Almesåkra group; Rifting, graben formation, sedimentation in the Vättern area; Visingsö group; ***brittle deformation in the cratonic Oskarshamn region?***
1,100-900	**Sveconorwegian orogeny**; formation of the Sveconorwegian Frontal Deformation Zone ("Protogine Zone"); WNW-ESE to E-W regional compression; intrusion of dolerites - E-W extension; Assembly of the supercontinent Rodinia; ***Brittle deformation in the cratonic Oskarshamn region as a far-field effect of orogenic reworking of the crust in southwestern Sweden?***
1,460-1,420	**Hallandian orogeny**; *Brittle deformation in the cratonic Oskarshamn region as a far-field effect?*
1,450	Intrusion of granite (e.g. Götemar and Uthammar granites)
1,610-1,560	**Gothian orogeny**; *Brittle deformation in the cratonic Oskarshamn region as a far-field effect?*
1,750-1,700	Transition from ductile to brittle tectonic régime
1,800-1,750	Formation of transpressive, ductile deformation zones in response to c. N-S to NNW-SSE regional compression under low-grade conditions. Deformation zones with NW-SE to WNW-ESE and NE-SW direction display dextral and sinistral horizontal component, respectively.
1,810-1,760	Intense igneous activity; Intrusion of granite-syenitoid-dioritoid-gabbroid ("Småland granite"), composite dykes; Sedimentation and volcanic activity
1,830-1,810	Regional, inhomogeneous deformation under (low)- to medium-grade conditions
1,830-1,820	Intrusion of granitoids; volcanic activity?
1,850(-1,800)	Formation of transpressive, ductile deformation zones with a dextral horizontal component of movement, in response to c. N-S to NNW-SSE regional compression under medium-grade metamorphic conditions; folding of foliation in pre-1850 Ma rocks
1,850	Intrusion of granite-syenitoid-dioritoid-gabbroid
1,890-1,850	Volcanic activity and sedimentation; regional deformation under medium- to high-grade conditions
1,960-1,750	**Svecokarelian orogeny**

3.2 Overburden including Quaternary deposits

3.2.1 Introduction

This section discusses the Quaternary history of Simpevarp area in a local and regional perspective. The Quaternary Period is the youngest in the earth's history, characterised by alternating cold glacial and warm interglacial stages. The glacial periods are further subdivided into cold phases, stadials and relatively warm phases, interstadials. A combination of climatic oscillations with a high amplitude, together with the intensity of the colder periods is characteristic of the Quaternary Period. At the Geological Congress in London, 1948 the age of the Tertiary/Quaternary transition, as used here, was determined to be 1.65 million years. More recent research, however, suggests that the Quaternary period started 2.4 million years /e.g. Šibrava, 1992; Shackelton, 1997/. The Quaternary Period is subdivided into two epochs: the Pleistocene and the Holocene. The latter represents the present interglacial, c. 11,500 years BP.

Oxygen isotope records in deep-sea sediment suggest as many as fifty glacial/interglacial cycles during the Quaternary /Shackelton et al, 1990/. The climate during the past c. 900,000 years has been characterised by 100,000 years long glacial periods interrupted by interglacials lasting for approximately 10,000–15,000 years. The coldest climate occurred toward the end of each of the glacial periods. Most research indicates that the long-term climate changes (> 10,000 years) are trigged by variations in the earth's orbital parameters. However, there is not a universal agreement on this point. Quaternary climatic conditions have been reviewed by e.g. /Morén and Påsse, 2001/.

The most complete stratigraphies used in Quaternary studies are from the well-dated cores from the deep sea that have been used for studies of e.g. oxygen isotopes /e.g. Shackelton et al, 1990/. The marine record has been subdivided into different Marine Isotope Stages (MIS), which are based on changes in the global climatic record. Quaternary stratigraphies from before the Last Glacial Maximum (LGM) from areas that have been repeatedly glaciated, such as Sweden, are sparse. Furthermore these stratigraphies are often disturbed by erosion and are difficult to date absolutely. Our knowledge of pre-LGM Quaternary history of Sweden is, therefore to a large extent based on indirect evidence from non-glaciated areas.

In most parts of Sweden, the relief of the bedrock is mainly of Pre-Quaternary age and has only been slightly modified by glacial erosion /Lidmar-Bergström et al, 1997/. The magnitude of the glacial erosion seems to vary considerably geographically. Pre-Quaternary deep weathered bedrock occurs in areas such as the inland of eastern Småland, southern Östergötland and the inner parts of northernmost Sweden /Lundqvist, 1985; Lidmar-Bergström et al, 1997/. Such saprolites indicate that these areas have only been affected to a small extent by glacial erosion.

In some areas, such as in large parts of inner northern Sweden, deposits from older glaciations have been preserved, which indicates that the subsequent glaciations have had a low erosional capacity /e.g. Hättestrand and Stroeven, 2002; Lagerbäck and Robertsson, 1988/.

Saprolites of Pre-Quaternary age occur 50 km west of the Simpevarp regional model area /Lidmar-Bergström et al, 1997/. The occurrence of such "old" deposits in the regional model area can, however, not be excluded.

3.2.2 The Pleistocene

The preserved geological information from the early Quaternary in Sweden is, as mentioned above, fragmentary. However, inorganic deposits such as glacial till have not been dated with absolute methods and deposits from early stages of the Quaternary period may therefore exist. Although, as mentioned above, the oxygen isotope record indicates numerous glaciations it is impossible to state the number of glaciations reaching as far south as the Simpevarp area.

There are traces of three large glaciations, the Elster (MIS 8), Saale (MIS 6) and Weichsel (MIS2-5d), that reached northern Poland and Germany. /e.g. Fredén, 2002/. The Saale had the largest maximum extension of any known Quaternary ice sheet. There were two interstadials, the Holstein and Eem, between theses three glacials.

The oldest Quaternary deposit in Sweden, dated by fossil composition, was probably deposited during the Holstein interglacial (MIS 7, c. 230,000 years ago) /e.g. Garcia Ambrosiani, 1990/. The till underlying the Holsteinian deposits is the oldest known Quaternary deposit in Sweden.

Deposits from the interglacial Eem (MIS 5e, 130,000–115,000 years ago) are known from several widely spread places in Sweden /e.g. Robertsson et al, 1997/. The climate was periodically milder than it has been during the present interglacial, Holocene. It is likely that the Simpevarp regional model area was covered by brackish water during large parts of the Eem interglacial.

3.2.3 The latest glaciation

The latest glacial, the Weichsel, started c. 115,000 years ago. It is characterised by colder phases, stadials, interrupted by milder interstadials. The model presented by e.g. /Fredén, 2002/ and /Lundqvist, 1992/ is often used to illustrate the history of Weichsel (Figure 3-11). Two interstadials

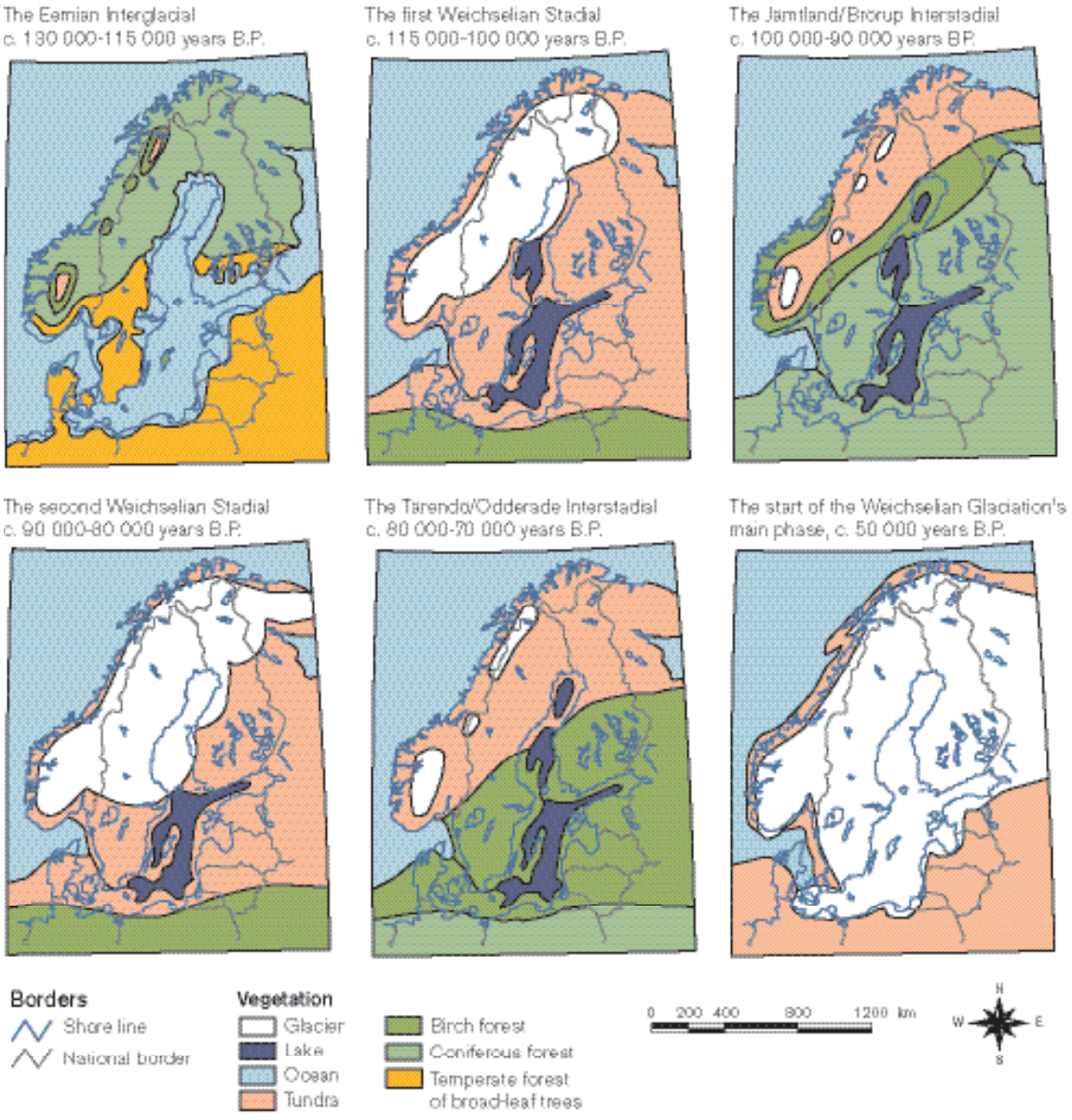

Figure 3-11. *The development of vegetation and ice cover in northern Europe during the latest interglacial (Eem) and first half of the latest ice age (Weichsel). The maps should be regarded as hypothetical due to the lack of well dated deposits from the different stages (from: Sveriges Nationalatlas, www.sna.se).*

took place during the early part of Weichsel, approximately 100,000–90,000 (MIS 5c) and 80,000–70,000 years ago (MIS 5a). Most of Sweden was free of ice during these interstadials, but the climate was considerably colder than today and tundra conditions probably characterised northern Sweden. The ice did not reach further south than the Mälaren Valley during the Early Weichselian stadials. The ice advanced south and covered the Simpevarp area first during Mid Weichselian (c. 70,000 years ago).

Most of Sweden, including Simpevarp, was then covered by ice until the deglaciation at around 12,000 years BP. The accuracy of the model presented by /Fredén, 2002/ and /Lundqvist, 1992/ can however be questioned. Most researchers agree that at least two interstadials, with ice-free conditions, did occur during the Weichselian glaciation. However, since the dating of such old deposits is problematic the timing of these interstadials is uncertain. Investigations from both Finland and Norway suggest that most of the Nordic countries were free of ice during parts of Mid Weichselian (MIS 3-4) /e.g. Olsen et al, 1996; Ukkonen et al, 1999/. That may imply that one of the interstadials attributed to Early Weichselian by /Fredén, 2002/ may have occurred during Mid Weichsel. In Simpevarp the total time of ice cover during Weichsel may therefore have been considerably shorter than previously has been thought.

Continental ice reached its maximum extent c. 20,000 years ago (MIS 2), c.f. Figure 3-12. The Weichselian ice reached as far south as the present Berlin, but had a smaller maximal extent than the two preceding glacials (Saale and Elster). According to mathematical and glaciological models, the maximum thickness of the ice cover in the Oskarshamn region was more than 1.5 km at 18,000 years BP /Näslund et al, 2003/. Glacial *striae* on bedrock outcrops as well as the orientation of eskers indicate a main ice movement direction from NW-NNW in the Simpevarp region. Subordinate older *striae* indicate more westerly and northerly directions.

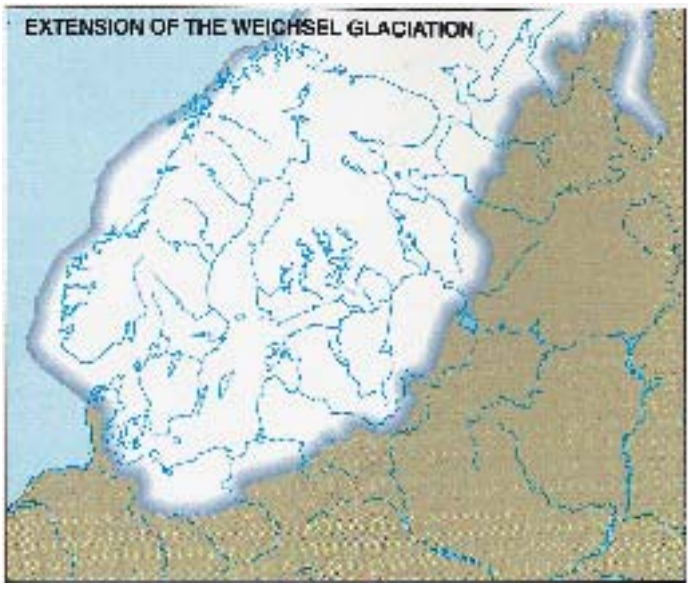

Figure 3-12. *The maximum extent of the Weichselian ice sheet approximately 20,000 years ago (from: Sveriges Nationalatlas, www.sna.se).*

3.2.4 Deglaciation

A marked improvement in climate took place about 18,000 years ago and the ice started to melt a process that was completed after some 10,000 years. The deglaciation of southeastern Sweden has been studied by using clay-varve chronologies /Kristiansson, 1986; Ringberg et al, 2002/.

The timing of the deglaciation of Sweden has been dated using several methods. These dates have recently been calibrated to calendar years /e.g. Fredén, 2002; Lundqvist and Wohlfarth, 2001/. According to the calibrated clay-varve chronology, the Oskarshamn area was deglaciated almost 14,000 years ago /Lundqvist and Wohlfarth, 2001/. The velocity of the retreat of the ice margin was c. 125–300 m/year /Kristiansson, 1986/.

3.2.5 Climate and vegetation after the latest deglaciation

Pollen investigations from southern Sweden have shown that a sparse *Betula* (birch) forest covered the area soon after the deglaciation /e.g. Björck, 1999/. There was a decrease in temperature during a cold period called Younger Dryas (*c.* 13,000–11,500 years ago) and the deglaciated parts of Sweden were consequently covered by a herb tundra. At the beginning of Holocene c. 11,500 years ago the temperature increased and southern Sweden was first covered by forests dominated *Betula* and later by forests dominated by *Pinus* (pine) and *Corylus* (hazel). The timing and climatic development of the transition between Pleistocene and Holocene has been discussed by e.g. /Björck et al, 1996/ and /Andrén et al, 1999/.

9,000–6,000 years ago the the summer temperature was approximately 2° warmer than at present and forests with *Tilia (lime)*, *Querus (oak)* and *Ulmus* (elm) covered large parts of southern Sweden. The temperature has subsequently decreased, after this warm period, and the forests became successively more dominated by coniferous trees. The ecological history of Sweden during the last 15,000 years has been reviewed by e.g. /Berglund et al, 1996/.

3.2.6 Development of the Baltic Sea after the latest deglaciation

The development of the Baltic Sea since the last deglaciation is characterised by changes in salinity and its history has therefore been divided in four main stages /Björck, 1995; Fredén, 2002/, which are summarised in Table 3-3. The most saline period occurred 6,000–5,000 years ago when the surface water salinity was 10–15‰ compared to approximately 7‰ today /Westman et al, 1999/.

A major crustal phenomenon that has affected and continues to affect northern Europe, following the latest melting of continental ice, is the interplay between isostatic recovery on the one hand and eustatic sea level variations on the other. During the latest glaciation, the global sea level was in the order of 120 m lower than the present /Fairbanks, 1989/.

In northern Sweden the heavy continental ice depressed the Earth's crust by as much as 800 m below its present altitude. As soon as the pressure started to decrease, due to the deglaciation, the crust started to rise (isostatic land uplift). The highest identified traces of the shoreline are at different altitudes throughout Sweden depending on how much the crust had been depressed. The highest shoreline in the Oskarshamn region is c. 100 m above sea level /Agrell, 1976/, and, thus the whole Simpevarp regional model area is situated below the highest shoreline.

Table 3-3. The four main stages of the Baltic Sea.

Baltic stage	Calender year BP	Salinity
Baltic Ice Lake	15,000–11,550	Glacio-lacustrine
Yoldia Sea	11,500–10,800	Lacustrine/Brackish /Lacustrine
Ancylus Lake	10,800–9,500	Lacustrine
Littorina Sea *sensu lato*	9,500–present	Brackish

Along the southern part of the Swedish east coast, the isostatic component was less and declined earlier during the Holocene, resulting in a complex shore line displacement with alternating transgressive and regressive phases. In the Simpevarp region, shoreline regression has prevailed and the rate of land uplift during the last 100 years has been c. 1 mm/year /Ekman, 1996/.

The estimated shore line displacement since the last deglaciation has been reviewed and modified by /Påsse, 2001, 1997/ (Figure 3-13). Påsse´s curve is similar to a curve presented by /Svensson, 1989/, who undertook stratigraphical investigations in the Oskarshamn area. However, according to /Svensson, 1989/ the shoreline dropped instantaneously c. 20 m due to drainage of the Baltic Ice Lake 11,500 years ago. Påsse, on the other hand, suggests a fast isostatic shoreline displacement at that time. The ^{14}C method does not have accuracy enough to tell if the drainage did occur or if the fast shoreline displacement during that time is caused by a fast isostatic rebound. Påsse´s curve (Figure 3-13) shows that the shoreline displacement has been regressive for most of the time since the deglaciation. There are, however, two transgressive periods, 10,000 years ago in the Ancylus Lake phase and 7,000 years ago in the Littorina Sea phase, c-f. Table 3-3.

/Risberg, 2002/ has studied a five meter long sediment core from Borholmsfjärden south of Äspö. The core comprises two main sediment sequences, the first accumulated in the Yoldia Sea (11,500–10,800) and the second during the last 3,000 years. As the site was exposed to the sea, there was no accumulation of sediment between the time of the Yoldia Sea and 3,000 years ago, The islands surrounding Borholmsfjärden had emerged from the sea some 3,000 years ago, which caused more sheltered conditions and the onset of sedimentation.

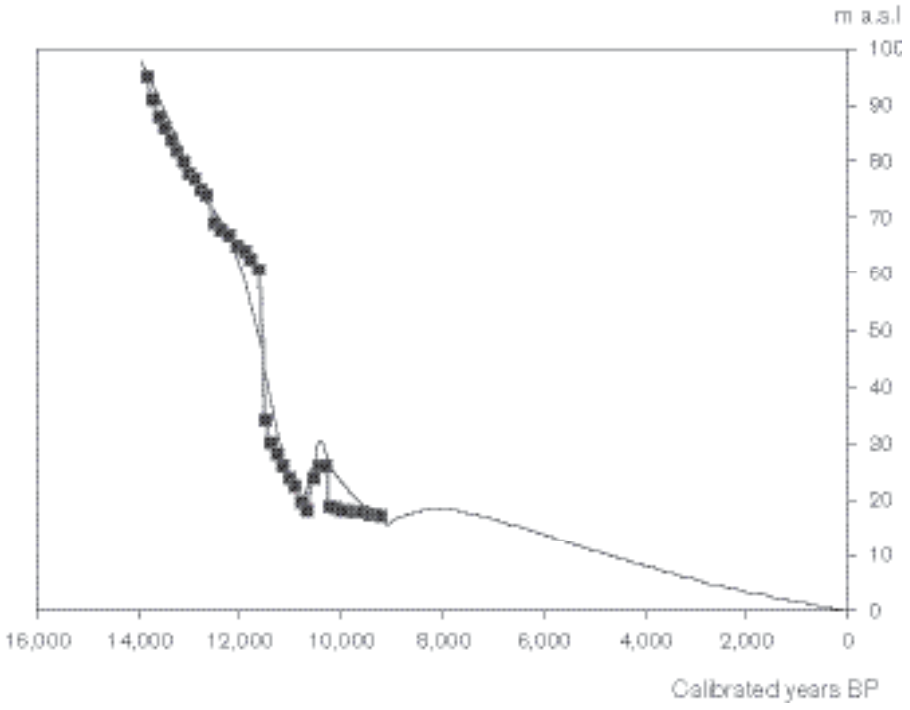

Figure 3-13. *The shore line displacement in the Oskarshamn area after the latest deglaciation. The blue symbols show a curve established by /Svensson, 1989/ after a study of lake sediments in the region. The curve without symbols has been calculated by the use of a mathematical model /Påsse, 2001/.*

3.3 Premises for surface water and groundwater evolution

3.3.1 Premises for surface water evolution

As shown in Figure 3-14, almost the whole regional model area was covered by sea water until 12,000 years ago. The salinity of the sea water since the melting of the latest inland ice, as used in model version Simpevarp 1.1, is shown in Figure 3-15. It should be emphasised that the salinity values for the Yoldia Sea period are associated with high uncertainty. The whole local model area emerged from the sea about 8,000 years ago. This means that the Quaternary deposits in the area have been exposed to groundwater recharge and soil forming processes for a rather long time. Figure 3-15 also shows the estimated lowest shore line at 9,750 BP (Before Present) before the transgression that continued until about 8,000 BP.

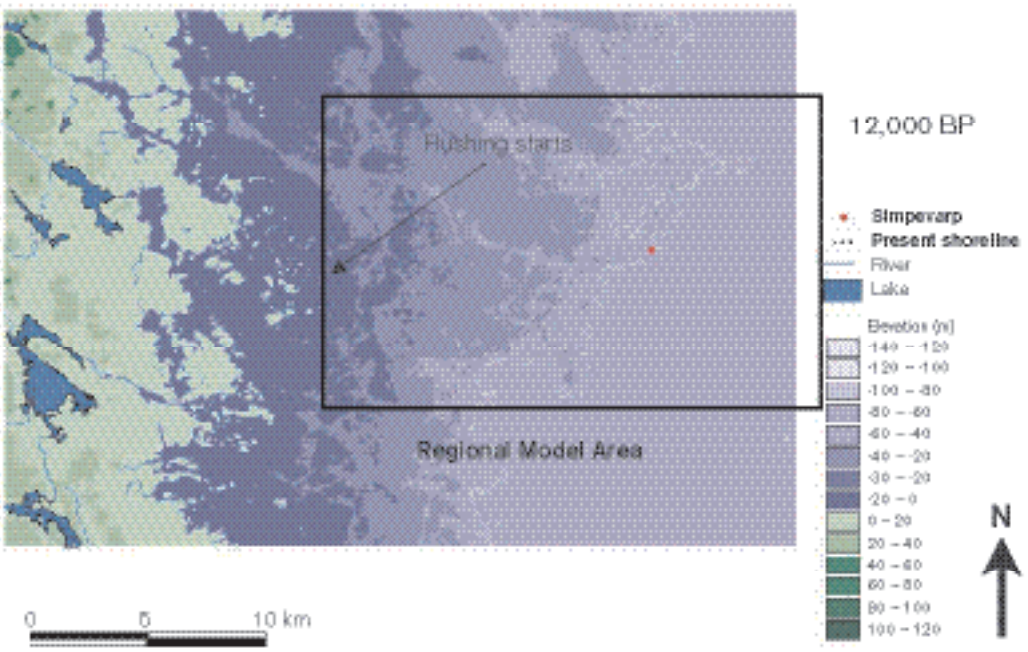

Figure 3-14. *Map of the Simpevarp area showing the shore line at 12,000 BP. Based on analysis by /Posse, 2001/ and /Brydsten, 2004b/.*

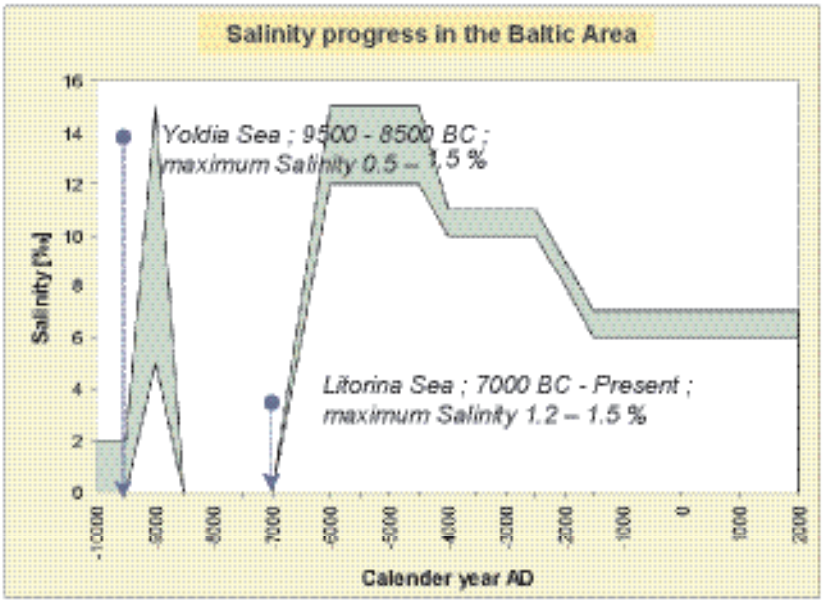

Figure 3-15. *The sea water salinity at Oskarshamn during Holocene. Modified after /Stigsson et al, 1999/ (Time scale: years AD (Anno Domini)).*

3.3.2 Post-glacial conceptual model of groundwater evolution

The first step in the groundwater evaluation is to construct a conceptual postglacial scenario model for the site (Figure 3-16) based largely on known palaeohydrogeological events from Quaternary geological investigations. This model can be helpful when evaluating data since it provides indications of the possible groundwater types that may occur. Interpretation of the glacial/postglacial events that might have affected the Simpevarp area is based on information from various sources including /Fredén, 2002/, /Påsse, pers. comm. 2003)/, /Westman et al, 1999/ and /SKB, 2002b/. This recent literature has resulted in some modifications to earlier views, for example, changes in the absolute ages of the different Baltic Sea evolution stages /Fredén, 2002/.

3.3.3 Development of permafrost and saline water

When the continental ice sheet was formed at about 100,000 BP permafrost formation ahead of the advancing ice sheet probably extended to depths of several hundred metres. According to /Bein and Arad, 1992/ the formation of permafrost in a brackish lake or sea environment (e.g. similar to the Baltic Sea) produced a layer of highly concentrated salinity ahead of the advancing freezing front. As this saline water would be of high density, it would subsequently sink to lower depths and potentially penetrate into the bedrock where it would eventually mix with formational groundwaters of similar density. Where the bedrock was not covered by brackish lake or sea water similar freeze-out processes would occur on a smaller scale within the hydraulically active fractures and fracture zones, again resulting in formation of a higher density saline component that would gradually sink and eventually mix with existing saline groundwaters. Laboratory experiments at the University of Waterloo, Canada /Frape, pers. comm. 2003/, indicate that the volume of high salinity water produced from brackish waters by this freeze-out process would be much less than initially considered by Bein and Arads (op. cit.) and would tend to form restricted pockets of high density saline water rather than a continuous horizon of high salinity as in the case of a lake or sea environment.

With continued evolution and movement of the ice sheet, areas previously subject to permafrost would eventually be covered by ice. This coverage would be accompanied by a rise in ground temperature due to the insulating properties of the ice and a slow decay of the underlying permafrost layer. Hydrogeochemically, this decay may have resulted in distinctive signatures being imparted to the groundwater and fracture minerals.

3.3.4 Deglaciation and flushing by melt water

During subsequent melting and retreat of the ice sheet the following sequences of events is thought to have influenced the Simpevarp area, c.f. Figure 3-16.

During the recession and melting of the continental ice sheet, glacial melt water was hydraulically injected into the bedrock (> 14,000 BP) under considerable head pressure close to the ice margin. The exact penetration depth is still unknown, but depths exceeding several hundred metres are possible according to hydrodynamic modelling /e.g. Svensson, 1996/. Some of the permafrost decay groundwater signatures may have been disturbed or destroyed during this stage.

Different non-saline and brackish lake/sea stages then transgressed the Simpevarp area during the period ca. 14,000–4,000 years BP. Of these, two periods with brackish water can be recognised; the Yoldia Sea (11,500 to 10,800 years BP) and the Littorina Sea starting at 9,500 years BP and continuing to the present. The Yoldia period has probably resulted in only minor contributions to the subsurface groundwater, as the water was very dilute to brackish because of the large volumes of glacial melt water it contained. Furthermore, this period lasted for only 700 years. The Littorina Sea period in contrast had a maximum salinity of about twice that of the present Baltic Sea and this maximum prevailed at least from 6,500 to 5,000 years BP; during the last 2,000 years the salinity has remained almost constant at the present Baltic Sea values /Westman et al, 1999 and references therein/. Because of increased density, the Littorina Sea water was able to penetrate the bedrock resulting in a density-driven turnover which affected the groundwater in the more conductive parts of the bedrock. The density of the intruding sea water relative to the density of the groundwater determined the final penetration depth. As the Littorina Sea stage was associated with the most saline groundwater, it is assumed to have had the deepest penetration depth, eventually mixing with the glacial/brine groundwater mixtures already present in the bedrock.

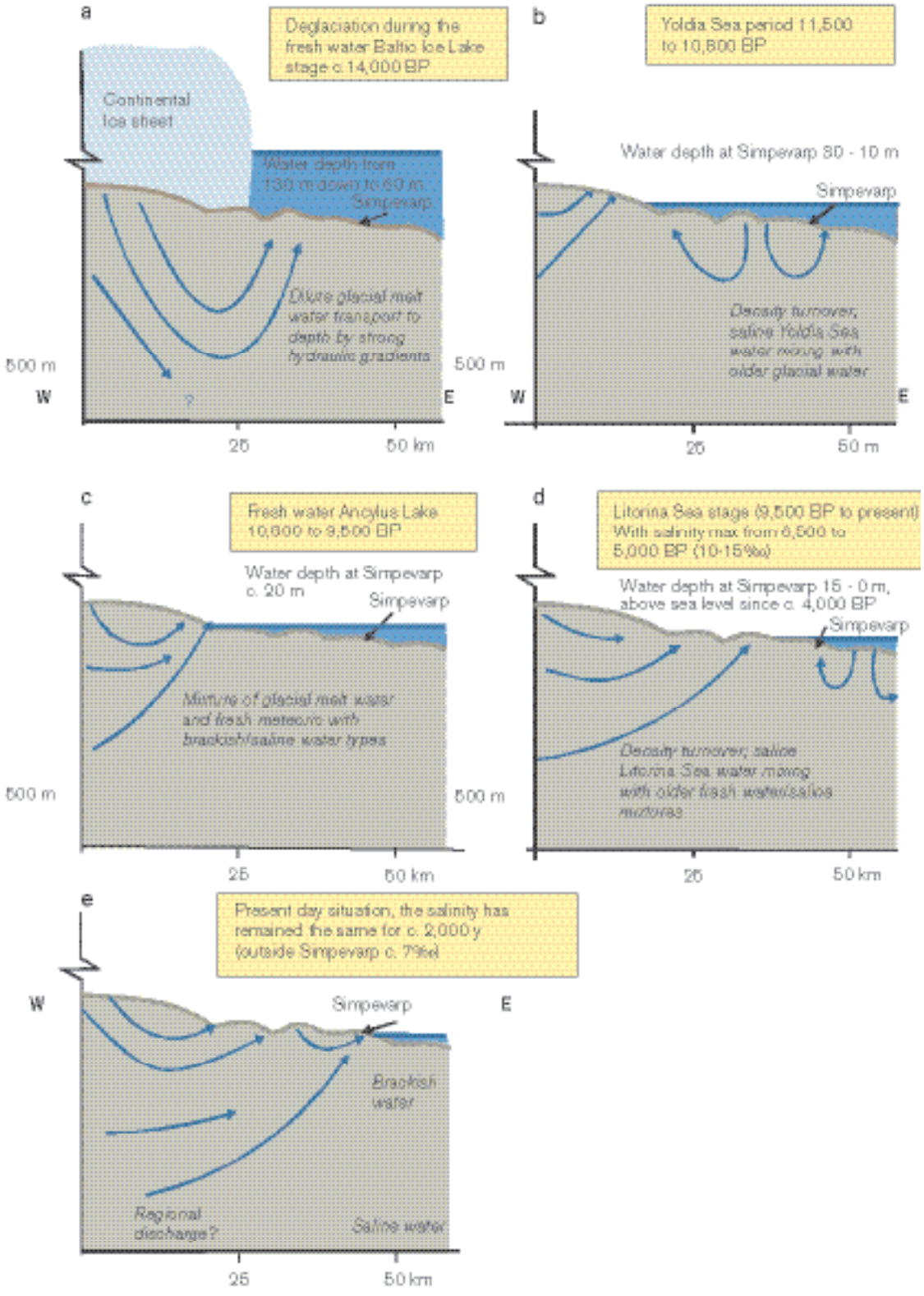

Figure 3-16. *An updated conceptual postglacial scenario model for the Simpevarp area. The figures show possible flow lines, density driven turnover events and non-saline, brackish and saline water interfaces. Possible relations to different known postglacial stages which may have affected the hydrochemical evolution of the site is shown: a) deglaciation of the continental ice, b) Yoldia Sea stage, c) Ancylus Lake stage, d) Littorina Sea stage, and e) present day Baltic Sea stage. From this conceptual model it is expected that glacial meltwater and deep and marine water of various salinities have affected the groundwater.*

When the Simpevarp region was subsequently raised above sea level 5,000 to 4,000 years ago, recharging fresh meteoric water formed a lens on top of the saline water because of its low density. However, local hydraulic gradients resulting from higher topography to the west of the Simpevarp area may have flushed out varying amounts of these older waters, at least to 100–150 m, with the freshwater lens for the most part occupying these depths today, depending on local hydraulic conditions.

Many of the natural events described above may be repeated several times during the lifespan of a deep repository (thousands to hundreds of thousands of years). As a result of these events, brine, glacial, marine and meteoric waters are expected to be mixed in a complex manner at various levels in the bedrock, depending on the hydraulic character of the fracture zones, groundwater density variations and borehole activities prior to groundwater sampling. For the modelling exercise which is based on the conceptual model of the site, groundwater end members reflecting, for example, Glacial meltwater and Littorina Sea water composition, were added to the data set /Laaksoharju, 2004b/.

The uncertainty of the updated conceptual model increases with modelled post-glacial time. The largest uncertainties are therefore associated with the stage showing the flushing of glacial melt water. The driving mechanism behind the flow lines in Figure 3-16 is the shore level displacement due to land uplift.

3.4 Development of surface ecosystems

Patterns observed in the present-day surface ecosystems are a result of physical and biological processes over time, e.g. land uplift, climate change, vegetation development and human impact. These processes are often combined, where one or more processes set the limits for others. For example, climate and land uplift often determine vegetation development, which in turn controls human settlements and land use. The strongest impact on the historical development of the surface ecosystems in the Simpevarp area is caused by direct or indirect effects of the latest glaciation. A direct effect, which still has some affect on the systems, is shoreline displacement, but other factors like soils, altitude, and the prerequisites for creation of lakes and watersheds were also determined by the latest glaciation.

3.4.1 The Baltic Sea

The glacial ice cover started to retreat about 14,000 years ago /e.g. Fredén, 2002/. The highest parts in the regional scale model area emerged from the Yoldia Sea (11,800 –10,550 years BP) /Brydsten, 2004b/, at that time a freshwater stage of the Baltic Sea. Approximately 1,500 years later, brackish water started to intrude into the Baltic Sea and this denotes the transition from the Ancylus lake to the next historical stage of the Baltic Sea, the Littorina Sea. From the onset of the Littorina stage until today, the Baltic Sea has been brackish with varying salinity and with an estimated maximum salinity level about twice as high as today, occurring during the period 6,500–5,000 years BP /Westman et al, 1999/. The post-glacial climate in the Baltic Sea area has changed several times between cold and warm periods, and the varying salinity may at least partly be related to climate variations with decreased salinity during periods of climate deterioration /Westman et al, 1999/.

The retreat of the glacial ice cover initiated a process of land uplift, and about 5,000 years BP the first islands appeared in the inner model area, Simpevarp /cf. Brydsten, 2004b/, at that time an outer archipelago in the region. Accordingly, the post-glacial ecosystems in the area have changed, and the oldest terrestrial or lacustrine ecosystems have existed for about 5,000 years. Because of the shoreline displacement, both the aquatic and the terrestrial ecosystems have gone through substantial changes during the post-glacial period, and there are still small changes near the shoreline as an ongoing effect of land uplift.

3.4.2 Lacustrine ecosystems

In Scandinavia, a majority of the present lakes were formed during the latest glaciation, when geomorphological processes substantially altered the entire landscape. As the ice retreated, erosion, transport, and deposition of material resulted in formation of numerous lake basins in the landscape. Immediately after formation of a lake, an ontogenetic process starts, where the basin ultimately is filled with sediments, and thereby develops towards extinction of the lake. Depending on local hydrological and climatic conditions, the lake may be converted to a final stage of a bog or to forest /Wetzel, 2001/. A usual pattern for lake ontogeny is the subsequent development of more and more eutrophic conditions as lake depth and volume decreases. In later stages, aquatic macrophytes speed up the process by colonising large areas of the shallow sediments /Wetzel, 2001/.

Freshwater lake basins have been continuously formed along the coast of Simpevarp as bays became isolated from the brackish water of the Baltic Sea. However, since land uplift is small, the lake forming processes are currently slow. Lake ontogeny has not been explicitly examined for the lakes in the Simpevarp area.

3.4.3 Vegetation

Vegetation development after the latest glaciation was primarily controlled by land uplift and climatic changes. The general vegetation development, after the retreat of the glacial ice cover, is documented in archipelagos along the Baltic coast, e.g. the Stockholm archipelago /Jerling et al, 2001/. The first islands in the Stockholm archipelago emerged early, some 11,000 years BP, as in the Simpevarp regional area. As the general processes controlling the successional development of vegetation are the same along the coast, it is presumable that the early vegetational development was very much the same also in the Simpevarp region.

Vegetation development has been examined by using data from pollen analysis /Jerling et al, 2001/. Such analyses have shown that the first vegetation in the archipelagos, after the ice retreat, was dominated by typical early colonising tree species like Pine (*Pinus sylvestris)*, Birch (*Betula spp*) and Hazel (*Corylus avellana*). Some tree species are fast colonisers and occur early in succession (Figure 3-17). However, a major part of the early succession species is short-lived herbs and grasses, but since they are light dependent they disappear later in succession, as a closed vegetation canopy develops. The Boreal period, approximately 10,000–9,000 year BP, was totally dominated by Birch (*Betula spp*) and Pine (*Pinus sylvestris*), whereas the warmer Atlantic period, approximately

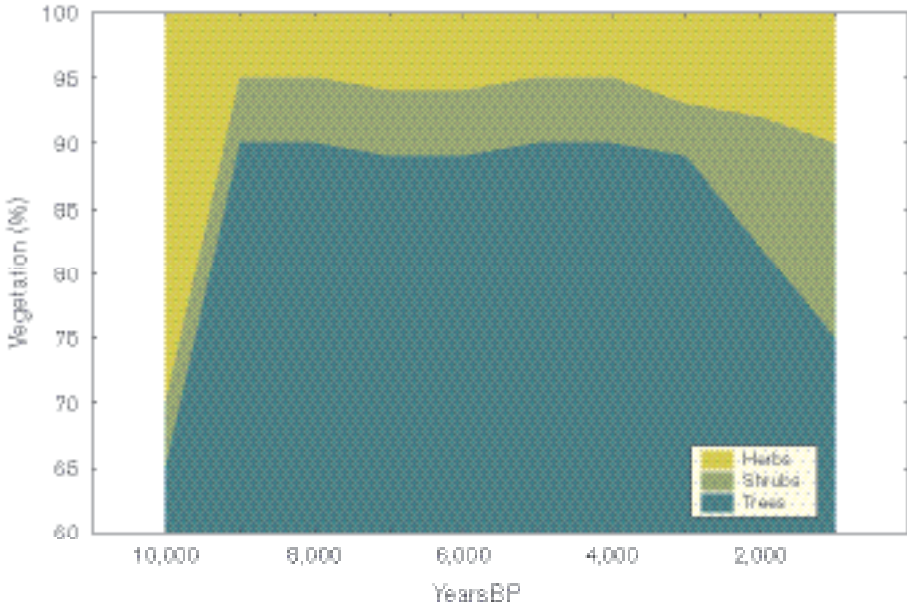

Figure 3-17. *Pollen diagram showing the relative amount of trees, shrubs and herbs in the Stockholm archipelago (after Jerling et al, 2001/.*

9,000–6,000 years BP**,** was characterised by the expansion of nemoral (thermophilous) forest trees, like Oak (*Quercus robur*), Elm (*Ulmus glabra*), Lime (*Tilia cordata)* and Ash (*Fraxinius excelsior)*, because of the warmer climate. Spruce (*Picea abies*) had its expansion much later, about 2,500 BP /Jerling et al, 2001/. In conclusion, due to the relatively early emergence of islands, most of the immigrating plants established early in the regional model area. Thus, the ecosystems in the area have the potential for being quite old.

Historical vegetation and land use development can be reconstructed by combining data from pollen analyses, old cadastral maps, soil and bedrock maps and archaeological data, with shoreline displacement models /Cousins, 2001/. Human activities have had a major impact on vegetation development in Simpevarp during the last 200 years, although this area has always had a small human population (see Section 3.4.5). Although land use alters the "natural" vegetation processes, all of the area has not been equally exploited through time, depending on differences in Quaternary deposits. There is documentation of early settlements in the region, suggesting that the vegetation has been affected by humans over a considerable period. However, since the regional model area has a large proportion of forested area with thin soils /Lindborg and Schüldt, 1998; Berggren and Kyläkorpi, 2002/, much of the land is unsuitable for agriculture /Lundqvist, 2004/.

It is difficult to evaluate the relative importance of natural factors affecting the coniferous forests. As the iron industry became more organised in the 16th century, forests all over Sweden were cut down to feed furnaces and mines with wood and charcoal. Many forests, including those in the Simpevarp region, were used during this period /Welinder et al, 1998/. Tar and lumber also became commercially important.

3.4.4 Wild fauna

Archaeological excavations make it possible to document the diet of early settlers and identify bones from wild animals /cf. Bratt, 1998/. However, abundances of specific species are not possible to estimate based on these findings. Food remains from the Stone Age in the Stockholm archipelago imply that seal and different kinds of fish were common, which probably holds also for the Misterhult archipelago. During the most intense hunting period, some two hundred years ago, many large terrestrial mammals were locally extinct in the area, e.g. bear, beaver, and wolf /Lindborg and Schüldt, 1998/. Documenting earlier fauna in the Simpevarp area specifically has not been done, and may be difficult due to few excavations in this area. However, information on the occurrence of large mammals during the last 50 years may be available for the Simpevarp area, based on bag records registered by local hunters /Cederlund et al, 2003/.

3.4.5 Population and land use

The first documented settlements in the Simpevarp regional area are from the Stone Age (approximately 6,000 BC) /Lundqvist, 2004/.The documented remains are, however, limited, and only some 20 settlements have been found in the area surrounding Misterhult. One of the settlements is located close to a bay of the Littorina Sea, today known as the "Döderhultsdalen" valley. As many of the early settlements were located close to the seashore, it is suggested that the migration of human populations occurred along the coast /Edenmo, 2001/.

The county of Kalmar is regarded as a being a rich Bronze Age landscape, with locally high concentrations of ancient graves. The Misterhult area is such a place /Lundqvist, 2004/, dominated by mounds of stone and stone circles. One of the most significant remains is located within the Simpevarp area, Stora Bashult/Värnamo. There are only limited remains from the Iron Age, which is puzzling. It has been suggested that the area suffered a severe decline in population after the Bronze Age, but the reason for this is unknown. The large extent of documented common lands, "allmänningar", at that time also supports the idea of a small population in the area. During the Medieval period the farms in the area were dominated by crown land ("Kronohemman").

More recent land use may be studied by using cadastral maps from the late 17th century and written historical documents. However, only land close to villages was mapped and only when the villagers requested redistribution of land. During the period 1,700–1,850, the communally owned land was divided and distributed to the individual farms, and the fields were reorganised. Evolving technology

also altered the cultural landscape as lakes and wetlands were drained and cultivated. Better iron tools made it possible to till the earth deeper and dig ditches and thus drain sodden areas. The area of agricultural land expanded and meadows and pastures became an important land use because of substantial cattle breeding /Gustafsson and Ahlén, 1996/. In the Simpevarp area, the population expanded first at the beginning of the 19th Century /Lundqvist, 2004/, but the population in the area has never been high. Documents from the 1550s show that the permanent settlements were at the same locvations as today /Lundqvist, 2004/. The permanent settlements, as we recognise them today, were probably established during the early Medieval.

Prehistoric and historic times in the Simpevarp area are characterised by limited opportunities for land cultivation, due to restricted occurrence of suitable soils /Lundqvist, 2004/. It has been suggested that only some 10–15% of the total area was suitable for cultivation. The area has better opportunities for cattle breeding, and islands in the outer archipelago were often used exclusively for livestock grazing and mowing. The area has always been self supporting to a high degree, based on fishing and cattle breeding, whereas crops were probably imported by trade. The fact that fishing was of major importance for the farmers is documented in local names of places and harbours.

The forests in the landscape have not been mapped to the same extent in historical time. Forests and wood land have only recently been regarded as an economical resource, which has implications for the historical documentation of forestry in the Simpevarp area. However, from the 17th centaury there is documentation of furnaces established in the Misterhult region, which gives some indication of the utilization of wood..

4 Evaluation of primary data

This chapter describes analyses and compilations of processed primary data that serve either as direct input to the subsequent modelling (material properties and boundary conditions), or data used for calibration/verification/conditioning, as reported in Chapter 5. The underlying primary data, as outlined in Chapter 2, either constitute old existing data or new data from the ongoing site investigations, or combinations of the two. Sections 4.1 through 4.3 plus 4.10 cover the "surface system", including evaluation of biota data. The analysis of primary data related to the "bedrock system" is treated in Sections 4.4 through 4.9.

4.1 Topography and bathymetry

The digital elevation model, DEM, is built from several different sources with different resolution and accuracy. Three regions of accuracy and resolutions are identified; sparse land, dense land and sparse sea, cf. Figure 4-1.

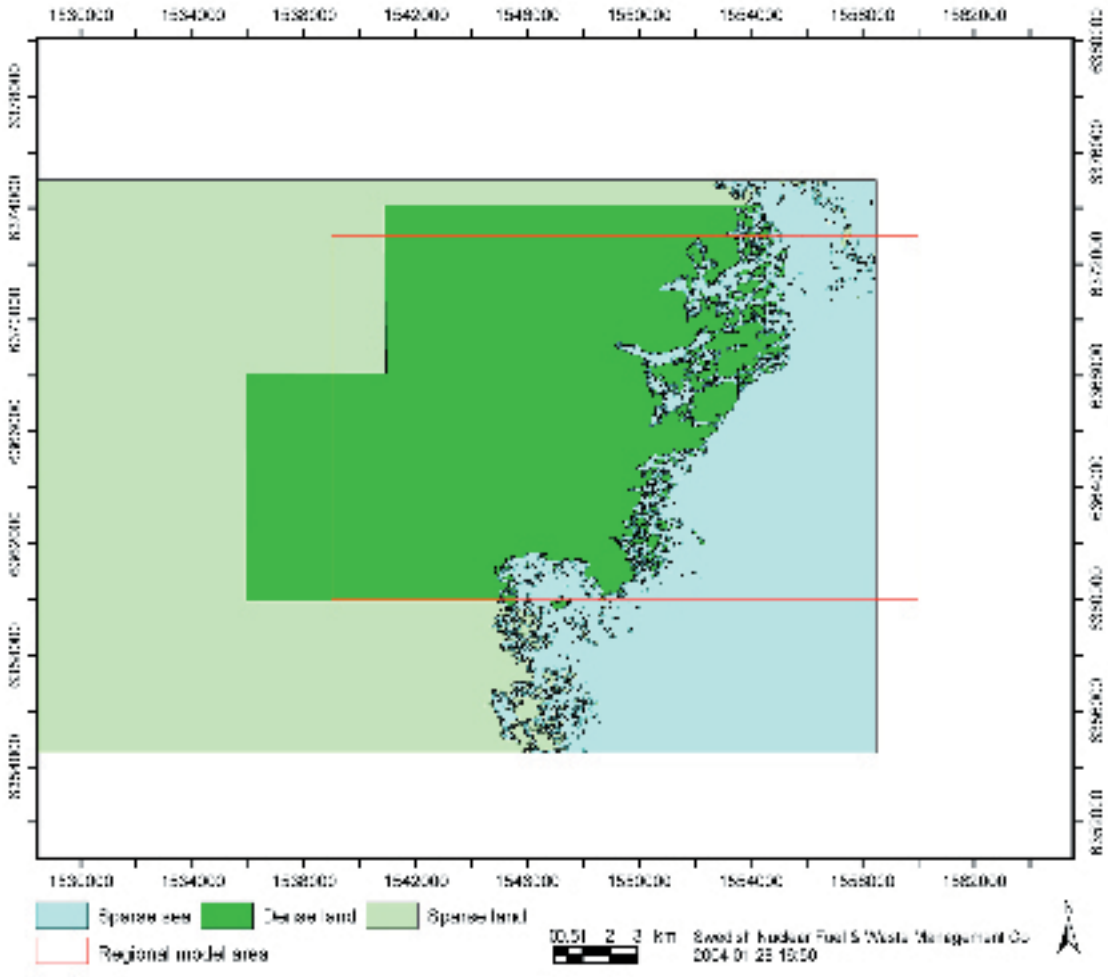

Figure 4-1. *Data density for the digital elevation model including the Simpevarp area. The given data density reflects the variable uncertainty in the resulting DEM model.*

According to /Brydsten, 2004a/, the sparse data on land is collected from two sources, partly the existing DEM from the Swedish national land survey on a grid with 50 m squares and partly elevation lines from the digital map with a scale of 1:10 000. The dense data on land come from a special survey on a grid with 10 m squares. Neither of these data sets contains any bathymetric data in the lakes and hence the elevation coincides with the water table.

Elevation at sea for the sparse area were obtained from the paper chart of the Swedish National Administration of Shipping and Navigation. From the paper chart, the depth contours for 3, 6, 10, 15, 25 and 50 m were digitised together with the point depths shown on the paper chart /Brydsten, 2004a/.

Some of the source data are not in the Swedish National Cartesian system, RT90, and hence had to be transformed to the national 2.5 gon V 0:–15, RT90 system.

Elevation data are available for the whole of Sweden from the GSD-Elevation database. These data are mappen on a 50 m grid through digitalisation and interpolation. They are attributed an average error less than 2.5 m (per large frame, i.e. 5x5 km^2). The accuracy is 1 m. In order to improve the elevation model, a site specific model has been produced on a 10 m grid using digital matching and interpolation of elevation in photogrammetric models, c.f. Figure 4-2. An area in the northwest is however still based on interpolation from the 50 m grid. The data are given with an accuracy (precision) of ±0.0001 m. The average error in the 10 m grid data is less than ±1 m in open terrain, and less than ±2 m in forested terrain.

The interpolated DEM is shown in Figure 4-2.

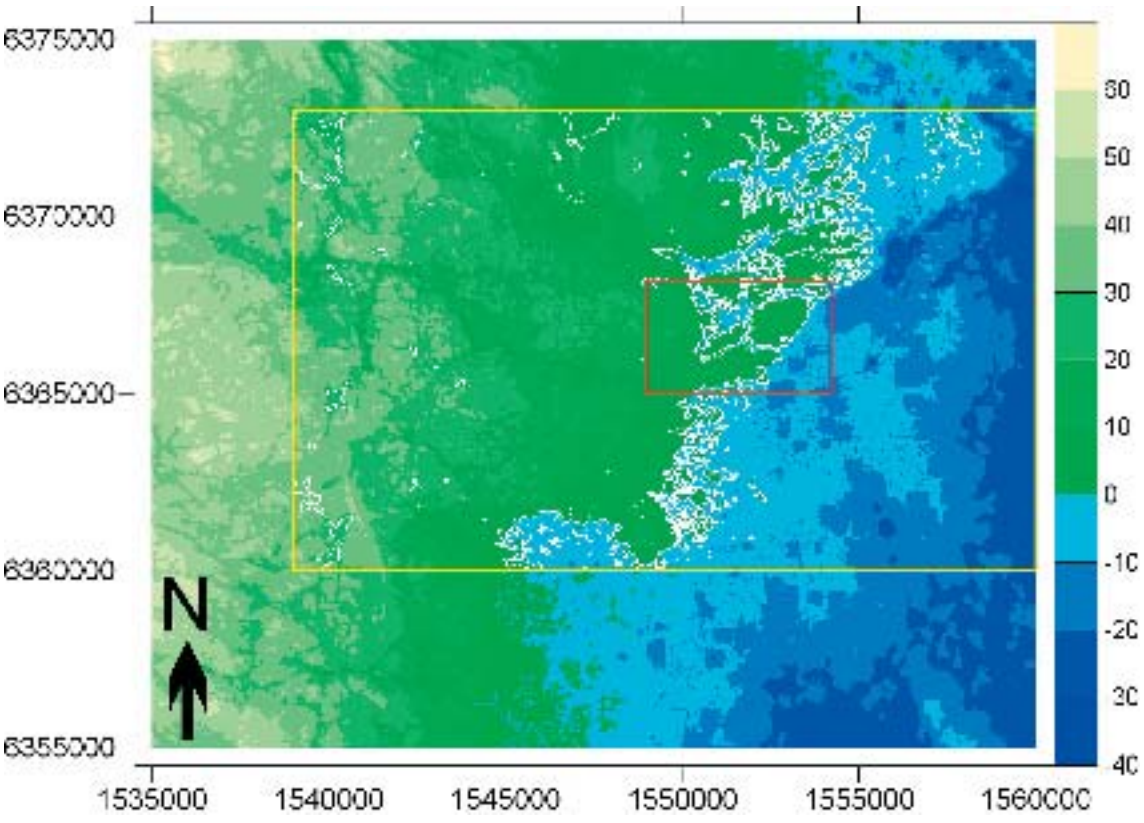

Figure 4-2. *The interpolated digital elevation model (DEM) of the Simpevarp area with outline of the Regional model area (yellow) and the Local model area (red) . Elevation of modelled surface is given in metres above sea level (masl).*

4.2 Geologic evaluation of surface-based data

4.2.1 Overburden including Quaternary deposits

The overburden includes marine and lacustrine sediments and peat. The overburden in the Simpevarp subarea was formed during the Quaternary period and is for the most part henceforth designated as Quaternary deposits. All known Quaternary deposits in the Simpevarp region were formed during and after the latest glaciation. Deposits related to earlier glaciations or interglacials are not known. The whole Simpevarp model area is situated below the highest coastline, which means that the environment, in the lowest parts of the landscape, has been favourable for the deposition of fine-grained, water-laid sediments. The division of Quaternary deposits according to genesis and the environment in which they were formed consists of two main groups: glacial and post-glacial.

Glacial deposits, which were deposited either directly from the continental ice sheet or from the water derived from the melting of this ice. Till was deposited directly by the ice whereas the melt water from the ice deposited glaciofluvial deposits. These last deposits comprise coarse material often forming eskers but also clay and silt, which often form flat fields.

Post-glacial deposits that were formed after the inland ice had melted and retreated from the area approximately 14,000 years ago. Post-glacial sediment and peat form the youngest group of the Quaternary deposits. In general, they overlie till and, locally, glacial clay or crystalline bedrock. The post-glacial deposits are dominated by organic sediment and re-deposited, wave-washed clay, sand and gravel.

The Quaternary geology within the investigation area had earlier been mapped by the Geological Survey of Sweden /Svedmark, 1904/. This information is relatively old and has only been presented on the scale 1:100 000. The map shows that the area is dominated by till and exposed bedrock. Some of the valleys are covered by peat. A map of the Quaternary deposits was presented in /Bergman et al, 1998/. That map is based upon interpretation of aerial photographs and indicates that most of the Simpevarp subarea is exposed bedrock. The information based on the ongoing site investigation shows, however, that Quaternary deposits cover a considerably larger part of the Simpevarp subarea. The old map by /Svedmark, 1904/ seems to give a better view of the distribution of Quaternary deposits than the the map from 1998. The old map has, however, been made using methods, that have a low accuracy of geographical positioning. In the Simpevarp subarea new and more reliable information concerning the distribution of Quaternary deposits is available. The information from the older maps is, therefore, not used further in this report.

The Simpevarp version 1.1 descriptive model incorporate results from the mapping of Quaternary deposits carried out during 2003 on the peninsula of Simpevarp and the adjacent islands of Ävrö and Hålö (4.4 km^2) all situated within the Simpevarp subarea.

The results presented here include:

- A map which can be presented in scale 1:10 000 and show bedrock exposures and Quaternary deposits with an area larger than 10 by10 m. The map shows the overburden at a depth of 0.5 metres below ground surface. The superficial boulder frequency of the till and the effects of wave washing are also shown on the map (Figure 7-1).
- Stratigraphical data that has been compiled from studies of trenches and 17 auger boreholes down to a depth of maximum 1.5 meters below the ground surface, cf. Figure 4-3.
- The direction of glacial *striae* on rock outcrops, which gives information of the direction of the ice movements during the latest ice age.

The uppermost deposits were mapped using a spade and a hand driven probe. GPS and aerial photos (infrared photographs taken from an altitude of 2,300 m, scale 1:15 000) were used for orientation. A mirror compass was used to measure the directions of the glacial *striae*. Before the mapping started, the aerial infrared photographs were interpreted and areas with exposed bedrock were marked.

The different Quaternary deposits were marked directly on the aerial photographs in the field. All Quaternary deposits that could be distinguished from other deposits and had an area larger than 10 by 10 m were marked on the map as surfaces. The map shows the distribution of Quaternary deposits at a depth of 50 cm. Some surface layers thinner than 50 cm are also shown on the map (e.g. peat overlaying other deposits).

Figure 4-3. *Location of boreholes used to assess the stratigraphy of the Quarternary deposits.*

Table 4-1. Auger boreholes used to assess the stratigraphy of the Quaternary deposits.

Site	Depth below ground surface	Quaternary deposit
PSM002591	0.0–0.1 0.10–1.0	Postglacial gravel Glacial clay
PSM002602	0.0–1.5	Glacial clay
PSM002603	0–0.3 0.3–1.0	Postglacial gravel Glacial clay
PSM002604	0.0–0.3 0.3–0.8 0.8–1.5	Peat Postglacial sand Glacial clay
PSM002605	0.0–0.8 0.8–2.0	Postglacial gravel Glacial clay
PSM002609	0.0–3.0	Postglacial gravel
PSM002610	0.0–0.4 0.4–0.7	Bog peat Fen peat
PSM002611	0.0–0.7	Postglacial gravel
PSM002621	0.0–0.5 0.5–0.8	Bog peat Fen peat
PSM002622	0.0–0.8 0.8–1.3	Fen peat Gyttja
PSM002623	0–0.5 0.5–1.5	Fen peat Glacial clay
PSM002624	0.0–3.0	Postglacial gravel
PSM002625	0.0–1.5	Glacial clay
PSM002626	0.0–2.0	Till, sandy
PSM006272	0.0–1.0	Glacial clay
PSM002659	0.0–1.2 1.2–?	Fen peat Gravel
PSM002660	0.0–0.1 0.1–0.2 0.2–1.5	Fen peat Postglacial gravel Glacial clay

4.2.2 Rock type distribution

Analysis of primary data

The available bedrock data relating to the distribution and description of rock types within the local model area are of variable quality, whereas the ages of the rock types are judged to be fairly well-constrained.

Detailed bedrock mapping and analytical work have been carried out in the Simpevarp subarea during 2003, in conjunction with the ongoing site investigation programme at Oskarshamn. The quality of the surface bedrock data is judged to be high in this area (Figure 4-4). However, in the remaining part of the local model area employed for Simpevarp 1.1 no detailed mapping of the bedrock has so far been carried out in connection with the site investigation programme. Consequently, the bedrock information in this area (western and northern part of the local model area) is based on the compilation in the Site Descriptive Model Version 0 /SKB, 2002b/. It is difficult to judge the quality of the bedrock information in this area, since it is partly based on bedrock maps on the scale 1:250 000 /Bergman et al, 1998, 1999; SKB, 2002b/. In order to visualise the differences between the bedrock map of the Simpevarp subarea and the bedrock map from model version 0 in a simplified manner, these maps are merged in Figure 4-5. The obvious mismatch between the two maps is visible in the western part of the Simpevarp peninsula.

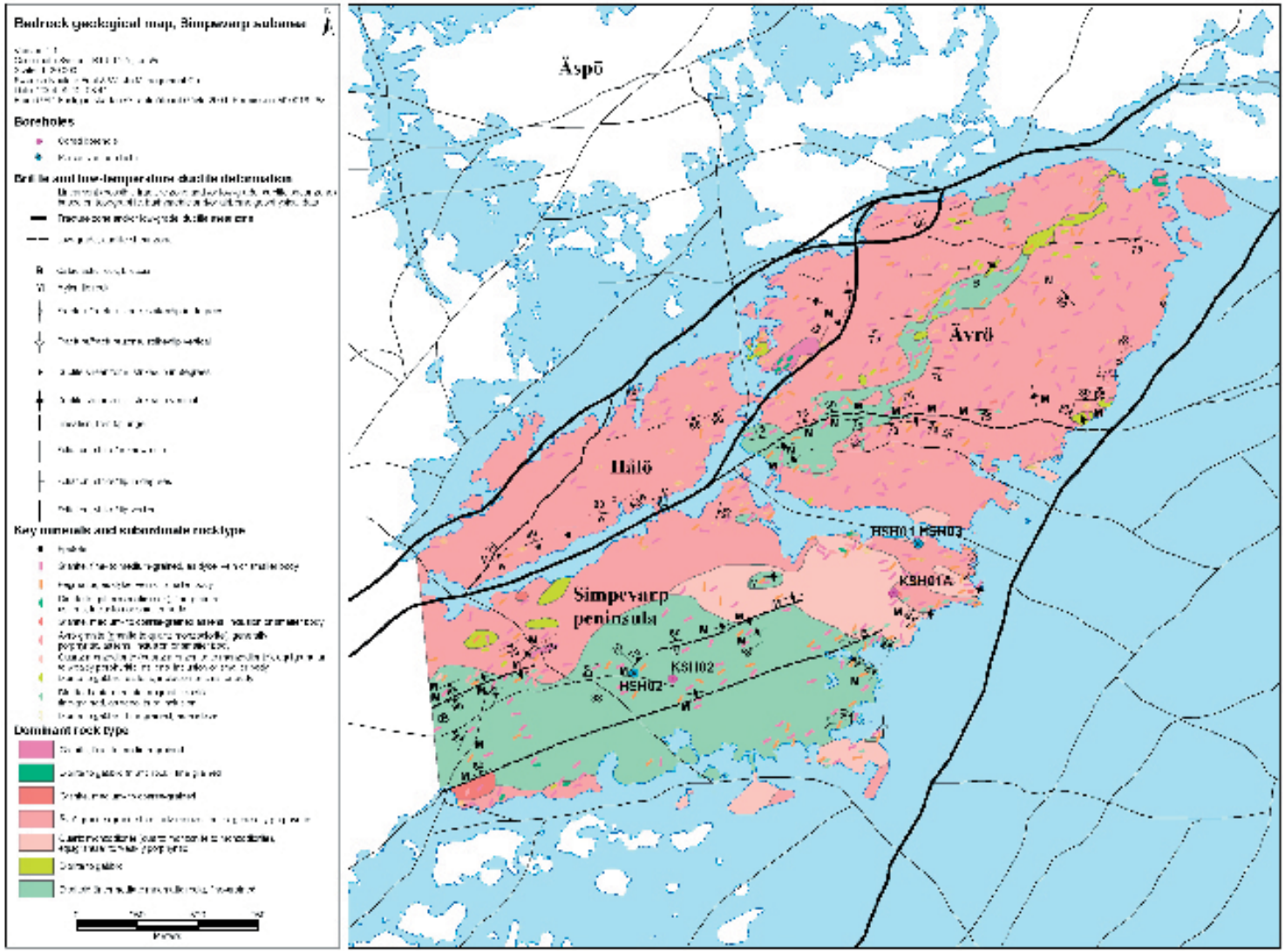

Figure 4-4. *Bedrock map of the Simpevarp subarea.*

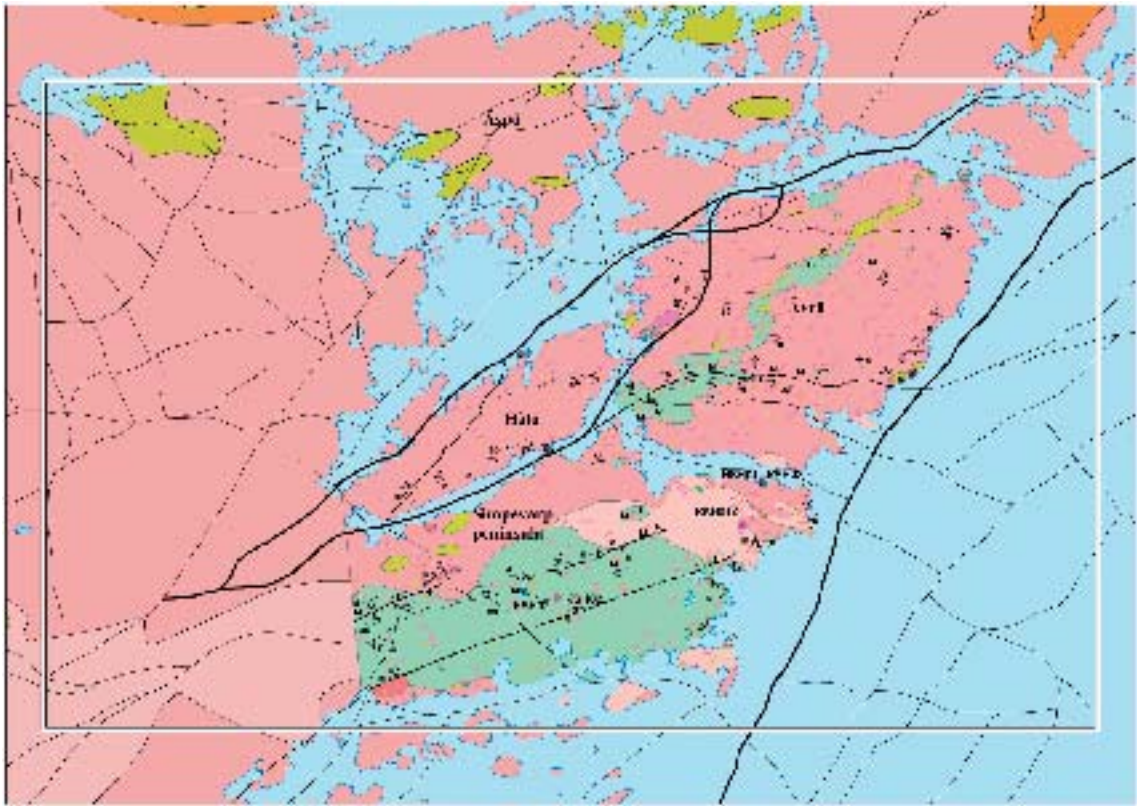

Figure 4-5. *Combination of the bedrock map from the model version 0 (dark pink=Ävrö granite, light pink=quartz monzodiorite, green =diorite to gabbro) and the bedrock map of the Simpevarp subarea (cf. Figure 4-4). The frame marks the local scale model area.*

The distribution, description and age of the various rock types in the local model area have been documented with the help of the following information that to a major extent has been generated during various recently performed site investigation activities in the Simpevarp subarea:

- An outcrop database with numerical and descriptive data from 353 observation points /Wahlgren et al, 2004/.
- 46 modal analyses (mineral composition) of surface samples, recalculated and plotted in a QAPF diagram in order to classify the various rock types /Wahlgren et al, 2004/.
- Chemical analyses of 31 surface samples, which have been used to chemically characterise the various rock types /Wahlgren et al, 2004/.
- Petrophysical data from laboratory measurements of samples from 10 locations /Mattsson et al, 2003/.
- *In situ* gamma-ray spectrometry data from 32 locations, including locations on the Äspö island /Mattsson et al, 2003/.
- U-Pb zircon and titanite dating of two of the dominant rock types /Wahlgren et al, 2004/.
- Bedrock geological map that was compiled with the help of the outcrop database and magnetic data from airborne geophysical measurements /Wahlgren et al, 2004/, c.f. Figure 4-4.

In this report, attention is focussed on the composition, grain size and texture of the rock types in the local model area. The characterisation of the rock types is mainly based on data from the Simpevarp subarea. The petrophysical properties are only briefly commented since the available information is very limited. Furthermore, the content of uranium is reported since, in particular, anomalously high values (≥ 16 ppm) of the dominant isotope ^{238}U can give rise to high values of ^{222}Rd.

Rock types

The local model area employed for Simpevarp 1.1 is dominated by intrusive igneous rocks that belong to the approximately 1,810–1,760 Ma BP generation of granite-syenitoid-dioritoid-gabbroid rocks in the 1,860–1,650 Ma BP Transscandinavian Igneous Belt (TIB). The rocks are mostly well-preserved and more or less isotropic, but a weak foliation is locally developed. However, low-grade ductile shear zones of mesoscopic to regional character do occur. The description of the rock types in the local model area is based on documentation produced in connection with the bedrock mapping of the Simpevarp subarea during 2003 /Wahlgren et al, 2004/.

The local model area is composed of three dominant rock types, namely:

- Dioritoid, fine-grained, unequigranular.
- Ävrö granite (granite to quartz monzodiorite), medium-grained, generally porphyritic.
- Quartz monzodiorite, medium-grained, equigranular to weakly porphyritic.

Subordinate rock types comprise:

- Granite, fine- to medium-grained.
- Pegmatite.
- Mafic rock, fine-grained.
- Granite, medium- to coarse-grained.
- Diorite to gabbro, medium-grained.

As can be seen in the QAPF and geochemical classification diagrams (see Figure 4-6, Figure 4-7 and Figure 4-8), the dominant rock types in the Simpevarp subarea display similar and overlapping compositional variations. Petrophysical data on the rock types in the Simpevarp subarea is very limited. However, the documentation of the magnetic susceptibility during the bedrock mapping of the Simpevarp subarea displays supporting similar and overlapping values (Figure 4-9). The most important criteria in distinguishing between different rock types are texture and grain size.

According to the International Union of Geological Sciences /LeMaitre, 2002/, the classification of rocks should be based on the modal composition. Thus, the geochemical classification diagrams, c.f. Figure 4-7 and Figure 4-8, should not be used strictly for classification purposes, but merely as an indication of the compositional trend of the different rock types.

The *fine-grained dioritoid* dominates the southern part of the local model area, and the central part of Ävrö island as a NE-trending, narrow, undulating belt (Figure 4-4). Furthermore, it occurs as minor bodies and inclusions in the Ävrö granite and the quartz monzodiorite.

The fine-grained dioritoid is grey and commonly unequigranular, with up to 3 mm large (exceptionally 5 mm) megacrysts of hornblende and plagioclase (Figure 4-10). Locally, megacrysts of pyroxene and biotite also occur. However, the pyroxene is generally more or less altered to hornblende. Thus, most of the hornblende megacrysts are inferred to be secondary after pyroxene.

A characteristic feature in the fine-grained dioritoid is an inhomogeneous coarsening of the grain size (Figure 4-11). It appears as diffusely delimited vein-like aggregates and patches. The coarsening makes the fine-grained dioritoid resemble the quartz monzodiorite, and consequently, these two rock types are occasionally difficult to distinguish from one another.

The contacts between the dioritoid and the country rocks are usually gradual, but locally the contact is sharp (Figure 4-12).

The compositional variation of the fine-grained dioritoid is displayed in the QAPF modal classification diagram in Figure 4-13. The average density is 2,803±52 kg/m^3.

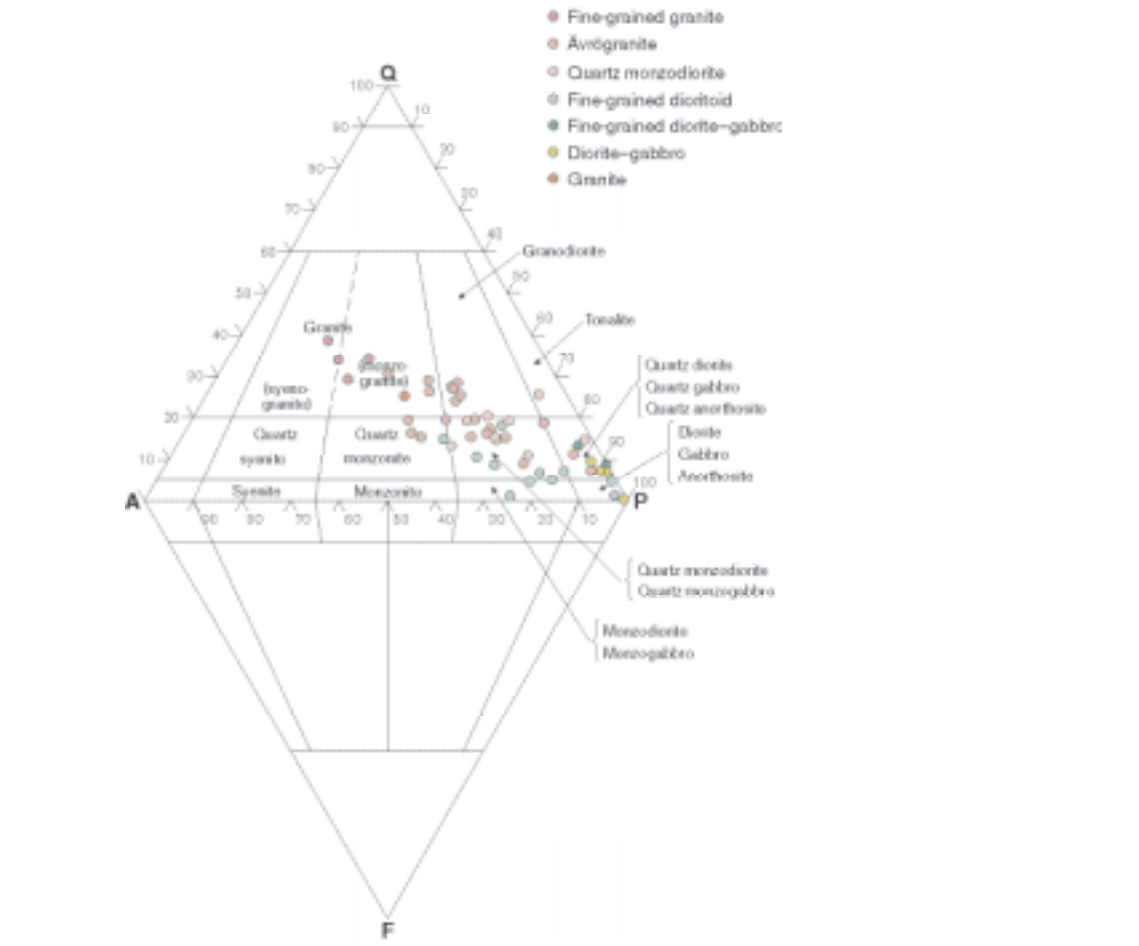

Figure 4-6. *QAPF modal classification /Streckeisen, 1976, 1978/ of rock types in the Simpevarp subarea. Modal analyses of samples from boreholes KSH01A/B are also included.*

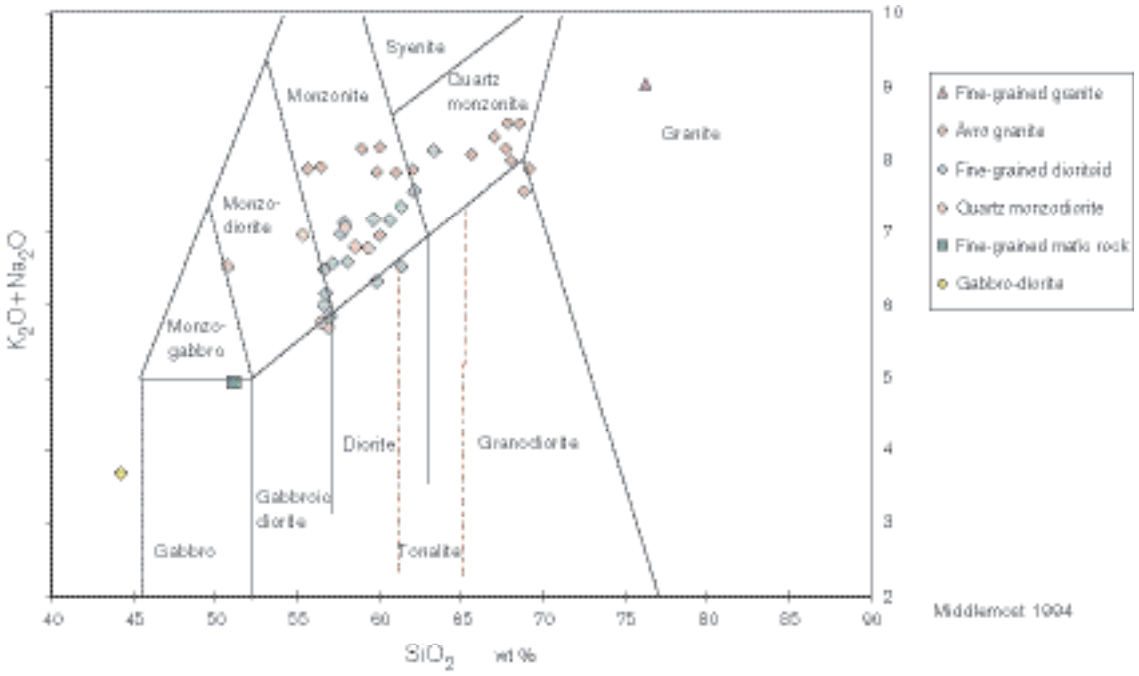

Figure 4-7. *Geochemical classification of rocks from the Simpevarp subarea according to /Middlemost, 1994/. In the diagram, 3 analyses from borehole KSH02 are also included.*

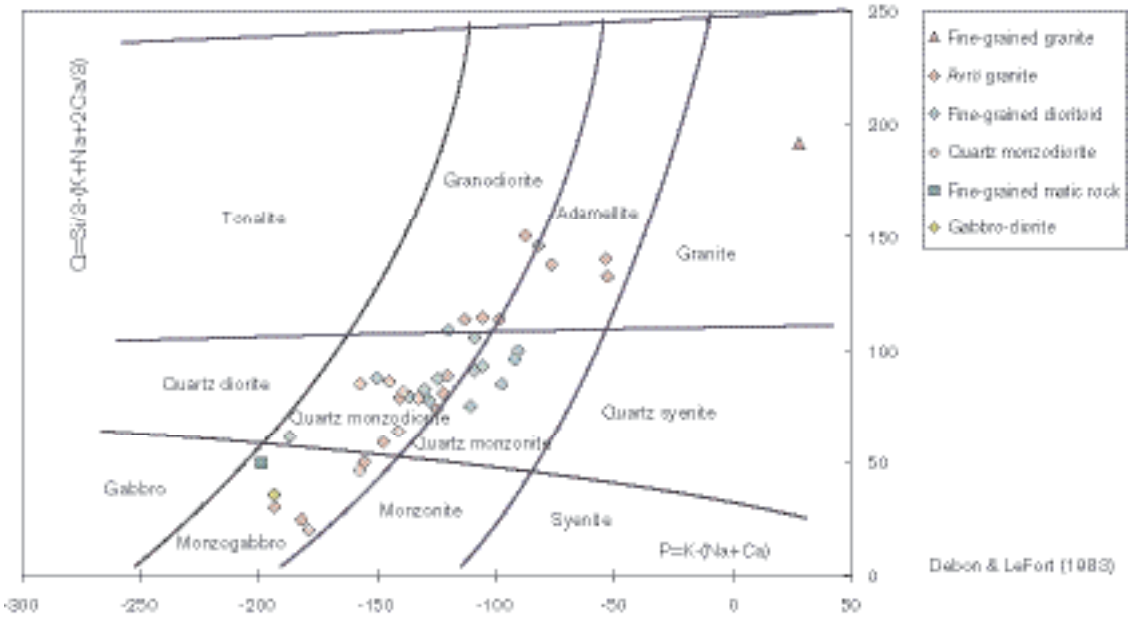

Figure 4-8. *Geochemical classification of rocks in the Simpevarp subarea according to /Debon and Le Fort, 1983/. In the diagram, 3 analyses from borehole KSH02 are also included.*

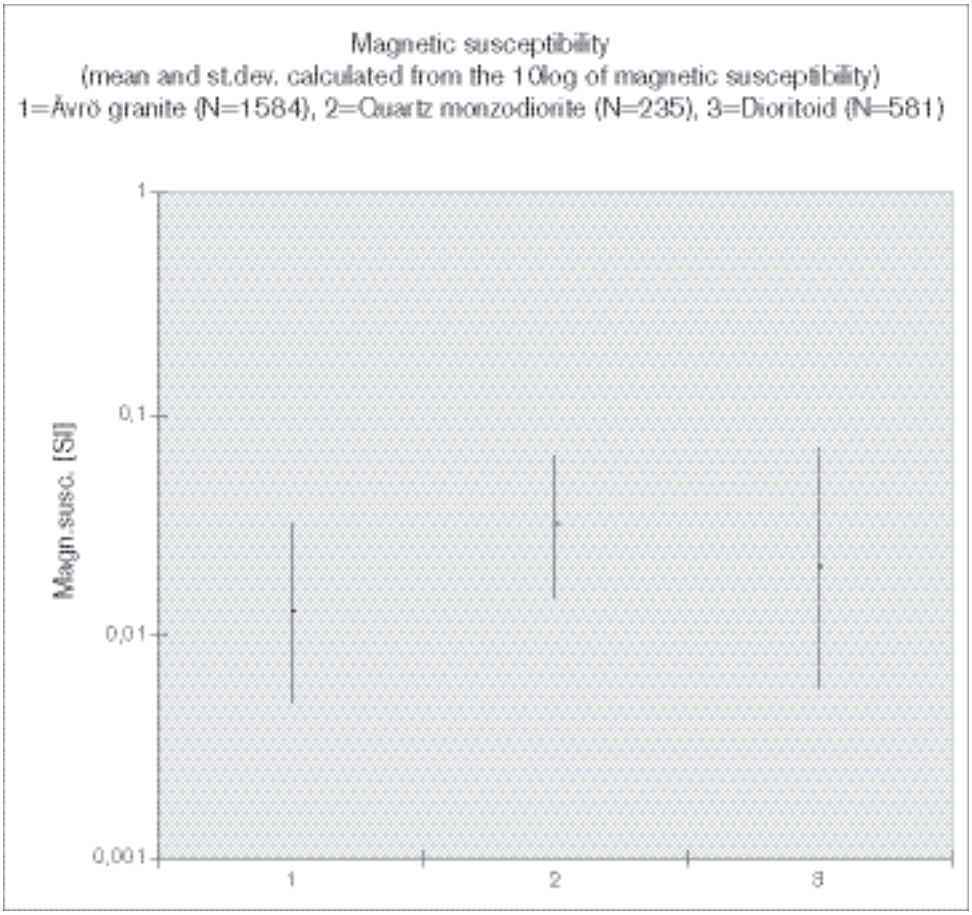

Figure 4-9. *Magnetic susceptibility of the dominant rock types in the Simpevarp subarea. Based on field measurements during bedrock mapping.*

Figure 4-10. *Fine-grained dioritoid with megacrysts of hornblende (dark grains) and plagioclase (white to light grey grains).*

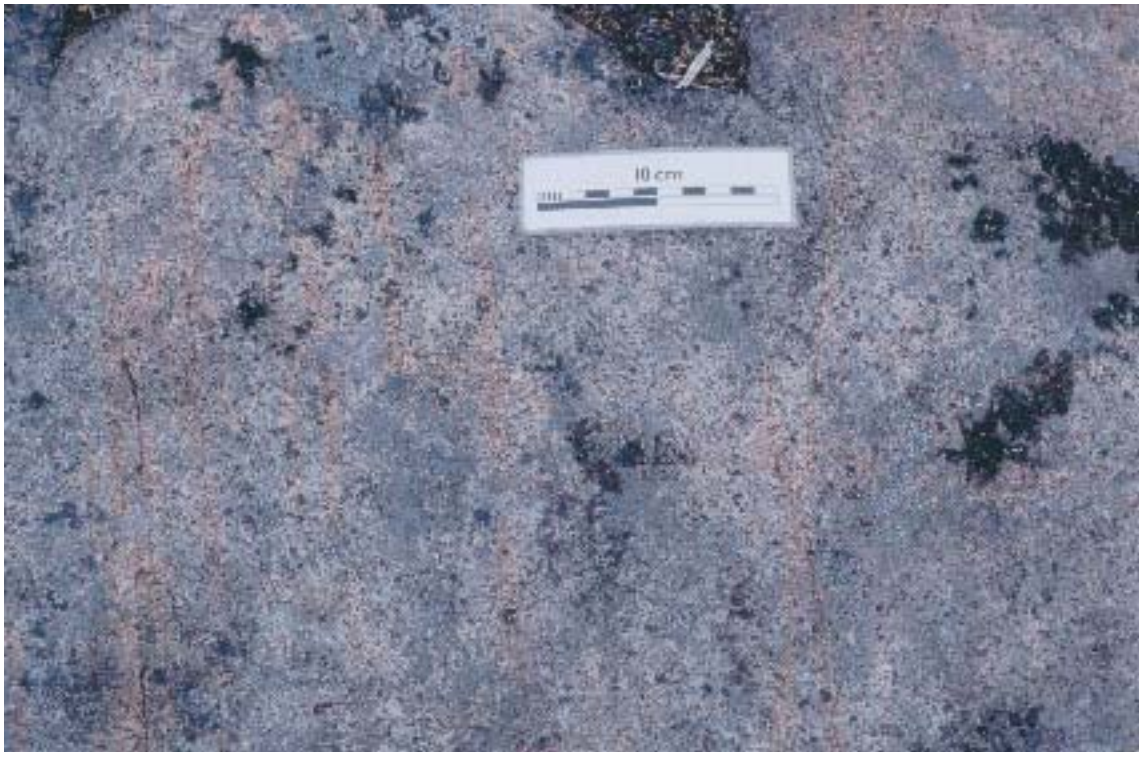

Figure 4-11. *Inhomogeneously coarsened, fine-grained dioritoid.*

Figure 4-12. *Contact between fine-grained dioritoid (lower part) and quartz monzodiorite (upper part).*

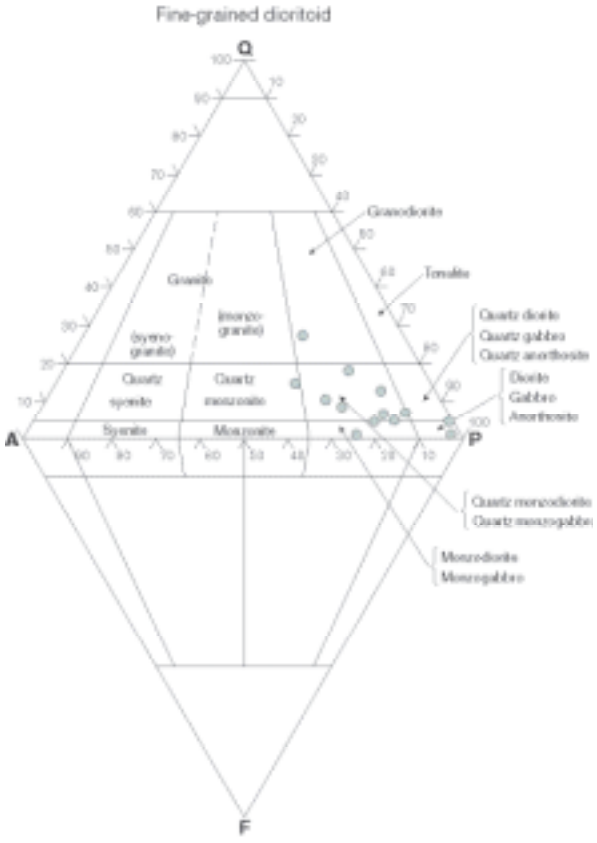

Figure 4-13. *QAPF modal composition of the fine-grained dioritoid.*

The fine-grained dioritoid has traditionally been classified as a volcanic rock of dacitic to andesitic composition /SKB, 2002b and references therein/. However, except for being fine-grained, no characteristic criteria indicating that the rock is of volcanic origin were found during the bedrock mapping of the Simpevarp subarea. An alternative interpretation is that the rock constitutes a high-level intrusion that subsequently was intruded by its parent magma, which is represented by the neighbouring quartz monzodiorite in the country rock. The characteristic, inhomogeneous coarsening in the fine-grained dioritoid is inferred to be a late-magmatic phenomenon, presumably due to a thermal input during the emplacement of the quartz monzodiorite and possibly also the Ävrö granite. The uncertainty in the interpretation of the origin of this fine-grained rock of intermediate composition is the primary cause of the more neutral classification as a dioritoid. However, this does not exclude that the rock may be of volcanic origin.

The *quartz monzodiorite* mainly occurs in the eastern part of the Simpevarp peninsula and neighbouring parts in southernmost Ävrö (see Figure 4-4). It is grey to reddish grey, medium-grained, commonly equigranular (Figure 4-12) and exhibits a relatively restricted compositional range (see Figure 4-14), which is similar to that of the fine-grained dioritoid. As can be seen in Figure 4-14, tonalitic and quartz dioritic varieties occur as well. Transitional varieties between typical quartz monzodiorite and fine-grained dioritoid occur, which further strengthens the inferred close relationship between these two rock types.

Ävrö granite is a collective name for a suite of more or less porphyritic rocks that vary in composition from quartz monzodiorite to granite, including quartz dioritic, granodioritic and quartz monzonitic varieties (Figure 4-15). It is the dominating rock type in the Simpevarp subarea, as well as in the whole local model area. The Ävrö granite is reddish grey to greyish red, medium-grained and the phenocrysts are usually 1–2 cm in size but scattered larger phenocrysts occur (Figure 4-16). A characteristic feature in the Ävrö granite is the occurrence of scattered cm to 0.5 metre large enclaves of intermediate to mafic composition. The average density is 2,681±16 kg/m^3. In the present context, the so-called Äspö diorite, due to textural and compositional similarities, is included in the Ävrö granite category.

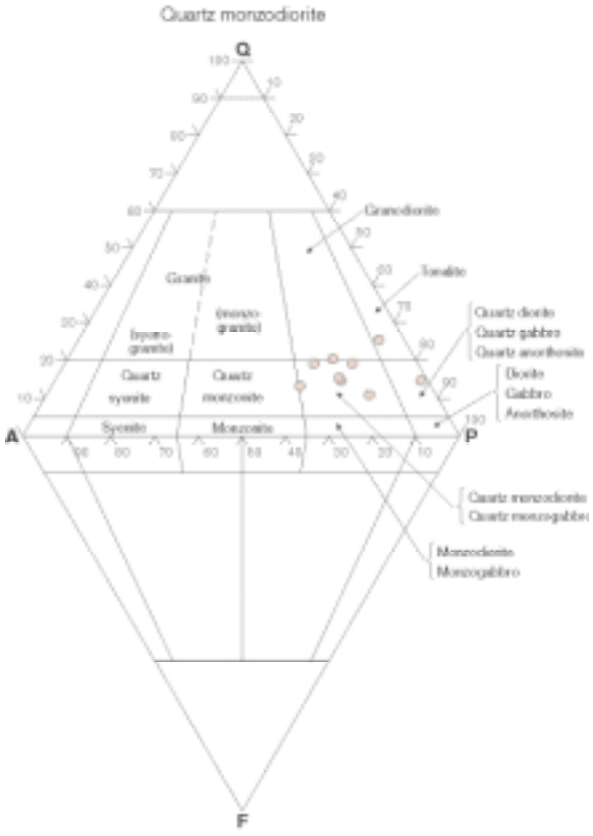

Figure 4-14. *QAPF modal composition of the quartz monzodiorite.*

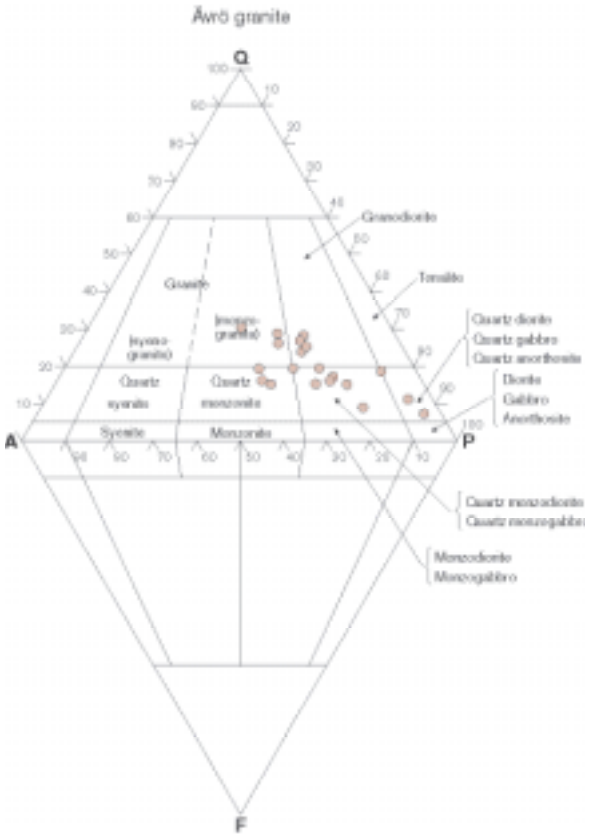

Figure 4-15. *QAPF modal composition of the Ävrö granite.*

Figure 4-16. *Sparsely porphyritic Ävrö granite.*

In the easternmost part of the Simpevarp peninsula, the quartz monzodiorite is mixed and mingled with the Ävrö granite. This is also evident in the cored borehole KSH01A. Gradual contact relationships are characteristic and strongly indicate that the quartz monzodiorite and the Ävrö granite formed more or less synchronously.

Diorite to gabbro occurs as scattered, minor bodies and as inclusions in the Ävrö granite and the fine-grained dioritoid (Figure 4-4). These minor bodies and inclusions usually display mixing and mingling relationships with the country rock. Furthermore, red to greyish red, *medium- to coarse-grained granite* occur, both as minor bodies in the western part of the subarea and as diffusely delimited small occurrences in the Ävrö granite (Figure 4-4).

A characteristic feature in the Simpevarp subarea is the frequent occurrence of *fine- to medium-grained granite*, usually as dykes but also as veins and irregular minor bodies (Figure 4-4 and Figure 4-17). In situ gamma-ray spectrometric measurements have shown that it has higher content of thorium than the other rock types in the area /Mattsson et al, 2002, 2003/.

Pegmatite frequently occurs (Figure 4-4 and Figure 4-17) and pegmatite cross-cutting granitic dykes and *vice versa* is observed. Consequently, at least two generations of fine- to medium-grained granite as well as pegmatite occur in the area. However, they are all interpreted to belong to the waning stages of the igneous activity that formed the majority of the rocks in the region.

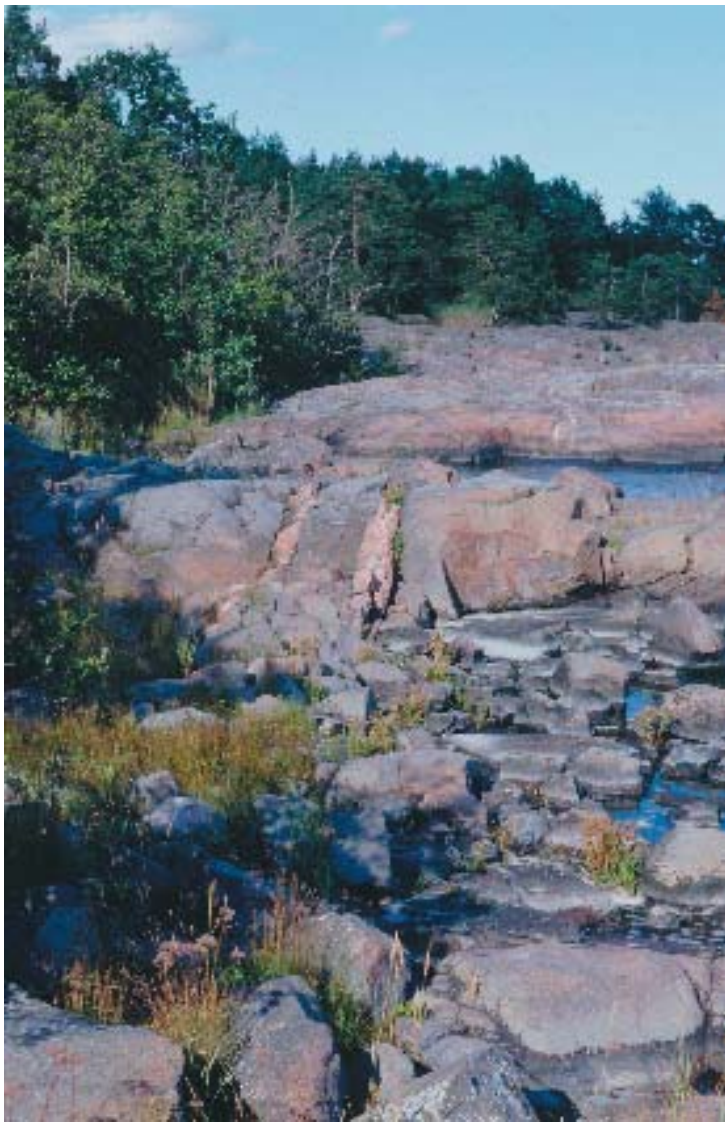

Figure 4-17. *Dykes of fine- to medium-grained granite and pegmatite (c.f. central part of the picture).*

Locally, a fine-grained *mafic rock* occurs as sheets, dykes or minor bodies (Figure 4-4). Generally, it is mixed (net-veined) with fine-grained granite, and, thus, they constitute composite intrusions (dykes).

In conjunction with the bedrock mapping, the Ävrö granite and the quartz monzodiorite were sampled for *U-Pb zircon and titanite dating*. The Ävrö granite was sampled at the stripped outcrop at the site for the cored borehole KAV01. The quartz monzodiorite was sampled in a road cut north of the OIII nuclear reactor, in the eastern part of the Simpevarp peninsula.

Zircon and titanite was analyzed in both samples. The Ävrö granite yielded an upper intercept zircon and titanite age of 1,800±4 Ma, and the quartz monzodiorite yielded an upper intercept zircon age of 1,802±4 Ma and a slightly younger titanite upper intercept age of 1,793±4 Ma. The obtained ages are in good agreement with earlier reported ages for intrusive rocks in the region (Table 4-2).

The mixing and mingling relationships and diffuse contacts between the dominant rock types in the Simpevarp subarea strongly support the view that they were formed more or less synchronously. However, based on field relationships, the following chronostratigraphy is indicated for the dominant and subordinate rock types:

Fine- to medium-grained granite and pegmatite **Youngest**

Fine-grained mafic rock

Medium- to coarse-grained granite

Ävrö granite

Quartz monzodiorite

Diorite to gabbro

Fine-grained dioritoid **Oldest**

All rock types in the Simpevarp subarea display low contents of uranium, except for pegmatite in which the uranium content locally exceeds 16 ppm (see Table 7-6). The latter is a critical value that corresponds to radium index=1, which must not be exceeded in rocks that will be used for engineering purposes /BFS, 1990/.

Bedrock heterogeneity can be assessed at different scales. The subordinate rock types in the Simpevarp subarea have been registered in the outcrop database at every observation point during the bedrock mapping. The bedrock map in Figure 4-4 reveals schematically the high content of subordinate rock types, especially fine-to medium-grained granite and pegmatite. However, quantitative estimates of the volume of subordinate rock types in the outcrops are lacking. The high content of fine- to medium-grained granite in particular, but also pegmatite, is characteristic for the Simpevarp subarea, and constitutes the most important factor in heterogeneity.

Table 4-2. Radiometric ages for intrusive rocks in the Simpevarp local model area.

Rock type	Northing (m)	Easting (m)	Depth (masl)	U-Pb zircon age (Ma)	Reference
Fine-grained granite	6367111.8	1551572.7	–124.8	1,794 + 16/–12	/Kornfält et al, 1997; Wikman and Kornfält, 1995/
Fine-grained granite	6367985.2	1551588.6	–395.7	1,808 + 33/–30	/Kornfält et al, 1997; Wikman and Kornfält, 1995/
Äspö diorite	6367669.2	1551455.3	–318.4	1,804 ± 3	/Kornfält et al, 1997; Wikman and Kornfält, 1995/
Quartz monzodiorite	6366200	1552295		1,802 ± 4	/Wahlgren et al, 2004/
Quartz monzodiorite	6366200	1552295		1,793 ± 4 (titanite)	/Wahlgren et al, 2004/
Ävrö granite	6367281	1553063		1,800 ± 4 (zircon+titanite)	/Wahlgren et al, 2004/

4.2.3 Lineament identification

Data and inferred lineaments

Lineaments in the local model area have been identified on the basis of a joint interpretation of different sets of lineaments, each of which has been identified separately from the following data sets /Rønning et al, 2003; Triumf et al, 2003; Wiklund, 2002/:

- Helicopter-borne geophysical survey data, i.e. data on the total magnetic field, electromagnetic (EM) multifrequency data and very low frequency electromagnetic (VLF) data.
- Fixed-wing airborne, very low frequency electromagnetic (VLF) data.
- Detailed topographic data (terrain model), c.f. Section 4.1.

Furthermore, offshore bathymetric information has also been used in the lineament identification.

The helicopter-borne magnetic, EM multifrequency and VLF data were obtained during 2002 /Rønning et al, 2003/. Measurements were performed along north-south flight lines with a spacing of 50 m. The nominal instrument flight altitude during the measurements was 30–60 m. In a smaller area immediately east of the Simpevarp nuclear power plants, measurements were made along 36 lines perpendicular to the coast with a line spacing of 100 m. No measurements were carried out over the area occupied by the power plants (Figure 4-18), which implies that a large portion of the Simpevarp peninsula is devoid of airborne geophysical data. Furthermore, there are local disturbances in the measured data induced along existing power lines.

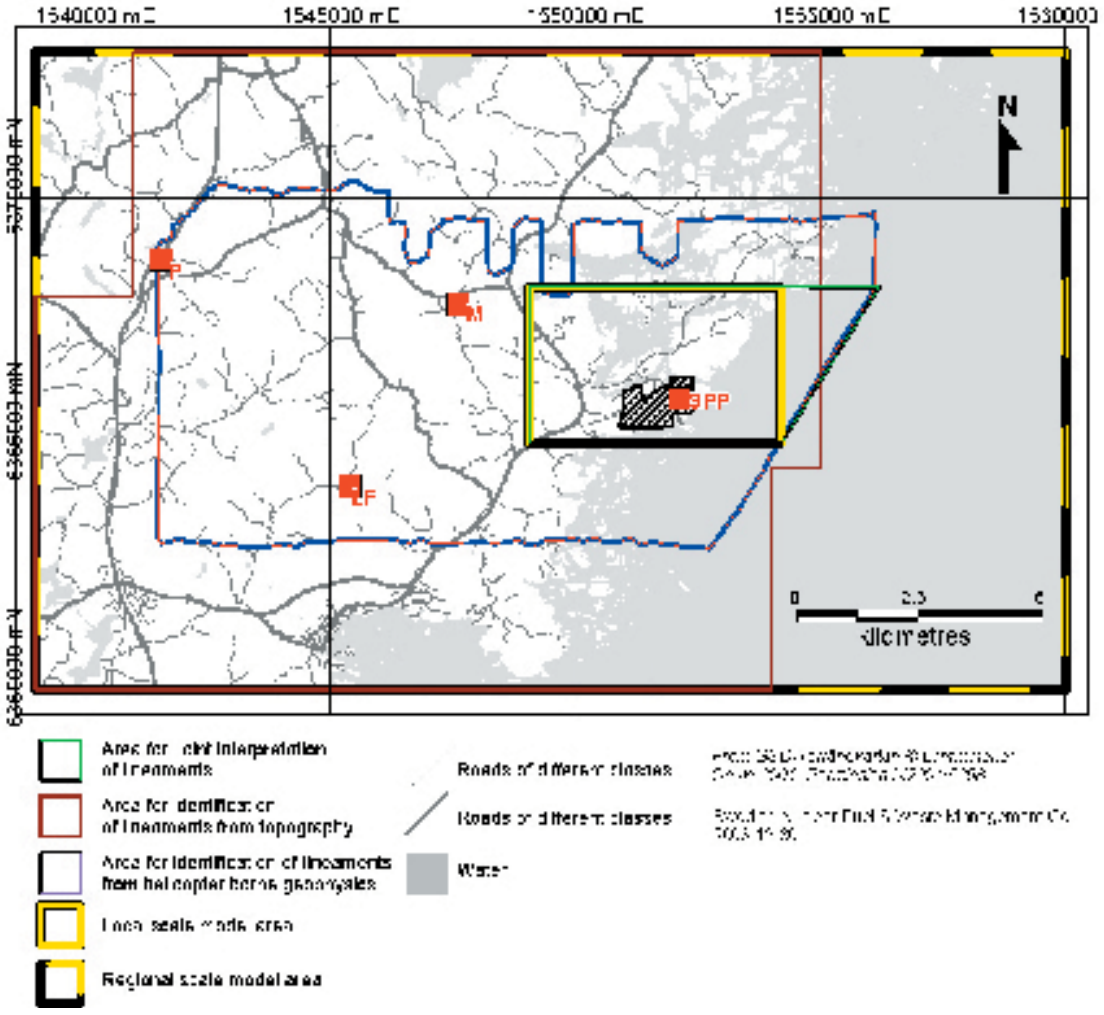

Figure 4-18. *Map showing helicopter-borne geophysical and topographic data coverage. Note that no data were acquired in the area that is occupied by the nuclear power plants and their infrastructure. Geographical labels employed : P =Plittorp, M=Mederhult, LF=Lilla Fjälltorpet and SPP=Simpevarp Power Plants.*

The data processing and methodology used in the interpretation of the helicopter- and fixed-wing borne geophysical survey data and the resulting different sets of identified lineaments are described in /Triumf et al, 2003/. Maps of the total magnetic field, apparent resistivity calculated from fixed-wing VLF data and apparent resistivity calculated from EM multi-frequency data are shown in Figure 4-19, Figure 4-20 and Figure 4-21, respectively.

The topographic data are based on detailed airborne photography carried out 2001 with an instrument flight altitude of 2,300 m and a spatial resolution of 0.2 m /Wiklund, 2002/. The processing of the data resulted in a new detailed digital terrain model (see section 4.1). The latter forms the basis for the identification of topographic lineaments. The processing of the topographic data, the methodology used in the interpretation work and the identified topographic lineaments are reported by /Triumf, 2003/.

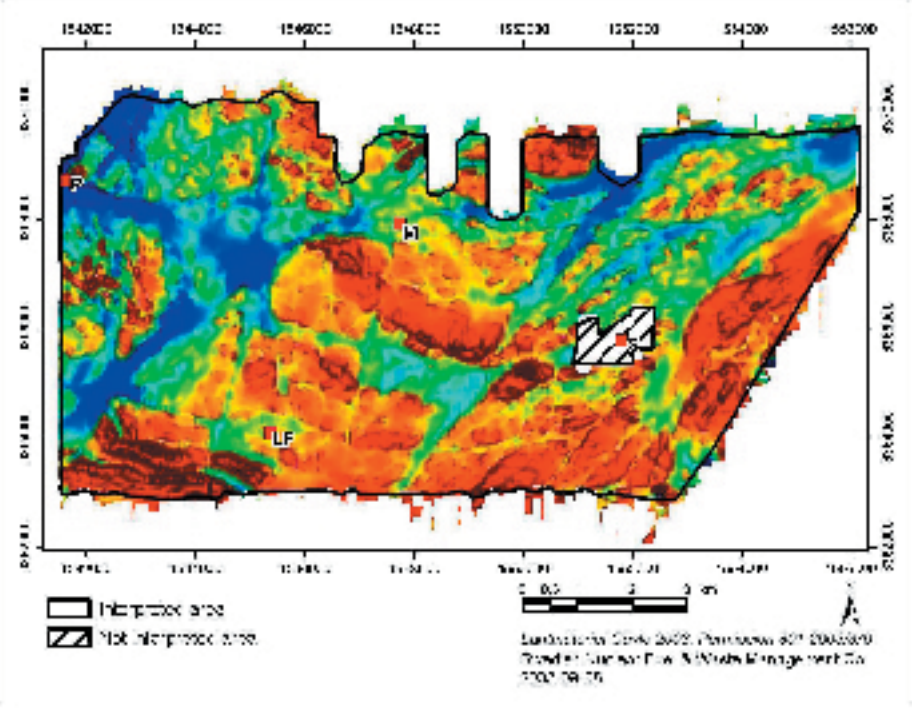

Figure 4-19. *Map showing the total magnetic field from the helicopter survey. Reddish brown colour = strongly magnetic bedrock, blue colour = weakly magnetic bedrock.*

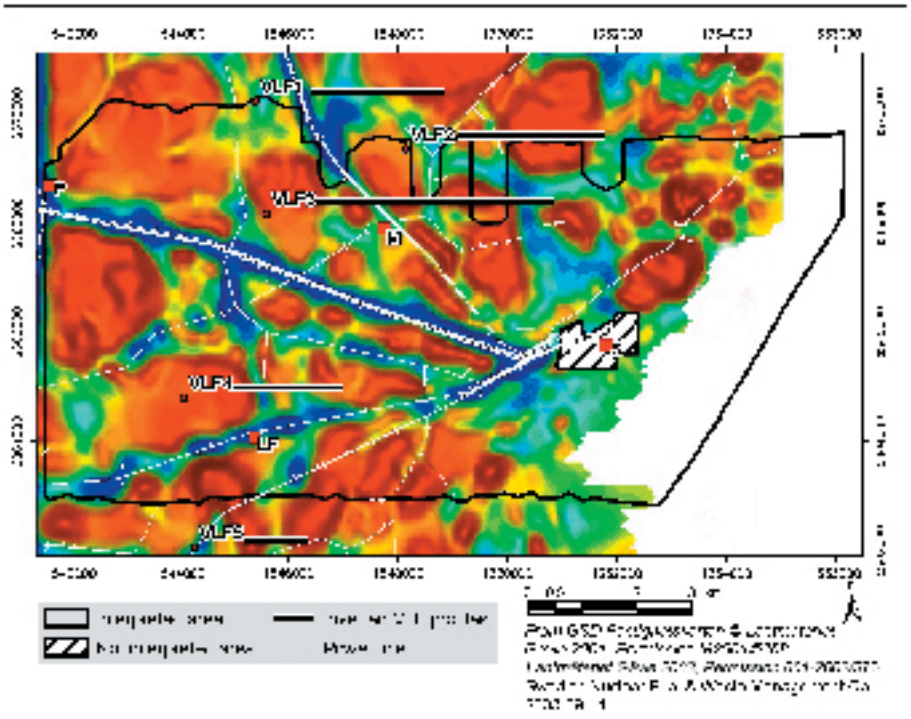

Figure 4-20. *Map showing apparent resistivity calculated from fixed-wing VLF data. Reddish brown colour = high resistivity, blue colour = low resistivity.*

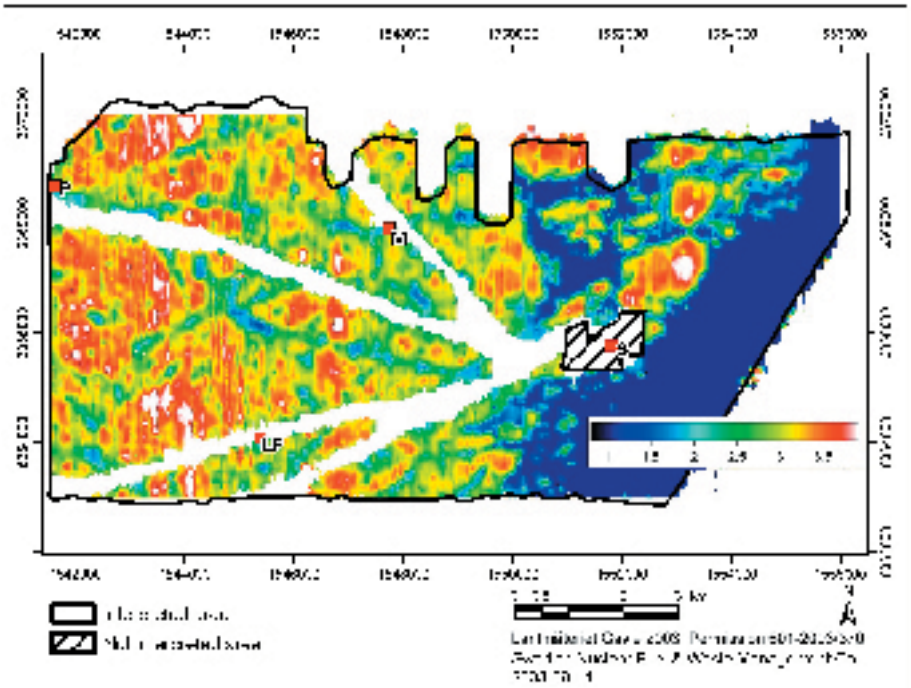

Figure 4-21. *Map showing apparent resistivity calculated from helicopter-borne EM multi frequency data. Reddish colour=high resistivity, blue colour=low resistivity.*

Evaluation

The process of joint interpretation of lineaments consists of the following major steps (c.f. Figure 4-22 and definitions in the adjoing text):

- Construction of “co-ordinated lineaments” from “method-specific lineaments”.
- Parameterisation of the “coordinated lineaments”.
- Construction of “linked lineaments”.
- Parameterisation of “linked lineaments”.

A “method-specific lineament is a lineament identified in a single and specific type of data set, e.g. topography, helicopter-borne magnetic data, multifrequency electromagnetic (EM) data. A “coordinated lineament” is a single interpreted lineament that accounts for all “method.-specific lineaments” along a section of a given single lineament. A “linked lineament” here implies a lineament composed of one or several “coordinated” lineaments with an extension in most cases longer than the underlying interpreted coordinated lineaments, c.f. Figure 4-22.

The final result of the joint interpretation is the map of linked lineaments. They have been assigned attributes relating to their origin and character /Triumf, 2004/. The linked lineaments identified in the Simepvarp 1.1 local scale model area are presented in Figure 4-23, where their assigned class (regional > 10 km or local major 1–10 km) and level of uncertainty are identified. The latter is an expert judgement that relates to the degree of clarity in surface expresion of the lineaments where 1=low, 2=medium and 3= high uncertainty. A weighted average is calculated according to the length of each segment in the linked lineament. For a more detailed explanation, see /Triumf, 2004/.

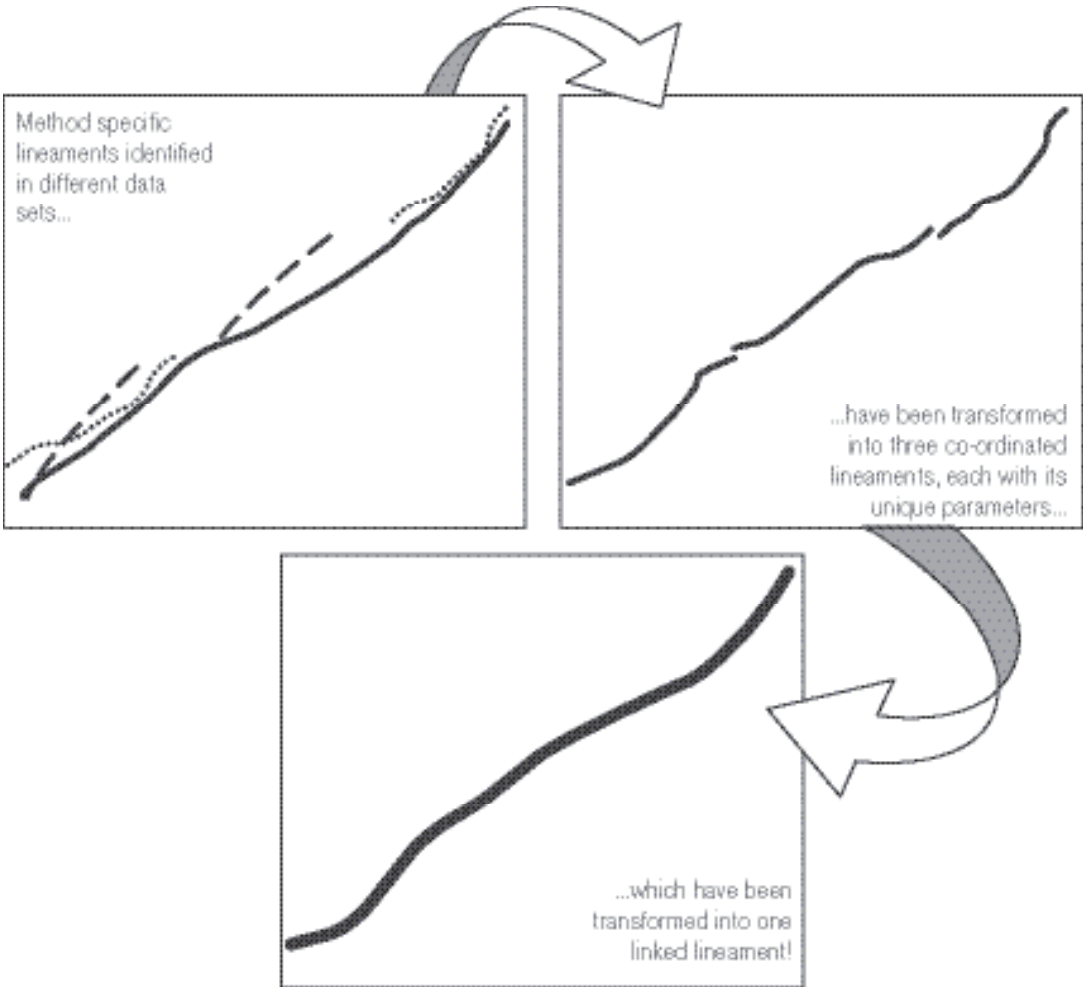

Figure 4-22. *Schematic explanation of the joint lineament interpretation process.*

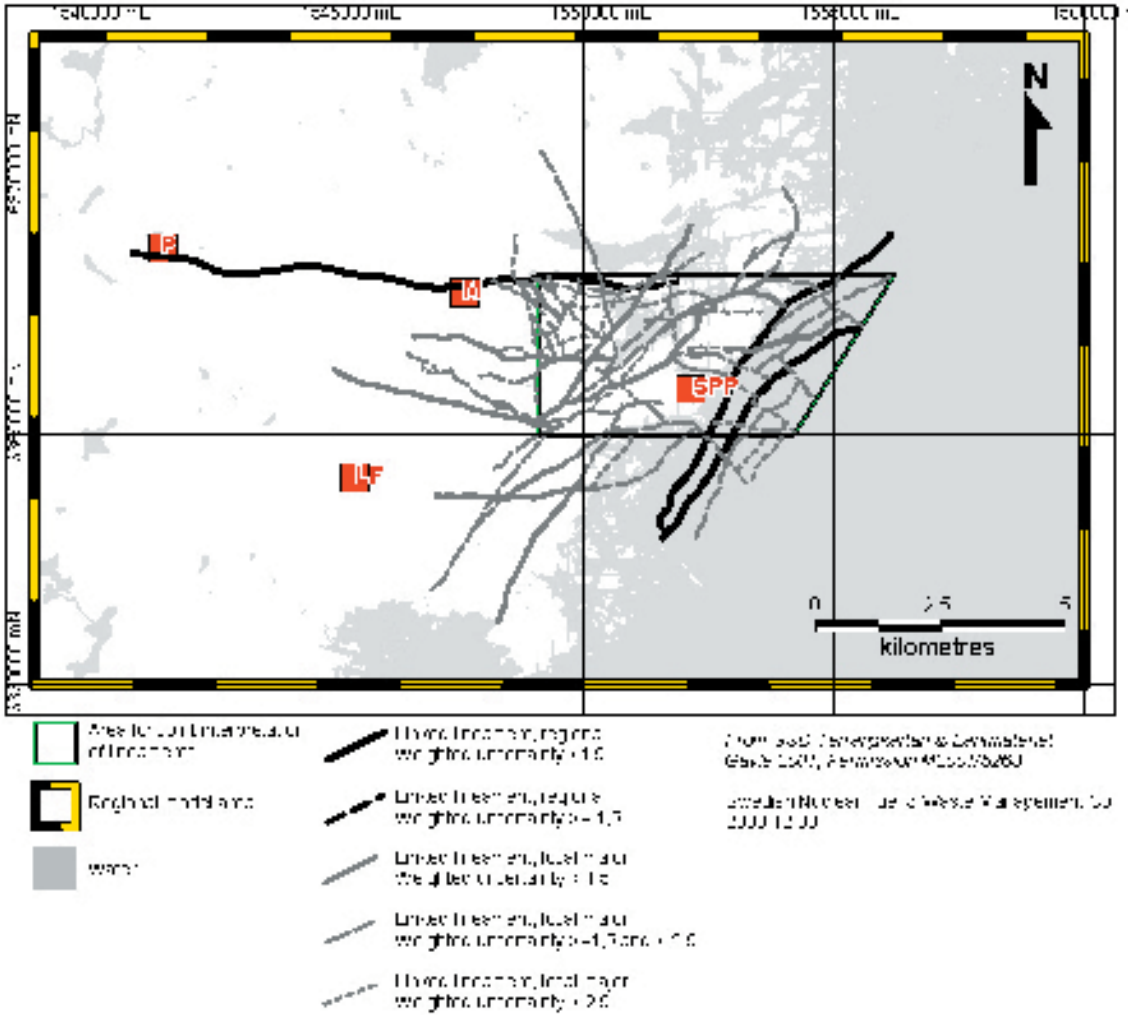

Figure 4-23. *Interpreted linked lineaments in the Simpevarp 1.1 local model area. Abbreviated geographical labels are given in caption of Figure 4-18.*

4.2.4 Ductile and brittle structures

Data that document the character and orientation of ductile and brittle structures at the surface are based mainly on observations made in connection with the bedrock mapping of the Simpevarp subarea during 2003. Available data comprise:

- Measurements of mainly ductile structures, as well as some brittle structures and bedrock contacts at 91 of the 353 observation points that were documented during the bedrock mapping /Wahlgren et al, 2004/.
- Laboratory measurements of the magnetic susceptibility (including anisotropy) of samples from 10 outcrops in the Simpevarp 1.1 local scale model area /Mattsson et al, 2003/.
- Documentation of fracture fillings by visual inspection at 100 of the 353 observation points referred to above /Wahlgren et al, 2004/.
- Detailed mapping of fractures (including fracture fillings) that are longer than 50 cm at four cleaned or (stripped) outcrops which are approximately 600 m^2 in areal extent /Hermanson et al, 2004/.
- Scan-line mapping of frequency and orientation of fractures that are longer than 100 cm at 16 of the 353 observation points referred to above /Wahlgren et al, 2004/ – fracture fillings were also noted.

Ductile structures

It is noted that the rocks in the Simpevarp subarea generally are well-preserved and more or less isotropic. However, locally a weak foliation is developed that is defined by the preferred orientation of biotite and in the porphyritic Ävrö granite, by oriented feldspar phenocrysts as well. The foliation is principally oriented in an east-west to northeast direction. Its dip is generally steep to vertical, but locally it is difficult to decipher.

However, the most spectacular and characteristic structures in the overall relatively well-preserved rocks are mesoscopic, low-grade ductile to brittle-ductile shear zones of the same character as the regional Äspö shear zone, c.f. Table 5-6 and Figure 5-3 (see Section 5.1.5). These are documented at 47 of a total of 353 observation points. The width varies from a decimetre to several metres and the shear zones are characterized by strong protomylonitic to mylonitic foliation (Figure 4-24). The dip is subvertical to vertical and the majority of the observed shear zones have E-W to NE strike. Kinematic indications suggest that they are characterised by a sinistral strike-slip and a south-side-up dip-slip component. The alignment of some of the observed shear zones implies that they form part of one and the same zone of local major character (see Figure 4-4).

The anisotropy of the magnetic susceptibility (AMS) measurements is a tool to calculate the principal directions and principal susceptibilities ($K_1 \geq K_2 \geq K_3$) of the magnetic susceptibility anisotropy ellipsoid for each sample /Mattsson et al, 2003/. By analysing the mean values of the principal magnetic susceptibilities, the degree of anisotropy and the shape of the anisotropy ellipsoid can be estimated. The latter may be prolate (dominated by magnetic lineation), spherical or oblate (dominated by magnetic foliation. By analysing the principal directions it is possible to estimate the magnetic fabric orientation in 3D, which is related to structural parameters of the rocks such as lineation and foliation. Thus, the AMS data may be an important and useful tool in revealing an anisotropic fabric in rocks that appear well-preserved and lack a clear visible tectonic fabric.

Figure 4-24. *Decimetre-wide, low-grade ductile shear zone in Ävrö granite.*

Despite a restricted number of AMS measurements from the Simpevarp subarea, the results are very consistent. The orientation of the mean magnetic foliation planes and the foliation documented during the bedrock mapping are very similar in the Simpevarp subarea, i.e. they display an east-west to northwesterly strike. Furthermore, the magnetic foliation, as well as the foliation measured during the bedrock mapping, have an orientation similar to the major lithological boundaries. However, the majority of the magnetic foliation planes display gentle to intermediate northerly dips, whereas the foliation documented during the bedrock mapping is characterised by steep to vertical dips. With few exceptions, the magnetic lineation is consistently west to northwest plunging between 0° and 53°. Due to the similarities in the orientation of the magnetic foliation and the lithological boundaries, it is inferred that the rocks carry a magnetic fabric that is related to the stress field that prevailed during the emplacement of the igneous rocks in the Simpevarp subarea.

The AMS data will be more fully evaluated in the future model versions when more data are expected to be available.

Brittle structures

Detailed fracture mapping has been carried out at 4 sites in the Simpevarp subarea. The sites were chosen on both geographical and lithological basis, i.e. the sites were distributed between different parts of, and between the various dominant rock types in, the Simpevarp subarea (Figure 4-25).

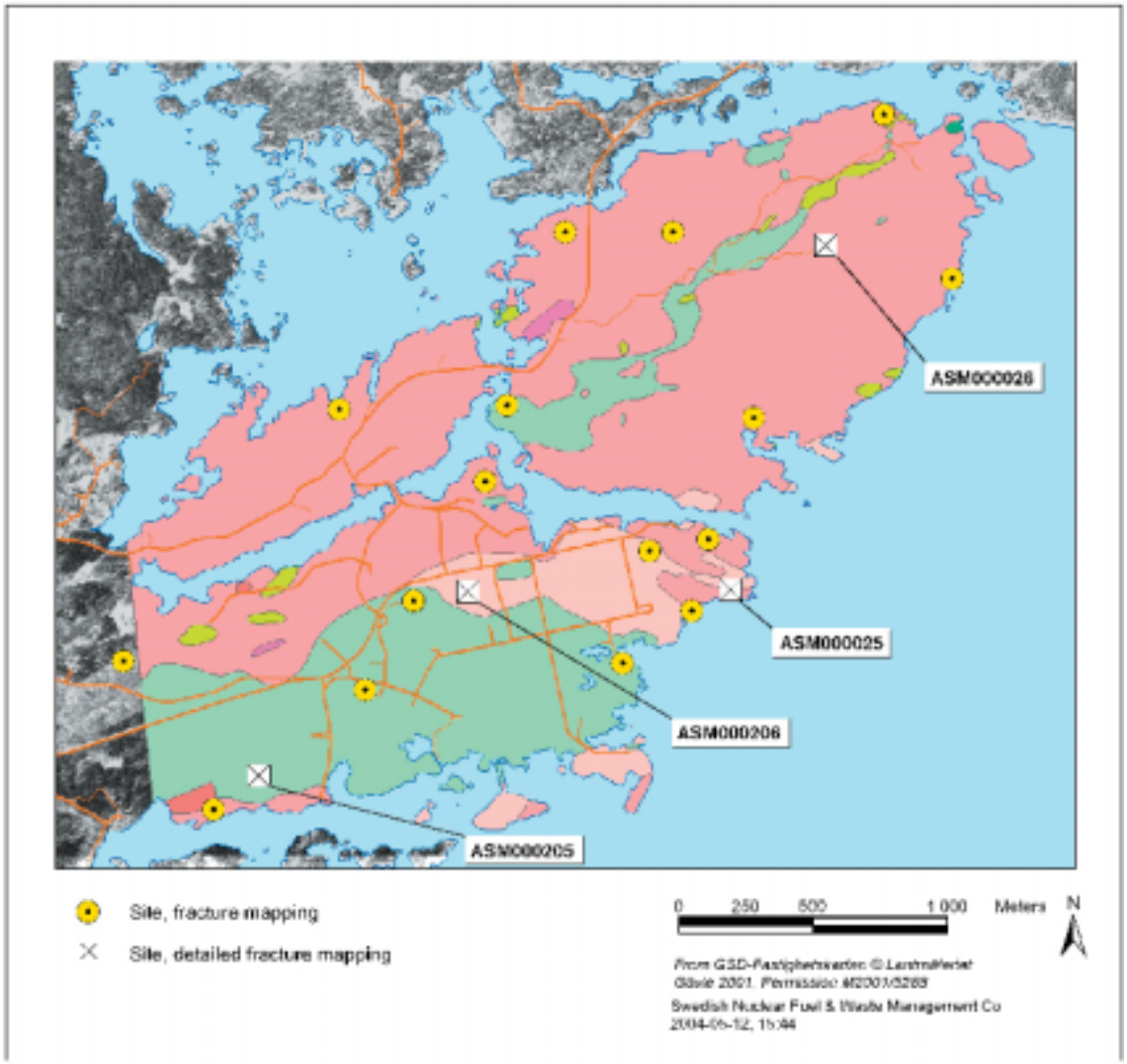

Figure 4-25. *Sites where detailed and scan line mapping of fractures have been carried out. For explanation of the coloured areas, see Figure 4-4 and Figure 4-26.*

Fracture trace maps that show fracture trace geometry, were produced for each outcrop during the detailed fracture mapping (c.f. Figure 4-26). The assembled data include the 3D geometry of fracture traces and their associated geological parameters, including mineralogy, undulation, trace length and characteristics of termination. The censoring of the trace data results in inclusion of fractures 50 cm long up to the maximum extent of the cleared outcrop. The number of fractures mapped at each site varied between 876 and 1,175 (Table 4-3). Scan line measurements were also completed at each site along NS and EW directions, employing a censoring in fracture length of 20 cm. The analysis of the data from the detailed mapping of fractures is presented in Section 4.6.

The simplified scan-line mapping of fractures at 16 locations (Figure 4-25) completed in connection with the bedrock mapping was carried out along two orthogonal lines with N-S and E-W orientation. The location and orientation of fractures, with a truncation length of 100 cm, were recorded during the mapping. In total, 616 fractures were measured. The fracture frequency varies between a minimum of 0.6 to a maximum of 3.5 fractures/metre, with an average of 1.9 fractures/metre. In Figure 4-27, rosette diagrams indicate the fracture frequency and strike for fractures with a dip steeper than 45° at each location. The dominance of fractures striking c. NW and NE is clearly evident. However, the fracture set that dominates varies between the different locations mapped in the Simpevarp subarea. The analysis of the fracture data obtained during the scan-line mapping will be evaluated in version Simpevarp 1.2 of the site descriptive modelling.

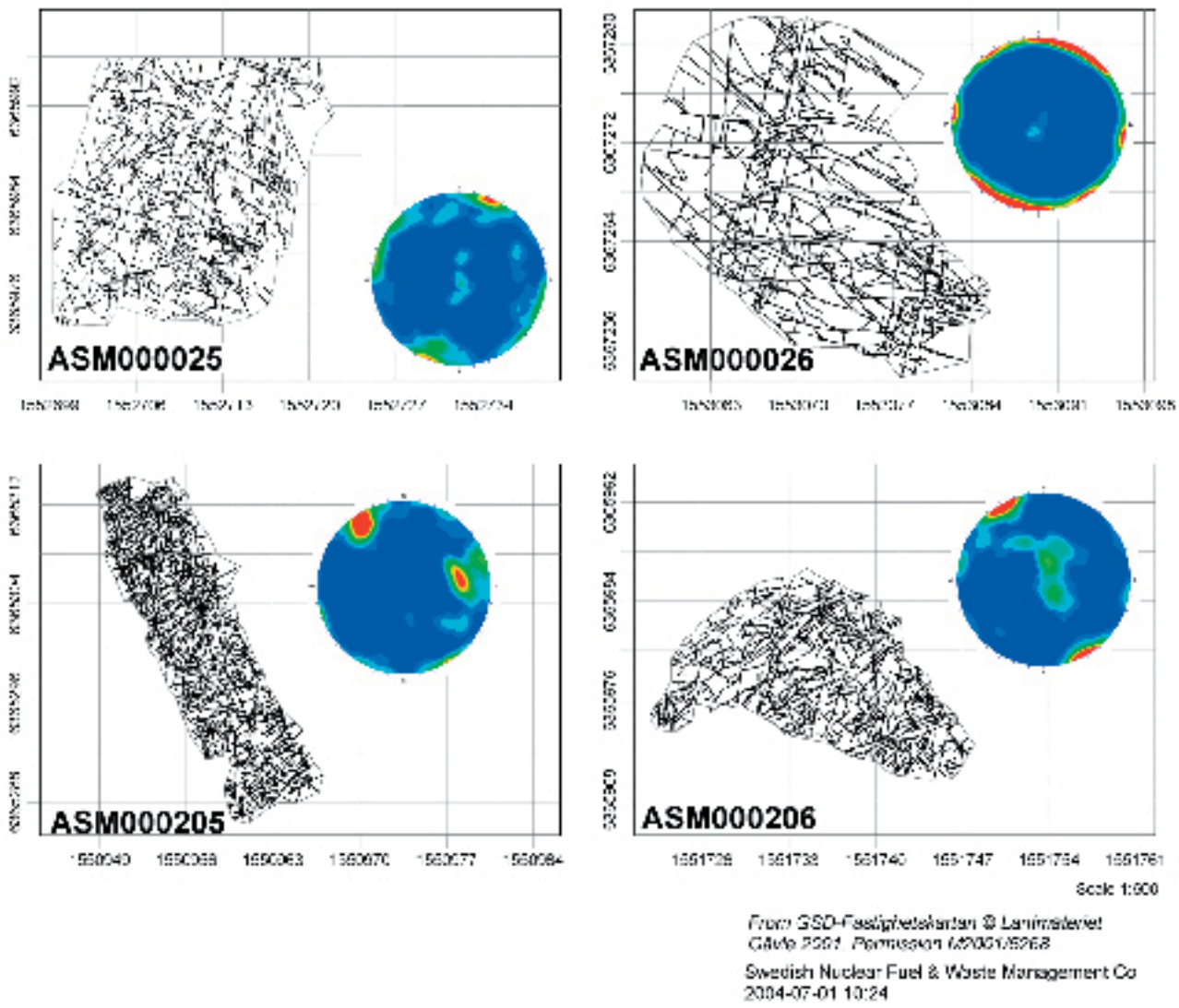

Figure 4-26. *Fracture trace maps and fracture lower hemisphere contour plots of fracture poles of the four outcrops cf. Figure 4-25, where detailed fracture mapping has been carried out.*

Table 4-3. The amount of fractures measured by the detailed fracture mapping, see also Section 4.4 for necessary definitions..

Outcrop ID	All fractures	Open Fractures	Sealed Fractures
ASM000025	917	147	770
ASM000026	876	138	738
ASM000205	1,175	126	1,049
ASM000206	940	200	740

Figure 4-27. *Orthophoto with diagrams showing fracture strike and frequency for fractures dipping 45 degrees or more at each outcrop.*

Epidote is the dominant fracture filling mineral observed during the bedrock mapping. Another common fracture filling is greyish white and is inferred to be dominated by prehnite. Furthermore, quartz, chlorite and calcite have been observed. Larger veins of hydrothermal quartz are also present.

So far, there are not sufficient data to evaluate the relationship between the fracture filling minerals and the orientation of the fractures. The fracture mineralogy is more extensively described in Section 4.4.3.

A characteristic phenomenon in the Simpevarp subarea is an extensive, inhomogeneous, red staining (oxidation) of the bedrock (Figure 4-28; cf. section 4.4.2). The red staining may at least partly have obliterated the primary magnetisation of the dominant rock types. At least in part, the inhomogeneouos oxidation is inferred to have caused the apparently overlapping magnetic susceptibility values recorded for the dominant rock types (see Figure 4-9). The red staining is caused by hydrothermal processes, and is principally concentrated along fractures. However, in many places the red staining has also affected the rock volumes in between mesoscopic fractures. Numerous, small-scale, sealed fractures occur in these rock volumes, and presumably these fractures acted as conduits for the penetrating hydrothermal fluids.

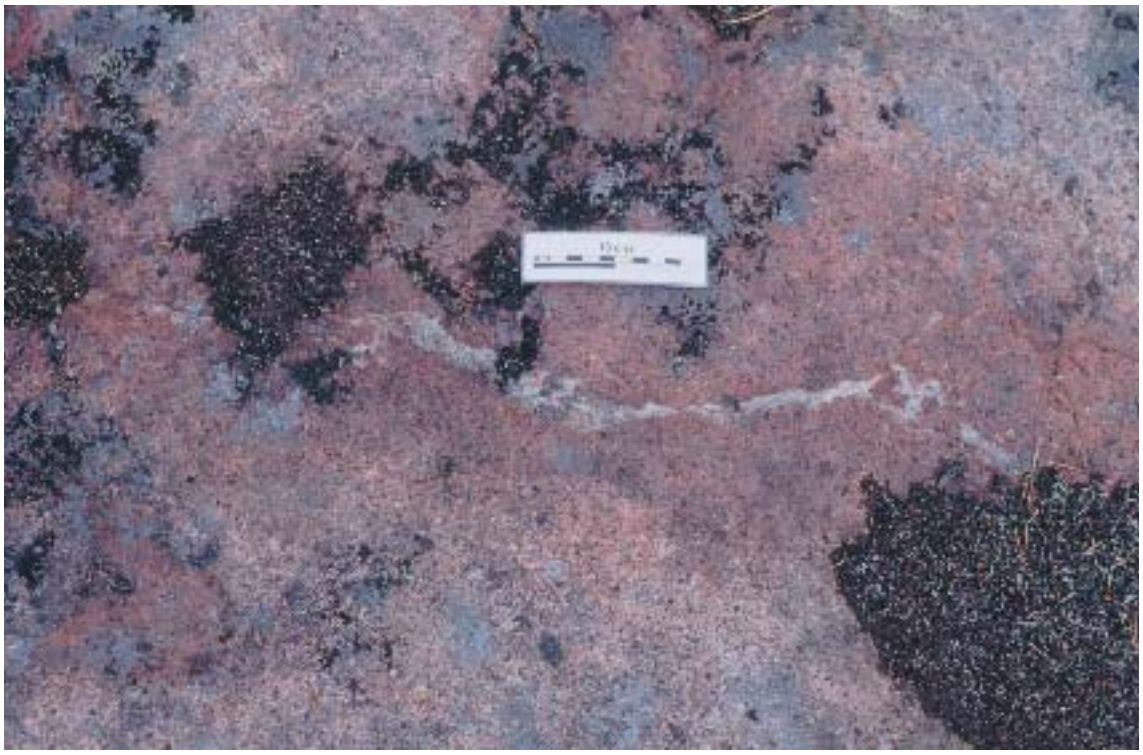

Figure 4-28. *Red-staining along a sealed fracture in fine-grained dioritoid. The mineral infilling is thought to be dominated by prehnite.*

4.2.5 Surface geophysics

Ground magnetic and slingram measurements have been carried out during 2003 for the siting of a new cored borehole in the central parts of Ävrö, and west of CLAB on the Simpevarp peninsula in order to improve knowledge of the position of earlier detected fracture zones. The results from measurements west of CLAB have been evaluated in the present modelling.

Within the Simpevarp peninsula area many of surface geophysical measurements were carried out during the investigation phases of OKG I–III and CLAB1–2. The resulting interpretations of major structures have been considered in the current project. However, due to the lack of the original raw data, no reassessment or reinterpretation of these data has been possible. In addition, since these surveys were followed up by drilling and excavation, a greater emphasis has been given to the results of tunnel and excavation mapping.

4.3 Meteorology, hydrology, near surface hydrogeology and oceanography

The same meteorological, discharge and oceanographical data is used for model version 1.1 as for version 0. Existing data were compiled by /Lindell et al, 1999/ and /Larsson-McCann et al, 2002/. Figure 4-29 shows the locations of the observation stations of interest for the Simpevarp area. All water chemical data are presented in Section 4.9.

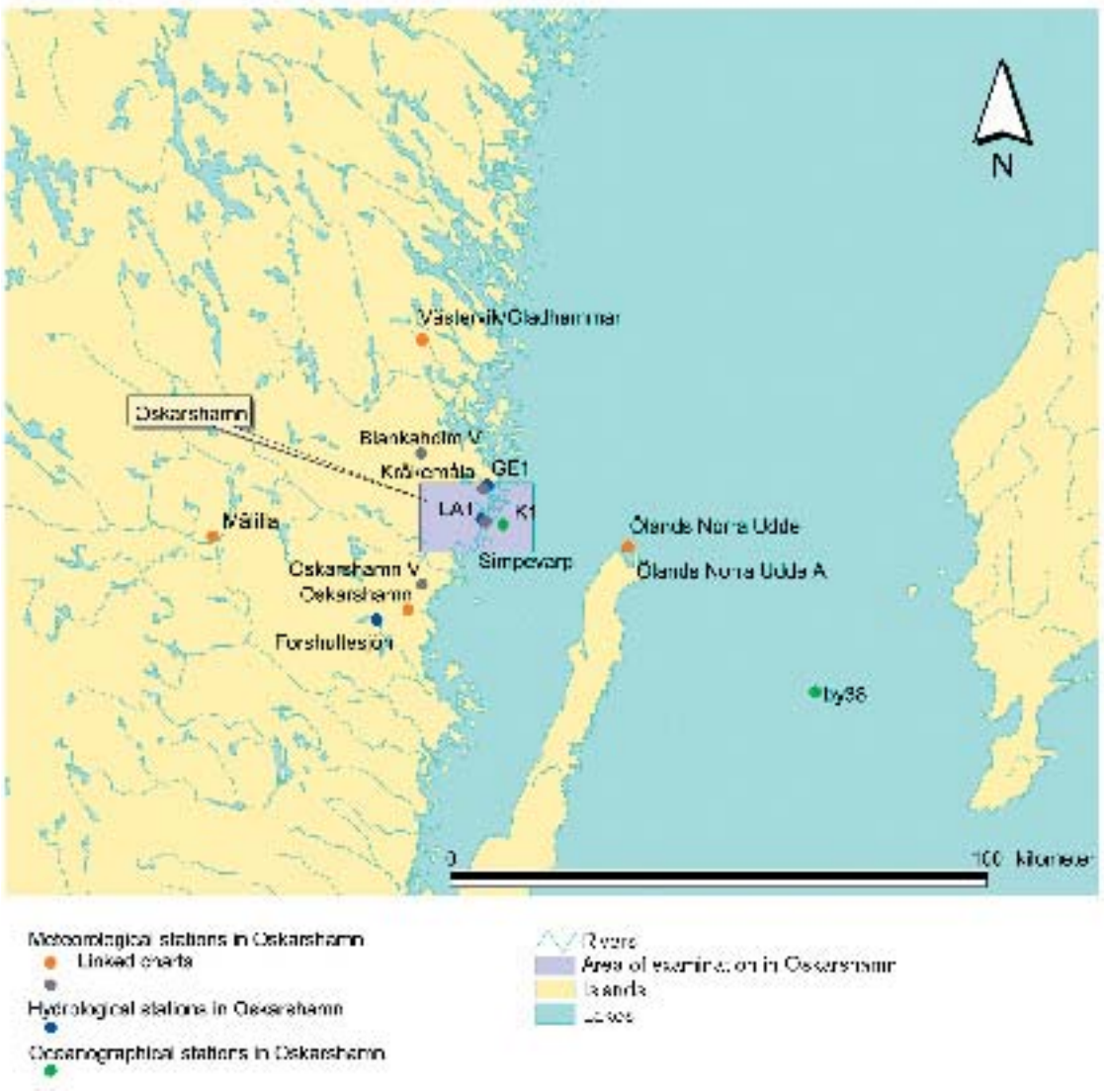

Figure 4-29. *Meteorological, hydrological and oceanographical stations of interest for site-descriptive modelling in theSimpevarp area. "Linked charts" (c.f. orange symbols) are meteorological stations run by the Swedish Meteorological and Hydrological Institute (SMHI) and stations represented by the grey dots are operated by the Swedish National Road Administration (SNRA) or the OKG Power Company /Larsson-McCann et al, 2002/.*

4.3.1 Meteorological data

In Table 4-4 the meteorological stations of interest for the Simpevarp area are listed.

The short description below of the meteorological conditions at the Simpevarp area is based on data compiled by /Lindell et al, 1999/ and /Larsson-McCann et al, 2002/. /Larsson-McCann et al, 2002/ described actual measurements in the Oskarshamn region and /Lindell et al, 1999/ described available stations in the municipalities of Oskarshamn and Hultsfred (and 4 other municipalities). For a more detailed description reference is made to these reports.

A wind rose from the station at Ölands norra udde (Ölands north tongue of land), which is judged to be representative for the Simpevarp area, is presented in Figure 4-30. The most frequent wind directions in southern Sweden are west and south-west. Compared to the West Coast of Sweden the climate is less maritime, which means that the differences are less pronounced between coastal sites and their inland neighbourhood than on the West Coast.

The average monthly mean temperature varies between –2°C in January–February and 16–17°C July, c.f. Figure 4-31. The winters are slightly milder at the coast than inland and the mean annual temperature at Ölands norra udde is about 2°C higher than at the more inland stations at Oskarshamn and Målilla. The vegetative period (daily mean temperature exceeding 5°C) is about 200 days.

The annual precipitation (measured) amounts to 500–600 mm in the region with a slight tendency of increase inland. The correction factor for the measured precipitation (measured precipitation is always smaller than the actual because of losses due to evaporation, adhesion and wind effects) is ca 1.15–1.2. The mean annual (corrected) precipitation at the stations Oskarshamn, Kråkemåla, Målilla and Ölands norra udde are 681 mm, 694 mm, 579 mm, and 507 mm, respectively, for the period 1991–2000. The average monthly and yearly precipitation values at Oskarshamn are shown in Figure 4-32 and Figure 4-33. About 20 % of the precipitation falls in the form of snow.

Potential evapotranspiration established for the stations Västervik/Gladhammar, Ölands norra udde and Målilla has been calculated by SMHI. The monthly potential evapotranspiration for Västervik/Gladhammar is shown in Figure 4-34.

The relative humidity is 80–100% in the winter and 70–90% in the summer. In each case the high values occur at night and the low at noon /Larsson-McCann et al, 2002/.

Table 4-4. Existing meteorological data[1] of interest for the Simpevarp area /Larsson-McCann et al, 2002/.

Station no	Station name	Co-ordinates, RT90 Northing (m)	Easting (m)	Period	Information
7722	Ölands norra udde	*636108*	*157776*	1880–1995	
7721	Ölands norra udde A	*636089*	*157763*	1996–	
7616	Oskarshamn	*634920*	*153660*	1918–	Only temp.prec.
7628	Kråkemåla	*637184*	*155073*	1990–	Only prec.
7524	Målilla	*636291*	*150033*	1931–	
7647	Västervik	*639977*	*153933*	1951–1995	
7642	Gladhammar A	*639819*	*153876*	1995–	
823	Blankaholm V[2]	*637848*	*153904*	1990–	
822	Oskarshamn[3]	*635398*	*153927*	1990–	
	OKG, Simpevarp[4]	*636570*	*155120*	1971–	

[1)] Parameters: Temperature, precipitation, relative humidity, air pressure, wind (direction and speed).

[2)] Vägverkets station, Not stored in SMHI:s database. Operates during winter only.

[3)] Vägverkets station, Not stored in SMHI:s database. Operates during winter and summer.

[4)] Wind speed and direction at 25 and 100 m above ground, temperature at 2 m, temperature difference at 2–70 m and 2–100 m. Available data for 1996–2000.

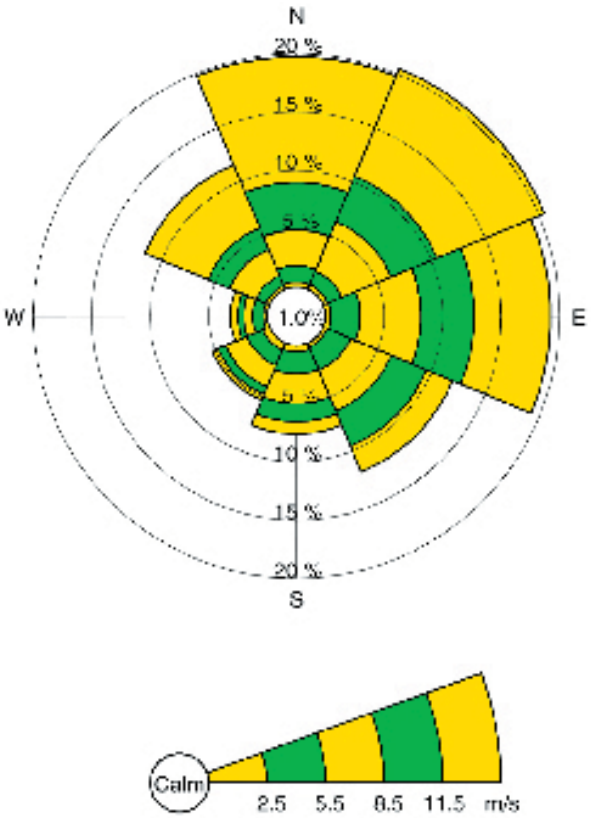

Figure 4-30. *Windrose based on data collected 1968–1995 from the SMHI meteorological station at the northern cape of the island of Öland (Ölands norra udde) /Larsson-McCann et al, 2002/.*

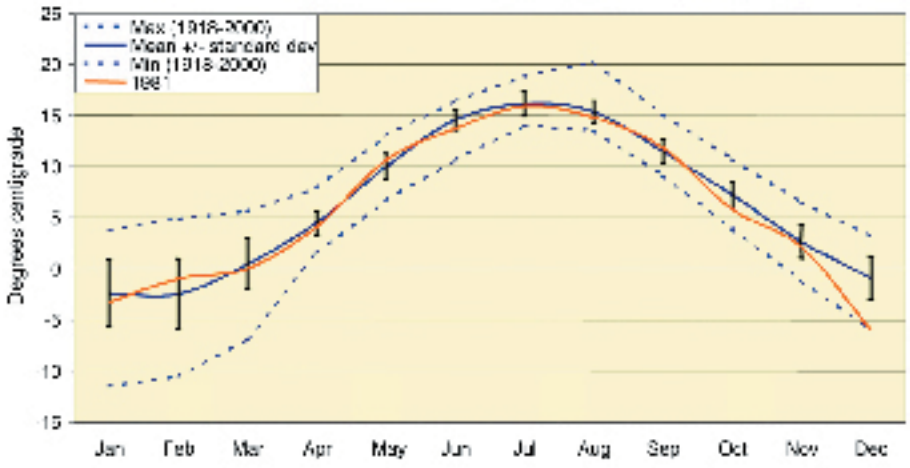

Figure 4-31. *Monthly mean temperature for the standard normal period 1961–1990, meteorological station at Oskarshamn. Vertical lines: One standard deviation. Dashed lines: Maximum and minimum of monthly mean temperature. Red line: Monthly mean for the selected (representative) year 1981. /Larsson-McCann et al, 2002/.*

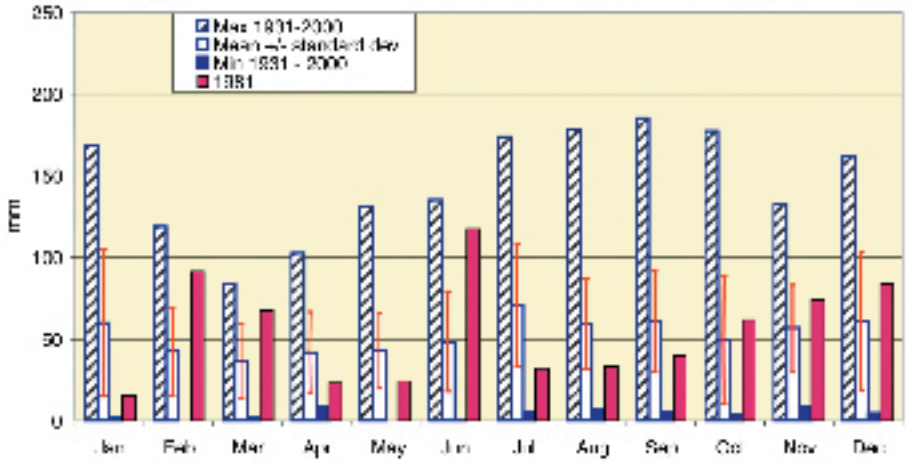

Figure 4-32. *Oskarshamn – Monthly mean, maimumx and minimum precipitation for the standard normal period 1961–1990 (mean and standard deviation) and extreme values for the period 1931–2000. Vertical lines: one standard deviation. Red bar: Monthly sums for the selected (representative) year 1981. /Larsson-McCann et al, 2002/.*

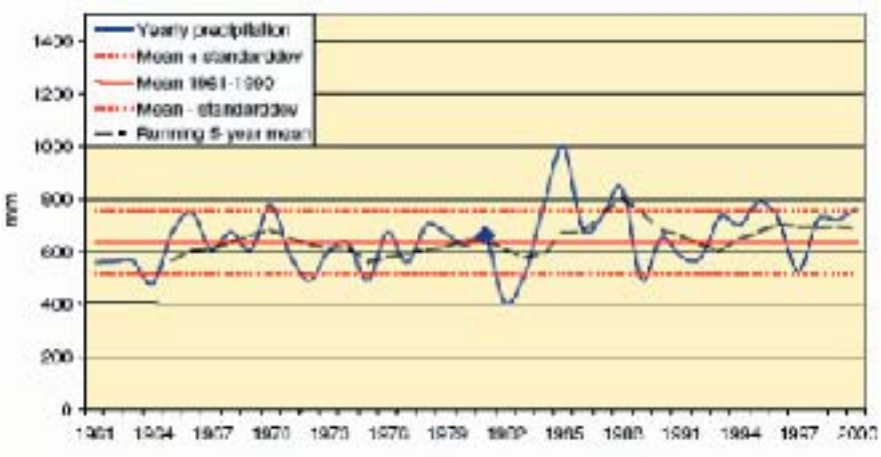

Figure 4-33. *Annual precipitation, 5-year running average precipitation and mean of the total annual precipitation for the standard normal period 1961–1990, station Oskarshamn. Dashed lines: one standard deviation from the mean. /Larsson-McCann et al, 2002/.*

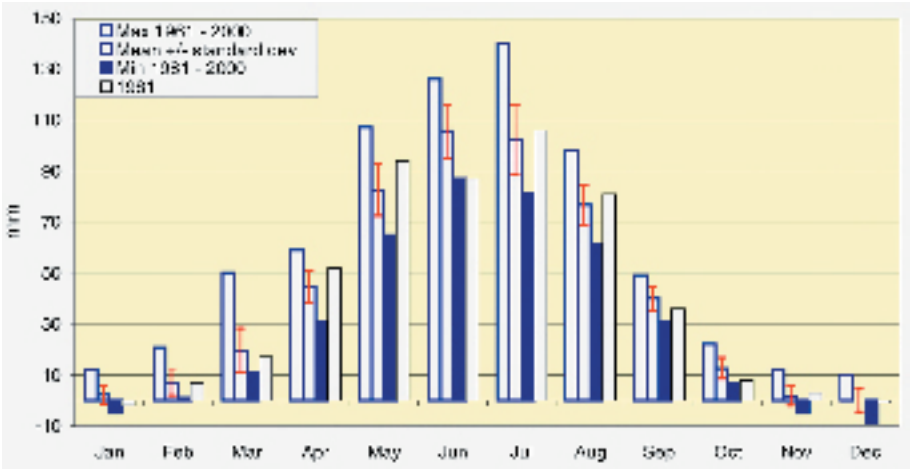

Figure 4-34. *Monthly mean, max and min of the sum of potential evapotranspiration per month for the standard normal period 1961–1990, station Oskarshamn. Vertical lines: one standard deviation. Unfilled bar: Monthly sums for the selected (representative) year 1981. /Larsson-McCann et al, 2002/.*

The annual hours of sunshine are about 1,800 hours on the coast and slightly lower inland. The annual cloudiness percentage is 60–65%, being slightly less in the summer and slightly more in winter. In the summer, the cloudiness tends to decrease near the coast compared to inland conditions. Based on synoptic observations at the station Ölands norra udde, the mean annual global radiation is calculated at 1,021 kWh/m^2, with mean monthly values varying from 8.5 kWh/m^2 in December up to slightly above 179.5 kWh/m^2 in June /Larsson-McCann et al, 2002/.

The ground is covered by snow about 75 days of the year with an average annual maximum snow depth of approximately 35–40 cm. The conditions on the coast do not differ much from those inland /Larsson-McCann et al, 2002/.

Air pressure is usually above 950 and below 1,050 hPa. The greatest air pressure variations are experienced in the winter and there are only small variations during May through August. More details can be found in /Larsson-McCann et al, 2002/.

Comments

One meteorological station was established on the island of Äspö during the autumn 2003 where precipitation, temperature, wind, humidity, air pressure and global radiation are measured. The island is situated partly inside the local sval modelling area used for Simpevarp 1.1. During 2004 another station is planned for the western part of the Simpevarp area, some 10 km due west of the established station on the Äspö island. Furthermore, snow depth and ground frost depth are currently measured at one location (Äspö island) and 1–2 further locations in the Laxemar subarea , immediately west of Simpevarp peninsula, and at Äspö will be established. However, no data from the established meteorological station, nor any data on snow or ground frost depth were available for Simpevarp v1.1.

4.3.2 Hydrological data

Although new discharge stations hace been established in the Simpevarp area, no new data from these ststions were available at the time of the Simpevarp 1.1 data freeze. Therefore, results were available only from pre-existing ststions in the region

Regional discharge data

The hydrological stations near the Simpevarp area are shown in Figure 4-29 and in Table 4-5.

The station at *Lake Forshultesjön nedre* was chosen by /Larsson-McCann et al, 2002/ to be the main representative station for the Oskarshamn area. The catchment area is 103.2 km^2 and the mean specific discharge is 5.7L/s/km^2 (approximately 180 mm/year). Monthly discharge values for the station *Lake Forshultesjön nedre* are shown in Figure 4-35.

Daily mean discharge was simulated for two sites within the area of interest, Gerseboån (GE1) and Laxemarån (LA1) rivers, c.f. Figure 4-36 and Figure 4-37. The calculated mean specific discharge for Gerseboån (GE1) and Laxemarån (LA1) are 4.7 and 5.4 L/s/km^2 (approximately 150 and 170 mm/year) respectively. Table 4-6 summarises the characteristic discharge values for the stations listed in Table 4-5.

Table 4-5. Hydrological stations near Oskarshamn. C. area: Catchment area. Coordinates in RT90. /Larsson-McCann et al, 2002/.

Stn No	Name	River	Lake area (%)	C. area (km²)	Northing (m)	Easting (m)	Period
1619	Forshultesjön	Lillån	5	103.2	634734	153084	1955–2000
	GE1	Gerseboån	1.2	24.8	637249	155155	1962–2001
	LA1	Laxemarån	0	41.3	636614	155041	1962–2001

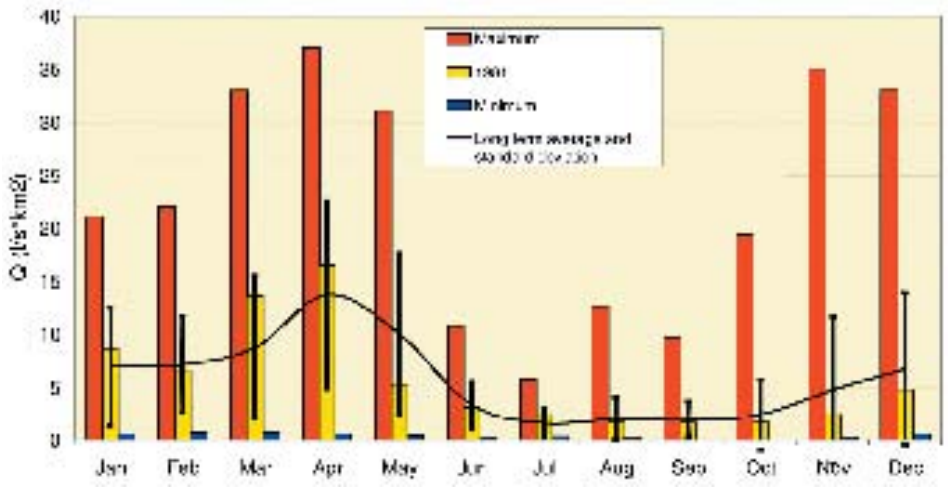

Figure 4-35. *Monthly discharge at hydrological station Forshultesjön nedre, 1955–2000. Maximum and minimum daily mean, long term average and standard deviation (L/s/km²). The year 1981 is selected as a representative year /Larsson-McCann et al, 2002/.*

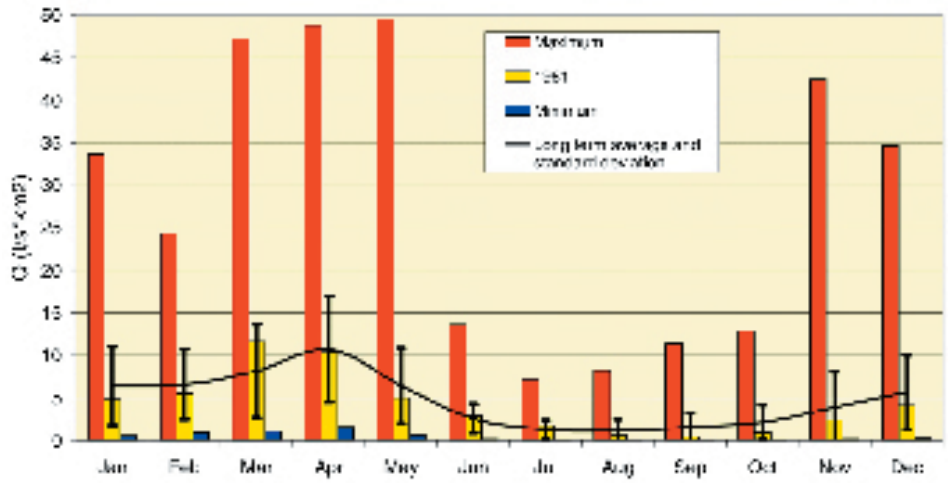

Figure 4-36. *Monthly simulated discharge at GE1 Gerseboån, 1962–2001. Maximum and minimum daily mean, long term average and standard deviation (L/s/km²). The year 1981 selected as a representative year /Larsson-McCann et al, 2002/.*

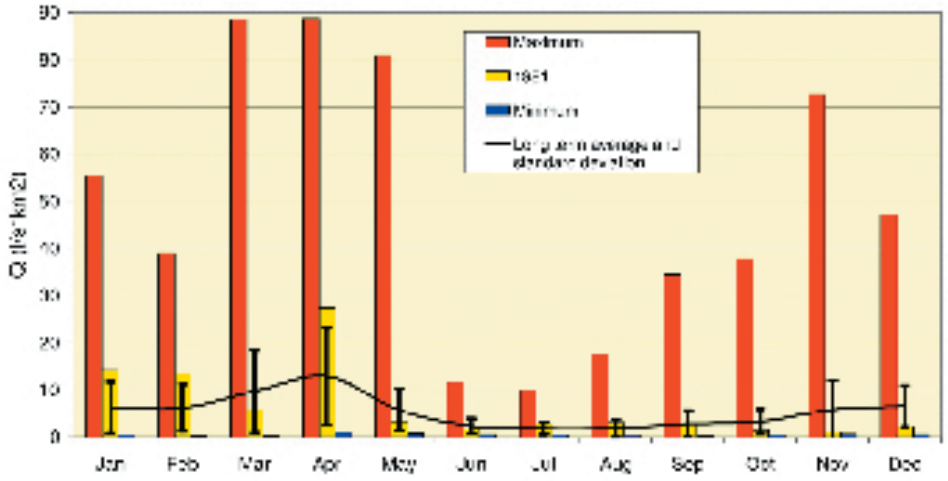

Figure 4-37. *Monthly simulated discharge at LA1 Laxemarån, 1961–2001. Maximum and minimum daily mean, long term average and standard deviation (L/s/km²). The year 1981 selected as an especially representative year /Larsson-McCann et al, 2002/.*

Table 4-6. Charactertistic discharge (L/(s · km²) for hydrological stations near Oskarshamn. Thr characteristic discharges, MLQ etc, are based on daily mean values. The HHQ50 and HHQ100 values are based on calculations /Larsson-McCann et al, 2002/. Results for GE1 and LA1 are based on calculations and that of Lake Forshultesjön is based on measurements.

Stn No	Name	Charactertistic discharge (L/(s · km²)						Period
		Obs min	MLQ	MQ	MHQ	HHQ50	HHQ100	
1619	Forshultesjön	0	0.58	5.7	26	59	66	1955–2000
	GE1		0.46	4.7	21	52	56	1962–2001
	LA1		0.24	5.4	43	99	111	1962–2001

MLQ= long-term average of annual minimum discharge, MQ= long-term average of annual discharge.
MHQ= long-term average of annual maximum discharge, HHQ50= highest maximum flow 50 years.
HHQ100= highest maximum flow 100 years.

Catchment areas

The catchment areas outlined in Figure 4-38 and Figure 4-39 are based on the interpretation by SMHI and are only to be regarded as preliminary. The underlying map will be updated during 2004 using topographical maps, aerial photographs and field checks conducted in the Spring and Summer of 2004 resulting in a detailed delineation of the catchment areas. Table 4-7 presents preliminary data on size and land use of the catchment areas with which discharge measurement stations are associated. The geometric data for the lakes have not been calculated and compiled, but will be presented in version Simpevarp 1.2.

Discharge measurement stations and water level measurement stations are shown in Figure 4-39. Some have been constructed during autumn 2003 and some will be constructed during 2004. No data was available for version Simpervarp 1.1. The planning for the discharge measurement stations is presented in /Lärke and Hillgren, 2003/.

Table 4-7. Size and land use of delineated catchment areas, cf. Figure 4-39, associated with discharge measurements (preliminary presentation) /SKB GIS, 2004/.

	Name	Catchment area (km²)	Forest (%)	Forest wetland (%)	Clear-cut area (%)	Agric. land (%)	Open land wetland (%)	Other open land (%)	Water (%)
1	Laxemar ån	40.99	(1)	(1)	(1)	(1)	(1)	(1)	1.15
2		18.43	(1)	(1)	(1)	(1)	(1)	(1)	0.07
3		2.32	(1)	(1)	(1)	(1)	(1)	(1)	0
4		0.93	(1)	(1)	(1)	(1)	(1)	(1)	0
5		8.73	(1)	(1)	(1)	(1)	(1)	(1)	0.49

(1): Not evaluated as part of descriptive modelling Simpevarp v1.1.

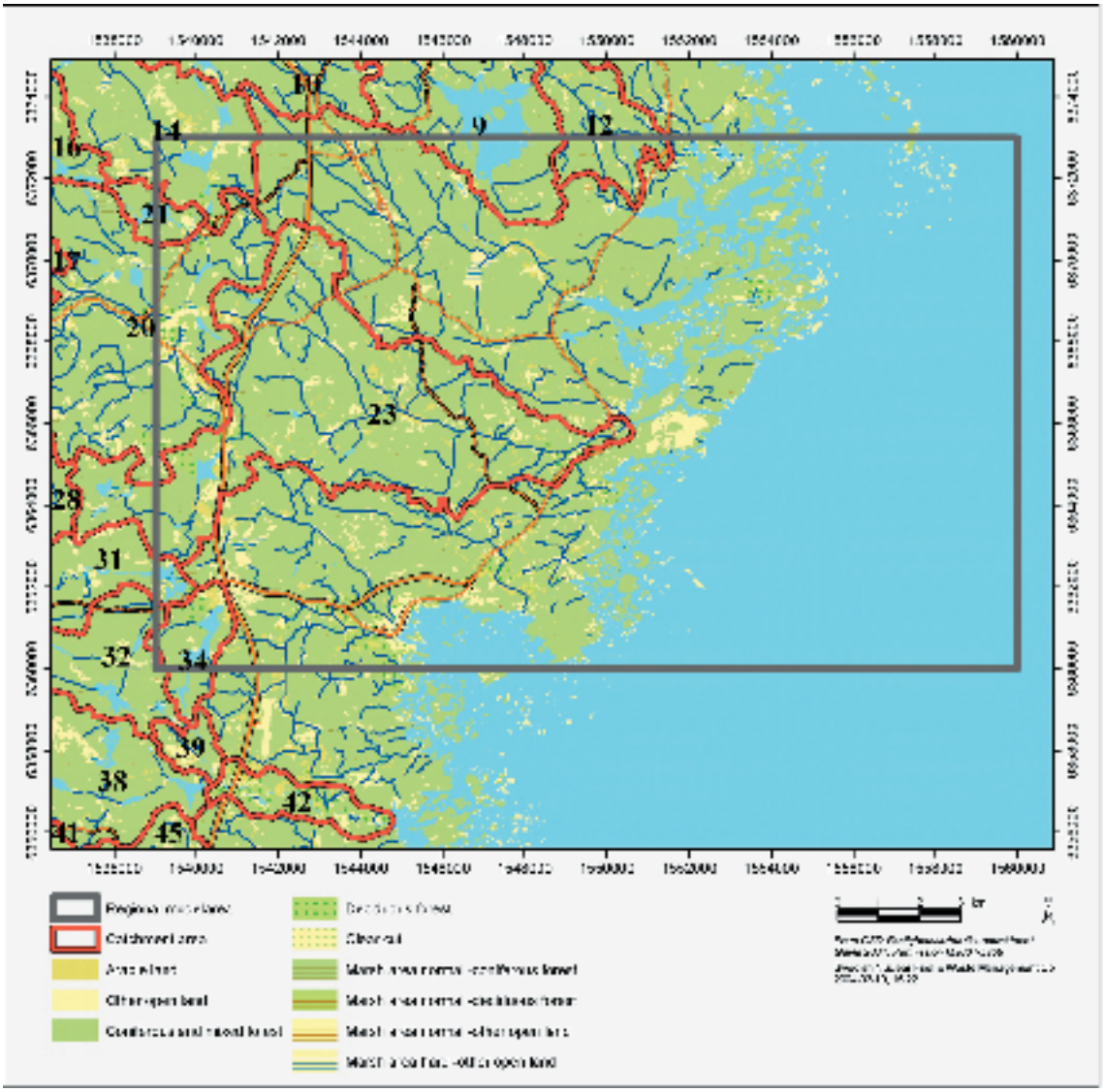

Figure 4-38. *Delineation of catchment areas (red outline) in the vicinity of the regional model area (outlined in solid black) /SKB GIS, 2004/.*

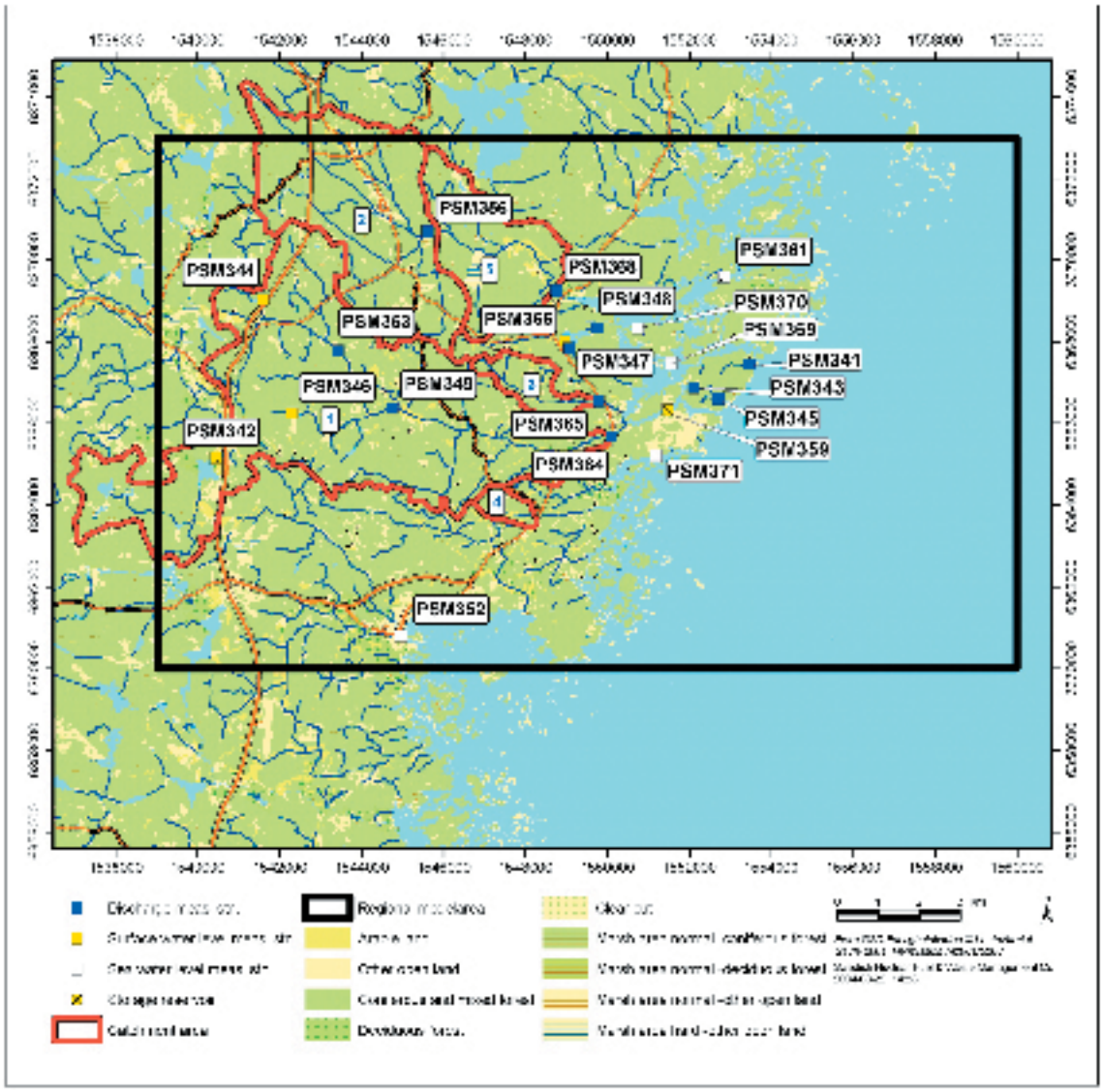

Figure 4-39. *Delineation of catchment areas with positions of measurement stations for discharge and water level measurements /SKB GIS, 2004/.*

Simple discharge measurements

Related to the surface water sampling, simple discharge measurements have been performed in running waters at a number of locations since summer 2003 (Figure 4-40). These measurements are not included in this report.

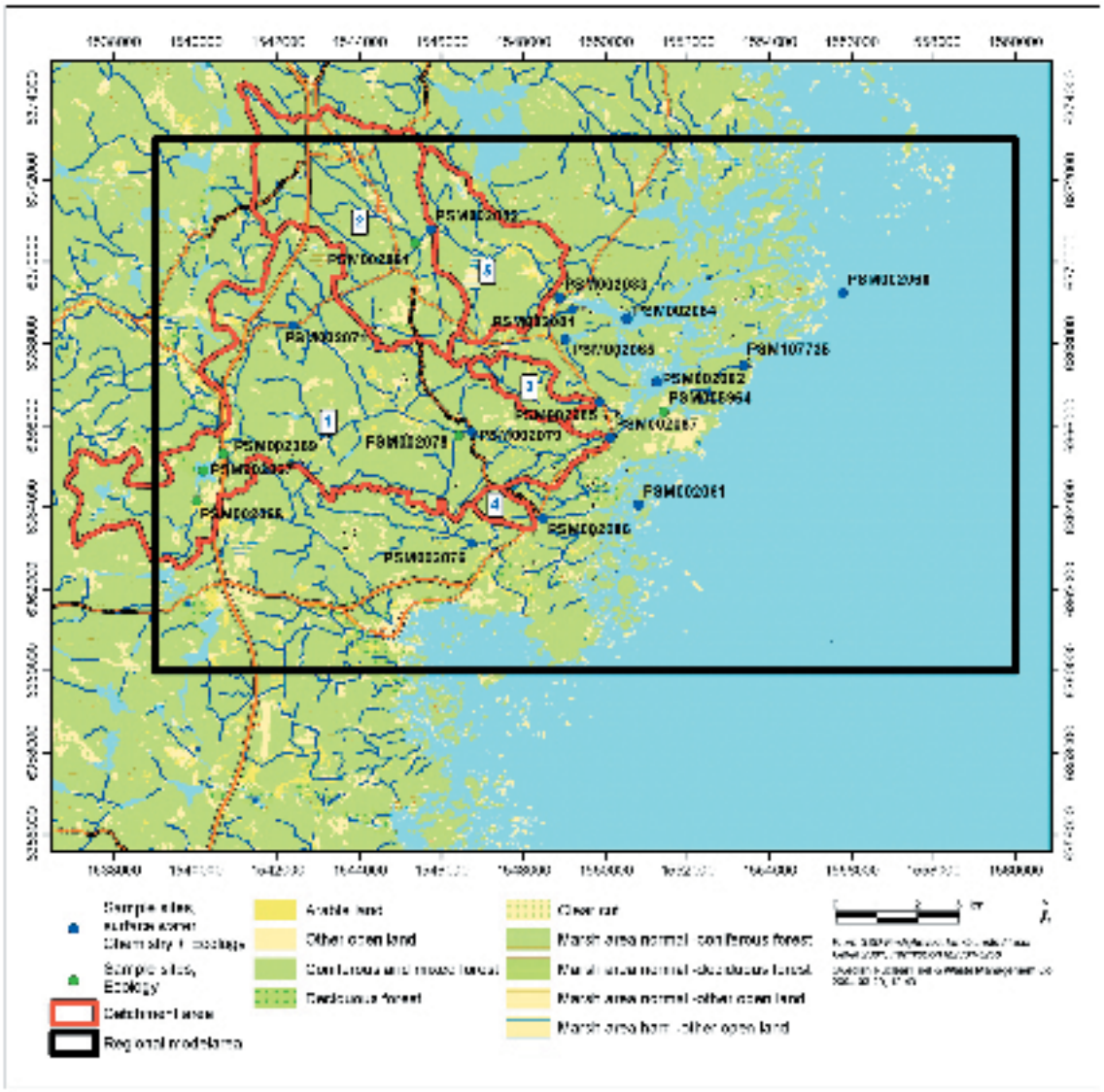

Figure 4-40. *Measurement locations for samling sites for Surface water chemistry (at locations used by Ecology and Hydrogeochemistry). Simple discharge measurements are made at a number of the locations shown. /SKB GIS, 2004/.*

4.3.3 Hydrogeological data for Quaternary deposits

No tests for determining the hydraulic conductivity of the contact zone between the Quaternary deposits (mainly till) and the bedrock surface, nor of the Quaternary deposits have been made so far, but such tests are planned to be conducted later during the initial site investigations.

The hydraulic conductivities attributed to Quaternary deposits are for version Simpevarp 1.1 based on generic data from /Knutsson and Morfeldt, 2002/, /Carlsson and Gustafson, 1997/.

4.3.4 Private wells

An inventory of private wells was made during 2001 through 2003 /Morosini and Hultgren, 2003/, c.f. Figure 4-41. The inventory is mainly intended to serve as a tool in the planning of a follow-up on environmental impact. The water level in the well at the time of inventory was documented for most wells, and in general shows a water level depth of between 1–10 m below ground surface. For a few of the wells it was possible to estimate their capacity.

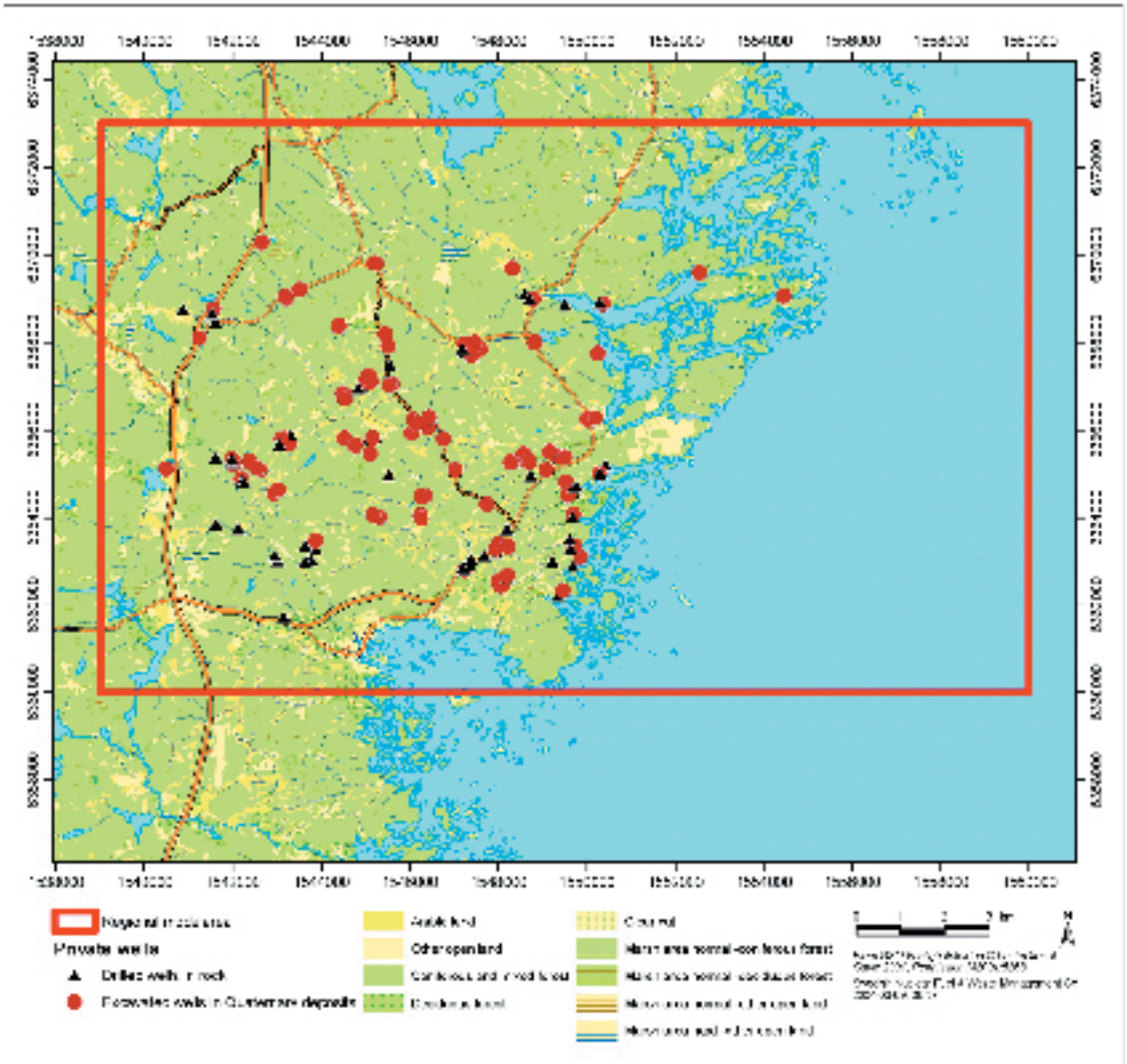

Figure 4-41. Location of private wells in the Simpevarp area. /SKB GIS, 2004/.

4.3.5 Oceanographic data

In this report, the term “oceanography” incorporates the physics and chemistry of the open sea. Geology of the sea bed and biology of the sea, are sometimes included in the term oceanography, but are here treated separately under the geology and biology (biota) headings, respectively. Furthermore, data on physical and chemical parameters in shallow bays, collected in the surface water programme, are here treated in the hydrogoechemistry section. No new site-specific oceanographic data are available at present. Previously available site-specific oceanographic data related to the Oskarshamn region are presented in /Engqvist and Andrejev, 1999; Lindell et al, 1999; Larsson-McCann et al, 2002/.

4.4 Geologic interpretation of borehole data

4.4.1 Geological and geophysical logs

New geological borehole data for model version 1.1 are available from:

- Core-drilled borehole KSH01A between c. –100 masl down to c. –1,000 masl.
- Core-drilled borehole KSH01B between c. 0 masl down to c. –100 masl.

- Percussion-drilled borehole data from the boreholes drilled around drillsite 1; HSH01, HSH02, HSH03 and the first one hundred meters of KSH01A.

Existing borehole data, used for model version 1.1 comes from:

- Core drilled borehole KLX02A between c. –200 m masl to c. –1,700 m masl.
- Core drilled borehole KLX01A down to c. 1,060 m masl.

The locations of the available boreholes are shown in Figure 4-42. The cored borehole KSH01A has been mapped using the BOREMAP system /Aaltonen et al, 2003/. The percussion boreholes have been subject to both geological (BIPS) interpretations and geophysical logging /Aaltonen et al, 2003/. The geophysical logs have been utilised in the single-hole geological interpretation, see Section 4.4.5.

Data available from the cored boreholes KSH01A, KLX02 and from the percussion drilled boreholes are shown in Table 4-8 and Table 4-9. Due to time constraints, the following data are considered most valuable for the construction of the geological model:

- Lithology (rock types).
- Alteration (weathering, tectonisation).
- Brittle deformation (i.e. observations of fracturing, core loss and crush).

The percussion holes contain lithological data (rock types), fracture location and orientation. The fractures are mapped only based on BIPS data. The mapping of rock types is a combination of BIPS data and observations of rock pieces retrived during drilling.

The data files used for the fracture analysis are listed in Table 4-10.

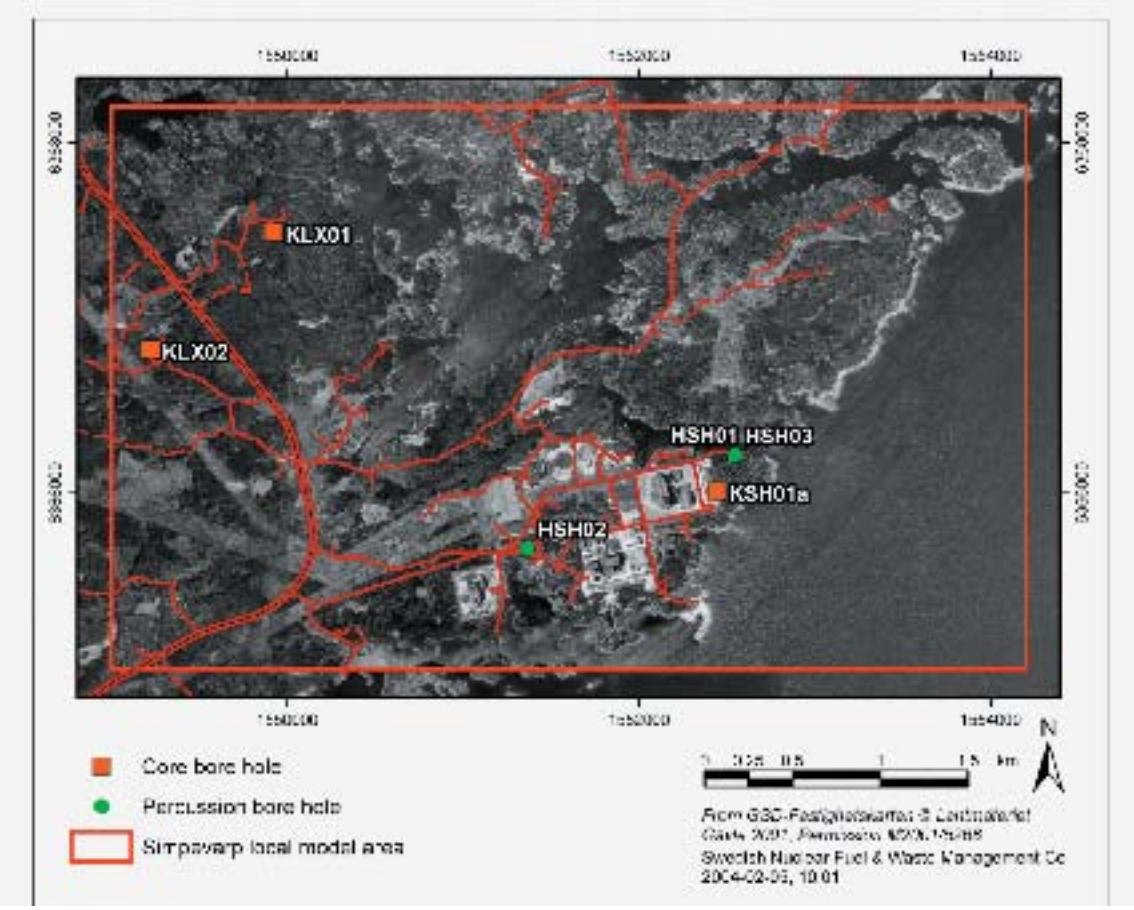

Figure 4-42. *Location of boreholes available for the geological model version Simpevarp 1.1.*

Table 4-8. Available geological data from cored boreholes KSH01A and KLX02.

Type of data	KSH01A, core drilled section 100–1,000 m (Boremap)	KLX02, core drilled section 0–1,700 m (Petrocore)
Lithology (rock types)	X	0–1,700 m
Fracture orientation	X	200–1,700 m
Fracture mineralisation	X	200–1,700 m
Weathering	X	X
Tectonisation	X	X
Core loss	X	X
Crush	X	X

Table 4-9. Available geological data from percussion-drilled boreholes.

Type of data	HSH01	HSH02	HSH03
Lithology (rock types)	X	X	X
Fracture location	X	X	X
Fracture orientation	X	X	X

Table 4-10. Data files used for the borehole fracture analysis.

File Name	Content
natural_fractures.xls	Data_request #03_29 from SICADA containing fracture data from KSH01A, KSH01B HSH01, HSH02, HSH03 and KLX02
sealed_fractures.xls	Data_request #03_29 from SICADA containing fracture data from KSH01A, KSH01B HSH01, HSH02, HSH03 and KLX02
KSH01A_Metod_1_2003-11-12.WCL	Visual display of KSH01A borehole geology
KSH01B_Metod_1_2003-11-12.WCL	Visual display of KSH01B borehole geology

Not all of the boreholes are associated with the same quality of fracture data, nor do they have the same coverage in variables/parameters. The boreholes with the most complete and consistent sets of data were the three percussion-drilled boreholes (HSH01 through HSH03) and the cored borehole KSH01A. The shallow cored borehole KSH01B (L=100 m) provided useful data for fractures classified as ”sealed”, but there was only one single entry for the ”open” fractures, which made this borehole not suitable for any type of analyses focusing on ”open”, or potentially conductive, fractures (see section on “Fracture classification” below for explanation of terminology used). The cored borehole KLX01 did not provide information on fracture orientation, and could consequently not be used for orientation studies.

The fracture data variables included for the boreholes previously identified are listed in Tabell 4-11.

These attributes comprise three classes of information. The primary geometrical information consists of the strike, dip and location. Variables that describe the geological basis of these data include the mineral filling, roughness, surface type, alteration type (degree and colour) and aperture. A third class of variables is associated with database referencing, data quality and source. These include such variables as “ACTIVITY_TEXT”, “CONFIDENCE” and “VISIBLE IN BIPS”.

The borehole fracture data have been used in two different ways; as a primary data source for assessing how fracture orientations and intensity may vary with depth, and what geological causes may account for these observed variations; and as corroborative data for hypotheses on regional fracture patterns and their controls derived from the outcrop analyses.

Tabell 4-11. Variables used for the fracture analysis.

Variable Name	Explanation of variable
ACTIVITY_ID	ID for the mapping activity
ACTIVITY_TEXT	Type of mapping technique, e.g. BOREMAP
IDCODE	Fracture ID
ADJUSTED SECUP	Location along the borehole axis
MIN1	Primary mineral filling
MIN2	Subordinate mineral filling in decreasing order of cntent
MIN3	Subordinate mineral filling in decreasing order of content
MIN4	Subordinate mineral filling in decreasing order of content
ROUGHNESS	Fracture surface roughness
FRACT_ALTERATION	Alteration around the fracture, such as epidotisation, oxidation
STRIKE	0 to 360 degrees
DIP	Right-hand rule
WIDTH	Fracture width including mineral filling
APERTURE	Fracture opening, measured from the BIPS
CONFIDENCE	Confidence in aperture measurement
VISIBLE_IN_BIPS	Visible in BIPS

4.4.2 Borehole rock types

The most abundant rocks in the core drilled borehole KSH01A are a combination of porphyritic granite to quartz monzodiorite, medium-grained and generally porphyritic (named Ävrö granite) and Quartz monzodiorite, which together characterise about 58% of the core, c.f. Table 4-12 and Figure 4-43. There is also a substantial amount of fine-grained dioritoid (37%) basically concentrated on the borehole section 200 m to 630 m. The more shallow percussion-drilled boreholes HSH01 and HSH03 show the same pattern of lithology as in the deeper parts of KSH01A, but major dioritoid sections are absent. However, HSH02 is situated in a rock mass west of the KSH01 drill site (see Figure 4-42), dominated by the fine-grained dioritoid (95%) with subordinate occurrence of granite (10%).

The Ävrö granite is mostly well-preserved and is more or less isotropic, but a weak foliation is locally developed. This is enhanced where faults and low-grade ductile shear zones of mesoscopic character are intersected by the borehole and locally influences the foliation. Thin, low-grade ductile and brittle faults and minor zones intersect the borehole at approximately thirteen locations. The bedrock is often moderately to strongly altered (epidotisised and oxidised) in the vicinity of mapped faults and deformation zones intersected by the borehole. The section between 200 m and 630 m borehole depth is dominated by fine-grained dioritoid which shows a slightly increased occurrence

Table 4-12. Occurrence of rock types along the core drilled part of KSH01A.

Rock name	Fine-grained dioritoid	Diorite/ gabbro	Quartz monzodiorite	Ävrö granite	Granite	Pegmatite	Fine-grained diorite – gabbro	Fine-grained granite
Rock type ID	501030	501033	501036	501044	501058	501061	505102	511058
Total rock occurence (m)	329.2	1.28	314.26	202.52	11.7	3.46	8.87	28.23
Percentage of total length	36.60	0.14	34.94	22.51	1.30	0.38	0.99	3.14

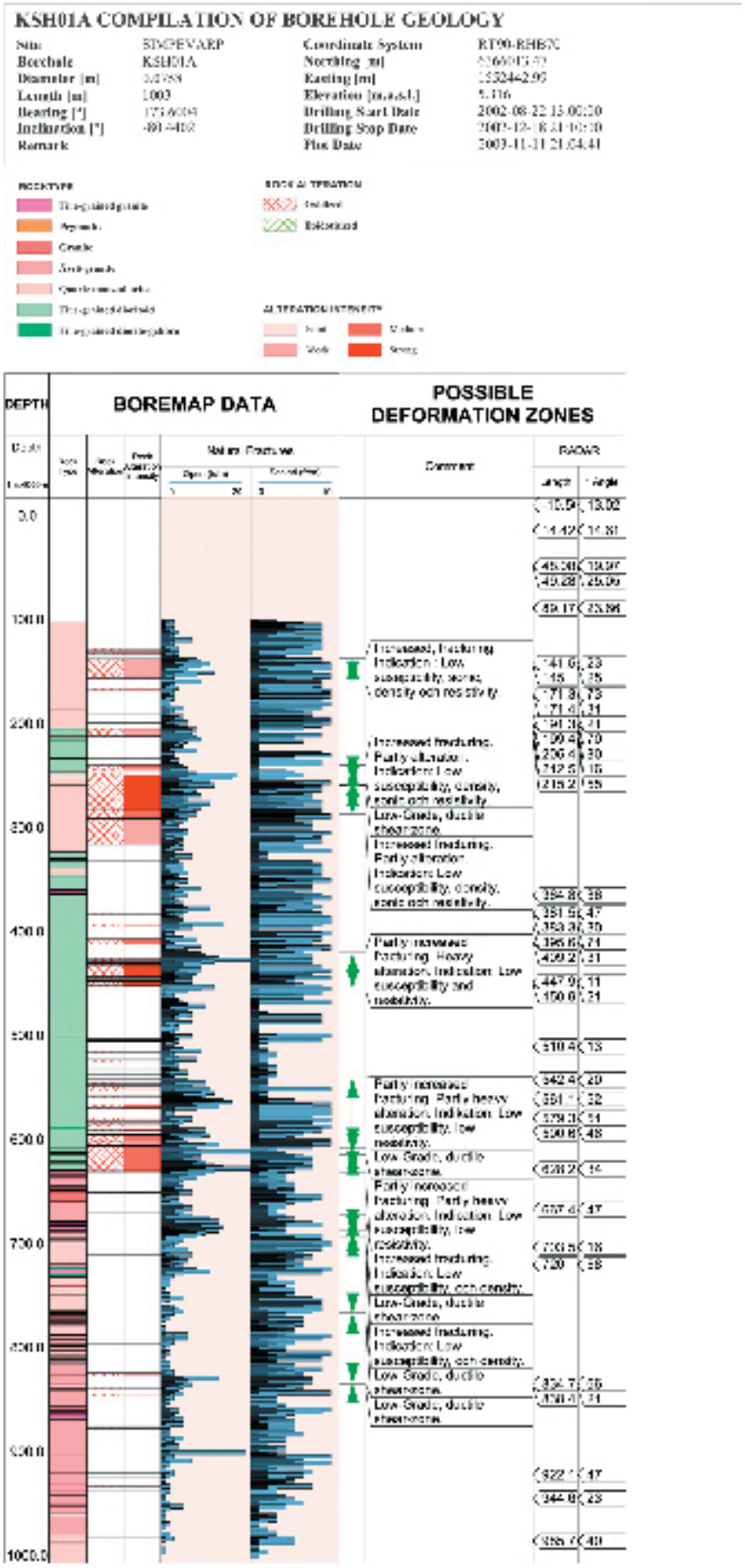

Figure 4-43. *Overview of the geology in core-drilled borehole KSH01A.*

Table 4-13. Occurrence of rock types along the percussion-drilled borehole HSH02.

Rock type	Fine-grained dioritoid	Granite
Rock ID	501030	501058
Total rock occurence (m)	189.56	10.14
Percentage of total length	94.92	5.08

of altered rock where ductile and brittle faults and minor zones are intersected compared to intersections of mapped zones in the Ävrö granite. It can also be noted that there seems to be a small depth dependence in the occurrence of minor zones and faults and no clear evidence that more zones are found in the fine-grained granite compared with the Ävrö granite. The contacts between the combination of Ävrö granite and quartz-monzodiorite and the dioritoid are sometimes diffuse, but can also be well defined, and are not necessarily coupled to mapped deformation zones or faults.

4.4.3 Borehole fractures

Fracture classification

SKB has developed a system for classification of fractures in parallel to this analysis stipulating how to treat fractures (open, partly open and sealed) based on aperture. This system was in progress to be fully implemented in SICADA to the effect that the old terminology of natural and sealed fractures should be replaced. At the time of this analysis, however, this change was not implemented.

The fractures in the boreholes as obtained from the SICADA database (see Table 4-10) are classified in two fracture groups; *natural* and *sealed*. In the present analysis, it is assumed that the group *sealed* fractures are cohesive and *natural* fractures are non-cohesive as observed in the drill core. It is further assumed that this classification does not take into account whether the fracture has been opened by the drilling or not.

If these assumptions are true, the classification does not provide reliable information on the real state of the fracture, i.e. whether it is truly open or sealed in the rock mass. The mapped fracture data also contains other parameters, e.g. aperture, that can be used to get closer to a true description of the state of the fractures. Cooonsequently, ans as stipulated in the terminology from SKB, the measured fracture aperture was used to divide fractures into the groups open and sealed.

Aperture is measured from the BIPS image during the BOREMAP survey of the core. The resolution of the BIPS image has a lower aperture detection limit of 1 mm. However, the geologist also has access to the core which gives further possibilities to estimate smaller apertures. In percussion-drilled boreholes, the source of fracture information comes from the BIPS image solely and the lower measurable aperture limit is 1 mm.

Fractures with an aperture larger than 0 mm are classified as open, out of which fractures with an aperture of 0.5 mm are classified as partly open. Fractures with no aperture are classified as sealed.

Table 4-14 and Table 4-16 present the original data set of mapped fractures in each of the groups natural and sealed in the cored boreholes KSH01A and KSH01B. Table 4-15 and Table 4-17 present the data interpreted according to the adopted classification of fractures into *open, partly open* and *sealed* in the corresponding cored boreholes, based on apertures measured using BIPS.

There are 197 fractures with apertures of 0.5 mm in the data mapped in KSH01A (classified as “partly open”). In total there are 509 fractures mapped with an aperture larger than 0 mm (classified as “open” or “partly open”). This gives 5% open or partly open fractures in KSH01A (or 3% “open” fractures and 2% “partly open” fractures).

In borehole KSH01B, there are no partly open fractures, and only one fracture with an aperture larger than 0 mm.

Table 4-14. Classification of fractures in KSH01A as delivered from SICADA.

Section (m)	Type	Number of fractures
100–1,000	Natural	3,046
100–1,000	Sealed	6,552
100–1,000	All fractures	9,598

Table 4-15. Fracture classification in the cored borehole KSH01A, based on measured aperture.

Section (borehole depth (m))	Type	Number of fractures
100–1,000 m	Open (aperture > 0 mm)	509
100–1,000 m	Partly open (0 mm < aperture < 1 mm)	197
100–1,000 m	Sealed (aperture = 0 mm)	9,089
100–1,000 m	All fractures	9,598

Table 4-16. Fracture classification in the cored borehole KSH01B, as delivered from SICADA.

Section (borehole depth (m))	Type	Number of fractures
0–100 m	Natural	0
0–100 m	Sealed	472
0–100 m	All	472

Table 4-17. Fracture classification in the cored borehole KSH01B, based on measured aperture.

Section (borehole depth (m))	Type	Number of fractures
0–100 m	Open (> 0 mm aperture)	1
0–100 m	Partly open (0 < aperture < 1 mm)	0
0–100 m	Sealed (aperture = 0)	471
0–100 m	All	472

The percussion-drilled borehole HSH01 contains 653 fractures with an aperture larger than 0 mm, of which 591 are partly open (aperture = 0.5 mm). There are 631 fractures that have 0 mm aperture. This gives 51% “open“or “partly open” fractures (or 46% “partly open” and 5% “open” fractures).

The percussion-drilled borehole HSH02 has 850 fractures with an aperture larger than 0 mm, of which 763 fractures are partly open and 348 fractures with an aperture of 0 mm This gives a relation of 71% “open” or “partly open” fractures (or 64% “partly open” fractures and 7% “open” fractures).

Borehole HSH03 contains 42% partly open fractures and 7% open fractures based on aperture.

Fracture orientations

The orientations of fractures in the boreholes are shown in Figure 4-44 through Figure 4-49. Each figure provides results for an individual borehole, and shows fracture orientations displayed as both contoured stereo plots and rose diagrams. Fractures are further subdivided into open (including partly open) and sealed based on the aperture measurements.

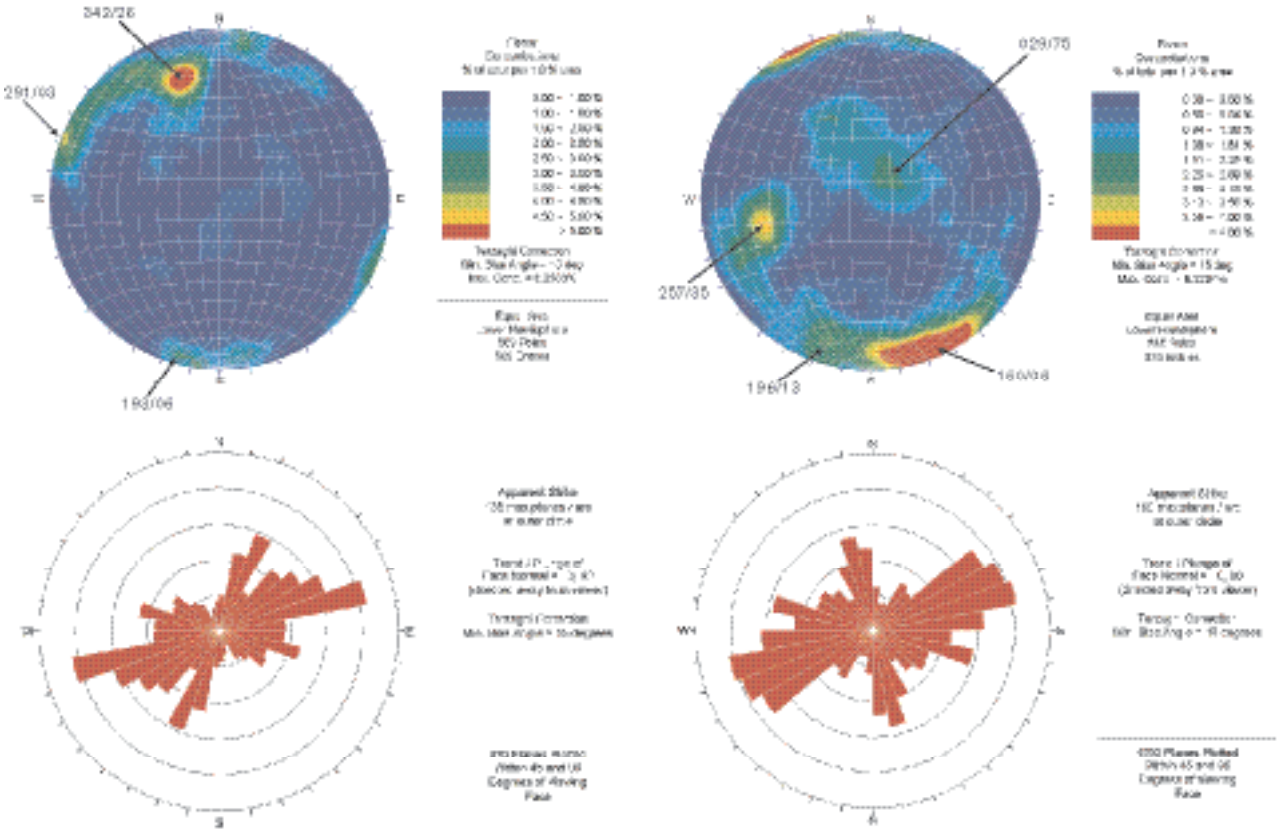

Figure 4-44. *Open fractures in percussion-drilled boreholes HSH01 (left) and HSH02 (right) plotted as poles to fracture planes, equal area, lower hemisphere projection (top) and in a rose diagram (bottom). Both plots are corrected for orientation bias.*

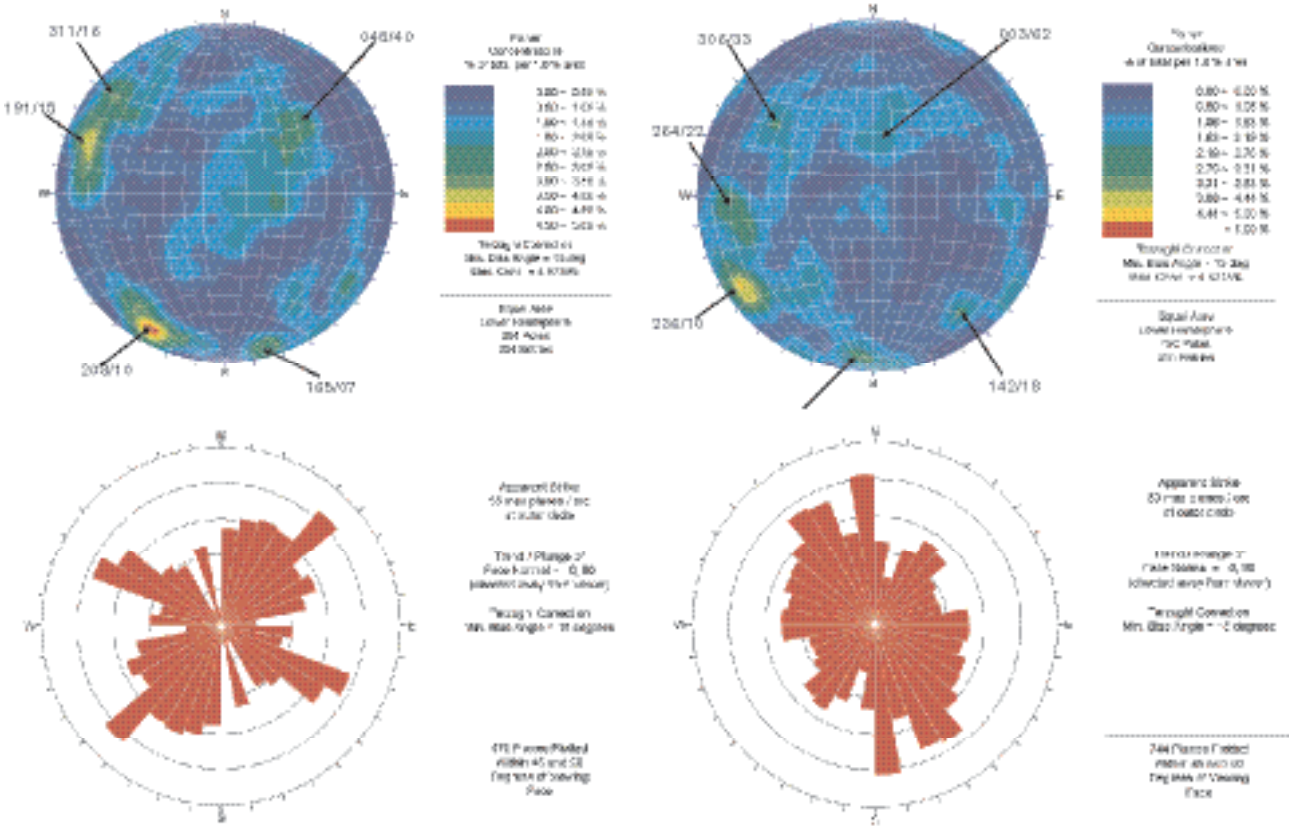

Figure 4-45. *Open fractures in boreholes HSH03 (left) and KSH01A (right) plotted as poles to fracture planes, equal area, lower hemisphere projection (top) and in a rose diagram (bottom). Both plots are corrected for orientation bias.*

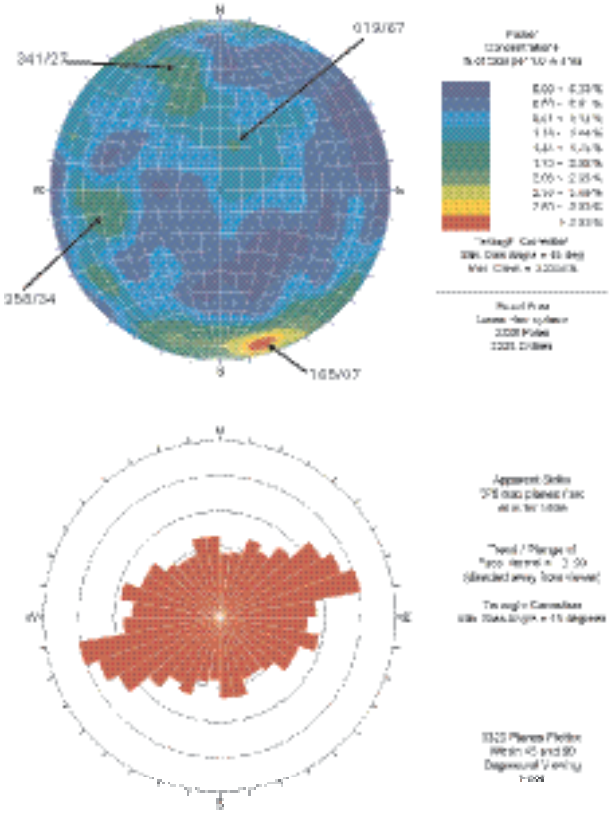

Figure 4-46. *All open fractures combined in boreholes HSH01, HSH02, HSH03 and KSH01A, plotted as poles to fracture planes, equal area, lower hemisphere projection (top) and in a rose diagram (bottom). Both plots are corrected for orientation bias.*

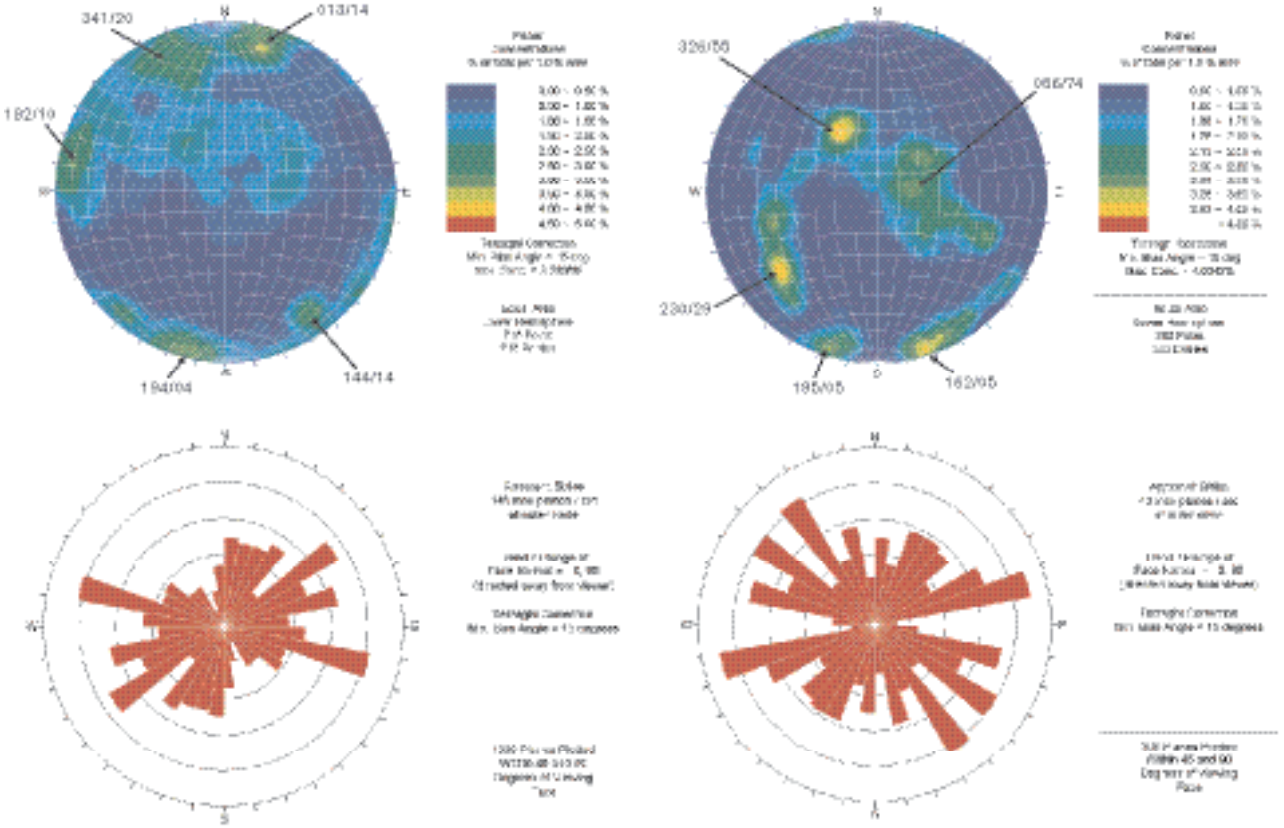

Figure 4-47. *Sealed fractures in boreholes HSH01 (left) and HSH02 (right) plotted as poles to fracture planes, equal area, lower hemisphere projection (top) and in a rose diagram (bottom). Both plots are corrected for orientation bias.*

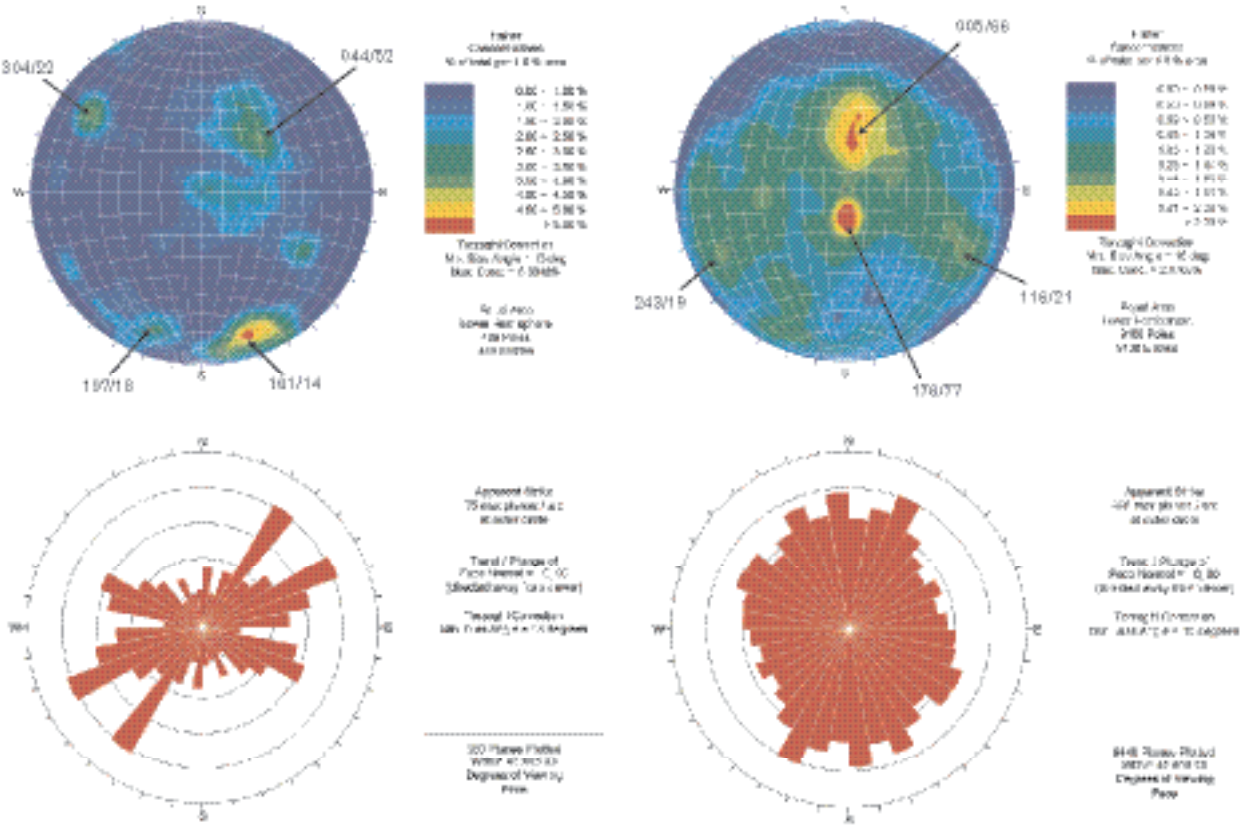

Figure 4-48. *Sealed fractures in boreholes HSH03 (left) and KSH01A (right) plotted as poles to fracture planes, equal area, lower hemisphere projection (top) and in a rose diagram (bottom). Both plots are corrected for orientation bias.*

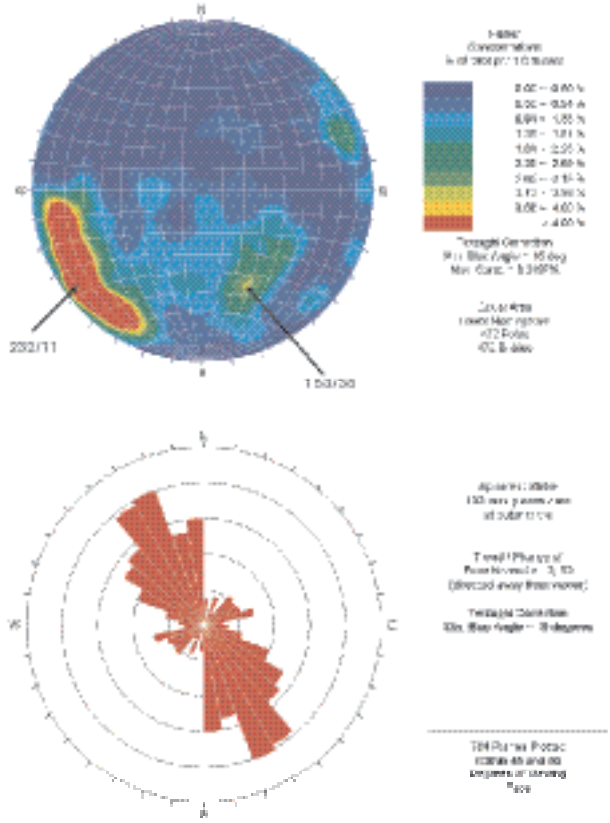

Figure 4-49. *Sealed fractures in cored-drilled borehole KSH01B plotted as poles to fracture planes, equal area, lower hemisphere projection (top) and in a rose diagram (bottom). Both plots are corrected for orientation bias.*

Table 4-18 summarises the modal pole orientations noted in Figure 4-44 through Figure 4-49. There are a number of sets present in each borehole, but there is typically a near-vertical, east-northeasterly set, a steeply dipping north-northwesterly set, and a steeply dipping west-northwesterly set for the open fractures, as shown in Figure 4-46. There is also a shallowly dipping set striking northwest and dipping to the southwest. The sealed fractures show similar patterns. There is a well-developed east-northeasterly, subvertical set, a west-northwesterly, subvertical set, a steeply dipping west-northwesterly set, and a north-northwesterly set with shallow dips to the southwest. The relative prominence of each set varies from borehole to borehole, and there is variability in the absolute orientations The orientations of these and other fracture data are more rigorously analysed in Section 5.1.6.

Fracture frequency

Fracture frequency is based on the number of fractures recorded in each borehole. Frequency was analysed separately for open (including partly open) and sealed fractures, and as a function of lithology and degree of alteration, in order to evaluate whether these factors are related to observed variations in fracture frequency. Sections of crush has not been analyzed for different reasons; 1) this data is mapped differently than the rest of the core, 2) lack of time. Crush represents sections of the core where fractures have not been mapped individually due to the large number of fractures present. Instead, the number of fractures in each section has been estimated.

Fracture frequency plots such as those presented in Figure 4-50 through Figure 4-54 provide visual indications of sections of higher and lower fracturing, and the dominant mineralisations. However, in boreholes where fracturing is variable and sparse, the intervals must of necessity be large in order to typically contain one or more fractures. If the interval size becomes too large, it may be difficult to detect discrete boundaries of fracture intensity domains. In this situation, a cumulative fracture intensity (CFI) plot, in which the intensity is normalized from 0.0 to 1.0, often proves more useful (c.f. Figure 4-55).

The intensity of these and other fracture data are more rigorously analysed in Section 5.1.6.

Table 4-18. Summary of Terzhagi-corrected orientation clusters from borehole fracture data.

Borehole	Modal Pole Orientations	Type
HSH01	324/26; 291/03; 193/06	Open
HSH01	013/14; 341/20; 182/10; 194/04; 144/14	Sealed
HSH02	160/06; 257/35; 196/13; 029/75	Open
HSH02	162/05; 230/29; 326/55; 195/05; 086/74	Sealed
HSH03	208/10; 191/15; 048/40; 311/16; 165/07	Open
HSH03	161/14; 044/52; 304/22; 197/18	Sealed
KSH01A	236/10; 264/22; 183/08; 306/33; 142/18; 003/62	Open
KSH01A	176/77; 005/86; 243/19; 116/21	Sealed
KSH01B	232/11; 153/38	Sealed

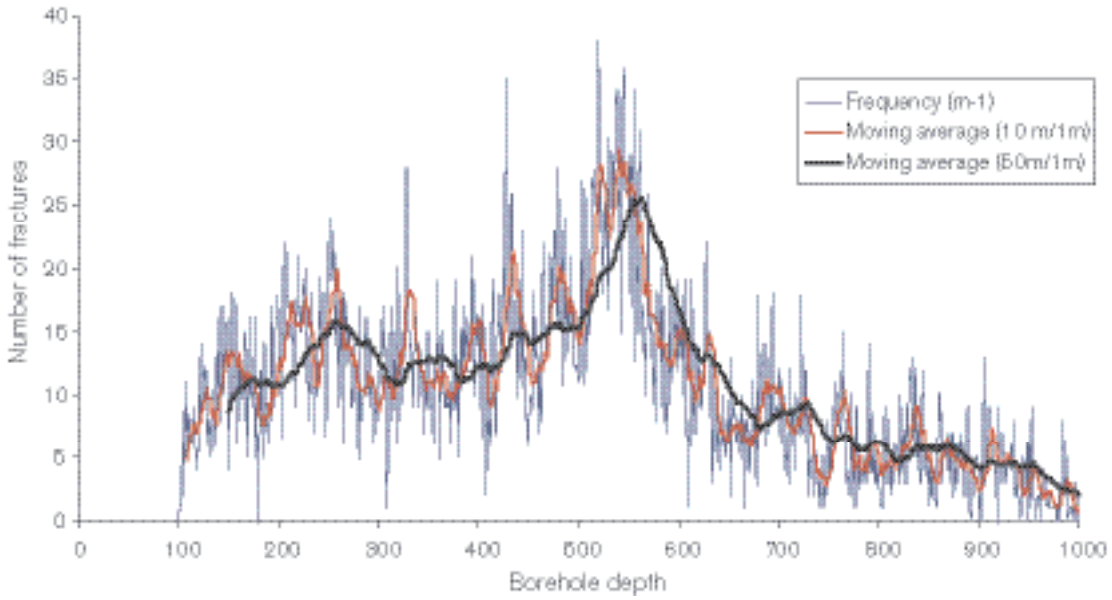

Figure 4-50. *Fracture frequency for open fractures as assessed for cored borehole KSH01A. Fracture frequency (m^{-1}) blue line, moving average with 10 m window and 50 m window, 1 m interval (red line) and (black line) respectively. Note that sections of crush has not been included in this frequency plot.*

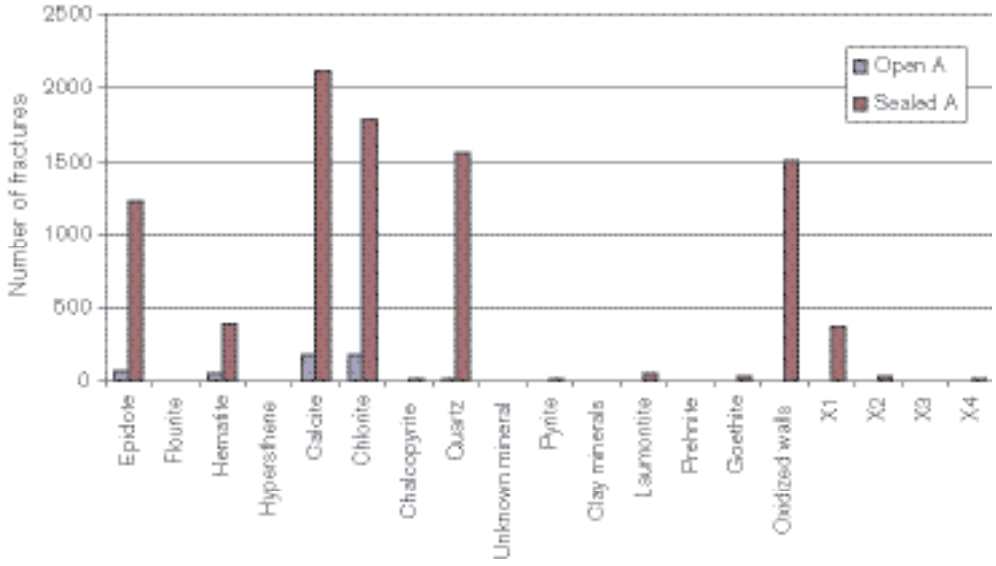

Figure 4-51. *Dominant mineral fillings (MIN1) in open and sealed fractures in cored borehole KSH01A. Minerals X1 through X4 are not identified.*

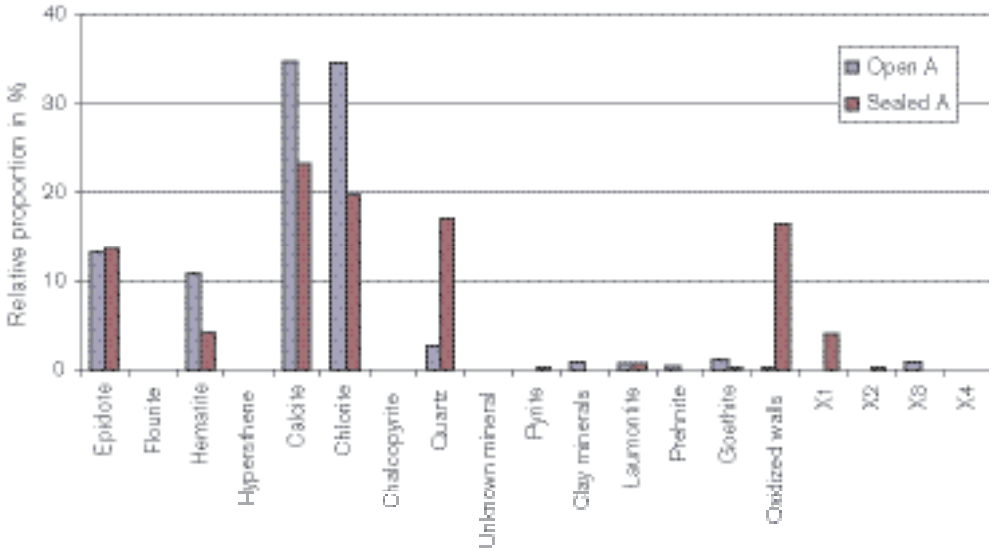

Figure 4-52. *Relative proportion of dominant mineral fillings for open and sealed fractures in cored borehole KSH01A. Minerals X1 through X4 are not identified.*

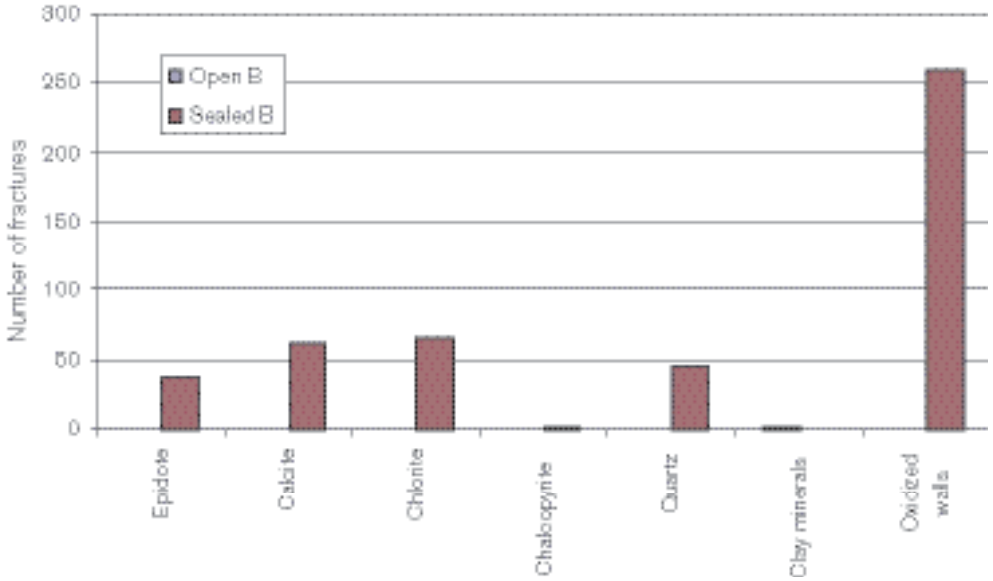

Figure 4-53. *Dominant mineral fillings in open and sealed fractures in cored borehole KSH01B. Note that there is only 1 open fracture mapped in KSH01B (filled with clay minerals).*

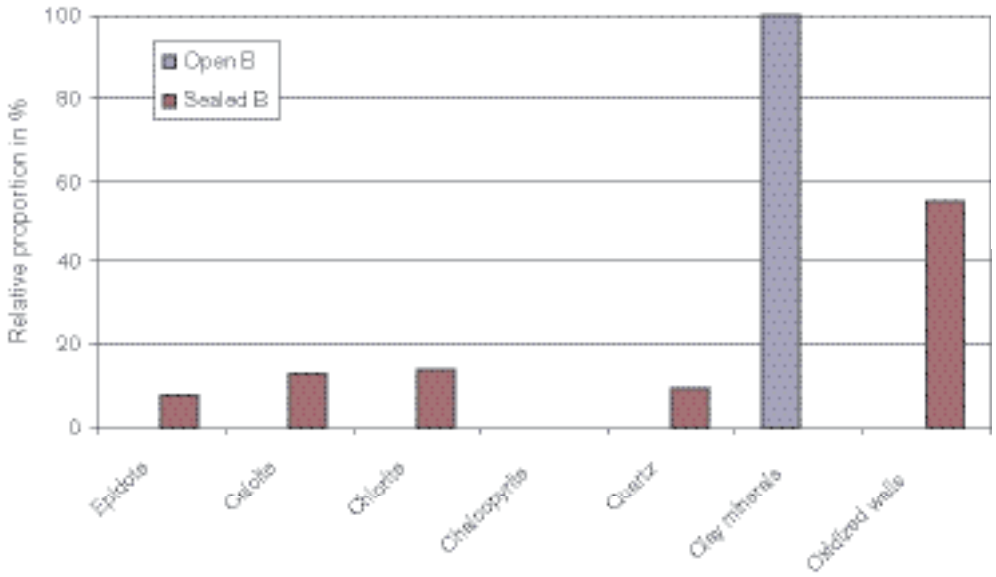

Figure 4-54. *Relative proportion of dominant mineral fillings for open and sealed fractures in cored borehole KSH01B.*

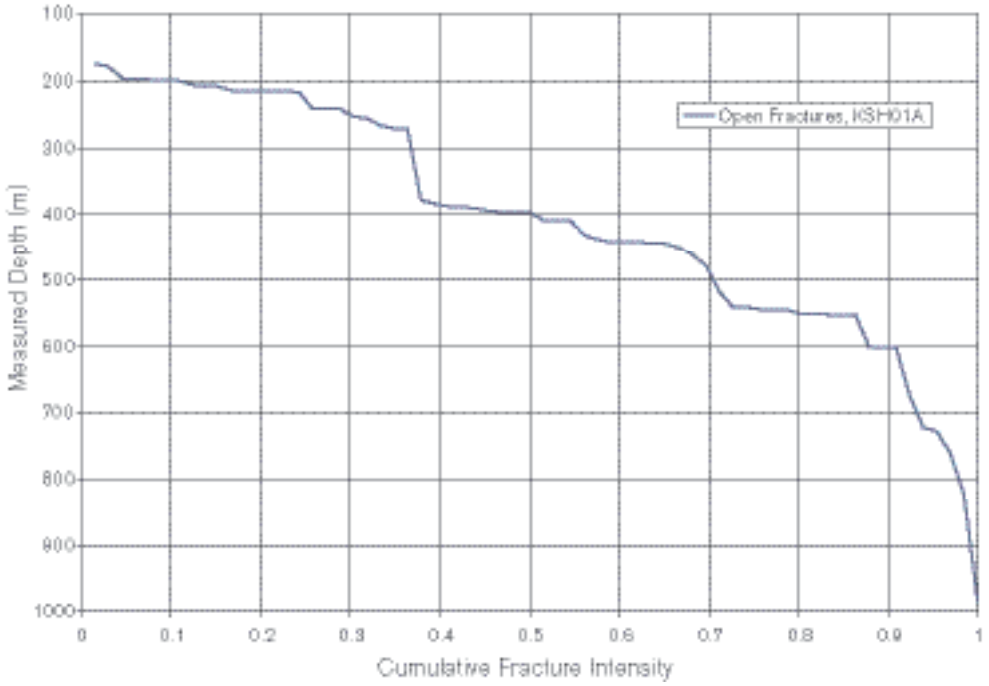

Figure 4-55. *Cumulative fracture intensity for open fractures, cored borehole KSH01A.*

Fracture mineralogy

Fracture minerals are determined macroscopically and are mapped within the Boremap system. However, many of the minerals are difficult to identify and small crystals are easily overlooked. Therefore, fracture mineral analyses have been carried out on samples from boreholes KSH01A and KSH01B for identification. These analyses have mainly comprised:

- X-ray diffractometry; especially used for identification of clay minerals and gouge material composition. All in all 23 samples have been analysed by XRD.
- Microscopy of fracture fillings; around 30 fractures from borehole KSH01A have been sampled and 30 thin sections and 5 fracture surfaces have been studied by SEM. /Drake and Tullborg, in manuscript/.

The most common fracture minerals are chlorite and calcite which occur in several different varieties and are present in most of the open fractures. Other common minerals are epidote, prehnite, laumontite, quartz, adularia (low-temperature K-feldspar), fluorite, hematite and pyrite. A barium-zeolite named harmotome has been identified in some fractures and apophyllite has been identified in a few diffractograms.

Clay minerals identified are, in addition to chlorite, made up of corrensite (mixed-layer chlorite/smectite or chlorite/vermiculite clay, the smectite or vermiculite layers are swelling), illite, mixed-layer illite/smectite (swelling) and a few observations of smectites.

Results from XRD analyses

Samples for XRD identification have mainly been taken from open and usually water conducting fractures with loose and clayish coatings, often of fault gouge type. All the fractures sampled are located in the uppermost 600 metres of the borehole (KSH01A+B) as the deeper part shows very low hydraulic conductivity and a low frequency of open fractures. The fine fraction from each sample has been separated and oriented samples on glass were prepared for the clay mineral identification.

Most of the samples contain quartz, K-feldspar, and albite in addition to calcite, chlorite and clay minerals (Table 4-19). From earlier studies of open fractures at Äspö (e.g. material from the TRUE experimental sites) it is known that altered rock fragments dominate the gouge material, /Andersson et al, 2002c/. It is therefore probable that most of the quartz and feldspars together with the few observations of amphibole and biotite belong to these rock fragments, although contamination due to incorporation of material from the wall rock cannot be ruled out. The total clay mineral content in the open fractures is very difficult to determine in an appropriate way and the XRD analyses should not be regarded as necessarily being representative for the entire filling, but more of the specific sample. However, in fractures filled with fault gouge, a reasonable estimate of the amount of clay mineral (chlorite not included) does not exceed 10–20 weight %. Thin coatings attached to the fracture wall can consist of 90–100% chlorite and clay minerals. The amounts are relatively small, as these coatings are usually thin (<100 μm) but their surface(-s) can be very large (cf. SEM photo of mixed-layer clay coating Figure 4-58).

Minerals constituting less than 5–10% of a sample by weight may not be detected in the diffractograms and particular minerals, e.g. hematite and pyrite, which have been detected in some of the XRD samples, are likely to be present in several of the other samples as well.

Smectite which is a significant swelling clay mineral, has been identified in three of the samples from KSH01A (at 3.7 m, 24 m and 289.8 m).

Table 4-19. XRD analyses of fracture material from open fractures in borehole KSH01A+B (Analyses carried out by the Geological Survey of Sweden, Uppsala).

Sample Core length	Qtz	Kfsp	Alb	Ca	Chl	Py	Hem	Amp	Bi	Pre	Epi	Apo	Clay	Corr	M-I Clay	Ill	Smec
3.7–3.87	x			xxx	(x)								xx	yy’			y
24.0	xx	xx	x		x	x		x					x				yy
67.8–67.9	xx	xx	xx	x	xx								x		yy	(y)	
81.35	xx	xx	xx	x	x								x		y	yy	
82.2	xx	xx	xx	x	xx								x		yy	y	
95.0		xx	xx	xxx	x			x			x		x	y	y	(y)	
130.83	xx		x	xxx	x			x					(x)*				
159.20 m (I)	xx	x	x	xxx	xx			x					x	yy			
159.20 m (II)	xx	xx	x	xx	xxx			x					xx*			y	
178.25–178.35			xx	xx	x							xxx	x	yy			
249.0	x	x	x	xx	x								(x)*				
250.4	xx	xx		x	xx		x						(x)			(y)	
255.78–255.93	xx	xx		x	xx		x						x	yy’			
259.3	xx	xx		xx	xx		x						x		yy	y	
267.97–268.02	xx	xx		xx	xx		x						xx	yy			
289.8–289.95	xx	xx			xxx								x				yy
290.9	xx	x	xxx	xx	xx								x	yy			
306.77	x	x	x	xxx	x								x	yy			
325.93	xx		x		x				xx			xx	x	yy			
447.34	xx	x			xx					xx	x	xx	x	yy			
514.46	xx			xx	xx								x	y	yy		
558.60–558.65	xx	xx		x	xx		x						x	yy			
590.35–590.52	xx	xx	xx		xx								x		y	yy	

Qtz=quartz, Kfsp=K-feldspar usually adularia, Alb =Na-plagioclase (albite), Ca= calcite, Chl= chlorite, Py=pyrite, Hem=hematite.

Amp=amphibole, Bi =biotite, Pre=prehnite, Ep=epidote, Apo=apophyllite, Clay = presence of clay minerals indicated in the random oriented sample, the clay minerals are identified in the fine fraction oriented sample, results are marked with y.

Corrensite = swelling mixed layer clay with chlorite/smectite or chlorite/vermiculite regularly interlayered, M-I clay = mixed layer clay with illite/smectite layers, ill = illite, Smec= smectite *= indicates swelling chlorite, ‘ =indicates corrensite without 1:1 layering.

xxx = dominates the sample, xx= significant component, x= minor component, OBS this is only semi-quantitative.
yy = dominating clay mineral in the fine fraction, y = identified clay mineral in the fine fraction.

( ) = potentially present.

Results from microscopy and SEM studies

The fractures sampled for microscopy comprise open as well as sealed fractures from the entire length of borehole KSH01A with a focus on the uppermost 600 metres (example shown in Figure 4-56). All sample descriptions and results from the SEM/EDS analyses of different fracture minerals are provided in /Drake and Tullborg, in manuscript/. The aim of the microscopy, in addition to identification of minerals, is to determine different mineral parageneses and their sequences of formation and also to establish the different chemical varieties of minerals present (primarily chlorite and calcite).

The fracture mineralogy as revealed in drill core KSH01A+B (c.f. Figure 4-57) shows several generations of mineralisations ranging from epidote facies (epidote, albite, quartz, calcite, pyrite and muscovite) in combination with ductile deformation, over to brittle deformation in combination with oxidation and formation of hematite, causing extensive red-staining of the wall rock along the fractures. Subsequent breccia sealing by prehnite-fluorite, calcite and Fe-Mg chlorite has occurred followed by adularia, hematite, Mg-chlorite and calcite formation. The latest hydrothermal mineralisation shows a series of decreasing formation temperature as follows; Mg-chlorite, adularia, laumontite (Ca-zeolite), pyrite, hematite, harmotome (Ba-zeolite), Fe-chlorite (sperulitic), calcite + REE-carbonates and clay minerals. There is an ongoing pilot study to attempt dating of the hydrothermal mineralisations using Rb-Sr and Ar-Ar techniques. Early results may be available for the Laxemar model version 1.2. Indirect dating of calcites using stable isotopes is ongoing and results will be available to the Laxemar model version 1.2.

Figure 4-56. *Drillcore sample KSH01A:603.11 m showing fracture sealed by prehnite (greenish) and cut by discordant calcite filling (white). Note the red staining and chloritisation of the wall rock. Blue line shows location of thin section.*

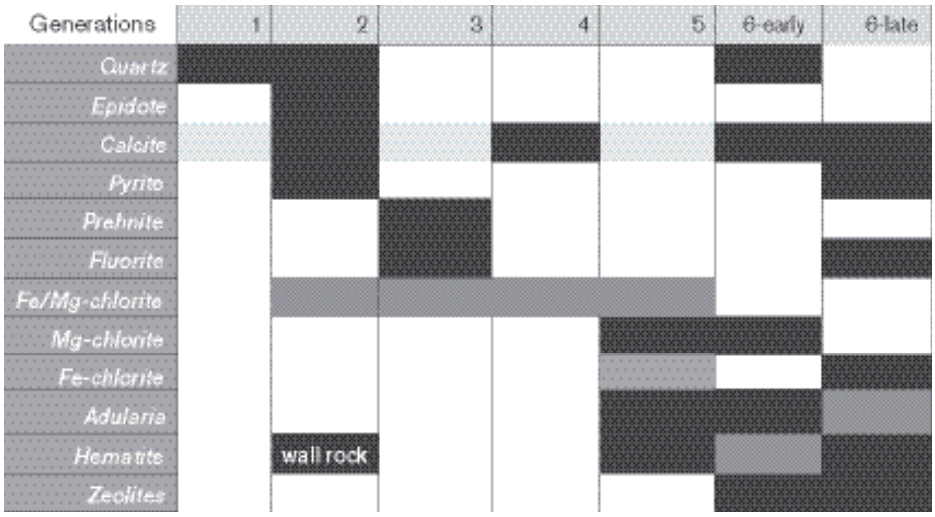

Figure 4-57. *Compiled results showing the paragenesis and different generations determined from microscopy and SEM/EDS (Drake and Tullborg, in manuscript). Black colour represents major mineral present in a generation. Dark and light grey represents minerals that are present, but not dominant and possibly present, respectively.*

The outermost coatings along the hydraulically conductive fractures consist mainly of clay minerals of illite and mixed layer clays (corrensite=chorite/smectite and illite/smectite), together with calcite and minor grains of pyrite. It is assumed that especially the calcite and pyrite formation is an ongoing process although the amounts of possible recent precipitates are low.

From the fracture mineral data available to date the following can be concluded.

The over all fracture mineralogy is very similar to earlier observations in the Äspö HRL /cf e.g. Landström and Tullborg, 1995; Andersson et al, 2002c/.

The drill core KSH01A+B is well preserved (flushing and grinding have been minimised), which has facilitated sampling of relatively undisturbed clay mineral samples.

Furthermore, it has been possible to study calcite and pyrite that have grown fracture edges as well as soft or brittle zeolites minerals. This has, for example, resulted in the identification of the previously overlooked Ba-zeolite harmotome.

The red-staining of the wall rock around many fractures and mapped fractures zones, corresponds to hydrothermal alteration/oxidation, which has resulted in saussuritisation of plagioclase, breakdown of biotite to chlorite and oxidation of Fe(II) to form hematite, mainly present as micrograins giving rise to the red colour. However, there is not always a perfect correspondence between the extent of hydrothermal alteration and red-staining /also cf. Landström et al, 2001/.

In the fractures, several generations of hematite and pyrite are present. The finding of small pyrite grains in the outermost layers of the fracture coatings is in agreement with the groundwater chemistry, indicating reducing conditions /cf. Laaksoharju et al, 2004b/. More detailed studies of the redox-sensitive minerals and the timing of the hydrothermal oxidation event/-s is ongoing and needs to be assessed in the next model version.

It has so far, not been possible to link different fracture minerals to different fracture orientations. The same difficulty was experienced in a corresponding analysis of a larger data set from Äspö, cf. /Munier, 1993/ and /Mazurek et al, 1997/.

- The sequence of minerals, going from epidote facies in combination with ductile deformation, over to brittle deformation and breccia sealing during prehnite facies and subsequent zeolite facies and further decreasing formation temperature series, indicates that the fractures were initiated relatively early in the geological history of the host rock and have been reactivated during several different periods of various physiochemical conditions.

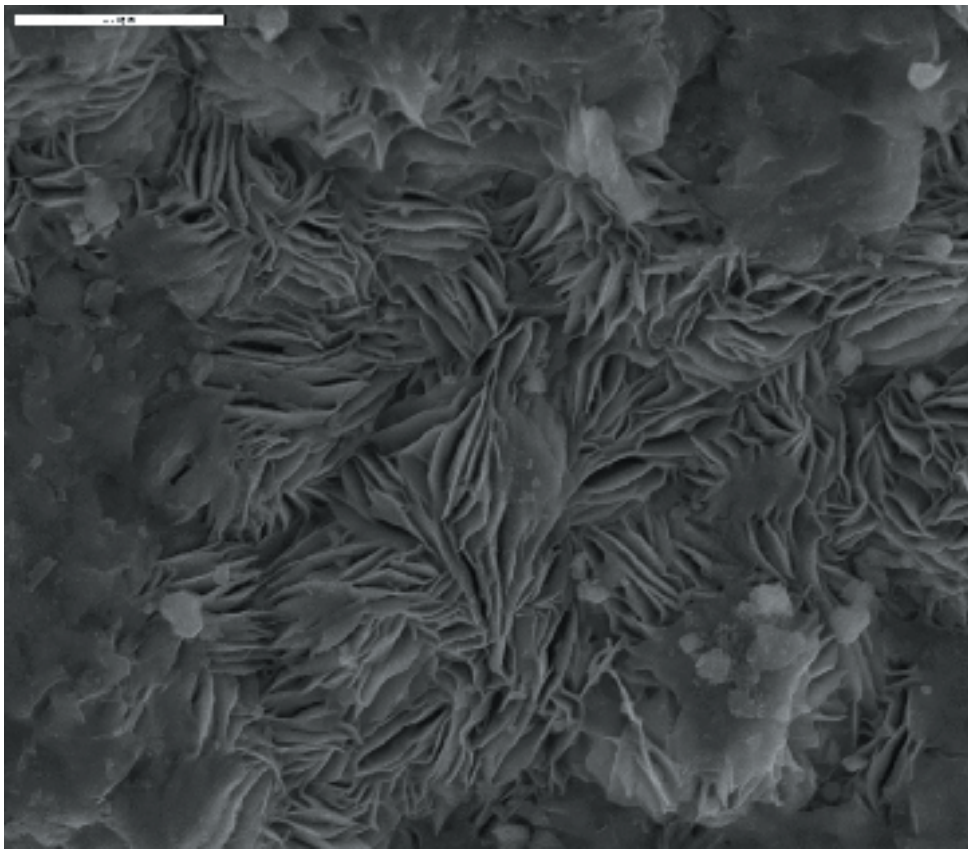

Figure 4-58. *SEM photo showing mixed layer clay on a fracture surface from borehole KSH01A (scale bar = 20 mm).*

- The locations of the hydraulically conductive fractures are mostly associated with the presence of gouge-filled faults produced by brittle reactivation of earlier ductile precursors or hydrothermally sealed fractures. The outermost coatings along the hydraulically conductive fractures consist mainly of clay minerals, usually illite and mixed layer clays (corrensite = chorite/smectite and illite/smectite) together with calcite and minor grains of pyrite.

4.4.4 Borehole radar

There are thirty-six identified radar reflections in boreholes KSH01A, HSH01, HSH02 and HSH03, evenly distributed over the sampled depth interval 0–200 m, c.f. Table 4-20. The radar information has not been analysed in detail in support of model version Simpevarp 1.1 and needs to be assessed further in future model versions.

Table 4-20. Distribution of identified structures from the radar investigation in boreholes KSH01A, HSH01, HSH02 and HSH03 /from Nilsson and Gustafsson, 2003/.

Table 4-20. Distribution of identified structures from the radar investigation in boreholes KSH01A, HSH01, HSH02 and HSH03 /from Nilsson and Gustafsson, 2003/.

Distribution of identified structures Site: Simpevarp Depth	KSH01A	HSH01	HSH02	HSH03
0–50	2	4	2	1
50–100	1	4	3	1
100–150		4	2	5
150–200		2	2	3

4.4.5 Geological single-hole interpretation

Geological data from the cored borehole are important for the construction of the geological 3D models, since the borehole constitutes the only available direct data at depth in the local scale model domain. A geological single hole interpretation for KSH01A was made at the site and is presented in Figure 4-59.

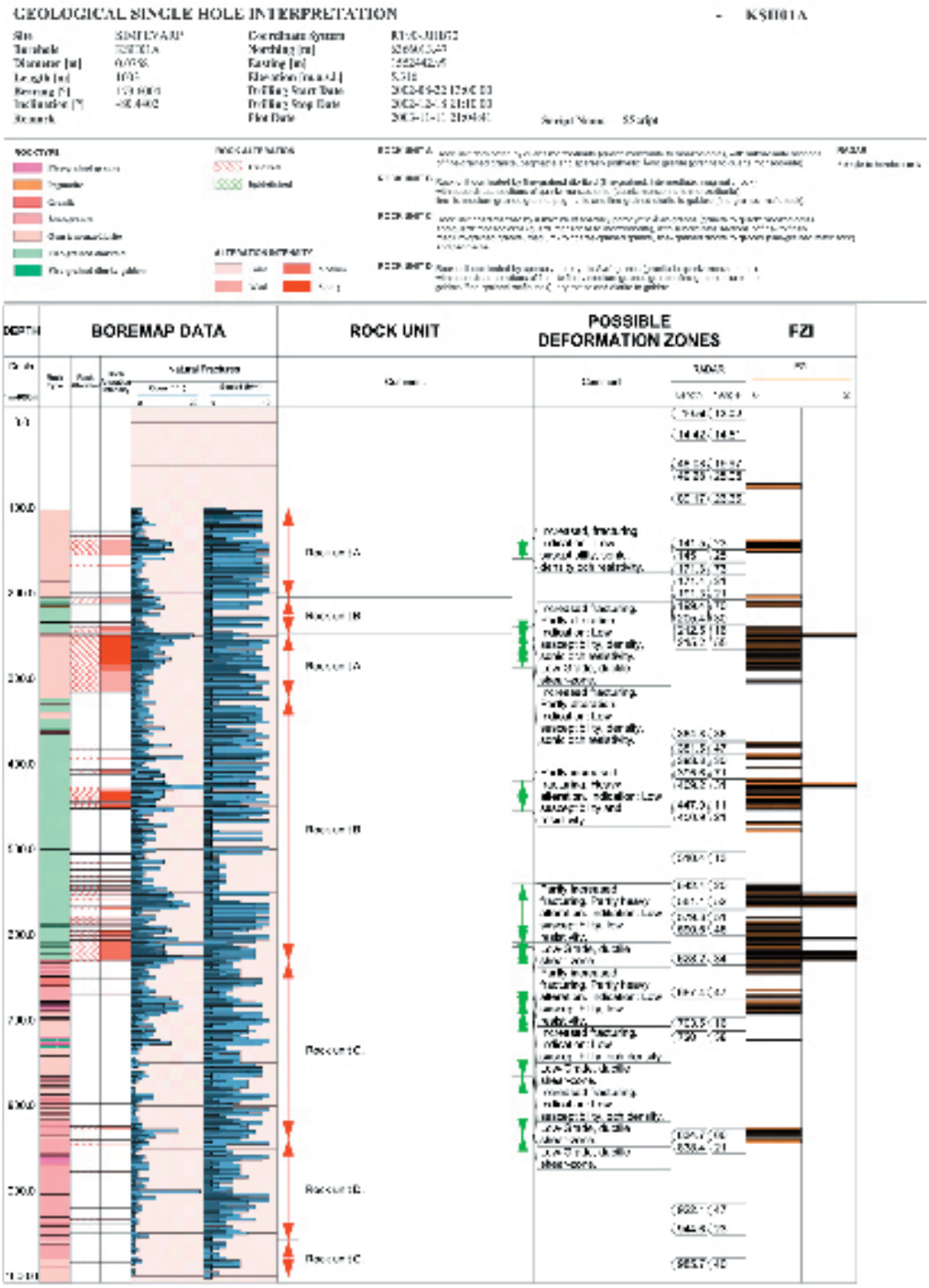

Figure 4-59. *Single hole geological interpretation of KSH01A.*

The division of the borehole in different units is mainly based on the complexity of lithology and alteration. Four main rock units are defined :

Unit A; dominated by quartz monzodiorite (quartz monzonite to monzodiorite), with subordinate sections of fine-grained granite, pegmatite and sparsely porhyritic Ävrö granite (granite to quartz monzodiorite),

Unit B; dominated by fine-grained dioritoid (fine-grained, intermediate, magmatic rock) with subordinate sections of quartz monzodiorite (quartz monzonite to monzodiorite), fine- to medium-grained granite, pegmatite and fine-grained diorite to gabbro (fine-grained mafic rock),

Unit C; characterised by a mixture of sparsely porphyritic Ävrö granite (granite to quartz monzodiorite) and quartz monzodiorite (quartz monzonite to monzodiorite), with subordinate sections of fine- to finely medium-grained granite, medium- to coarse-grained granite, fine-grained diorite to gabbro (fine-grained mafic rock) and pegmatite,

Unit D; dominated by sparsely porphyritic Ävrö granite (granite to quartz monzodiorite), with subordinate sections of fine- to finely medium-grained granite, fine-grained diorite- to gabbro (fine-grained mafic rock), pegmatite and diorite to gabbro.

A simplified version of the identified units in the single hole interpretation of cored borehole KSH01A has been used in the 3D geometrical modelling of rock domains. In the 3D lithological modelling, units A, C and D have been considered to belong to the same rock domain, but are separeteed from unit B, as is further explained in Sections 5.1.3 and 7.3.1.

Mapped deformation zones have been delineated in the geological single hole interpretation and a fracture zone index (FZI) has been devised based on the geophysical logs. Thirteen possible deformation zones have been mapped in borehole KSH01A.

Borehole fracture data and other fracture data are more rigorously analysed in Section 5.1.6.

4.5 Hydrogeologic interpretation of borehole data

4.5.1 Hydraulic evaluation of single hole tests etc

Methods for measurement and evaluation of parameters

A number of hydraulic tests are used as (more or less) standard methods in boreholes drilled during the site investigations. These are summarized in Table 4-21. Slug tests and tests with the pipe string system (PSS) were not used to provide as input data for Simpevarp v1.1.

Data available

A few boreholes have been tested during the early stages of the initial site investigations and were available for the Simpevarp 1.1 modelling. In the cored borehole KSH01A, c.f Figure 2-1, hydraulic tests with the Posiva flow logging tool (PFL) and the wire-line probe (WLP) were performed. Some data based on WLP were however not available in SICADA at the time of the evaluation. In percussion holes HSH01-03, c.f. Figure 2-1, some data was available in SICADA but a few more tests are to be reported.

Single-hole hydraulic tests and interference tests conducted prior to the onset of the ongoing initial site investigations (historical data) were carried out in the Äspö, Ävrö, Hålö, Mjälen, Laxemar and Simpevarp areas /e.g. Rhén et al, 1997b/. Some of these data are commented on in this section, but have not been re-evaluated and are only partly included in the analysis for Simpevarp 1.1 due to the limited time available.

Table 4-21. Principal methods used during initial site investigations for measurement and evaluation of hydraulic parameters.

Measurement equipment	Acronym for method	Acronym for method variant	Type of test performed	Comments
Pipe String System	PSS		Pumping or injection tests performed as constant rate tests. Impulse test is ab option.	Transient data collected. Evalution based on transient or stationary conditions. Tests in core-drilled boreholes.
Hydraulic test system percus-sion boreholes	HTHB		Pumping or injection tests performed as constant rate tests. Flow logging with impellar is an option.	Transient data collected. Evalution based on transient or stationary conditions.
Wire Line Probe	WLP	WLP-pt	Pumping tests with WLP in core drilled bore holes.	Transient data collected. Evalution based on transient or stationary conditions.
		WLP-ap	Absolute pressure measurement. with WLP in core-drilled bore holes.	Transient data collected.
Posiva Flow Log	PFL	PFL-s	Difference flow logging (sequential). Electrical conductivity (EC) and temperature of the borehole fluid as well as Single Point resistance (SP) is measured during different logging sequences.	Purpose to estimate test section transmissivity and unbdisturbed pressure. Two logging sequences. Evalution based on stationary conditions.
		PFL-o	Difference flow logging-overlapping.	Purpose to estimate flow distribution and use PFL-s to estimate transmis-sivity for fractures/features. One logging sequence.
Slug test			Slug or bailer test.	Normaly just performed in boreholes in the overburden.

During 2000–2002 an inventory of private wells in the Simpevarp area was made /Morosini and Hultgren, 2003/, c.f. Figure 4-41. For the most part the well design and water level were documented. There are altogether 218 private wells, of which 213 have been documented. Some 110 are dug wells in the Quaternary deposits. Only a few of the wells have a recorded flow rate capacity, but for most wells a water level was measured. These data have not been used in the evaluation as they are not considered to provide any significant contribution to the understanding of the area. Thhhese data were collected mainly for use in Environmental Impact Assessment (EIA).

Evaluation of data from single hole tests – general

Data from the hydraulic tests performed in the cored borehole KLSH01A have been compiled and univariate statistics have been calculated and compared with data from other cored boreholes in the area, where similar tests have been conducted. The geological single-hole evaluation for KSH01A was not available at the time of the hydraulic single-hole evaluation, which means that hydraulic properties for interpreted rock units could not be defined.

Furthermore, analyses of the newly available hydrogeological data have not been coordinated with the geological structural model, as it was not available in time for the evaluation.

Due to the circumstances mentioned above, it was not possible to compile a data set for the numerical groundwater flow modelling based on an integrated evaluation of geological and hydro-geological data. The modelling that was undertaken is described in more detail in Section 5.4.

Hydraulic conductivity (or transmissivity) evaluated from hydraulic tests with the same test section length often fit rather well to a lognormal distribution. When the test section length decreases, the number of tests below the lower measurement limit increases. The data set is henced “censored”, which has to be taken into account when choosing a statistical distribution that should describe the measured values above the measurement limit as well as possible. Below the measurement limit the fitted distribution can predict the properties, but of course it is not known whether it is a good

prediction. When performing modelling based on the fitted distribution it has to be motivated if extrapolation is reasonable and if there also is a lower limit (below the lower measurement limit) for the property in question due to e.g. conceptual considerations.

The standard procedure in describing the hydraulic material properties from single-hole test data is to fit the logarithm of the data to a normal distribution, and taking the censored data into account. The associated statistics normally shown is the mean and standard deviation (std) of Y, $Y=\log_{10}(X)$, X= hydraulic conductivity (K) or transmissivity (T), where the mean of $\log_{10}(X)$ corresponds to the geometric mean. Usually, the number of measurements below the lower measurement limit is greater than above, and it is here argued that the methodology above is an appropriate way by which to describe the data above the lower measurement.

Evaluation of data from single hole tests – available data

The single-hole hydraulic tests conducted in the cored borehole KSH01A and percussion boreholes HSH01–03 are listed in Table 4-22 and Table 4-23, respectively. The hydraulic tests conducted in the percussion boreholes were performed as open-hole pumping tests combined with flow logging. Some tests were also conducted with a single packer, making it possible to pump the section above or below the packer. The hydraulic tests performed in the cored borehole were made during drilling as pumping tests and included measurements of absolute pressure made with the SKB-developed Wire-Line Probe (WLP). After completion of the drilling, the Posiva Flow Log (PFL) was applied in the cored borehole. The sequential logging (PFL-s) was made with a test section length of 5 m and the overlapping logging (PFL-o) was made with a test section length of 1 m and a step length of 0.1 m when moving the test section along the borehole.

Table 4-22. Hydraulic tests performed in cored borehole KSH01A (WLP: WireLine probe (tests during drilling), PFL: Posiva Flow Logging).

Total bore-hole length (m)	Upper limit in bh Secup (m)	Lower limit in bh Seclow (m)	No. of tests	Type of test performed	Test scale (m)	Step length (for moving test section) (m)
1,003	95	997.98	179	PFL-s, difference flow logging-sequential	5	5
	100	850	–	PFL-o, difference flow logging-overlapping	5	0.1
	100	1,003	9	Pumping tests with WLP	≈100	–
	102	842	5	Abs. Press. Meas. with WLP	≈100	–

Table 4-23. Hydraulic tests performed in percussion boreholes HSH01–HSH03.

Bore-hole ID	Bore-hole length (m)	Upper limit in bh Secup (m)	Lower limit in bh Seclow (m)	No. of tests	Type of test performed	Test scale (m)	Step length (for moving test section) (m)
HSH01	200	12.03	200	1	Airlift test	≈200	–
HSH02	200	12.03	200	1	Airlift test	≈200	–
HSH03	201	12.03	201	1	Pumping test	≈200	
HSH03		29	198.7	1	Flow logging		≈2 , anomalies 0.5
HSH03		12.03	103	1	Pumping test	≈100	
HSH03		80.5	201	1	Injection test	≈100	
HSH03		12.03	201	1	Step-drawdown test (after hydr.fract)	≈200	

The drilling process and the tests during drilling in borehole KSH01A are described by /Ask et al, 2003/. The drilling and some simple hydraulic tests in boreholes HSH01, HSH02 and HSH03 were reported by /Ask and Samuelsson, 2004/. Hydraulic tests after drilling in HSH03 were reported by /Ludvigson et al, 2003/ and the PFL in KSH01A by /Rouhiainen and Pöllänen, 2003/. Evaluation methods and data are presented in those reports.

The PFL-s, c.f. Table 4-21, provides the transmissivity distribution on a test scale of 5 m along the borehole. Based on the distribution of flow measured by PFL-o and the evaluated transmissivity for a given test section by PFL-s, a transmissvity can be estimated for hydraulic features (normally individual fractures). By combining this interpretation with the information from the Boremap log it is also possible to link geologically mapped information with the hydraulic features identified by PFL-o. A test of the methodology for correlating flow anomalies from overlapping flow logging (PFL-o) with Boremap data, individual or groups of fractures (based on core mapping and BIPS images), will be made for Simpevarp1.2 as the fracture mapping data for KSH01A was in the process of being updated at the time for this report.

The difference flow logging (PFL-o) conducted in KSH01A indicates that the rock is of very low transmissivity below the casing shoe at c. -100 masl. Out of a total of 179 test intervals, only 46 intervals were found to yield a flow above the lower measurement limit of the test equipment, corresponding to a hydraulic conductivity of approximately $K=8 \cdot 10^{-11}$ m/s ($T=4 \cdot 10^{-10}$ m^2/s) in this particular borehole /Rouhiainen and Pöllänen, 2003/. The "theoretical" lower measurement limit for PFL (under optimal conditions) is estimated at $T=1.6 \cdot 10^{-10}$ m^2/s /Rouhiainen and Pöllänen, 2003/. Due to effects of fine particles or gas, the measurement limit that is considered in the evaluation is in general higher. Most of the conductive sections were found between c. –100 and –300 masl, see Figure 4-60. The univariate statistics of the test data are shown in Figure 4-61 and Table 4-24. The average hydraulic conductivity K is found to be low compared to results from other old cored boreholes in the area where similar test scales have been used, see Table 4-25.

Only one percussion-drilled borehole, HSH03, was tested with HTHB, c.f. Table 4-26. The other two percussion boreholes, HSH01 and HSH02, were judged to be low-conductive from the flushing after drilling, and only a rough value of the specific capacity Q/s is available. In borehole HSH03, one major hydraulic anomaly at a depth of 58.5–59.5 m and one minor anomaly at a depth of 53–56 m were observed.

Table 4-24. Univariate statistics for hydraulic tests performed in cored borehole KSH01A. Method employed: PFL-s, Sequential Posiva Flow Logging.

Test type	Upper limit in bh Secup (m)	Lower limit in bh Seclow (m)	Test scale (m)	Lower meas. limit[1] (m/s)	Sample size	K Mean of Log10(K) (m/s)	K Std dev Log10(K) (m/s)
PFL-s[2]	95	997.98	5	8 E–11	179	–12.25	2.83

[1)] Measurement limit estimated from field results.

[2)] PFL-s: Theoretical lower measurement limit (under optimal conditions) is 3.2E–11 m/s.

Table 4-25. Data from KSH01A compared to data reported in /Rhén et al, 1997/ and /Andersson et al, 2002b/.

Bore hole	Test type	Secup (m)	Seclow (m)	Test scale (m)	Sample size	Mean Log10 K (m/s)	Std Log10 K (m/s)
KSH01A	PFL-s	103	1,000	5	179	–12.25	2.83
KLX01	Inj.Test	106	688	3	197	–10.5	1.75
KLX02	PFL-s	207	1,398	3	398	–10.3	1.6
KAS02–KAS08	Inj.Test	Ca 100	500–800	3	1,105	–7.8 to –9.7	1.12 to 2.08

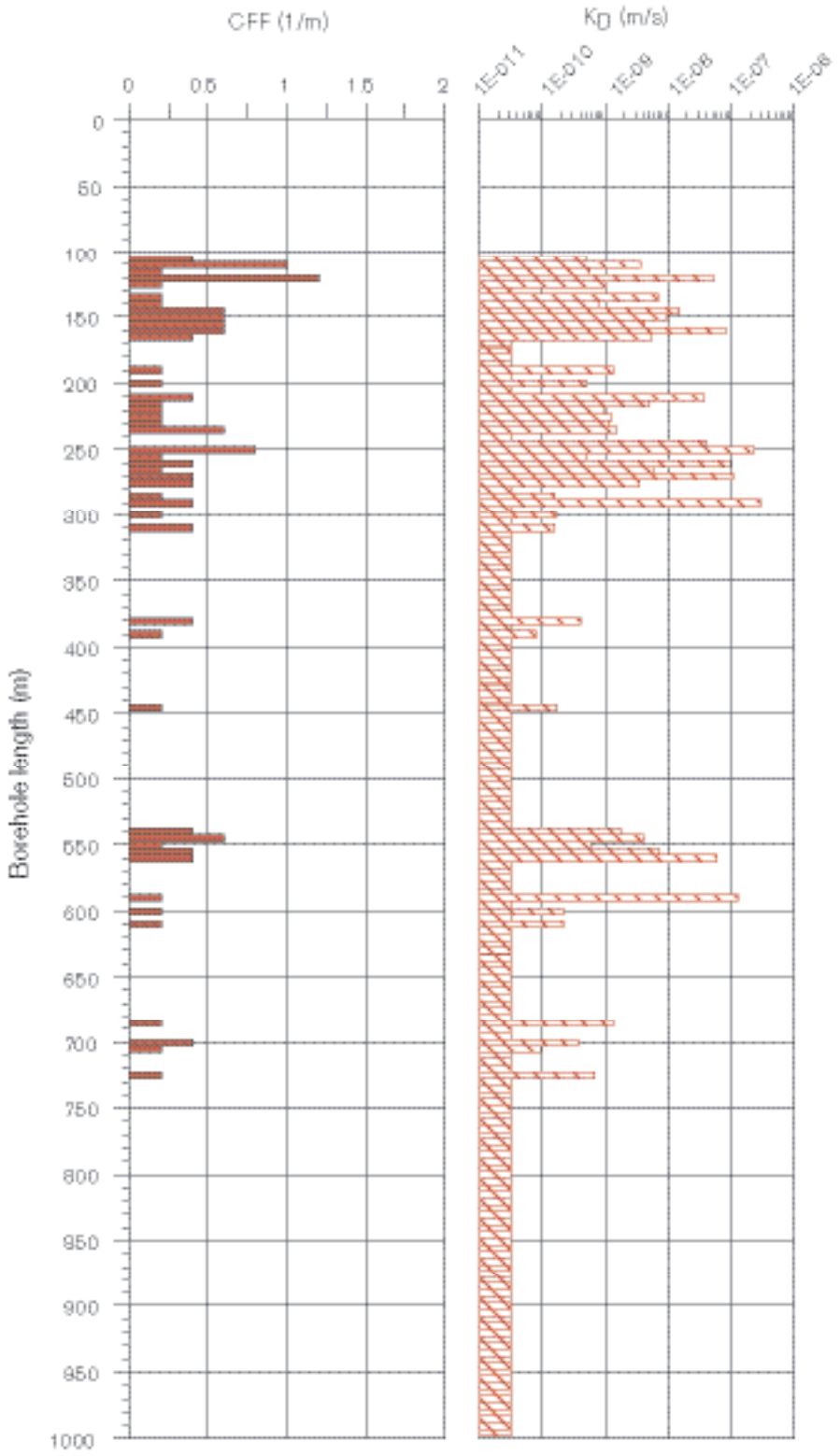

Figure 4-60. *Plot of the evaluated hydraulic conductivity K_D (K based on Differential flow logging) based PFL-s (5 m test sections) and conductive fracture frequency (CFF) based on PFL-o in borehole KSH01A. The plotted measurement limit of K_D is based on the theoretical limit: $K=3.2 \cdot 10^{-11}$ m^2/s m/s ($T=1.6 \cdot 10^{-10}$ m^2/s). CFF is based on the interpreted number of anomalies by PFL-o within a 5 m section. The measurements and the interpretations are reported by /Rouhiainen and Pöllänen, 2003/.*

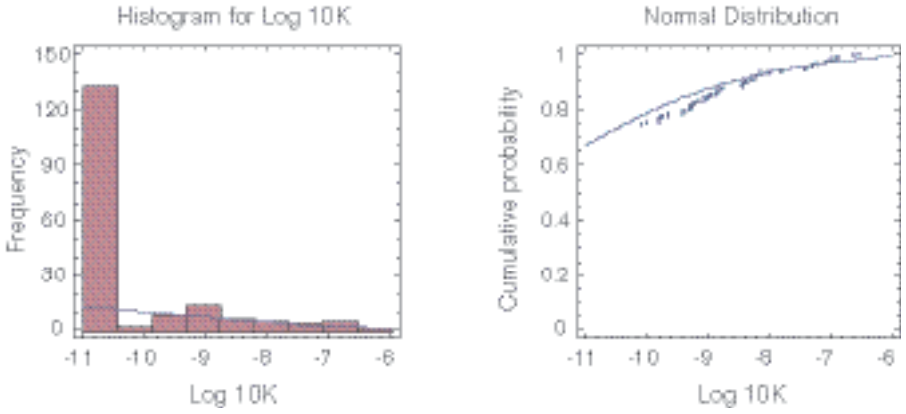

46 of 179 test sections (test section length 5 m) are above the (field estimated) measurement limit K=8 E–11 m/s

Fitted normal distribution:
mean log 10 (K)= –12.25
standard deviation Log10(K)= 2.83

Figure 4-61. *Univariate statistics for hydraulic conductivity ($log_{10}K$ in m/s) from borehole KSH01A as evaluated from the 5 m PFL-s data (difference flow logging) presented in Figure 4-60, /Statgraphics, 1998/.*

Table 4-26. Univariate statistics for hydraulic tests performed in percussion-drilled boreholes. Methods used: HTHB-p: Pumping test or injections test, HTHB-f: flowlogging, c.f. Table 4-21.

Borehole ID	Test type	Upper limit in bh Secup (m)	Lower limit in bh Seclow (m)	Test scale (m)	Lower meas. Limit1 (m/s)	Sample size	K Log10(K) (m/s)	K Mean Log10K (m/s)	K Std Log10K (m/s)
HSH01, 02, 03[1]	HTHB-p	12	200	≈200	≈2 E–8	3		–8.1	0.8
HSH01	HTHB-p	12	200	≈200	–	1	(–9.0)[2]		
HSH02	HTHB-p	12	200	≈200	–	1	(–8.1)[2]		
HSH03	HTHB-p	12	201	≈200	≈2 E–8	1	–7.1		

[1)] Mixed tests: airlift tests and pumping tests. Parameters evaluated from airlift tests are uncertain.

[2)] Preliminary values.

/Rhén et al, 1997b/ estimated a geometric mean $K=1.6 \cdot 10^{-8}$ m/s with a standard deviation ($Log_{10}K$) of 0.96 for well data obtained from the well archive of the Swedish Geological Survey (area approximately corresponding to the NE part of the municipality of Oskarshamn) and percussion holes located in the Äspö, Ävrö, Mjälen. Hålö and Laxemar areas. The test scale was approximately 100 m. Subsequently, /Follin et al, 1998/ estimated a geometric mean $K=6.3 \cdot 10^{-8}$ m/s for wells sunk in the bedrock within the municipality of Oskarshamn found in the SGU well archive. The test scale in this case varied between 10 and 100 m. Both analyses included fracture zones, if present.

4.5.2 Hydraulic evaluation of interference tests

Methods for measurement and evaluation of parameters from hydraulic interference tests

Methods will be discussed in conjunction with future site descriptive models when data become available.

Data available

No interference tests have been made.

4.5.3 Joint hydrogeology and geology single hole interpretation

No joint interpretation has been possible, due to late development of the geological single-hole interpretation.

4.6 Rock mechanics data evaluation

4.6.1 Stress measurements

New stress measurements in the Simpevarp subareahas been performed only in the cored borehole KSH02, and in this hole only successfully at one single location. However, measurements have been performed within the framework of research at Äspö HRL, in several boreholes and using different methods. Further, results from a borehole (KOV01) at SKB's Canister Laboratory in Oskarshamn have been included in the compilation of data that have been used as a base for the estimation. In total measurements from 12 boreholes have been used.

The results as presented in four diagrams in Figure 4-62. The first diagram shows the results from the measurement of the minimum principal stress and the second diagram shows the results from measurements of the maximum principal stress, botrh obtained using the overcoring technique. This method is described in /Sjöberg, 2004/. The modelling approach is described in Section 5.2.1.

The third diagram shows the minimum horizontal stress measured with the hydraulic fracturing method. These data have been used to estimate the minor principal stress in the Simpevarp area, cf. Section 5.2.1.

The forth diagram presents results from both hydraulic fracturing and overcoring measurements. The orientation of the maximum horizontal stress is given for hydrofracturing results and the trend for the maximum principal stress tensor is shown for the overcoring results. (In cases where the actual tensor trend was larger than 180 degrees, 180 degrees was subtracetd, to make all data fall in the span 0–180. This means that this diagram does not represent differences in dip for the maximum principal stress, which is most often subhorizontal). The choice of model span is described in Section 5.2.1. The locations of Äspö, CLAB and the boreholes KSH02 and KLX02 can be seen in Figures 2-1 and 2-2.

Intact rock mechanical tests

No new laboratory tests have yet been performed within the site investigation program. However existing laboratory test data have been compiled. One of the standard test results is the uniaxial compressive strength (USC) and a histogram for this parameter is given in Figure 4-63.

The rock samples from Äspö are from different rock types, but these have not been distinguished because the naming critera in these old data may not be those that are now used. Further, the measurement procedures for the old data may differ slightly from each other and from current test procedures. However the results, summarized in Table 4-27, show typically high strength values, normal for brittle crystalline rock, but a large spread. There is no obvious difference in strength between the rock samples from CLAB and Äspö. At CLAB the dominating rock type is the fine grained dioritoid and at Äspö the quartzmonzodiorite and the Ävrö granite, but also other rock types may be included in the data set from the Äspö laboratory.

Schmidt hammer tests were performed on core samples taken from borehole KSH01A /Chryssanthakis, 2003/. From such tests, a UCS value may be determined indirectly. The mean UCS for the whole set of samples is 174 MPa, and the range of variation between 134 and 208 MPa (Table 4-28) on average, except for the mafic rocks, the values of the UCS are very homogeneous for all the observed rock types along the borehole. The values in Table 4-28 are in agreement with the results of the uniaxial compressive tests (Table 4-27).

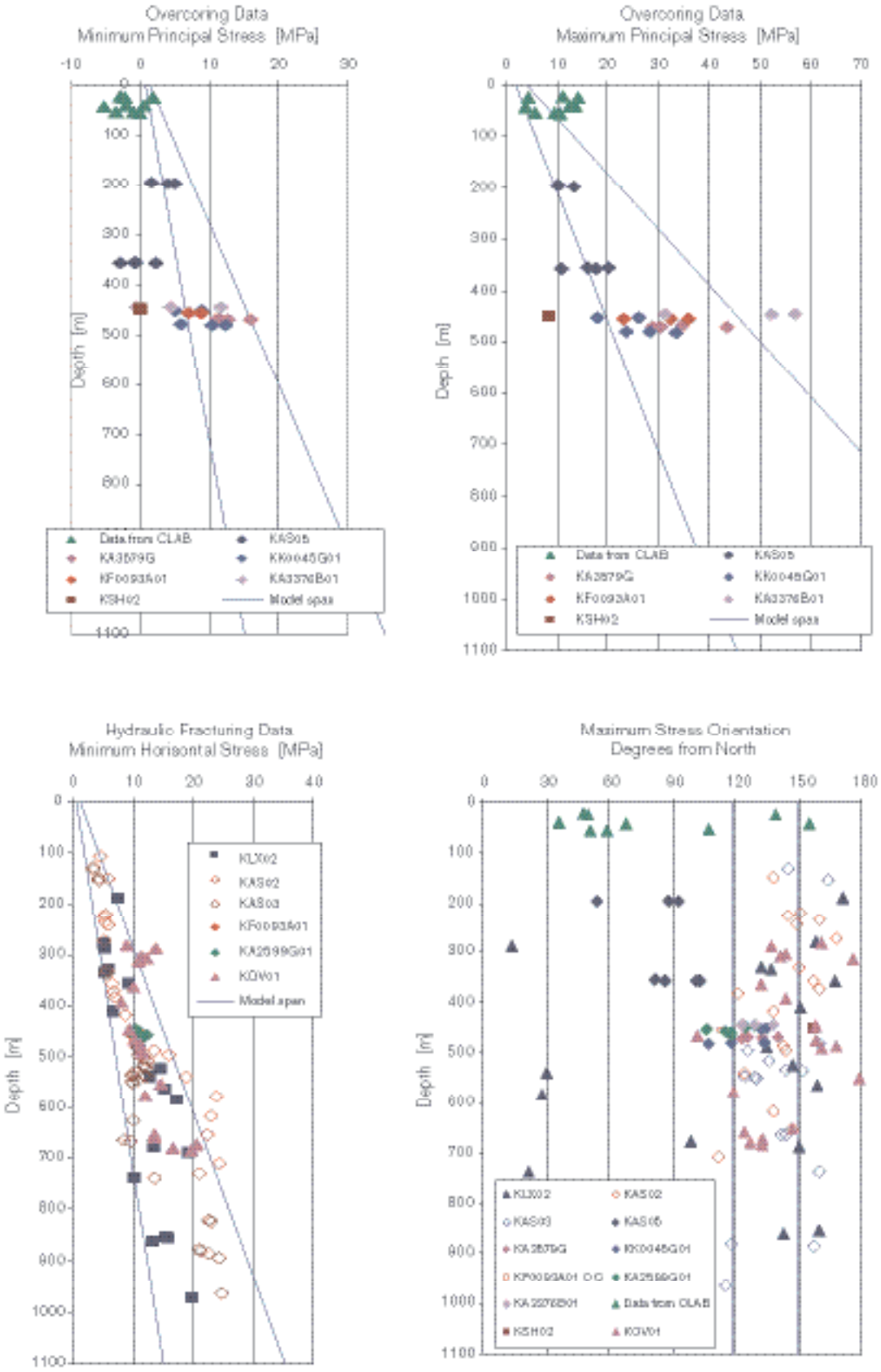

Figure 4-62. *Stress measurement results: From overcoring a) minimum and b) maximum principal stress magnitudes. From hydraulic fracturing c) minimum principal stress. d) Measured orientations for maximum principal stress. Data with romb symbols are from the Äspö HRL.*

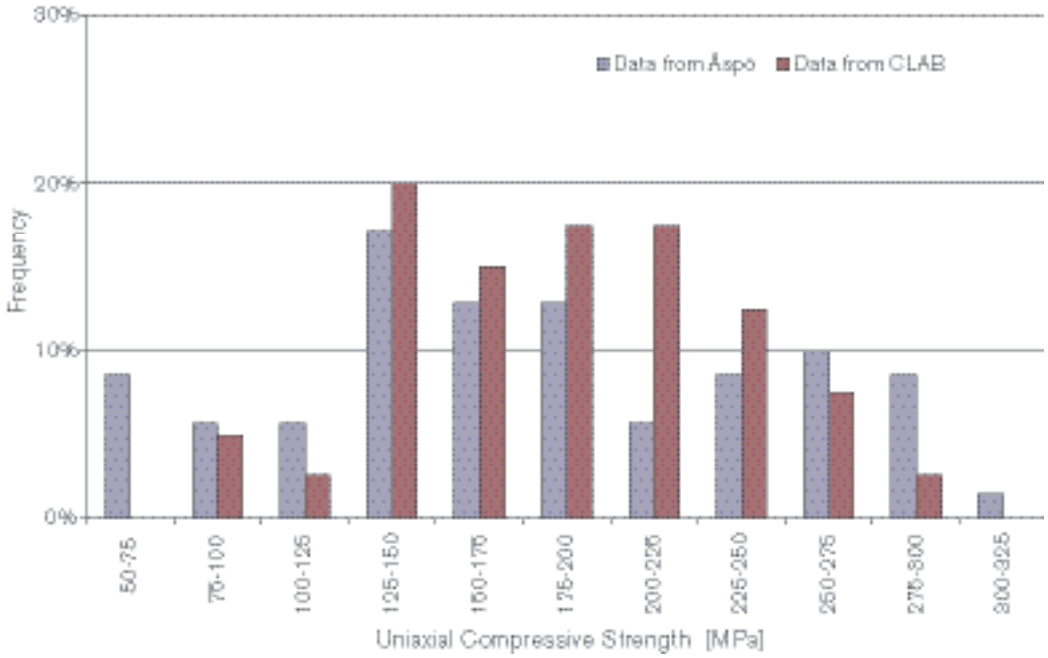

Figure 4-63. *Histogram of the uniaxial compressive strength obtained from loading tests on rock core samples collected at Äspö and CLAB, respectively.*

Table 4-27. Summary of the mechanical properties from uniaxial compressive tests. Data collected from the Äspö laboratory /SICADA/ and CLAB /Moberg et al, 1995/.

	No. of samples	Mechanical property	Minimum	Mean	Maximum	Standard deviation
Data from Äspö	70	UCS [MPa]	52	183	348	72
	58	E* [GPa]	15	64	80	16
	42	v* [–]	0.15	0.23	0.29	0.03
Data from CLAB	40	UCS [MPa]	77	187	284	49
	4	E [GPa]	87	92	97	5
	1	v [–]	–	0.27	–	–
All data	110	UCS [MPa]	52	184	348	64
	62	E [GPa]	15	66	80	17
	43	v [–]	0.15	0.23	0.29	0.03

* Values from uniaxial compressive tests.

Table 4-28. Summary of the uniaxial compressive strength estimated from Schmidt hammer tests /Chryssanthakis, 2003/ The values are obtained through an empirical relation with the rebound of the Schmidt hammer and the density of the rock.

Rock type	No. of samples	UCS, Mean [MPa]	Standard dev. [MPa]	UCS, Minimum [MPa]	UCS, Maximum [MPa]
Ävrö granite	5	183	15	170	208
Fine-grained dioritoid	8	174	11	158	183
Quartz monzodiorite	5	180	15	158	196
Diorite-gabbro	9	167	21	134	195
All rock types	27	174	16	134	208

Tensile strength tests have not been performed from the new boreholes in the subarea. However, the results from tests performed at the Äspö laboratory, using the so called Brazilian test, have been collected from SICADA (Table 4-29). These test results have been used for the estimation of the intact rock tensile strength, cf. Section 5.2.

Table 4-29. Summary of the mechanical properties from indirect tensile tests.

Boreholes	Total no. of samples	Mean Tensile Strength [MPa]	Standard Deviation	Minimum	Maximum
KA3376B01 KA3545G KQ0064G01	11	14.8	1.25	12.9	16.5

4.6.2 Mechanical tests on fracture samples

Fracture samples were collected approximately each 18–20 m along the core of borehole KSH01A /Chryssanthakis, 2003/. Three tilt tests were performed on each sample and three roughness profiles were measured at the same time. No obvious differences between fracture sets along the borehole could be observed. Table 4-30 summarises the results.

Table 4-30. Tilt tests on fractures from KSH01A, from /Chryssanthakis, 2003/.

	Number of samples	Basic friction angle [°]	JRC0 (100 mm)	JCS0 (100 mm)	Residual friction angle [°]
Mean values for all fractures	51	31	6.0	79	27

4.6.3 Rock mechanical interpretation of borehole data

Two empirical classification schemes, for determining Q and RMR indexes, have been applied to data from borehole KSH01A. The details of these two well-known schemes are further described in /Röshoff et al, 2002/. The results from the classification based on the data from Boremap logging, are given in Figure 4-64. In this figure the mean values for each 5 m section along the borehole, using both Q and RMR systems, are shown. The UCS values used for the intact rock in the classifications were: minimum 75 MPa, average 185 MPa and maximum 300 MPa, respectively (cf. Figure 4-63).

It can seem noted that both Q and RMR indicate that the rock mass of the borehole mainly falls in the rock mass quality classes “fair” to “very good” rock (since the ranges of quality classes are not the same for the two systems the classes are not directly comparable). In the centre column of Figure 4-64 the division of the borehole into units with similar geological conditions (presented in Section 4.4), is shown for comparison. It is noted from the Q-values that at depth, where Ävrö granite starts to dominate (units C and D in the geological single-hole interpretation, c.f. Section 4.4.5), the rock quality improves. Parallel to this classification, the core from KSH01A was also classified directly by /Barton, 2003/ (without the use of Boremap data). Table 4-31 and Table 4-32 show the resulting Q-values for the more intact parts of the core and for the fractured zones, respectively. A UCS value of 200 MPa was assumed, for the whole borehole, in the estimations of Young’s modulus, also shown in the tables (See further Section 5.2).

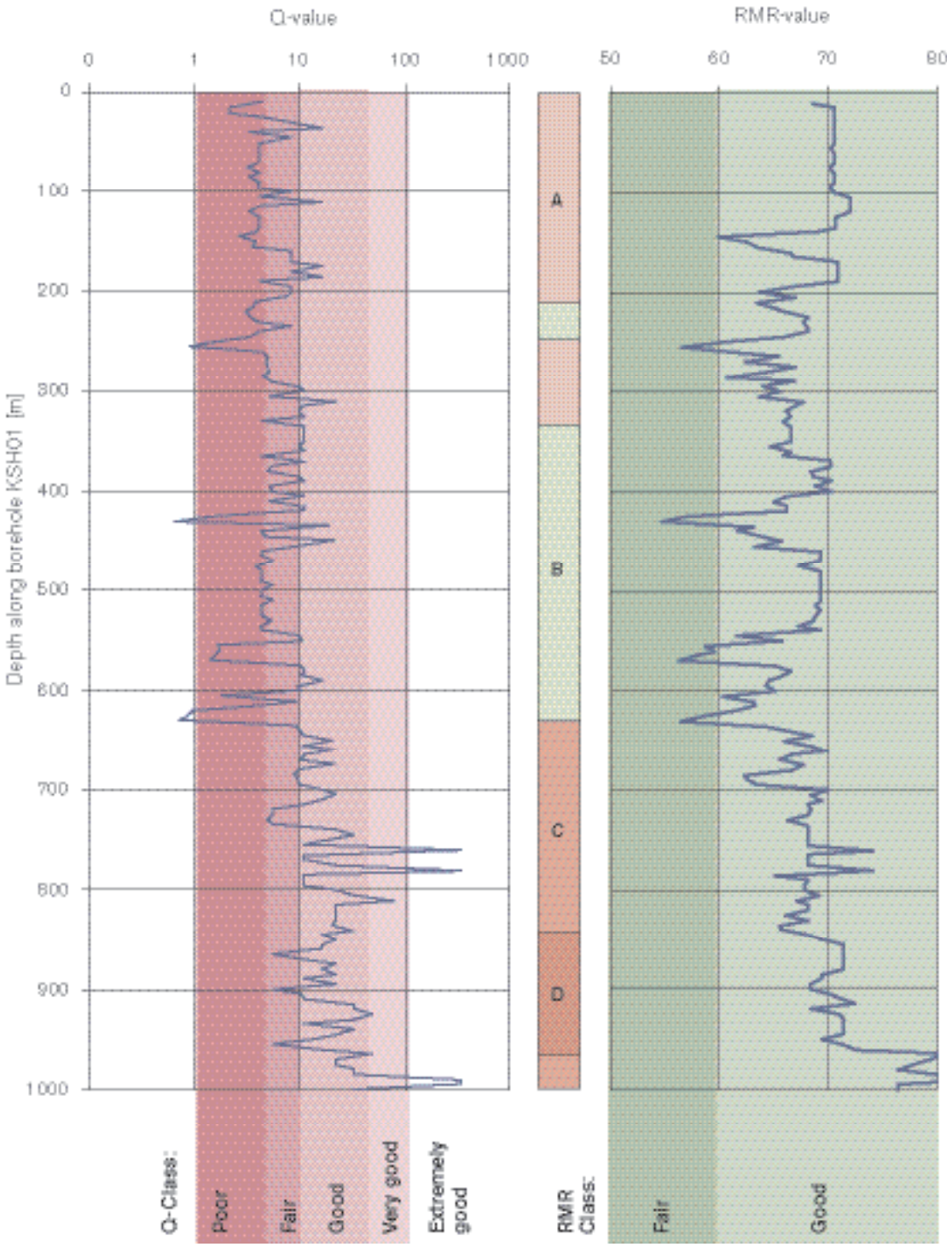

Figure 4-64. *Rock mass rating results along borehole KSH01A using the empirical methods Q and RMR. The classification was performed based on the results from Boremap logging of the drill core, i.e. from the logging results stored in SICADA and without the core itself. In the middle of the figure the result from the geological single hole interpretation is given, dividing the core into units A-D in accordance with the single-hole geological interpratation, see Section 4.4.5.*

Table 4-31. Variations of Q with depth for the 'background rock mass' (i.e. 7 fracture zones excluded) in KSH01A /Barton, 2003/ and depth-adjusted estimates of the deformation modulus (E_m), based on the Q values /Barton, in prep/.

Borehole Depth (m)	Q (most frequent)	Q (mean)	Em (most frequent) (GPa)	Em (mean) (GPa)
1.3–100.8	24.8	6.3	45.7	31.6
100.8–199.9	31.4	12.9	52.9	43.7
199.9–302.9	13.9	6.0	48.6	41.1
302.9–398.8	31.4	16.8	57.1	52.5
398.8–500.1	15.8	15.3	55.4	55.0
500.1–600.6	49.5	17.9	68.7	57.1
600.6–699.5	62.7	14.0	71.9	58.4
699.5–798.8	133.0	48.3	83.2	73.0
798.8–901.2	133.0	59.4	83.8	78.2
901.2–1,003.0	150.0	71.7	85.8	77.6

Table 4-32. Q-statistics for the four principal fractured zones identified from Q-parameter changes in KSH01A, and depth-adjusted estimates of E for the rock mass in these zones (E_m), /Barton, 2003/ and /Barton, in prep/.

Fracture Zone Borehole Depth (m)	Q (most frequent)	Q (mean)	Em (most frequent) (GPa)	Em (mean) (GPa)
138.5–154.5	5.3	2.2	36.3	29.7
420–437	3.8	1.4	41.1	36.3
541–570	2.3	1.3	41.7	38.0
619–637	2.7	1.1	46.1	40.4

4.6.4 Rock mechanical interpretation of surface data

The surface rock at ten locations has also been empirically classified with the Q-system /Barton, in prep/. Table 4-33 shows a summary of these results. A general uniformity of rock conditions appears to be the main result of this surface logging. There is also quite good similarity to the general results of the core logging of KSH01A/B close to the ground surface (Figure 4-64, Table 4-31 and Table 4-32). The fractured zones in the core are for obvious reasons not accurately represented (in a statistical sense) in the surface exposures, due to selective erosion of such zones at the surface. There is a great consistency in the number of fracture sets, and the number of sets is considered unusually high (3–4 sets) /Barton, in prep/.

Table 4-33. Summary and comparison of Q-logging results for ten selected surface outcrops, mainly in the eastern part of the Simpevarp subarea /Barton, in prep/.

Location	Qmean	Qmost freq.	Qtypical range
#1, #A, #2, #3, borehole KAV01, ridge, borehole KAV02, Åvrö village	3.4	4.4	0.5–20.0
#4, #5, Åspö tunnel ramp, N road cuts	2.3	3.3	0.4–13.3
#6, coast close to borehole KSH03	2.65	4.2	0.2–20.0
#7, #11, close to borehole KSH01A, and east facing rock cuts	2.26	2.6	0.5–13.3
#8, #9, CLAB ramp, rock cuts at road junction	2.53	3.1	0.4–13.3
#10, road cuts along Kustvägen	2.57	2.2	0.4–13.3

4.7 Thermal properties data evaluation

4.7.1 Measurement of thermal properties

No new results from direct laboratory measurements of thermal properties on samples from Simpevarp are available in this model version. However, tests have been made previously on rock samples from the Äspö area close to the Simpevarp subarea. These results are reported in /Sundberg, 2002/ and /Sundberg, 2003a/ and are used in the modelling described in Section 5.3.

Indirectly, the thermal conductivity may be estimated from the mineral composition or from the rock density /Sundberg, 2003a/. The input data for such estimations are given in the following sections and the method and results are described in Section 5.3.

4.7.2 Calculation of thermal conductivity from mineral composition

The mineral composition of surface and borehole samples from the Simpevarp area has been investigated. The composition of 56 samples from the SICADA database (39 surface samples, 8 samples from KSH01A and 9 additional samples from KSH02) have been used in order to calculate the thermal conductivity.

The chemical composition of the plagioclase and pyroxene that influences the thermal properties is not known. Instead, assumed or typical values for the chemical composition are used /Horai, 1971; Horai and Simmons, 1969; Berman and Brown, 1985/. The sampling was made by the geologists to investigate different variants of the rock units and not to get a mean mineral composition in proportion to the total mass of each rock unit. Therefore the proportions of minerals, as shown by these samples, are not necessarily representative of the mineral composition in the rock on average.

4.7.3 Calculation of thermal properties from density measurements

Correlation has been found between thermal conductivity and rock density for some rock types at the Äspö HRL /Sundberg, 2003a/. Gamma-gamma density logging has been performed in KSH01A /Nielsen and Ringgaard, 2003/ and the result is shown in Figure 4-65.

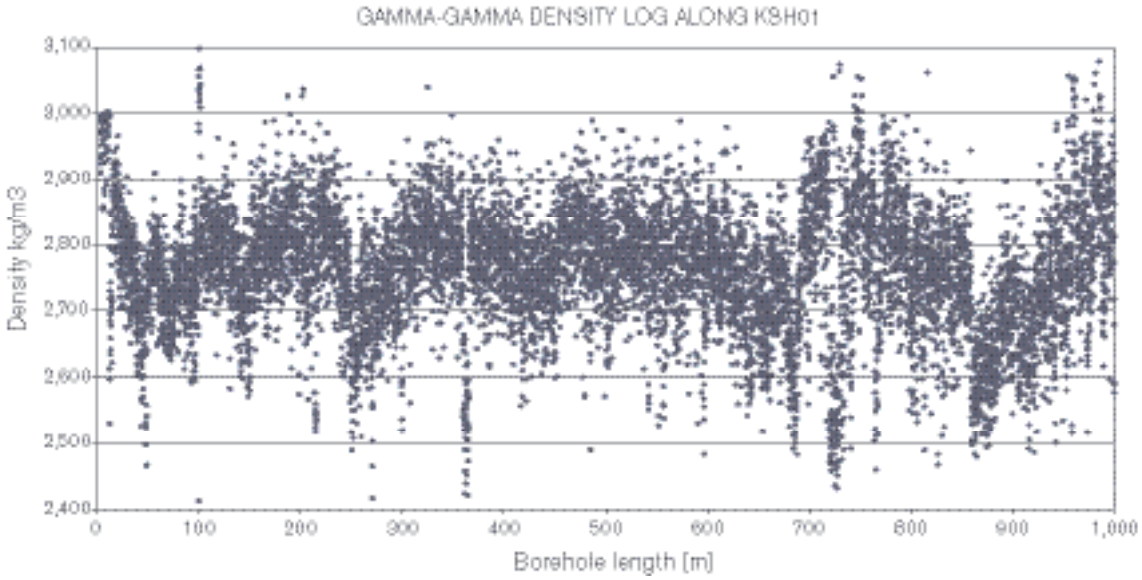

Figure 4-65. *Results from gamma-gamma density logging in borehole KSH01A. Each dot corresponds to a measurement taken at every 0.1 m. The measurement gives an average value for the rock over 0.2 m segment of the borehole /Nielsen and Ringgaard, 2003/.*

4.7.4 Thermal expansion of rock

No measurements have been made on thermal expansion of the rock on samples from the Simpevarp subarea. However, three samples from the Äspö HRL have been tested by /Staub et al, 2004/ and are used in this model version, c.f. Table 4-34.

Table 4-34. Summary of results from thermal expansion tests /Staub et al, 2004/.

Rock Sample location	Rock type	Porosity (%)	Wet density (kg/m³)	Coeff. of thermal expansion, 20–40°C (mm/mm°C)	Coeff. of thermal expansion, 40–60°C (mm/mm°C)	Coeff. of thermal expansion 60–80°C (mm/mm°C)
KQ0064G01 6.60–6.85	Ävrö granite Code 501044	0.35	2,750	7.1E–6	6.0E–6	7.5E–6
KQ0064G01 6.85–7.10	Ävrö granite Code 501044	0.36	2,760	6.7E–6	6.6E–6	7.9E–6
KQ0064G05 5.77–6.01	Ävrö granite Code 501044	0.15	2,750	8.1E–6	6.6E–6	6.7E–6

4.7.5 In-situ temperature

The temperature of the borehole fluid has been logged in KSH01A and KSH02 /Nielsen and Ringgaard, 2003/. The result of the logging in KSH01A is presented in Figure 4-66. The mean gradient over 100 m, successively calculated, is also shown in the figure. It can be notred that the temperature gradient increases with depth from about 13°/km to 16°/km. The temperature logging results from borehole KSH02 are similar to those from KSH01.

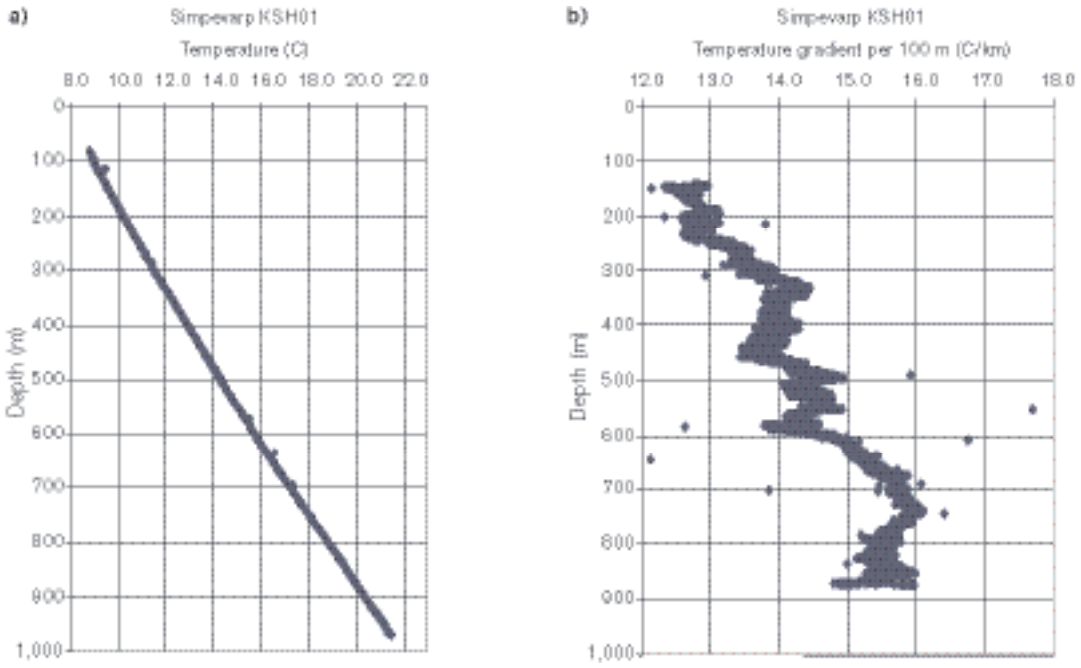

Figure 4-66. *a) Temperature versus depth for borehole KSH01A. b) Temperature gradient calculated per 100 m (approximately) and the corresponding depth for the midpoint of each 100 m interval.*

4.8 Hydrogeochemical data evaluation

This section describes the evaluation of the primary hydrogeochemical data. Most of these data are from waters sampled at various surface locations and in a few boreholes. The evaluation essentially aims at identifying representative datasets which subsequently are used for further analysis and to provide a first conceptualisation of the origin and evolution of the Simpevarp groundwaters.

The dataset available consists in total of 535 water samples /cf. Laaksoharju et al, 2004b/. Samples reflecting surface/near-surface conditions (precipitation, streams, lakes, sea water and shallow waters collected in soil pipes) comprise a total of 419 samples. Of the remainder, 11 samples are from percussion-drilled boreholes and 105 samples from core drilled boreholes; some of these borehole samples represent repeated sampling from the same isolated borehole section or samples of the water column in an open borehole (using a tube sampler). Overall, there is a significant bias at this stage in the site characterisation towards water samples from surface and near-surface environments. Evaluation of the hydrochemical situation at greater depth is restricted to a limited number of borehole sampling points.

In the total dataset, only 86 surface samples, 4 samples from percussion-drilled boreholes and 21 samples from core-drilled boreholes were analysed for all the major elements, stable isotopes and tritium at the time of the "data freeze". This means that only 21% of the samples could be used for more detailed evaluation concerning the origin of the water. How the dataset was used in the different models is described in /Laaksoharju et al, 2004b/.

4.8.1 Surface chemistry data

As noted above, a total of 86 surface water samples were analysed sufficiently enough to be used in the detailed evaluation. Analysed data include: major cations and anions (Na, K, Ca, Mg, Si, Cl, HCO_3^-, SO_4^{2-}, S^{2-}), trace components (Br, F, Fe, Mn, Li, Sr, DOC, N, PO_4^{3-}, U, Th, Sc, Rb, In, Cs, Ba, Tl, Y and REEs) and stable (^{18}O, ^{2}H, ^{13}C, ^{37}Cl, ^{34}S, ^{10}B) and radiogenic (^{3}H, ^{14}C, ^{226}Ra, ^{228}Ra, ^{222}Rn, ^{238}U, ^{235}U, ^{234}U, ^{232}Th, ^{230}Th and ^{228}Th) isotopes, but only for some samples. In addition, for some samples there are data on nutrients and organics including NH_4, NO_2, NO_3, N_{Tot}, P_{Tot}, PO_4, poP (particulate organic P), poN (particulate organic N), poC (particulate organic C), Chlorophyll A, Chlorophyll C, Pheopigment, TOC, DOC, DIC and O_2. Water temperature, pH, conductivity, salinity, turbidity and oxygen concentration values were determined at the nearby chemical laboratory of the Äspö HRL shortly after sampling. There are no measured Eh and temperature values. The surface sampling locations are shown in Figure 4-67.

4.8.2 Chemistry data from borehole samples

Two cored boreholes have been sampled, KSH01 and KSH02. With respect to nomenclature, the first 100 m of each borehole (the initial percussion drilled portion) is referred to as 'B' (i.e. KSH01B and KSH02B) and from 100 m to the hole bottom (by core drilling) is referred to as 'A' (i.e. KSH01A and KSH02A). Since all hydrogeochemical data originate from the cored borehole length, all references in the text are to KAS01A and KSH02A.

The borehole sampling locations in the Simpevarp area are shown in Figure 4-68 and the sampling and analytical data have been reported for the groundwaters by /Wacker, 2003/. In the data evaluation 116 groundwater samples have been used. The analytical programme included: major cations and anions (Na, K, Ca, Mg, Si, Cl, HCO_3^- SO_4^{2-}, S^{2-}), trace elements (Br, F, Fe, Mn, Li, Sr, DOC, N, PO_4^{3-}, U, Th, Sc, Rb, In, Cs, Ba, Tl, Y and REEs) and stable (^{18}O, ^{2}H, ^{13}C, ^{37}Cl, ^{10}B, ^{34}S) and radioactive (^{3}H, ^{226}Ra, ^{228}Ra, ^{222}Rn, ^{238}U, ^{235}U, ^{234}U, ^{232}Th, ^{230}Th and ^{228}Th) isotopes. Note that the samples had not been analysed for all these elements at the time of the "data freeze" /cf. Laaksoharju et al, 2004b/.

The various results obtained with different analytical techniques for Fe and S have been confirmed with speciation-solubility calculations and checks of their effect on the charge balance. The values selected for modelling were those obtained by ion chromatography (SO_4^{2-}) and spectrophotometry (Fe), assuming no colloidal contribution. The selected pH and Eh values correspond to available downhole data /cf. Laaksoharju et al, 2004b/.

Figure 4-67. *Surface water sampling locations in the Simpevarp area.*

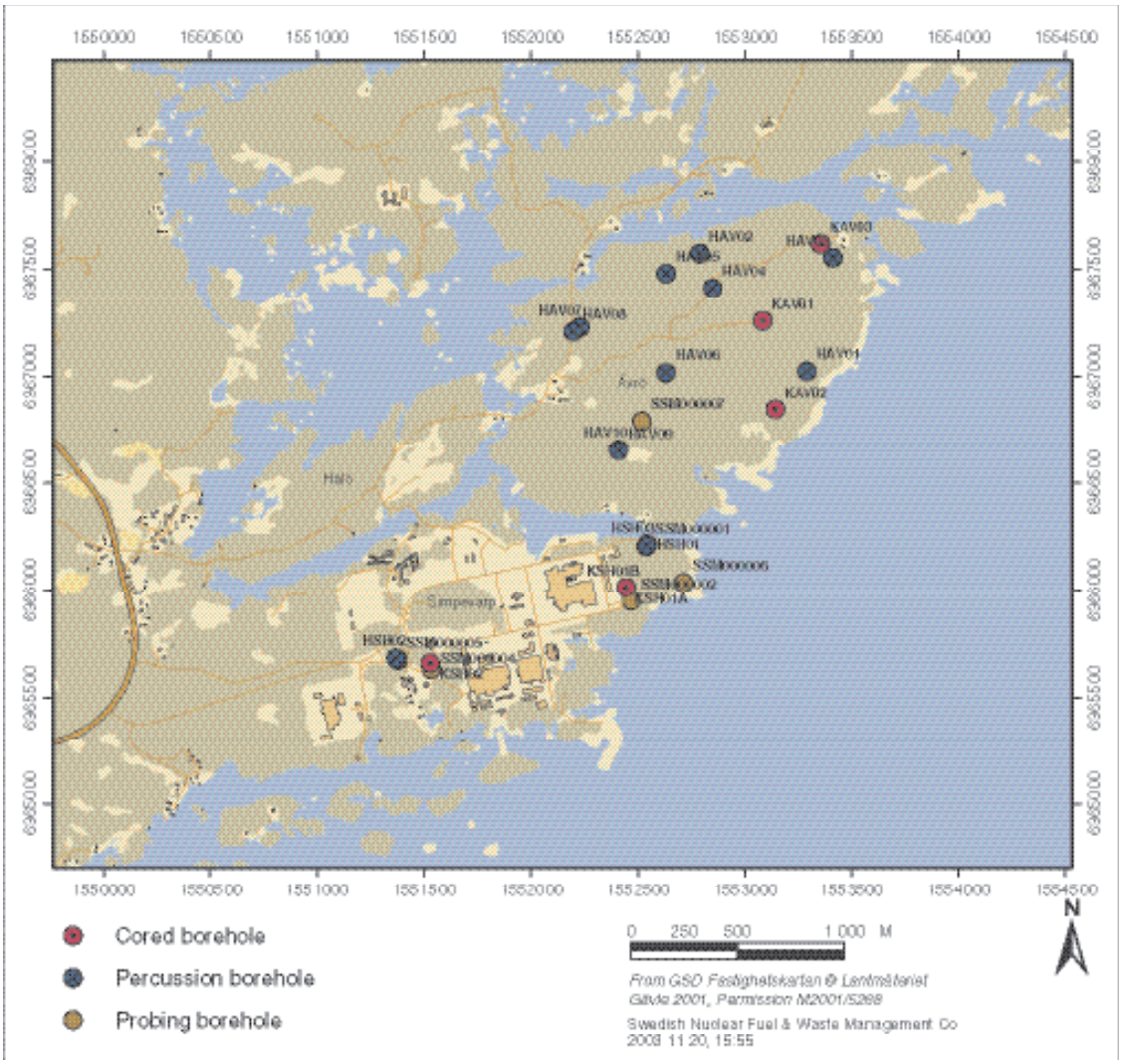

Figure 4-68. *The sampling locations for groundwater in the Simpevarp subarea.*

4.8.3 Representativity of the analysed data

By definition, a high quality sample is considered to be that which best reflects the undisturbed hydrological and geochemical *in-situ* conditions for the sampled location or borehole section. A low quality sample may contain *in-situ*, on-line, at-line, on-site or off-site errors such as contamination from tubes of varying composition, air contamination, losses or uptake of CO_2, long storage times prior to analysis, analytical errors etc. The quality may also be influenced by the rationale in locating the borehole and selecting the sampling points. Some errors are easily avoided, others are difficult or impossible to avoid. Furthermore, chemical responses to these influences are sometimes, but not always, apparent.

A sampling and analytical protocol is established prior to each sampling campaign. This protocol is based on established sampling routines or special requirements associated with the sampling campaign. The sampling and analytical protocols used in the sampling campaigns for the Simpevarp subarea are described by /Wacker, 2003/. The analytical precision for the major components: Na, K, Ca, Mg, HCO_3, Cl and SO_4 was checked by ion balance calculation, in which the difference between the anions and cations was calculated. The charge balance calculated for 326 surface samples (made both manually and through speciation-solubility calculations with PHREEQ-C for all the samples) indicates that half of the samples show errors within the range of ± 10%; only these samples were used in the detailed modelling. The calculated charge balances for the 25 groundwater samples with complete analytical data indicate that the error is almost always in the range ± 5%. Only samples 5177 and 5174 from borehole KSH01A fall outside this range, with errors of +8.46% and +16.91%, respectively.

The pre-sampling Chemac in-situ monitoring data for O_2, Eh, electrical conductivity and temperature are available for borehole KSH01A but not for KSH02. Additional information requested and received included the actual sampling dates of the groundwater samples tabulated in the database received for evaluation, and also included the range of data from which the tabulated values were selected. Only some on-line monitored *in-situ* field pH values were measured; most recorded values are laboratory-derived and lie about 0.6 pH units below the *in-situ* values.

Based on flushing water content, borehole activities and subsequent data evaluation a detailed assessment of the representativeness of borehole data is presented in /Laaksoharju et al, 2004b/. As a general conclusion, the open hole tube samples are not representative for the KSH01A borehole and should be discarded. The sections KSH01A:156.50–167.00 m and KSH01A: 245.00–261.50 m were considered representative. The sections KSH02:6.65–100.50 m and 739.0–755.0 m were regarded as not representative, whereas the section KSH02: 411.85–467.07 m can be considered as fairly representative.

The drilling event is considered to be the major source for contamination of the formation groundwater. During drilling, large hydraulic pressure differences may occur due to uplifting/lowering of the equipment, pumping and injection of drilling fluids. These events can facilitate unwanted mixing and contamination of the groundwater in the fractures, or the cutting at the drilling head itself can change the local hydraulic properties of the fractures intercepted by the borehole. It is, therefore, of major importance to analyse events during the drilling in detail. From this information not only the uranine-spiked drilling water can be traced, but also the major risks of contamination and disturbance from foreign water volumes can be directly identified. The effects of too low or excessive extraction of water from a fracture zone prior to sampling can be calculated by applying the DIS (Drilling Impact Study) modelling concept /Gurban and Laaksoharju, 2002/.

Hydraulically active fracture zones in two isolated sections in borehole KSH01A were the subject of DIS modelling (156.5–167 m and 245–261.5 m). The modelling carried out for these fracture zones was based on the Posiva differential flow meter logging (PFL) with the main aim of modelling the amount of the contamination (Figure 4-69) for each fracture zone /cf. Laaksoharju et al, 2004b/.

For section KSH01A:156.5–167 m, the DIS calculations show that the section was contaminated with 21.22 m^3 of “foreign water”, of which a maximum of 5% consisted of drilling water consumed when penetrating this section. Subsequent drilling activities could potentially have increased the amount of contamination, due to the relatively high hydraulic conductivity of the section. The results from the pumping and sampling show 3.7% remaining drilling water in the first sample at the start of pumping, and 2.39% remaining drilling water in the final sample during pumping. The duration of the pumping was from 28.03.2003 to 30.04.2003 (600 hours), with an average flow rate 200 mL/min /Wacker, pers. comm. 2003/. The volume removed was calculated at 7.2 m^3 of drilling water mixed with groundwater. This can be compared with the maximum 21.22 m^3 volume of foreign water that contaminated the section in question. The average amount of drilling water remaining in the fracture system connecting to the section is therefore 14 m^3. The sampling showed a drilling water content of 2.39% after some 600 hours of pumping. The DIS calculations show that the pumping should have continued further in order to remove the remaining 14 m^3. After some 49 days at a pump rate of 200 ml/min the drilling water would theoretically be removed entirely.

For section KSH01A:234–261.5 m, the calculations show that the section was contaminated during the drilling with 54.47 m^3 of “foreign water” of which a maximum of 18% consisted of drilling water. As stated above, subsequent drilling activities could have increased the amount of contamination, due to the relatively high hydraulic conductivity of the section. The results from the sampling show 8.02% drilling water in the last sample. The duration of the pumping was from 24.04.2003 to 20.5.2003 (some 900 hours), with an average flow rate of 200 ml/min. The volume removed was calculated to be, 10.9 m^3 of drilling water mixed with groundwater. This can be compared with the maximum volume of 54.47 m^3 foreign water that contaminated the section. The sampling showed a drilling water content of 8.02% after 912 hours of pumping. The DIS calculations show that the pumping should have continued further in order to remove the remaining 43.5 m^3. In the future, the DIS calculations should be performed prior to sampling in order to support and guide the on-going sampling programme.

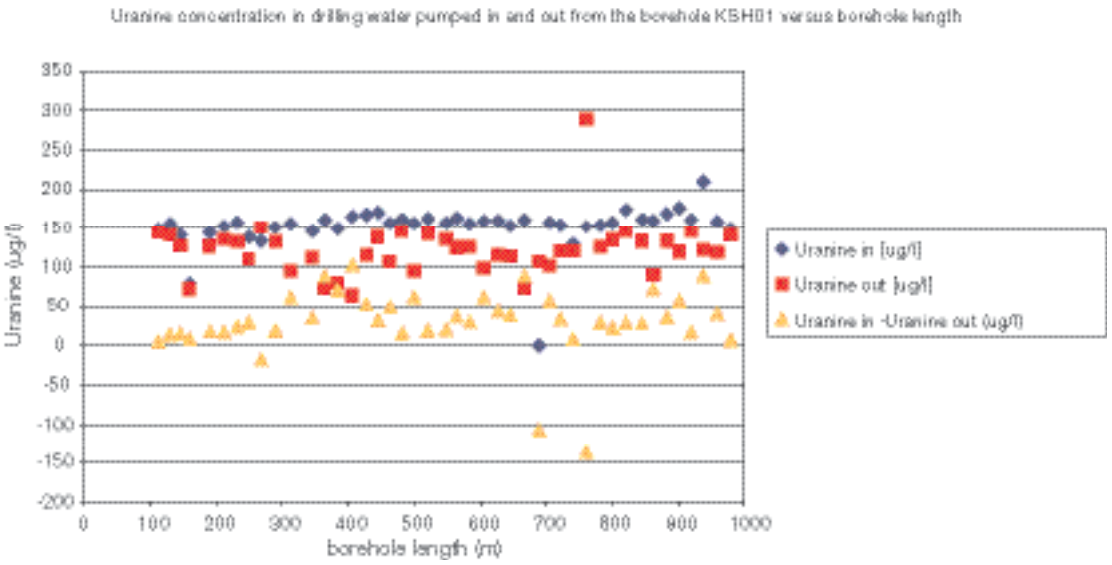

Figure 4-69. *Concentration of added tracer to drilling water (Uranine) in pumped in and pumped out water from borehole KSH01A.*

4.8.4 Exploratory analysis

One fundamental question in modelling is whether uncertainties associated with the data lead to a risk of misunderstanding the information therein. Generally, the uncertainties from the analytical measurements are lower than the uncertainties associated with the modelling, but the variability observed during sampling is generally higher than the modeling uncertainties.

A commonly used approach in groundwater modelling is to start the evaluation by exploratory analysis of different groundwater variables and properties. The degree of mixing, the type of reactions and the origin and evolution of the groundwater can be evaluated by applying such analysis. Of major importance is also to relate, as far as possible, the sampled groundwater to the near-vicinity geology and hydrogeology.

Because of incomplete data, or data below detection limits, or suspect values at the time of the 'data freeze', evaluation of, e.g. the radiogenic isotopes, ^{87}Sr, ^{10}B, REEs and other trace elements, have not been included in the current Simpevarp 1.1 modelling.

Evaluation of scatter plots

The hydrochemical data have been expressed in several X-Y plots to derive trends that may facilitate interpretation. Since chloride is generally conservative in normal groundwater systems, its use is appropriate to study hydrochemical evolution trends when coupled to ions, both conservative and non-conservative, to provide information on mixing, dilution, chemical sources/sinks etc. Many of the X-Y scatter plots therefore involve chloride as one of the variables. The following is a preliminary evaluation of the various geochemical and isotopic trends apparent in the Simpevarp groundwaters. A more detailed evaluation of the major components and isotopes can be found in /Laaksoharju et al, 2004b/.

Evaluation of the hydrogeochemical data considers all sampled locations jointly in order to understand the overall large-scale dynamics and evolution of the groundwater system. However, since the most quantitative hydrogeochemical data are from two borehole sections in KSH01A with Class 5 (a higher class of a sample indicates a more extensive analytical program, for details see /Smellie et al, 2002/) data located at 156.50–167.00 m and 245.00–261.50 m, respectively, Class 3 data from one section at 197.00–313.42 m, and Class 3 data from one section in borehole KSH02A at 411.85–457.50 m, these data provide the main focus of the hydrogeochemical evaluation. Although considered unrepresentative, the open hole tube sampling data are also included for completeness, but will be omitted in the next modelling phase. The following discussions therefore relate only to groundwater samples obtained from specified packed-off borehole sections.

General comparison of Cl vs depth with results from other sites

Considering samples from KSH01A (156.50–167.00 m and 245.00–261.00 m) and KSH02A (411.85–467.07 m), chloride increases from ~5,500 to ~6,400 mg/L over this depth interval. At shallower depths chloride ranges from ~12 to ~ 55 mg/L which reflects the composition of the drilling water extracted from open percussion-drilled boreholes HSH03 and HSH02, respectively. Comparison with data from the Forsmark, Laxemar and Olkiluoto (Finland) sites, c.f. Figure 4-70, is shown in Figure 4-71. It may be argued that such a comparison should be treated with caution since Forsmark and Olkiluoto are geographically distant, have had a somewhat different palaeo-evolution and represent different hydrogeological regimes. Furthermore, Laxemar, although close by, represents more a mainland environment and involves greater depths. However, since the Fennoscandian basement hydrogeochemistry probably shares general similarities irrespective of geographic location, Figure 4-71 may serve a useful purpose, particularly with respect to establishing whether a Littorina component is present in the Simpevarp groundwaters.

The Laxemar data show dilute groundwater extending to approximately 600 m depth in KLX01, and in the case of KLX02 to around 1,000 m before a rapid increase in salinity to maximum values of around 47 g/L Cl at 1,700 m. Olkiluoto shows an initial sharp increase in chloride at around

Figure 4-70. *Geographical locations of the Simpevarp/Laxemar, Forsmark and Olkiluoto sites.*

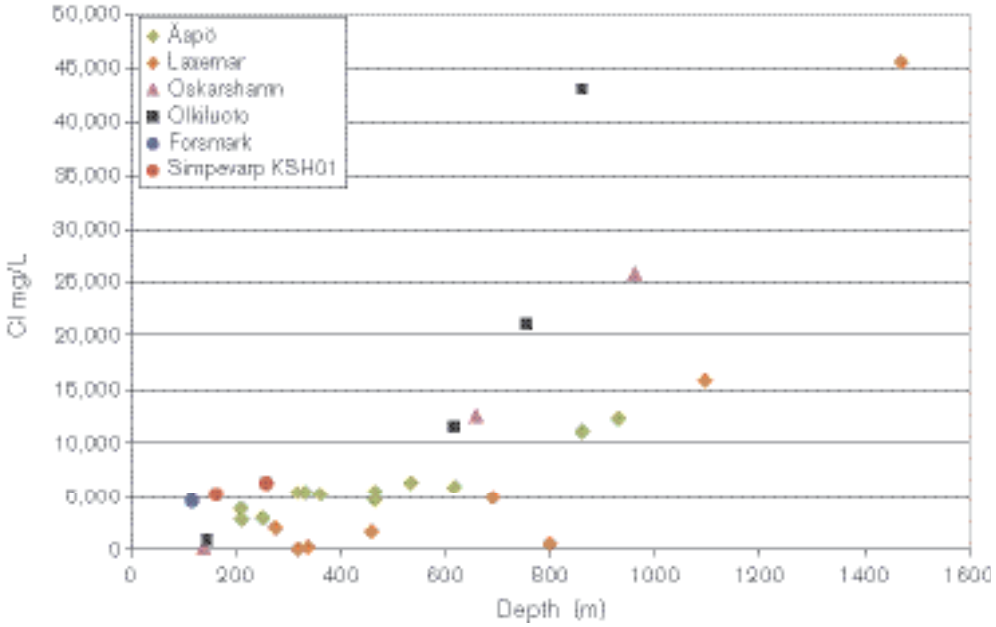

Figure 4-71. *Comparison of chloride vs. depth using data from Simpevarp (KSH01A), Forsmark, Laxemar, Äspö, Olkiluoto and an experimental borehole in Oskarshamn (KOV01).*

600 m with a levelling off at 5 g/L Cl which continues to 450 m; from which there is a relatively steady increase to values of around 20 g/L Cl at 900 m depth (a maximum value of 44 g/L Cl was recorded). The available Forsmark data show a close similarity to the initial Olkiluoto trends, and the Simpevarp data, whilst also limited, also fall along the general plateau ranging from around 5.1–6.3 g/L Cl. For the future, it will be interesting to see whether Simpevarp will follow the same rapid increase in salinity with increasing depth as at Olkiluoto and Laxemar. In common with the Forsmark data, an initial observation at this juncture is that the levelling out at 5 g/L Cl at Olkiluoto has been interpreted as possibly reflecting a Littorina Sea water component. Whether this may also be the situation at Simpevarp is further discussed below.

pH vs Cl for all Simpevarp data

Superficial fresh waters show a wide range of pH values as a consequence of their multiple origins (Figure 4-72). The lowest values are associated with waters with a marked influence of atmospheric and biogenic CO_2; the highest values are associated with the most diluted groundwater samples from percussion boreholes. Overall this gives a decreasing trend with chloride when the rest of the groundwater samples are taken into account. However, this trend is partially defined by contaminated samples and affected by uncertainties of pH measurements in the laboratory, so it should be interpreted with care.

/Laaksoharju et al, 2004b/ presents an analysis of the uncertainties associated with pH values. Broadly speaking, the main features of the trend in pH can be correlated with other Fennoscandian sites with similar waters (e.g. Äspö and Olkiluoto; /Laaksoharju and Wallin, 1997/ and /Pitkänen et al, 1999/ respectively) also affected by uncertainties in pH /e.g. Pitkänen et al, 1999/.

Alkalinity vs Cl for all Simpevarp data

Alkalinity, or more specifically, (HCO_3^-) is, together with chloride and sulphate, the third major anion in the system, being the most abundant in the non-saline waters. Its concentration increases to equilibrium with calcite in surface waters as a result of weathering; then it decreases dramatically as a result of mixing and calcite precipitation (Figure 4-73). It is worth noting that the samples contaminated with flushing water (pale red circles dubbed “uncertain” in Figure 4-73a) fit very well the trend defined by the rest of the samples. This alkalinity trend is similar to that observed at the nearby sites Äspö and Oskarshamn (borehole KOV01) (e.g. Figure 4-73b).

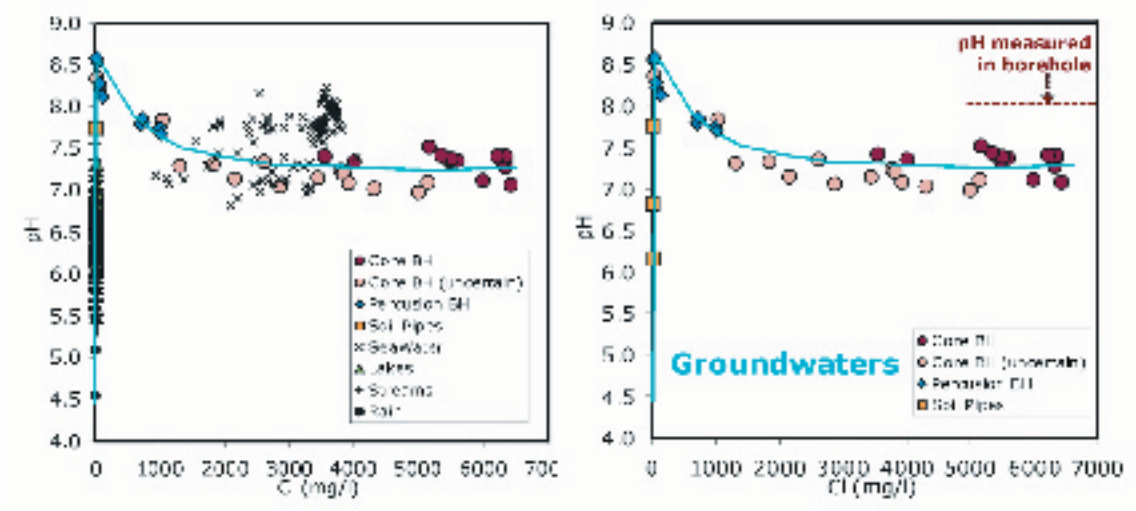

Figure 4-72. *pH vs. chloride content (increasing with depth) in the Simpevarp waters.*

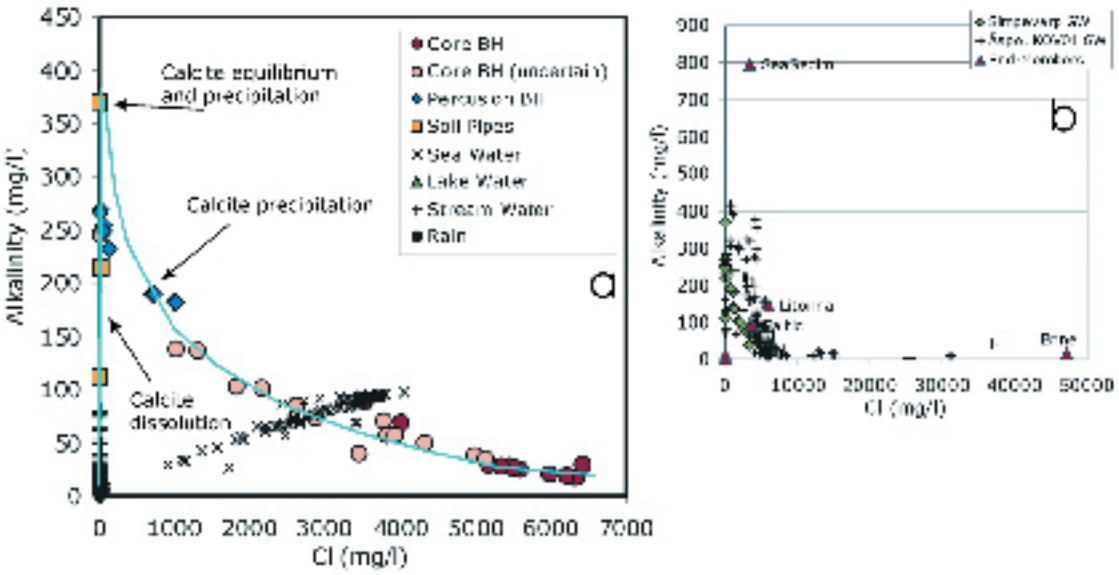

Figure 4-73. *Alkalinity vs. Cl in water for all Simpevarp data (a) and comparison with Äspö and Oskarshamn (b). Figure (b) also indicates the main end members for the Simpevarp area, i.e. Sea Sediment, Brine, Littorina, Baltic and modern Meteoric (Lakes, Streams, Precipitation) unnamed symbols at the origo of the diagram.*

SO_4 vs Cl for all Simpevarp data

Figure 4-74, showing SO_4 vs Cl, indicates an obvious modern Baltic Sea water dilution trend with the cored borehole samples possibly representing a separate saline dilution trend, although there are inadequate data at this stage to be more specific. The reliable sulphate values for borehole KSH01A are generally low (32–51 mg/L) and show no correlation with Cl; Borehole KSH02A contains greater amounts of SO_4 (177 mg/L) but this may be a function of increasing sulphate with depth (in conformity with the Äspö data). The sulphur isotope data /cf. Laaksoharju et al, 2004b/ support a marine origin for the sulphate in the two sampled sections in borehole KSH01A. However, the SO_4/Cl ratio is much too low to be representative of a Littorina Sea water, and later modification caused by sulphate-reducing bacteria is thought to have caused the observed increase in sulphur isotope ratios.

In general, these data for the representative groundwaters from the cored borehole lend support to an absence of a significant postglacial marine component, instead suggesting mixing with deeper, more saline waters of a non-marine origin.

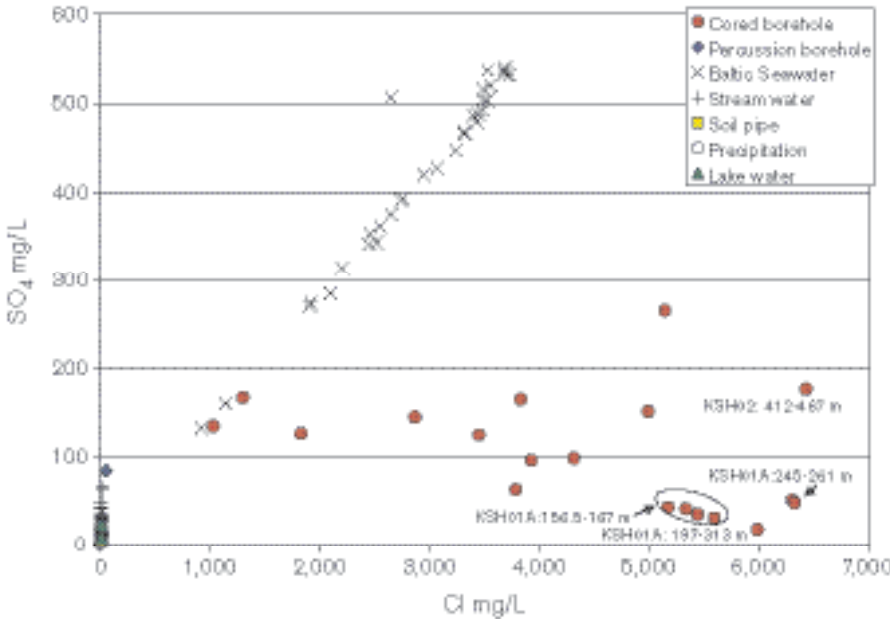

Figure 4-74. *Plot of SO_4 vs Cl for all Simpevarp data. (Note: Cored borehole samples not labelled represent open hole mixing and should be ignored).*

Comparing all the Simpevarp SO_4 vs Cl data with the Forsmark site (Figure 4-75) further underlines the distinction between Forsmark, characterised by a strong marine (Baltic Sea plus Littorina Sea) signature, and Simpevarp which trends towards a non-marine or mixed non-marine/marine signature.

Mg vs Cl for all Simpevarp data and comparison with other Swedish sites

Figure 4-76 (also c.f. Figure 4-68) shows, in common with Figure 4-75, two clear observations/ distinctions: a) an obvious modern Baltic Sea water dilution trend, and b) a clear isolated "borehole groundwater" grouping, probably forming part of a different saline dilution trend that may become more evident with additional future data. Borehole KSH02 (411.85–457.07 m) has a significantly lower Mg content (10 mg/L at 6,426 mg/L Cl) than the three KSH01A samples.

With respect to the modern Baltic Sea water dilution trend, the plotted data generally show a large spread to more dilute mixing compositions, and extreme examples exist where only small amounts of Cl are present. Because of this mixing there is no distinct clustering of the data that would indicate a representative Baltic Sea composition, although a small concentration of values occurs between 3,300 and 3,700 mg/L Cl.

According to /Ericsson and Engdahl, 2004/, two distinct environments have been sampled for 'Baltic Sea' water; one close to the open sea with only a few small surrounding islands (locations PSM002060/61), and that situated close to the mainland, surrounded by large islands and more subject to dilution from seasonal run-off effects from the mainland (PSM002062/64). This would explain the nature of the Baltic Sea dilution line and also may explain the three anomalous samples around 2,500 mg/L Cl (from localities PSM002060/61).

A further observation from Figure 4-76 is the spread of Mg values at low Cl contents for the samples from Soil Pipes (0.91–5.37 mg/L). This may reflect: a) contact with an older marine water followed by cation exchange reactions and subsequent flushing out of chloride, or b) water-rock interaction of recharge with minerals in the soil.

There is no indication from these borehole data of a significant Littorina Sea component; for example the Mg values are too low (10–72 mg/L) compared to the estimated values for the Littorina Sea composition (Mg ~448 mg/L; Cl ~6,500 mg/L) as derived by /Pitkänen et al, 1999/.

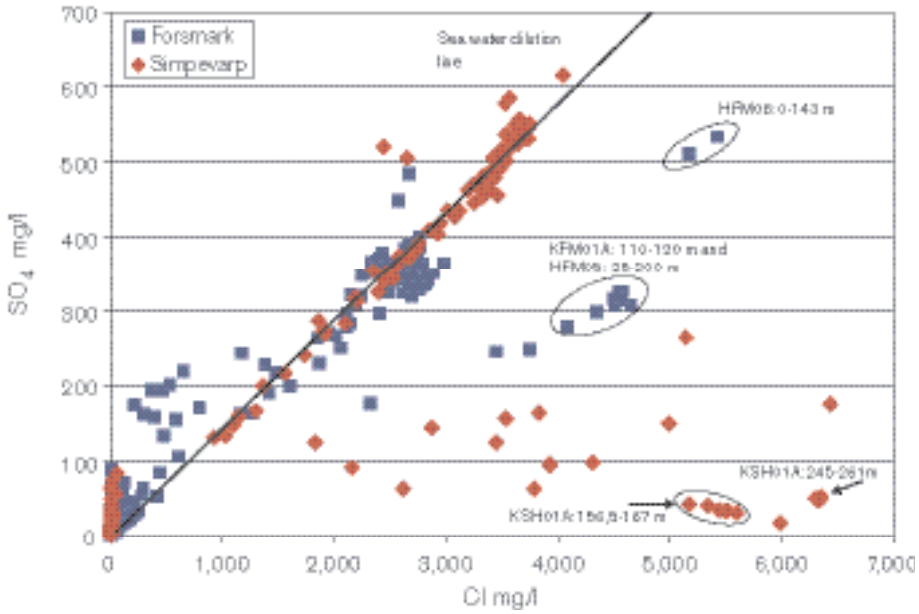

Figure 4-75. *Plot comparing all Simpevarp SO_4 vs Cl data with corresponding data from the Forsmark site.*

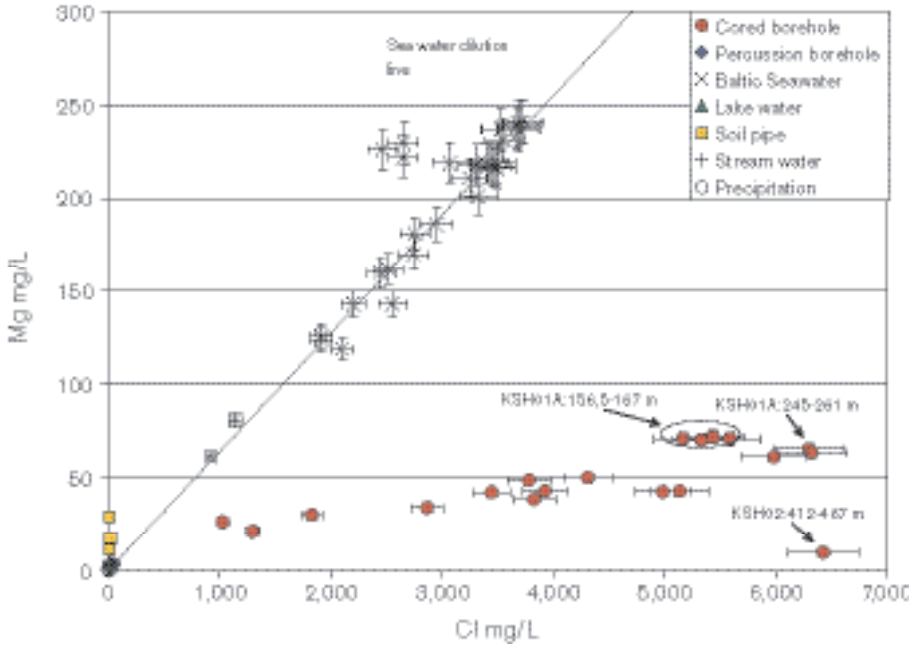

Figure 4-76. *Plot of Mg vs Cl for all Simpevarp data including analytical error bars ±5%. (Note: Cored borehole samples not labelled represent open hole mixing and should be ignored).*

Ca/Mg vs Br/Cl comparing all Simpevarp data with other Fennoscandian sites

By plotting Ca/Mg vs. Br/Cl, Figure 4-77 provides an opportunity to indicate those data of marine origin versus data with a non-marine or a non-marine/marine mixing origin. For comparison, the Simpevarp data have been plotted with data for other Fennoscandian sites (Finnsjön, SFR, Forsmark, Äspö, Laxemar, Olkiluoto and Stripa). The Yellowknife-Thompson data have been included because they represent highly evolved basement brines in Canada (Northwest Territories) where a significant marine component is unlikely.

The figure shows clearly the clustering of modern Baltic Sea water data; these values can be compared to the other extreme, the Stripa groundwaters, which are considered to be more representative of a non-marine origin since this area was not transgressed by the Littorina Sea or subsequent transgressions /Nordstrom et al, 1985/. Between these two extremes fall the range of Finnsjön and Äspö groundwaters considered to have a marine component of varying amounts /Smellie and Wikberg, 1991; Laaksoharju et al, 1999a/, and the Olkiluoto groundwaters which trend to a less marine component at greater depths /Pitkänen et al, 1999/. The Laxemar data, of deep basement origin, plot off the diagram, further emphasising their non-marine character. The Forsmark borehole groundwaters cluster toward a dominant marine component, more similar to the SFR data than the Finnsjön groundwaters, although the Forsmark samples from the cored borehole do extend towards a slightly less marine component.

The groundwater data from cored boreholes at Simpevarp plot well within the range of the Äspö HRL samples, suggesting a more non-marine signature when compared with the data from Simpevarp percussion-drilled boreholes and the Forsmark waters. A more non-marine Simpevarp signature is further supported by plotting Br vs Cl /cf. Laaksoharju et al, 2004b/.

Na vs Cl for all Simpevarp data

Sodium shows a positive and very good linear correlation with chloride concentration (Figure 4-78a), which reflects that mixing is the main process controlling the Na content. The deviation of representative groundwater samples from the sea water dilution line can be interpreted as a small influence of the saline end member or as Na removal due to cation exchange reactions.

Sodium contents and the trend of the representative cored borehole samples fit fairly well with the less saline Äspö and KOV01 data set (Figure 4-78b) although they seem to be more enriched in Na in Simpevarp.

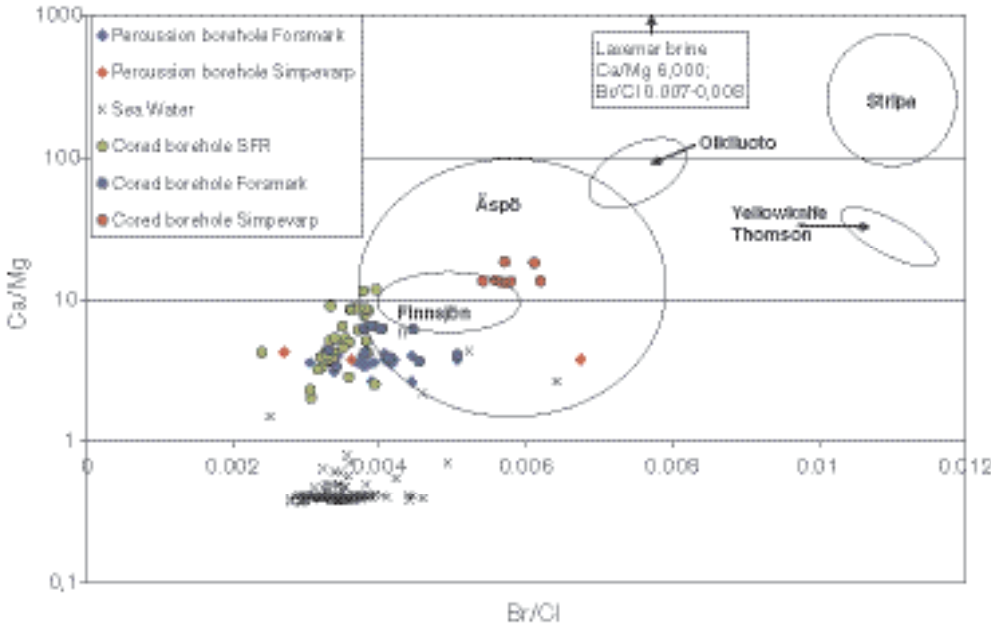

Figure 4-77. *Plot comparing all Simpevarp Ca/Mg vs Br/Cl data with other Fennoscandian sites and deep Canadian brines.*

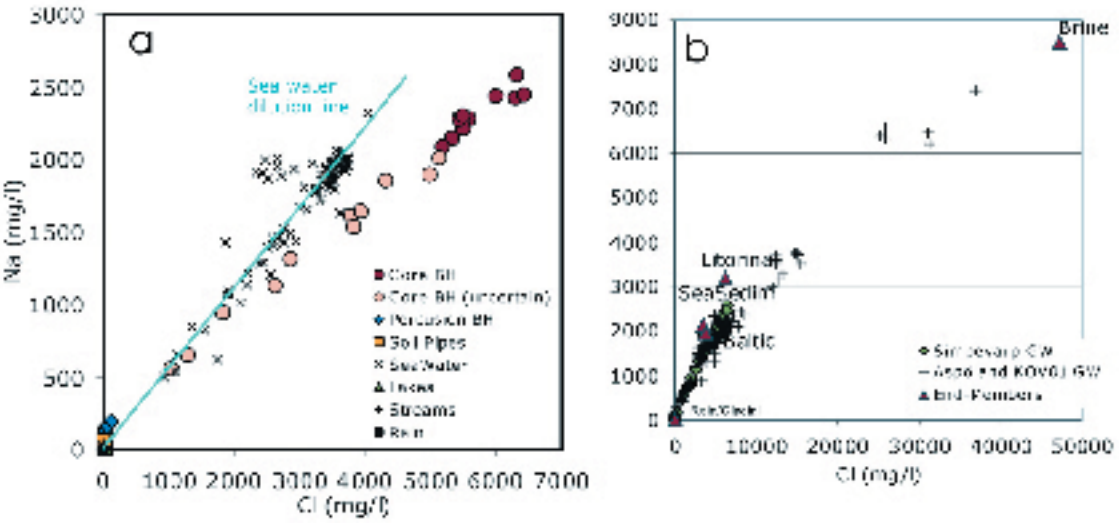

Figure 4-78. *Plots of (a) Na vs Cl for all Simpevarp data and (b) comparison with Äspö HRL data and data from test borehole KOV01 in Oskarshamn.The end members used in the plots are defined in Section 5.5.3.*

Si vs. Cl for all Simpevarp data

The content of dissolved SiO_2 in surface waters indicates a typical trend of weathering, whereas in groundwaters it has a narrow range of variation indicative of a steady state (Figure 4-79a). The general process evolves from an increase in dissolved SiO_2 by dissolution of silicates in surface waters and shallow groundwaters to a progressive decrease related to the participation of silica polymorphs and aluminium silicates which control dissolved silica as the residence time of the water increases. Silica contents of the representative cored borehole samples and their trend fit fairly well with the less saline Äspö and Oskarshamn (KOV01) data set (Figure 4-79b).

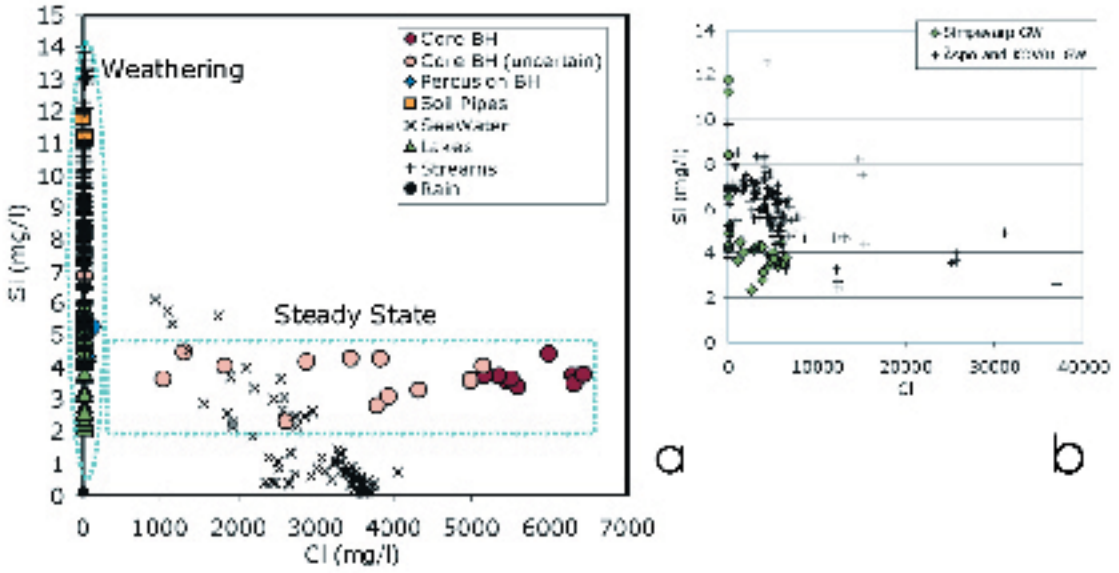

Figure 4-79. *Plots of (a) SiO2 vs.Cl for all Simpevarp data and (b) comparison with data from the Äspö and the test borehole KOV01 in Oskarshamn.*

δD vs $\delta^{18}O$ for all Simpevarp data and comparison with the Finnsjön and SFR sites

Figure 4-80 details the Simpevarp samples which plot on or close to the Global Meteoric Water Line (GMWL) indicating a meteoric origin. Three clear groups are indicated: a) Baltic Sea and Lake waters (($\delta^{18}O$ = –9.6 to –6.7‰ SMOW; δD = –72.7 to –54.1‰ SMOW), b) Stream Water ($\delta^{18}O$ = –11.7 to –9.7‰ SMOW; δD = –85.0 to –70.4‰ SMOW), and c) Waters from Cored Boreholes ($\delta^{18}O$ = –14.1 to –12.6‰ SMOW; δD = –102.5 to –93.6‰ SMOW). The two $\delta^{18}O$ values related to precipitation represent a large spread ranging from –15.5 to –10.9‰ SMOW and δD from –116.9 to –80.6‰ SMOW. There is a clear indication of the Cored Borehole groundwaters representing cold recharge conditions, particularly from sections 245.0–261.5 m and 197.0–313.42 m in borehole KSH01A where recorded $\delta^{18}O$ and δD values are lowest (–14.1 to –13.4‰ SMOW and –102.5 to –100.0‰ SMOW, respectively).

On closer inspection, the Baltic Sea and Lake waters plot further from the GMWL in a trend (evaporation trend?) that intersects the GMWL. There is no evidence of a mixing line towards the Baltic Sea samples as indicated in other regions (e.g. Olkiluoto; /Pitkänen et al, 1999/. The depleted deuterium samples may be the result of surface evaporation which, at Simpevarp, would appear to be the likely case since the two sample groups (Baltic Sea and Lake waters) would be most subject to evaporation due to their large surface area exposure.

$\delta^{18}O$ vs Cl for all Simpevarp data and comparison with the Finnsjön and SFR sites

The Lake and Stream waters from the Simpevarp area (Figure 4-81) show a wide variation of $\delta^{18}O$ values (–11.7 to –6.7‰ SMOW) at low chloride contents; in turn there is a clear distinction between Lake Water (–6.7 to –9.6‰ SMOW) and Stream Water (–9.7 to –11.7‰ SMOW) with no major evidence of mixing. At higher chloride contents, and reflecting the above described plots, there is a clear Baltic Sea water dilution trend quite separate from the cored borehole group which may more obviously form part of a separate saline dilution trend when additional data become available. This conforms to the present hydrogeological interpretation that the near-surface and deep groundwater environments represent two distinct hydrogeological systems.

Figure 4-82, comparing Simpevarp with Forsmark, SFR and Finnsjön data, shows the Simpevarp KAH01A and KSH02 groundwaters plotting towards an increasing non-marine brine signature.

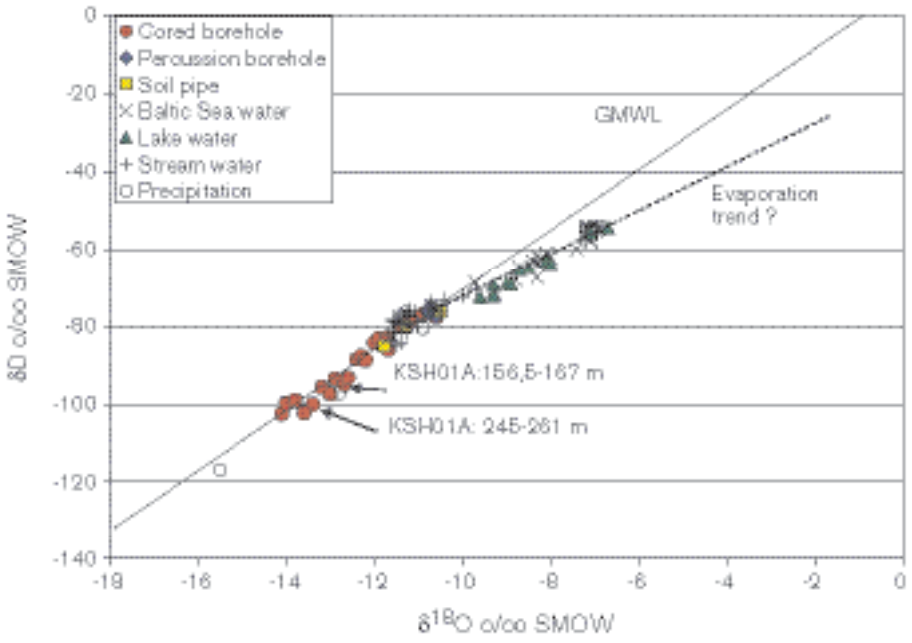

Figure 4-80. *Plot of δD vs $\delta^{18}O$ for all Simpevarp data (GMWL = Global Meteoric Water Line). (Note: Cored borehole samples not labelled represent open hole mixing).*

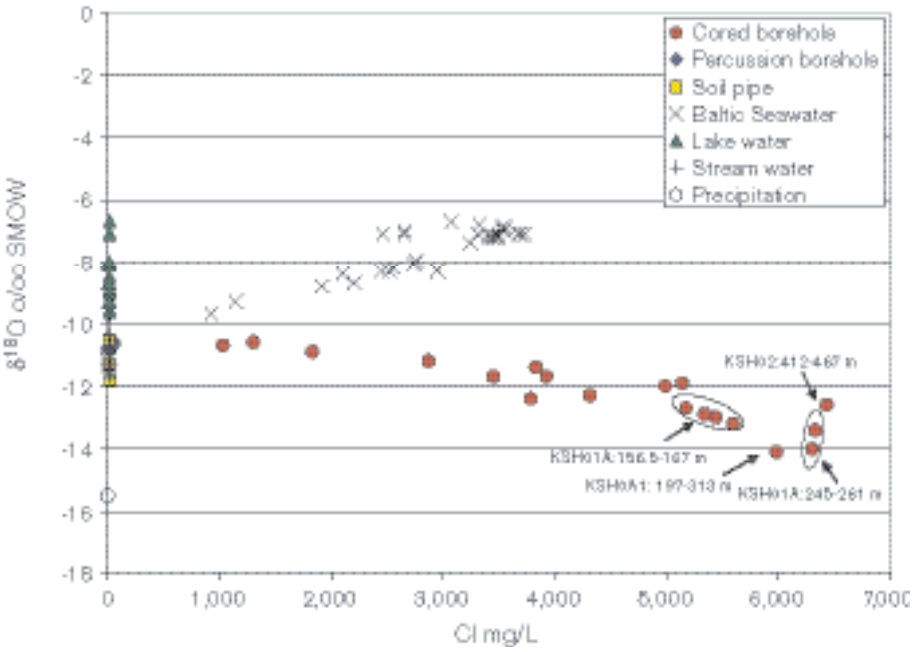

Figure 4-81. *Plot of $\delta^{18}O$ vs Cl for all Simpevarp data. (Note: Cored borehole samples not labelled represent open hole mixing and should be ignored).*

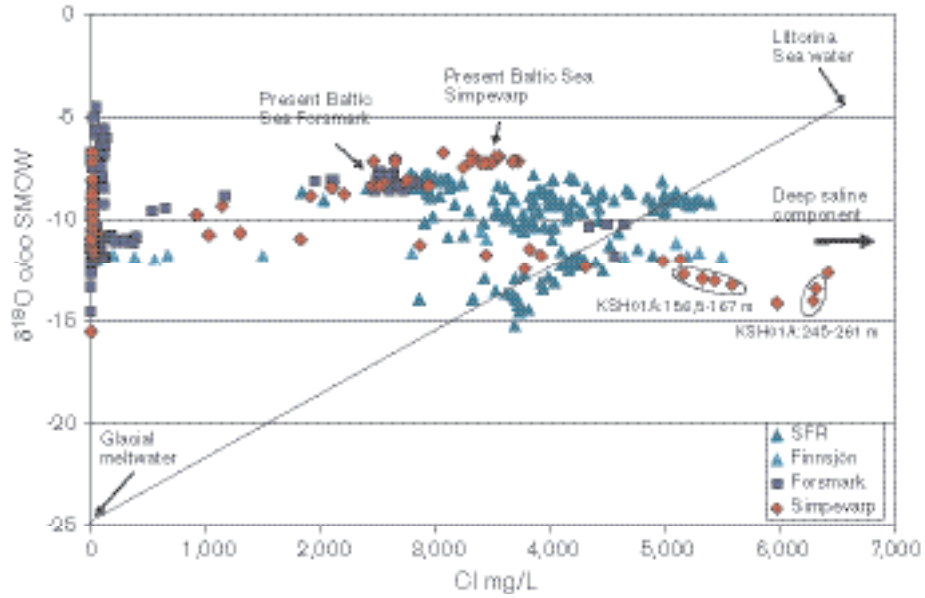

Figure 4-82. *Plot of $\delta^{18}O$ vs Cl, comparing Simpevarp with Forsmark, SFR and Finnsjön.*

Furthermore, the data from Simpevarp correspond generally to plotted areas for Baltic Sea, Lake and Stream waters. Of more significance is the absence of any of the Simpevarp samples plotting near, or on the Littorina Sea dilution line. So far Simpevarp seems to lack a significant Littorina Sea component, even though it is reasonable to assume that Littorina Sea water entered the bedrock during the several thousand year long period when it covered the Simpevarp area (approximately from 7,000 BP to 4,000 BP). However, this water seems to have been subsequently removed (possibly flushed out by meteoric recharge, c.f. Chapter 3). Less likely is the possibility that there in fact never was a Littorina Sea component.

$\delta^{18}O$ vs tritium for all Simpevarp data

Figure 4-83 shows a wide range of $\delta^{18}O$ and tritium values; the present-day average precipitation of 10–15 TU is associated with the Baltic Sea water and the Lake and Stream waters, as would be expected. The deepest samples from the cored borehole sections are tritium-free apart from one sample from the series taken from KSH01A (156.50–167.00 m) of about 4 TU. This value probably represents some residual flushing water contamination from percussion borehole HSH03 (4.7–10 TU).

The range of $\delta^{18}O$ distinguishes very clearly between Baltic/Lake waters and Stream Water, whereas tritium values differentiate between the Baltic Sea and Lake waters. This may be due to a large surface area for evaporation of Lake and Baltic waters relative to a small surface area for evaporation of Stream water. Alternatively, it may reflect longer residence times for these surface/sub-surface waters at shallow depths in the overburden where local recharge/discharge (plus some soil interaction) may have influenced their chemistry. More information is required on the near-surface/surface environment of the streams chosen for sampling to resolve these issues.

The groundwaters from the cored borehole show diminishing tritium values with depth, coupled with an increasing cold climate recharge $\delta^{18}O$ signature. The presence of tritium probably reflects some residual drilling water contamination. The percussion borehole data (with one exception) plot close to Stream Water compositions.

Water classification

The aim of water classification is to simplify the groundwater information. First the data set was divided into different salinity classes. Except for sea waters, most surface waters and some groundwaters from percussion boreholes are fresh waters according to the classification used for Äspö groundwaters /Laaksoharju and Wallin, 1997/. The rest of the groundwaters are brackish (Cl <5,000 mg/L), except for three samples from KSH01A (at 253 m and 439 m depth) which are saline (>5,000 mg/L). Most surface waters are of Ca-HCO_3 or Na-Ca-HCO_3 type and by nature the sea water is of Na-Cl type. The deeper groundwaters are mainly of Na-Ca-Cl type. These water classes are illustrated by using different standard plots in Figure 4-84 and the results are listed for all samples in /Laaksoharju et al, 2004b/. The Ludwig-Langelier plot in Figure 4-84 for instance indicates processes that link Cl–, SO4–, Na+ and K+ concentrations.

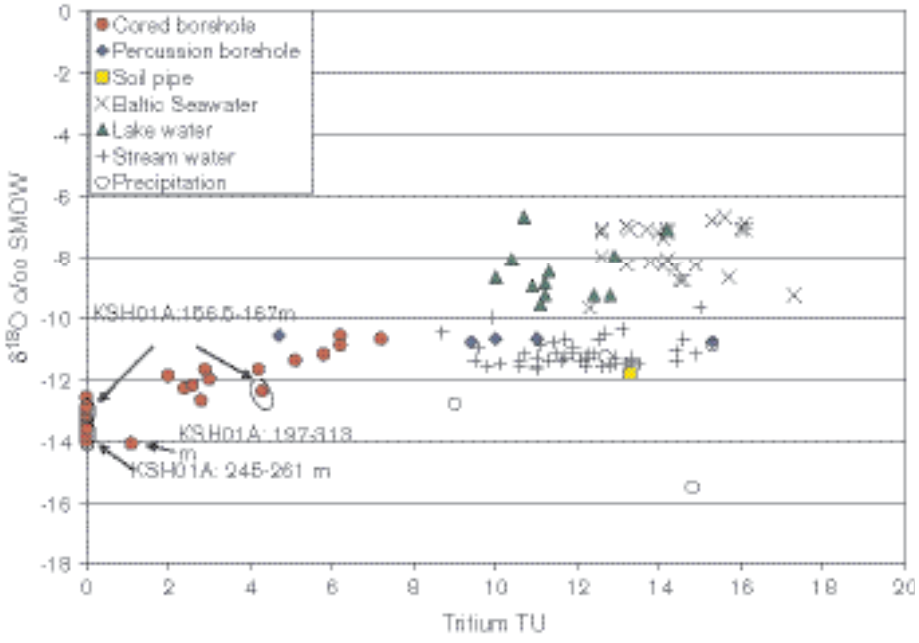

Figure 4-83. *Plot of $\delta^{18}O$ vs ^{3}H for Simpevarp data.*

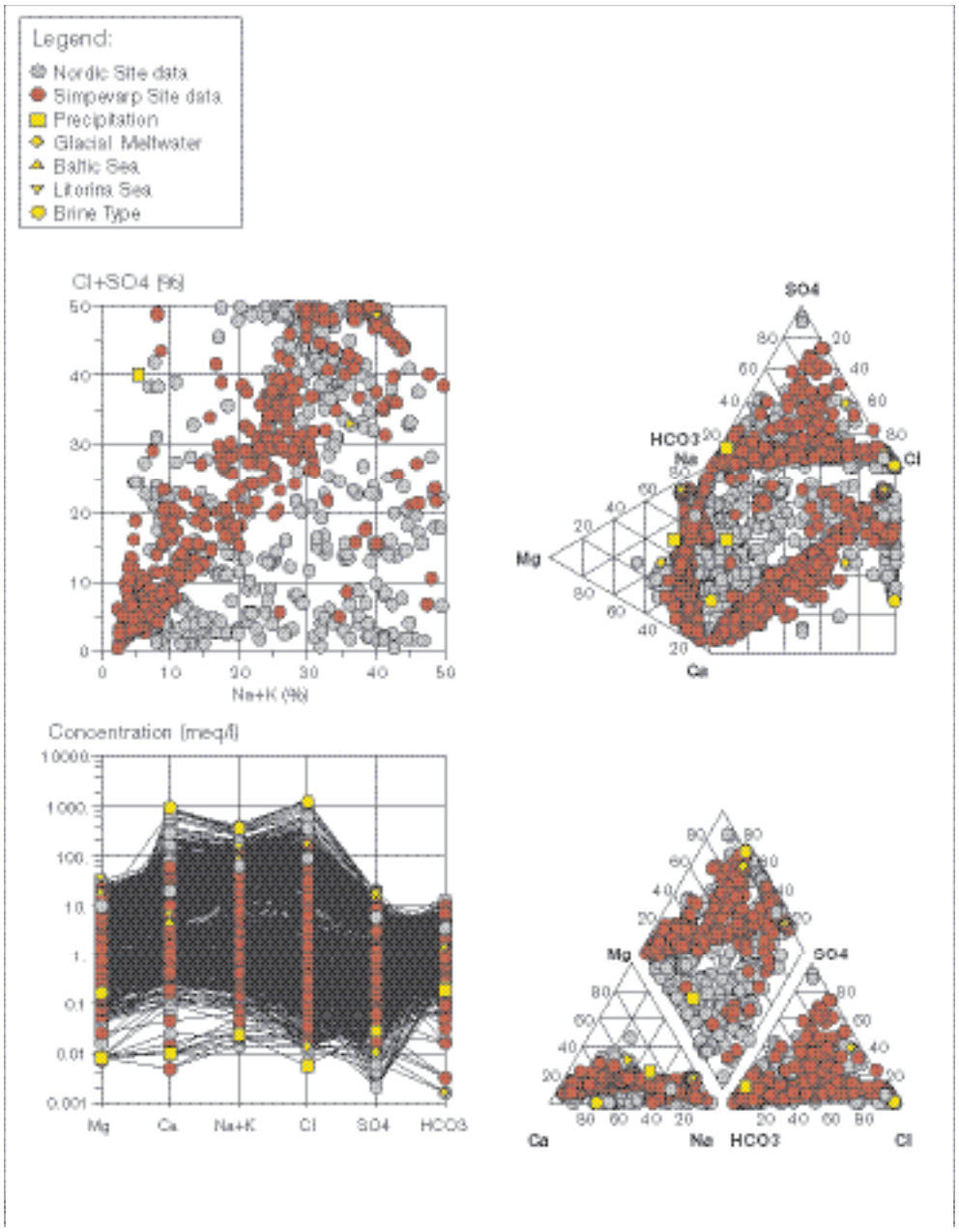

Figure 4-84. *Multicomponent plots used for classification and applied to all Simpevarp groundwater data. Clockwise from top to left: Ludwig-Langelier plot, Durov plot, Piper plot and Shoeller plot. Plots produced using AquaChem.*

4.9 Transport data evaluation

The investigation programme for the transport properties of the rock produces primary data on the diffusion and sorption properties of geological materials (intact rock, altered rock in the vicinity of fractures, fracture-filling materials). According to the guidelines for the site descriptive modelling /Berglund and Selroos, 2003/, these data will be evaluated and presented as a "retardation model" consisting of interpreted parameter values for different rock types and "type structures". The parameters included in the retardation model are the porosity, θ_m, the effective diffusivity, D_e, and the linear equilibrium sorption coefficient, K_d. The programme also includes methods for measuring advection parameters (the groundwater flow velocity and its spatial variations), primarily through different types of tracer tests *in situ*.

Until now, the site investigation programme for the transport properties of the rock has been focused on sampling of drill cores and initiation of laboratory measurements. Commencing the time-consuming laboratory measurements is one of the main goals of the present initial stage of the site investigation /SKB, 2001a/. Laboratory measurements are under way, but no results were available for Simpevarp 1.1 data freeze. This means that the transport modelling in the present model version is based on data from previous investigations only. Furthermore, methods for *in situ* measurements of transport parameters are being tested in the boreholes at Simpevarp. These methods are presently under evaluation. Therefore, data from *in situ* measurements are not included in the present model version.

4.9.1 Transport data from drill cores

Since site investigation transport data are not available, activities related to data compilation and evaluation have concerned generic data only. Generic data, broadly defined as data not obtained within the framework of the Simpevarp site investigation, can be grouped into two main categories: (i) Äspö HRL data, and (ii) data from other sites. Äspö is situated in the immediate vicinity of the Simpevarp area, which means that Äspö data could include data on specific geological materials that are also present within the Simpevarp area, cf. below. In the present work, generic data from other sites are represented by the databases compiled during the SR 97 project: /Ohlsson and Neretnieks, 1997/ for diffusion data, and /Carbol and Engkvist, 1997/ for sorption data.

The main methods employed within the laboratory programme are through-diffusion tests and resistivity measurements to obtain diffusion parameters, and batch sorption tests /Widestrand et al, 2003/. Thus, available data from previous investigations at Äspö were compiled and assessed with the basic restriction that data must have been measured and evaluated with methods similar to those in the site investigation programme. In addition, geological data (mineralogy) and information on the water compositions used in the experiments were required, such that the usefulness of the Äspö HRL data for describing the transport properties of the rock within the Simpevarp area could be judged.

The assessment of the compiled Äspö HRL database shows that information on the mineralogical compositions of the various drill core samples is available in many cases, whereas the relation between the water composition used in a given experiment and that at the corresponding sampling site is often unclear. The general conclusion is that the amount of data that can be used within the site descriptive modelling context is very limited. The main source of such data is the laboratory measurements that were carried out during the TRUE project /Byegård et al, 1998/. The results of further data selection, based on a joint transport-geological-hydrogeochemical evaluation of the Äspö data, are described in Section 5.6.

4.9.2 Transport data sampled in boreholes

No data from *in situ* measurements are available for the present model version. Ongoing field tests include *in situ* resistivity measurements and single-well tracer tests. If found useful, these methods will provide data for future site descriptive models.

4.9.3 Joint evaluation of transport, geological, hydrogeological and hydrogeochemical borehole data

Further evaluation and selection of diffusion and sorption data from previous projects at Äspö has been performed. The objective of this work was to identify the geological materials within the investigated area that can be parameterised by use of Äspö data, and to quantify the parameters. The evaluation was based on the lithological model of the Simpevarp area and on petrophysical data, primarily porosities, for the main rock types there /Mattsson et al, 2003/. Fracture mineralogy data were not used in the Simpevarp 1.1 transport modelling, primarily due to the delayed delivery of the geological model. In future model versions, this type of data will be used in the development of retardation models and for supporting analyses of retention processes /Berglund and Selroos, 2003/.

Due to the limited availability of both transport data and supporting data and models from other disciplines, no retardation model has been developed for the present version of the site descriptive model. Thus, the descriptive modelling is based on a limited amount of data on specific rock types, rather than a retardation model with interpreted parameters for “typical” materials, and on an evaluation of whether these data provide a sufficient basis for assigning other parameter values than those recommended in the existing databases /Ohlsson and Neretnieks, 1997; Carbol and Engkvist, 1997/. Since there is no clear distinction between data evaluation and descriptive modelling in this case, the joint data evaluation outlined above is described in detail in the section on descriptive transport modelling (Section 5.6).

4.10 Biota data evaluation

This section gives a compilation of site-specific primary data concerning biota, i.e.. producers, consumers and decomposers, as well as humans and human activities. Biotic primary data may concern both characterisation (e.g. species composition or habitat distribution) and processes (e.g. production or respiration).

Only primary data used for characterisation and modelling of ecosystems are presented in this section. All available data concerning objects and areas of environmental and/or cultural concern in the regional model area have been collected and compiled in the “accessibility map”, which is a GIS-product describing the location and spatial distribution of these objects and areas (see Section 4.10.3).

4.10.1 Producers

Terrestrial producers

Vegetation mapping from satellite data of the Simpevarp regional model area was conducted by /Boresjö Bronge and Wester, 2003/. Other site specific and generic information has been presented by /Berggren and Kyläkorpi, 2002/, /Jerling et al, 2001/, /Jacobsson, 1978/ and /Svensson, 1989/. The vegetation map has been used together with some new information to produce models for biomass and production of the terrestrial vegetation of the Simpevarp regional model area. In order to arrive at such models of standing crop biomass and production, a number of different steps were undertaken :

1. Definition of habitat categories for the tree layer and for the bush, field and ground layers.
2. Assembly of the different habitat categories based on the vegetation map.
3. Production of habitat maps for these new tree, bush, field and ground layers.
4. Calculations of biomass and production values for the different habitat categories.
5. Assignment of these values to the habitat categories on the maps.

As far as possible, site-specific data were used in the modelling process. However, since some of the information needed for the study has not been measured on the site, generic data was used for some calculations and some conversions of site-specific data into units necessary for the study. Table 4-35 shows the input data that have been used for modelling of biomass and production in the different vegetation layers.

Table 4-35. Input data for modelling of biomass and production of terrestrial vegetation in the Simpevarp regional model area.

Variable group	Variable	Data source
Biomass	Tree layer	Forestry management plan, AssiDomän 1999
	Other layers	In situ studies of standing crop forrom bush, field, and ground layers in the Forsmark area /Fridriksson and Öhr, 2003/
	All layers	Generic data on dry weight and carbon content of biota /Jerling et al, 2001/
Primary production	Tree layer	Data obtained from the plots of the National Forest Survey /Berggren and Kyläkorpi, 2002/
	Other layers	In situ studies of standing crop forrom bush, field, and ground layers in the Forsmark area /Fridriksson and Öhr, 2003/
	All layers	Generic data on dry weight and carbon content of biota /Jerling et al, 2001/

Aquatic producers

Limnic

No new site-specific data concerning primary producers in lakes and streams is available for version Simpevarp 1.1.

Marine

Biomass and distribution of macroscopic benthic primary producers (algae and vascular plants) is presented in /Fredriksson and Tobiasson, 2003/. In this report, the cover of dominant species has been interpolated from quantitative sampling to determine a total biomass for the investigated area. A digital map, presenting cover and dominant species distribution is available in the SKB GIS-database. Interpretations of under water videos with quantitative cover estimates of vegetation are presented in /Tobiasson, 2003/. Some point sample data of occurrence of benthic macrophyte species is presented in /Borgiel, 2003/. In /Lingman and Franzén, 2003/ literature on benthic macroalgae are cited presenting data for two stations north and south of Simpevarp that were monitored during the 1980's and 1990's.

Primary producing plankton is estimated from chlorophyll A (laboratory) and measurements of fluorescence in the field 18 times per year at 5 sites (2003) and 4 sites (2004). Data from October 2002 until October 2003 are presented in /Ericsson and Engdahl, 2004/. A survey of the species composition and biomass of the planktonic community started in July 2003 and will continue for one year. Data will be presented in fall 2004.

There are no site specific data on benthic microproducers in the marine system at the time of writing.

4.10.2 Consumers

Terrestrial consumers

Terrestrial consumers in the Simpevarp region in this version are only represented by wild mammals and birds, since no site-specific data are available for amphibians, reptiles or invertebrates /Berggren and Kyläkorpi, 2002/. Domestic animals such as cattle, sheep and pigs are presented under Humans and land use (Section 4.10.3).

Mammals

A study of wild mammals was conducted in the areas surrounding Simpevarp during 2003 /Cederlund et al, 2004/. The aim was to survey a major part of the large mammals, both terrestrial and aquatic, expected to be found in the Simpevarp region. Selected species were: wolf, lynx, otter, marten, mink, red fox, wild boar, red deer, fallow deer, roe deer, moose, European hare and Mountain hare.

Birds

A survey of bird populations in the regional model area was performed during 2002 and the results are presented in /Green, 2003b/. The survey will continued during 2003 and 2004, and thereafter a more thorough analysis of the results will be performed. Therefore, the results from the bird population survey have so far mainly been used for a qualitative characterisation of the bird fauna in Simpevarp.

Aquatic consumers

Limnic

No new site-specific data concerning consumers in lakes and streams were available for version Simpevarp 1.1.

Marine

Abundance and biomass of soft-bottom macrofauna is presented in /Fredriksson and Tobiasson, 2004/. The data are based on sampling at 40 stations in the regional area. Hard-bottom fauna are partly described in /Fredriksson and Tobiasson, 2003/, here fauna associated with macro vegetation are described. There are no site-specific data on non-phytobenthic hard-bottom fauna, i.e. hard-bottom fauna from below the vegetated zone, i.e. at depths of greater than approximately 10 m. In /Lingman and Franzén, 2003/ literature on soft-bottom fauna are cited, presenting results from two bottom- fauna stations north and south of Simpevarp that were monitored during the 1980's and 1990's.

Fish are being sampled in specific sites within the regional area in a number of programmes by the Swedish National Board of Fisheries, primarily for recipient control of the Simpevarp nuclear power plant. The dataset from this sampling is in terms of indices and there are no actual population size estimations at the time of writing, but this is planned for the summer 2004. In /Lingman and Franzén, 2003/ literature concerning fish sampling during the period 1962–2002 are reviewed. In conjuction with geophysical measurements, fish sampling subsequent to blasting was undertaken in late fall 2003 and the data are presented in /Engdahl and Ericsson, 2003/.

Coastal birds breeding in the regional area hasvebeen counted during 2003 and the data are presented in /Green, 2003b/. Concerning mammals, data on a neighbouring colony of grey seals have been collected by the Swedish Museum of Natural History /Helander et al, 2003/.

4.10.3 Humans and land use

In order to arrive at a feasible assessment of the human population and human activities in the model area, a wide range of various human-related statistics were acquired from Statistics Sweden. These statistics include data and times series on demography, labour, health situation, land use, agriculture etc. Beside this, some additional information was searched for and obtained from other sources, such as the National Board of Fisheries, the Swedish Association for Hunting and Wildlife Management, the County Administrative Board. The data sources used for the variables describing humans and land use are listed in Appendix 4, and a more thorough presentation of the data and results is given in /Miliander et al, 2004/.

5 Descriptive and quantitative modelling

5.1 Geological modelling

5.1.1 Overburden including Quaternary deposits

The data presented here comes from the mapping of Quaternary deposits in the Simpevarp area. The aim of that activity is to describe and characterise the formation, grain size composition, chemical and physical properties, distribution of the uppermost Quaternary deposits and, as far as possible, the thickness and stratigraphical condition of all deposits above the bedrock surface. Besides, this investigation determines the extent of areas with exposed bedrock.

The map, which shows the areal distribution of Quaternary deposits, is presented in Section 7.1.4. The proportional distribution of overburden and exposed bedrock is shown in Table 5-1. In the following, for a detailed account of sampling point locations and detailed stratigraphy, reference is made to Figure 4-3 and Table 4-1, respectively.

The Simpevarp subarea is relatively flat, and is dominated by exposed bedrock and glacial till. In some places, there are distinct valleys, which partly are covered with water-laid sediments and/or peat. Glaciers have polished the bedrock surface to a large extent. The *striae* can be found all over the area but they occur most frequently close to the shoreline. The *striae* probably reflect ice movement close to the ice margin during ice recession. The dominating ice movement in the area was, according to the *striae* directions, from N40–50°W. At the northernmost cape of Hålö (PSM002590), a more northerly, probably older, direction (N30°W) was observed.

Till is the dominating Quaternary deposit and covers about 35% of the area (Table 5-1). The morphology of the till normally reflects the morphology of the bedrock surface. The thickness of the till is often between 0.5 and 3 m. In some areas, as on the western part of Hålö, the till may be thicker, which will be revealed from excavations in the future.

The matrix of most till is sandy, but gravelly till was observed in some trenches (PSM002643, PSM002642). It was impossible to separate these two till types in the field. Therefore, all till areas have been shown as sandy till on the map (Figure 7-1).

The boulder frequency of the till is, in most areas, normal. There are, however, areas with a high boulder frequency, especially on the peninsula of Simpevarp and on the western part of the island of Hålö. There are also a few small areas with a high frequency of large boulders on northern Ävrö.

Glacial clay occurs as a cover in many valleys and is often covered by postglacial sediments, such as sand and gravel (Table 4-1). The thickness of the glacial clay is often approximately 1 metre. Three drillings on Ävrö and one on the Simpevarp peninsula (PSM002660) showed that the total thickness of glacial clay was more than 1.5 m.

Postglacial sand, gravel and cobbles cover about 6% of the investigated area and occur on the coast, on the eastern part of Ävrö and on the southern part of the Simpevarp peninsula.

Table 5-1. The proportional areal distribution of Quaternary deposits and exposed bedrock on the peninsula of Simpevarp and the islands of Ävrö and Hålö.

Quaternary deposit	Coverage (%)
Peat	1.89
Gyttja sediment	0.05
Glacial clay	1.06
Postglacial sand and gravel	5.80
Glacial till	35.04
Man-made fill	17.93
Precambrian bedrock	38.22

Flat areas and small beach ridges consisting of gravel occur in many places in the investigated area, most frequently in the coastal zone on the north-eastern part of Ävrö. There is a well-developed, 200 m long, cobble field north of Korsbergen on Ävrö. Gravel exploitation has occurred in a small pit (PSM002609) about 200 m south-west of Korsbergen. The thickness of the gravel in the pit is more than 3 m. Littoral sand is of small extent and occurs in depressions, where it often covers glacial clay.

The mires are divided in two types: bogs and fens. A coherent cover of Sphagnum-species characterises the bogs. There are few, small, not raised, bogs on the northern part of Ävrö. The thickness of the bog peat (Sphagnum peat) is about 0.5 m. The bog peat is underlain by fen peat and gyttja (Table 4-1). The fens are characterised by sedges of different species, reed, moisture-seeking herbs etc. The fens are small and are situated in depressions. The largest fen in the investigated area is Örnkärren/Stora mossen. The peat thickness in that particular fen is almost 1 m (PSM002622 and PSM002623).

Around the nuclear power station the ground has been changed by human activities. These areas were mapped as artificial fill and cover 18% of the total investigated area, c.f. Table 5-1. On the island of Hålö, there is a large area with artificial fill, which consists of bedrock material from the excavation of the access tunnel to the Äspö HRL.

5.1.2 Lithological model – regional scale

No three-dimensional modelling of the distribution of rock domains has been carried out at the regional scale in the site descriptive modelling version Simpevarp 1.1. This will be carried out in version 1.2. During the work with the model version 0 of the site descriptive model /SKB, 2002b/, the various rock units that had been recognised at the surface were only distributed on the top surface of a three-dimensional block. No extrapolation to depth was carried out. Only small amounts of new primary data were available to allow a detailed documentation of the properties of rock domains or rock types on a regional scale for version Simpevarp 1.1.

5.1.3 Lithological model – local scale

Modelling assumptions and input from other models

No previous, three-dimensional local scale model for the distribution of rock domains has been presented that comprises the entire Simpevarp local model area. As mentioned above, no three-dimensional model was presented in the version 0 site descriptive model /SKB, 2002b/. A lithological model as a vertical section across Äspö is presented in /Rhén et al, 1997b/. However, a tentative three-dimensional lithological model has been presented for Ävrö /Markström et al, 2001/. Furthermore, as a result of the testing of the methodology for the site descriptive modelling procedure, a three-dimensional lithological model was presented for Laxemar /Andersson et al, 2002b/, i.e. the westernmost part of the present local model area used for the Simpevarp 1.1 SDM. However, this model has not been evaluated and incorporated in the present lithological model, mainly because the mentioned Laxemar project was designed only as a methodology test. Furthermore, there were significant limitations in the input data and the scope of analysis.

This section describes how the three-dimensional lithological model of the Simpevarp local model area has been constructed. The terms rock units and rock domains are used here according to the terminological guidelines for geological site descriptive modelling given in /Munier et al, 2003/. Rock units are defined on the basis of the composition, grain size and texture of the dominant rock type. In particular, composition and grain size are judged to have some relevance for the construction of a repository. Rock domains are defined on the basis of an integration of the rock units taking into account these geological criteria. In addition, a complex and intimate mixing of rock units has also been used as a criterion in the definition of a given rock domain.

Although, three deep cored boreholes (KLX01, KLX02 and KSH01) and a number of shallow percussion boreholes are available in the Simpevarp local scale model area, the construction of the rock domain model (see Section 4.2.2) is principally based on surface data from the bedrock mapping.

The first stage in the modelling procedure is the identification of rock domains at the surface. This involves the use of four principal rock units that have been distinguished on the basis of the composition, grain size and texture of the dominant rock type (Table 5-2). Note that these rock units should not be confused with the simplified units introduced in the geological single-hole interpretation of borehole KSH01A, c.f. Section 4.4.5.

Since the bedrock in the local model area employed for Simpevarp 1.1 is dominated by more or less pristine igneous rocks, there are no ductile structural frameworks that can be adopted as a guide for the three-dimensional geometric modelling of the rock domains. Due to the lack of subsurface data that relates to depth extension of the interpreted rock domains, the following assumption has been adopted in the modelling procedure:

- With the exception of the dominating porphyritic granite to quartz monzodiorite (Ävrö granite), assumed to extend to the bottom of the model volume, the other rock domains have been extended to a depth that equals the width of the rock domain at the surface. In addition, the width of the rock domains decreases gradually with increasing depth. The assumption that the porphyritic granite to quartz monzodiorite extends to the bottom of the model volume is confirmed by the character of the dominating rock in the cored boreholes KLX01 and KLX02.

The above assumption is the basis for the geometric three-dimensional modelling of the rock domains in the local scale model volume. It should also be noted that the character and occurrence of rock types in the cored borehole KSH01 (c.f. Section 4.4) are similar to those observed at the surface. This supports the interpreted extension of this rock domain to a depth of approximately 1,000 m, i.e. to the bottom of the local scale model volume. The three-dimensional model is presented in conjunction with the description of the site (c.f. Section 7.2.1).

A proposed alternative assumption is that the larger rock domains extend vertically to the bottom of the model volume, whereas the minor rock domains should only modelled to a depth that equals their width at the surface.

Geometric modelling

The following working stages have been followed during the geometric modelling:

- Some simplification of the geological map that has been produced for the Simpevarp subarea during 2003 in connection with the site investigation programme.
- Integration of the bedrock map of the Simpevarp subarea with the bedrock map that was used in the version 0 Simpevarp SDM /SKB, 2002b/.
- Definition of the areal extension of rock domains at the surface using the bedrock components defined above (Table 5-2).
- Projection of the rock domains downward in the local model volume.

Table 5-2. Bedrock components used in the modelling procedure and their principal characteristics and encoding.

Rock units − composition, grain size and texture of dominant rock type			
Code (SKB)	**Composition**	**Complementary characteristics**	
501044	Granite to quartz monzodiorite	Medium-grained	Porphyritic
501036	Quartz monzodiorite	Medium-grained	Equigranular
501030	Dioritoid	Fine-grained	Unequigranular
501033	Diorite to gabbro	Medium-grained	Equigranular

In order to carry out the modelling properly, it was necessary to simplify the bedrock map of the Simpevarp subarea (Figure 4-4). Minor rock units on the geological map were included as subordinate rock types within the surrounding principal rock unit. This process reduced the number of minor rock units and resulted in minor bodies of fine-to medium-grained granite, medium-grained granite, diorite to gabbro and fine-grained dioritoid.

The next stage in the modelling involved an integration of the bedrock map of the Simpevarp subarea with the bedrock map compiled in conjunction with the Simpevarp site descriptive model version 0 /SKB, 2002b/. This procedure was necessary because the new bedrock map of the Simpevarp subarea did not cover the entire Simpevarp 1.1 local scale model area. As the fine-grained dioritoid was not separated as a mappable unit in the version 0 bedrock map, the extension of the fine-grained dioritoid west of the Simpevarp subarea was based on the bedrock map by /Kornfält and Wikman, 1987/.

The simplification and integration procedures applied to the surface data have yielded a geological map that shows rock domains over the local scale model area (Figure 5-1). The rock domains have been given different denominations (Figure 5-1), where rock domains denominated with the same capital letter are dominated by the same rock type.

On this basis, 17 rock domains have been identified at the surface of the local model volume. All these domains have subsequently been modelled at depth.

The final stage in the modelling work concerns the projection of the rock domains that have been recognised at the surface to a depth of –1,100 m, i.e. to the base of the local model volume. The key assumptions adopted in this procedure have been summarised earlier in this section.

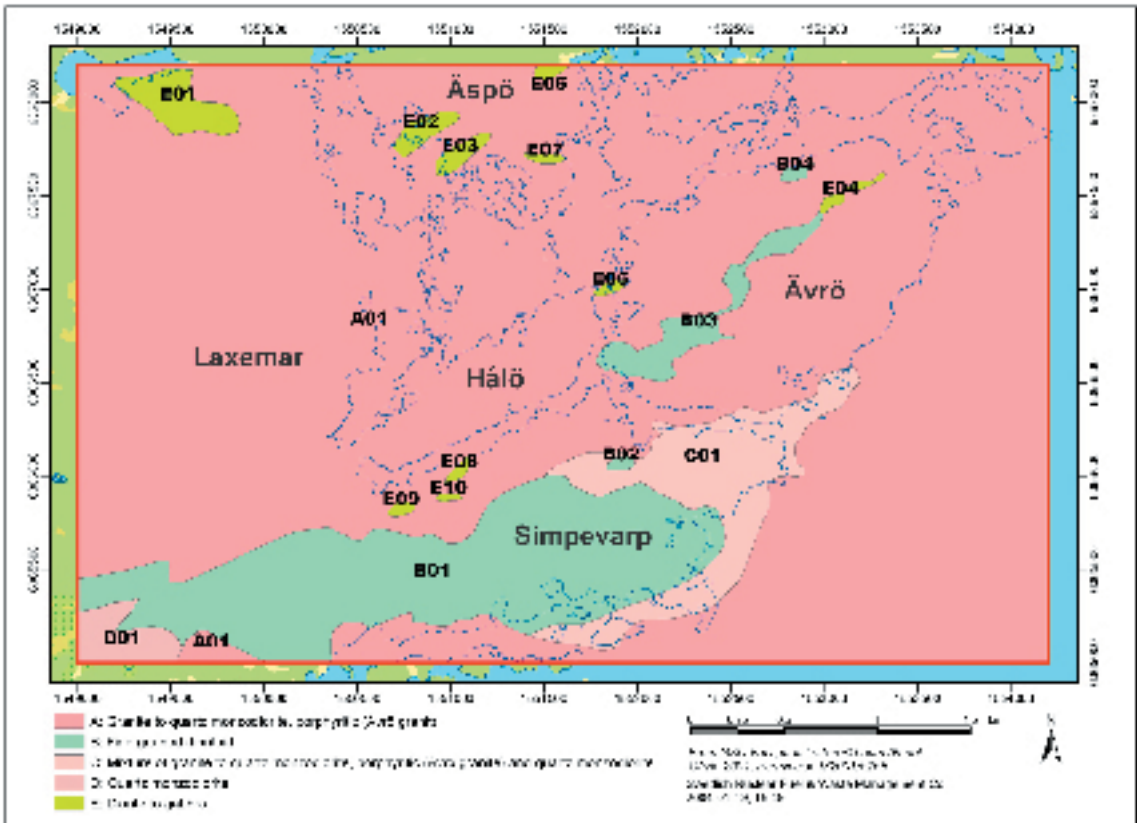

Figure 5-1. *Rock domains (N=17) used in the modelling procedure. Surface view of the local scale model area.*

Assignment of properties

Each rock domain has been assigned a set of properties (Table 5-3), including the dominant and subordinate rock types in the domain. Furthermore, the properties of the different rock types (Table 5-4) have also been defined. All these properties are presented in tabular format in the description of the site (Section 7.2).

For the rock domains situated within the Simpevarp subarea, the properties of the rock domains (Table 5-3) have been extracted from the outcrop database (see Section 4.2.2). In rock domain RSMC01 (mixture of Ävrö granite and quartz monzodiorite), additional information on rock type is available in the data from the cored borehole KSH01A and the percussion boreholes HSH01 and HSH03 (see Section 4.4). Only limited information is available from the bedrock compilation for rock domains or those parts of rock domains that are situated outside the Simpevarp subarea (see Section 4.2.2).

Critical properties are the composition, grain size and texture of the different rock types in the various domains. By using the information in the outcrop database from the Simpevarp subarea (see Section 4.2.2), it has been possible to estimate qualitatively the relative amounts of the different rock types in each domain.

For example, in rock domain RSMA01, the lithology that forms the dominant rock type is the Ävrö granite, i.e. a medium-grained, porphyritic granite to quartz monzodiorite (Figure 5-2). However, fine-grained granite, pegmatite, fine-grained dioritoid, diorite to gabbro, fine-grained diorite to gabbro, granite and quartz monzodiorite form subordinate rock types (Figure 5-2). Similar semi-quantitative information concerning the proportions of dominant and subordinate rock types in most of the remaining rock domains are presented in Appendix 1.

Table 5-3. Properties assigned to each rock domain.

Rock property
Rock domain ID (RSM***, according to the nomenclature recommended by SKB).
Volume.
Dominant rock type.
Subordinate rock types.
Degree of inhomogeneity.
Low temperature alteration.
Low-grade, ductile deformation.
Low-temperature alteration around fractures (if data are available).
Fracture filling (if data areis available).

Table 5-4. Properties assigned to each rock type.

Property
Rock code (according to the nomenclature recommended by SKB).
Rock name.
QAPF values (%).
Grain size (classification according to SGU).
Texture.
Age (million years).
Density (kg/m^3).
Porosity (%).
Magnetic susceptibility (SI units).
Electrical resistivity in fresh water (ohm m).
Uranium content based on gamma-ray spectrometric measurements (ppm).
Uranium content based on geochemical measurements (ppm).
Total gamma radiation. Natural exposure (µR/h).

Based on the mapped rock types in the cored borehole KSH01A in rock domain RSMC01, it has been possible to quantify the total occurrence in terms of borehole length in metres and the percentage of the total length of the core for the different rock types (see Section 4.4). This quantification is another estimate of the relative amounts of different rock types in rock domain RSMC01 that complements the estimate based on the outcrop database.

The key properties that define the various rock types (Table 5-4) have been obtained from the petrographic, geochemical and petrophysical analyses of surface samples or, in the case of the gamma-ray spectrometric data, from the measurements carried out directly on the outcrop (see section 4.2.2). Mean and standard deviation values as well as the number of samples analysed are provided for each property and rock type (Section 7.2).

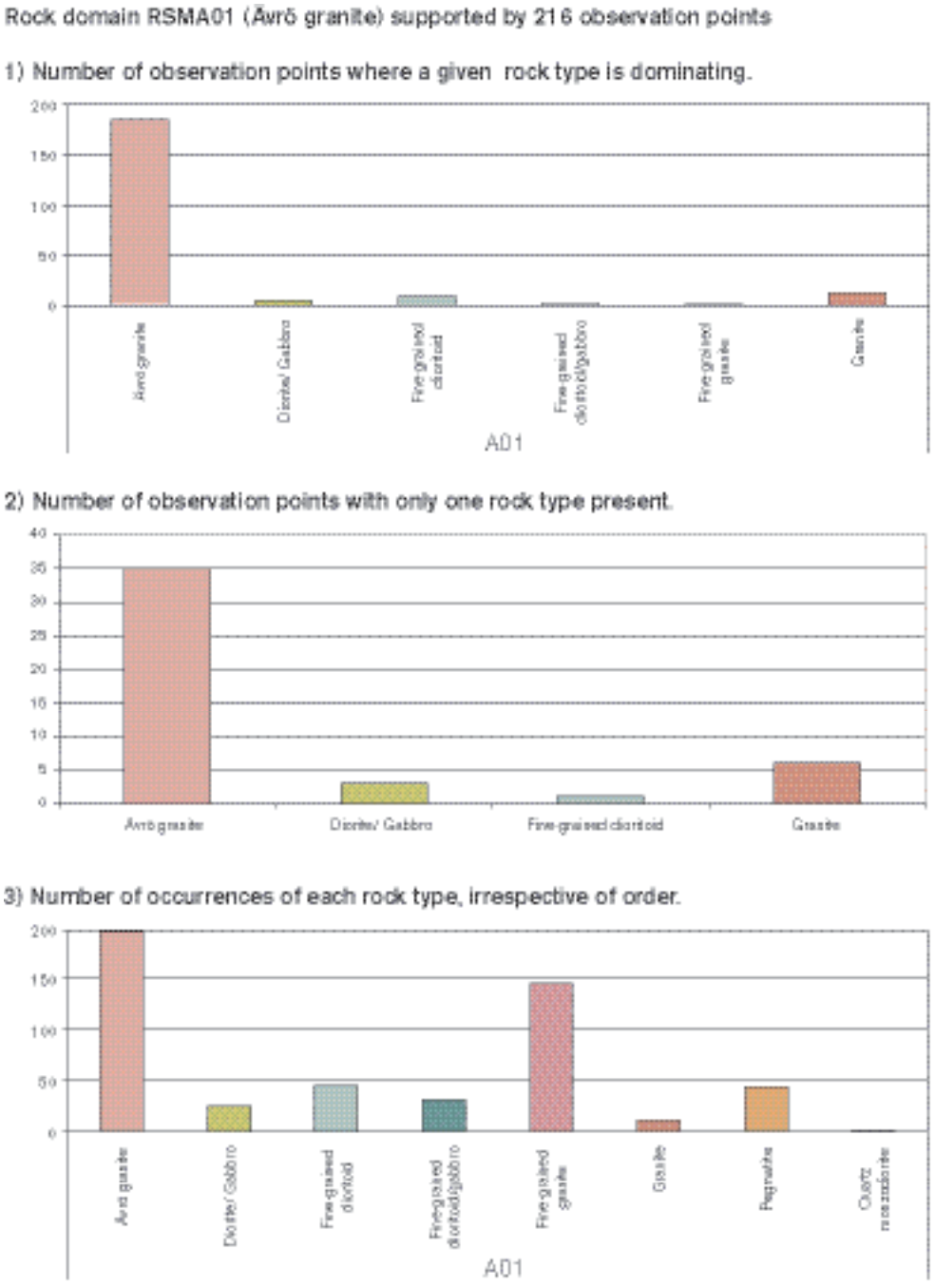

Figure 5-2. *Qualitative assessment of dominant and subordinate rock types in rock domain RSMA01 (Ävrö granite) based on surface outcrop data. The translation of the rock codes to rock type is provided in Appendix 1.*

Evaluation of uncertainty

The variation in the quality of the surface geological data across the local scale model area (c.f. Section 4.2.2) is important to consider in the modelling procedure. Since no additional surface information will be available for the Simpevarp subarea in the next model version, the uncertainties described here will remain valid also for the version 1.2 site descriptive model for the Simpevarp subarea. Apart from some possible local updating of the lithologies outside the Simpevarp subarea, the attributed uncertainties will presumably remain valid throughout the site investigation programme.

The uncertainties mainly concern the location of the boundaries between the different rock units, especially in areas where outcrops are limited or where only reconnaissance bedrock information is available. Furthermore, there remains an uncertainty as to whether some minor inhomogeneous rock domains possibly could be treated as subordinate rocks and integrated in the surrounding major rock domain. There is also insufficient information concerning the character of the inhomogeneity of the rock domains. In particular, this concerns the frequency and spatial distribution of subordinate rock types.

As there is a lack of subsurface lithological data, there remain considerable uncertainties concerning the extension and geometry of rock domains at depth. Apart from the dominating rock domain RSMA01 (Ävrö granite), which constitutes the “matrix” in the lithological model, and the rock domain RSMC01 (mixture of Ävrö granite and quartz monzodiorite), which has been verified to a depth of 1,000 metres in the cored borehole KSH01A, the depth extensions of the remaining rock domains are uncertain. However, the fine-grained dioritoid of rock domain RSMB01 is verified to a depth of at least c. 200 m in the percussion borehole HSH02. In particular, the geometrical relationships between the different rock domains are considered highly uncertain. This problem will presumably persist throughout the site investigation programme for most of the rock domains. However, reduction of this uncertainty may be achieved by future modelling of airborne or ground geophysical data and information collected from cored and percussion-drilled boreholes. The uncertainty associated with the western part of rock domain RSMB01 (see above) at the surface will be resolved during the future detailed mapping of the corridor between the Laxemar and Simpevarp subareas.

With the above considerations in mind, an attempt has been made to assess, at least qualitatively, the confidence in the occurrence and geometry of the interpreted 17 rock domains (Table 5-5). Confidence is expressed at three levels; “high”, “medium” and “low”.

The information concerning the properties of the different rock domains (Table 5-3) originates primarily from the surface outcrop data (c.f. Section 4.2.2). Subsurface data are only available from rock domains RSMA01 and RSMC01 (c.f. Section 4.4). Despite the fact that it has been possible to estimate from the surface data the relative importance of the different rock types in a specific domain, there remains an uncertainty concerning the quantitative proportions of the different rock types. This characteristic is a basis for the uncertainty assessment related to the bedrock heterogeneity in the rock domains. Based on a qualitative estimation, the frequently occurring fine- to medium-grained granite is judged to be evenly distributed both in individual rock domains and between the various rock domains.

The assigned properties of most rock types (Table 5-4) are incomplete and are based only on available data from the Simpevarp subarea. Whether the properties of the rock types of the Simpevarp subarea are also valid for the rock types of the remaining part of the Simpevarp 1.1 local scale model area is a factor contributing to uncertainty.

Table 5-5. Table of confidence related to interpreted rock domains in the local scale model domain employed for the Simpevarp 1.1 descriptive model.

Domain ID	Basis for interpretation	Confidence at the surface	Confidence at depth
RSMA01	Bedrock geological map, version 1.1 and version 0	High	High
RSMB01	Bedrock geological map, version 1.1 and /Kornfält and Wikman, 1987/, KSH01, HSH02	Medium	Medium
RSMB02	Bedrock geological map, version 1.1	Medium	Low
RSMB03	Bedrock geological map, version 1.1	High	Low
RSMB04	Bedrock geological map, version 1.1 (based on /Kornfält and Wikman, 1987/)	Medium	Low
RSMC01	Bedrock geological map, version 1.1, KSH01, HSH01, HSH03	High	Medium
RSMD01	Bedrock geological map, version 0	Medium	Low
RSME01	Bedrock geological map, version 0	Medium	Low
RSME02	Bedrock geological map, version 0	Medium	Low
RSME03	Bedrock geological map, version 0	Medium	Low
RSME04	Bedrock geological map, version 1.1	High	Low
RSME05	Bedrock geological map, version 0	Medium	Low
RSME06	Bedrock geological map, version 1.1	High	Low
RSME07	Bedrock geological map, version 0	Medium	Low
RSME08	Bedrock geological map, version 1.1	Medium	Low
RSME09	Bedrock geological map, version 1.1	Medium	Low
RSME10	Bedrock geological map, version 1.1	Medium	Low

5.1.4 Modelling of deformation zones – regional scale

Since no new integrated lineament interpretation was available at the time of the postponed data freeze for Geology in mid December, no regional scale modelling of deformation zones has been performed. Hence, the version 0 regional scale model of deformation zones is valid also for Simpevarp 1.1.

5.1.5 Modelling of deformation zones – local scale

Modelling assumptions and input from other models

The deterministic model of deformation zones on a local scale has made use of:

- The identification of linked lineaments completed during the ongoing site investigation programme (see Section 4.2.3).
- The regional structural model presented in version 0 of the site descriptive model /SKB, 2002b/.
- The structural model of the Äspö HRL (Äspö 96 model), /Rhén et al, 1997b/.
- The GEOMOD structural model /Berglund et al, 2003/.
- The Ävrö RVS model /Markström et al, 2001/.
- The Laxemar model test /Andersson et al, 2002b/.
- Measurements of mainly ductile structures, as well as some brittle structures and bedrock contacts at 91 of the 353 observation points that were documented during the bedrock mapping during 2003 /Wahlgren et al, 2004/ (see section 4.2.4).
- A variety of structural geological data covering the Simpevarp peninsula, Hålö and Ävrö, as assembled in /Curtis et al, 2003a/ and /Curtis et al, 2003b/.

- Borehole and seismic reflection data that have been assembled in connection with the ongoing site investigation programme (see sections 4.4 and 4.2, respectively).

The local scale structural model addresses the deformation zones that are inferred to be of length 1 km or longer, i.e. local major and regional deformation zones according to the terminology of /Andersson et al, 2000/. Structures that are considered to be shorter than 1 km are handled in a statistical way and are described and characterised in the stochastic description in Section 5.1.6.

For the modelling of deformation zones in the Simpevarp 1.1 local scale model, it is assumed that the linked-lineaments can provide the necessary detailed information about the location and extent at the surface of possible deformation zones and are regarded as preferred surface information in comparison with existing older lineament data.

The version 0, Laxemar model test, GEOMOD and Ävrö models have been checked systematically relative to the linked-lineament map of the local scale model domain. Interpretations that are related to the new linked-lineament map are always preferred, unless there is other additional supportive information from geophysics, boreholes or tunnels.

A key question in the modelling procedure concerns the extent of the deformation zones at depth. It is assumed that the deformation zones that are vertical or steeply dipping, and can be recognised at the surface as linked lineaments, extend downwards the same distance that they can be traced as a lineament at the surface. This assumption implies that the frequency of deformation zones decreases with depth. Despite the restriction inherent in this assumption, the majority of deformation zones in the structural model extend to the base of the local model volume, as their surface length exceeds the depth of the model (1,100 m).

Each interpreted deformation zone has also been ranked based on confidence of its existence being high, medium or low. Zones that have high confidence ratings have, in addition to lineament indications, also supportive information from geophysics, boreholes and/or tunnels.

Interpreted zones with medium confidence have strong lineament indications from more than one lineament attribute, those attributes being from topography, magnetics, EM or other indirect indications such as seismics or ground geophysics.

Interpreted zones with low or very low assigned confidence have lineament indications based only on one lineament attribute (such as topography etc), or weak indications based on a combination of several indirect sources.

Geometric modelling

An initial step in the modelling procedure made use of the previous models established in the Simpevarp area. Each of the zones in these models was checked against the linked-lineaments and updated interpretations were generated in each case.

The subsequent modelling work was executed by placing the following groups of deformation zones in the local scale model volume, in the order indicated below:

- The regional deformation zones, and their associated splays, which have linked-lineament support and have been included in older existing structural models.
- The local major fracture zones which have linked-lineament support and have been included in older structural models or are supported by new borehole data.
- The possible deformation zones that have been inferred solely on the basis of the interpretation of linked lineaments.

The modelling procedure has made use of the key assumptions concerning the relationships between dip and the along-strike and down-dip extents of a single deformation zone, as outlined in the previous section.

Fourteen deformation zones, recognised as deformation zones with high confidence, have been included in the model. These zones have been included in one or several of the previous models. Each one of these interpreted zones is observed both indirectly, through lineament or geophysical

data, and directly through borehole or tunnel observations. An exception is the Mederhult zone (ZSMEW002A) which has not been observed in boreholes or tunnels. These high confidence deformation zones, as interpreted in model version Simpevarp 1.1, are summarised in Table 5-6 and illustrated in Figure 5-3.

Table 5-6. Summary of deformation zones that have been included in the deterministic structural model at the local scale.

Zone ID, SDM version 1.1	Alternative name	Zone ID, in other models	Basis for interpretation
ZSMEW002A	Mederhult deformation zone	Combination of a short section of XSM013A0 with v0 ZSM0002A0.	Topographic data, airborne geophysics (magnetic data, VLF data), ground geology, seismic refraction.
ZSMEW004A		XSM0010A0, B0 & XSM0016A0 from V0 model.	Airborne geophysics (magnetic 100% along the length, low uncertainty), Position on surface and Äspö tunnel (tunnel lengthchainage 0/318 m).
ZSMEW007A		ZLXEW02 in the Laxemar model test.	Airborne geophysics (magnetic 100% along the length, electrical data, low uncertainty), topography. Borehole KLX02.
ZSMEW009A		EW3 in the GEOMOD model.	Topography, ground geology, Äspö tunnel (1,407–1,421 m), borehole KAS06 (60–70 m).
ZSMEW013A		ZLXNW04 in the Laxemar model test.	Airborne geophysics (magnetic 100% along the length, electrical data, low uncertainty), topography, borehole KLX01 (750 m).
ZSMNE005A	Äspö shear zone	EW1b in the GEOMOD model. ZSM0005A0, ZSM0004A0 in the V0 model. ZLXNE01 in the Laxemar model test.	Airborne geophysics (magnetic 100% along the length, low to medium uncertainty), Ground geology, ground geophysics, Boreholes (KA1755A, 90–100 m), Äspö data.
ZSMNE006A		NE1 in the GEOMOD model. ZSM0006A0 in the V0 model. ZLXNE06 in the Laxemar model test.	Airborne geophysics, topography, Äspö tunnel (chainage 1/290 m).
ZSMNE012A		Linked lineaments XSM0012A0, (part of B0), A1, A3 & B1. NE4 in the Äspö 96 model. Z15 in the Ävrö model.	Airborne geophysics (magnetic 100% along the length, low to medium uncertainty) Äspö tunnel, borehole.
ZSMNE016A		Northern section of linked lineament XSM0016A0. ZSM0004A0/B0 in the v0 model.	Airborne geophysics, topography, tunnel.
ZSMNE024A		Z13 in the Ävrö model.	Airborne geophysics (magnetic 91% along the length), nuclear power plantOKG cooling water intake tunnel.
ZSMNE040A		ZSM0003A0 in the v0 model. ZLXNE04 (part ZLXNE03) in the Laxemar model test.	Airborne geophysics (magnetic 60% along the length), boreholes KLX01 and KLX02.
ZSMNS017A ZSMNS017B		NNW4 in the GEOMOD model.	Topography, borehole KA2048B and tunnel evidence (chainage 1/876, 1/979, 3/083 m).
ZSMNW004A		Z14 in the Ävrö model.	Airborne geophysics (magnetic 100% along the length, low to medium uncertainty) ground geophysics, topography.
ZSMNW007B		ZSM0007A0 in the v0 model. ZLXNS01 in the Laxemar model test.	Airborne geophysics (magnetic >70% along the length, medium uncertainty) topography.

Possible deformation zones based solely on the interpretation of linked lineaments that was completed during the ongoing site investigation programme.

49 unspecified possible deformation zones in four orientation sets (divided into 59 segments).

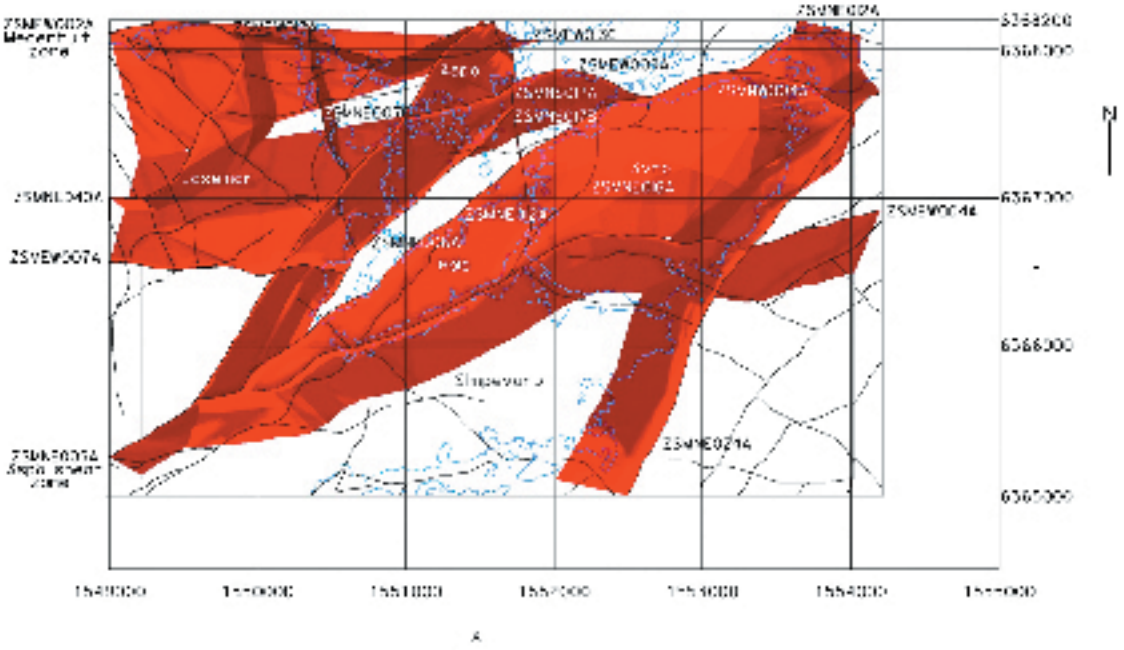

Figure 5-3. *The fourteen interpreted high confidence deformation zones in the Simpevarp 1.1 local scale model domain, see also linked-lineament map in Figure 4-23.*

The positions of these zones at the surface have been redefined on the basis of the interpretation of the linked lineaments in the ongoing site investigation programme (see Section 4.2.3). These lineaments are based primarily on the topographic data, and also to some degree on magnetic and electric data. Since the interpretations of the new airborne geophysical and topographic data have provided a more precise siting of these zones on the surface and, thereby, their mean strike, there are changes in these attributes relative to those reported in the site descriptive model version 0 for Simpevarp /SKB, 2002b/.

The dip of each of these fourteen zones has been estimated using geophysical data plus borehole or tunnel observations. These observations are in several cases identical to observations made in support of the related models, but the redefinition of lineaments on the surface has resulted in changes to the dip of the zones.

Fourty-nine deformation zones with medium or low confidence have also been included in the deformation zone model. These zones are based only on the linked lineament interpretation.

Deformation zones correlated to zones in model version 0

Seven of the high confidence zones are based, in parts, on zones included in the version 0 model /SKB, 2002b/, c.f. Table 5-6.

The regional Mederhult deformation zone, ZSMEW002A, follows the interpretation made in model version 0 (zone ZSM0002A0) and a short section of the linked-lineament XSM013A0. The zone can be traced westward to the boundary of the regional model domain following the version 0 interpretation. The surface extent is interpreted to be at least 30 km. It is argued here that the linked lineament XSM013A0 provides a more precise extension eastward than the previous interpretation used in version 0. The detailed lineament map shows that there are no indications from magnetics or topography that suggest a zone extension eastward as suggested in version 0. The linked-lineament XSM013A0, on the other hand, is well indicated by topography, magnetics and EM. The zone has been verified by ground magnetic and VLF measurements /Stenberg and Sehlstedt, 1989/, a refraction seismic survey /Rydström and Gereben, 1989/ and surface geology /Stanfors and Erlström, 1995/. Results from the VLF measurements indicate that the zone has a steep southerly dip, whereas observations on the surface suggest a more gentle dip to the southeast. The zone is not interpreted to intersect borehole KLX02, but to pass beneath its termination. The interpreted mean

orientation in the local scale model of deformation zones is 76/55. The conclusion in the version 0 model regarding dextral movements of the Mederhult deformation zone during the Phanerozoic has not been verified and remains an open issue.

The local major zone ZSMEW004A, is based on the magnetic lineaments XSM0010A0, XSM0010B0 and XSM0016A0. The dip of the zone is observed in the Äspö tunnel at chainage 0/318 m, which also corresponds with the version 0 zone ZSM0004A0, c.f. Figure 5-4. The interpretation of ZSMEW004A deviates from version 0 zone ZSM0004B0 on Ävrö, mainly based on the pronounced nature of the XSM0010A0 lineament together with surface observation on Ävrö. The lateral extension is estimated to be at least 8 km.

The regional Äspö shear zone, ZSMNE005A, is reinterpreted from the version 0 model zone ZSM0005A0 based on the new linked lineament data, c.f. Figure 5-5. The southernmost section of the Äspö shear zone is interpreted to link into the southern part of version 0 zone ZSM0004A0 due to a better defined linked lineament that runs through the whole local scale model domain (XSM0005A0). The lineament is a strong magnetic anomaly that does not follow the earlier south-west extension of the shear zone, but turns more west along version 0 zone ZSM0004A0. This zone also corresponds (further north) with NEHQ3 and EW-1b in the GEOMOD model and ZLXNE01 in the Laxemar model.

The surface outcrop of the local major zone ZSMNE006A is based on the linked lineament XSM0015B0, which corresponds well with the version 0 surface outcrop of zone ZSM0006A0. The dip of the zone is adjusted based on the GEOMOD model and the Äspö access tunnel at chainage 1/290 m. The reinterpreted dip is 65 degrees towards the NW compared to 70 degrees in the version 0 model. This zone also corresponds with ZLXNE06 in the Laxemar model test and NE-1 in the GEOMOD model.

The surface intersection of the local major zone ZSMNE016A is based on the north section of linked lineament XSM0016A0 and shows a medium magnetic anomaly and a strong topographic depression. The interpreted surface outcrop corresponds well with the southern part of version 0 zone ZSM0004B0. However, with the current orientation and northern termination of ZSMNE016A it does not intersect borehole KAV01, as does the corresponding version 0 zone. The zone is bounded in the south by ZSMEW004A and in the north by ZSMNE012A.

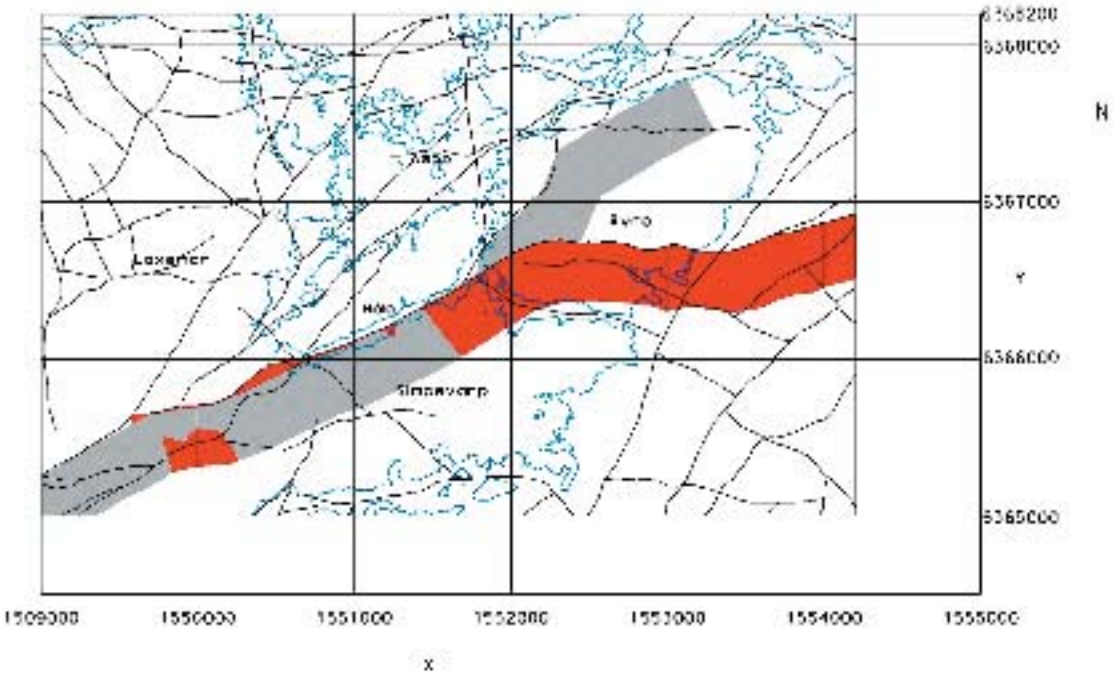

Figure 5-4. *Interpretations of deformation zone ZSMEW004A in model version Simpevarp 1.1 (red) and ZSM0004A0 and ZSM0004B0 in version 0 (grey). The interpreted linked lineaments are shown in black.*

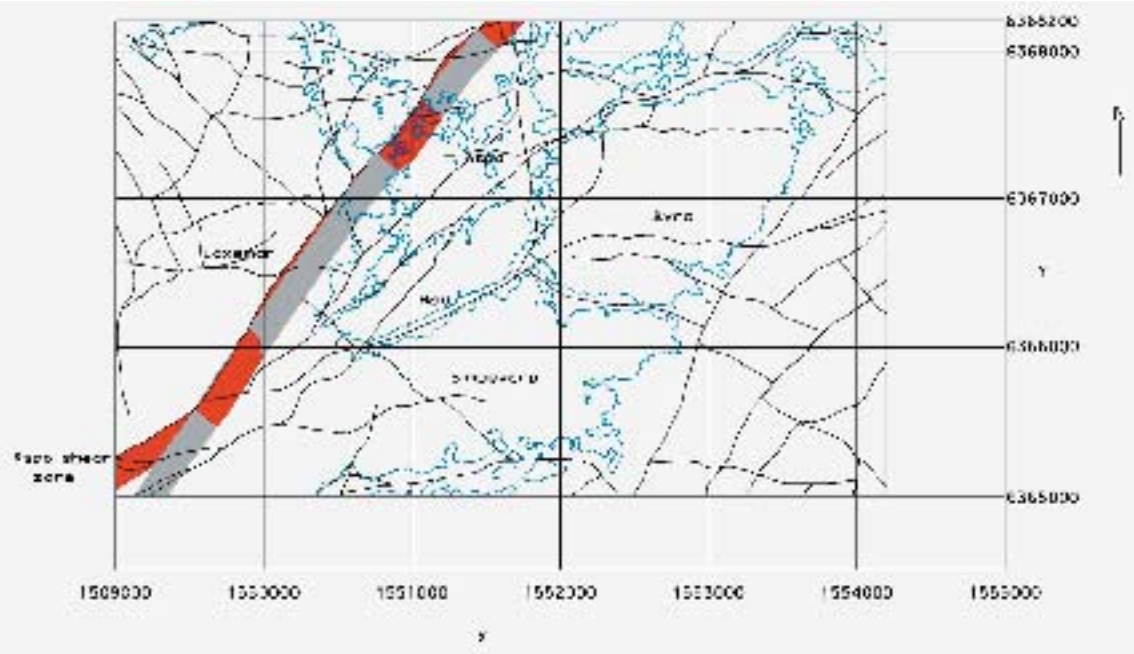

Figure 5-5. *Interpretations of the Äspö Shear zone (ZSMNE005A) in model version Simepavarp 1.1 (red) and version 0 (grey). Note the new interpretation of the southwestern branch along lineament XSM0005A0. The linked lineaments are shown in black.*

The interpreted surface outcrop of the local major zone ZSMNE040A is based on the linked lineament XSM0040A0, which has strong topographic and electromagnetic anomalies and a medium magnetic anomaly. The zone follows the northern section of the version 0 zone ZSM0003A0 well at the surface, except for the southern end where the linked lineament flexes to the west. The dip (63 degrees SE) deviates from the version 0 interpretation (90 to 60 degrees west) and is based on interpreted intersections with boreholes KLX01 (421 m) and KLX02 (1,040 m), c.f . Figure 5-6. The report on the Laxemar model test accounts for two zones which in part follow the interpreted deformation zone; ZLXNE03 and ZLXNE04.

The local major zone ZSMNW007B is based on the linked lineament XSM0003A1 which exhibits strong magnetic and topographic anomalies. This zone corresponds with the version 0 zone ZSM0007A0, but has a slightly different mean orientation because of the new lineament interpretation. The new orientation (165/90) also corresponds well with the Laxemar alternative model zone ZLXNS01.

Deformation zones correlated to zones in the Laxemar, Ävrö or GEOMOD models

There are seven more high confidence zones that are, to certain degrees, based on the GEOMOD, Laxemar or Ävrö models and are based on both indirect and direct observations.

The local major zone ZSMEW007A has a surface intersection based on the linked lineament XSM0007A0, which is a significant topographic, magnetic and electric anomaly. The interpreted zone is interpreted to intersect borehole KLX02 at approximately 340 m and is parallel to the zone ZLXEW02 included in the Laxemar model test, c.f. Figure 5-7.

The local major zone ZSMEW009A has a surface outcrop based on the linked lineament XSM0009A0. The interpreted zone is parallel to the GEOMOD zone EW3 which is confirmed in dug trenches on the Äspö island, in the Äspö tunnel (TASA 1/407 m) and in borehole KAS06 (66 m). The dip of the zone is based on EW3 as interpreted in the GEOMOD model.

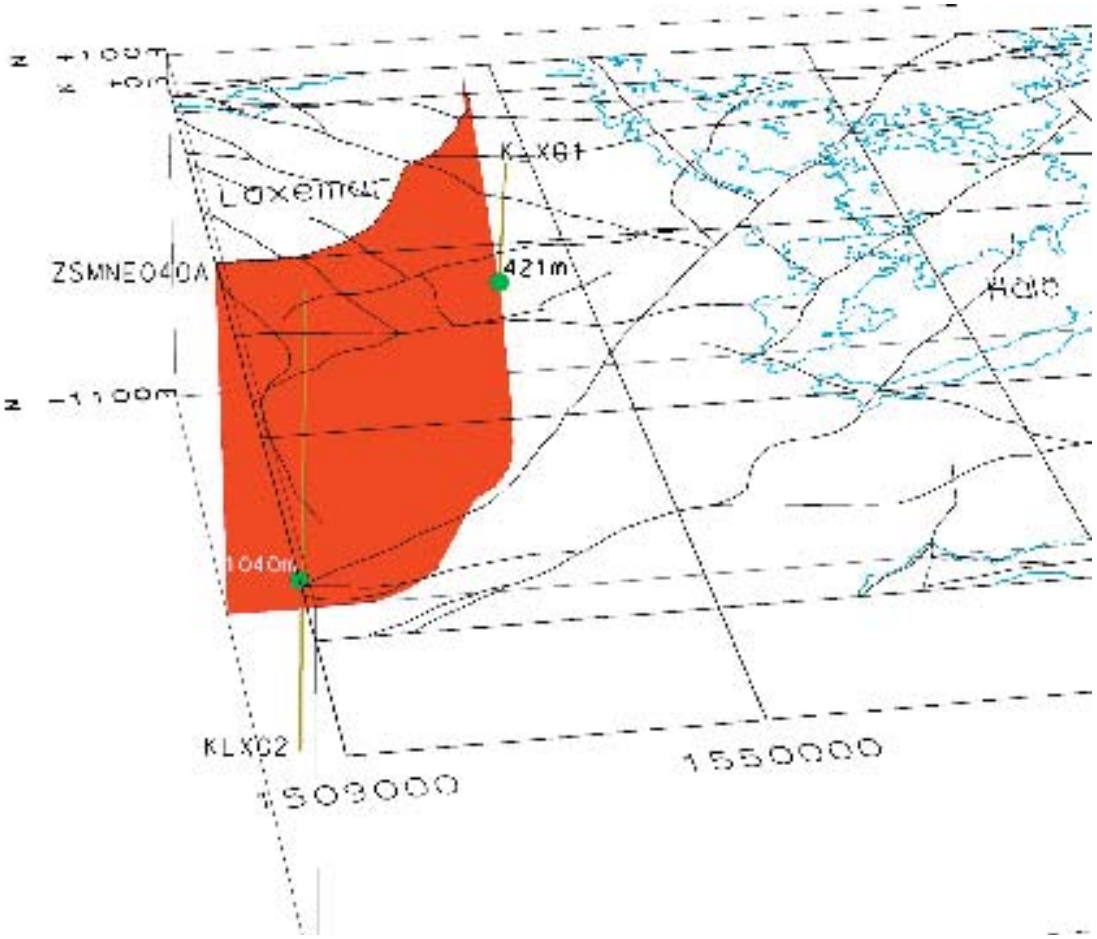

Figure 5-6. *Interpreted deformation zone ZSMNE0040A and its intersections with boreholes KLX01 at 421 m and KLX02 at 1,040 m.*

The local major zone ZSMEW013A is based on the linked lineament XSM0013A0 which shows a magnetic anomaly along its full extent with a medium confidence. The interpreted zone is modified to terminate against ZSMEW002A (western boundary) and at the eastern end of the linked lineament XSM0014A0. This zone corresponds to zone ZLXNW04 in the Laxemar model test, which has been possibly intersected in the percussion borehole HLX02 /Andersson et al, 2002b/.

The local major zone ZSMNE012A is based on the linked lineaments XSM0012A0, 12A1, 12B1 and 12A3. A part of the zone is based on lineament 12A0, which can be correlated with zone ZLXNE02 of the Laxemar model test and zone Z15 in the Ävrö model. The zone section based on lineament 12B1 is correlated with the Äspö access tunnel, chainage 0/827 m and zone Z15 in the Ävrö model. The portions of the zone based on lineaments 12A3 and 12A1 are correlated with zone Z15 in the Ävrö model.

The local major zone ZSMNE024A is based on the linked lineament XSM0024B0 which is indicated by a strong offshore magnetic and topographic anomaly immediately east of Ävrö and the Simpevarp peninsula. This zone is correlated with an observation in the OKG III cooling water intake tunnel (distributed over a 175 m section). It is also correlated with zone Z13 of the Ävrö model in its northern part, which in turn is based on seismics. The zone is interpreted to dip 60 degrees NW under Ävrö Island (see Figure 5-3).

The local major zone ZSMNS017 is divided into two segments, A and B separated by zone ZSM0012A. The former zone is correlated with NNW4 in the GEOMOD model and is also identified in the Äspö access tunnel at chainages 1/876 m, 1/979 m and 3/083 m, as well as in selected boreholes sunk at Äspö (see Appendix 2).

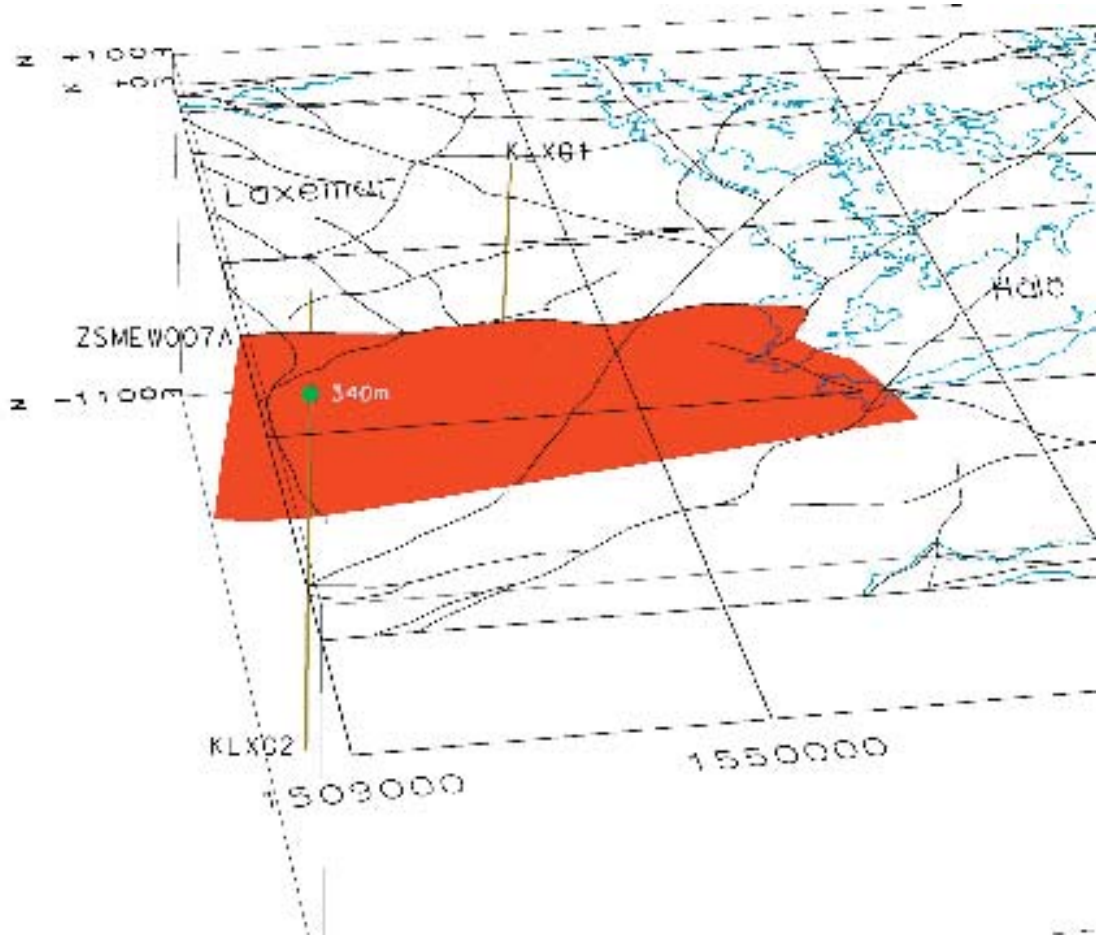

Figure 5-7. *Interpreted deformation zone ZSMEW007A and its intersection with borehole KLX02 at 340 m borehole depth.*

The local major zone ZSMNW004A is based on the topographic linked lineament XSM0004B0 and is sub-parallel to zone Z14 of the Ävrö model.

There remains a clear possibility that one or more additional deformation zones will be recognised/interpreted in later modelling phases, following completion of more surface and borehole investigations in the Simpevarp and Laxemar subareas.

Possible deformation zones inferred solely from the interpretation of lineaments

The remaining 49 possible deformation zones included in the local structural model correspond to the linked lineaments that are 1 km or more in length. It is assumed that the strike of the possible deformation zones correspond to the trends of the corresponding linked lineaments. All these deformation zones are assumed to be vertical (90° dip).

The presented Simpevarp 1.1 model of deformation zones consists of only one “base case” model. Alternative models for deformation zones have not yet been considered, mainly due to time constraints. Alternative models are likely to be presented for the subsequent model version Simpevarp 1.2.

Property assignments

Key properties, and numerical estimates of the uncertainty in some of these parameters, have been attributed to each of the fourteen high confidence deformation zones that are based on a variety of geological or geophysical information or deduced from older models (Table 5-7). The properties of the deformation zones are presented in tabular format in the description of the Simpevarp subarea (Section 7.3.1).

The properties of the seven deformation zones that were classified as being highly probable to certain in the SDM version 0 have been extracted primarily from /SKB, 2002b/. For example, the strike and length of the Mederhult zone are based on the interpretation of linked lineaments (see Section 4.2.3) and references to SDM version 0. Since an estimate of the total length of these seven deformation zones was completed during the model version 0 work /SKB, 2002b/, the total length of these regionally important zones, and their associated splays, is also provided in the property tables in Appendix 2.

The properties of the remaining seven deformation zones that were recognised from either the Laxemar model test, Ävrö or GEOMOD models have been extracted primarily from the data tabulated in the Laxemar model test report /Andersson et al, 2001/ and the report on the Ävrö model /Markström et al, 2001/. The GEOMOD model was provided without any description and therefore references are made to properties related to the Äspö model /Rhén et al, 1997b/.

There are few data available at the present time that relate to the properties (including numerical estimates of uncertainty) of the interpreted possible deformation zones, which are based solely on the interpretation of linked lineaments, c.f. Table 5-8. The data available are presented for each orientation set – NW, NE, NS and EW – in the description of the site (Section 7.2.1). Both the NW and NS orientation sets are divided into two subsets that relate to the regional and local major deformation zones, respectively.

Table 5-7. Properties assigned to the fourteen high confidence deformation zones along which there are, to variable extents, supporting geological and geophysical data.

Property	Comment
Deformation zone ID	ZSM******, in two places plus thewith additional letter A, B, C, D and E (according to the nomenclature recommended by SKB).
Position	With numerical estimate of uncertainty.
Strike and dip	With numerical estimate of uncertainty.
Width	With numerical estimate of uncertainty.
Length	With numerical estimate of uncertainty.
Ductile deformation	Indicated if present along the zone.
Brittle deformation	Indicated if present along the zone.
Alteration	Indicated if present along the zone.
Fracture orientation	In places, with numerical estimate of uncertainty.
Fracture frequency	With numerical estimate of uncertainty.
Fracture filling	Mineral composition.

Table 5-8. Properties assigned to the 49 possible deformation zones that are based solely on the interpretation of linked lineaments.

Property	Comment
Orientation set	Each zone within the set is identified with a ZSM****** code, in two places plus with additional letters A and B or A, B and C (according to the nomenclature recommended by SKB).
Position	With numerical estimate of uncertainty.
Strike and dip	With numerical estimate of uncertainty. Statistical analysis.
Width	With numerical estimate of uncertainty. Assumption − no data available.
Length subset	Regional (>10 km) or local major (1−10 km).
Ductile deformation	Indicated if present along the zone.
Brittle deformation	Indicated if present along the zone.

Estimates of the mean value of the strike and dip of the possible deformation zones for each of these sets (or subsets) are provided on the basis of the statistical analysis of fractures and lineaments in the DFN model (see Section 5.1.6). The estimates of width are based solely on a comparison with the fourteen deformation zones where more data are available. In essence, the given estimates represent an assumption.

Estimated properties are reported in Appendix 2.

Evaluation of uncertainty

In summary, in the whole model there are 63 deformation zones that are made up of 74 zone segments.

An expert judgement on the level of confidence for the occurrence of the various deformation zones is provided in Table 5-9 through Table 5-13. Fourteen deformation zones are allocated a high confidence of occurrence. One of these zones, ZSMNS017, consists of two segments (A and B).

39 deformation zones are allocated a medium confidence of occurrence. Once again, the different segments have been distinguished using letter notation (A, B and C) according to the denomination of the linked lineaments. Six deformation zones are allocated a low confidence of occurrence and four deformation zones are allocated a very low confidence of occurrence.

All the fourteen zones that are based, at least in part, on supporting geological and geophysical data are included in the deformation zones with a high confidence of occurrence. Since there is considerable uncertainty concerning the interpretation of the geological significance of the linked lineaments, the 49 deformation zones that are based solely on the interpretation of these lineaments are assigned a lower degree of confidence. Strictly, they form a group of possible deformation zones. For the reasons outlined in the evaluation of the primary data (see Section 4.2.3), both the character and the clarity of expression of the linked lineaments are used to assess the level of confidence in occurrence of the respective possible deformation zones that have been identified solely from lineaments.

The most important uncertainties in the properties of essentially all the interpreted deformation zones are related to their dip, their continuity along-strike and their down-dip extension. In the present model, the dip of most of the deformation zones is assumed to be 90°. Since there is little control on the dip of most of the zones, a presentation of different alternative models of deformation zone geometry has not been considered viable at this stage. Consequently, only a base model is presented for the along-strike continuity and down-dip extension of the interpreted deformation zones.

Quantitative estimates of the uncertainty in position, orientation, width and length of the fourteen deformation zones with high confidence of occurrence are provided in the tabulation of the properties of these zones in the site description (Section 7.2.1). Corresponding estimates of the uncertainty in the orientation and frequency of fractures along these zones have been given for some of the zones. Quantitative estimates of the uncertainty in the position of the interpreted possible deformation zones, which are based solely on the interpretation of linked lineaments, are also available in the various property tables presented in Section 7.2.1.

The detailed tectonic evolution of the deformation zones included in the Simpevarp 1.1 model is not well known, and hence little is known about the terminations of the individual zones against each other. The linked lineaments have been used as a guide where evidence is lacking.

Finally, there remains an overall conceptual uncertainty concerning the possible occurrence of gently dipping or sub-horizontal fracture zones in the Simpevarp area. Available data from the Äspö HRL provide little (or no) evidence of sub-horizontal zones, nor does the interpreted seismics presented in previous models. However, it is anticipated that work will be performed to analyse the possible existence of subhorizontal zones within the target area as more data become available.

Table 5-9. Table of confidence for the occurrence of deformation zones, high confidence.

Zone ID	Basis for interpretation	Confidence	Comments
ZSMEW002A (Mederhult zone)	Linked lineaments, VLF, seismic refraction. Ground geology.	High	Position on surface: combination of a short section of XSM013A0 with v0 (Version 0, ref: R-02-35) ZSM0002A0.
ZSMEW004A	Airborne geophysics (magnetic 100% along the length, low uncertainty), tunnel. v0.	High	Position on surface and Äspö tunnel. Based on XSM0010A0, B0 & XSM0016A0. Ref: R-02-35.
ZSMEW007A	Airborne geophysics (magnetic 100% along the length, electrical data, low uncertainty), topography. borehole.	High	Ref: ZLEW02 alternative Laxemar model test /TR-02-19/.
ZSMEW009A (EW3)	Topography, ground geology, tunnel, borehole.	High	Ref: EW3 GEOMOD model.
ZSMEW013A	Airborne geophysics (magnetic 100% along the length, electrical data, low uncertainty), topography, borehole.	High	Ref: ZLXNW04 alternative Laxemar model.
ZSMNE005A (Äspö shear zone)	Airborne geophysics (magnetic 100% along the length, low to medium uncertainty), Ground geology, ground geophysics, Borehole, Äspö data.	High	’Äspö shear zone’ Ref: NEHQ3, EW1b GEOMOD model. Ref: ZSM0005A0, ZSM0004A0 in R-02-35. Ref: ZLXNE01 alternative Laxemar model.
ZSMNE006A (NE1)	Airborne geophysics (magnetic 100% along the length, low to medium uncertainty), tunnel, boreholes, Äspö data.	High	Ref: NE1 GEOMOD model. Ref: ZSM0006A0 in R-02-35. Ref: ZLXNE06 alternative Laxemar model.
ZSMNE012A (NE4)	Airborne geophysics (magnetic 100% along the length, low to medium uncertainty) Tunnel, borehole.	High	Linked lineaments XSM0012A0, (part of B0), A1, A3 & B1. Ref : NE4, Äspö 96, TR97-06. Ref: Z15 Ävrö model, R-01-06.
ZSMNE016A	Airborne geophysics, topography, tunnel.	High	Only N section of lineament XSM0016A0. Ref: ZSM0004A0/B0 in R-02-35.
ZSMNE024A	Airborne geophysics (magnetic 91% along the length) tunnel.	High	Ref: OKG 3 intake tunnel. Ref: Z13 Ävrö model.
ZSMNE040A	Airborne geophysics (magnetic 60% along the length) boreholes.	High	Ref: ZSM0003A0 in R-02-35. Ref: ZLXNE04 (part ZLXNE03) alternative Laxemar model.
ZSMNS017A ZSMNS017B	Topography, borehole BH and tunnel evidence.	High	Ref: GEOMOD model, NNW4.
ZSMNW004A	Airborne geophysics (magnetic 100% along the length, low to medium uncertainty) ground geophysics, boreholes, topography.	High	Ref: Z14 Ävrö model.
ZSMNW007B	Airborne geophysics (magnetic >70% along the length, medium uncertainty) topography.	High	Ref: ZSM0007A0 in R-02-35. Ref: ZLXNS01 alternative Laxemar model.

Table 5-10. Table of confidence for the occurrence of deformation zones, EW striking zones.

Potential Zone	Basis for interpretation	Confidence level	Comments
EW set of possible deformation zones ZSMEW006A ZSMEW013B ZSMEW013C ZSMEW014A ZSMEW014B ZSMEW023A ZSMEW028A ZSMEW038B ZSMEW039A ZSMEW039B ZSMEW042A ZSMEW052A	Airborne geophysics (magnetic ≥70% along the length ± electrical, low to medium uncertainty) ± topography.	Medium	
ZSMEW026A ZSMEW027A ZSMEW038A	Airborne geophysics (magnetic <70% along the length ± electrical, medium to high uncertainty) ± topography.	Low	
ZSMEW023B	Topography.	Very low	

Table 5-11. Table of confidence for the occurrence of deformation zones, NE striking zones.

Potential Zone	Basis for interpretation	Confidence level	Comments
NE set of possible deformation zones ZSMNE008A ZSMNE011A ZSMNE012D ZSMNE018A ZSMNE019A ZSMNE020A ZSMNE021A ZSMNE022A ZSMNE029A ZSMNE031A ZSMNE032A ZSMNE033A ZSMNE033B ZSMNE034A ZSMNE036A ZSMNE041A ZSMNE044A ZSMNE044B ZSMNE044C ZSMNE045A ZSMNE050A	Airborne geophysics (magnetic ≥70% along the length ± electrical, low to medium uncertainty) ± topography.	Medium	ZSMNE018A, an interpreted splay of this zone has been identified by ground geophysics Ref: P-03-66.
ZSMNE043A	Topography.	Very low	

Table 5-12. Table of confidence for the occurrence of deformation zones, NS striking zones.

Potential Zone	Basis for interpretation	Confidence level	Comments
NS set of possible deformation zones ZSMNS037A ZSMNS046A ZSMNS049C	Airborne geophysics (magnetic ≥70% along the length ± electrical, low to medium uncertainty) ± topography.	Medium	
ZSMNS001A	Topography (ref:Laxemar model in TR-02-19).	Very Low	XSM0003A1 outside the local domain, ZLXNS04 Laxemar model test within the domain volume present at depth- not on surface.

Table 5-13. Table of confidence for the occurrence of deformation zones, NW striking zones.

Potential Zone	Basis for interpretation	Confidence level	Comments
NW set of possible deformation zones ZSMNW025A ZSMNW025D ZSMNW030A ZSMNW035A ZSMNW035D ZSMNW047A ZSMNW048A ZSMNW048B ZSMNW049A ZSMNW051A ZSMNW051B	Airborne geophysics (magnetic ≥70% along the length ± electrical, low to medium uncertainty) ± topography.	Medium	ZSMNW047A confidence based on Laxemar model test. Partial coincidence with ZLXNS03 and ZLXNW01.
ZSMNW028B ZSMNW035B ZSMNW035C ZSMNW049B	Airborne geophysics (magnetic <70% along the length ± electrical, medium to high uncertainty) ± topography.	Low	
ZSMNW007A ZSMNW025C	Topography.	Very low	

5.1.6 Stochastic DFN modelling – local scale

Modelling assumptions and input from other models

The assumptions for the local stochastic model of fracturing are described below, along with the rationale for why the assumptions are reasonable given the current state of knowledge about the Simpevarp area.

Assumption 1:

The outcrops and boreholes contain data that span the range of expected geological conditions in the regional rock volume. This assumption is important, as there are several lithological domains in the regional rock volume, and at present, a limited number of fracture analyses from boreholes and outcrops. If the properties of the fracture system are lithology-dependent, then it is necessary to have at least sufficient information to bracket the range of expected conditions in lithologies where no direct data have been obtained to date. Otherwise, the uncertainties for these portions of the rock volume are unknown.

Rationale for Assumption 1:

It is not necessary to sample every lithology if the controls on fracture intensity and orientation can be determined, and these controls can be shown applicable to unsampled lithologies. For example, if it was found that fine-grained rock has a characteristic intensity that differed from that of coarse-grained rock, then it would not be necessary to sample every fine-grained or coarse-grained lithology individually in order to construct a useful, defensible preliminary model. As the mechanical properties of intrusive crystalline rocks generally vary by composition/mineralogy, depth and grain-size, it should be possible to assess these controls with the existing data set and establish the necessary relationships. However, this assumption needs to be validated.

Assumption 2:

All fracture data are equally valid. Data comes from many different sources and tools. There are outcrop data, borehole data and lineament data. Lineaments, for example, may reflect features other than fractures, and the quality of the fracture data in core may reflect whether the core was obtained from rotary coring or percussion drilling. Since all inferences are based on the data without regard to possible differences in quality, any conclusions based upon a particular data set could be weaker or stronger depending upon the relative quality of that data set.

Rationale for Assumption 2:

It is difficult without co-located information of different types to assess the quality of the various data types. This assumption could be validated in the future by locating new boreholes where there are existing outcrops.

While there remain various other hypotheses to be tested, there are no other assumptions required for this model.

Data sources for the DFN analysis

Data from five different sources have been used in the DFN analysis;

- Linked lineament map presented in Section 4.2.3.
- Outcrop maps ASM000025, ASM000026, ASM000205 and ASM000206, presented in Section 4.2.4.
- Cored borehole data from KSH01A, KSH01B and KLX02, presented in Section 4.4.
- Percussion-drilled data from HSH01, HSH02 and HSH03, presented in Section 4.4.
- The single-hole interpretation from KSH01A presented in Section 4.4.5.

Geometrical modelling

The methodology for the geometrical DFN modelling is given in Appendix 3. Below follows the analysis and results of the DFN model.

Identification of fracture sets

Figure 4-26 shows the traces mapped in the outcrops ASM000025, ASM000026, ASM000205 and ASM000206. Equal-area stereoplots corrected for outcrop orientation are also displayed for each outcrop. The stereoplots indicate two or three dominant, near-vertical fracture sets at each location. However, the trace maps show that this is an oversimplification; there are many more sets, but they are close enough in orientation such that the contouring obscures them.

The trace maps were further examined to refine these sets into two or more subsets. The results are shown for outcrop ASM000025 in Figure 5-8. Details of all other set orientations for outcrops are given in Appendix 3. These figures show that there are typically 6 sets visible in each outcrop, and further that the same sets are often present in all four outcrops. The azimuth range used to define each set is also shown as an inset in the figures.

The azimuthal range shown on each of the trace maps reflects the angular range used to select the traces from the entire trace set for each outcrop. However, it does not represent a statistical orientation model for those traces. This was done by testing and evaluating alternative statistical models to determine; 1) the mean orientation and dispersion for each set; and 2) the goodness-of-fit for alternative models. The results are shown in Table 5-14.

Note that most of the fracture sets are poorly represented by a Fisher distribution. Other models, such as Bivariate Bingham, were also assessed, but none of the alternative models proved significant either.

The lack of fit might be due to the uncertainty in measuring the dip of a fracture in outcrop, since very little of the surface is visible. In any event, the lack of fit is not an issue for building a site-scale model because orientations can be Bootstrapped if necessary. Moreover, individual sets identified in outcrop were combined into lineament-related and non-lineament related sets, and re-estimated, as is described in the section on analysis of lineaments below.

Prior to consideration as to whether the same sets are present in all of the outcrops, it is useful to consider the relative chronology of the sets using the criteria set out in Appendix 3. The trace maps shown in Figure 5-9 show all the fractures mapped in the outcrops.

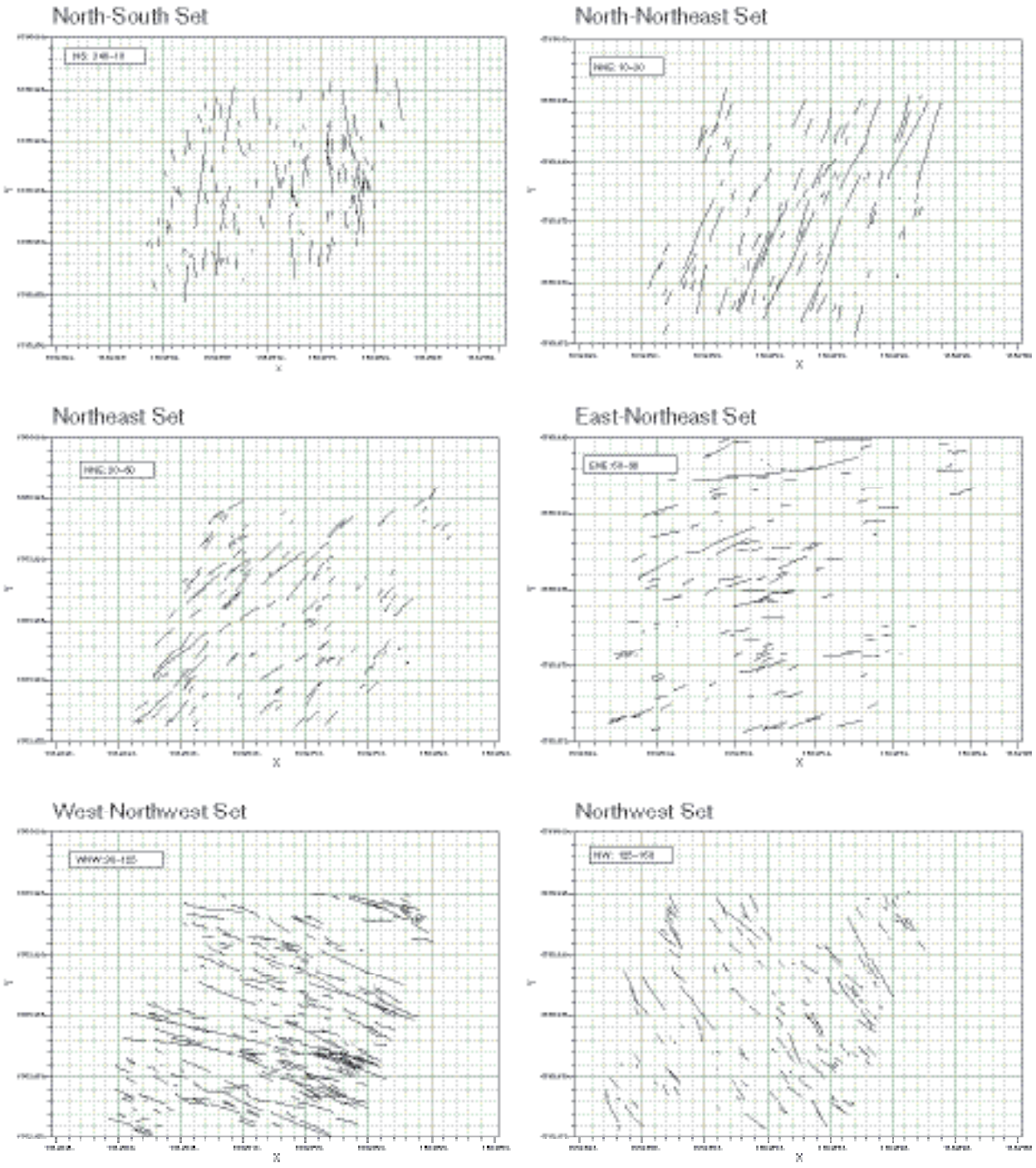

Figure 5-8. *Sets of fracture traces identified in outcrop ASM000025.*

Table 5-14. Statistical parameters for fracture sets identified in outcrops.

Set Name	Mean Pole Trend/ Plunge/Dispersion	Model	K-S
ASM000025NS	87.5/3.2/10.47	Fisher	not significant
ASM000025NNE	110.0/3.7/19.31	Fisher	not significant
ASM000025NE	135.5/3.0/12.78	Fisher	not significant
ASM000025ENE	346.2/3.6/7.31	Fisher	not significant
ASM000025WNW	199.0/0.04/10.7	Fisher	not significant
ASM000025NW	51.5/5.2/8.73	Fisher	1.8%
ASM000026EW	186.3/1.2/32.15	Fisher	not significant
ASM000026NE	334.5/0.4/30.34	Fisher	not significant
ASM000026NNE	310.1/0.8/30.47	Fisher	not significant
ASM000026NS	103.1/1.7/25.92	Fisher	not significant
ASM000026NNW	67.5/0.2/19.36	Fisher	not significant
ASM000026NW	214.3/0.8/25.71	Fisher	not significant
ASM000205NS	101.5/12.3/12.21	Fisher	not significant
ASM000205NE	128.6/3.3/10.97	Fisher	91.3%
ASM000205ENE	335.4/6.8/13.92	Fisher	not significant
ASM000205WNW	16.0/1.0/11.11	Fisher	not significant
ASM000205NW	50.7/3.1/8.86	Fisher	4.1%
ASM000205NNW	79.1/13.6/14.04	Fisher	not significant
ASM000206NNE	103.5/0.4/7.43	Fisher	not significant
ASM000206NE	314.8/4.2/6.7	Fisher	not significant
ASM000206ENE	335.9/4.6/8.53	Fisher	not significant
ASM000206EW	359.6/24.6/3.75	Fisher	27.8%
ASM000206WNW	27.2/26.9/3.79	Fisher	39.6%
ASM000206NW	50.5/10.9/6.42	Fisher	not significant
ASM000206NNW	252.6/0.2/6.14	Fisher	not significant

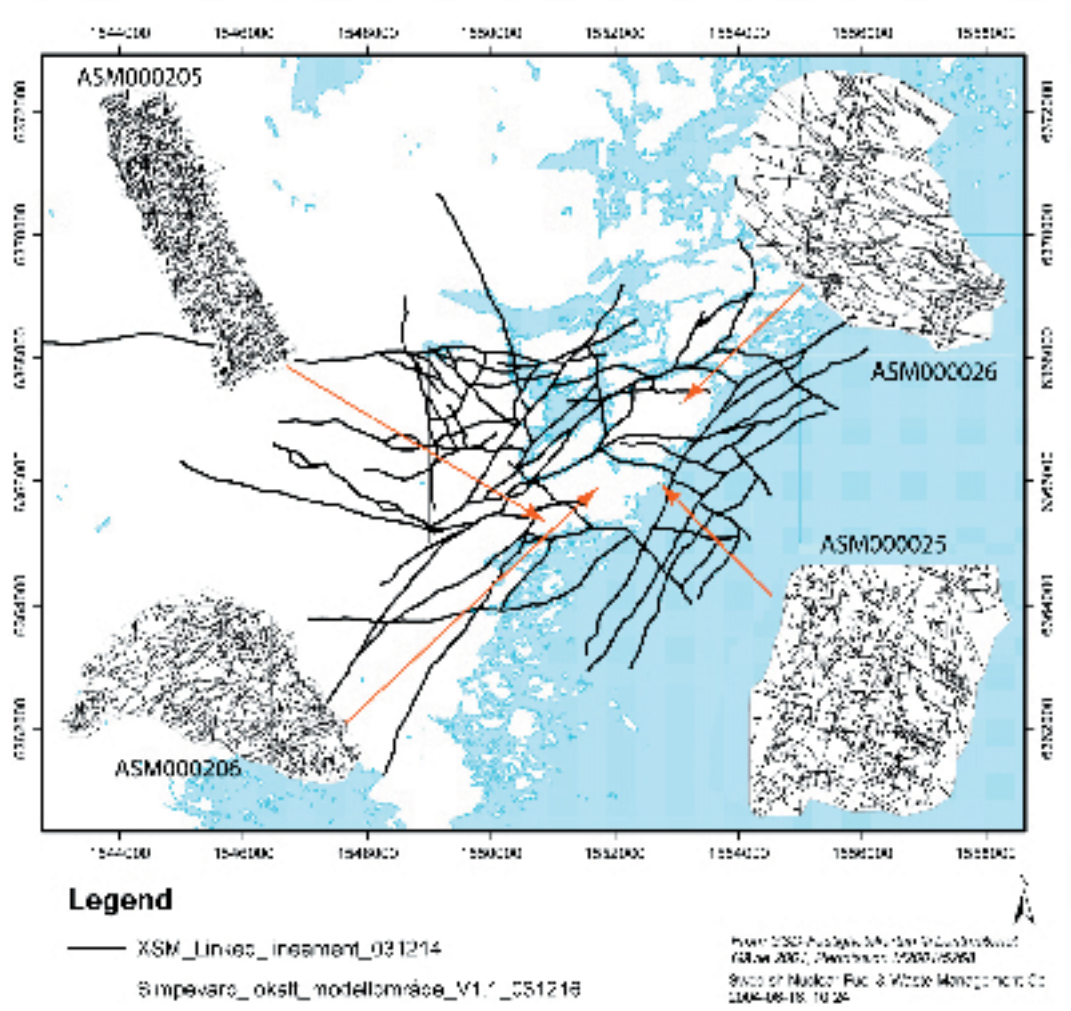

Figure 5-9. *Outcrop trace maps superimposed on lineament maps and rock domains. Note the similarity between adjacent lineament trends and the dominant fracture sets at outcrop.*

The figure shows that there appear to be consistent, dominant older sets in each of the outcrops. If terminations of each set is estimated and compared with other sets in each outcrop, the relatively oldest set typically strikes northeast or north-northeast. There are also prominent, older sets striking west-northwest and northwest. However, there is enough variation in the set azimuths to conclude that the oldest sets do not have constant mean orientations for all four outcrops.

Figure 5-10 through Figure 5-12 show the linked lineament traces and the trace azimuth rosettes. There are two sets present in the regional lineament group, wheras there are three sets present in the local major lineament group.

One of the interesting differences between the regional and local major sets is the 10°–20° difference in the northeast set. For the regional lineaments, the modal azimuth is between 20° and 30°, whereas for the local major lineaments, the modal azimuth varies between 40° and 60°. This is not unlike the difference seen at outcrop for the early-formed north-northeast to northeast set.

Figure 5-9 shows this correspondence more clearly. For example, ASM000025 has a dominant, early north-northeasterly fracture set that is nearly parallel to the adjacent lineament trend. Moreover, this same outcrop shows an early-formed west-northwest set that also parallels an adjacent lineament trend. ASM000206 has a more north-easterly trending fracture set that is early, but the local lineament trend, for example immediately to the northwest of the outcrop, also shows a more north-easterly azimuth rather than a north-northeasterly trend.

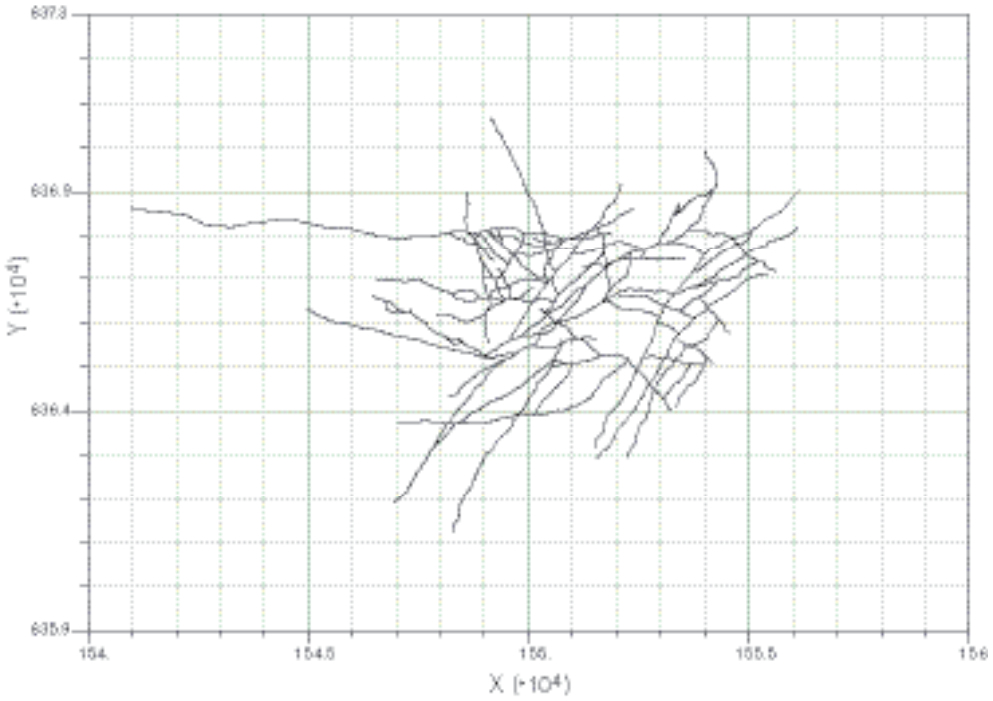

Figure 5-10. *Lineament traces for the Simpevarp area. The trace map shows both regional and local major lineament groups (See Section 4.2.3 for discussion of lineament classes).*

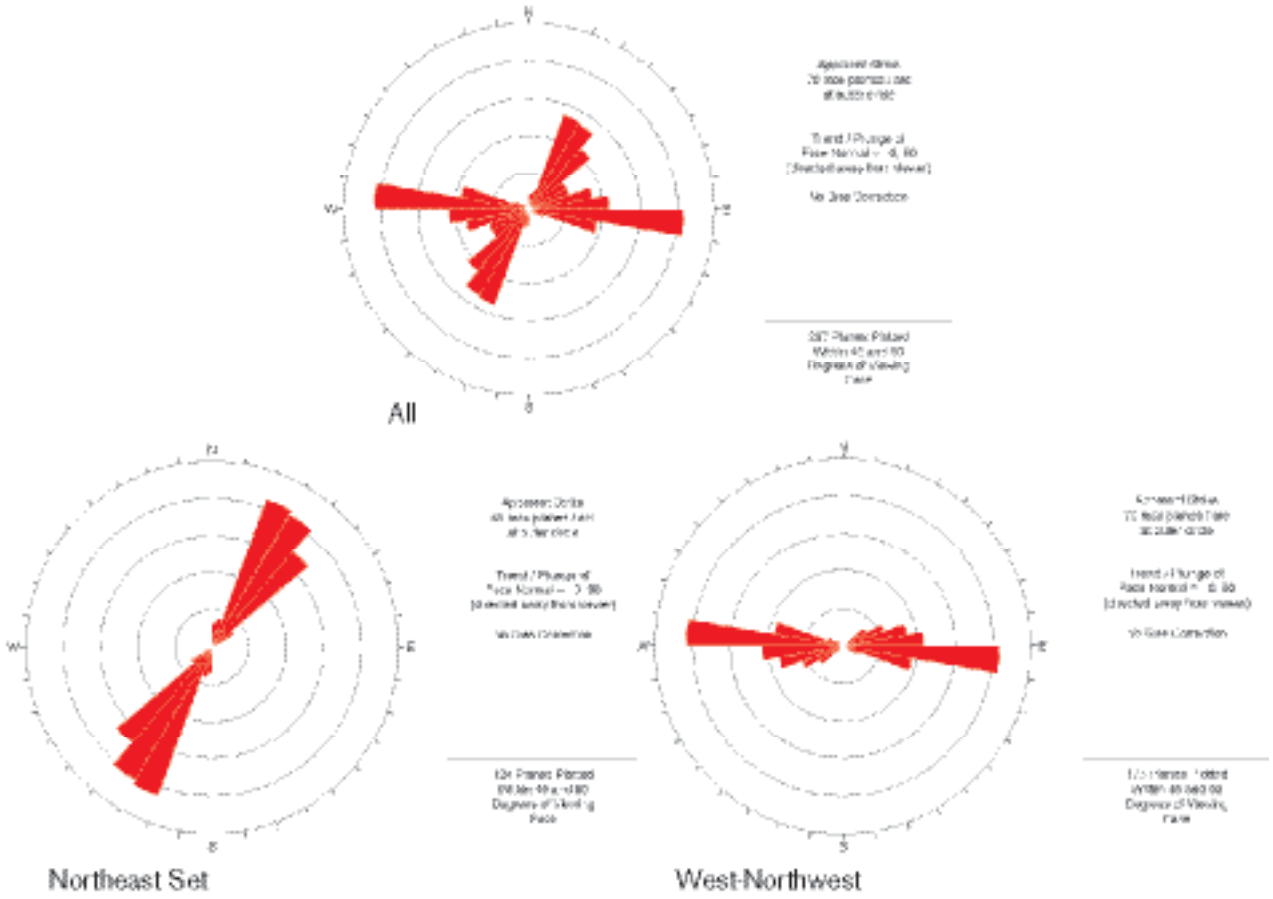

Figure 5-11. *Rosettes for lineaments belonging to the regional group.*

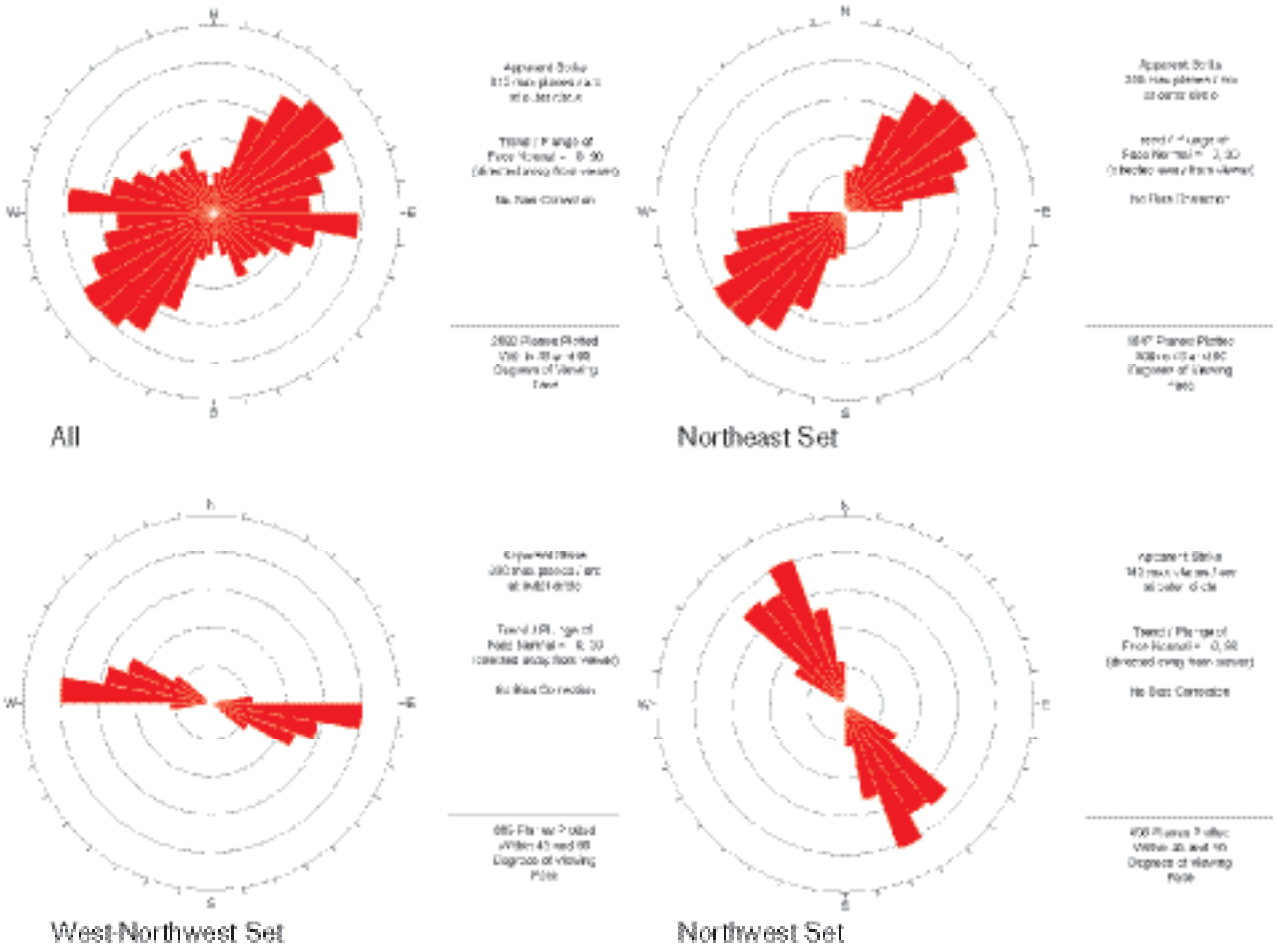

Figure 5-12. *Rosettes for lineaments belonging to the local major group.*

Although these visual similarities are not conclusive, they increase confidence that the early-formed fractures, that form a “backbone” or framework for fracturing seen in outcrop, are related to the neighbouring lineaments. As the lineament pattern changes locally across the Simpevarp regional scale model area, so does this fracture framework.

This conceptual model for the fracturing suggests that assigning a single mean fracture orientation to the lineament-related set would be inaccurate, since the local fracturing at outcrop and lineament scales varies spatially. In terms of developing a regional scale model, this implies that:

- Some fracture sets identified at outcrop appear to be related to nearby lineaments in terms of orientations.
- Orientations of lineament-related fracture sets, whether at the scale of meters or kilometres, change locally according to the dominant orientations of adjacent lineaments.
- Assignment of a mean orientation for any lineament-related fracture set would be inaccurate. Orientations should be assigned based on adjacent lineament trends, using the dispersion values calculated from the outcrop analyses of the respective sets (Table 5-15).

The outcrop fracture sets that are not part of one of the three lineament-related sets can be combined to see if they show consistency between outcrops. The resulting equal-area stereo plot is shown in Figure 5-13.

This stereo plot shows that there are two dominant, spatially consistent vertical sets with modal poles orientations at 325/04 and 277/01, a minor vertical set with a pole of 211/01, and two sub-horizontal sets with poles of 357/69 and 153/75.

Table 5-15. Mean dispersion (κ) for lineament-related fracture sets based on averaging outcrop values for each set.

Lineament-Related Fracture Set Identifier	Mean pole Trend/plunge/dispersion (Fisher)
NNE-NE	118.0/1.9/17.3
EW-WNW	17.1/7.3/11.2
NW-NNW	73.1/4.7/13.7

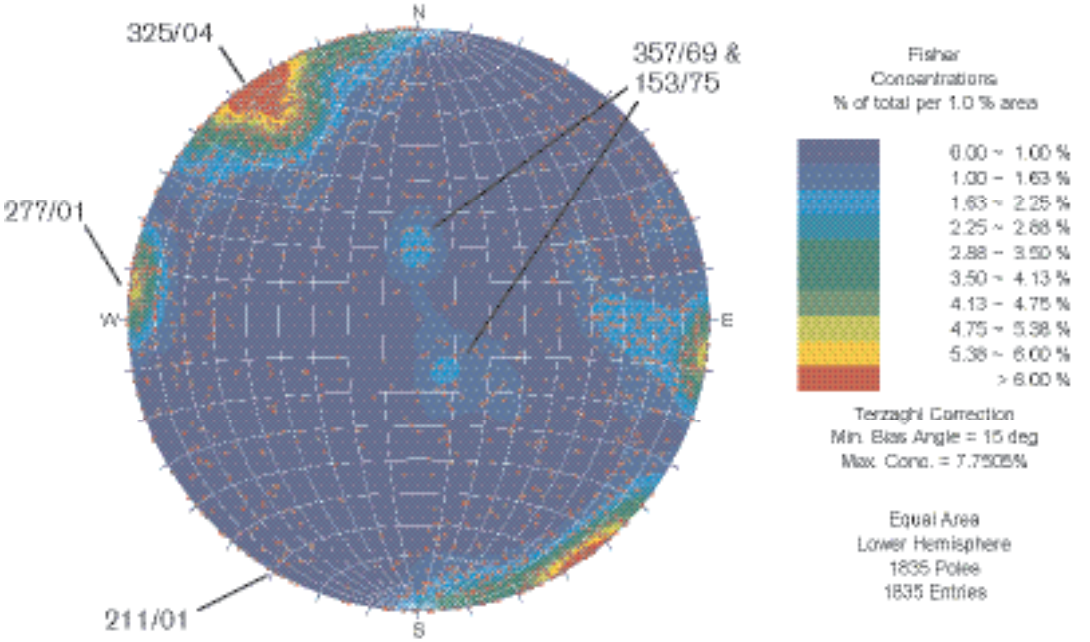

Figure 5-13. *Equal-area stereo plot of fracture sets not identified as lineament-related in outcrops ASM000025, ASM000026, ASM000205 and ASM000206. The plot is corrected for orientation bias.*

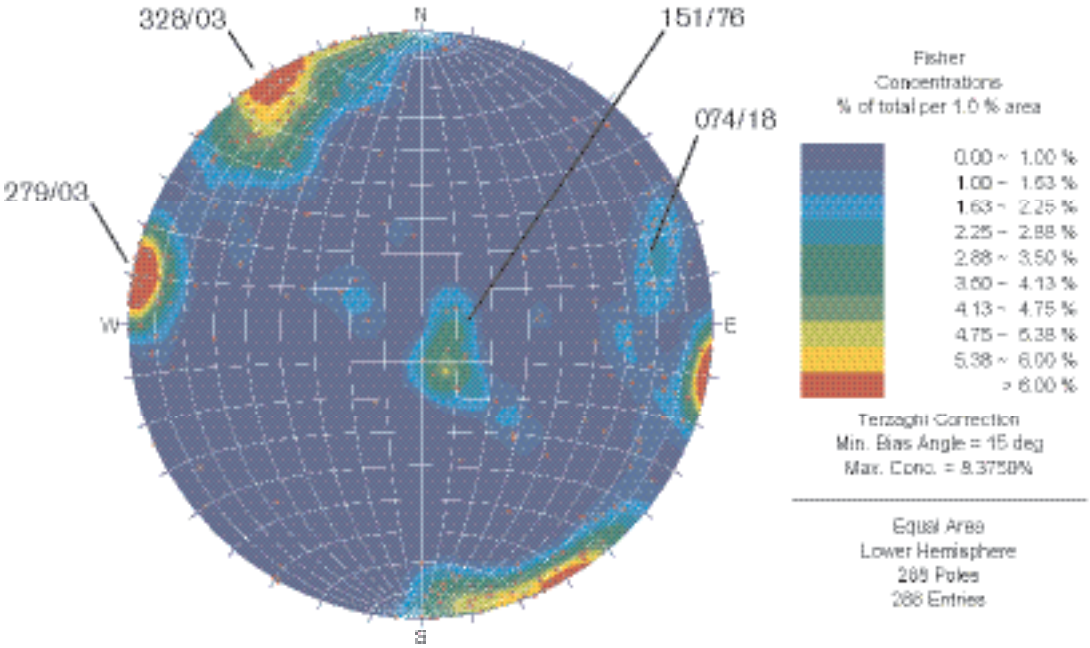

Figure 5-14. *Orientation of open non-lineament related fractures in outcrop.*

These stereo plots suggest that:

- The background fracturing is consistent among the four outcrops and not related to local lineament azimuth variations.
- There are two, possibly three subvertical background sets and one subhorizontal set.
- Open and sealed fractures show similar orientations.
- Background sets should be specified based upon the mean pole orientations and dispersions shown in Table 5-16 , which were calculated from the combined sets.

The stereo plots do not provide any evidence to suggest that the non-lineament-related fracture sets are older or younger. However, reference to the fracture set chronology previously discussed (see also Appendix 3) indicates that they are likely to be younger.

As was seen for the lineament-related sets, the northeasterly-striking set is the most numerous. The lineament-related fracture sets are designated Group 1 sets, wheras the background fracture sets are designated as Group 2 throughout the remainder of this report.

Estimation of fracture size

The size distribution parameters were estimated in two different ways: all sets identified at outcrop were individually fit by finding a fracture radius distribution whose trace length statistics matched the actual trace length statistics for that set (termed the FracSize approach), and through area-renormalization for the Group 1 sets in which the outcrop and corresponding lineament trace lengths were combined into a single plot and analysed. In all cases the best fitting radius model was a lognormal model.

FracSize size estimates were also made on the lumped Group 2 (Table 5-16) fracture data. These results are presented in Table 5-17. The fits are not statistically significant at the 5% level, suggesting that it would be more accurate to bootstrap the size distribution from the empirical data, rather than to generate fractures from a lognormal distribution. Inspection of the fractures mapped at outcrop and identified as belonging to Group 2, suggests that many of the traces truncate against other fracture sets. This truncation may be responsible for the poor statistical fit to parametric distributions such as the lognormal.

The Group 1 renormalization calculations were carried out by plotting both the Euclidean (area) and intensity-scaling renormalizations (fractal). In order to select and carry out the most appropriate renormalization, it was first necessary to determine whether the intensity scaling followed a Power Law, and if so, to compute the parameters needed for the fractal renormalization.

Table 5-16. Orientation parameters for background fracture sets (Group 2, all fractures in outcrop).

Set Name BG (back-ground fracture set)	MeanPole Trend/ Plunge/Dispersion	Model	K-S	Relative % of group 2	Relative % of group 1 and group 2	Comments
BGNE	326.3/5.5 K1:17.65 K2:18.14	Bivariate Fisher	0.041/45.4%	41.5%	17.87%	Univariate Fisher also significant at 43.9% (K=16.9)
BGNS	96.8/3.8/20.32	Fisher	not significant	34.4%	14.84%	
BGNW	22.1/2.4 K1:5.36 K2: 6.66	Bivariate Fisher	0.051/61.3%	15.0%	6.45%	Weakly-developed set; Bivariate normal also significant at 18.8%
BGHZ	123.0/55.3 K1:83.58 K2:15.97 K12=–0.05	Bivariate Normal	0.072/24.2%	9.1%	3.91%	Bivariate Bingham also signifnicant at 6.2%

Mass dimension plots and tables for each identified outcrop fracture set are given in Appendix 3. The mass dimension analyses for each fracture data set shows that intensity does not scale, except in rare cases, linearly with area. In other words, the scaling behaviour is rarely Euclidean. In general, the regression through the locus of the mean for each mass dimension plot indicates that a fractal scaling behaviour is a valid model for these fracture sets. As a result, the renormalization for Group 1 fracture sets was undertaken using the fractal renormalization as well as the Euclidean.

The results of the intensity-scaling renormalization and the Euclidean renormalisation are summarised in Table 5-18. The results of the mass dimension renormalisation are also shown in italic type in for completeness. They were only performed on Group 1 sets, as Group 2 sets are not related to the lineaments.

The diagrams for power law fits can be found in Appendix 3. However, note that the values of k and X_0 shown in these diagrams are for the trace lengths, not for the radius distribution of the parent fracture population. To calculate the correct fracture radius value for all fractures in a 3D volume, it is necessary to add 1.0 to the value shown. The radius exponent is obtained by adding 1.0 to these values, as has been done in Table 5-18 . It is important to note that some software specifies the power law distribution in terms of a different exponent, b, which is 1.0 greater than k_r. The user of these values should determine what their particular software requires.

Note also that the value of X_0 in the diagrams in Appendix 3 refers to the fracture trace length, not the radius. The transformation of this value into a fracture radius minimum size is described by Equation A3-6, in Appendix 3. The parent radius distribution is shown in Table 5-18 .

Table 5-17. Radius distribution for aggregated background fracture sets (Group 2).

SET	Size model	Lognormal (radius distribution)		
		Arithmetic space Mean [(1/n) Σ xi] (meter)/ Standard deviation	Log10 space Mean [(1/n) Σ log10 xi]/ Standard deviation	LN space Mean [(1/n) Σ ln xi]/ Standard deviation
BGNE	Lognormal	0.48/0.55	–0.50/ 0.60	–1.15/ 0.92
BGNS	Lognormal	0.67/0.82	–0.37/0.63	–0.86/0.96
BGNW	Lognormal	0.45/1.00	–0.73/0.88	–1.69/1.33
SubH	Lognormal	0.57/1.86	–0.78/1.03	–1.79/1.57

Table 5-18. Power Law parameter values calculated from the trace length renormalisation plots from outcrop and lineament data (Appendix 3). Note that the parameters k_r and X_{r0} refer to the radius distribution and X_{t0} to the minimum trace length. The corresponding trace length exponent, k_t, can be obtained as k_r–1. Estimates are given both for intensity-scaling (mass) and euclidian (euc) renormalization, respectively, an as a span (upper, median, lower).

Fracture set	Size model (preferred)	Powerlaw (radius distribution)		
		Upper kr/Xt0/Xr0 (mass) (euc)	Median kr/Xt0/Xr0 (mass) (euc)	Lower kr/Xt0/Xr0 (mass) (euc)
NNE-NE	Powerlaw	2.68/0.6/0.38 2.85/0.43/0.27	2.58/0.36/0.23 2.82/0.31/0.20	2.50/0.20/0.13 2.69/0.15/0.10
EW-WNW	Powerlaw	2.93/0.63/0.40 2.99/0.71/0.45	2.80/0.36/0.23 2.82/0.32/0.20	2.67/0.18/0.11 2.78/0.21/0.13
NW-NNW	Powerlaw	2.97/0.75/0.48 3.02/0.54/0.35	2.87/0.49/0.31 2.91/0.35/0.22	2.62/0.13/0.08 2.83/0.14/0.10

Significance tests were not carried out on the power law models for Group 1, as the fits were based on visual identification and removal of data points that may have been related to truncation effects. Hence, the significance would be based upon this expert judgement, and does not capture the uncertainty in the data to the extent that fitting bounding models does.

Uncertainty in the fracture size parameters was estimated as described in Appendix 3 by bracketing or fitting bounding models of the Power-Law fits to the renormalised trace length plots (provided as upper and lower parameter estimates in Table 5-18).

A graphical illustration of this uncertainty calculation is shown in Figure 5-15. In this graph, the upper and lower bounds are shown by dashed lines. These lines are visual estimates of the span of possible power law models that could be fit to the data. The results are shown in Table 5-18.

Surface vs. subsurface fracturing

In building a regional scale model of fracturing, it is necessary to determine if surficial stress-relief has altered the fracture pattern. Stress-relief enhancement of fracture set size, intensity, aperture or other factors may impact whether and to what extent outcrop and lineament data may be analysed combined with borehole data.

If stress-relief has altered the surficial fracturing, then the following effects might be present:

1. Stress-relief effects should produce higher fracture intensity near the surface, especially for subhorizontal fractures.
2. Fractures near the surface should have a lower percentage of alteration than deeper fractures, since any newly generated surficial fractureswould not have been subject to older hydrothermal effects.
3. Effects of items 1 and 2, if seen, should be seen to approximately the same depth in all boreholes within a region.

As Figure 5-16 illustrates, the demarcation between horizontal and vertical fractures is gradational. For the analyses that follow, a subhorizontal fracture was taken as any fracturing dipping shallower than 45°, whereas a vertical fracture was one that dipped steeper than 70°.

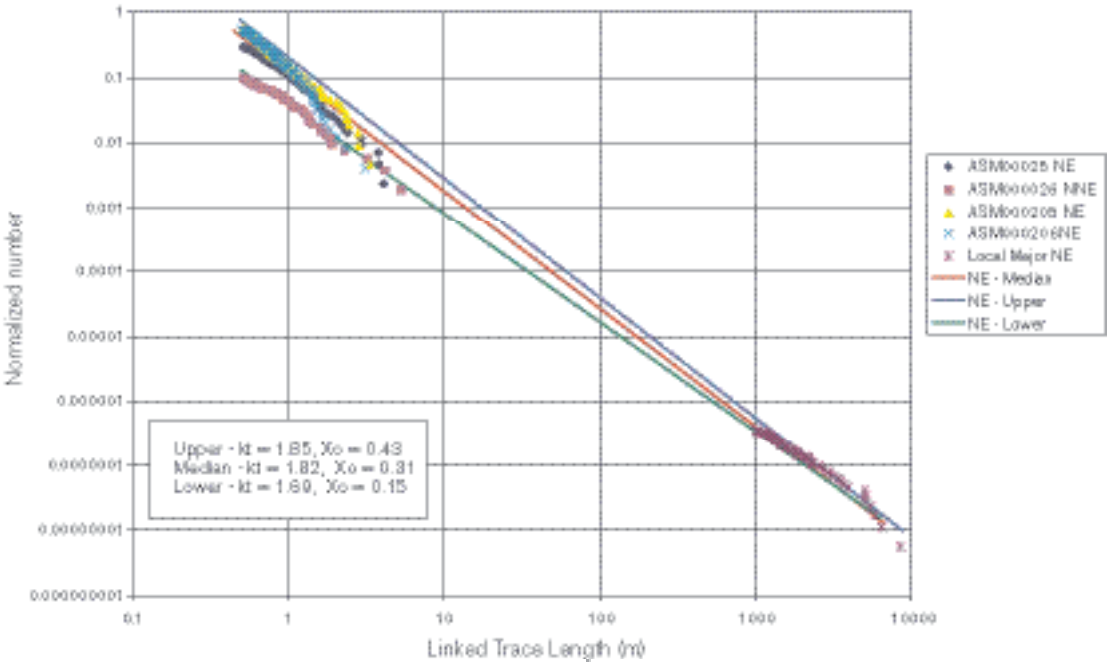

Figure 5-15. *Example of the calculation of uncertainty for the northeast lineament-related fracture set. Dashed lines indicate visual upper and lower bounds for fitting the data.*

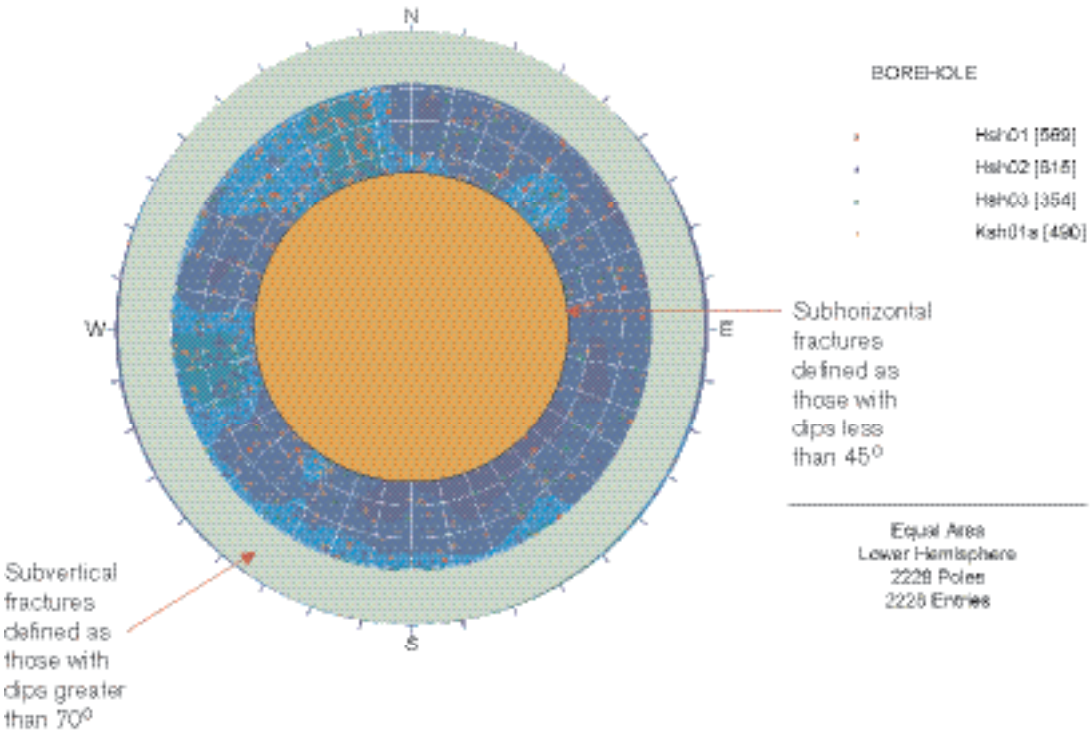

Figure 5-16. *Operational definition of subhorizontal and subvertical fractures. Poles to all open fractures in the boreholes listed in the figure have been plotted as background example of fracturing.*

The dip value of 70° to map out vertical fractures was chosen to capture the girdle of poles on the stereoplot without including the cyan-coloured clusters that lie between the two shaded bands. The value of 45° to map out horizontal fractures was selected to also avoid these clusters, and also to include a statistically reasonable number of fractures for analysis. Neither of the the slected bounds is unique, and others certainly could be used if deemed appropriate.

To examine more closely the possible impact of stress-relief, cumulative fracture intensity plots (CFI) were constructed as previously described.

In particular, the plots were closely examined to identify possible shallow slopes near the surface, which indicate a higher fracture intensity. Plots were made by borehole and for groupings of the data including open fractures, sealed fractures, and fractures that were unaltered, filled with calcite or filled with epidote. Unaltered or calcite-filled fractures might be evidence of near-surface conditions and recent formation, whereas epidote mineralisation is likely to be quite old and to have occurred at a depth well below the surface. Figure 5-17 through Figure 5-19 show the CFI plots for vertical open fractures.

The HSH boreholes begin their respective fracture records within 10 m of the surface, whereas KSH01A and KLX02 start much deeper, and may begin below the depth where surface effects might occur. However, none of the boreholes shows any evidence of a high fracture intensity zone within a few meters or tens of meters of the surface, followed by much lower fracture intensities below. In fact, HSH02 shows higher intensity at depth, as does HSH01, whereas HSH03 shows no depth dependence whatsoever.

Vertical fractures may be less prone to stress relief effects than horizontal or subhorizontal ones, the latter which are more favourably oriented for being affected by such effects.

Figure 5-20 through Figure 5-21 present CFI plots for the subhorizontal fractures in the HSH-, KSH- and KLX-boreholes, respectively.

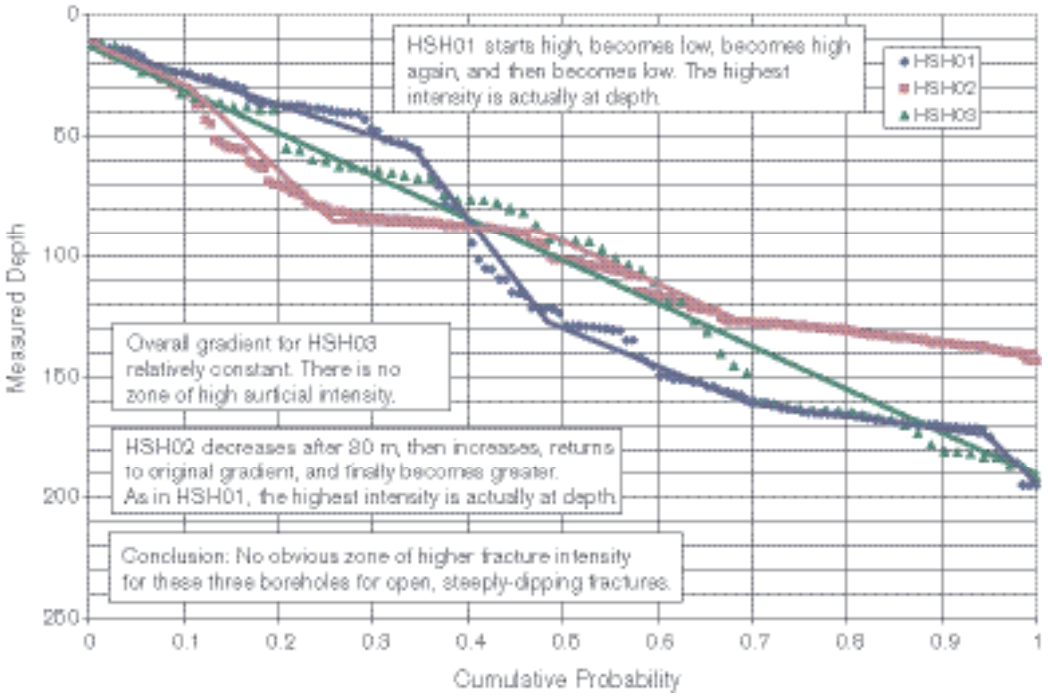

Figure 5-17. *CFI plot for open vertical fractures in the percussion-drilled boreholes HSH01 through HSH03.*

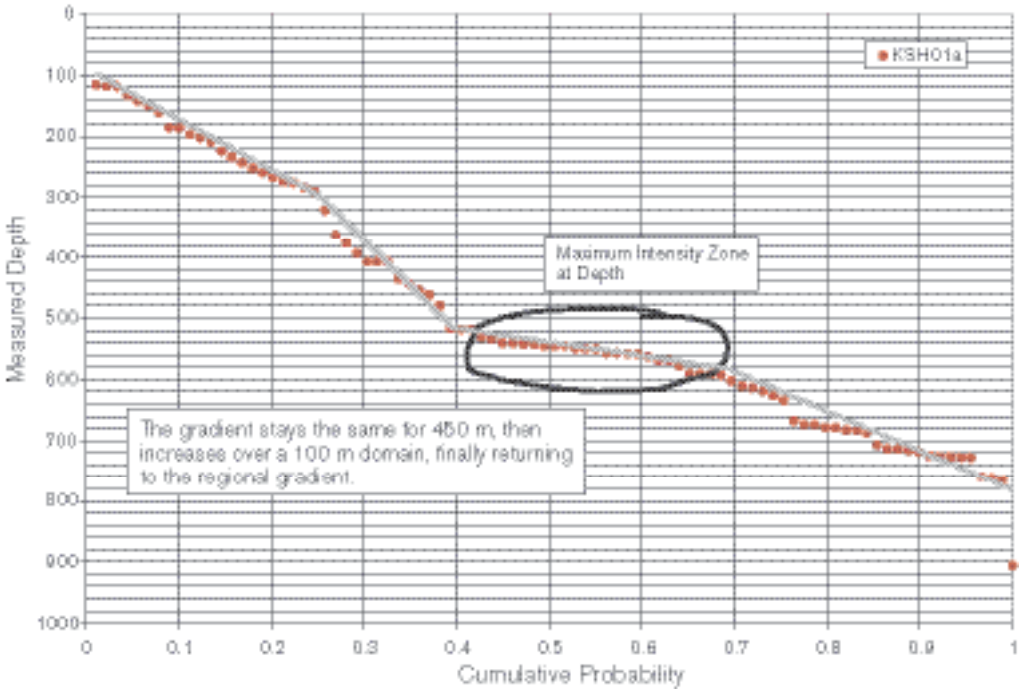

Figure 5-18. *CFI plot for open vertical fractures in cored borehole KSH01A.*

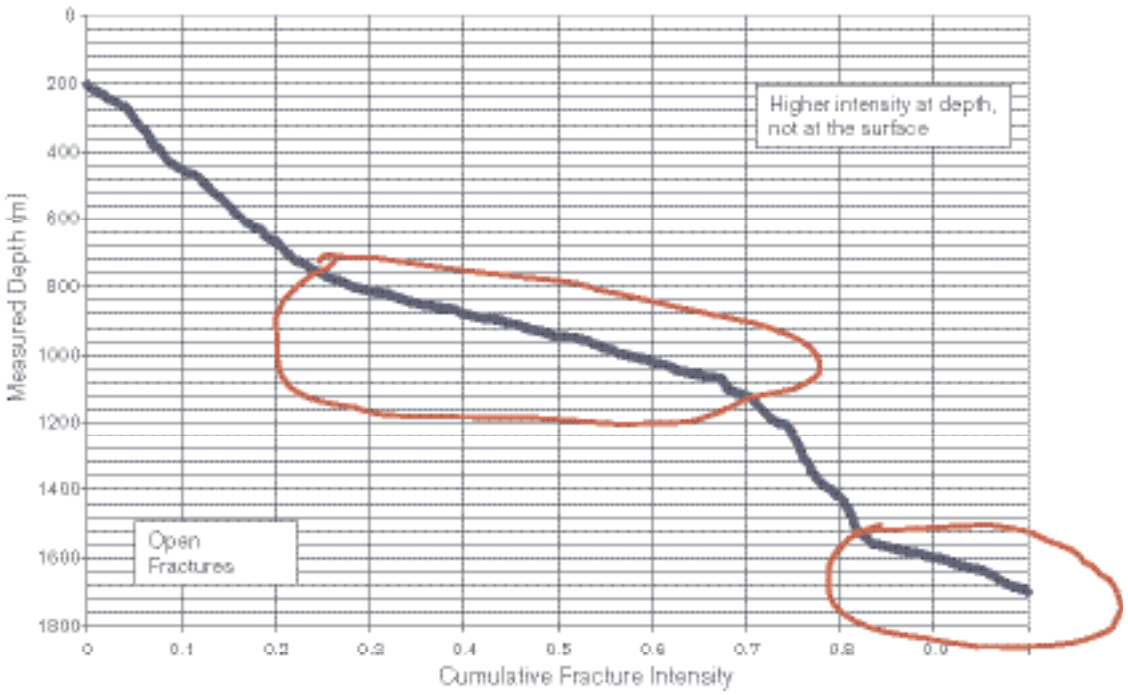

Figure 5-19. *CFI plot for open vertical fractures in borehole KLX02.*

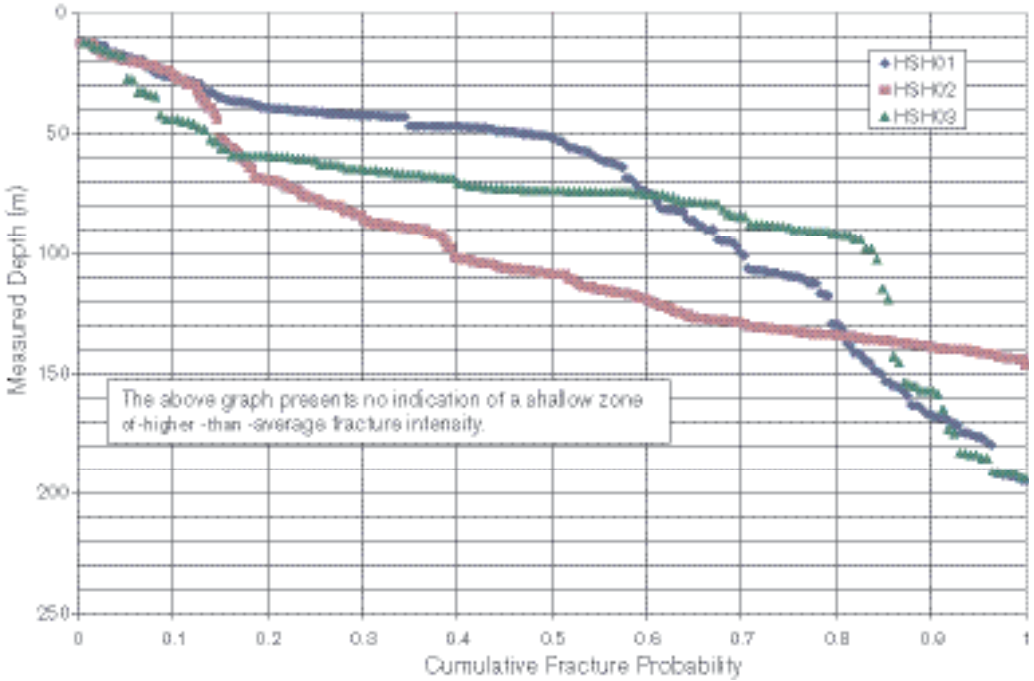

Figure 5-20. *CFI plot for open, subhorizontal fractures in percussion-drilled boreholes HSH01 through HSH03.*

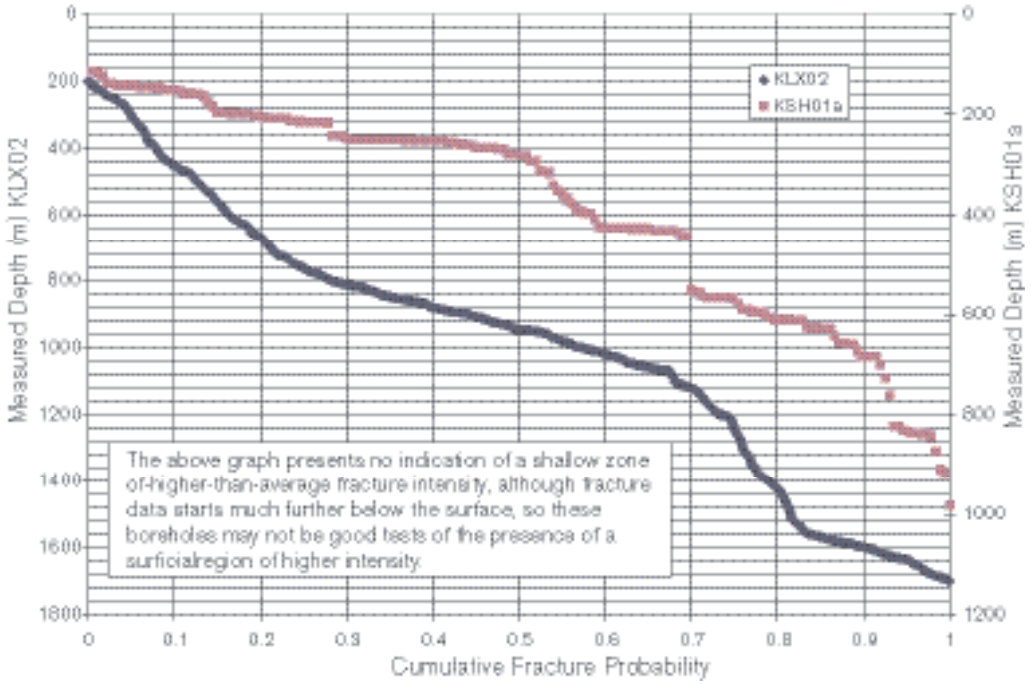

Figure 5-21. *CFI plot for open subhorizontal fractures in cored boreholes KSH01A and KLX02.*

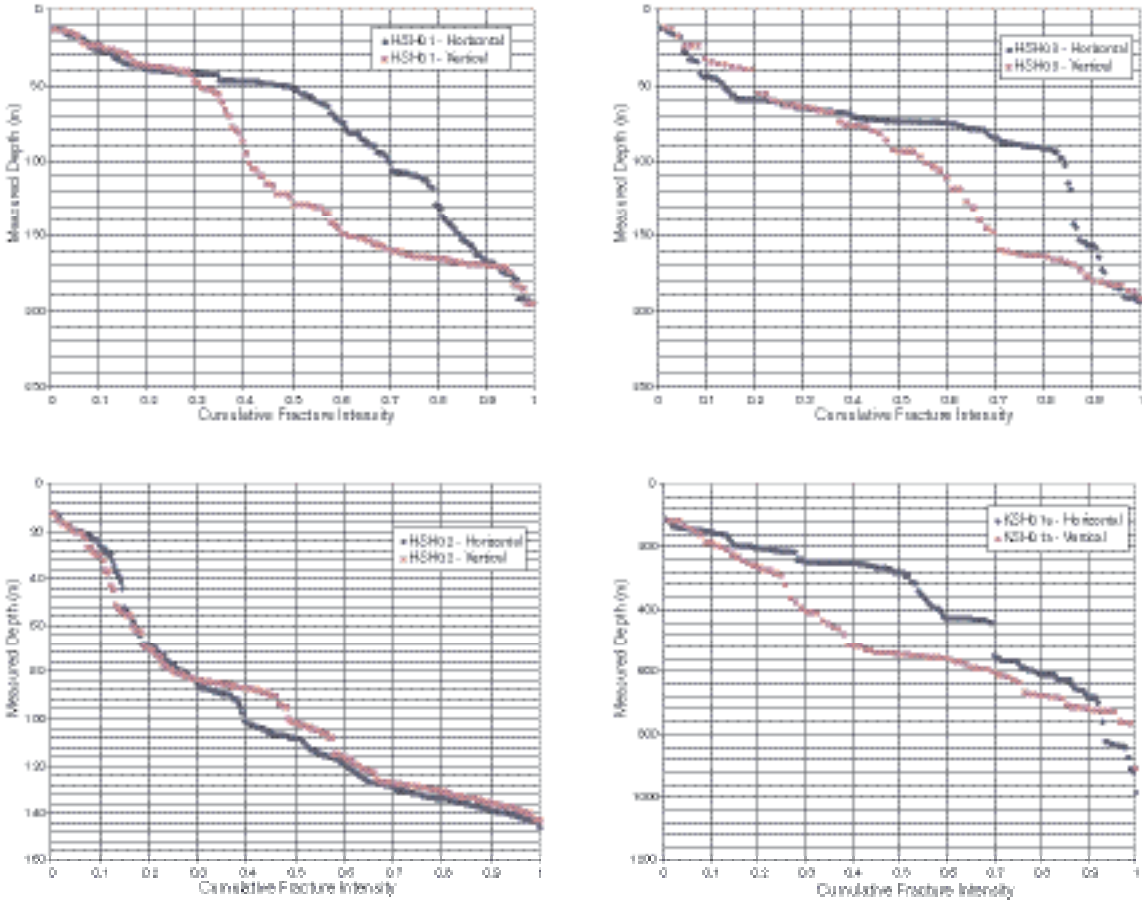

Figure 5-22. *CFI plots for both open horizontal and open vertical fractures, boreholes HSH01, HSH02, HSH03 and KSH01A.*

These figures show no evidence of effects of stress relief. HSH01 actually shows a higher intensity zone below 40 m, whereas HSH02 shows its highest intensity at depths greater than 100 m, and HSH03 shows its highest intensity between 60 m and 100 m. Likewise, neither KSH01A nor KLX02 show any indication of higher fracture intensity near the surface.

Figure 5-22 compares open subvertical and subhorizontal fractures mapped in four of the boreholes. What is striking is the lack of conformity to the behaviour expected if there were surface stress relief effects. If stress relief was important, then the relative intensity of horizontal fractures should exceed that of the vertical. However, HSH01 and HSH02 show that they are the same at the top of the hole; HSH03 actually shows higher vertical relative intensity than horizontal at the top of the hole, while KSH01A possibly shows a slightly higher horizontal intensity at the top of the borehole. However, in the latter borehole, the record starts at 100 m so surface effects are unlikely to be the cause of its distinction, given the lack of other supporting evidence.

Figure 5-23 and Figure 5-24 present CFI plots for fresh vs. altered, vertical and horizontal open fractures, respectively. Stress relief may manifest in higher relative intensity of fresh fractures near the surface and diminish with depth. However, none of the CFI plots show any evidence that there is a higher relative intensity of fresh fractures near the surface. In fact, fresh and altered fractures track each other quite closely, and show zones of high intensity at depth, rather than at the surface, which suggests that the fresh fractures are notdue to recent stress-relief effects.

Figure 5-25 shows a CFI plot for KSH01A based on the primary mineral filling. Only four mineral fillings were plotted, as other mineral types had insufficient data for analysis. Figure 5-25 shows no evidence that calcite-filled fractures are more numerous near the surface. In fact, there is a zone of high intensity from 100 m to nearly 300 m, and an equally intense zone below 500 m;

Epidote-filled fractures (and also hematite and chlorite) show relative intensity patterns very similar to calcite.

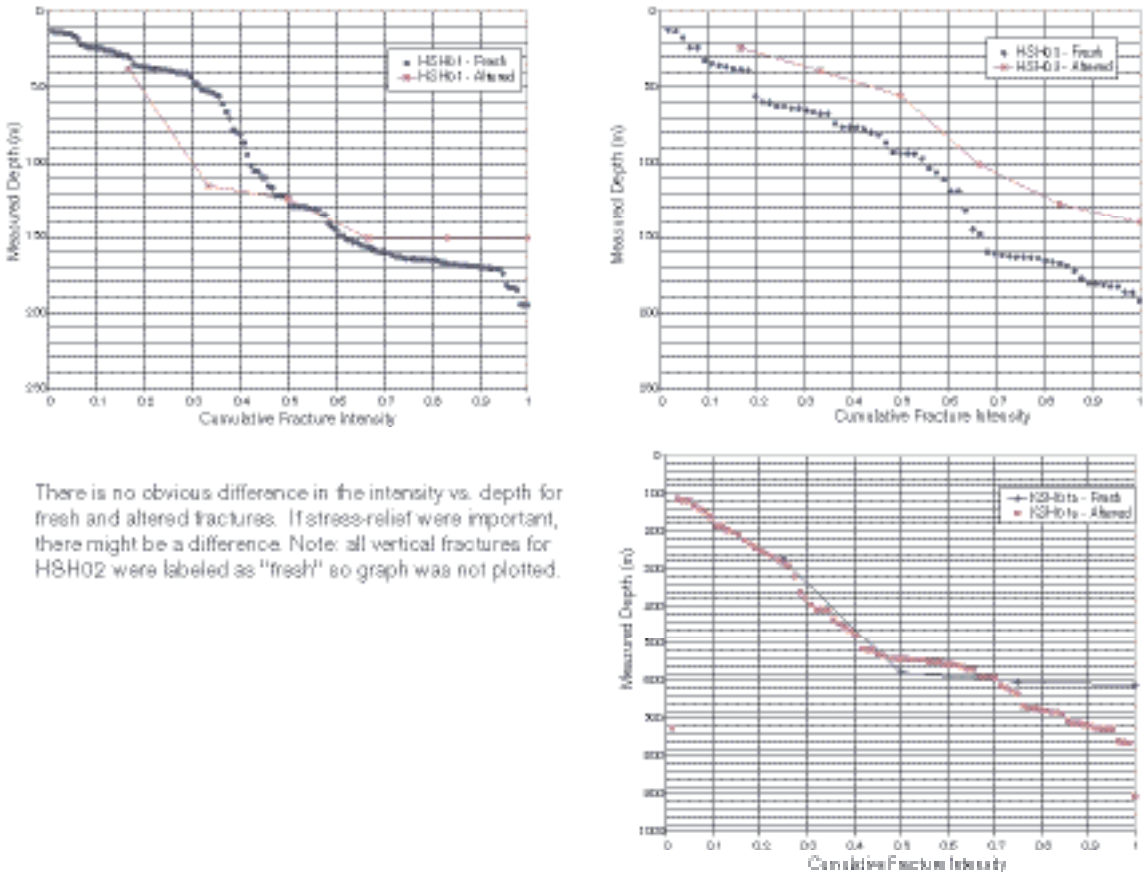

Figure 5-23. *CFI plots for fresh vs. open vertical fractures with alteration.*

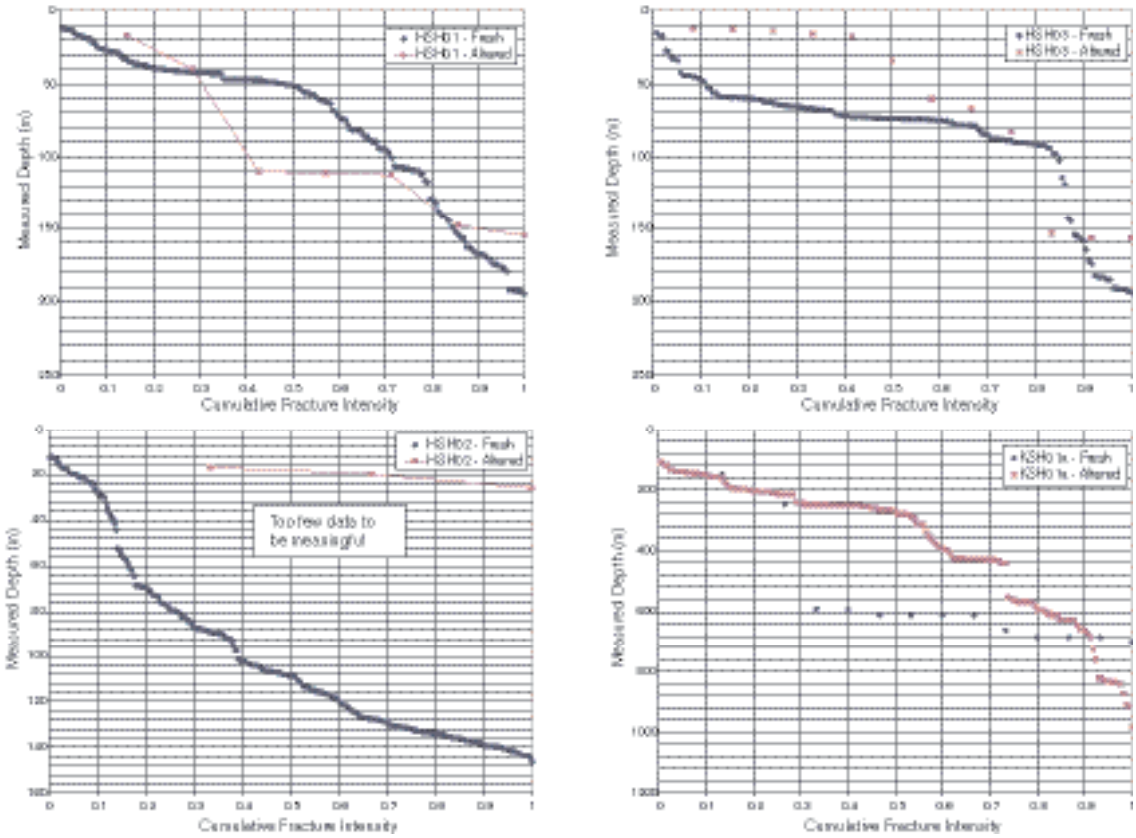

Figure 5-24. *CFI plots for fresh vs. open horizontal fractures with alteration.*

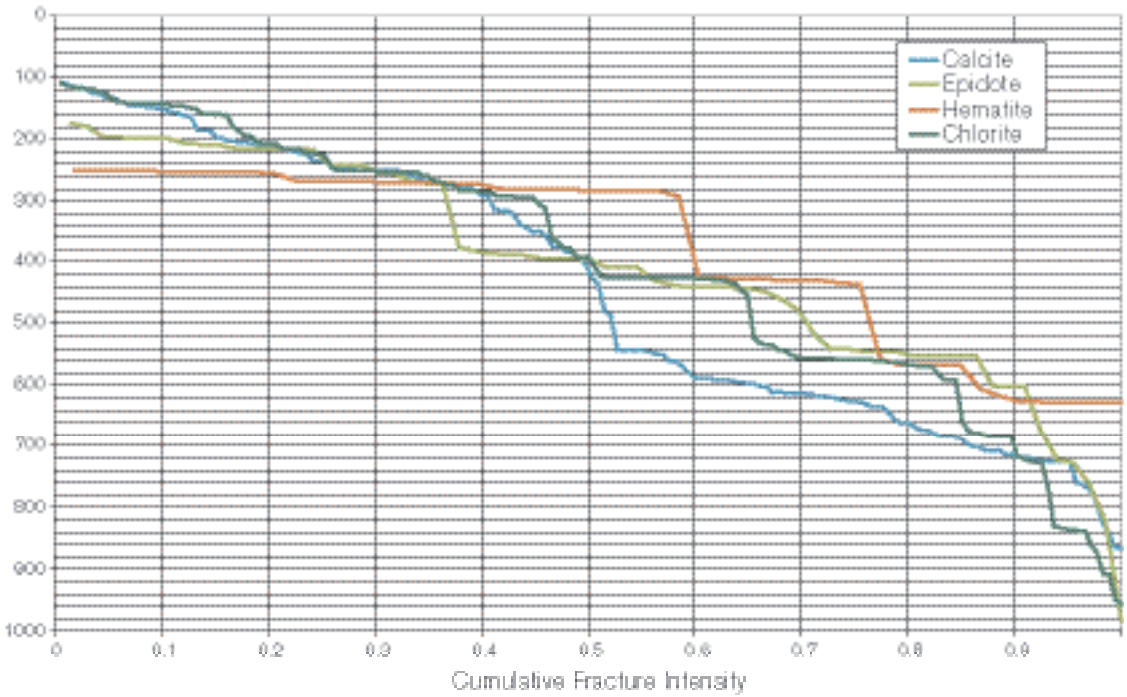

Figure 5-25. *CFI chart for open, filled fractures for KSH01A. Only four primary mineral fillings had enough data for plotting. Note distinct zones of higher intensity for all fractures, regardless of primary filling mineralogy.*

Unfortunately, it is not possible to assess the primary fracture mineral filling for the shallower HSH boreholes, as over 98% of the recorded primary fillings seen in these boreholes are composed of chlorite. Although information from KSH01A provides no direct evidence for the top 100 m of the borehole, the close correspondence seen in all four primary mineral fillings suggests that calcite does not show any obvious departure from the other mineral fillings.

Another possible expression of surface effects would be a different orientation among open fractures at the surface as opposed to at depth. However, this is not seen in any of the boreholes, as shown in Figure 5-26 or Figure 5-27.

Although intensity may vary, there is no evidence that near-surface open fractures have different orientations than open fractures at depth. Also note that intervals of higher fracture intensity are evident at depth, rather than at the surface.

Thus, surface fracturing at outcrop does not appear to be affected by surficial stress-relief mechanisms.

Relationship between fracture intensity and geology

Currently, only borehole KSH01A, and to a lesser extent, KSH01B provide sufficient data and geological variability to evaluate possible geological controls on fracture intensity. Figure 5-28 shows CFI plots for KSH01A, in which fractures are divided into open, sealed and all fractures, and KSH01B, which only had fractures designated as sealed.

The interpreted open fractures in KSH01A show a visual correlation with the presence of alteration zones (the red-hatched and shaded zones in columns 2 and 3 of each plot). Sealed fractures show no variation in intensity throughout the full length of KSH01B, nor in the interval 100 m to 500 m in KSH01A. There is a slight increase in the intensity of sealed fractures between 500 m to 550 m, afterwhich the intensity of sealed fracture intensity diminishes. The the intensity of open fracture is higher higher intensity in units A and B, but this is due at least in part to the presence of the alteration zones, see also Section 4.4.

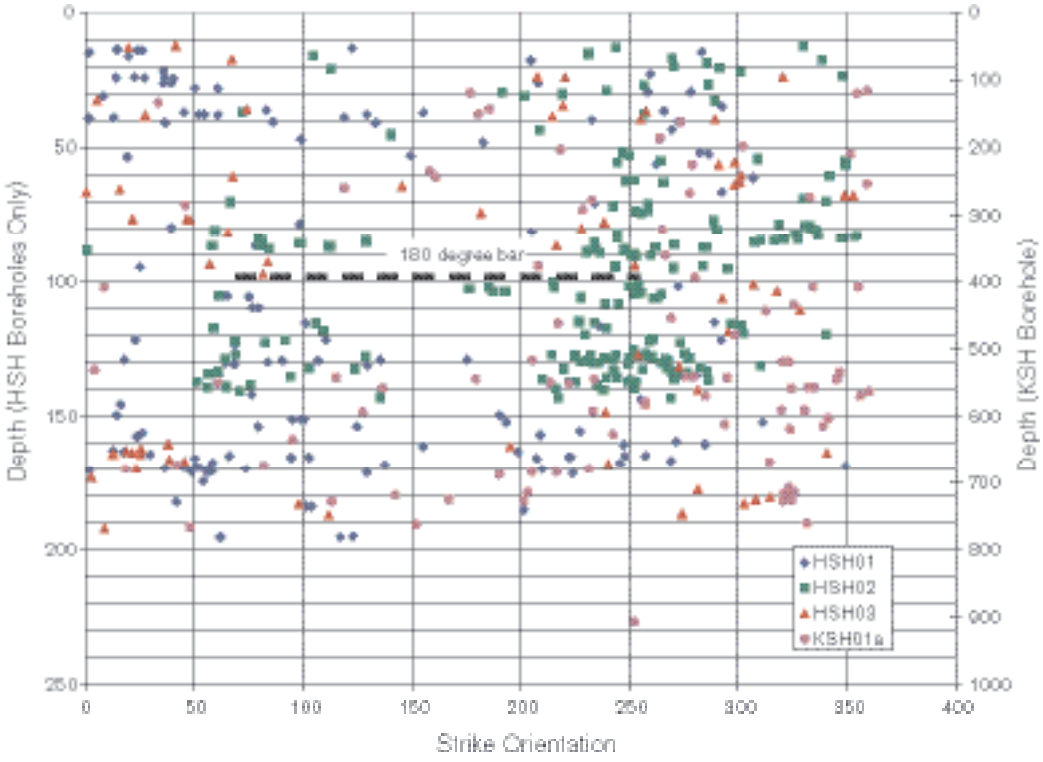

Figure 5-26. *Variation in strike of open vertical fractures as a function of depth.*

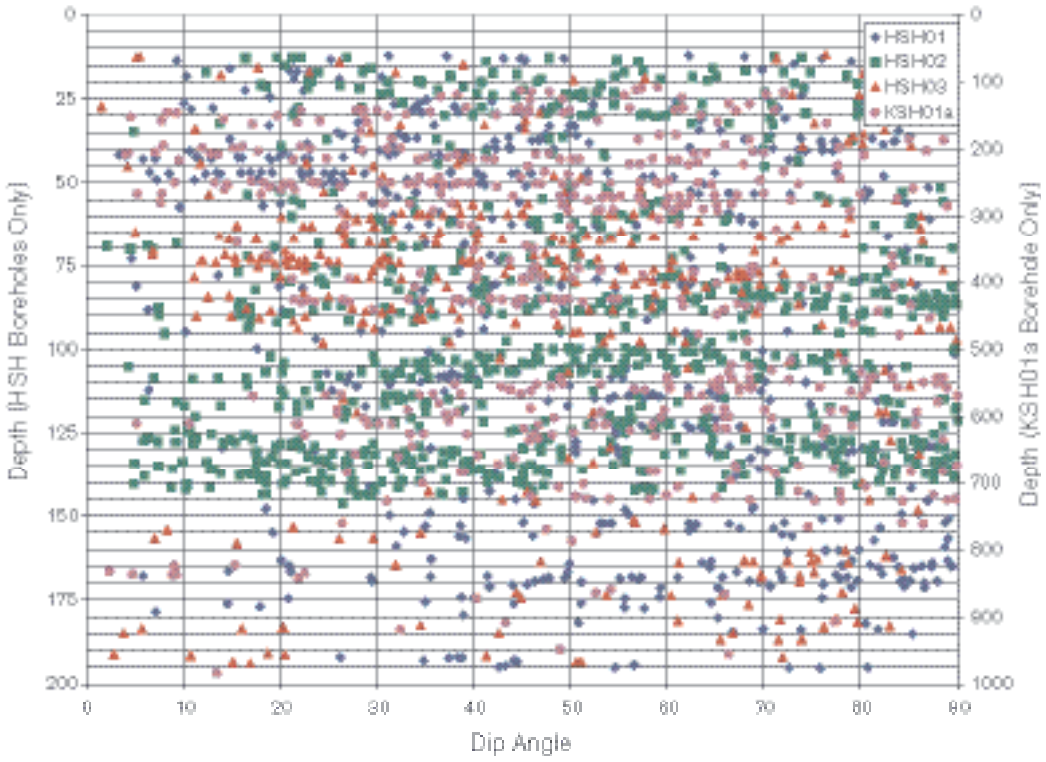

Figure 5-27. *Variation in dip angle for all open fractures as a function of depth.*

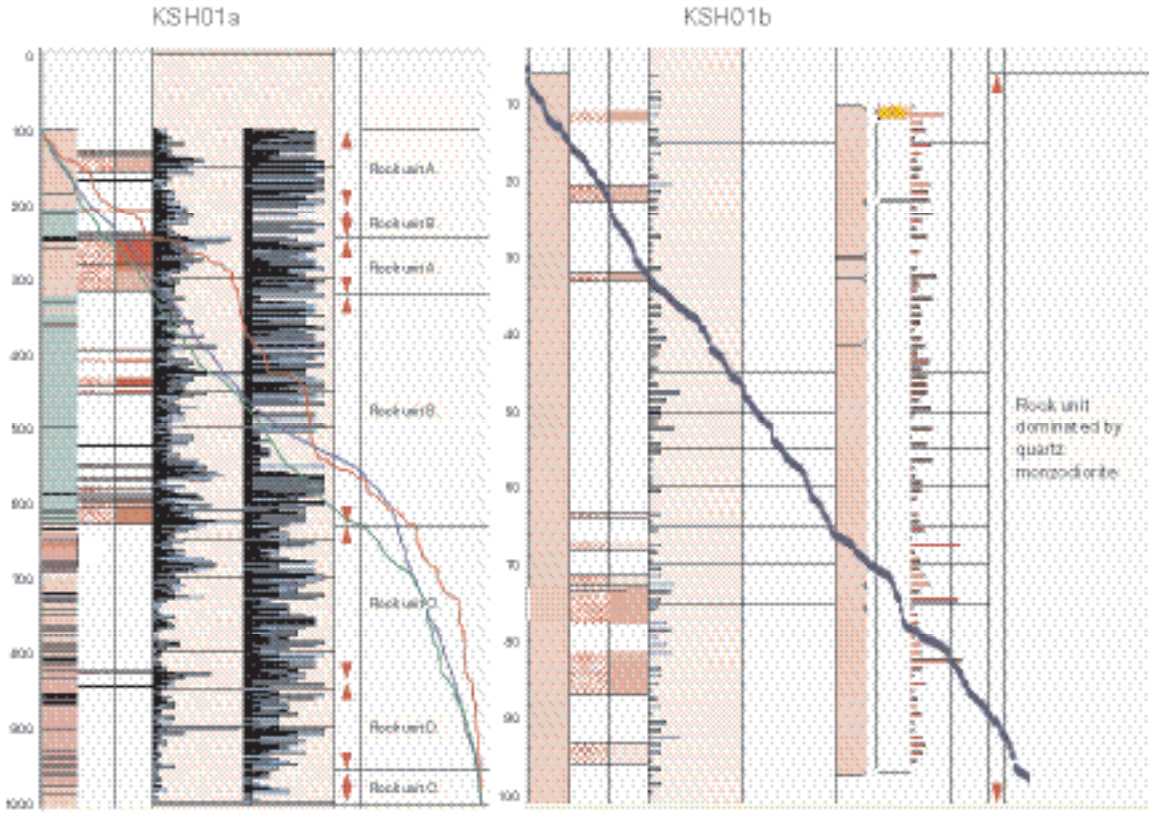

Figure 5-28. *Relation between zones of variable fracture intensity zones to mapped geological parameters in KSH01A (left) and KSH01B boreholes (right). Red line in the left graph is for open fractures only; blue line is for sealed fractures only; green line represents all mapped fractures (sealed and open). The blue line in the right-hand graph is for sealed fractures only (open fractures were not present). Note different length scale.*

The open fractures were further subdivided by type of mineral infilling (Figure 5-29). Mineral-filled fractures seem to be associated with alteration zones. It appears also that the alteration zones have given rise to more fractures, which are more prone to be filled with fracture minerals.

Subsequently, the fracture intensity vs. lithology and alteration type were calculated and results show how fracture intensity varies with lithology. This has been done for borehole KSH01A specifically, as this borehole provides the most data, and for all boreholes aggregated together (see Appendix 3).

Table 5-19 compares fracture intensity for boreholes and outcrops. The numbers cannot be compared directly, since intensity is given for boreholes as the number of fractures per unit length P_{10} [m^{-1}] and at outcrop as the fracture length per unit area P_{21} [m^{-1}], but the relative intensity as a function of lithology still holds. The yellow shading indicates lithologies that are found in both boreholes and outcrops (or are very similar to one another). The table shows that the relative order of the fracture intensity in terms of lithology measured in boreholes is also found in outcrops. The standard deviation shown for borehole P_{10} values is calculated for each of the lithology intervals in the boreholes, and as such, quantifies the spatial uncertainty in the intensity estimation for each rock type. However, the quartz monzonite is more fractured at the surface than in the boreholes. This may indicate that this rocktype is more prone to surface erosion.

Examination of intensity as a function of alteration shows an even stronger correlation than with lithology. Specifically, an analysis of the intensity as a function of alteration in KSH01A and KLX02 reveals that fracture intensity correlates with the degree of rock alteration. Fracturing in zones where alteration is weak, moderate or strong tends to be 2 to 3 times higher than the intensity in unaltered zones.

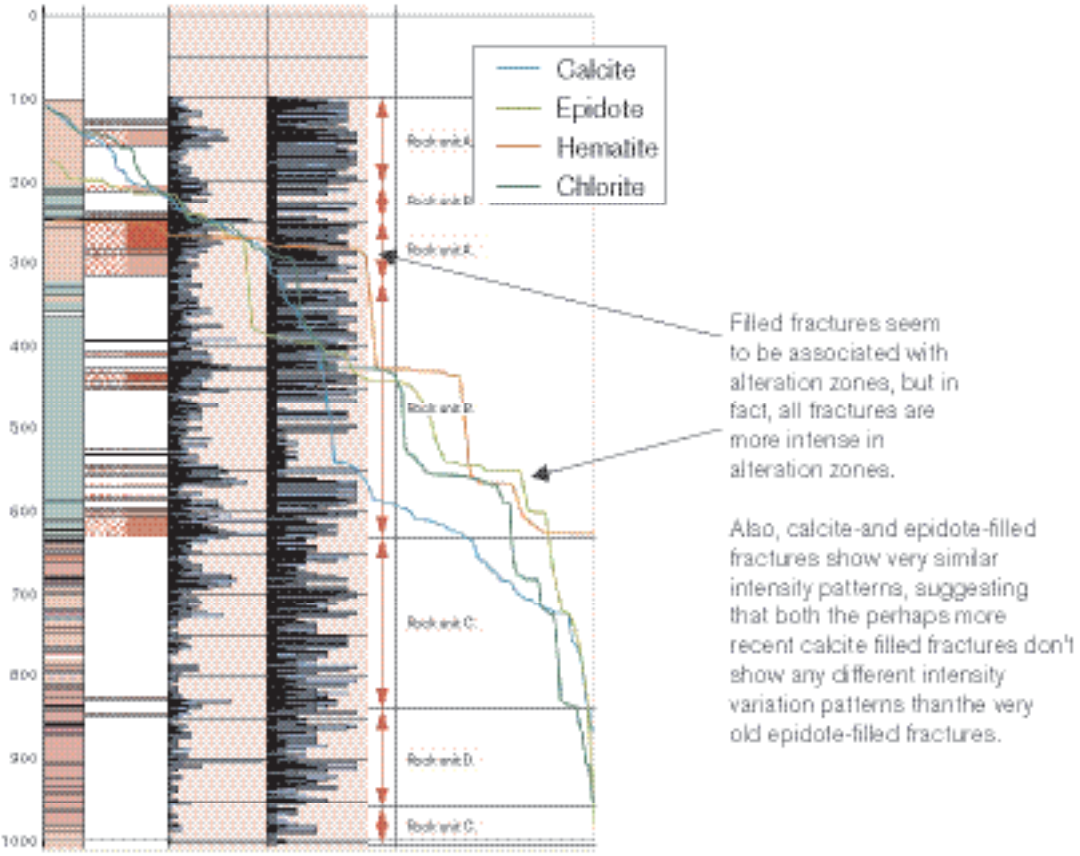

Figure 5-29. *CFI plot of mineral fillings in KSH01A superimposed on single-hole geological interpretation.*

Table 5-19. Comparison of outcrop and borehole fracture intensity as a function of rock type. Yellow shaded lithologies are found both in boreholes and outcrops.

Outcrop	Rock Type	Rock Name	No. Fractures	% of Total	Total Trace Length (m)	Approx P_{21}
ASM000025	501030	Fine-grained dioritoid (Metavolcanite, volcanite)	188	11.18%	122.366	
ASM000025	501044	Granite to quartz monzodiorite, generally porphyritic	1494	88.82%	1010.695	2.23
ASM000026	501044	Granite to quartz monzodiorite, generally porphyritic	1822	99.67%	113.295	2.11
ASM000026	501061	Pegmatite	4	0.22%	1.547	
ASM000026	511058	Granite, fine- to medium-grained	2	0.11%	0.445	
ASM000205	501030	Fine-grained dioritoid (Metavolcanite, volcanite)	2798	99.40%	1063.693	4.8
ASM000205	511058	Granite, fine- to medium-grained	17	0.60%	4.988	
ASM000206	501036	Quartz monzonite to monzodiorite, equigranular to	1853	85.73%	695.368	3.18
ASM000206	501061	Pegmatite	36	1.65%	15.224	
ASM000206	511058	Granite, fine- to medium-grained	274	12.61%	92.859	

Yellow shaded rows indicate dominant rock type at each outcrop. P_{21} is calculated as if the entire outcrop area belongs to the dominant rock type.

Rock Code	n	Mean	SD	Description
501044	61	0.29	0.78	Granite to quartz monzodiorite, generally porphyri
501036	55	0.97	1.71	Quartz monzonite to monzodiorite, equigranular to
501061	6	1.18	1.89	Pegmatite
511058	20	1.54	2.11	Granite, fine- to medium-grained
503105	39	1.76	2.22	Intermediate volcanic rock (quartz latite to andes
501058	11	1.94	2.10	Granite, medium- to coarse-grained
505102	5	2.62	2.72	Mafic rock, fine-grained

The same relative order of fracture intensity is seen in both boreholes and outcrops.

The noted correlation is associated with some uncertainties due to limited sample coverage, but in general, rocks from Rock domain A have the lowest intensity, followed by Rock domain C with Rock domain B having the highest intensity, c.f. Section 5.1.3. There is some evidence that intensity increases as grain size decreases, but the data are not conclusive. The fine-grained dioritoid (Rock domain B) seems to have the highest intensity. The latter may possibly be attributed in part to the greater alteration seen in this rock domain.

Statistical tests of the hypothesis that the median fracture intensity does not depend upon alteration class have been performed and is reported in Appendix 3. The test used, Kruskal-Wallis, evaluates the null hypothesis that the medians are the same. The tests confirm that fracture intensity is a function of alteration degree.

Some final investigations on possible geological controls on fracturing were carried out using two-way contingency table analysis. This showed that irregular, stepped and undulating fractures tend to have slightly larger apertures than planar fractures (Appendix 3)

It is noted that mineral fillings have little relation to aperture. Individual probabilities for the various combinations of mineral filling and aperture class show little statistical difference from the marginal probabilities. This lack of correlation also corroborates the lack of observed stress-relief effects, as the calcite-filled fractures do not seem to be related to aperture, and have statistical affinities very similar to all other filled fractures.

Fracture intensity

Volumetric fracture intensity for each fracture set is expressed as the fracture surface area per unit volume of rock, or P_{32} [m^{-1}]. This parameter is not directly measurable from borehole or outcrop fracture data, but must be inferred either from the number of fractures per unit length (P_{10}) in a borehole, or the fracture trace length per unit surface area (P_{21}) at outcrop.

The conversion factors required to go to P_{32} from measured outcrop data were calculated from 25 realisations of a DFN fracture model using the parameters found for each of the outcrop sets. The mean estimate of the parameter was used to estimate the values of P_{32} reported in Table 5-20.

The calculation of the volumetric intensity from the borehole data is somewhat more problematic, as the linear intensity, P_{10}, changes along the borehole due to changes in lithology and degree of alteration. Moreover, the orientation of the fractures in these intervals changes, so that the value of the factor relating P_{10} to P_{32} can change somewhat between intervals. For this reason, Low, Best and High values of P_{32} are provided which represent, in addition to the average, the combinations of the

Table 5-20. Values of P_{32} for all fractures, calculated from the trace length intensity for the fracture sets associated with the four outcrops.

Set Name	P_{21} (m^1/m^2)	P_{32} (m^2/m^3)
ASM000025NS	0.47	0.60
ASM000025NNE	0.50	0.42
ASM000025NE	0.40	0.33
ASM000025ENE	0.37	0.30
ASM000025WNW	0.54	0.95
ASM000025NW	0.42	0.33
ASM000026NS	0.49	0.36
ASM000026NNE	0.24	0.13
ASM000026NE	0.08	0.12
ASM000026ENE	0.37	0.29
ASM000026WNW	0.24	0.23
ASM000026NW	0.69	0.97
ASM000205NS	0.66	0.67
ASM000205NE	0.54	0.54
ASM000205ENE	1.60	1.64
ASM000205WNW	0.46	0.41
ASM000205NW	0.77	0.76
ASM000205NNW	0.77	0.84
ASM000206NNE	0.57	0.53
ASM000206NE	0.54	0.53
ASM000206ENE	1.03	1.08
ASM000206EW	0.19	0.23
ASM000206WNW	0.35	0.36
ASM000206NW	0.25	0.40
ASM000206NNW	0.25	0.14

P_{10} and P_{32}/P_{10} conversion that produces the lowest and highest value, respectively. This alternate way of quantifying bounds on uncertainty in P_{32} is useful when the standard deviations of intensity are equal to, or much greater than the mean intensity. In the latter case measures such as the mean minus one standard deviation produce meaningless negative values. Values of P_{10} calculated for each borehole, lithologic class and alteration class are also provided in Table 5-21, Table 5-22 and Table 5-23, respectively.

Estimated intensity as a function of lithology (Table 5-21) show, for some lithological groups, much higher values than the results for the outcrop trace lengths, but may reflect the prevalence of intermediate and basic fine-grained volcanic rock in the subsurface at the borehole locations. These lithologies, not well-represented in the outcrop data, tend to have much higher fracture intensities than the other, more felsic and coarse-grained rock groups. Another factor is that the outcrop data is subdivided by fracture sets. When the sets are combined according to lithology, the estimated P_{32} values are much closer to one another (Table 5-22), and in fact, the estimated P_{32} intensities for outcrops are somewhat higher than the borehole-based estimates, probably due to the inclusion of both open and sealed fractures for the outcrops. The fracture intensity, based on fracturing in borehole KSH01A, was also estimated as a function of alteration degree of the rock, c.f. Table 5-23.

Table 5-21. Estimates of P_{32} for all fractures based on borehole data as a function of lithology.

Borehole	Mean P_{10}	Rock Name	P_{32} Range		
			Low	Best Guess	High
HSH01	0.00	Granite, fine- to medium-grained	0.00	0.00	0.00
HSH01	1.53	Intermediate volcanic rock (quartz latite to andesite	1.84	2.14	4.44
HSH01	2.27	Quartz monzonite to monzodiorite, equigranular	2.73	3.18	6.59
HSH01	4.17	Granite, medium- to coarse-grained	5.00	5.84	12.09
HSH02	4.59	Intermediate volcanic rock (quartz latite to andesite	5.51	6.43	13.32
HSH02	4.67	Granite, fine- to medium-grained	5.60	6.53	13.54
HSH03	1.84	Granite to quartz monzodiorite, generally porphyritic	2.21	2.58	5.35
HSH03	2.23	Granite, medium- to coarse-grained	2.67	3.12	6.45
HSH03	2.68	Quartz monzonite to monzodiorite, equigranular	3.21	3.75	7.76
KSH01A	0.04	Granite, medium- to coarse-grained	0.05	0.06	0.12
KSH01A	0.12	Granite to quartz monzodiorite, generally porphyritic	0.15	0.17	0.35
KSH01A	0.52	Quartz monzonite to monzodiorite, equigranular	0.63	0.73	1.51
KSH01A	0.53	Granite, fine- to medium-grained	0.63	0.74	1.53
KSH01A	0.93	Intermediate volcanic rock (quartz latite to andesite)	1.12	1.30	2.70
KSH01A	1.18	Pegmatite	1.42	1.65	3.43
KSH01A	2.62	Mafic rock, fine-grained	3.15	3.67	7.60

Table 5-22. Estimates of P_{32} for borehole and outcrop data.

Rock type	Key to rock domains Including comments	Boreholes (Open fractures)	Outcrop (All)	Outcrop (Open fractures)
Granite to quartz monzodiorite, generally porphyritic (Ävrö granite)	A01 Estimated to be >90% Ävrö granite	0.41	2.78	0.62
Fine-grained dioritoid (Metavolcanite, volcanite)	B01 94.2% Fine-grained dioritoid	3.67	4.94	0.69
Quartzmonzodiorite, equigranular	C01 is a mix between Ävrö granite (51.5%) and quartz monzodiorite (34.1%) and other subordinate rock types (14.4%). KSH01 is dominated by C01 with a section of B01.	1.36	3.29	0.93

Table 5-23. Estimates of P_{32} for open fractures in KSH01A as a function of degree of alteration of the rock.

Alteration Class	P_{10}	Borehole Low P_{32}	Borehole Best P_{32}	Borehole High P_{32}
Unaltered rock	0.79	0.95	1.11	2.29
Altered rock	2.04	2.45	2.86	5.92

Spatial model

The spatial model is not a simple homogeneous stochastic model, but rather a combination of geological and fractal models that produces a heterogeneous stochastic conceptual model. Primary geological controls on fracture orientation are the orientation of nearby structural lineaments. These control the orientations of the Group 1 fracture sets. Intensity appears to be a function of both lithology and degree of alteration, as observed above. Lithologies that are quartz-rich and coarser-grained appear to have a lower fracture intensity than lithologies that are more basic and fine-grained. This implies that Rock domain B is more fractured than Rock domain C and A, an

observation consistent with the observed differences in P_{21} fracture intensity among the outcrops ASM000025, ASM000026, ASM000205 and ASM000206 and the boreholes HSH01, HSH02, HSH03 and KSH01A.

Part of the explanation for the higher intensity in Rock domain B may also be that it contains (at least in borehole KSH01A) many zones of alteration, which are statistically correlated with higher fracture intensity.

Conceptual model uncertainty

The uncertainty in the model has been quantified in the previous sections. For each fracture set, the uncertainty is quantified by the dispersion and the model for dispersion (Table 5-15 for Group 1 sets; Table 5-16 for Group 2 sets). For fracture size, the range in sizes for Group 1 sets were bracketed for each set by estimating a minimum slope, a maximum slope and a "best guess" slope to the combined lineament and outcrop trace data (Table 5-18). For Group 2 fracture sets, the size uncertainty is quantified by the standard deviation of the trace fits (Table 5-17).

Total fracture intensity uncertainty was quantified by depth, rock type and alteration degree (Table 5-20 through Table 5-23). Thus, in assigning spatial fracture intensity values through the local model region, it is necessary to consider both the lithology and the degree to which the rock may contain alteration zones. A range of values for P_{32} has been provided in this report for all lithologies and alteration classes found in outcrop or borehole data sets, which should enable the modeller to select values that are locally appropriate for the model, or conservative if desired.

5.2 Rock mechanics modelling

5.2.1 Modelling of state of stress

Modelling assumptions and input from other models

Tectonic forces are the dominating source for the prevailing stress field in the whole of Sweden, resulting in a compressive horizontal stress clearly larger than the vertical stress. The regional stress field expected from the tectonic forces on the Fennoscandinan shield suggests a NW orientation of the major horizontal stress, /Slunga et al, 1984; Müller et al, 1992/.

Two main factors may influence the in situ stress field, stiffness differences in the bedrock material and the presence and characteristics of fracture zones /Hakami et al, 2002/. For the geological conditions at Simpevarp the difference in stiffness of the rock mass will not be sufficient to cause considerable stress differences. Fracture zones are expected to be the major possible cause for stress variations. By 'stress variation' is here meant variation in magnitude or orientation apart from the commonly seen magnitude increase with depth, which is related to the gravitational forces.

It is assumed that the measurements within the region (not all within the Simpevarp subarea) are representative of the stress field. The geological model does not, at this stage, indicate any sign of any important gently dipping structure in the area (c.f. Section 5.1.5). However, the amount of measurement data from the region are limited and there are almost no data from the Simpevarp subarea. There is no reason at this stage to expect a specific stress variation within the region or within the local area. Therefore, the same stress estimates are assumed to apply to the whole area, both at the regional and the local scales. However, an alternative stress model is also discussed.

Principal stress magnitudes

Estimates of the minor principal stress are made based directly on the measurement results from hydraulic fracturing. The minor principal stress is assumed to vary linearly with depth (see above) and the least squares best-fit trendline for the hydraulic fracturing data is used (c.f. Figure 4-62). The major principal stress is estimated based on the calculation of the ratio between minor and major principal stress from the overcoring results, according to the proposed approach /Hakami et al, 2002/. This ratio is, for this case, 3 on the average, (See Table 2-2 and Figure 4-62). The

measurements from CLAB are not included in the representative ratio for two reasons. Firstly, the measurements are shallow and, therefore, not appropriate to use for predictions at depth. Secondly, the approach of using the ratio does not give realistic values when stresses are very low or tensional. Therefore, the lower KAS05 measurements are also excluded.

Principal stress orientation

The stress orientation is estimated directly as the mean of the borehole measurements, giving each borehole the same weight, regardless off geographical position and number of measurements in the borehole. For each borehole, the median value was used as the representative value for orientation. The mean of the principal stress was estimated to be 132 degrees from north, i.e. giving a NW-SE direction of the largest stresses. This major principal stress is estimated to be subhorizontal, which is supported by the data and also by general knowledge of the stress pattern in Sweden. The intermediate principal stress is estimated to be vertical on the average, with minor local variations. However, the magnitude of the intermediate and the minor stresses might well be similar at some depth and therefore have an uncertain dip in the plane perpendicular to the major stress.

Evaluation of uncertainties in stress model

The sources of uncertainty in the stress model may be distinguished into two main categories: measurement reliability and scarcity of data. Both categories contribute significantly to the uncertainty in the stress model in this version.

Stress measurements were not successful in KSH01A and only one result is available from this borehole. Further, the reliability of this single datum is questioned.. Even when stress measurements are successful, they have uncertainties in the interpretation due to the need for the Young's modulus. The biaxial tests are not always easy to interpret giving an uncertain modulus. Also, anisotropy and non-linearity in the results may add to the difficulties.

The data used are biased such that many of them are located on Äspö. This means that the model may be biased towards the stresses prevailing there. The tests from CLAB are both old, shallow and give scattered results. They do therefore not help in the estimations of stresses at depth.

An uncertainty span was selected, as a percentage, such that most of the existing data fall within the span. With such a proportional uncertainty, the absolute span gets larger with depth, which is considered appropriate. The measurement accuracy is estimated to about 25% /Amadei and Stephansson, 1997/, but the lack of data, and potential bias and uncertainty in the deformation zone model imply that the uncertainty should be larger, and a total span of ± 40% was selected. The model is shown together with available data in Figure 4-62 and summarized in Tables 7-11 and 7-12.

Alternative stress model

Most of the stress data are from Äspö and Laxemar, which are both located NW of the Simpevarp subarea. Inside the subarea, there are only data from CLAB, showing low and scattered stress values. The new datum from borehole KSH02 shows very low stress (Figure 4-62) even though it is from 450 m depth. If it is assumed that this is a correct measurement, the explanation could be that there is a different stress domain in the local model area.

A possible case that could give such conditions would be if there was a gently dipping major fracture zone that could have caused a stress release due to shear slip in the direction of the regional major principal stress. If one of the lineaments striking NE between Äspö and Hålö (c.f. Figure 5-3) has fairly small dip towards SE, then the rock mass located above this zone could have stress levels corresponding to the gravitational forces rather than the tectonic forces. The large NW trending regional stresses would then be distributed to the rock mass below the zone. This case would thus give the possibility for having large variations in stress inside the subarea. This alternative model will be strengthened if the forthcoming data from Ävrö also shows low stresses. The existence and orientation of major fracture zones in the area will also be further investigated.

5.2.2 Mechanical properties

Modelling assumptions and input from other models

Borehole KSH01A is assumed representative of the Simpevarp subarea. The division of the borehole geology follows the preliminary division presented in conjuction with the single-hole geological interpretation (Section 4.4.5).

It is also assumed that the geometrical elements in the geological model are correct. Thus, the uncertainty associated with geometrical uncertainties in the geological model is not included in the spans of parameter values estimated here..

Intact rock mechanical properties

Uniaxial compressive strength

The uniaxial compressive strength is the maximum load a small core sample can sustain before failure. The sample has no confining stress in this standardized test (SKB MD-190.001). The result from the old data from Äspö shows a total spread from 52 MPa to 348 MPa (cf. Table 4-27). At this stage, when old data have to be used and these data cannot be legitimately filtered, and the detailed rock types are not known, a large span must be selected to cover the possible actual values. The selected value span should also cover potential properties for rocks situated at a large distance from Äspö. The potential Äspö bias in the data introduces an additional uncertainty to the estimation. The available data from Äspö was chosen to estimate the properties for quartzmonzodiorite and Ävrö granite, and the available data from CLAB to estimate the properties of fine-grained dioritoid (cf. the geological description Section 5.1.3).

However, the span size for parameter estimation must be somewhat limited because it would not be relevant to have a model span entirely covering the tails of the distribution. The very rare values would not be useful for characterization purposes. If the parameter is normally distributed, 3 standard deviations around the mean correspond to about 80% of the distribution, which was judged to be a reasonable coverage. The value 183 MPa is selected for the mean and about 3 standard deviations total span (i.e. mean ±1.5 SD) gives a span from 75 to 300 MPa. Numbers are rounded to the closest 5 or 10, such that undue false precision in the estimate is not implied by the model. This applies to all parameters in the description.

Deformation modulus

The deformation modulus for the intact samples is directly estimated from the test results. The tests are in this case performed on the same scale as the definition of the parameters. The spread in the old data resulted in estimates with a large span. This span may become narrower later when the well-defined, newer laboratory tests are performed. The total span is taken as about 3 times the standard deviation based on the test from Äspö. The middle of the span was 64 GPa and the standard deviation 16 GPa, and the span thus becomes 40–90 GPa and is taken to apply to both the rock types Ävrö granite and Quartzmonzodiorite. The CLAB-data shows slightly higher values, although the data are few (4), and therefore the span 70–100 GPa was selected. It also seemed reasonable to estimate a slightly higher deformation modulus for the “fine-grained dioritoid” because the fine-grained texture and the lower porosity (c.f. Sections 5.1.3 and 5.6.3), also imply a stiffer behaviour.

Poisson’s ratio

The Poisson’s ratio for the intact rock is similarly estimated from the Äspö HRL data (42 samples). The mean value is 0.23, which is within the value range expected from previous experience.

Tensile strength

Existing data are presented in Table 4-29. The mean value seen from the tests is about 15 MPa. The standard deviation in this case is small, but since the number of samples is small and all samples were taken from the Äspö HRL, a larger uncertainty span, 10–20 MPa, was judged appropriate. This span also fits roughly to the “rule of thumb” that the tensile strength tends to be related to the compressive strength as a 1:10 relation. For the fine-grained dioritoid no laboratory data exist. The same span for all rock types was considered an appropriate basis for this model version.

Rock mass mechanical properties

On the larger scale, the “rock mass” scale, all parameters are here based on empirical relations between Q and RMR and the desired parameters. The equations used to correlate the Q and RMR values to the different mechanical property parameters are given in /Röshoff et al, 2002/.

Uniaxial compressive strength

This parameter is difficult to define because the strength of a rock mass is very dependent on the conditions (fracture geometry, stress levels, anisotropy etc). By rock mass, what is meant here is a scale of a block with 30 m side. Actual testing on this scale is not possible. Q and RMR values were determined along KSH01A for both 5 and 30 m sections of the core (Figure 4-64 shows the results for 5 m sections). The mean and the standard deviation (SD) from the 30 m sections of each unit defined in the single-hole interpretation of KSH01A were used as base for the estimates, since this length corresponded to the selected parameter scale. The lowest and highest calculated values, corresponding to minimum and maximum Q and RMR, were also determined to give an indication of the uncertainty in the estimates. However, these results were not directly used in the estimation of the expected spans.

Table 5-24 shows a summary of the results from calculations of the mechanical parameters, for the units A–D along the KSH01A core, c.f. Section 4.4.5, based on the empirical indices Q and RMR, respectively.

The results for units A and B combined and for units C and D in combination, were generally similar to each other (cf. Q and RMR values in Figure 4-64 and Table 5-24). Therefore, it was decided that only one estimate should be made for each pair of combined units. The selection of values was performed with these steps: 1) Take the average of the two mean values (from two units) from Q-estimation. 2) Calculate ±1.5 SD (of Q estimations values) around the mean. 3) Round off the number to be divisible by 5 such that the RMR mean values for the two units fall inside the span, preferably in the centre. 4) Judge if there are other specific reasons to adjust the span.

Deformation modulus

The deformation modulus of a rock mass in situ is expected to increase with confining stress. Therefore, the parameter selected for the characterisation is defined such that it is the deformation modulus for low confining stress (0–5 MPa). This is the situation believed to correspond the best to the cases on which the empirical systems are based. In order to obtain the actual deformation modulus prevailing at a particular depth, one must add the stress dependency to the value. This stress dependency is here suggested to be about 2.5 GPa per MPa of confining stress (above 5 MPa), based on estimates in /Röshoff et al, 2002/.

The model descriptions are made in order to be generally applicable in the area, irrespective of depth, and this is why the deformation modulus has not been determined according to the depths at which the units happened to exist in borehole KSH01A. It is assumed that the variations in Q and RMR with depth seen in the borehole can be explained by differences in geological conditions, and not by the depth as such. This also agrees with the conclusion on this issue in Section 5.1.6. No, depth-dependency for the fracture statistics was found, but correlations were noted with lithology and alteration.

The span for the deformation modulus was selected in a way analogous to the uniaxial compressive strength, based on the values from the empirical estimations given in Table 5-24. The results for each unit along KSH01 is shown in Table 5-25.

The above estimates may be compared with the values estimated for the background rock mass by /Barton, in prep/, c.f. Table 4-31. It should be noted here that in the latter table the the values given were the modulus for a certain depth and therefore higher than the numbers in Table 5-25. However, the values compare fairly well with the estimated span if the suggested stress-dependency is considered, e.g. at 500–600 m depth the confining stress (the minimum stress) is expected to be about 15 MPa and the estimate is, for low stress (according to Table 5-25), 15–40 GPa for unit B. The addition of 2.5*10 = 25 GPa to the span gives an estimate of 40–65 GPa, for the actual stress

Table 5-24. Summary of result from estimation of rock mechanics parameters, based on empirical indices Q and RMR. One value for each 30 m along KSH01A was determined. The borehole was divided into units according to the geological single- hole interpretationof borehole KSH01A (c.f. Section 4.4.5).

Rock Unit	A		B		C		D	
	Mean	St Dev	Mean	St Dev	Mean	St Dev	Mean	St Dev
Q30m	5	3	5	3	17	7	19	6
RMR30m	69	3	69	4	72	5	73	2
UCSQ[MPa]	10	5	10	6	31	14	36	12
UCSRMR [MPa]	51	10	50	12	59	14	62	6
Em,Q [GPa]	21	3	20	4	31	5	33	4
Em,RMR [GPa]	31	5	30	7	36	10	38	4
ΦFm,Q [°]	27	6	20	3	20	1	18	1
ΦFm,RMR [°]	37	0	37	0	37	0	37	0
Cm,Q [MPa]	19	9	22	9	32	1	32	0
Cm,RMR [MPa]	13	2	12	3	15	4	15	2

Table 5-25. Predicted rock mechanical properties for the rock mass along the borehole KSH01A. The borehole is divided into different units according to the geological interpretation in Section 4.4.5.

Parameter for the rock mass (30x30x30 m scale)	Unit A Quartzmonzodiorite dominating	Unit B Finegrained dioritoid dominating	Unit C Mainly mix of quartzmonzodiorite and Ävrö granite	Unit D Ävrö granite dominating
Uniaxial compressive strength*	5–35 Mpa	5–35 MPa	5–55 MPa	5–55 MPa
Friction angle**	20–40°	20–40°	20–40°	20–40°
Cohesion**	5–25 MPa	5–25 MPa	10–30 MPa	10–30 MPa
Deformation Modulus*	15–40 GPa	15–40 GPa	20–75 GPa	25–75 GPa
Poisson's ratio*	0.05–0.20	0.05–0.20	0.05–0.25	0.10–0.25

*For low confining stress. See text.

**Linear model between 10 and 20 MPa confining stress

level. The estimate by /Barton, in prep/ is 57 GPa as a mean value. This value may be compared with the upper part of the span because this estimation was for the "background rock", i.e. for the rock outside the minor deformation zones along the hole. For the minor deformation zones in the borehole /Barton, in prep/ has estimated a modulus of 38 GPa at this depth (c.f. Table 4-32), which compares well with the lower part of the estimated span for the unit (a unit includes all rock masses both the best parts and the rock mass inside minor deformation zones).

Poissons' ratio for the rock mass

The Poisson's ratio is a parameter that describes the relation between the amount of deformation in directions parallel and perpendicular to direction of applied load. The rock mass behaviour, in general, is very much determined by the fractures of the rock mass, and this is the case also for this parameter. Closure of the fractures will be a major part of the rock mass deformation. An empirical means of estimating the Poisson's ratio is to assume that the ratio between the deformation modulus of the rock mass and the modulus of the intact rock is equivalent to the ratio between the corresponding Poisson's numbers. The deformation modulus for the rock mass is here estimated to be about 15% of that of the intact rock (at the lowest) and reaching a value corresponding to the modulus for intact rock in the case when confinement is high. Therefore, a span of 0.05–0.20 and 0.2–0.25 was selected as possible Poisson's ratios for the units A-B and C-D, respectively (cf. Table 5-25).

Friction angle and cohesion for rock mass

The friction angle (Φ) has been estimated using the Q and RMR systems that also include empirical relations for the friction angle (see Table 5-28). For empirical index systems, such as Q and RMR, the division into classes causes results in certain numbers being estimated in a stepwise manner. Therefore, the situation may arise where several spans get exactly the same number, as in the case of the friction angle based on RMR. This should not be interpreted as if there is no uncertainty in the estimation. The Q-value is a more sensitive index and therefore this index shows more spread. In this case a friction angle span from 20 to 40° was selected for rock mass in all units along borehole KSH01A, since this span covers both the Q and the RMR estimates.

The cohesion was similarly estimated based on values in Table 5-24 to be in the span 5 to 25 MPa for the units A and B and 10–30 MPa for units C and D. The higher values for the latter two units is a direct effect of the higher Q and RMR values calculated for these parts of the borehole. The selected span covers estimates based on both the Q and RMR system.

Rock mechanics description for rock domains

The rock mechanics description is here applied to the geological rock domains of the Simpevarp local area, which were defined and described in Section 5.1.3. So far results from empirical classifications are only avialbel from only one borehole, KSH01A. However, all the main rock types occur in this borehole, so it was assumed that the properties of the units along borehole KSH01A should be used for obtaining estimates applicable to the whole area for Simpevarp 1.1. It was judged reasonable to assume that Rock domain A (dominated by Ävrö Granite) should have properties corresponding to the units C and D, (these two were already given the same estimated span). The properties of Rock domain B (dominated by fine-grained dioritoid) was assumed the same as the properties estimated for the unit B of borehole KSH01A. Rock domain C consists of a mix of Ävrö granite and Quartzmonzodiorite. Therefore, the span for this domain was selected such that the minimum and maximum values of both units A and C-D in comnbination (in Table 5-24) were covered. Rock domain D (dominated by Quartzmonzodiorite) was assumed to have properties similar to the ones estimated for unit A. The resulting spans for all parameters in the four defined rock domains are given in Table 5-26.

Table 5-26. Predicted rock mechanical properties for the rock mass (including naturally occurring fractures) in the Simpevarp local model area. The area is divided into different rock domains according to the geological model in Section 5.1.3.

Parameter for the rock mass (30x30x30 m scale) [5]	Rock Domain A Ävrö granite dominating Min–Max	Rock Domain B Finegrained diorito-toid dominating	Rock Domain C Mix of Ävrö granite and quartz monzo-diorite	Rock Domain D Quartzmonzodiorite dominating	Rock inside Deformation Zones[4] [5]
Uniaxial compressive strength[1]	5–55 MPa	5–35 MPa	5–55 MPa	5–35 MPa	1–15 MPa
Friction angle[2]	20–40°	20–40°	20–40°	20–40°	10–35°
Cohesion[2]	10–30 MPa	5–25 MPa	10–30 MPa	5–25 MPa	0–20 MPa
Deformation Modulus[3]	25–55 GPa	15–40 GPa	15–55 GPa	15–40 GPa	1–10 GPa
Poisson's ratio	0.05–0.25	0.05–0.20	0.05–0.25	0.05–0.20	0.05–0.20

[1] This description parameter is not a standard parameter, it refers to the strength of a block of 30 m size with low confinement at boundaries. The conditions inside the block are not really uniaxia.

[2] Linear model between 10 and 20 MPa confining stress.

[3] For low confining stress, 5 MPa and lower. For higher stresses the modulus should be adjusted, See text.

[4] This is meant to refer to the larger deterministic deformation zones included in the deformation zone model.

[5] The properties of the rock inside minor deformation zones (or effects on rock mass blocks from minor zones) are also included in the parameter span for the rock domains. Minor zonez are the zones that are not part of the deterministic model of deformation zones.

The rock mechanics parameter values estimated for the deformation zones are uncertain, because we do not have borehole information from any major deformation zone at this stage. The values were selected based on the lower values noted in borehole KSH01A were minor deformation zones are intersecting the borehole. The estimates are also based on general experience and judgement where the strength in the major deformation zones should be ntably lower compared to the ordinary rock mass between the deformation zones.

Evaluation of uncertainties in mechanical property model

Applicability of empirical relations

Empirical relationships using Q and RMR, as reported in scientific articles have been used for different parameters /Röshoff et al, 2002/. However, the applied empirical equations were not developed for the type of excavations planned at a future repository site. Most of the excavations in the underlying cases were probably located closer to ground surface and possibly the considerations involved in these cases were others than will be of main concern for a geological repository.

Comparison between different empirical systems

The two systems, Q and RMR, did not give exactly the same results for estimations of the mechanical parameters. This introduces some additional uncertainty to the model. There are also other systems that could have been used for the characterisation. However, the systems would start with the same input data, more or less, and the uncertainty due to the input data quality and due to any possible bias from borehole KSH01A would be similar no matter what system is used. Figure 4-64 shows the Q and RMR for borehole KSH01A. The empirical approach gives a fairly large uncertainty in the absolute model parameter values, but should be quite reliable when used for comparisons between boreholes, or between sites, as long as classifications are identically applied. A useful and alternative way of appreciating rock mechanics differences between boreholes or sections in boreholes, is to compare directly the input data used to calculate the empirical indices.

Comparison between Q based on Boremap data and direct Q-logging

A comparison between the two classifications (direct Q-logging at the core and logging with the use of Boremap data) has been performed. The main differences in estimated parameter values originate from differences in the way the stress-dependency has been treated. The input parameter Ja (Joint alteration number) was associated with some uncertainty when determined from the Boremap logging, but this did not give any major differences in determined Q-values. The input parameters that may cause the largest differences in estimates are the ones that are not based on what is observed on the core, SRF (Stress Reduction Factor) and Jw (Joint water reduction number) /See further Röshoff et al, 2002/. All in all, both methods gave similar results.

Comparison with conditions at existing excavations at Äspö and CLAB

A back-calculation of the rock mass deformation modulus has been performed at the APSE site in the Äspö HRL. This study showed that the modulus is about 55 GPa, at a depth of 460 m. /Staub et al, 2004/. This value falls within the span selected for the rock domains dominated by Ävrö granite and quartzmonzodiorite, which are the rock types mostly occurring at Äspö. Although fracture intensity ins considered to be more important to rock mass mechanical properties than rock type, the performed geological DFN modelling also shows that the fracture intensity is expected to vary between the rock domains of the Simpevarp local area (See Table 5-22). Several factors, such as fracture intensity, rock type and stress conditions should thus be considered carefully before extrapolating the results from one site within the area to other sites.

Estimates from back-analysis of data collected at CLAB /Fredriksson et al, 2001/ similarly showed a deformation modulus of about 40 GPa. This value lay within the selected model span for Rock domain B. This value is for an excavation built at comparatively shallow depth.

Lack of theoretical approach

According to the strategy for rock mechanics description /Andersson et al, 2002a/ not only the empirical but also a "theoretical" approach should be applied to make the property estimates. This has not been undertaken for this version of the model, due to lack of laboratory test data, and this adds to model uncertainty, in particular for rock mass properties at depth. The parameters and scales to be used in the site-descriptive modelling to best satisfy the needs for safety assessment and repository design are difficult to determine. Some of the processes of importance may be on a scale that is larger than intact scale, i.e. large enough to include many open and sealed fractures, but still so small that elastic equivalent material parameters for 30 metre blocks may be inappropriate. This means that the set of parameters selected for the description may have to be reconsidered and extended in later model versions.

5.3 Thermal properties modelling

5.3.1 Thermal conductivity modelling

Thermal conductivity from mineral composition

The thermal conductivity of composite materials, such as crystalline bedrock, can be calculated from its mineral composition. In /Sundberg, 1988/, an overview of different approaches to the subject is given. For calculations of thermal conductivity of rock from mineral compositions, the self-consistent approximation (hereafter named SCA) of an n-phase material has been suggested /Sundberg, 1988; 2003a/. Chemical and mineralogical composition will be determined using the methods ICP, SEM and EDS /SKB, 2001a/. /Horai, 1971/, /Horai and Simmons, 1969/ and /Berman and Brown, 1985/ have determined values that can be used for the thermal conductivity and heat capacity of different minerals.

The geology of the Simpavarp site and the different rock types are described in Section 5.1.3. Table 5-27 presents the thermal properties for different rock types calculated from existing modal analyses using the SCA method. In addition to the dominating rock types mentioned in Table 5-27, fine medium-grained granite dikes and pegmatite occur, subordinated and occasionally copious (c.f. Section 5.1.3). However, the effects of these subordinate entities on the thermal properties have not been considered in the calculation. For Ävrö granite 15 thermal conductivity values have been used for the statistical analysis. At onset there were 17 samples but two outliers were removed after further examination of the data.

Statistical tests were performed to decide if the data are best described by a normal or a lognormal distribution. In Figure 5-30 the data from each rock type and best-fitting distribution, log-normal or normal, is indicated. Calculation of confidence limits was performed using the Maximum Likelihood method.

Table 5-27. Results of thermal conductivity estimation for different rock types, estimated with the SCA method. The mean values and the standards deviation values are given for the actual sample values. The confidence intervals for the mean of best fit distribution are also given.

Rock type	Number of samples	Mean value (W/m·K)	St. dev. (W/m·K)	2-sided 95% confidence interval for the mean		Best fitting distribution model (mean/st dev or loc/scale)
				Lower	Upper	
Granite to quartz monzodiorite (Ävrö granite)	15	2.67	0.25	2.55	2.80	Normal (2.673/0.2528)
Fine-grained dioritoid	22	2.24	0.18	2.16	2.32	Lognormal (0.8024/0.08294)
Quartzmonzodiorite	19	2.38	0.10	2.34	2.43	Normal (2.384/0.1040)

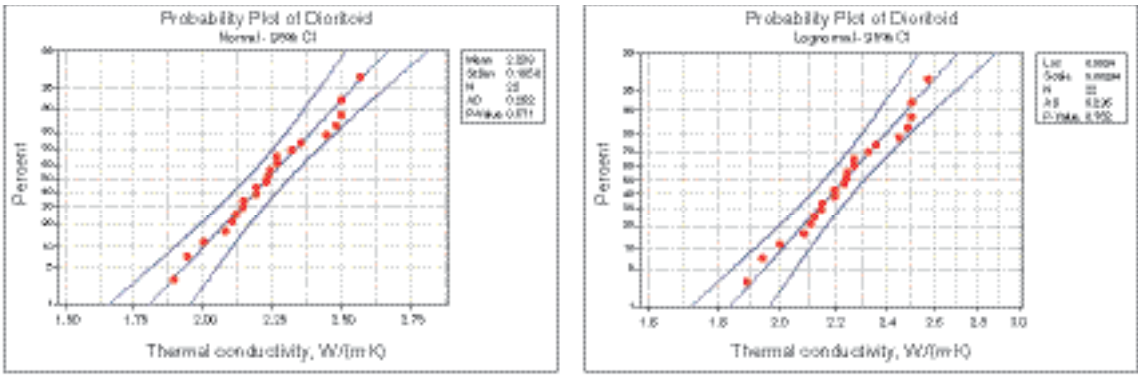

Figure 5-30. *Thermal conductivity – Probability plots of all data for three major rock types: Ävrö granite, finegrained dioritoid and quartz monzodiorite. The best fitting distributions, normal or lognormal, are also shown.*

Thermal conductivity from density measurements

The density log data (obtained from downhole logging) were divided into sections in accordance with the units along borehole KSH01A, as described in the section describing the geological single-hole interpretation (c.f. Section 4.4.5). The empirical relation between thermal conductivity and rock density proposed in /Sundberg, 2003b/ was used to estimate the thermal conductivity, based on the mean density averaged over each successive metre of borehole. The results are shown in Table 5-28.

As there are no laboratory data from the Simpevarp subarea to test the empirical density-thermal conductivity relation, the estimate based on the mineral composition was judged more reliable for the modelling at this stage. However, it is noted that both approaches give similar values for the thermal conductivity (compare mean values in Table 5-28 and Table 5-27).

It is noted that the standard deviation of the density data decreases with 20 to 35% when comparing the single data point scale with the 1 metre scale. This indicates that much of the variation in density data from the latter log is due to small scale variation. The measurement fluctuations seen may be explained by a combination of natural small-scale density variations and effects of the relative measurement accuracy of the logging tool (estimated at ±30 kg/m^3 /Mattsson and Thunehed, 2004/).

Table 5-28. Estimation of thermal conductivity for the interpreted units along KSH01A, based on density logging (c.f. Figure 4-65). A measurement is taken every 0.1 m and the length of a single measurement is about 0.25 m.

Unit (See Section 4.4.5)	Mean density [kg/m^3]	Stand. dev. Single points, [kg/m^3]	Stand. dev. for av. density over 1 meter [kg/m^3]	Stand. dev. for av. density over 2 meter [kg/m^3]	Thermal Cond. for Mean value [W/m·K]
A. Quartzmonzodiorite	2,768	101	78	69	2.42
B. Fine-grained dioritoid	2,783	77	51	47	2.34
C. Mixture of Quartz monzo-diorite and Ävrö granite	2,762	102	78	71	2.45
D. Ävrö granite	2,663	69	44	40	3.32

Thermal conductivity for rock domains

The density logging results imply that larger-scale variability (variability between rock blocks of larger size) should be less than the variability on the small scale, i.e. the result from the SCA analysis. This is reasonable, considering that the influence of local scale mineralogy variation within the same rock type would be negligible at a larger scale. The use of density log data has been similarly discussed and demonstrated within the framework of the APSE project at the Äspö HRL /Staub et al, 2003/. The results from this project support the finding that most of the density variation seen from the density log, within the same rock type, is concentrated to a length scale smaller than a metre.

On the other hand, there is a factor pointing in the opposite direction. The selection of the rock samples for the SCA analysis did not include samples from the non-dominant rock types that exist within the defined rock domains (a rock domain consists of different rock types to variable extent). The influence of this added mixing would entail an increase in the variance for the domain compared to the result of the present SCA calculation. The difference in composition of the samples included in the SCA analysis compared with the expected actual mix in the defined rock domains has not been quantified.

The average value for a cubic rock volume of 1x1x1 metre was selected as a relevant parameter scale for the description of the thermal properties, as it corresponds to the deposition-hole scale (the planned deposition hole-diameter is approximately 2 m). A decision on how to upscale from the SCA scale to the selected support scale for the rock domains had to be made. For Simpevarp 1.1 it was assumed that the two factors mentioned above give an effect on the standard deviation of the same order of magnitude, but cancelling each other out, such that the standard deviation obtained from the SCA analysis for a certain rock type becomes a reasonable estimate of the spread also at the 1 metre length scale in the rock domains dominated by this particular rock type.

For the mixed Rock domain C, a distribution was fitted to the samples from both quartzmonzodiorite and Ävrö granite, by simply assuming that the mixing was about the same as the number of samples turned out to be (15 to 19). The resulting distribution models for the four rock domains are given in the Table 5-29, and are visualised in Figure 5-31. It is noted that there is a fairly large difference in the mean thermal conductivity between the Rock domain B (dominated by fine-grained dioritoid) and Rock domain A (dominated by Ävrö granite), 2.2 W/mK compared to 2.7 W/mK, respectively.

Table 5-29. Descriptive model for the thermal conductivity of the four largest rock domains (cf. Section 5.3). The distribution functions are selected based on the results from estimations from samples of the dominating rock type (See Table 5-27). For rock domain C the descriptive model is based on statistics for all samples from both quartz monzodiorite and Ävrö granite. For discussion about scale and uncertainty see text.

Rock Domain (See Section 5.1.3, Figure 5-1)	Model distribution for Thermal conductivity Scale 1x1 m [W/m·K]		
	Function type	Mean value	Standard deviation
A Dominated by granite to quartz monzodiorite (Ävrö granite)	Normal	2.673	0.2528
B Dominated by fine-grained dioritoid	Lognormal	0.8024 (= ln2.231)	0.08294
C Dominated by a mixture of quartz monzodiorite and Ävrö granite	Lognormal	0.9168 (= ln2.501)	0.09140
D Dominated by quartzmonzodiorite	Normal	2.384	0.1040

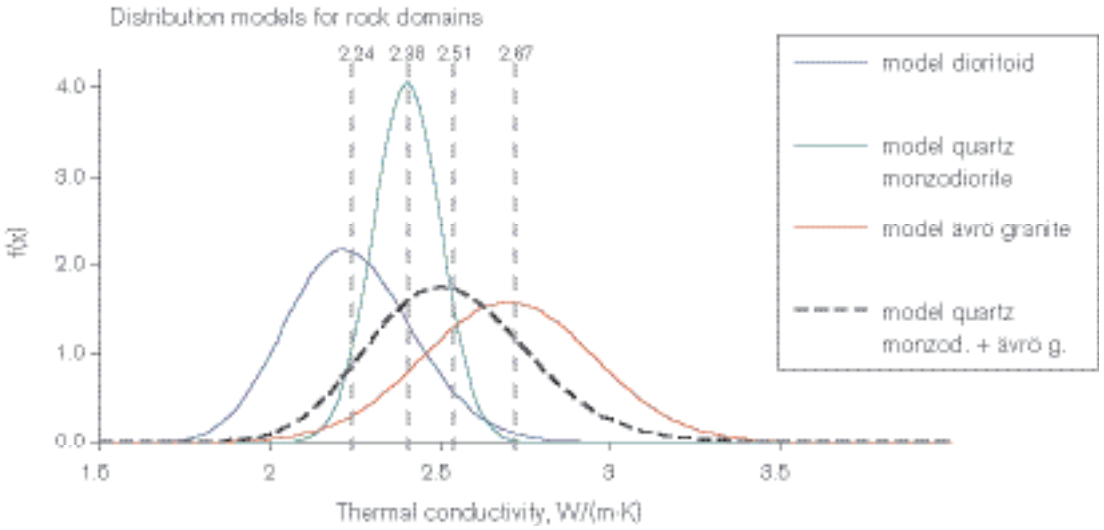

Figure 5-31. *Distributions of thermal conductivity for the rock domains. The mean values are indicated by dashed vertical lines.*

5.3.2 Specific heat capacity modelling

There are no laboratory test data on the specific heat capacity from the site investigation at this stage. Therefore the estimation was based on the empirical relationship presented in /Sundberg, 2003b/ between rock density and specific heat capacity. Assuming that the density for all rock types in the Simpevarp subarea lie in the span 2,600 to 2,900 kg/m^3 (c.f. Figure 4.65), the corresponding values for specific heat capacity range from 2.0 to 2.3 MJ/m^3 K. Bearing in mind that this parameter will not be important for repository design and safety assessment, and since it does not influence the equilibrium temperatures (only the transient development), it was judged sufficient to use the same span for all defined rock domains.

5.3.3 Thermal expansion coefficient

In absence of laboratory test results for the thermal expansion coefficient from the Simpevarp subarea, the test results from the APSE area at the Äspö HRL were used (c.f. Table 4-34). The minimum and maximum of the available data, although limited, were assumed to give a span covering the probable average values for 1 metre cubic rock blocks in all identified rock domains. It is not expected that this parameter will show any major scale or ”mixing” effect as the thermal expansion depends on the mineral content, and the composition is roughly similar for all rock types. The selected span is $6.0 \cdot 10^{-6}$ to $8.0 \cdot 10^{-6}$ mm/mm°C.

5.3.4 In-situ temperature

The available data on in situ temperature is provided in Section 4.7.5. The basic modelling assumption is that data from boreholes KSH01A and KSH02 are representative for the Simpevarp subarea. This assumed valid because in situ temperature does not normally show large local variation. From these data it is concluded that the temperature is about 16°C at a depth of 600 m. The temperature gradient is increasing from about 13°C/km, at a depth of 200 m, to about 16°C/km at about 900 m. In addition, the temperature gradient measured in borehole KSH01A is influenced by natural disturbances in the temperature measurement. The explanation for this could be changes in the thermal conductivity (a lower thermal conductivity gives rise to a higher gradient at a given constant heat flow), climate changes (changes during the last 200–300 years can be measured down to about 250 m), or perturbations by drilling and induced water flow. If variation in thermal rock conductivity is the actual cause, the change in gradient indicates a reduction in thermal conductivity of about 20% at larger depths compared to the situation at shallow depth.

5.3.5 Evaluation of uncertainties

A general description of uncertainties is provided in the strategy report for the thermal site descriptive modelling /Sundberg, 2003a/. Here, some specific uncertainties related to the data are discussed.

Modelling from mineral composition

There is currently an overall uncertainty associated with the thermal properties of individual minerals and an uncertainty in the chemical composition of, primarily, plagioclase in the investigated area.

Comparison between measured thermal conductivity values and those calculated by the SCA method has been made using data from the Äspö HRL. In Table 5-30, measured values based on density variations are compared with values calculated using the SCA method. In earlier work at the Äspö HRL, the rock type "Äspö diorite" was studied specifically. The rock type Quartzmonzodiorite used in the geological modelling of the Simpevarp area is closest in composition, but it is not identical, to "Äspö diorite".

If the TPS-measured values from the laboratory are assumed to be "true" the SCA method underestimates the thermal conductivity for the different rock domains in this model with approximately 5 to 10%. No correction has been made to the SCA values calculated for the current model version, due to lack of laboratory measurements on comparable samples.

Upscaling from core samples to rock domains

The mean value for the thermal conductivity seems to be fairly certain at this stage. However, direct laboratory tests of the thermal conductivity due for the upcoming model version will increase the confidence substantially. Of greater concern is the uncertainty in the spatial variation of the thermal conductivity. It is not evident how to make the up-scaling from small rock samples to larger rock volumes. A comprehensive and dense sampling of the drill core and subsequent laboratory testing is not realistic, due to the number of tests needed. However, if the results from density borehole logging, and the relation between density and thermal conductivity are shown to be reliable, this log provides a possible basis to study spatial correlation as described tentatively above and in more detail in /Sundberg, 2002/ and /Staub et al, 2003/.

Table 5-30. Comparison between thermal conductivity determined from laboratory measurements using the transient plane source method (TPS) /Gustafsson, 1991/ and determined using the SCA method (self-consistent approximation) for the same rock samples (the number of samples limited to 2–5 for each rock type) . Modified from /Sundberg, 2003a/.

Method	Äspö diorite[1] λ, W/(m·K)	Äspö diorite[2] λ, W/(m·K)	Ävrö granite λ, W/(m·K)	Finegrained granite λ, W/(m·K)
Calculated (SCA)	2.24	2.35	3.01	3.45
Measured (TPS)	2.41	2.56	3.24	3.63
Difference in %	–7.1%	–8.2%	–7.1%	–5.0%

[1,2] Comparisons from two different reports, see /Sundberg, 2003a/.

5.4 Hydrogeological modelling

The hydrogeological descriptive model should provide data that are useful for modelling advective flow in the groundwater system, including density driven flow. More specifically, groundwater flow models should be able to calculate groundwater flow within a given volume under natural (undisturbed) conditions. Modelling, that includes the fully open or back-filled deep repository is subsequently carried out by Repository Design and Safety Assessment. In the undisturbed system, the flow paths within the modelled volume are important for the hydrogeochemical interpretation, while the flow paths from the repository area to discharge areas are important for Safety Assessment. Shoreline displacement must also be taken into account when modelling the long-time evolution of the groundwater flow.

A primary objective for hydrogeological description is to;

- Determine and motivate hydraulic properties, boundary and initial conditions based on Primary Data and numerical modelling.

The numerical groundwater flow modelling serves three main purposes:

- *Model testing:* Simulations of different major geometric alternatives or boundary conditions in order to try to disprove a given geometric interpretation or boundary condition, and thus reduce the number of alternative conceptual models of the system.
- *Calibration and a sensitivity analysis:* to explore the impact of different assumptions of hydraulic properties, boundary and initial conditions.
- *Description of flow paths and flow conditions:* useful for the general understanding of the groundwater flow system at the site.

The numerical groundwater flow simulations are thus helpful for the description of the hydraulic properties, boundary and initial conditions and associated uncertainties, as well as for enhancing the general understanding of the site. The interaction between the geology and hydrogeology disciplines, but also the disciplines of hydrogeochemistry, transport and surface ecosystems, in interpreting the available data, is essential in order to obtain consistent models, and the numerical groundwater flow models play an important role in this context.

A given version of the site description, with its groundwater flow models, subsequently forms the basis for further analysis by Repository Design and Safety Assessment and for the planning of new investigations. Exploratory groundwater flow simulations are considered when planning field investigations or solving specific Repository Design and SA questions.

Overview of work done for Simpevarp 1.1

It was not possible to base the evaluation of the hydrogeological data on the geological model version Simpevarp 1.1 due to the delayed delivery of the geological model. It was, therefore, decided that the regional scale structural model version 0 should be used jointly with reasonable estimates of hydraulic properties to obtain a first insight into the groundwater flow situation in the Simpevarp area. Because of the above reasons, the numerical groundwater flow model with its input data presented in Section 5.4 should mainly be regarded as a semi-generic study and cannot be directly interpreted in the context of the local scale geological model presented in Chapter 5.1.3. Furthermore, it is emphasised that the present description relates to the regional scale only.

The modelling done for Simpevarp 1.1 comprises estimates of hydraulic properties based on data from the Laxemar area, but also Äspö HRL and Forsmark model version 1.1 information, as well as numerical groundwater flow simulations. The numerical groundwater flow modelling based on structural model version 0 and the estimates of hydraulic properties was performed by two different modelling teams each using the numerical codes **DarcyTools** /Svensson et al, 2004; Svensson and Ferry, 2004; Svensson, 2004/ or **ConnectFlow** /Hartley et al, 2003a,b; Hartley and Holton, 2003; Hoch and Hartley, 2003; Hoch et al, 2003/, respectively. The main focus for the groundwater flow modelling was to assess the different hydraulic properties, initial and boundary conditions and implications of the description of past and present salinity distribution.

5.4.1 Modelling assumptions and input from other models

The descriptive hydrogeological model of the Simpevarp area is based on four different sources of information. The four sources are: (i) mapping of Quaternary deposits and bedrock geology (rock type, lineaments and deformation zones) (ii) meteorological and hydrological investigations, (iii) hydraulic borehole investigations and monitoring, and (iv) hydrogeological interpretation and analysis. The model may be described by means of parameters, which detail:

- The geometric and hydraulic properties of the crystalline bedrock and the Quaternary deposits.
- The hydrological processes that govern the hydraulic boundary conditions and hydraulic interplay between surface water and groundwater, including groundwater flow at repository depth.

Figure 5-32 illustrates schematically SKB's systems approach to hydrogeological modelling of groundwater flow. The division into three hydraulic domains (overburden (soil), rock and conductors) constitutes the basis for the numerical simulations carried out in support of the site descriptive model.

From a hydrogeological perspective, the geological data and related interpretations constitute the basis for the geometrical modelling of the different hydraulic domains. Thus, the investigations and documentation of the bedrock geology and the overburden (Quaternary deposits) provide input to:

- The geometry of deterministic fracture zones (and/or linked lineaments) (HCD) and the bedrock in between (HRD).
- The distribution of Quaternary deposits (overburden) (HSD), including genesis, composition, stratification, thickness and depth.

Likewise, the investigations and documentation of the present-day meteorology, hydrology and near-surface hydrogeology (in terms of mapping of springs, wetlands and streams, surveying of land use (ditching and dam projects), resources for water supply, nature conservation areas, etc) together with the shoreline displacement throughout the Holocene constitute the basis for the hydrological process modelling. This information provides input to:

- Present-day interpretation of drainage areas, as well as recharge and discharge areas.
- Estimates of the average present-day precipitation and run-off, distribution of heads and flows in watercourses.
- Estimates of boundary conditions since the last glaciation.

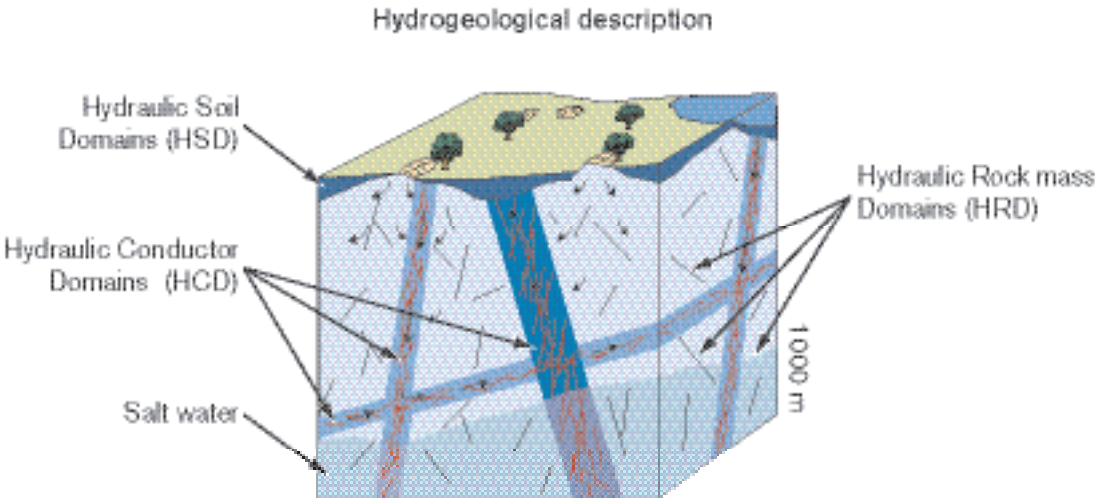

Figure 5-32. *Division of the crystalline bedrock and the overburden (Quaternary deposits) into hydraulic domains representing the overburden,(HSD) and the rock mass volumes (HRD) between major fracture zones (conductors, HCD). Within each domains the hydraulic properties are represented by mean values, or by spatially distributed statistical distributions. /Rhén et al, 2003/.*

Results from hydraulic borehole investigations and monitoring are of interest for the definition of hydraulic properties of the different hydraulic domains. There are basically two main sources of information for the bedrock hydrogeological properties:

- Hydraulic tests and hydrogeological monitoring in deep boreholes within the Simpevarp area.
- Hydraulic tests and other hydrogeological observations in boreholes drilled in overburden (Quaternary deposits) in the Simpevarp area.

Hydrogeological interpretation and analysis form the hydrogeological part of site descriptive model. The work has three main parts.

- Primary interpretation of hydrogeological data.
- Integrated evaluation between disciplines to obtain consistent models.
- Groundwater flow simulations for testing and evaluating the implications of describe the dite descriptive model version.

5.4.2 Hydrology

A good understanding of the surface hydrological conditions is essential, as it serves as a basis for assigning boundary conditions to the groundwater flow simulations. The surface hydrological conditions are also important for interpreting hydrochemical conditions near surface and in water-courses and lakes.

The description below forms the initial conceptual basis for near-surface hydrological conditions. As few site specific data currently exist, the description is mainly based on what can be expected based on general knowledge of hydrology in central Sweden. No quantitative surface hydrological modeling has been performed in model version Simpevarp 1.1.

General near-surface hydrological conditions

From the description of the topography and Quaternary deposits of the Simpevarp area, as provided in Chapters 4 and 5, it can be concluded that the area is characterised by a limited topographic relief, with relatively small-scale topographical undulations and relatively shallow Quaternary deposits. Almost the entire area is below 50 metres above sea level (masl). The Quaternary deposits are, for the most part, less than 20 m thick in the regional scale model area and rock outcrops are frequent. Till is the dominant deposit, cf. Sections 4.2.1 and 5.1.1. Coniferous and deciduous forests cover most of the area and wetlands are found in places.

Geometry of catchment areas and water courses

The small-scale topography with the large number of small streams form a large number of small catchments with local, shallow groundwater flow systems within the regional scale model area, see Section 4.3.2.

Discharge and recharge areas

In recharge areas, the soil water deficit has to be satisfied before any major groundwater recharge can take place. By-pass flow in different types of macro-pores may take place but can be assumed to be insignificant from a quantitative point of view.

In discharge areas, defined as areas where the groundwater flow has an upward component, by definition no groundwater recharge takes place. However, not all discharge areas are saturated to the ground surface. Rather, water flows in the uppermost most permeable part of the soil profile, or along the overburden interface with the bedrock. In unsaturated discharge areas the soil water deficit is usually very small and these areas respond quickly to rainfall and snowmelt events.

Lakes are considered to be permanent discharge areas. The hydraulic contact with the groundwater zone is highly dependent on the hydraulic conductivity of the bottom sediments. Borings in the lakes sediments have not yet been made to show the type of sediments, but probably the lake bottoms are covered with fine sediments of low hydraulic conductivity.

Streams are also considered as permanent discharge areas. However, some are dry during parts of the year.

Wetlands (bogs and mires) can either be in direct contact with the groundwater zone and constitute typical discharge areas, or be separate systems with tight bottoms and little or no hydraulic contact with the groundwater zone. Information needs to be collected to clarify the hydraulic contact between groundwater and the major wetlands. Probably, fine sediments of low permeability are present in the subsurface.

In flat terrain, the extension of recharge and discharge areas may vary during the year.

Groundwater recharge and discharge

The infiltration capacity exceeds rainfall and snowmelt intensity with few exceptions. Unsaturated (Hortonian) overland flow may occur over short distances on agricultural land covered with clayey soils and on frozen ground where the soil water content was high during freezing. Also, on outcropping bedrock, unsaturated overland flow may occur but only over very short distances before water meets open fractures or the contact zone between bedrock and soil. Initially, unsaturated overland flow can be assumed to be negligible in the quantitative hydrological modeling, and the groundwater recharge in recharge areas can be set equal to the specific runoff. Saturated overland flow appears in discharge areas where the groundwater level reaches the ground level.

The uppermost metre of the Quaternary deposits is generally much more permeable and porous than deeper-lying deposits. The probable permeability and storage characteristics of the soil profile mean that very little water needs to be added to raise the groundwater table at depths below approximately one metre. A groundwater recharge of 10 mm is estimated to give rise to a 20 to 50 cm increase in groundwater level. In periods of abundant groundwater recharge, the groundwater level in most recharge areas reaches the shallowest part of the soil profile where the hydraulic permeability is much higher and significant lateral groundwater flow will take place. However, the transmissivity of this upper layer is so high that the groundwater level does not reach much closer to the ground surface than 0.75–1 m in typical recharge areas.

By use of Oxygen-18 as a tracer, information can be obtained on the runoff generation process as well as on groundwater reservoir volumes /Lindström and Rodhe, 1986; Johansson, 1987a; Rodhe, 1987b/. /Rodhe, 1987b/ studied the runoff generation process by consideration of oxygen isotope ratios in several small Swedish catchment areas. The results showed that in peak runoff events, groundwater (pre-event water) often constitutes the dominant fraction of the discharge. The infiltrating water pushes out the “old” water to form the peak runoff. Also, in an area with shallow Quaternary deposits, like the Simpevarp area, the total reservoir volume in the till is much larger than the annual groundwater recharge. The water stored in a 3 metre thick saturated till profile corresponds to 3–4 years of groundwater recharge. In traditional hydrological (linear) reservoir modeling, the active storage used is usually much smaller than the total storage. However, in hydrogeochemical and contaminant transport modeling the total storage is also of major interest.

Groundwater recharge from the Quaternary deposits to the bedrock aquifer is probably small due to the generally higher permeability of the Quaternary deposits compared with the bedrock. Only a small fraction of the total recharge will reach below the uppermost (more fractured/weathered)) zone of the bedrock, probably < 10%.

Discharge from the groundwater system in the bedrock probably mostly takes place in the topographically defined major discharge areas.

Water table

The shallow groundwater flow in the Quaternary deposits can be assumed to follow the topography. Groundwater levels are probably also shallow, usually less than a few metres below ground in recharge areas and < 1 m in discharge areas. The annual groundwater level fluctuation is probably a few metres in recharge areas and about 1 m in discharge areas /Rhén et al, 1997b/. Sea-level fluctuations probably have insignificant influence on the absolute groundwater levels and the groundwater level fluctuations in large parts of the regional area.

Water balance – precipitation and run-off

Annual precipitation is relatively low in the Simpevarp area, 600–700 mm, increasing somewhat further inland. The specific runoff is approximately 150–180 mm. Most of the specific runoff can be expected to be discharging groundwater, as the combined area of surface waters and peat lands is small compared to the total area. The unsaturated (Hortonian) overland flow is not expected to generate significant flows directly to surface waters (as mentioned above), The discharge areas near surface waters and peat lands (generating subsurface flows to surface waters and peat lands) also probably make a relatively small contribution.

The over-all, long-term, water balance in the area can be formulated in different ways depending on the hydrological system studied and the components considered essential to represent /e.g Domenico and Schwartz, 1998; Dingman, 2002; Freeze and Cherry, 1979/. In Figur 5-33, the elements of the hydrological cycle for a catchment area are indicated. The components of the figure are:

P : Precipitation,

E : Evaporation,

T_T : Total Transpiration,

T_G : Transpiration (from groundwater),

F : Infiltration,

S_E : Unsaturated upward flow to surface due to evaporation,

S_{EG} : Unsaturated upward flow from the groundwater due to evaporation,

R_N : Recharge to the groundwater from the unsaturated zone,

$Q_{G\text{-}IN}$: Inward groundwater flow across the catchment's boundaries,

$Q_{G\text{-}OUT}$: Outward groundwater flow across the catchment's boundaries,

$Q_{G\text{-}S}$: Groundwater flow to the streams,

$Q_{S\text{-}G}$: Recharge to the groundwater from streams,

Q_O : Overland flow to streams,

Q_I : Inter-flow to streams,

Q_R : Runoff, flow in streams out of the catchment area.

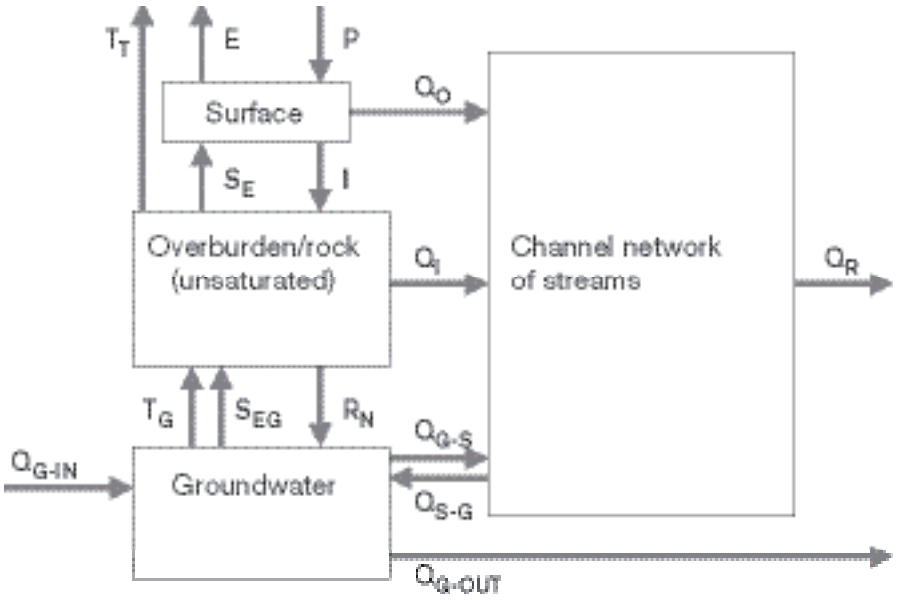

Figur 5-33. *Elements of the hydrological cycle of a catchment /modified after /Domenico and Schwartz, 1998/.*

Assuming a long-time average (no storage effects in the subsurface waters and surface waters) and that further there is an insignificant groundwater flow over the catchment boundaries ($Q_{G\text{-}IN=}$ $Q_{G\text{-}OUT}$ =0) a simplified hydrologic equation can be formulated as below.

$P=ET+Q_R$,

where

ET : Evapotranspiration (Sum of transpiration (T_T) and evaporation (E)).

Assuming that Q_O and Q_I are small the net groundwater recharge (R_N-T_G-S_{EG}) can be approximated as Q_R. Using relevant meteorological and hydrological data from Section 4.3, the estimated average annual groundwater recharge amounts to some 150–180 mm, c.f. Table 5-31.

Evaluation of uncertainty

The estimates of precipitation and runoff are probably fairly correct but other surface hydrological characteristics are very uncertain, as no site-specific data are yet available.

5.4.3 Hydrogeology of Quaternary deposits

The upper surface of the groundwater flow models have to be adapted to the topography and the Quaternary deposits and are a part of the groundwater flow model. The hydraulic properties of these deposits are expected to differ significantly from the bedrock properties. Both the geometric and hydraulic properties of these deposits have to be adequately characterised to underpin a realistic description of groundwater flow near the surface.

General considerations relating to modeling of Quaternary deposits

No 3D geological description of the Quaternary deposits could be produced for Simpevarp 1.1 due to lacks of spatially distributed data. Furthermore, geometrical description of HSDs and their properties could not be made for Simpevarp 1.1 and a very simplified geometrical model was, therefore, applied in the numerical groundwater simulations.

For model version S1.1 no site-specific hydrogeological data for Quaternary deposits were available, but the till is expected to be sandy and occasionally gravelly. Therefore, only concepts considered relevant to the Simpevarp area and associated generic data are described here.

Preliminary geometrical assumptions

The overburden (mainly Quaternary deposits) is treated in a very simplified way in the numerical groundwater simulations as a layer of constant thickness and homogeneous hydraulic properties. Consequently, in the Simpevarp v1.1 groundwater flow modelling only one HSD is represented over the entire area.

The soil cover in the area is thin with numerous outcrops of bedrock. It is assumed that the soil cover can be approximated as a 3 m thick layer over the entire regional scale modeling area.

Table 5-31. A crude water balance for the Simpevarp area (P: Precipitation, ET: Evapotranspiration, Q_R: Run-off, Q_G: Groundwater recharge).

P (mm)	ET (mm)	Q_R (mm)
600–700	420–550	150–180

Assignment of properties

As no site-specific data as to the hydraulic conductivity of Quaternary deposits are available, the model parameters have been based on generic data from e.g. /Knutsson and Morfeldt, 2002/ and similar textbooks, c.f. example in Table 5-32.

In the upper approximately one metre section of the Quaternary deposits, the hydraulic conductivity and effective porosity are much higher than further down the soil profile /Lundin, 1982; Johansson, 1986, 1987a,b; Espeby, 1989/. This is mainly due to soil forming processes, with ground frost probably the single most important process. However, wave washing also implies that the till, at exposed locations, is coarser at the soil surface and, at some locations, coarse outwashed material has been deposited. The hydraulic conductivity in the upper one metre can typically be 10^{-5}–10^{-4} m/s. The effective porosity typically varies between 10 and 20%.

Below the depth strongly influenced by the soil-forming processes, the hydraulic conductivity and the effective porosity of the till will be much lower. Depending on the type of till, the hydraulic conductivity typically varies between 10^{-10} and 10^{-5} m/s, with the lower values for the clayey till. The effective porosity is typically in the order of 2–5%.

The properties assigned for the Simpevarp 1.1 hydrogeological modeling were the same as assigned for the Forsmark 1.1 descriptive model /SKB, 2004/, see Table 5-33.

Evaluation of uncertainty

The uncertainty of the geometrical model and the associated material properties is high due to lack of data.

Table 5-32. Expected range for hydraulic conductivity of various Quaternary deposits.

Type of Quaternary deposits	Expected range of hydraulic conductivity (K) (m/s)	Ref.
Till, near surface 0–1 m	10^{-3}–10^{-6}	1
Till, gravelly	10^{-5}–10^{-7}	2
Till, sandy	10^{-6}–10^{-8}	2
Till, silty	10^{-7}–10^{-9}	2
Till, clayey	10^{-8}–10^{-10}	2
Clay till	10^{-9}–10^{-11}	2
Gravel	10^{-0}–10^{-3}	1, 2
Sand	10^{-3}–10^{-6}	2
Silt	10^{-5}–10^{-9}	2
Clay	10^{-9}–10^{-12}	2

1) /Knutsson and Morfeldt, 2002/.

2) /Carlsson and Gustafson, 1997/.

Table 5-33. Hydraulic property assigned to Hydraulic Soil Domain (HSD).

HSD	Type of Quaternary deposits	Thickness (m)	Hydraulic conductivity (m/s)	Expected range of hydraulic conductivity (K) (m/s)	Kinematic porosity, n_e %
1	Till- near surface type	3	$1.5 \cdot 10^{-5}$	10^{-3}–10^{-6}	5

5.4.4 Oceanography

No new model has been developed since model version 0.

Groundwater flow simulations

The oceanographic conditions at the top surface of the model domain have to be specified for groundwater flow models connected to the sea. Present and past conditions are presented in Section 5.4.8.

5.4.5 Numerical groundwater flow model of the bedrock with potential alternatives

The Regional Model Domain in the Simpevarp area has its bottom surface at –2,100 masl and the horizontal dimensions are 21 km times 13 km, c.f. Figure 2-3. Figure 5-34 shows the model domain in a perspective view with the physical dimensions to scale. The top surface follows the topography and bathymetry as defined for the Simpevarp version 0 site descriptive model /Brydsten, 1999/. Below the thin layer of Quaternary deposits (HSD), the fractured bedrock consists of Hydraulic Conductor Domains (HCD) and Hydraulic Rock Domains (HRD), c.f. SKB's systems approach /Rhén et al, 2003/ shown in Figure 5-32. The areal extent of the regional scale model domain is defined by the Simpevarp version 0 model /SKB, 2002b/, see also Section 2.8.2 for explicit definition of the regional model area.

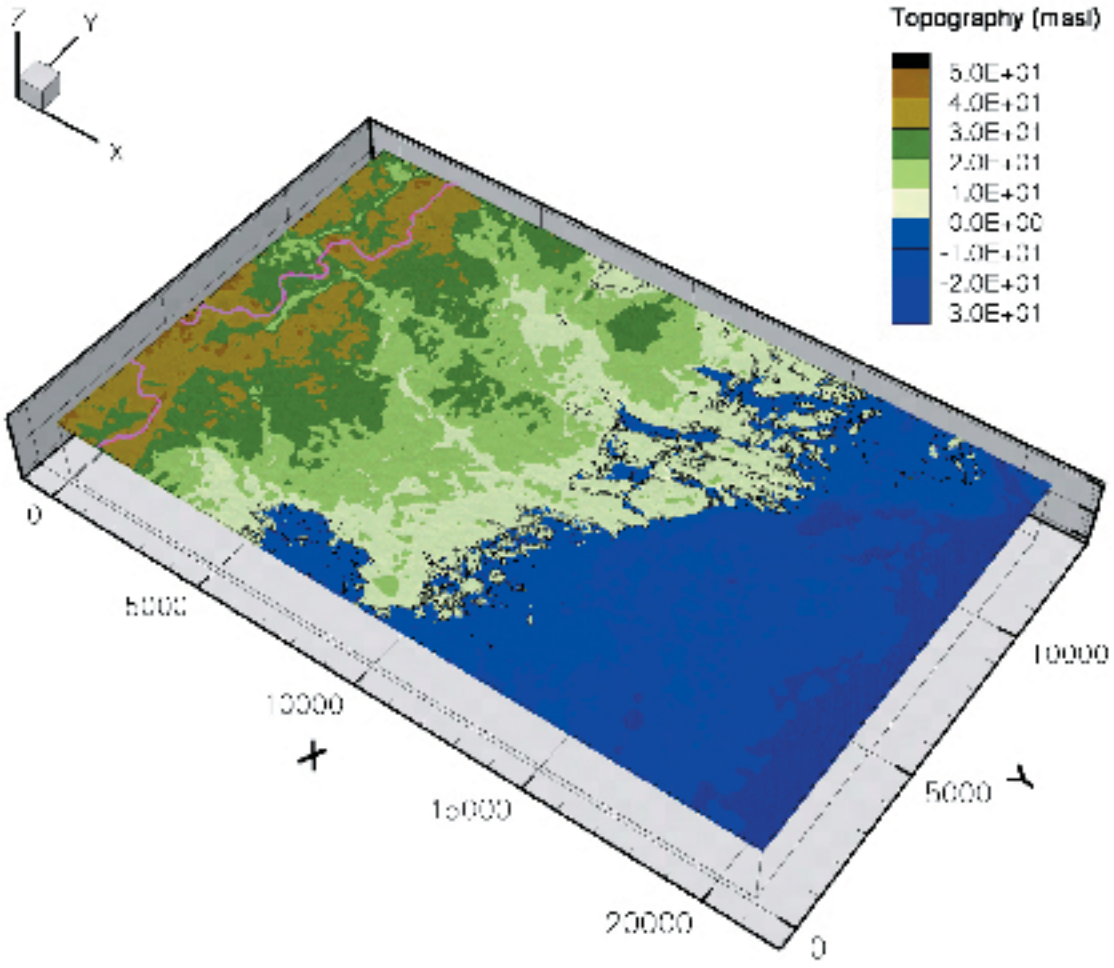

Figure 5-34. *The regional scale model domain as defined for the Simpevarp 1.1 site descriptive hydrogeological models including superimposed topography and bathymetry /Follin et al, 2004/.*

The deformation zones interpreted in the Simpevarp version 0 model, shown in Figure 5-35, constitute the primary geometrical input for the division of the bedrock into HCDs and HRDs. As pointed out in the beginning of Section 5.4, the reason for using this structural model is that the Simpevarp version 1.1 geological model was not available at the start of the groundwater flow simulations.

The deformation zones are of different size and confidence level. The lower trace length threshold for inclusion as a deterministic deformation zone was set to one kilometre and the depth was assumed no greater than the trace length on the surface. These imposed constraints are not well-informed by field information, but should be considered working hypotheses for the Simpevarp 1.1 site descriptive model.

The version 0 deformation zones were used in the hydrogeological modelling regardless of their designated level of confidence. That is, each fracture zone segment was treated as a conductor without taking any associated uncertainty into account. All zones should be considered as having a low or medium confidence of existence.

Alternative geometric interpretations were not treated due to lack of time.

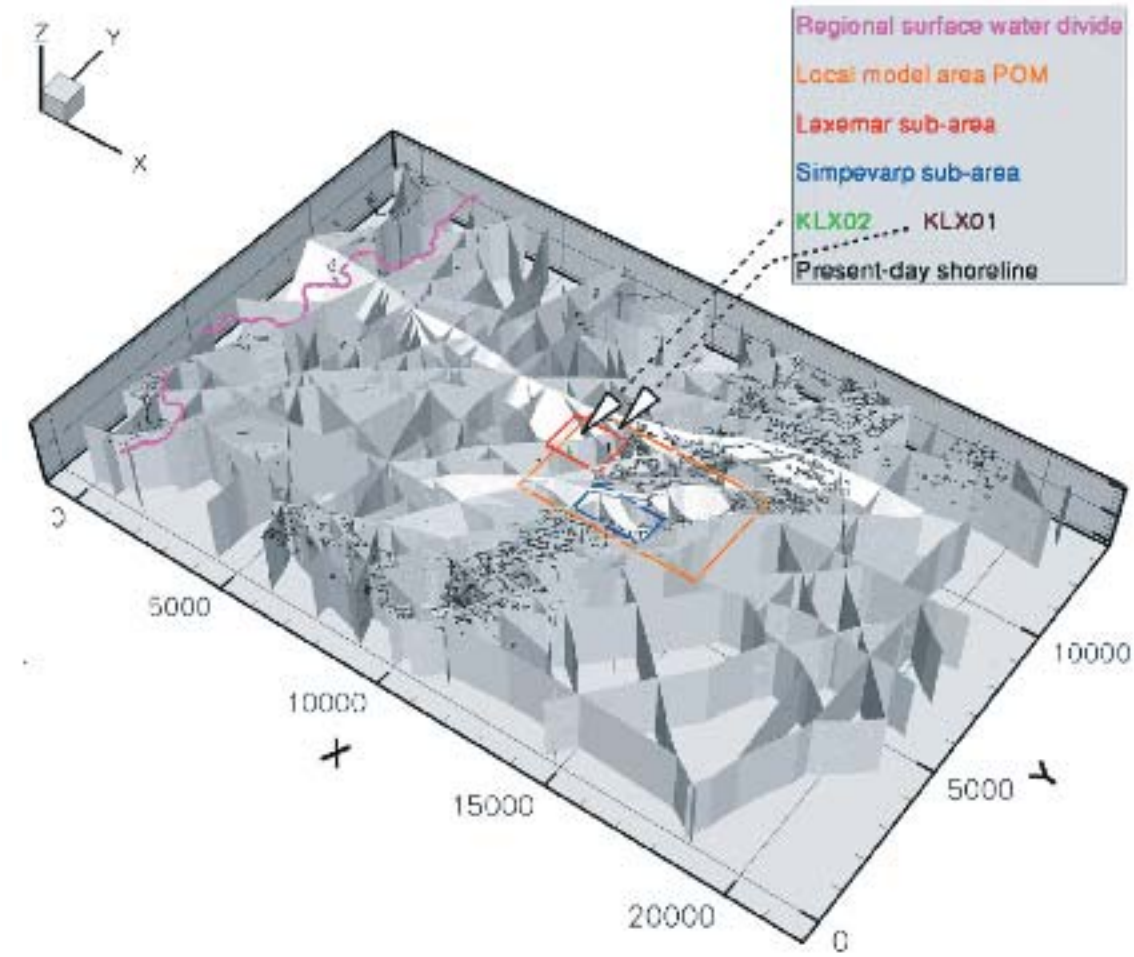

Figure 5-35. *Visualisation of the version 0 structural model employed for the Simpevarp 1.1 hydro-geological modelling. The interpreted deformation zones are combined from 171 zone segments. /Follin et al, 2004/. Simpevarp 1.1 local scale model area is shown for reference.*

5.4.6 Estimation of hydraulic properties in the bedrock – regional scale

As pointed out in the beginning of this section the present description is not integrated with the geological model version 1.1. To be able to assign properties to HCDs and HRDs, data from the construction of the Äspö HRL /Rhen et al,1997b/, some of the results from experiments at Äspö HRL /e.g. Andersson et al, 2002c; Winberg et al, 2000; Rhen and Forsmark, 2001/ have be used, as well as some results from the Forsmark site descriptive model version 1.1 /SKB, 2004/.

Assignment of hydraulic properties to the HCDs

Table 5-34 summarises the hydraulic properties of the HCDs included in the Simpevarp 1.1 descriptive hydrogeological model. The properties are based on results from the pre-construction investigation and the construction of the Äspö HRL. The geometric mean of the transmissivities of HCDs from Äspö HRL was used; $T=1.3 \cdot 10^{-5}$ m^2/s, with a standard deviation of Log_{10} (T) =1.55 /Rhen et al, 1997b/. No sensitivity analyses of the numerical groundwater flow modelling were carried out at this stage.

The hydraulic thickness (10 to 50 m) was based on the geological interpretation of zone thickness made for structural model version 0, see Table 5-34 .

There is rather limited information concerning storage coefficients of fracture zones in the Simpevarp area. In /Rhén et al, 1997b/ the storage coefficient of fracture zones was estimated based on large-scale interference tests, and in /Rhen and Forsmark, 2001/ the storage coefficient (S) was estimated for larger and smaller fracture zones, see Table 5-35. In /Rhen et al, 1997b/ it was commented that the S values seem to become unrealistically low for low T values (the number of results from interference tests considered reliable for the evaluation of S-T relationship was limited). Based mainly results from the Prototype Repository $S=2.5 \cdot 10^{-5}$ was chosen.

Likewise, the database for the kinematic porosity (n_e) is also very limited. The values given in Table 5-34 have no basis in data from Simpevarp on-going investigations. Rather they constitute a reasonable estimate based on data reported from tests conducted at Äspö HRL /Rhén et al, 1997b/.

Table 5-34. Summary of the properties assigned to the HCDs in the version 0 model.

Name of HCD RVS ID	Geological confidence High/Medium/Low	Hydraulic thickness (m)	Transmissivity (m^2/s)	Storage coefficient (–)	Kinematic porosity (–)
ZSM0003A0	Medium/Low	50	1.30E–05	2.0E–05	2.0E–05
ZSM0001B0	Medium/Low	10	1.30E–05	2.0E–05	1.0E–04
ZSM0004B0	Medium/Low	50	1.30E–05	2.0E–05	2.0E–05
ZSM0005A0	Medium/Low	40	1.30E–05	2.0E–05	2.5E–05
ZSM0007A0	Medium/Low	50	1.30E–05	2.0E–05	2.0E–05
ZSM0009A0	Medium/Low	50	1.30E–05	2.0E–05	2.0E–05
ZSM0012A0	Medium/Low	40	1.30E–05	2.0E–05	2.5E–05
ZSM0006A0	Medium/Low	10	1.30E–05	2.0E–05	1.0E–04
ZSM0004A0	Medium/Low	50	1.30E–05	2.0E–05	2.0E–05
ZSM0008A0	Medium/Low	20	1.30E–05	2.0E–05	5.0E–05
ZSM0010A0	Medium/Low	20	1.30E–05	2.0E–05	5.0E–05
ZSM0001A0	Medium/Low	10	1.30E–05	2.0E–05	1.0E–04
ZSM0011A0	Medium/Low	10	1.30E–05	2.0E–05	1.0E–04
ZSM*	Medium/Low	20	1.30E–05	2.0E–05	5.0E–05

Table 5-35. Estimation of storage coefficient (S) from transmissivity (T). $S=a \cdot T^b$.

Approx. test scale (m)	a	b	Reference
100	0.0092	0.79	/Rhén et al, 1997/
5–30	0.027	0.64	/Rhén and Forsmark, 2001/

Assignment of hydraulic properties to the HRDs

General modelling concepts

Groundwater flow through the HRDs is governed by the geometric and hydraulic properties of the fracture networks in the rock mass between the HCDs. The hydraulic properties of the rock are generally heterogeneous and sometimes anisotropic. Hence, a combined use of the geological geometrical description of fractures with hydraulic test results provides the best basis for the description of the hydraulic properties. One major objective for the hydrogeological description is to establish Discrete Feature Network model(s) (DFN) with associated hydraulic properties.

The rock in the groundwater flow model may be represented using a DFN or a Continuum Porous Medium (CPM) approach. Using a CPM, the assignment of properties may be based on a stochastic model, or a DFN may be incorporated to calculate the cell properties. The codes used for the groundwater flow calculations presented below used the DFN model with specified fracture hydraulic properties to calculate the cell properties in a CPM.

Figure 5-36 shows the representation of discrete features in the HRD. As indicated in Figure 5-36, the minimum size (length) of the HCDs (fracture zones) was set to 1,000 m. In this study**,** the stochastic fracturing of the HRD between the HDCs was modelled as a network of discrete features representing local minor deformation zones ranging between 100 m and 1,000 m in size, each of which consists of a large number of small fractures ranging between decimetres to metres in size (not modelled here). (A case with zones ranging between 50 and 1,000 m was also tested.)

The locations of the deterministic fracture zones and their connectivity to the stochastic network govern the heterogeneity and anisotropy of the computational grid. The spatial resolution of the computational grid was set to 100 m. The choice of scale affects the derivation of the grid cell properties. The hydraulic properties of the grid cells that were not intersected by deterministic/stochastic fracture zones were modelled as a isotropic homogeneous continuum.

The properties of the DFN of local minor deformation zones were modelled by means of statistical distributions for orientation, size, intensity, spatial model and transmissivity. The sizes were modelled as a truncated power-law distribution. Some of the above properties are described in a general sense below followed by tables showing the suggested model parameters for the DFN model, called “model cases for XX-parameter” in the tables. These “model cases for XX-parameter” are the basis for the sensitivity analyses performed in relation to the subsequent groundwater flow simulations.

The frequency distribution of fracture (or rather feature) size is based on a power law distribution formulated as follows:

$$f(L) = \frac{\left(k_L \ L_0^{k_L}\right)}{\left(L^{1+k_L}\right)} \quad L_0 \le L < \infty \qquad (5\text{-}1)$$

L_0 is the minimum feature size of L and k_L is the shape parameter of the distribution. The shape parameter k_L is dependent on the dimension that the features are described for, generally 2D (surface) or 3D (volume): $k_{L3D}=k_{L2D}+1$. The evaluated size distribution may differ from what is actually used in the modelling; the distribution used in the modelling may have a higher value of truncation than L_0, if the smaller features below the chosen level of truncation is considered not to contribute significantly to the properties on the model/discretisation chosen. The implication is that a given intensity P_{32} related to L_0 has to be transformed using a minimum size $L_{min} \neq L_0$. L was truncated in

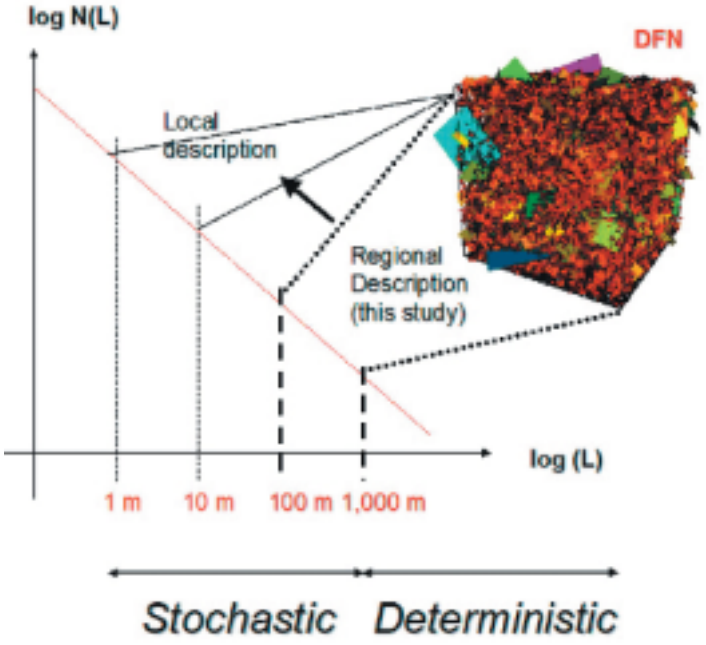

Figure 5-36. *Schematic conceptual model of the representation of deformation zones in the Simpevarp 1.1 hydrogeological modelling. The treatment of the bedrock in the numerical model depends on the scale and properties of the associated fracturing. The illustration indicates that a power-law size distribution is advocated /Follin et al, 2004/.*

the numerical simulations to match the window between the smallest fracture zone size, 1,000 m, and the resolution of the discretisation mesh, i.e. 100 m. For the truncation the following equation was used

$$P_{32}[L_{\min}, L_{\max}] = P_{32}[L \geq L_0]\left(L_{\max}^{[2-k_L]} - L_{\min}^{[2-k_L]}\right)/\left(-L_0^{2-k_L}\right) \qquad (5\text{-}2)$$

Different models for the transmissivity assignments are possible. In this modelling task it was assumed that the transmissivity was a function of (feature) length as below:

$T = a \cdot L^b$

This relation was proposed by /Dershowitz et al, 2003/. One argument for it is that, at least for deformation zones, the zone width increases with size, and thus generally the number of individual fractures per unit area of the fracture zone (with the fracture zone treated as a “plane”). If the transmisivity distribution for individual fractures is the same, the effective transmissivity for the fracture zone should increase with the size of the fracture zone. The values of a and b were estimated by means of numerical simulation using the method described in /SKB, 2004/. The formulation has major implications for the HRD properties and has to be further investigated.

Simpevarp S1.1

No geological DFN model for Simpevarp 1.1 was available at time of the groundwater flow modelling and it was decided to undertake a more or less generic study. Approximate values were estimated (partly by expert judgement) based on data evaluated from the cored boreholes KLX01 and KLX02 (in the Laxemar subarea) and the parameterisation of the DFN-model for Forsmark 1.1 /SKB, 2004/.

The area including the Äspö HRL is more conductive, possibly for structural reasons. KSH01A indicates a lower hydraulic conductivity compared with KLX02, but preliminary indications provided by data from new boreholes on the Simpevarp peninsula (data not available for version S1.1) appear to indicate a higher conductivity than KSH01A. Borehole KLX02 may possibly be representative for the regional area, as it seems to have rather similar hydraulic properties to the new boreholes on the Simpevarp peninsula.

In terms of conductive fracture frequency, there are similarities between the Forsmark borehole KFM01 and KLX02 that give some justification to chosing some of the interpreted hydraulic properties the same as those of the DFN model in Forsmark model version 1.1.

Thus, the DFN with hydraulic properties for hydrogelogical model S1.1 is partly based on data from the Laxemar area and partly on Forsmark version 1.1. It is pointed out that the evaluation in the test application of the methodology described by /Andersson et al, 2002b/ may not be fully consistent with evaluations made during the initial site investigations, but still give useful data for the modelling when other data are not available.

Fracture sets were evaluated in /Andersson et al, 2002b/ and shown in Table 5-36. Only data from KLX02 were used, as the data set from KLX01 was incomplete. The orientations of the fracture sets are assumed to be the same throughout the regional model domain. However, it is noted that the geological model in Section 5.1 indicates that orientations of fractures may be affected in the close proximity of interpreted deformation zones.

The measures of the one-dimensional, P_{10}, intensity of fractures along the borehole for KLX02, as reported by /Andersson et al, 2002b/ are compared with similar information for KFM01A in Table 5-37. KLX02 was used because P_{10} data for conductive fractures (P_{10c}) were not available for KLX01 but is plausibly the same, as the P_{32} for the open fractures ("natural") in KLX02 and KLX01 are about the same. It can further be noted that the measurement limit for T and the value of P_{10c} is about the same for boreholes KLX02 and KFM01.

As the minimum size of the deformation zones in Forsmark model version 1.1 was about the same as in Simpevarp model version 0, as was the fracture intensity in a few boreholes (Table 5-37) it was assumed that the derived model for Forsmark version 1.1 could be used as a first approximation. Assuming a similar length distribution and size interval of the stochastic features for the Simpevarp area as adopted in the Forsmark model 1.1 the P_{32c} for Simpevarp 1.1 should be approximately equal to that at Forsmark at depths from 10–400 m, applying a minimum modelled fracture size L_{min} =100, but can be increased somewhat due to a slightly higher P_{10c}:

Rock Layer 2: [(–10 masl) – (–400 masl)], Forsmark: P_{32c} =0.0311 m^2/m^3.

Rock Layer 1: [(–5 masl) – (–2,100) masl], Simpevarp: P_{32c} = 0.0371 m^2/m^3.

Table 5-36. Fracture sets based on data from KLX01 /Table 3-15, Andersson et al, 2002b/.

Fracture set	Mean pole trend	Mean plunge	Dispersion	Model
1	262	3.8	8.52	Fisher
2	195.9	13.7	9.26	Fisher
3	135.9	7.9	9.36	Fisher
4	35.4	71.4	7.02	Fisher

Table 5-37. Fracture intensity. Comparison between data from cored boreholes KLX01, KLX02 and KFM01A.

Borehole	P_{10} all open fractures (1/m)	P_{10c} all conductive fractures above meas. lim. for T (1/m)	Meas.limit fracture T (m^2/s)	Reference
KLX01	2.4	–	–	P_{10} : Table 3-4, /Andersson et al, 2002b/.
KLX02	2.3	0.135	3E–10	P_{10} : Table 3-4, /Andersson et al, 2002b/. P_{10c} : Table 3-24, /Andersson et al, 2002b/.
KFM01A	2.07	0.113	1.5E–10	P_{10} : Forsmark Site descr. ver 1.1 /SKB 2004/, depth 100–400 m. P_{10c} : Forsmark Site descr. ver 1.1 /SKB 2004/, depth 100–400 m.

Three cases for intensity were used in the modelling, as shown in Table 5-38. Cases 1 and 2 were initially suggested, but the DarcyTools team found that both these cases appeared to be too conductive and therefore defined and analysed the indicated case 3.

Fracture sizes and the spatial model derived for the Forsmark version 1.1 description were assumed to be valid on the basis of the above discussion. The model, presented in Table 5-39, is described by a power-law function with lengths (L) between 100 and 1,000 m (corresponding to equivalent radii of R=56 to 564 m): L_{min}=100 m and exponent k_{L3D} (3D representation) =2.6. The stochastic fracturing is constrained to representation of features between 100 and 1,000 m of size. The lower size limit was mainly determined by computational constraints, whereas the upper size limit coincides with aforementioned threshold used in identification of deformation zone segments.

The fracture centres were assumed be Poisson distributed in space. The transmisivity distribution was also based on Forsmark version 1.1, see Table 5-40. A relationship between transmissivity and size of the hydraulic features was used. This was parameterised as shown in Table 5-40.

Table 5-41 aggregates effective values of the hydraulic properties assigned to the HRDs, i.e. the flowing features between the HCDs. Table 5-42 shows the proposed hydraulic properties to be assigned to the rock mass (including naturally occurring conductive fractures) in-between the HCDs and the structures defined by the DFN (i.e. sub-grid material properties). The large differences in kinematic porosity used by the modelling teams are due to the concepts in the codes. ConnectFlow could, for the S1.1 analysis only handle single porosity and had to use a rather high value to match the data. In DarcyTools the multi-rate model can take into account water in the matrix and stagnant pools from which saline water may diffuse to the advective flow paths, thus keeping kinematic porosity lower than ConnectFlow.

Figure 5-37 shows an example of a realisation showing how the spatial distribution of the fracturing described by the DFN in the Regional Model Domain may look using the statistics presented in this section (HCDs included).

Table 5-38. Conductive fracture intensity (P_{32c}) with L_{min}=100 m for Simpevarp 1.1.

Parameter case for P_{32c}	P_{32c} (m^2/m^3)	Comment
1	0.0371	Only tested by Connectflow team
2	0.1855	Case 1 increased by a factor of 5 times
3	0.00742	Case added by DarcyTools team

Table 5-39. Size distribution of features in the DFN model. Power law model.

Parameter case for size distribution	L_{min} (m)	k_{L3D}	Spatial model	Comment
1	100	2.6	Poisson	Same as Forsmark ver 1.1, Used by DarcyTools
2	100	3.6	Poisson	Used by ConnectFlow
3	50	3.6	Poisson	Used by ConnectFlow

Table 5-40. Transmissivity assignment of DFN model. $T=a \cdot L^b$ (L: (m), T: (m^2/s)).

Model case for T assignment	a	b	Comment
1	2.47E–12	1.791	Same as Forsmark ver 1.1. Used by DarcyTools and ConnectFlow
2	24.7E–12	1.791	Useed by ConnectFlow
3	0.247E–12	1.791	Used by DarcyTools

Table 5-41. Summary of the hydraulic property assignment to the rock mass between HCDs.

Feature size interval M	Geological characterisation Determ./Stoch.	Hydraulic thickness (m)	Specific storativity (m^{-1})	Kinematic porosity (–)
100–200	Stochastic	2	1E–5	1E–5
200–500	Stochastic	1	5E–6	5E–6
500–1,000	Stochastic	0.5	2E–6	2E–6

Table 5-42. Hydraulic properties of the rock mass between HCDs and structures defined by the DFN.

Postion	Hydraulic conductivity (m/s)	Specific storativity (m^{-1})	Kinematic porosity (–)	Comment
Surface –3 m to bottom of model	1E–9	–	1E–3	Used by ConnectFlow team
Surface to –3 m from surface	1E–9	–	1E–3	Used by DarcyTools team (No quarternary deposits was included in the model)
3 m below surface to bottom of model	1E–12		1E–5	Used by DarcyTools team

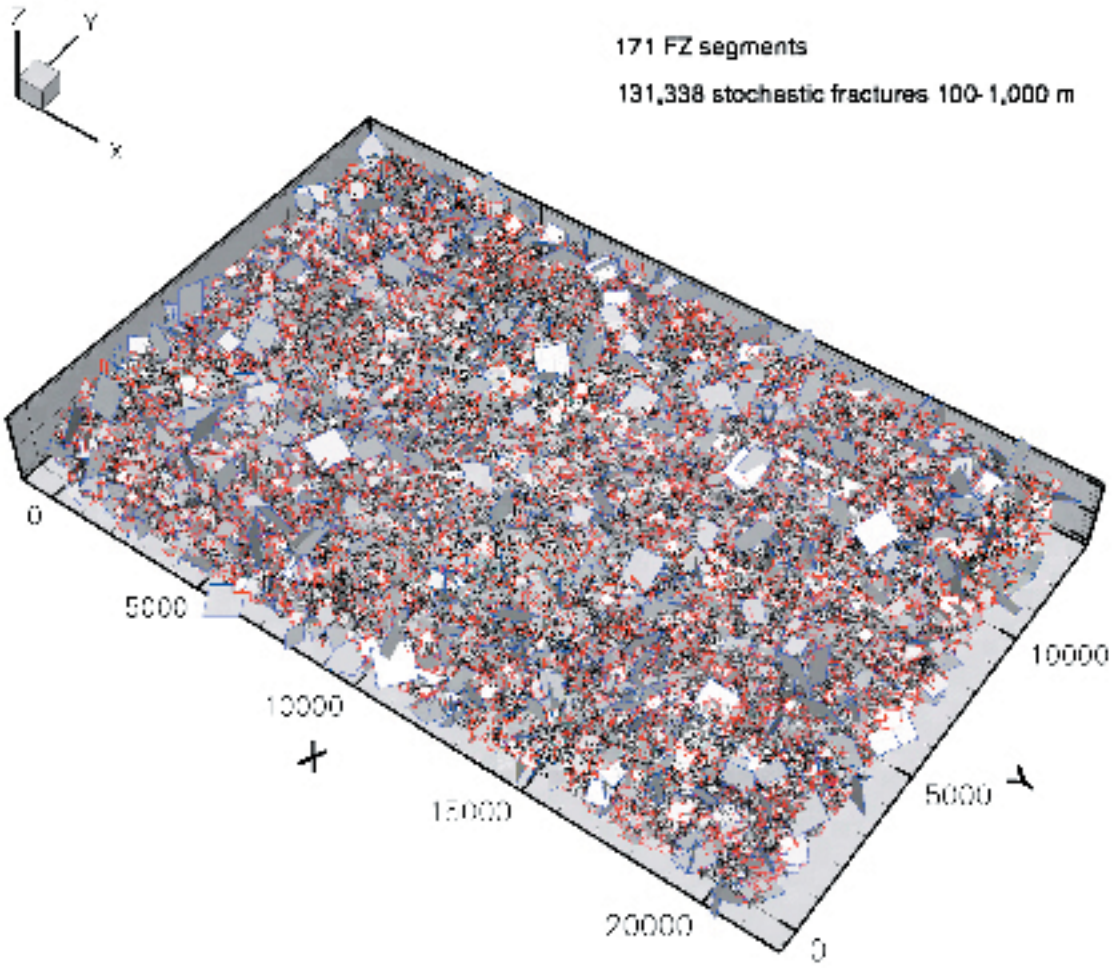

Figure 5-37. *Example simulation showing a realisation of a DFN stochastic fracture network with P_{32c}=0.00742 and HCDs /Follin et al, 2004/.*

5.4.7 Estimation of hydraulic properties in the bedrock – local scale

No estimation was made for the local scale model volume as no groundwater flow model was developed at this scale for Simpevarp 1.1.

5.4.8 Boundary and initial conditions for paleohydrological simulations

The information contained in Figure 3-14 and Figure 5-38 below constitutes the basis for a discussion of initial and boundary conditions used for testing the Simpevarp 1.1 site descriptive model in the context of analysing the paleohydrogeological development and distribution of saline waters in the area. Figure 3-14 shows the development of the salinity in the Baltic Sea during Holocene and Figure 5-38 shows the associated shoreline displacement process at Simpevarp during the same period. The map in Figure 3-13 shows a snapshot of the shoreline at Simpevarp at 12,000 years before present (BP).

The conditions experienced at 12,000 BP, Figure 3-13, were considered a suitable starting point for paleaohydrogeological modelling of the Simpevarp. At that time the surface water conditions in the Baltic region were governed by the Baltic Ice Lake characterised by freshwater. The groundwater composition at depth at this time, on the other hand, is more or less unknown. The working hypothesis used for Simpevarp 1.1 assumed an initial condition with fresh groundwater resting on top of a more saline groundwater body. The depth to, and origin of, the saline groundwater are probably variable and complex, but, given the information available from Olkiluoto and Laxemar, it is possible to advocate that a major source for the salinity is old groundwater of brine type.

There are a few data included in the data freeze for Simpevarp 1.1 that reveal the current chemical situation, but the few data are from the uppermost part of the bedrock in borehole KSH01A, see Figure 4-72. These data indicate chloride contents at depth similar to those found at similar depths at Äspö and higher than those at corresponding depths in the Laxemar area. The deep data from Olkiluoto and Laxemar, shown in Figure 5-39, suggest that the current groundwater salinities at those two sites are moderate (less than 1 mg/L) down to several hundreds of metres below sea level. The salinities then rapidly increase and reach a value of c. ten percent by weight at a depth of about two kilometres. However, the data shown for KLX02 in Figure 5-39 down to a depth of about 950 m should be considered as uncertain, as circulation in the borehole probably affected the samples on which the data in the plot are based.

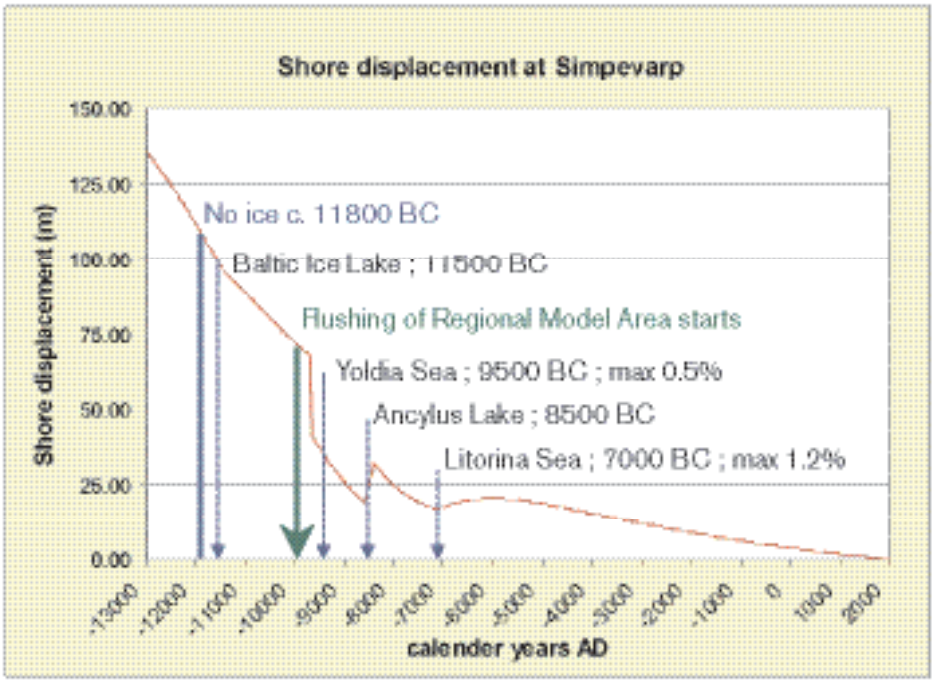

Figure 5-38. *The shoreline displacement process in the Simpevarp area during Holocene. Modified after /Påsse, 1996/.*

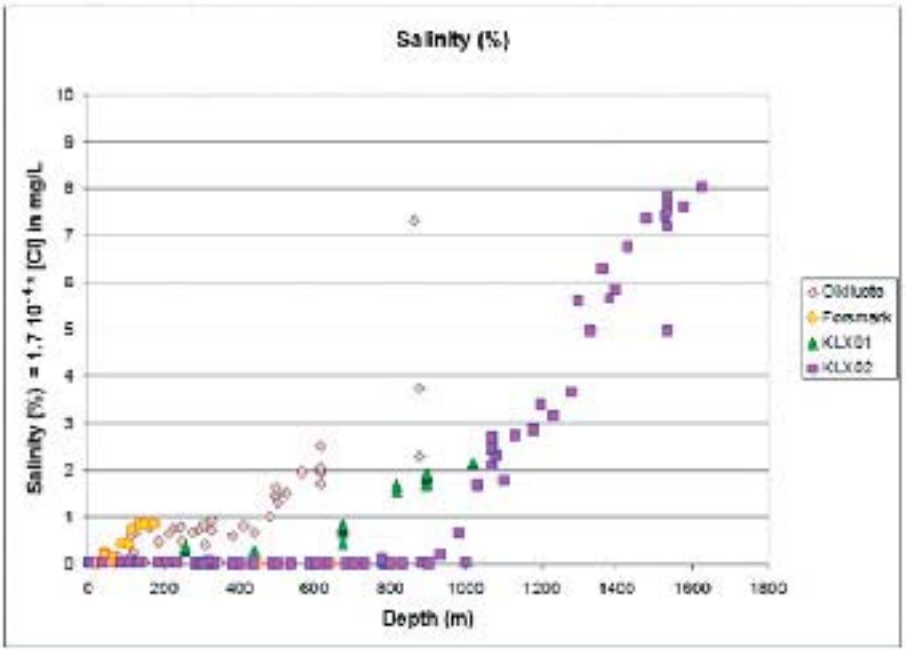

Figure 5-39. *Plot showing the salinity content in borehole groundwater versus depth. The plot shows data from Forsmark, Olkiluoto and Laxemar (two boreholes) /Follin et al, 2004/.*

A comparison between the Olkiluoto and Laxemar salinity profiles shown in Figure 5-39 is of greatest applicability to Forsmark. Like Forsmark, Olkiluoto was covered by seawater until quite recently, c. 900 AD, whereas the flushing of Laxemar started about 3,500 BC.

The working hypothesis used in the hydrogeological modelling for the model version Simpevarp 1.1, assumed a value of ten percent by weight for the salinity at the end of the last glacial period, i.e. 10,000 BC, and that this value still prevails at a depth of around 2,000 m. The main arguments for this boundary condition are, among other things, the flat topography and that the fact that water with a salinity of 10 mg/L has a high density and is not easily displaced by hydraulic gradients imposed at the surface.

Concerning the initial state groundwater composition as a function of depth at 10,000 BC, the working hypothesis used for model Simpevarp 1.1 is a freshwater system down to either –500 masl (alterantive1), –1,000 m (alternative 2) or –100 m (alterantive 3). Below this level, the salinity was assumed to increase linearly up to ten percent by weight at –2,100 masl, see Figure 5-40.

Water types, based on the M3 modelling concepts were provided by hydrogeochemistry discipline from boreholes KLX01 and KLX02, c.f. Figure 5-41, and used by the DarcyTools team. The salinity distribution described above, was used by both modelling teams to compare with the simulations.

The hydrological conditions on the top surface of the Regional Model Domain were simplified by assuming spatially and temporally varying Dirichlet conditions for both pressure and salinity at all times between 10,000 BC and 2,000 AD. From a hydrogeological point of view it may be advocated that the subsequent rise of the ground surface associated with the shoreline displacement should be associated with a Neumann condition, i.e. infiltration, instead of a specified pressure (fixing a fresh groundwater table at the topographic relief) and concentration, However, given the simplified representation of the Quaternary deposits, cf. Section 5.4.3, a Dirichlet condition was considered sufficient for model version Simpevarp 1.1. As the information about the Quaternary deposits improves, based on more data points and/or a better spatial analysis (interpolation) of existing data, a Neumann condition for flow is likely to be adopted as a part of the development and refinement of the top layer description in forthcoming numerical simulation models.

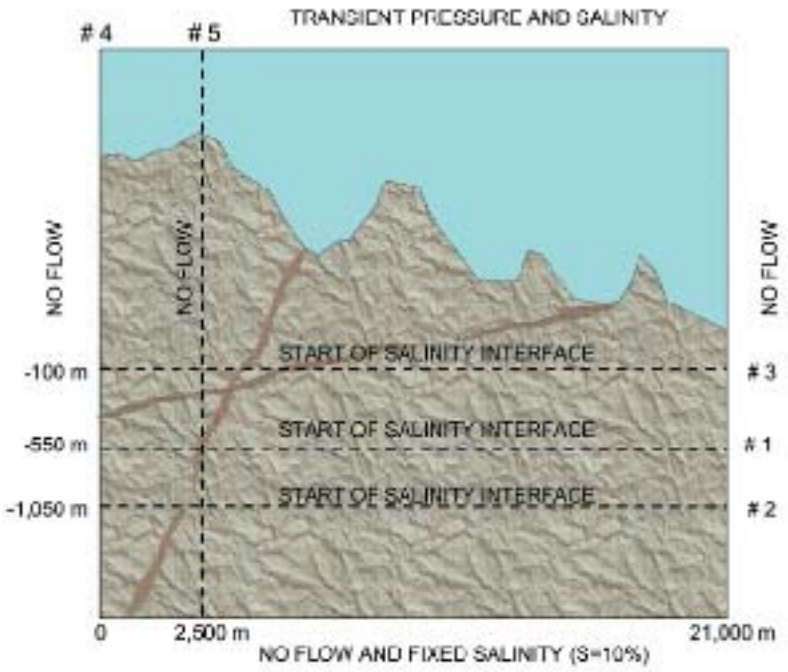

Figure 5-40. *Schematic illustration of the initial and boundary conditions used. (Start of the saline interface at –100 m and a moving western boundary to a more eastern position was only represented by the DarcyTools Team.) /Follin et al, 2004/.*

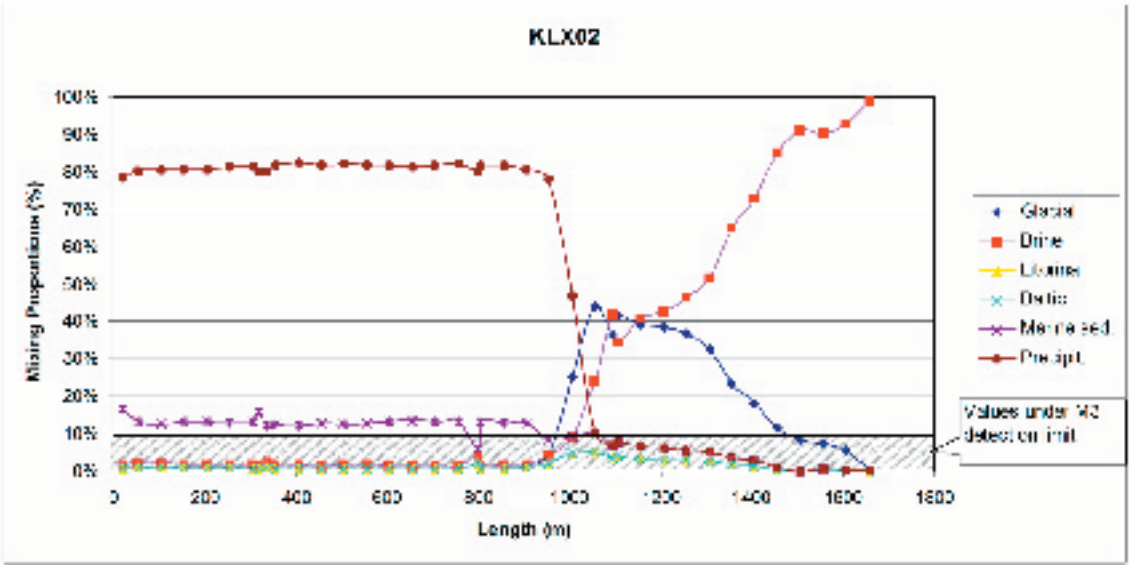

Figure 5-41. *Water types in KLX02 interpreted using the M3 method, c.f. Section 5.5. Observe that no Yoldia, Littorina or Baltic water types were found. Vertical lines indicate values used in the comparison with the numerical model simulations. /Follin et al, 2004/.*

The hydrogeological boundary conditions on the lateral (vertical) sides and the bottom surface of the Regional Model Domain are more or less uncertain. Since none of the lateral sides coincides with a major surface water divide, they must be considered artificial boundaries rather than physical. The regional topographic gradient is quite consistent and parallel to the longest axis of the rectangular model domain. This condition allows for a common simplification often used in numerical modelling, i.e. the parallel groundwater flow outside the along-gradient lateral sides is assumed not to interact with the flow inside the model domain, hence no-flow boundaries are assigned.

Concerning the “artificial” upstream boundary a different situation prevails. Between the artificial upstream boundary of the regional model and the western border of the Simpevarp subarea there exists a major surface-water divide, see Figure 5-35 and Figure 5-42.

Although, a small part of the water divide extends west of the regional model area, the working hypothesis used for Simepvarp 1.1 is that the major surface water divide to the west may be treated as a no-flow boundary. While this hypothesis remains to be tested, it is advocated here that a no-flow upstream boundary is a reasonable assumption for model version Simevarp 1.1. The assumption of a no-flow boundary is regarded as being less problematic as it is located far from the Simpevarp and Laxemar subareas. It is also reasonable to assume no-flow boundary conditions along the water divides south and north of the regional model area. These no-flow boundary conditions may also be justified on the basis that the north and south boudaries of the regional model area approximately follow stream lines because the topographic relief fairly uniformly declines from west to east.

Finally, as a consequence of the high salinity at depth, the bottom surface of the model domain at –2,100 masl was considered to be a no-flow boundary. It is also located sufficiently far away from the part of the model domain of interest that the positioning of assumed boundary conditions is of limited importance.

Two studies have been carried out that support the choice of adopted hydraulic boundary conditions /Follin and Svensson, 2003; Holmén et al, 2003/. The major conclusion from these two studies was the potentially strong impact of local topographic gradients, which easily dominate the potential impact of the regional topographic gradient.

The position of the model boundaries was treated somewhat differently by the modelling teams. This is further described in Section 5.4.12.

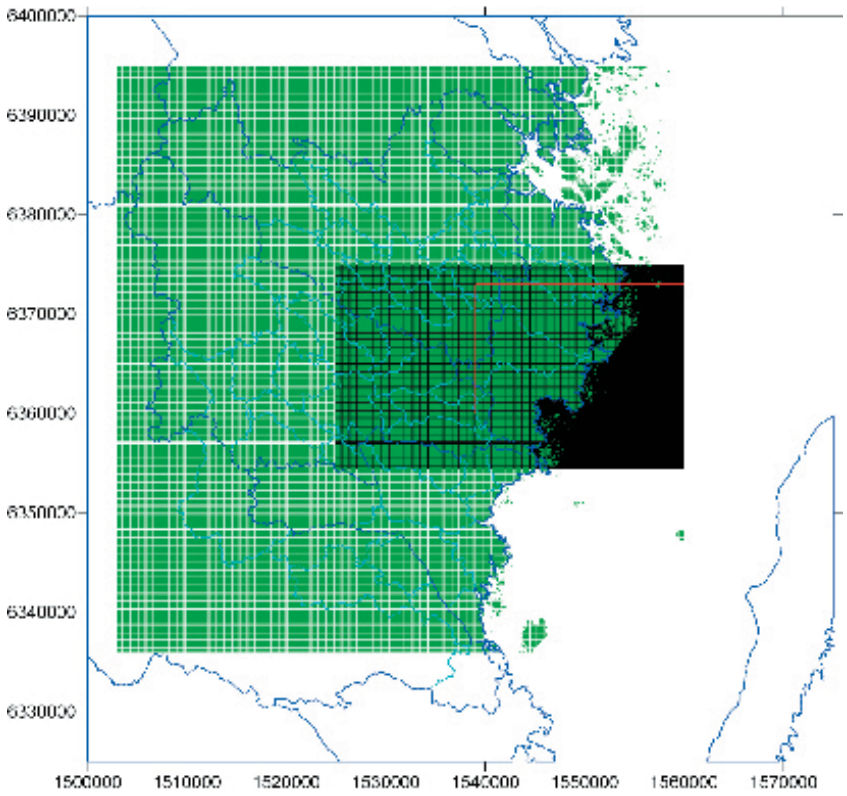

Figure 5-42. *Overview of regional water divides (dark blue) and the regional model area (red outline) (shown in the figure is also the area with available topographic data (shaded)). /Follin et al, 2004/.*

5.4.9 Simulation/calibration against hydraulic tests

No calibration against hydraulic tests was made for S1.1.

5.4.10 Overview of groundwater simulation cases

In this section and following sections, examples of simulation results are presented from DarcyTools Team (DT) and the Connectflow Team (CF), as reported by /Follin et al, 2004/ and /Hartley et al, 2004/, respectively. In Table 5-43 and Table 5-44 the model cases explored in these reports are summarised. The model cases discussed in the ensuing text refer to the cases presented in these tables.

Table 5-43. Model cases explored using ConnectFlow (CF) employing transient flow and saline transport calculations. Other properties used correspond to the defined base case of the modelling. /Hartley et al, 2004/. K: Geometric mean hydraulic conductivity of up-scaled DFN model (see Section 5.4.12). DFN model V1-V3 dicussed in Section 5.4.12.

CF model case	Initial condition. SALINITY of water in model	Kinematic Porosity for HRD	K[m/s]	DFN	Comment
1, pom11_1v2	1 (zero salinity at depth 500 m)	Low porosity, ($1.0 \cdot 10^{-3}$)	$8 \cdot 10^{-6}$	V1	~320,000 fractures
2, pom11_1v3	1	High porosity, ($5.0 \cdot 10^{-3}$)	$1.5 \cdot 10^{-6}$	V1	
3, pom11_1v4	1	Intermediate porosity, ($2.0 \cdot 10^{-3}$)	$4 \cdot 10^{-6}$	V1	
4, pom11_1v5	1	Intermediate porosity, ($2.0 \cdot 10^{-3}$)	$1.2 \cdot 10^{-4}$	V2	5 times higher P_{32} compared to V1, ~1,600,000 fractures time step dt=20 years
5, pom11_1v6	1	Intermediate porosity, ($2.0 \cdot 10^{-3}$)	$5 \cdot 10^{-6}$	V3	Lower truncation of Lmin (50 m), ~4,400,000 fractures
6, pom11_1v7	2 (zero salinity at depth 1,000 m)	Intermediate porosity, ($2.0 \cdot 10^{-3}$)	$4 \cdot 10^{-6}$	V1	
7, pom11_1v5vt1	1	Intermediate porosity, ($2.0 \cdot 10^{-3}$)	$1.2 \cdot 10^{-4}$	V2	Same as pom11_1v5, but dt (time step)=10 years
8, pom11_1v5vt2	1	Intermediate porosity, ($2.0 \cdot 10^{-3}$)	$1.2 \cdot 10^{-4}$	V2	Same as pom11_1v5, but dtime step t=5 years

Table 5-44. Model cases explored by the DarcyTools (DT) team. Overview of studied model cases ("variants" in /Follin et al, 2004/) and their parameter settings. Model case 1 met the Base Case specification in the original TD 1.5 for initiating the modelling. The results of model case 1–4 led to model case 5, which constituted the Base Case (5) for the remaining model cases 6–14. Note that cells left blank indicate properties identical to the cell to the left with a given data entry. Transport calculations were not performed for all cases. (T: Transmissivity, t: Hydraulic thickness, S: Storage coefficient, θ: Kinematic porosity, D_e: Effective diffusion coefficient, L: Side length of hydraulic feature modelled as a square, β_t: Capacity ratio for immobile volume and mobile volumes (See /Follin et al, 2004/ for details).

DT model case / Parameter	1	2	3	4	5	6	7	8	9	10	11	12	13	14
Pos. of the salinity interface (masl)	–550				–550	–1,050	100							
Surface water divide model boundary	No				No			Yes						
HCD,Determ. deform. zone T (m^2/s)	1.3E–5				1.3E–5									1.3E–6
HCD, Determ. deform. zone t (m)	20				20									
HCD, Determ. deform. zone S (-)	0				0									
HCD, Determ. deform. zone θ_f (-)	5E–3	1E–3		1E–3	5E–3				1E–3					
HCD, Determ. deform. zone D_e (m^2/s)	5E–12	1E–12		1E–12	5E–12				1E–12					
Random number seed (-)	1,234				1,234							5,678		
Stoch. deform. zone CCDF slope (-)	–2.6				–2.6									
Stoch. deform. zone minimum L (m)	100				100									
Stoch. deform. zone maximum L (m)	1,000				1,000									
Stoch. deform. zone P_{32c} (-)	3.71E–2		7.42E–3	7.42E–3	7.42E–3									
Stoch. deform. zone a (m^2/s) ; $T = a L^b$	2.47E–12				2.47E–12								2.47E–11	2.47E–11
Stoch. deform. zone b (-) ; $T = a L^b$	1.791				1.791									
Stoch. deform. zone t (m)	0.01 L				0.01 L									
Stoch. deform. zone S (-)	0				0									

Table 5-44. Cont.

Parameter \ DT model case	1	2	3	4	5	6	7	8	9	10	11	12	13	14
Stoch. deform. zone θ_f (-)	5E–3	1E–3		1E–3	5E–3				1E–3					
Stoch deform. zone D_e (m^2/s)	5E–12	1E–12		1E–12	5E–12				1E–12					
Background rock K (m/s)	1E–12				1E–12									
Background rock S_s (m^{-1})	0				0									
Background rock θ_p (-)	5E–5				5E–5									
Background rock D_e (m^2/s)	5E–15				5E–15									
Background rock β_t (-)	10				10					20	50			
Spec. flow wetted surface (m^2/m^2)	2				2									
Superficial rock K (m/s)	1E–9				> 1E–9									
Superficial rock S_s (m^{-1})	0				0									
Superficial rock t (m)	13				13									
Superficial rock θ_p (-)	1E–3				1E–3									
Superficial rock D_e (m^2/s)	1E–12				1E–12									

5.4.11 Simulation of block properties

/Hartley et al, 2004/ explored how different assumptions regarding the DFN model affected the up-scaled hydraulic conductivity in a 1 km^3 cube using 9·9·9 cubes with 100 m sides, see Figure 5-43. Somewhat different values for the fracture size distribution than proposed in the preceding section were employed: power-law function with length's (L) between 100 and 1,000 m or 50 and 1,000 m and an exponent k_{L3D} (3D representation) of 3.6 (instead of 2.6).

These results can be presented as a statistical distribution assigning each sub-block a data value. For 9·9·9 100 m blocks we have 729 data values. Figure 5-44 shows the distribution of the geometric mean permeability (the mean of the principal components of the permeability tensor) for the three DFN versions. The geometric mean is used as a simple scalar for comparison.

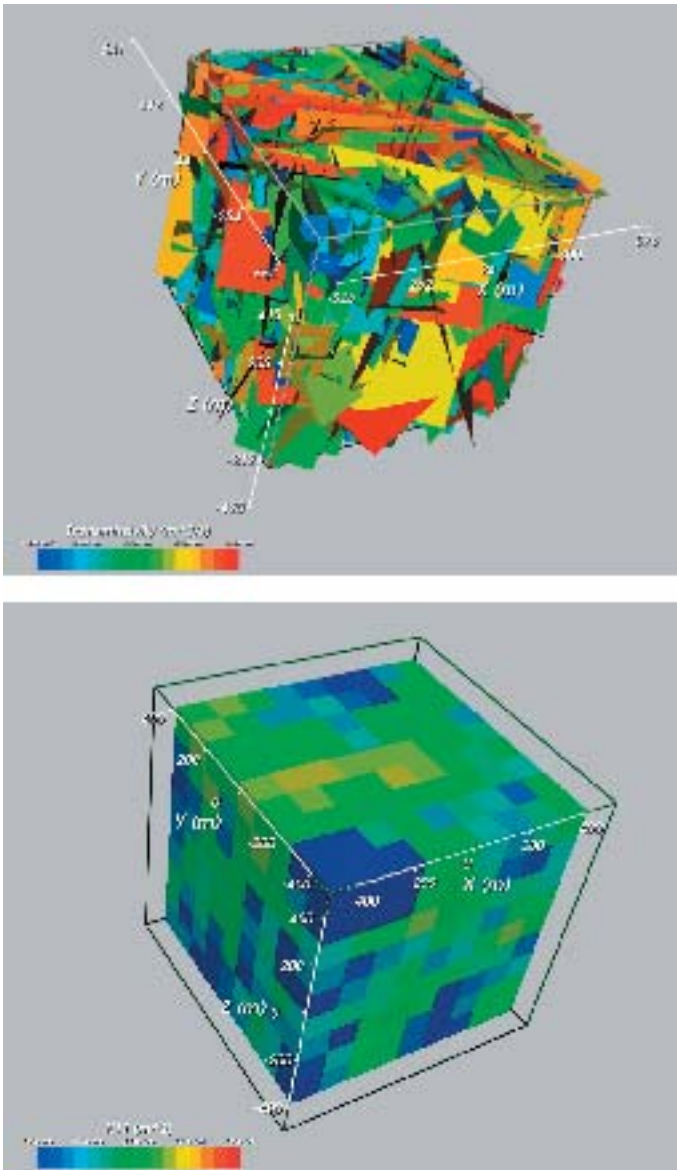

Figure 5-43. *Top: Log T for sets of fractures in the DFN-model (Parameter case 1 in Table 5-38 and Table 5-40 and summary of model cases in Table 5-43) in a generic 1 km block. Fractures are coloured by Log (T). Se also summary of modelling cases in Table 5-43. Bottom: Upscaled equivalent permeability (Log (k) (m^2) on 9·9·9 element cubes with 100 m sides, grid based on the same case as in the top figure. /Hartley et al, 2004/.*

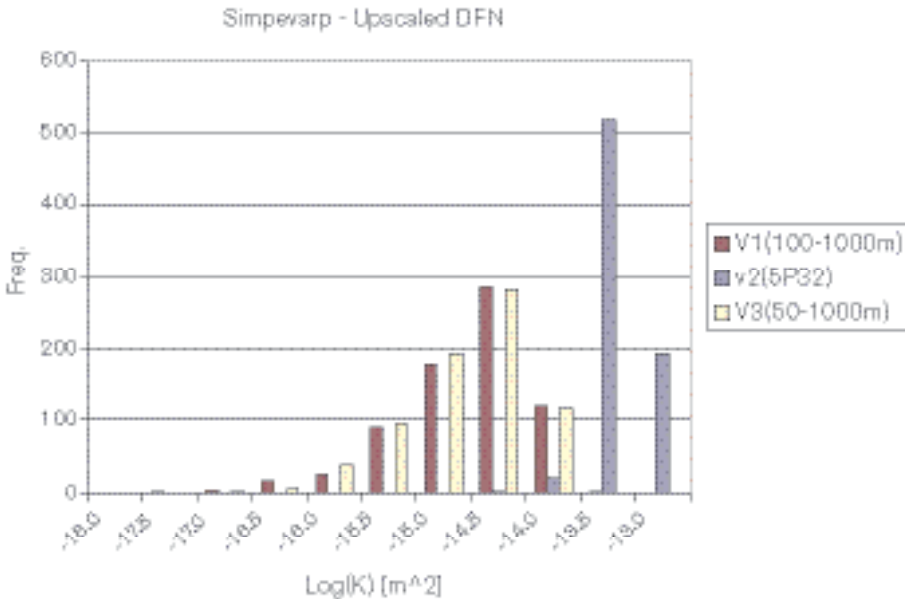

Figure 5-44. *Histogram of permeability k_g (m^2) in 100 m cells for the upscaled DFN-models. V1 corresponds to intensity parameter case 1 Table 5-38, V2 corresponds to intensity parameter case 2 in Table 5-38, both V1 and V2 with size distribution parameter as in case 2 in Table 5-39. V3 corresponds to parameter case 1 in Table 5-38 with size distribution according to parameter case 3 in Table 5-39, respectively. See also summary of modelling cases in Table 5-43. Total number of observations =729. /Hartley et al, 2004/.*

V3 displays a very similar distribution to V1, but there few values below $k=1.0 \cdot 10^{-16}\ m^2$ ($K=1.0 \cdot 10^{-9}$ m/s) due to the extra connectivity provided by the smaller 50–100 m fractures added in this case compared with the truncation at 100 m applied in the other two cases. This suggests that it is valid to truncate the DFN model at a threshold of about 100 m for the purposes of modeling bulk flow on the regional scale for 100 m elements. However, in practice no elements should have a hydraulic conductivity less than about $1.0 \cdot 10^{-9}$ m/s, because the smaller-scale fractures omitted from the regional DFN model give a background permeability of this magnitude.

The variability in the distribution for V1 suggests that a 100 m block is a sub-Representative Elementary Volume (REV) and that the network is not uniformly well-connected. In contrast, V2 represents a k-distribution with less variance and higher mean, suggesting a well-connected network and that 100 m is close to an REV.

5.4.12 Examples of simulation of evolutionary development

The main objective of the preliminary simulations was to study the past hydrogeological (paleohydrogeological) evolution, using different material properties and different initial conditions at 10,000 BC.

Boundary conditions

The DarcyTools Team modelled all but one case with boundaries corresponding to those defined for the regional model. To test the sensitivity to the western boundary position, this boundary was moved eastward for one case.

The ConnectFlow team made use of the water divides to the west and north and the defined regional model boundary to the south and east, see Figure 5-45.

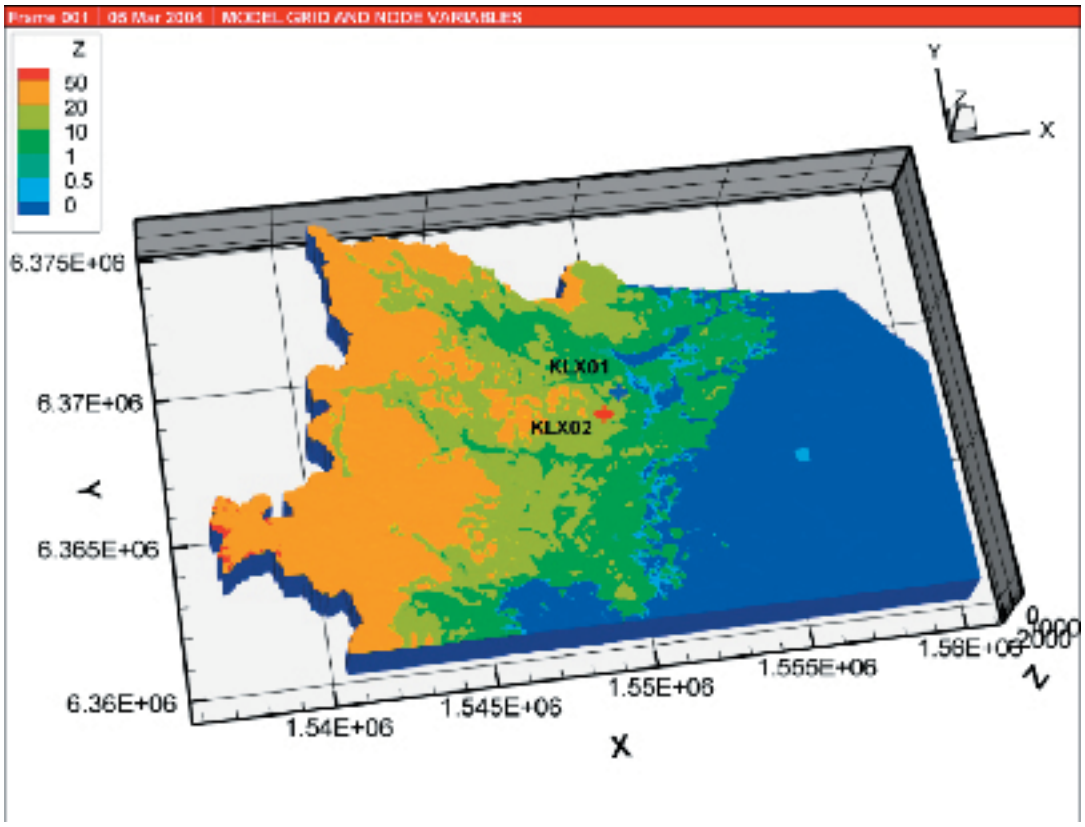

Figure 5-45. *Model boundary used by the ConnectFlow Team. The figure shows the present day elevation data superimposed on the model and the location of the boreholes KLX01 (blue marker) and KLX02 (red marker). /Hartley et al, 2004/.*

Results ConnectFlow

The two initial conditions, three cases of DFN models and several cases with different values of the total porosity (n)* were used to see how well the model was able to reproduce the salinity profiles at boreholes KLX01 and KLX02. The total porosity (n) was varied from 1E–3 to 5E–3 for the HRD and for the HCD from 1E–3 to 1E–2, respectively. One example of the results is shown in Figure 5-46. The other modelled cases show similar developments as a function of time. The final salinity distribution along the boreholes KLX01 and KLX02 is compared in Figure 5-47.

The results suggest that Littorina water should have infiltrated. Comparing results for 2,000 AD the present day situation at KLX01 appears insensitive to the cases modelled, they all cluster around initial condition case 1 and are rather close to the three measured points. The situation at KLX02 is more interesting as there are more measured data to compare with. However, the temporal discretisation was tested on case 4 and found to give a different salinity profile, see case 7, 1v7 in Figure 5-47. Although most cases were made with a time-step of 20 years, test cases 7 and 8 used time-steps of 10 and 5 years respectively. Cases 7 and 8 give similar results. This result is of course important for the further simulations that will be performed, but it means that no major conclusions should be made based on the present results.

* The code version used implements a single porosity model and it was not possible to retain the salt in the model with the suggested kinematic porosities. Therefore the porosities used for the calculation of the salinity field were denoted “total porosity” to be distinguished from “kinematic porosity” used for the transport calculations.

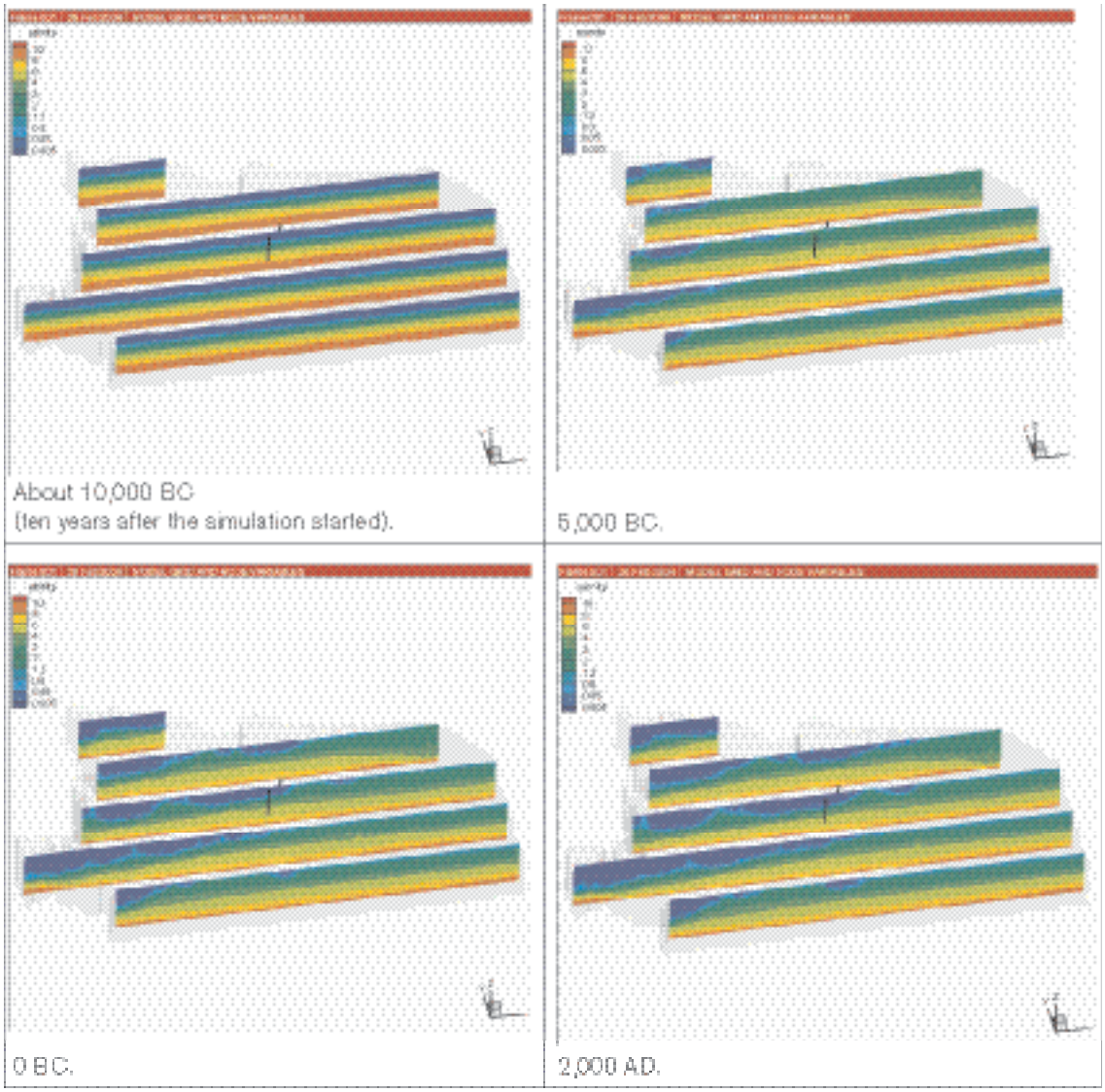

Figure 5-46. *Salinity distribution in vertical slices in E-W direction for Parameter case 1: version 1 DFN model (Parameter case 1 in Table 5-38 and Table 5-40), initial conditions 1 (Freshwater down to 500 m depth) and n=1E–3. See also summary of modelling cases in Table 5-43. The positions of KLX01 (rear) and KLX02 (front) are shown for reference. /Hartley et al, 2004/.*

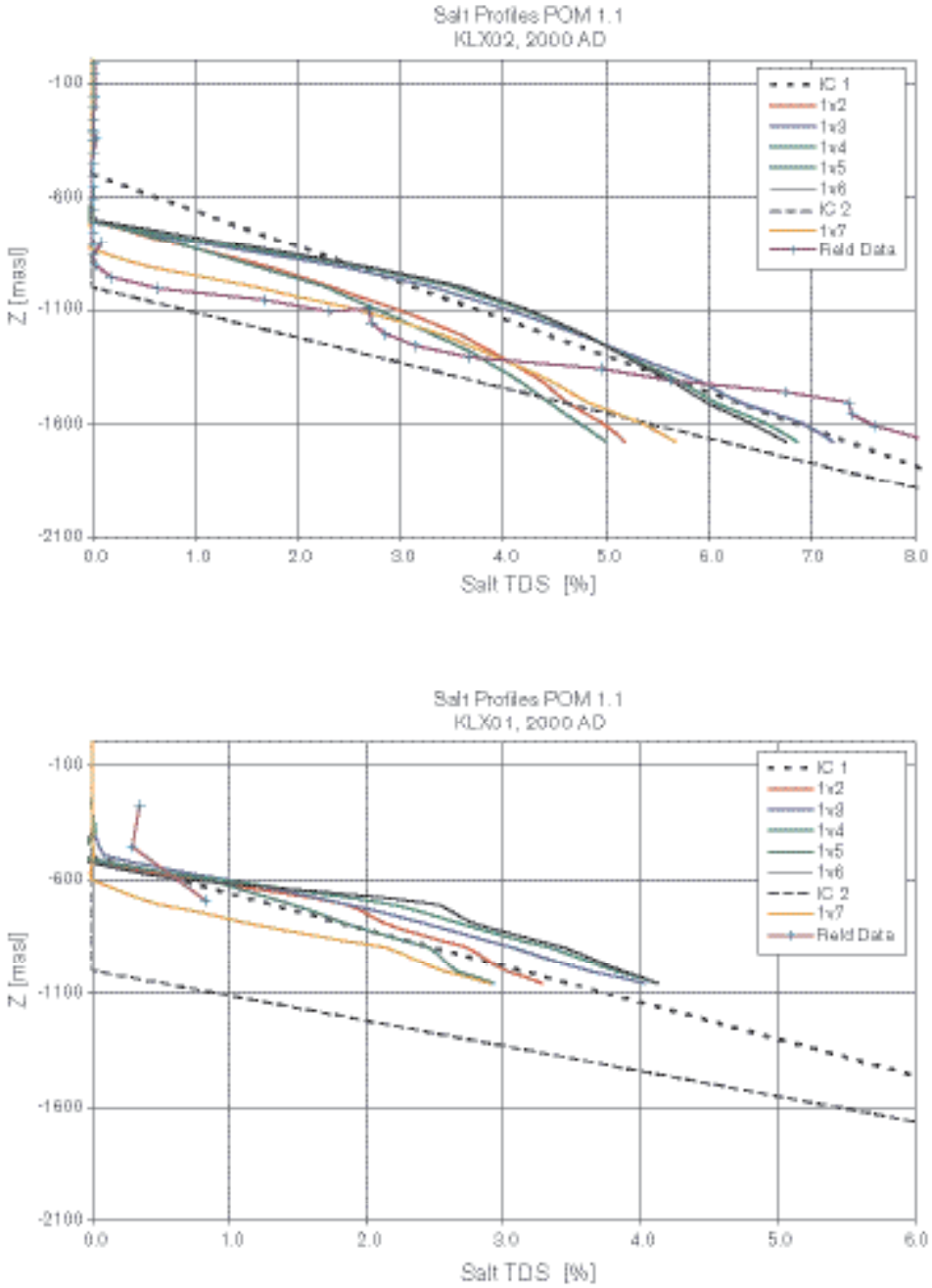

Figure 5-47. *Salinity profiles at 2,000 AD for different cases for the borehole KLX01 (bottom) and KLX02 (top). Field data and results for both initial conditions are included. /Hartley et al, 2004/.*

Results DarcyTools

The modelling was based on two DFN models according to modelling cases 5 and 7 in Table 5-44. A large number of simulations with different initial conditions, different hydraulic properties and one test of a different boundary condition in the western part of the model were performed and compared with the measured sanity distributions in KLX01 and KLX02, as well as the interpreted water types in KLX02. It was concluded that:

- The hydraulic connection of the HCDs to the upper part of the bedrock and Quaternary deposits has a great influence on the infiltration rates of waters from the Yoldia and Littorina seas. A well-connected system with HCDs reaching the Quaternary deposits was considered most realistic. However, it is not known if the HCDs generally are well-connected to more permeable layers of overburden or if there exist areas with low-conductive (clayey soils) covering outcropping HCDs, e.g, in the large valleys or below the sea.

- It was only possible (in both KLX01 and KLX02) to match both salinity and water types using the low fracture intensity case 3 and with an initial condition where salinity start to increase at a depth of 550 m. The match between simulated and measured/interpreted data was surprisingly good, see Figure 5-48 through Figure 5-50. Different realisations of the DFN did not have a significant effect on the salinity distribution and water types. The topography controls much of the spatial distribution of salinity and water types at depth.
- An order of magnitude decrease of the average transmissivty assigned to the DFN has a significant effect on the distribution of water types but minor effects on the salinity distribution.
- The simulations indicate Littorina water can possibly be found near the coast and offshore below the Baltic.

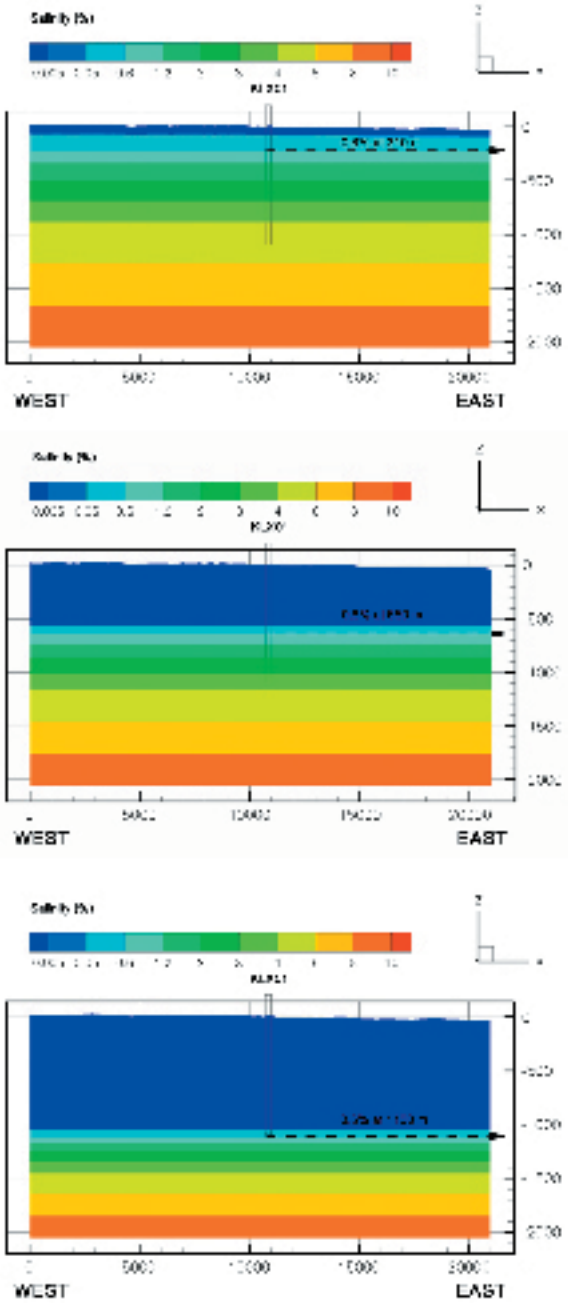

Figure 5-48. *Initial salinity conditions for modelling cases 7 (top), 5 (middle) and 6 (bottom), c.f. Table 5-44. /Follin et al, 2004/.*

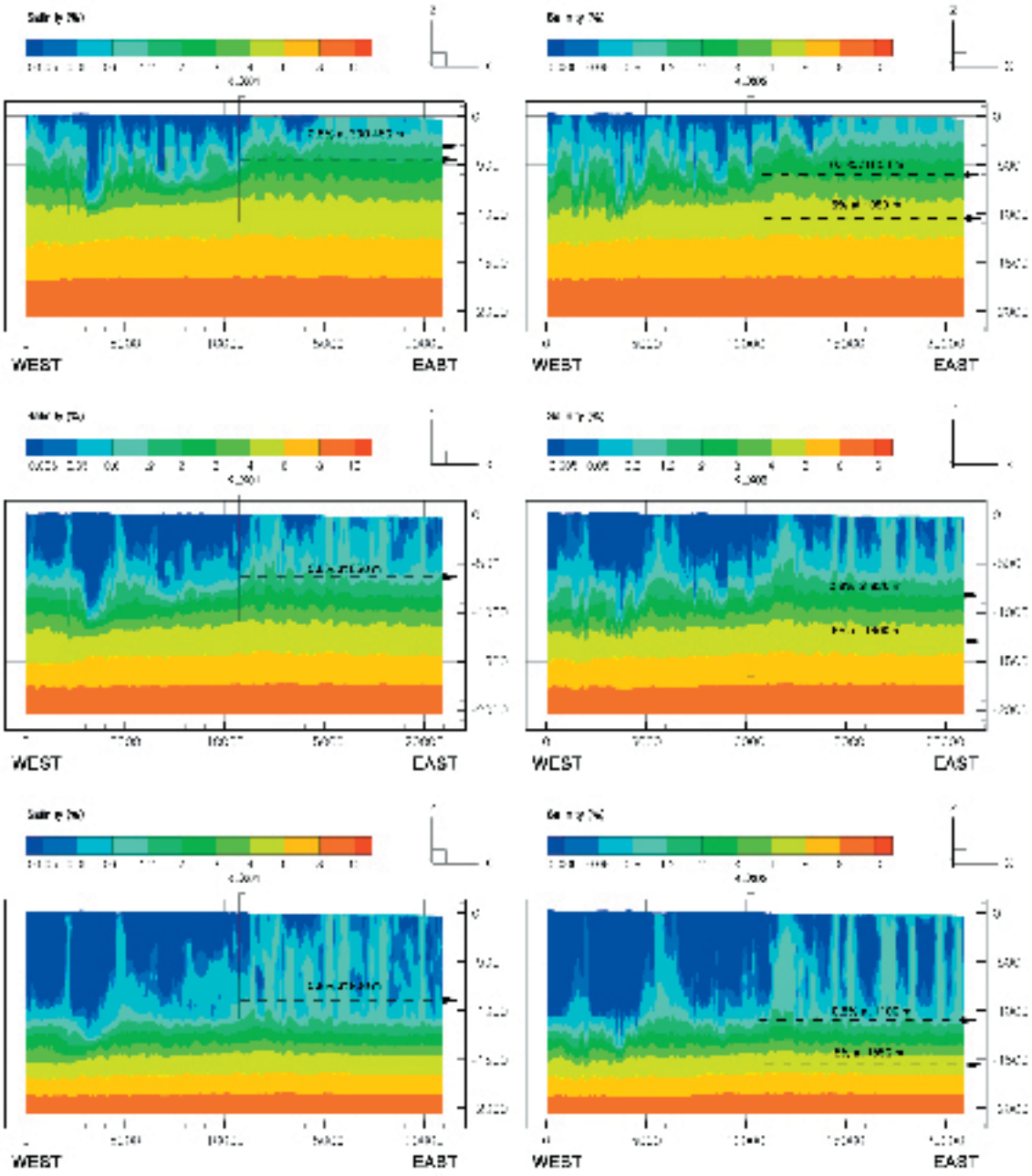

Figure 5-49. *Visualisation of the salinity distribution in the groundwater at 2,000 AD in two parallel profiles running from west to east through the locations of boreholes KLX01 (left column) and KLX02 (right column). The top row, the middle row and the bottom row show the results for modelling cases 7, 5 and 6, respectively, c.f. Table 5-44. /Follin et al, 2004/.*

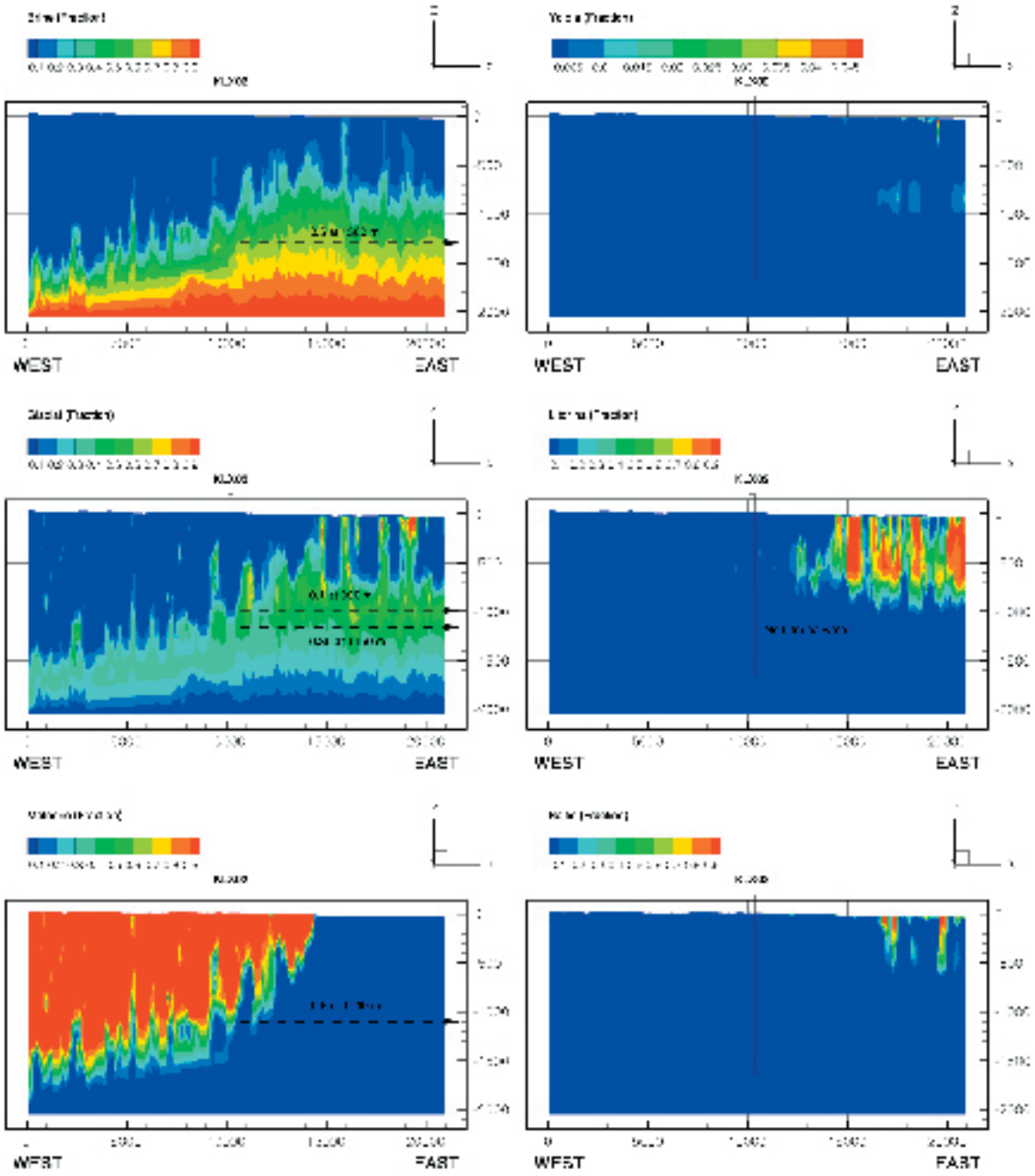

Figure 5-50. *Visualisation of the fractional occurrence of Brine, Glacial melt water, Meteoric water (left column) and Yoldia Sea, Littorina Sea and Baltic Sea (right column) at 2,000 AD in a profile running from west to east through the location of the borehole KLX02. Modelling Case 7, c.f. Table 5-44. /Follin et al, 2004/.*

- Moving the western boundary 2.6 km eastwards did not significantly affect the flow or the salinity distribution.
- The flushing out of the saline water is deeper with an assigned kinematic porosity in HCDs of 0.1% compared with 0.5%, but the difference is not very large. The difference in the distribution of Littorina water is greater, more Littorina water is found to the east in the model for an assigned kinematic porosity of 0.5%.
- The salinity distribution is sensitive to the capacity ratio between the immobile and mobile pore volumes. Only minor tests were made and additional principal studies are required to better characterise the multi-diffusion model included DarcyTools.

5.4.13 Examples of simulation of current flow conditions – regional scale

To get an insight in the present day flow field, the flow rate distribution was visualised for a few simulation cases at various depths. Also the flow paths from 500 m depth from an area below the Laxemar and Simpevarp subareas were simulated. A few examples are shown in this section.

Results Connectflow

Flow distribution

Contours of the vertical Darcy velocity under present-day flow conditions are shown in Figure 5-51 superimposed on a number of horizontal sections at different depths. Near the surface, at –10 masl and at –100 masl the calculated flow is mainly downwards (recharge, negative sign), with magnitudes around –0.001 to –0.01 m/year in the rock mass. Discharge areas are to the east (positive values) associated with the Baltic Sea and a few onshore discharge areas mainly

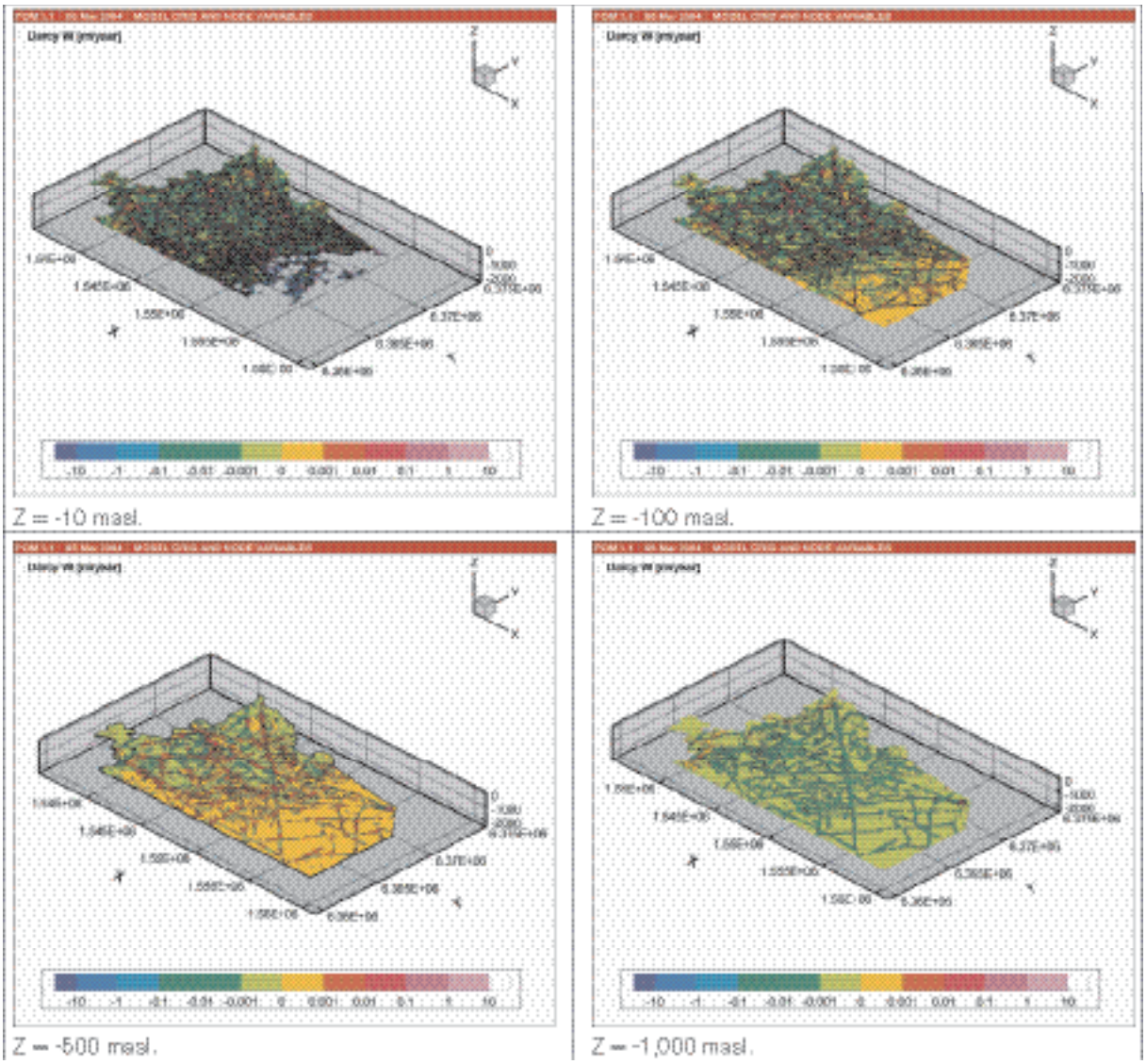

Figure 5-51. *Contours of vertical Darcy velocity (m/year) at present day conditions as mapped on horizontal sections at various depths. For ConnectFlow (CF) case 3 (Intensity case 1 in Table 5-38 and transmissivity case 1 Table 5-40), initial conditions CF 1 (Freshwater down to 500 m depth) and n=2E–3.), see also Table 5-43 for a summary of modelling cases. /Hartley et al, 2004/.*

associated with interpreted deformation zones. Discharge rates in the deformation zones are 0.01 to 0.1 m/year in some areas. Deeper in the bedrock, for example at a potential repository depth of –500 masl, the flow rates are generally less than 0.001 m/year, although some higher upward flows rates are observed in some deformation zones. The area of recharge on this horizontal section is much further inshore compared to the horizontal section at –100 masl. Clearly, inshore the freshwater only penetrates to –500 masl below the higher topography and is then pushed up and over the dense brine for the remaining majority of the model area. At –1,000 masl flow rates are very low in magnitude.

Flow paths

Figure 5-52, top figure, shows the set of starting points (on a regular grid) for transport calculations for the two subareas: Laxemar (north-west) and Simpevarp (south-east). The starting points are coloured according Log(travel time) for surface discharge and the deformation zones are indicated for reference. This visualisation reveals some interesting results. Firstly, the deformation zones have a significant influence on travel times. Secondly, travel times are generally shorter in the case of Laxemar than in the case of Simpevarp. Figure 5-52, bottom illustration, shows a corresponding plot for the exit points. There are several short paths that run almost vertically up along some deformation zones, and many discharge points are located close to their respective starting points.

Results DarcyTools

Flow distribution

The recharge and discharge pattern is show in Figure 5-53 for the top layer of the bedrock and at a depth 500 m for the case with the lowest conductive fracture intensity with model parameters that gave the best correspondence between calculated and measured salinity and water type distributions as shown above (with the lowest conductive fracture intensity and freshwater down to 500 m depth as initial conditions.).

The simulation results suggest that the Laxemar subarea is predominantly subjected to recharging flow conditions at (–500) masl in contrast to the Simpevarp subarea, which is predominantly subjected to discharging flow conditions.

Flow paths

Particles were released evenly distributed across two rectangular “release areas” at 500 m depth and traced in the present-day flow field. The results of these simulations are described in detail in Section 5.5.

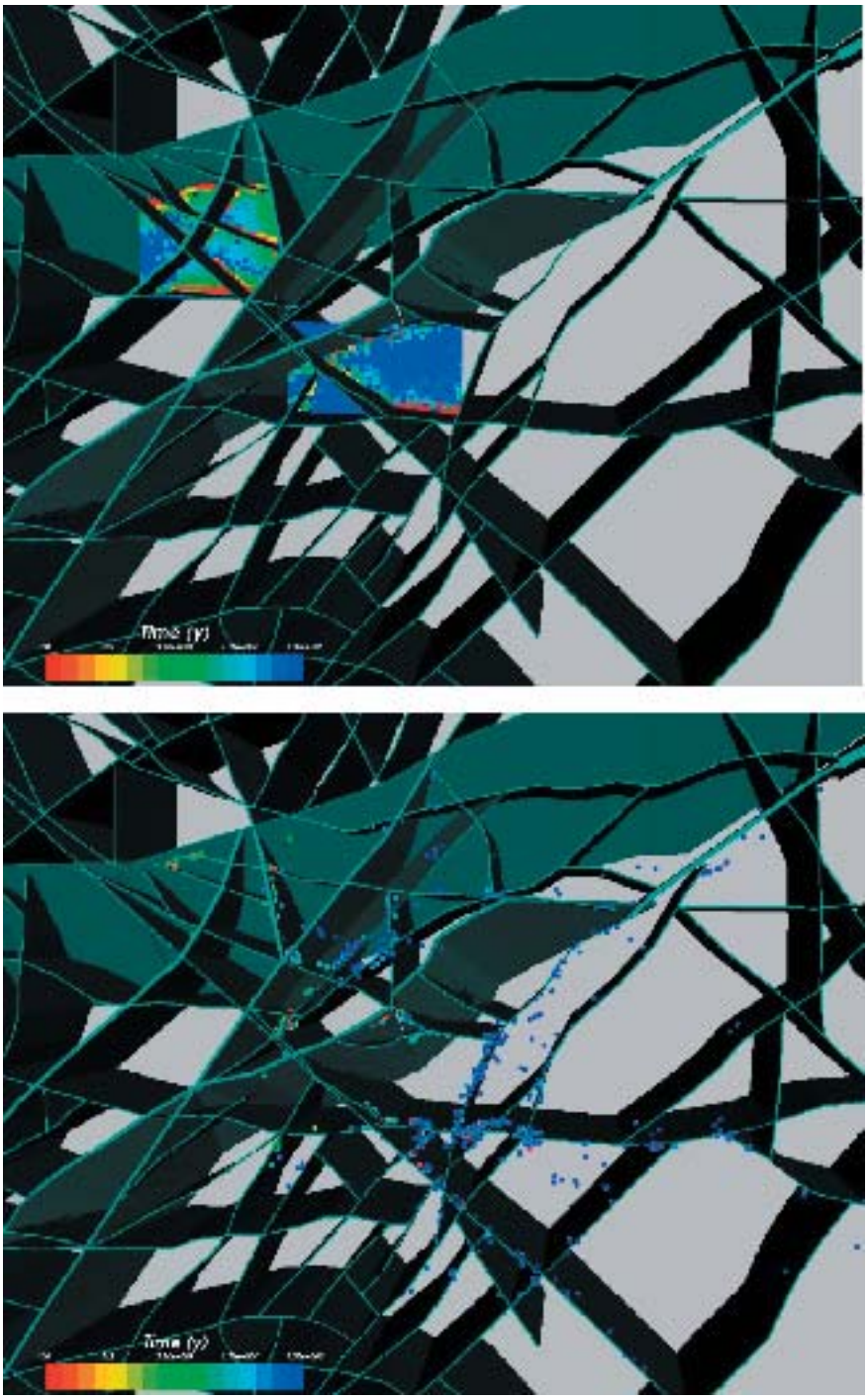

Figure 5-52. *Top: CF Case 3 – start points coloured by total travel time (Log-scale 100–10,000 years) and fracture zones, c.f. Table 5-43. Bottom: Case 3, low K/φ – exit points colored by total travel time (Log-scale: (red) 100– (blue) 10,000 years) and fracture zones.*

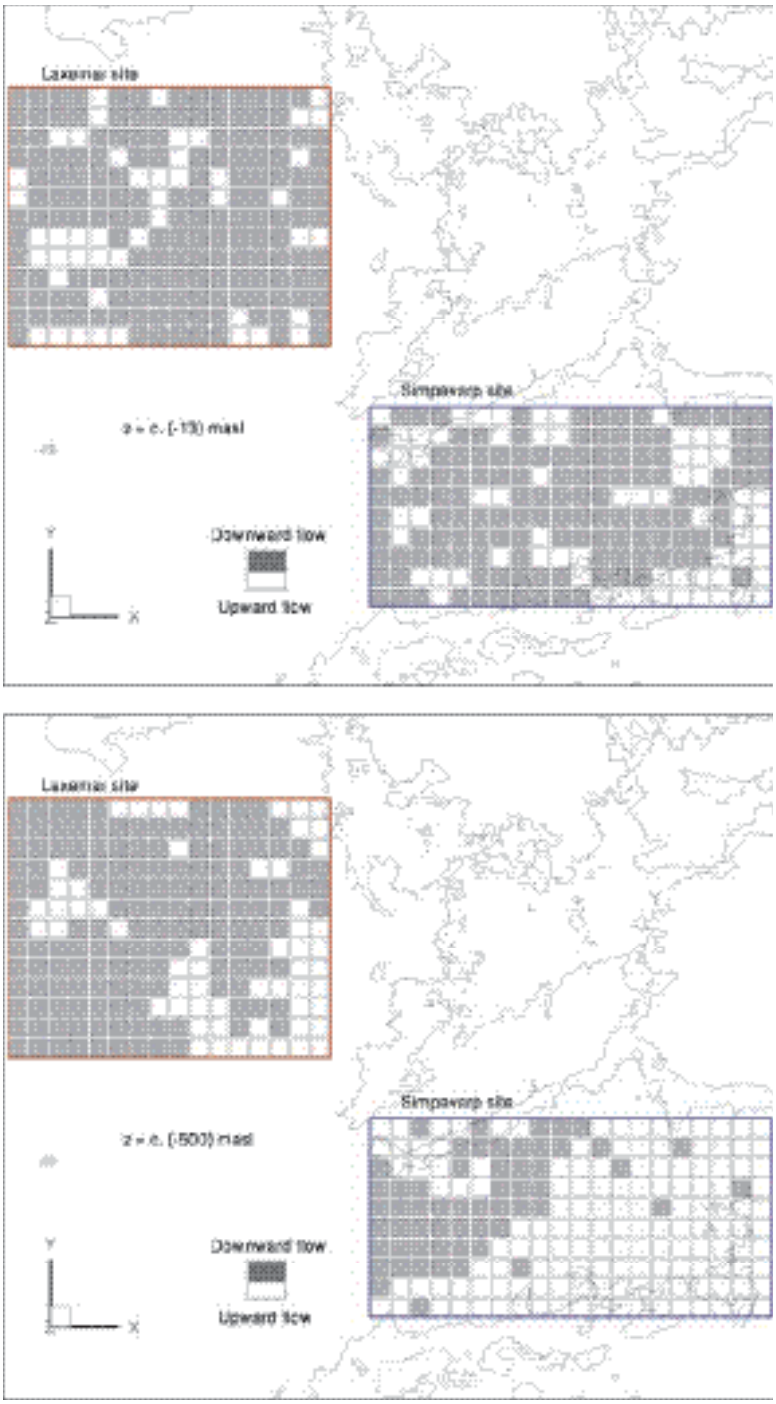

Figure 5-53. *Visualisation showing an example of the pattern of areal distribution of recharge and discharge in the Laxemar and Simpevarp subareas. Results are shown for a situation below the superficial rock layer (top) and at (–500) masl (bottom). (The rectangles do not however directly relate to the defined subareas as defined in Chapter 1) /Follin et al, 2004/.*

5.4.14 Evaluation of uncertainties in the hydrogeological description

Model version Simpevarp 1.1 is a first step towards a realistic site description of the in situ hydrogeological conditions in the Simpevarp area, and the Simpevarp subarea in particular. However, the performed groundwater flow modelling should be regarded as a more or less a generic study as it was not possible to establish a hydrogeological description based on the corresponding geological description for Simpevarp 1.1 for reasons described elsewhere in this report. The hydrogeological descriptive model Simpevarp 1.2 will be based on more integrated models based on rather limited data but some of the uncertainties listed below will be resolved then, whereas others will always be a part of the hydrogeological descriptive model regardless of the extent of the investigations. The latter arises for two main reasons:

- Large areas located far from the designated target areas and will never be investigated.
- The number of boreholes in the target area must be limited, among other things to safeguard the integrity of a possible future deep repository.

It is in this framework that numerical hydrogeological modelling comes into play as an important tool for analysing the impact of both heterogeneity (variable parameter values) and various conceptual uncertainties.

For the development of future model versions more and/or better data concerning the following hydrogeological issues are particularly emphasised:

Hydraulic conductor domains (HCD)

- The structural geological model of the target area, in particular, the occurrence and extensions of HCDs needs to be extended in scope and refined.
- The hydraulic characteristics and potential differences between deformation zones of varying geological confidence.

Hydraulic rock domains (HRD)

- The geological fracture network description, in particular, surface variability in fracturing in relation to fracturing at depth, and the geological classification of conductive fractures.
- The database for the deduction of fracture transmissivity, in particular, the motives for assigning set-specific differences (including possible geometric anisotropy). Concepts and motives for models underlying assignment of transmissivity to the DFN model are considered important.

Hydraulic soil domains (HSD)

- The spatial variability of the thickness of the overburden (Quaternary deposits), the topography of the bedrock surface.
- The type of overburden above HCD, to show whether the overburden is of low conductivity or not. This consideration is important for the paleohydrogeological simulations.
- Seasonal variations in the groundwater table, which describe the expected level of the water table and the relative role of evapotranspiration.

Link to hydrogeochemistry

- The description of the present groundwater salinity and water types versus depth in the kinematic fracture system based on borehole information.
- The description of salinity of immobile groundwater in the low-conductive rock.
- Evidence for discharging deep groundwater.

5.5 Hydrogeochemical modelling

The data evaluation and modelling becomes a complex and time-consuming process when the information has to be decoded. Manual evaluation, expert judgment and mathematical modelling must normally be combined when evaluating groundwater information. A schematic presentation of how a site evaluation/modelling is performed and its components is shown in Figure 5 54. The methodology applied in this report is described in detail by /Smellie et al, 2002/.

For the groundwater chemical calculations and simulations the following standard tools were used:

For evaluation and explorative analyses of the groundwater:

- AquaChem: Aqueous geochemical data analysis, plotting and modelling tool.

Mathematical simulation tools:

- PHREEQC with the database WATEQ4F: Chemical speciation and saturation index calculations, reaction path, advective transport and inverse modelling /Parkhurst and Appelo, 1999/.
- M3: Mixing and Mass balance Modelling /Laaksoharju et al, 1999b/.

Visualisation/animation:

- TECPLOT: 2D/3D interpolation, visualisation and animation tool.

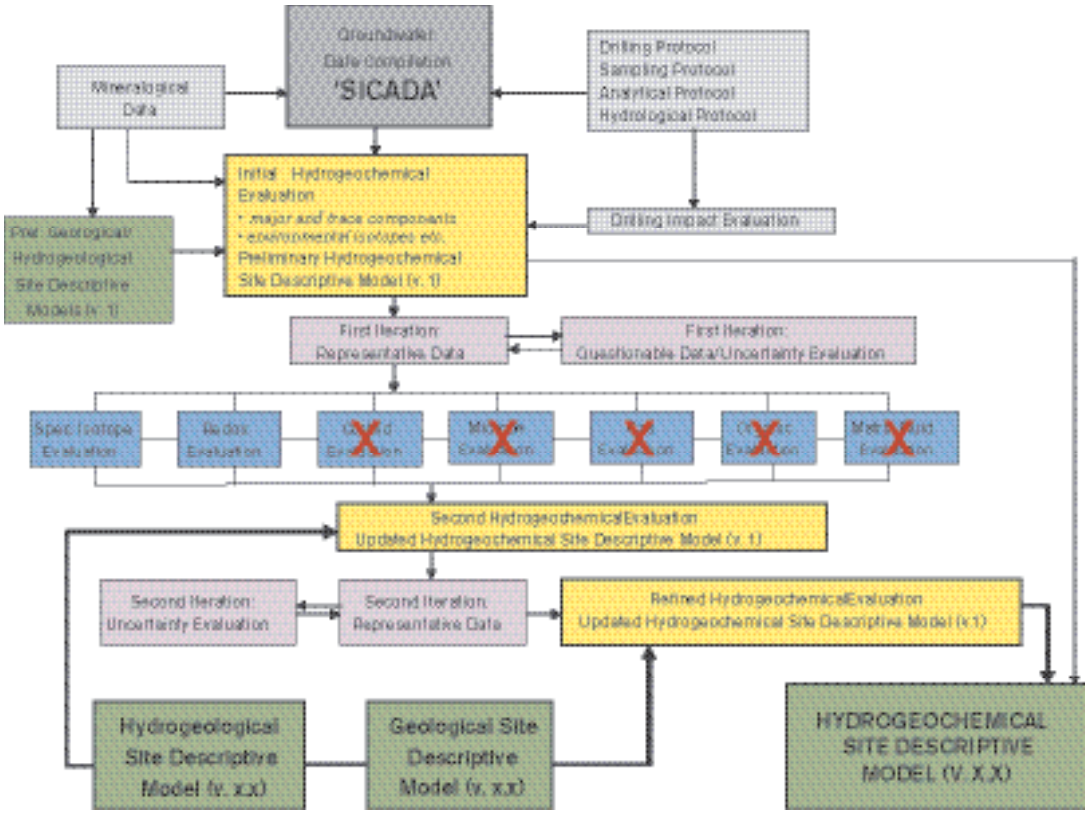

Figure 5-54. *The evaluation and modelling steps used in this report. The struck out evaluation steps (crosses in red) were not performed due to lack of data. After /Smellie et al, 2002/.*

5.5.1 Modelling assumptions and input from other models

Hydrogeochemical modelling involves the integration of different geoscientific disciplines such as geology and hydrogeology. This information is used as background information, supportive information or as independent information when models are constructed or compared. The following sections describe how geological information can be used in the modelling and how speciation, mass-balance, coupled modelling and mixing modelling can be applied to data from the Simpevarp area.

Geological information is used in hydrogchemical modelling as direct input in mass-balance modelling, but also to judge the plausibility of the results from e.g. saturation index modelling. For this particular modelling exercise, geological data were summarised, the information was reviewed and the relevant rock types, fracture minerals and mineral alterations were identified /cf. Laaksoharju, 2004b/.

The underlying geometrical model of deformation zones model provides important information on potentially water-conducting fractures and is used for the understanding and modelling of the hydrodynamics. A cross section used for visualisation of groundwater chemical properties is generally selected with due consideration for the geological model. The results from the modelling are generally presented by employing 2D/3D visualisation tools. Unfortunately, the lack of data at depth in the Simpevarp subarea precludes a 3D interpolation and production of 2D sections for this model version.

5.5.2 Conceptual model with potential alternatives

Because of the lack of hydrogeochemical data at depth (> 400 m) only a limited number of alternative models were explored. Those tested included some based on different reference waters at the local and regional scales /cf. Laaksoharju, 2004b/. Various modelling tools and approaches were applied to the data set.

5.5.3 Speciation, mass-balance and coupled modelling

Speciation modelling

Speciation-solubility modelling was carried out with PHREEQC /Parkhurst and Appelo, 1999/ using the WATEQ4F thermodynamic database. In these types of calculations, starting from the concentration of a set of elements in a water sample and other relevant parameters (temperature, pH, Eh, total or carbonate alkalinity, and, in some cases, density), the concentration and activity of all the relevant species in the system and the saturation indices with respect to a predefined set of minerals are computed. This is a purely thermodynamic calculation, in which it is assumed that all dissolved species are in a state of mutual homogeneous equilibrium. This approach defines the proximity of a solution to equilibrium with a relevant phase through a saturation index defined as:

(5-3)

where IAP is the ionic activity product and K(T) is the equilibrium constant of the dissolution-precipitation reaction of the relevant phase. A positive value indicates that thermodynamically a mineral can precipitate, and a negative value that it can dissolve. A value close to zero indicates that the mineral is at equilibrium and at saturation and, therefore, is not reacting. The saturation index indicates the potential for the process, not the rate at which the process will proceed. From this information, conclusions concerning possible major reactions taking place in the system can be drawn.

The calculations are used to investigate the processes that control water composition in the Simpevarp subarea. This section is divided into two main subsections, the first concerning the state of non-redox elements and phases, and the second focussed on the redox state of the modelled system.

The procedure deals only with plausible controlling minerals in the system, i.e. those that can reach equilibrium with the groundwater. Therefore, clearly undersaturated mineral phases are not included in this description. In addition, only mineral phases actually identified in the Simpevarp subarea were considered. A more detailed description of the modelling performed can be found in /Laaksoharju, 2004b/.

Carbonate system

Calculated saturation states with respect to calcite in most groundwater samples indicate a generalised equilibrium state (considering the commonly accepted ± 0.5 uncertainty in the SI of this mineral when uncertainties in pH are evaluated (Figure 5-55a). The valid groundwater samples plot below the Saturation Index (SI=0) line because laboratory pH have been used for the calculations. The scatter in the values is mainly due to uncertainties in the pH of the samples (see detailed discussion of the pH uncertainties in /Laaksoharju, 2004b/. Surface and shallow subsurface waters are mostly undersaturated with respect to this mineral.

The computed P_{CO_2} values do not show any clear trend with chloride due to the problems with the non-representative brackish samples (Figure 5-55b) sampled with the tube sampler in the open borehole. Basically, the trends of alkalinity, pH and the saturation state of calcite could be explained with a water-rock interaction model (dissolution-precipitation of fracture-filling calcite and silicate hydrolysis) proposed by /Nordstrom and Puigdomenech, 1989/ for Stripa groundwaters and verified at other Swedish and Finnish sites.

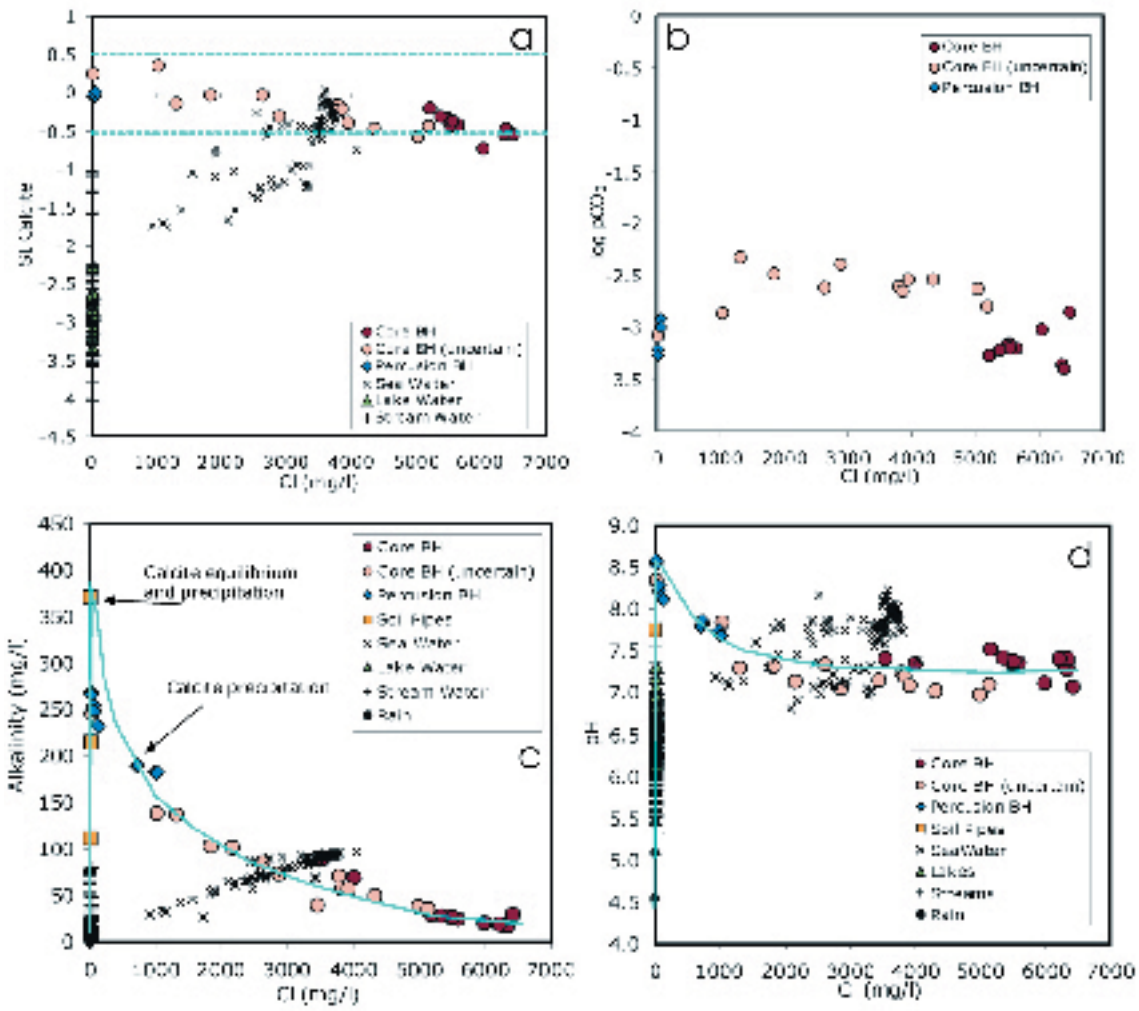

Figure 5-55. *Evolution of the carbonate system in the Simpevarp waters (a and b); Calculated calcite saturation indices and partial pressure of CO2 against chloride (c); and (d) Alkalinity and pH against chloride. The dashed lines in Figure 5-2a represent the uncertainty associated with SI calculations.*

The initial steep rise in alkalinity (Figure 5-55c) and pH (Figure 5-55d) that affects superficial waters is related to weathering of the bedrock, causing calcite dissolution and the hydrolysis of silicates. Calcite reaches saturation (or oversaturation) at the alkalinity peak and the subsequent depletion in alkalinity can be attributed to calcite precipitation. This precipitation process is induced by calcium enrichment in groundwaters associated with mixing with a saline source.

The pH usually increases slightly beyond the alkalinity peak. As calcite precipitation produces a decrease in pH, it has been assumed that the pH increase is associated with the effect of silicate hydrolysis (i.e. consuming proton reactions) deep in the bedrock. The trend observed in Simpevarp groundwaters shows a pH decrease, apparently with minor or no silicate hydrolysis compensation.

Nevertheless, this pH decreasing trend in the Simpevarp subarea can be magnified by the high pH peak developed in the more recent superficial waters (the existence of older recharge groundwaters with a less developed pH peak could modify the interpretation on the pH pattern) and mainly by the presence of the non-representative tube samples along the pattern.

Silica system

The weathering of rock-forming minerals is the main source of dissolved silica. Superficial waters have a variable degree of saturation with respect to silica phases (quartz and chalcedony), compatible with the weathering hypothesis.

Saline groundwaters are oversaturated in quartz and close to equilibrium with chalcedony (Figure 5-56). Saturation indices of these phases are relatively constant and independent of chloride content; this suggests that the groundwater has already reached a stationary state associated with the formation of aluminium silicates or secondary siliceous phases like chalcedony, which control the concentration of dissolved silica.

The lack of quality assured aluminium data for Simpevarp groundwaters precludes a speciation-solubility analysis of aluminosilicates. Therefore, activity diagrams were used to study the relationship between silicate minerals and their stability. The accuracy of these diagrams depends on pH and is therefore affected by the uncertainties in the pH measurements. Uncertainties in the equilibrium constants of the aluminosilicates (especially phillosilicates) also affect the conclusions drawn from these diagrams. This last source of uncertainty has been investigated considering more than one equilibrium constant for some phases and different assumptions or mineralogical relations when constructing the diagrams. Nevertheless, the conclusions are preliminary because few representative groundwater samples are available.

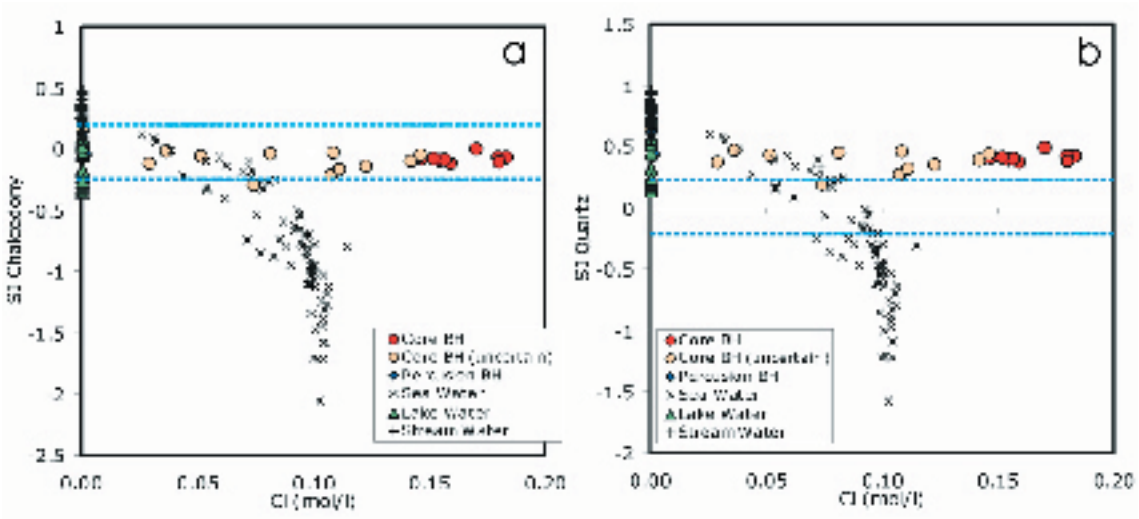

Figure 5-56. *Saturation indices of chalcedony (a) and quartz (b) as a function of Cl in Simpevarp waters. The dashed lines represent the uncertainty associated with SI calculations /Deutsch et al, 1982/.*

Figure 5-57 shows several activity diagrams based on data from /Helgeson, 1969/ calculated at 7°C (similar diagrams have been used in Olkilouto by /Pitkänen et al, 1999/. The diagrams plot clay minerals and, apart from the stability of kaolinite in superficial waters and in some groundwaters, they suggest an association of Ca and Mg to clay minerals in saline samples and samples from percussion boreholes, leading to the stabilisation of montmorillonite.

Figure 5-58 shows three additional stability diagrams for other mineral phases identified as fracture fillings in the KSH01A borehole: adularia, albite, prehnite, laumontite and chlorite. The diagrams are based on data calculated at 15°C by /Grimaud et al, 1990/ for the Stripa groundwaters. These diagrams show that the most valid saline groundwaters and samples from percussion boreholes are near to or in the albite stability field and some of them near or in the chlorite stability field.

Finally, Figure 5-59 plots stability diagrams that include illite. Diagram (a) was used in the Cigar Lake natural analogue study /Cramer and Smellie, 1994/, and is based on data from /Helgeson, 1969/ and /Helgeson et al, 1978/. Diagram (b) was constructed with data from /Garrels, 1984/. Both diagrams suggest that illite could play an important role in these groundwaters, in agreement with the presence of this mineral in the studied fracture fillings.

Cation exchange processes are probably more important than clay mineral recrystallisation during short-term water-rock interactions at low temperature, but in waters with long residence times these exchange processes may cause irreversible changes in clay minerals as the solubility diagrams suggest /Pitkänen et al, 1999/.

Redox pairs calculations

The available analytical data (measured dissolved Fe^{2+}, total Fe, total sulphide and sulphate concentrations) allow a standard redox pair calculation only for samples at 161.75 m (samples 5257 and 5259 to 5263) and 253.25 m depth (samples 5266 and 5268) in the KSH01A borehole. For these two depths there is also continuous Eh logging which gives a stable Eh reading of –220 mV at 161.75 m and –210 mV at 253.25 m, c.f. /Laaksoharju, 2004b/. These data enable a comparison to be made between the two approaches.

A temperature value is known only for the 161.77 m samples (7°C). The temperature at 252.15 m has also been fixed at 7°C for the speciation calculations. It is thought that this assumption does not substantially affect the final uncertainty, as the uncertainty due to temperature efects is smaller than the uncertainty associated with some redox pairs whose empirical calibration was carried out at 10°C, Sweden's mean groundwater temperature, or even at 25°C. Because redox calculations depend on pH and there are significant differences between in situ and laboratory pH, they add an a priori extra uncertainty to the results of the redox pair calculations. To quantify this uncertainty, the following calculations have been performed at three different pH values: laboratory pH, in situ pH (8.1 at 161.75 m and 8.05 at 253.25 m; see Appendix A in /Laaksoharju, 2004b/, and computed pH assuming equilibrium with calcite.

Previous studies in "granitic" groundwaters from Sweden and Finland /Nordstrom and Puigdomenech, 1989; Smellie and Laaksoharju, 1992; Grenthe et al, 1992; Glynn and Voss, 1999; Bruno et al, 1999/ have found that various iron and sulphur redox pairs/buffers are the most reliable couples controlling the redox state of these groundwaters. Therefore, for the Simpervarp groundwaters the selected redox couples are the dissolved Fe^{3+}/Fe^{2+} and SO_4^{2-}/S^{2-} redox pairs and the heterogeneous $Fe(OH)_3/Fe^{2+}$, pyrrhotite/SO_4^{2-} and pyrite/SO_4^{2-} couples. Also, results with the Fe^{3+}-clay/Fe^{2+}-clay redox pair proposed by /Banwart, 1999/ were determined /cf. Laaksoharju, 2004b/.

Several methods to model the redox potential obtained with the $Fe(OH)_{3(s)}/Fe^{2+}$ pair were employed. Results using the calibration from /Grenthe et al, 1992/ are very sensitive to uncertainties in pH but always provide a more reducing redox potential than the electrochemically measured downhole values at both depths. This is especially true for the Eh values (from –390 to –400 mV) obtained using the measured downhole pH values.

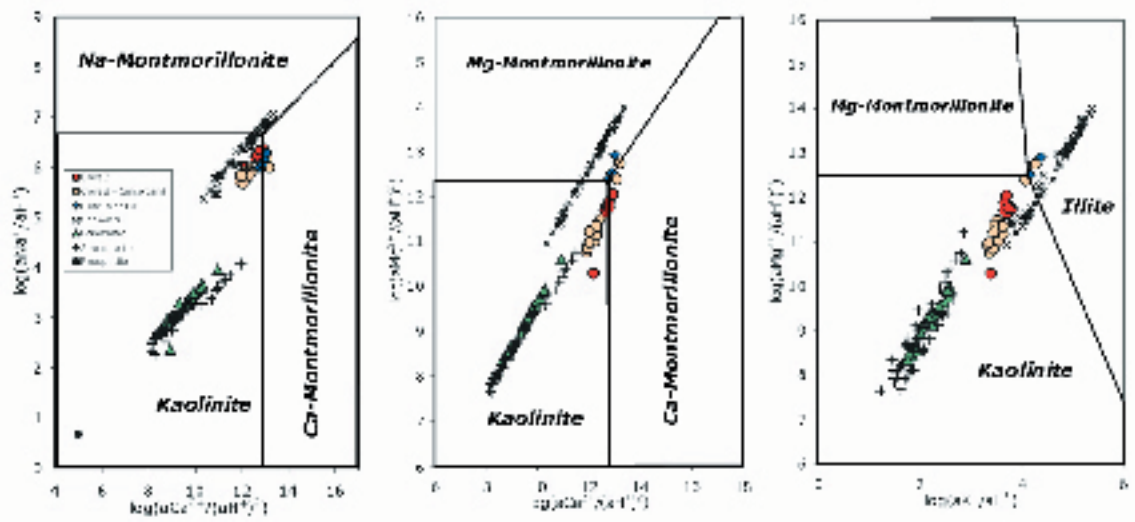

Figure 5-57. *Aqueous activity diagrams for some aluminosilicate minerals at 7°C, 1 bar. The field boundaries were calculated with data from /Helgeson, 1969/ and a logarithmic silica activity of −4.*

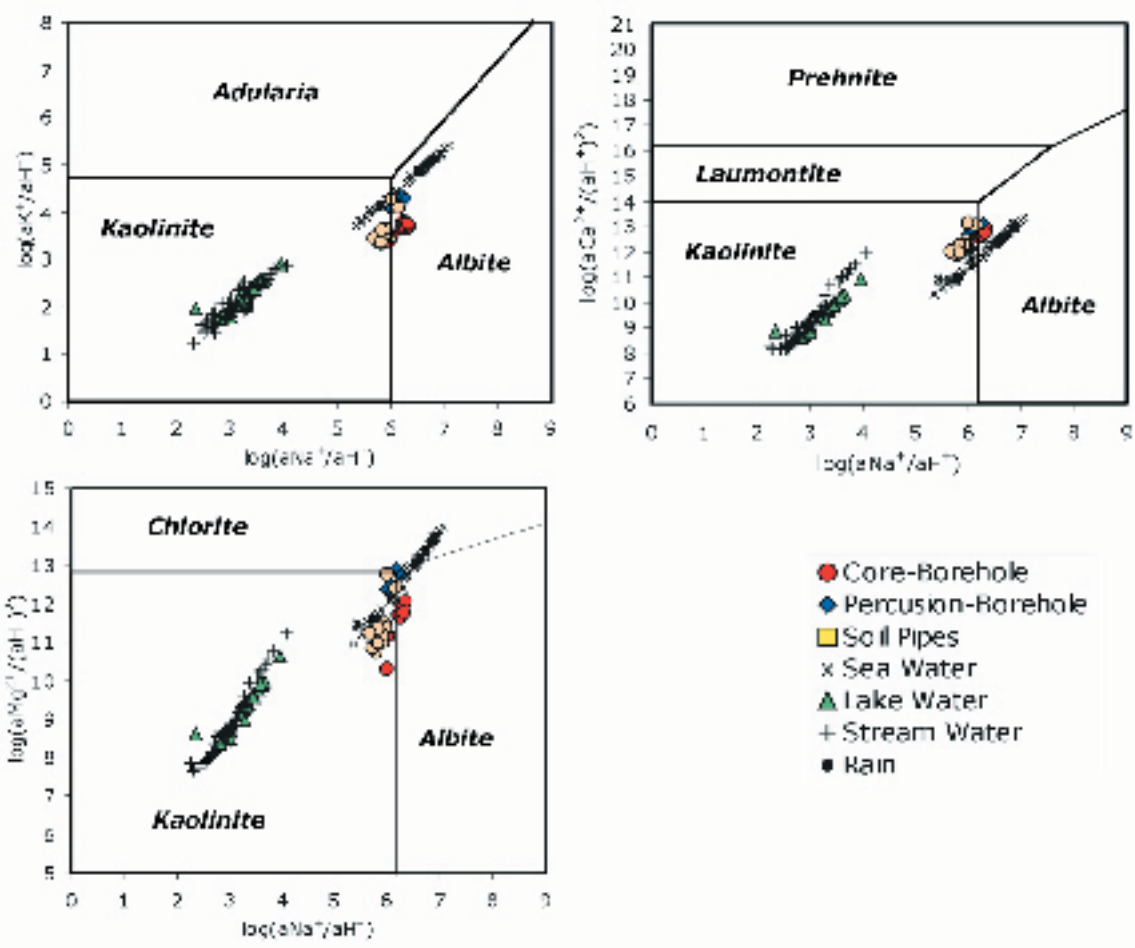

Figure 5-58. *Aqueous activity diagrams for some aluminium silicate minerals at 15°C, 1 bar. The field boundaries have been calculated from the data of /Grimaud et al, 1990/. The displacement from the model line for some of the trends in data could be due to incorrect pH values.*

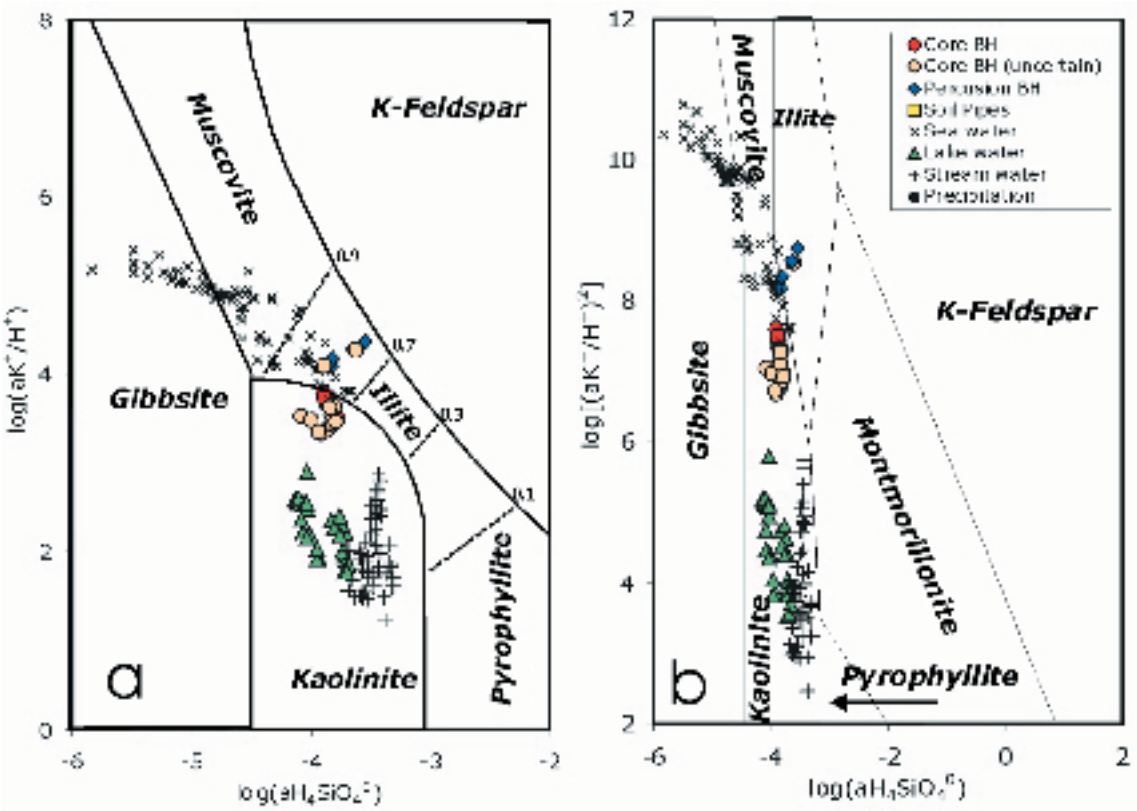

Figure 5-59. *Aqueous activity diagrams for some aluminium silicate minerals at 25°C, 1 bar, including illite. The field boundaries have been calculated using data from /Helgeson, 1969/ and /Helgeson et al, 1978/ in graph (a) and from /Garrels, 1984/ in graph (b). In graph (a) the illite field is contoured to show the stability of different illite fractions in I/S.*

The method based on the $Fe(OH)_{3(s)}/Fe^{2+}$ pair suggested by /Bruno et al, 1999/, using the thermodynamic data for two end members including crystalline and amorphous $Fe(OH)_3$ gave the best agreement with the measured values. The results obtained with this approach and using different pH values to assess the uncertainties, are shown in Figure 5-60. Obviously, without a detailed knowledge of the exact type of hydroxide involved and its crystallinity, this approach incorporates an additional uncertainty which, together with the pH uncertainty, broadens the Eh range from +30 to –240 mV. An excellent agreement between the redox potential obtained with the $Fe(OH)_3/Fe^{2+}$ pair and the in situ one is obtained if the amorphous hydroxide phase controls the pair at the pH measured in borehole KSH01A (Figure 5-60).

The redox potential deduced from the dissolved SO_4^{2-} pair shows less sensitivity to uncertainties in pH with differences of less than 50 mV for the pH interval examined. Furthermore, the Eh values provided by this redox pair (–210 to –230 mV) when using the in situ downhole pH measurements (or the calculated pH in equilibrium with calcite) are very similar.

Results obtained with the pyrite/SO_4^{2-} and pyrrhotite/SO_4^{2-} buffers from /Bruno et al, 1999/ are presented in Figure 5-61. Overall, the Eh values calculated with these pairs range from –210 to –270 mV and are not very sensitive to pH. This range is in fairly good agreement with the measured Eh.

Finally, results with the Fe^{3+}-clay/Fe^{2+}-clay redox pair proposed by /Banwart, 1999/ provides Eh values close to the measured downhole in situ values (around –170 to –174 mV) when using the downhole in situ pH measurements see /Laaksoharju, 2004b/.

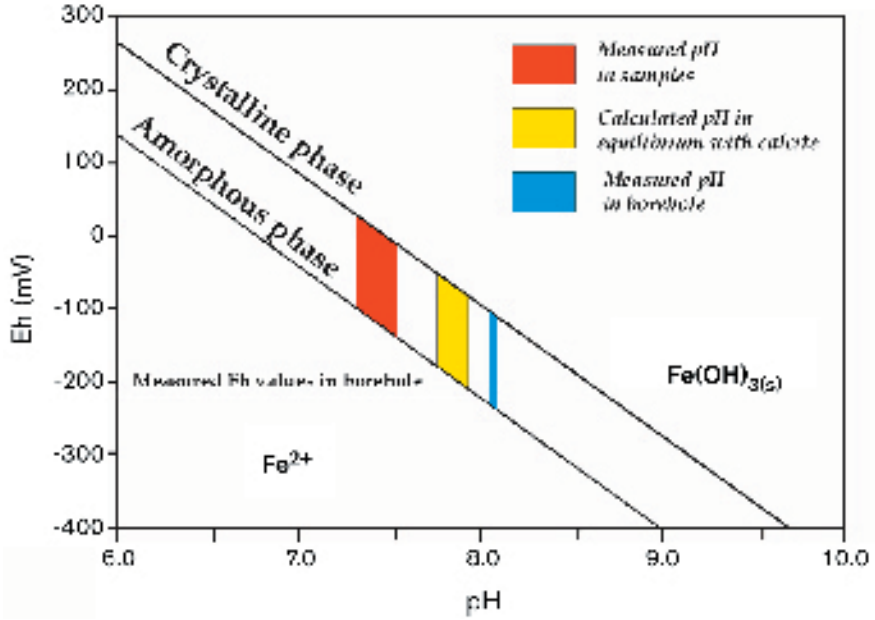

Figure 5-60. *Eh-pH diagram with $Fe(OH)_3(s)/Fe^{2+}$ phase boundaries for crystalline (log K=3) and amorphous (log K = 5) $Fe(OH)_3$ phases. The diagram has been drawn using data from the Palmottu natural analogue study /Bruno et al, 1999/ assuming a concentration of $Fe^{2+} = 3 \cdot 10^{-5}$ M. The coloured areas represent the pH ranges measured from the KSH01A borehole in samples from the 161.75 and 253.5 m depth intervals (in situ, blue, and in the laboratory, red), and those calculated assuming equilibrium with calcite (yellow). The uncertainty associated with the crystalline nature of the solid phase and the pH uncertainty, together give rise to a maximum variation in Eh of +30 to –240 mV. The in situ measured Eh is consistent with control by the amorphous hydroxide phase at the pH measured in the borehole (i.e. the intersection of the "Amorphous phase" line and the blue band).*

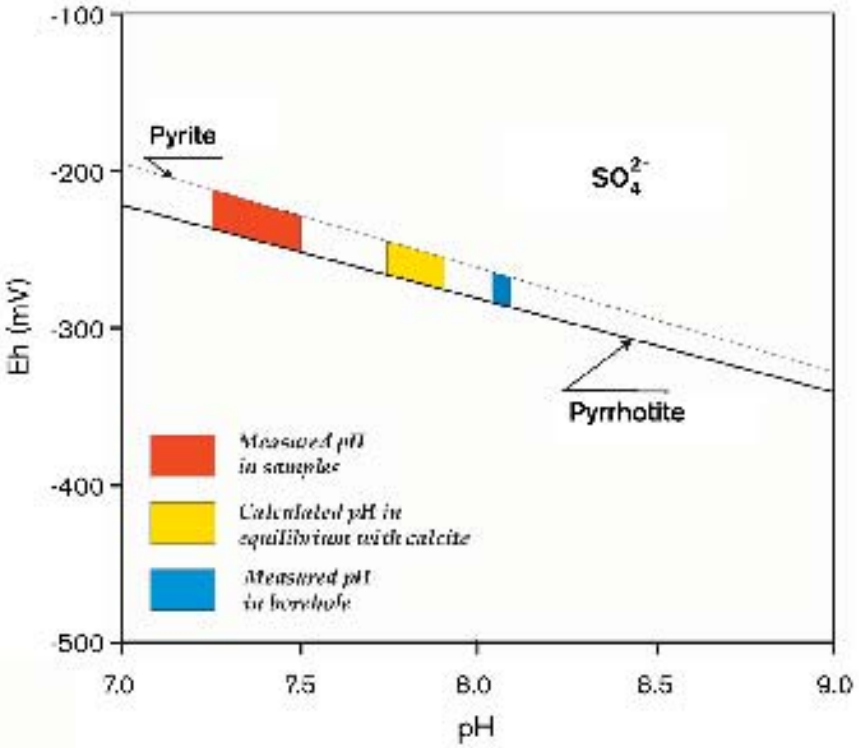

Figure 5-61. *Eh-pH diagram with SO_4^{2-}/pyrite and SO_4^{2-}/pyrrhotite phase boundaries for KSH01A saline groundwaters. Coloured areas show the pH ranges measured in-situ at 161.75 and 253.5 m depth (blue), in the laboratory (red) and computed assuming equilibrium with calcite (yellow).*

The above results suggest that the redox state of the saline waters from the 161.57 m and 253.25 m depth intervals in borehole KFM01A are buffered by the presence of iron oxides and hydroxides and by redox reactions between phyllosilicates. Nevertheless, the good match between the electrochemical and sulphur redox-pair Eh values points to sulphide minerals as the main redox buffers for the groundwaters at both depths. These reducing conditions are also suggested by the low and similar U concentrations at both depths. The fracture coatings in the modelled sections contain chlorite and clay minerals (mainly corrensite and mixed-layer illite-smectite clays) and pigmentation/impregnation caused by haematite in the fracture zone at 245 to 300 m depth in borehole KSH01A; the presence of minor amounts of pyrite post-dating the haematite is indicated. In section 158 to 162 m coatings with chlorite, corrensite, calcite and pyrite are found.

The buffering of the sulphur system has also been identified in other Swedish and Finnish groundwaters /Nordstrom and Puigdomenech, 1989; Glynn and Voss, 1999; Bruno et al, 1999/ and, together with the presence of dissolved sulphides, suggests the development of an anoxic-sulphidic environment mediated by sulphate-reducing bacteria (SRB). Microbial analysis data are not available for KFM01A groundwaters but other lines of reasoning support the presence of this bacterial process.

The precipitation of typical sulphide minerals associated with the sulphidic environment is suggested by the equilibrium between the waters and several sulphide phases, as deduced from speciation-solubility calculations for waters at 161.75 m depth. No reliable conclusion can be made from the 253.25 m depth downward due to lack of reliable samples. However, the concentration of dissolved Fe^{2+} at this depth is lower (1.27 to 1.34 mg/L) than at the shallower depth (1.4 to 1.74 mg/L), which is consistent with precipitation of these phases.

Finally, available $\delta^{34}S$ data for waters from both depths (between 20.2 and 22.8‰) show an enrichment with respect to values found in shallower bicarbonate waters (e.g. waters from percussion-drilled borehole HSH02 with $\delta^{34}S$ values between 12.1–17.2 ‰ and have values similar to those seen in some Finnish sites, that have been related to bacterial sulphate reduction /Haveman et al, 1998; Snellman et al, 1998; Pitkänen et al, 1998, 1999/.

The absence of key analytical data (Fe, sulphide, methane, concentrations etc) at the time of the "data freeze" for the rest of the samples in the area rules out a better characterisation of the sequence of redox conditions developed at depth.

Mass balance and mixing calculations with PHREEQC

The inverse approach via mass balance and mixing calculations for the purpose of tracking the hydrogeochemical evolution of the groundwaters in the Simpevarp subarea has been carried out on the few available samples that have a complete, and free of contamination, analytical data set. These comprise of five samples of fresh and non-saline groundwaters and two samples of saline waters. As a consequence, the geochemical evolution path has only been calculated for two groundwater types with extreme hydrogeochemical characteristics and widely different apparent ages: (1) fresh, non-saline waters with a bicarbonate imprint, low residence times (tritium values above detection limit) and chloride concentrations from 12–132 mg/L (samples from percussion boreholes HSH02 and HSH03), and (2) saline waters with longer residence times (tritium values below detection limit) and chloride concentrations ranging from 5,500–6,300 mg/L (samples from core-drilled borehole KSH01A at 156.5–167 and 245–261.5 m depth; see /Laaksoharju, 2004b/.

This limitation in sample types, together with the scarcity of detailed mineralogical data and the lack of a hydrogeological model, precludes the elaboration of a detailed evolutionary model for the groundwaters. Consequently, the results summarised in this section are to be regarded as preliminary. They are mainly focussed on the analysis of saline waters, and are based only on: (1) general premises regarding the type of waters and reactive phases involved, and (2) an inter-comparison with analogous systems (to select water end members). The code PHREEQC /Parkhurst and Appelo, 1999/ was used for all mass balance and mixing calculations employing the following chemical and isotopic data: Cl, HCO_3^-, SO_4^{2-}, SiO_2, Ca, Mg, Na, K, Fe, S^{2-}, $\delta^{18}O$ and δ^2H.

Model results for fresh, non-saline groundwaters

In common with the Forsmark area, these groundwaters have an important a priori water-rock interaction component, with an added marine contribution in the high-Cl members /Laaksoharju, 2004a/. Mass balance and mixing calculations carried out following the methodology developed for the Forsmark site /Laaksoharju, 2004a/ confirm this hypothesis.

The evolution of the low Cl-waters from this group is dominated by the decomposition of organic matter, the dissolution of calcite, plagioclase, biotite and sulphides, and by Na-Ca exchange and precipitation of some phyllosilicates, all with very low mass transfers. High Cl-waters from this group could have, however, a small (< 10%) mixing contribution with a marine end member, but in general the reaction model is preserved. The lack of more detailed mineralogical data from the overburden and bedrock, and the lack of a hydrogeological model for this zone, preclude more specific conclusions to be drawn; in consequence, no more effort has been invested in characterising these waters further.

Model results for saline groundwaters

As already pointed out, these waters have a longer residence time and their general character indicates that mixing between multiple end members is the principal mechanism controlling their chemistry as has been seen in this type of saline groundwaters at other Swedish and Finnish sites /e.g. Laaksoharju and Wallin, 1997; Pitkänen et al, 1999; Puigdomenech, 2001/. It is important to note that this type of modelling is relative, describing the reactions taking place when the different water types mix. The model is not absolute, describing the actual reactions that formed the end member composition, e.g. the compostion of the brine. The advantage with the employed modelling approach is that processes taking place during ambient conditions can be identified and separated, e.g. from processes associated with high temperature. To verify these general assumptions, the inverse modelling capabilities of PHREEQC to compute multiple end member mixing proportions and reactions have been used. The mixing proportions are computed with respect to end members of known composition and the reactions with respect to a predefined set of likely solid phases. Each solution given by PHREEQC is termed a model.

The chosen water end members, i.e. Rain 60, Littorina, Sea Sediment, Glacial Meltwater, and Brine, have been used elsewhere in the Fennoscandian Shield for modelling purposes. In addition, the end member Lake Water, used in M3 calculations for the Simpevarp subarea, has also been included for comparative purposes. The selection of these general end members is useful to interpret the mixing processes under the general framework of all investigated Swedish sites.

Due to the lack of detailed bedrock mineralogical data, likely reacting solid phases include the most common phases used in similar systems elsewhere supported additionally by available information from observed fracture fillings at Simpevarp. The set of chosen phases and reactions is shown in /Laaksoharju, 2004b/.

From the end members used as initial waters, and from reactions with respect to a predefined set of solid phases, PHREEQC computes all the possible combinations of mixing and reaction that satisfy the chemistry of the final waters (the selected samples, see below). The reactions influence the mixing proportions and not all end members are used by PHREEQC in all the modes found (see /Laaksoharju, 2004b/ for detailed results). Therefore, the mixing proportions obtained by PHREEQC strongly depend on the number of end members considered in the model, and to a lesser degree on the set of selected reactions.

Brine and Glacial Meltwater are the only end members that appear in all models, the former with a smaller variation range. The Glacial end member is generally the most abundant and shows up to a 20% variation in mixing proportion (30–50%) depending on the meteoric end member in the model.

Rain 60 and Lake Water were not used simultaneously in one subset of the models, but they were used in another test run using a different subset of data. In this case, the total mixing proportion of meteoric water (Rain + Lake Water) ranged from 30% to 40%, similar to the individual mixing proportions of each meteoric end member in models where only one of the two appeared.

Sea Sediment and Littorina behave in a similar way to Rain 60 + Lake Water. Here, one subset of the models included only one of the two, and the other more minor subset included both end members. The total contribution of both end members is low (13–17% for Sea Sediment and <10% for Littorina). All the models have, at least, one of these marine end members.

The differences in mixing proportions between the two saline samples (with different Cl concentrations) selected for these calculations are small. At most, the high-Cl sample tends to show a somewhat larger contribution of the Glacial and Brine end members, but this difference can be considered as insignificant due to the uncertainties associated with the selection of the reacting phases.

The heterogeneous reactions identified during the mixing processes in these saline waters include: a) organic matter decomposition, b) dissolution of plagioclase, biotite and Fe-chlorite (or Fe $(OH)_3$), c) precipitation of calcite, illite and SiO_2 phases (or phyllosilicates), d) the possible occurrence of bacterial sulphate reduction processes with the simultaneous precipitation of iron sulphides, and finally, e) the ionic exchange between Na and Ca. Detailed description of the sets of phases and heterogenous reactions is shown in /Laaksoharju, 2004b/.

Discussion of the results

The chemistry of fresh, non-saline groundwaters is controlled only by water-rock interaction processes for the low-Cl members. The identified heterogeneous reactions are: organic matter decomposition, dissolution of calcite, plagioclase, biotite and gypsum (or sulphides), and Na-Ca exchange and precipitation of some phyllosilicates, all of them with very low mass transfers. The high-Cl members (132 mg/L) could show a small contribution from mixing with a marine end member.

The chemistry of saline groundwaters is mainly controlled by mixing of a saline end member (Brine) with several “dilute” end members. Among these dilute end members, Glacial Meltwater is always present, with a contribution of 30–50%, together with a meteoric end member with a similar contribution. The presence of a marine end member (Littorina or Sea Sediment) is uncertain because they always appear in low proportions (< 17%).

These results agree fairly well with the ones obtained by M3 (see below). The mixing proportions predicted by M3 and PHREEQC (but only considering the models containing exactly the same end members as M3) for the two saline samples modelled are shown in Table 5-45.

Table 5-45. Variation ranges in the mixing proportions as computed by PRHEEQC and M3 for saline groundwaters from the Simpevarp subarea (Borehole KSH01A).

	Sample 5260 at 161.75 m		Sample 5266 at 253.25 m	
	PHREEQC	M3	PHREEQC	M3
Brine	9.2–10.5	9.5	9.5–11.5	10.8
Glacial	34.0–42.1	46.02	36.4–44.8	51.7
LitorinaLittorina	0–9.3	9.5	0.0–7–4	9.4
Sea Sediment	0–17.0	9.5	0.0–14.9	9.4
Rain 60	17.4–36.0	16.0	17.5–35.1	9.4
Lake water	5.3–13.6	9.5	4.5–14.2	9.4

M3 modelling

An additional modelling approach which is useful in helping judge the origin, mixing and major reactions influencing groundwater samples is the M3 modelling concept (Multivariate Mixing and Mass-balance calculations) detailed in /Laaksoharju et al, 1995/ and /Laaksoharju et al, 1999b/.

Introduction and model description

M3 is a water classification model and the results describe a possible occurrence of different water types in the bedrock and how these water types relate to each other in terms of mixing and reactions. The results should not be misinterpreted as a flow modelling of the site, but rather as a description of the similarities or differences between samples. M3 modelling uses a statistical method to analyse variations in groundwater compositions so that the mixing components, their proportions, and chemical reactions are revealed. The method estimates the contribution to hydrochemical variations by mixing of groundwater masses in a flow system by comparing groundwater compositions to identified reference waters. Subsequently, contributions to variations in non-conservative solutes from reactions can be calculated.

The M3 method consists of 4 steps where the first step is a standard principal component analysis (PCA), selection of reference waters, followed by calculations of mixing proportions, and finally mass balance calculations (for more details see /Laaksoharju et al, 1999b; Laaksoharju, 1999/). The PCA applied to data from the Simpevarp area (regional model) and data from all Nordic Sites is illustrated in Figure 5-62, where 223 samples from the Simpevarp area were used in the calculations. The numerical values are presented in /Laaksoharju, 2004b/ where also the M3 results using only data from the Simpevarp subarea (local model) are presented. The regional model is discussed further, since it better reflects the Simpevarp data in relation to other Nordic Site data such as Forsmark. In the future, when more data become available from the Simpevarp subarea, the local model will be used for site modelling and visualisation of the mixing proportions.

The reference waters used in the regional M3 modelling have been identified from: a) previous site investigations (e.g. Äspö HRL and Laxemar), b) the evaluation of the Simpevarp primary data set in Chapter 4 (for groundwater analytical data c.f. Table 5-46), and c) selecting possible compositions of Meteoric (Precipitation and Lake water), Marine (Littorina Sea and Modified Sea), Glacial and Brine reference water which, according to the post-glacial conceptual model (cf. Figure 3-14) may have affected the site. The selected reference waters are more extreme than actually present at Simpevarp (e.g. Rain-60 or Littorina Sea). Their function is a) to be able to compare differences/similarities of the Simpevarp groundwaters with possible end-members, b) to be able to model all available Nordic data used in the regional model. For the local model, local end-members will be used c.f. /Laaksoharju, 2004b/. The reference waters should not be regarded as point sources of flow but rather as possible contributors to the obtained water type.

- **Brine water:** Represents the sampled deep brine type (Cl = 47,000 mg/L) of water found in KLX02: 1,631–1,681 m /Laaksoharju et al, 1995/. The origin (autochthone/allochtone) of this water type has been discussed e.g. by /Laaksoharju and Wallin, 1997/, Processes such as water rock interaction, mixing, diffusion and leaching have altered the composition of this water type. An old age for the Brine is suggested by the measured 36Cl values indicating a minimum residence time of 1.5 Ma for the Cl component /Laaksoharju and Wallin, 1997/. The sample contains some tritium (TU 4.2) which is believed to be contamination from borehole activities. In the modelling the measured values were used for this sample.
- **Glacial water:** Represents a possible melt-water composition from the last glaciation >13,000BP. Modern sampled glacial melt water from Norway was used for the major elements and the $\delta^{18}O$ isotope value (−21 ‰ SMOW) was based on measured values of $\delta^{18}O$ in calcite surface deposits /Tullborg and Larson, 1984/. The $\delta^{2}H$ value (−158 ‰ SMOW) is a calculated value based on the equation ($\delta H = 8 \times \delta^{18}O + 10$) for the meteoric water line.
- **Littorina Sea:** Represents old marine water and its calculated composition has been based on /Pitkänen et al, 1999/. This water is used for modelling purposes to represent past Baltic Sea water composition.

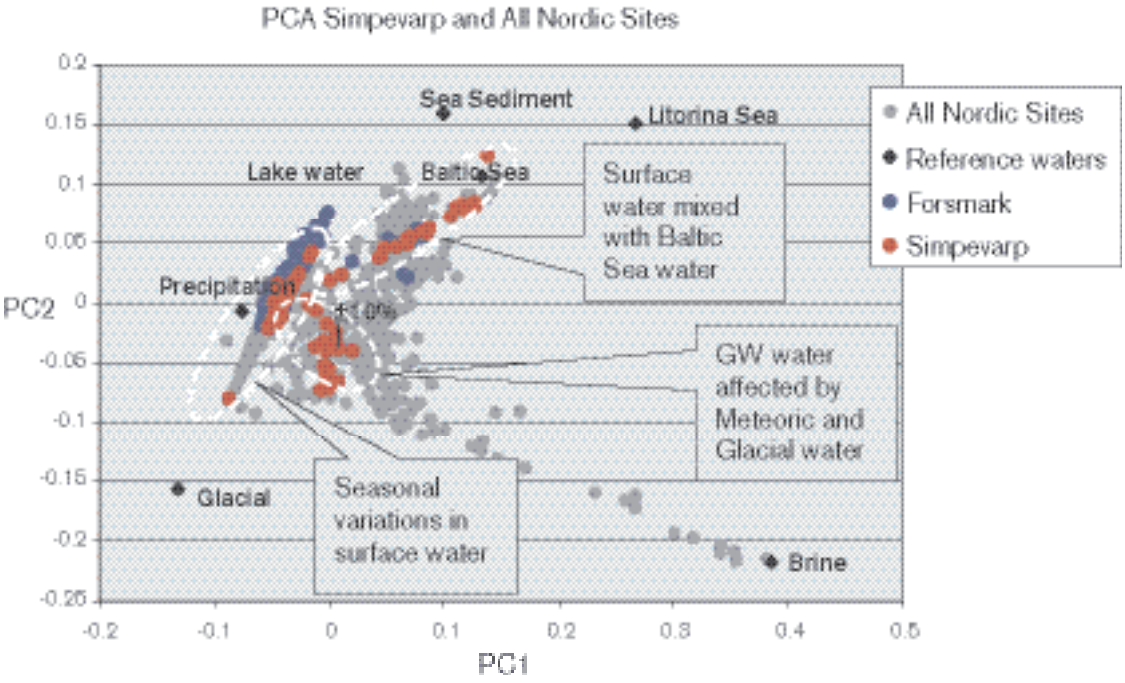

Figure 5-62. *This figure shows the principal components analysis and the location of the identified reference waters (Variance: First principal component: 0.42223, First and second principal components: 0.67221, First, second and third principal components: 0.77987). The figure shows the Nordic samples, the Simpevarp data (in red) and the Forsmark data (in blue). The Lake water (Forsmark), Sea sediment, Marine (Littorina), Brine, Glacial and Precipitation reference waters are used as end members for the modelling. The model uncertainty ±10% is shown here as error bar (in black); the analytical uncertainty is ±5% and represents therefore half of the error bar.*

Table 5-46. Groundwater analytical or modelled data* used as reference waters in the M3 regional modelling for Simpevarp.

	Cl (mg/L)	Na (mg/L)	K (mg/L)	Ca (mg/L)	Mg (mg/L)	HCO_3 (mg/L)	SO_4 (mg/L)	^3H (TU)	δ^2H ‰	$\delta^{18}O$ ‰
Brine	47,200	8,500	45.5	19,300	2.12	14.1	906	4.2	–44.9	–8.9
Glacial	0.5	0.17	0.4	0.18	0.1	0.12	0.5	0	–158*	–21*
LitorinaLitto-rina sea*	6,500	3,674	134	151	448	93	890	0	–38	–4.7
Sea Sediment	4,920	2,300	29	730	233	1,200	36	14	–50.4	–7.3
Precipitation	0.23	0.4	0.29	0.24	0.1	12.2	1.4	2,000*	–80	–10.5
Lake water	45.8	21	3.21	30.3	5.9	110	16.18	7.6	–44.3	–4.5

- **Modified Sea water (Sea sediment):** Represents sea water affected by microbial sulphate reduction.
- **Precipitation:** Corresponds to infiltration of meteoric water (the origin can be rain or snow) from 1960. Sampled modern meteoric water with a modelled high tritium (2,000 TU) content was used to represent precipitation from that period.
- **Lake water:** Corresponds to lake water affected by evaporation indicated by high $\delta^{18}O$ values and a slight evaporation modification of the deuterium value.

Based on past experience (e.g. from the Äspö HRL and Laxemar sites), the following six reactions have been considered in the M3 modelling:

Organic decomposition: This reaction is detected in the unsaturated zone associated with Meteoric water. This process consumes oxygen and adds reducing capacity to the groundwater according to the reaction: $O_2 + CH_2O \rightarrow CO_2 + H_2O$. M3 reports a gain of HCO_3 as a result of this reaction.

Organic redox reactions: An important redox reaction is reduction of iron III minerals through oxidation of organic matter: $4Fe(III) + CH_2O + H_2O \rightarrow 4Fe^{2+} + 4H^+ + CO_2$. M3 reports a gain of Fe and HCO_3 as a result of this reaction. This reaction takes place in the shallow part of the bedrock associated with influx of Meteoric water.

Inorganic redox reaction: An example of an important inorganic redox reaction is sulphide oxidation in the soil and the fracture minerals containing pyrite according to the reaction: $HS^- + 2O_2 \rightarrow SO_4^{2-} + H^+$. M3 reports a gain of SO_4 as a result of this reaction. This reaction takes place in the shallow part of the bedrock associated with influx of Meteoric water.

Dissolution and precipitation of calcite: There is generally a dissolution of calcite in the upper part and precipitation in the lower part of the bedrock according to the reaction: $CO_2 + CaCO_3 \rightarrow Ca^{2+} + 2HCO_3^-$. M3 reports a gain or a loss of Ca and HCO_3 as a result of this reaction. This reaction can take place in any groundwater type.

Ion exchange: Cation exchange with Na/Ca is a common reaction in groundwater according to the reaction: $Na_2X_{(s)} + Ca^{2+} \rightarrow CaX_{(s)} + 2Na^+$, where X is a solid substrate such as a clay mineral. M3 reports a change in the Na/Ca ratios as a result of this reaction. This reaction can take place in any groundwater type.

Sulphate reduction: Microbes can reduce sulphate to sulphide using organic substances in natural groundwater as reducing agents according to the reaction: $SO_4^{2-} + 2(CH_2O) + OH^- \rightarrow HS^- + 2HCO_3^- + H_2O$. This reaction is of importance since it may cause corrosion of the copper canisters. Vigorous sulphate reduction is generally detected in association with marine sediments that provide the organic material and the favourable salinity interval for the microbes. M3 reports a loss of SO_4 and a gain of HCO_3 as a result of this reaction. This reaction modifies the seawater composition by increasing the HCO_3 content and decreasing the SO_4 content.

Model results

The M3 modelling indicated three water types (Figure 5-62), one dominated by meteoric water and the second affected by marine water and the third saline groundwater affected by glacial and meteoric water. The surface meteoric type shows seasonal variations. Closer to the coast the influence of marine water is detected for the shallow samples. At depth, glacial and meteoric waters have affected the saline groundwater. The deviation calculations in the M3 mixing analysis show the potential for organic decomposition/calcite dissolution in the shallow water. Indications of ion exchange and sulphate reduction have been modelled. These M3 results essentially support the initial evaluation of primary data in Section 4.9 and the PHREEQC results described in previous parts of this section.

Model uncertainties

The following factors result in uncertainties in the M3 calculations:

- Errors in input hydrochemical data originating from sampling errors caused by the effects from drilling, borehole activities, extensive pumping, hydraulic short-circuiting of the borehole and uplifting of water which changes the in situ pH and Eh conditions of the sample, plus analytical errors.
- Conceptual errors such as wrong general assumptions, selection of wrong type/number of end-members and mixing samples that are not well mixed.
- Methodological errors such as oversimplification, bias or non-linearity in the model, and the systematic uncertainty that is attributable to use of the centre point to create a solution for the mixing model.

An example of a possible conceptual error is the assumption that the groundwater composition is a good tracer for the groundwater flow system. The water composition is not necessarily a tracer of mixing directly related to flow beacause there is not a point source as there is when labelled water is used in a tracer test.

Uncertainty in mixing calculations is smaller near the boundary of the PCA polygon and larger near its centre. The uncertainties have been handled in M3 by calculating an uncertainty of 0.1 mixing units (with a confidence interval of 90%) and stating that a mixing portion <10% is under the detection limit of the method. The similarities with the PHREEQC mixing modelling, although the approaches are very different, do lend support to the results obtained.

Visualisation of the groundwater properties

The 3D/2D visualisation of the Simpevarp Cl values was performed with the Tecplot code.

Figure 5-63 shows the 3D and the 2D visualisation of Cl at the 118 sampling points with values used in M3 calculations at Simpevarp. The few samples from depth did not allow any 3D interpolation of the Cl distribution or of the M3 mixing calculations.

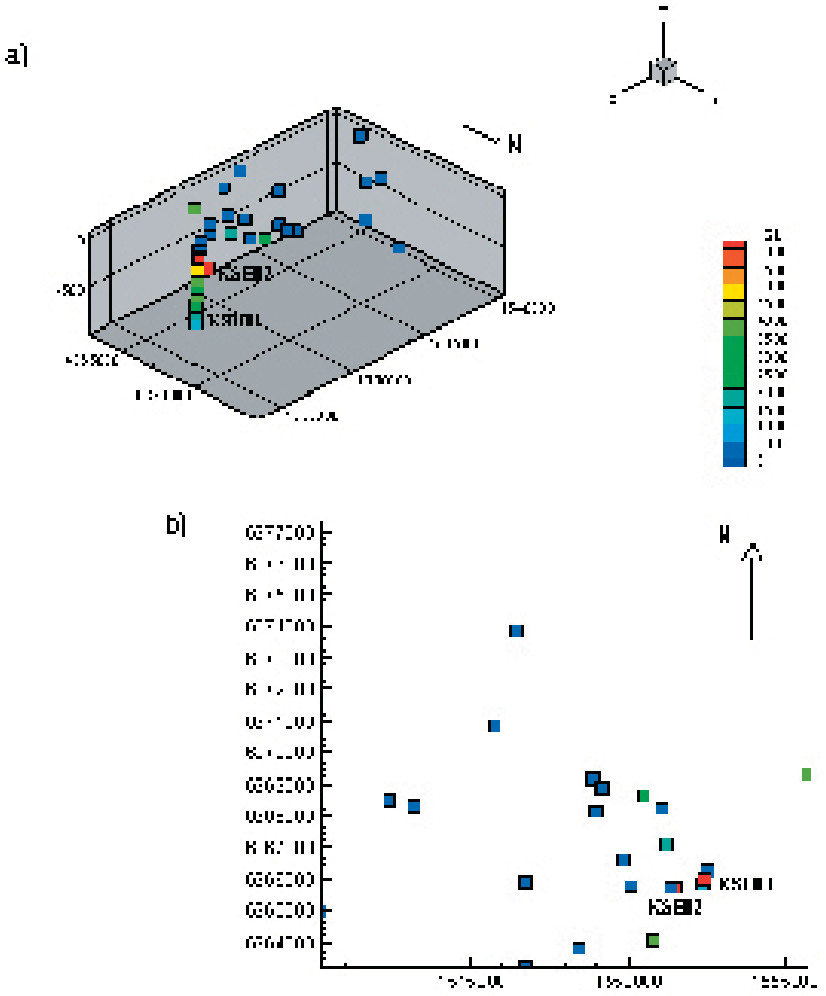

Figure 5-63. *3D (a) and 2D (b) visualisation of the Cl distribution and sampling points at Simpevarp. The x, y, z coordinates represent the Easting, Northing and elevation of the middle point of the sampling section as the locastions of the sampling points, and are expressed in metres. The continuous sampling in KSH01A is from tube sampling and does not reflect the salinity in the fractured rock.*

5.5.4 Comparison between hydrogeological and hydrogeochemical models

Since hydrogeology and hydrogeochemistry deal with the same geological and hydrodynamic media when describing the bedrock groundwater properties, these two disciplines should complement each other when modelling the studied groundwater system. Testing such an integrated modelling approach was the focus of a SKB project (Äspö Task Force Task 5) based on data from the Äspö HRL /Wikberg, 1998; Svensson et al, 2002; Rhen and Smellie, 2003/. The advantages with such an approach were identified as follows:

- Hydrogeological models will be constrained by a new data set. If, as an example, the hydrogeological model cannot produce any Meteoric water at a certain depth and the hydrogeochemical data indicates that there is a certain fraction of this water type at this particular depth, then one or other models has to be revised.
- Hydrogeochemical models generally focus on the effects from reactions on the obtained groundwater rather than on the effects from transport. An integrated modelling approach can describe flow directions and hence help to understand the origin of the groundwater. The turnover time of the groundwater system can indicate the relative age of the groundwater, and knowing the flow rate, this information can be used to indicate reaction rates. As groundwater chemistry is a result of reactions and transport, only an integrated description can be used to correctly describe the measured data.
- By comparing two independent modelling approaches a consistency check is made. As a result greater confidence in the characterisation of active processes, geometrical description and material properties can be gained.

Recent major developments in hydrogeological modelling of the Simpevarp area, c.f. Section 5.4, represents further progress since the Task 5 exercise /Rhén and Smellie, 2003/. The present modelling should further facilitate future comparison and integration between hydrochemistry and hydrogeology. The hydrogeological model can potentially provide predictions of the salinity in the connected rock matrix, in the flowing groundwater and be used for dynamic predictions over time for the different water types (meteoric, marine, glacial, and brine). Furthermore, the hydrodynamic model can, independently from hydrogeochemistry, predict these salinity features at any point of the modelled rock volume, and the predictions can be checked by direct hydrochemical measurements or calculations. The mixing proportions from the hydrogeological model could in the future, for example, be directly compared with the mixing calculations from the hydrochemical modelling or, conversely, the hydrochemical model could be used to predict the chemistry that results from transport alone and which, in turn, can be compared with that obtained from reactions. The modelling will increase the understanding of transport, mixing and reactions and will also provide a tool for predicting future chemical changes due to alterations in climate.

5.5.5 Evaluation of uncertainties

At every phase of the hydrogeochemical investigation programme – drilling, sampling, analysis, evaluation, modelling – uncertainties are introduced that have to be accounted for, addressed fully and clearly documented to provide confidence in the end result, whether for use in the site descriptive model or repository safety analysis and design /Smellie et al, 2002/. Handling the uncertainties involved in constructing a site descriptive model has been documented in detail by /Andersson et al, 2001, 2002b/. The uncertainties can be conceptual uncertainties, data uncertainty, spatial variability of data, chosen scale, degree of confidence in the selected model, precision, accuracy and bias in the predictions. Some of the identified uncertainties recognised during the Äspö HRL modelling exercises e.g. /Laaksoharju, 1999/ are discussed below.

The following data uncertainties have been estimated, calculated or modelled for the Simpevarp data; these are based on models used for the nearby Äspö HRL Model Domain /Laaksoharju, 1999; Smellie et al, 2002/ where similar uncertainties are considered to affect the present modelling (the uncertainties indicate the possible variation in % from reported values):

- disturbances from drilling; may be ± 10–70%,
- effects from drilling during sampling; are <5%,

- sampling; may be ± 10%,
- influence associated with the uplifting of water; may be ± 10%,
- sample handling and preparation; may be ± 5%,
- analytical error associated with laboratory measurements; is ± 5%,
- mean groundwater variability during groundwater sampling (first/last sample); is about 25%.
- The M3 model uncertainty; is ±0.1 units within 90% confidence interval.

Conceptual errors can occur in, for example, the palaeohydrogeological conceptual model. The influences and occurrences of end members representing old water in the bedrock can only be indicated by using certain elements or isotopic signatures. The uncertainty generally increases with the age of the end member. The relevance of an end member participating in groundwater formation can be tested by introducing alternative end member compositions, or by using hydrodynamic modelling to test if old water types can reside in the bedrock at prevailing hydrogeological conditions.

Uncertainties in the PHREEQC code depend on which version of the code is being used. Generally the analytical uncertainties and uncertainties concerning the thermodynamic data bases are of importance (in speciation-solubility calculations). Care is also required to select mineral phases that are realistic (better still if they have been positively identified) for the systems being modelled. The errors can be addressed by using sensitivity analyses, alternative models and descriptions. Such analysis was regarded to be outside the scope of work for version Simpevarp 1.1, due to lack of groundwater data.

The uncertainty inherent in 3D interpolation and visualisation depends on various issues, i.e. data quality, distribution, model uncertainties, assumptions and limitations introduced. The uncertainties are, therefore, often site specific and some of them can be tested, such as the effect of 2D/3D interpolations, by comparing with measured outcomes. The site-specific uncertainties can be tested by using quantified uncertainties, alternative models, and comparisons with independent models, such as hydrogeological simulations. However, tests concerning the Simpevarp subarea were not possible because of the lack of groundwater data.

The discrepancies between different modelling approaches can be due to the differences in the boundary conditions used in the models or in the assumptions made. The noted discrepancies between models should be used as an important contribution to validation and confidence building, which will be used to guide further modelling efforts.

5.6 Modelling of transport properties

5.6.1 Modelling assumptions and input from other models

The site descriptive transport modelling presents two types of transport parameters: retardation (diffusion and sorption) parameters associated with geological units (rock mass and structural units), and flow-related parameters associated with flow paths. The process of site descriptive modelling is described by /Berglund and Selroos, 2003/. The methods within the transport programme produce primary data on the retardation parameters, that is, the porosity, θ_m, the effective diffusivity, D_e, and the linear equilibrium sorption coefficient, K_d. These retardation parameters are evaluated, interpreted and presented in the form of a retardation model that constitutes the final product of the data evaluation.

The development of retardation models relies to large extent on interactions with other disciplines, primarily geology and hydrogeochemistry. Specifically, geology provides lithological and structural models where the rock types, fractures and fracture zones are described, as well as the mineralogical compositions of intact and altered materials. Hydrogeochemical information is important for the selection of water compositions in laboratory measurements of retardation parameters. Furthermore, hydrogeochemical data, and results from geological-hydrogeochemical analyses of fracture materials, are important inputs to the development of a site-specific understanding of the retention processes.

In the three-dimensional modelling, retardation parameters are assigned to the geological units of the site descriptive model. Generally, these units include both intact rock mass and structures (fractures and fracture zones). The latter could be parameterised by assigning “type structures” with a set of layers of altered and/or gouge materials. However, the present model is restricted to retardation parameters for intact rock only.

The flow-related parameters considered in the present model are the F parameter (“F-factor” or “transport resistance”), and the advective (water) travel time, t_w. These parameters are obtained from particle-tracking simulations in groundwater flow models provided by hydrogeological work. The site descriptive model is focused on flow-related transport parameters associated with the present groundwater flow situation, whereas other scenarios will be considered in the particle tracking simulations performed by Safety Assessment. However, for reasons described in Section 5.6.4 the flow-related transport parameters obtained from the large-scale flow simulations in Simpevarp 1.1 should not be regarded as equivalent, or even comparable, to Safety Assessment performance measures. In the present context, the transport parameters are used as generalised measures of the properties of flow paths associated with the relatively large-scale structures included in the flow models.

A key assumption of the model development is the selection of retardation parameters to be measured and included in the site descriptive models, that is, the assumption that diffusion and sorption are the main retention mechanisms. In future model versions, this assumption should be substantiated by field observations and/or modelling. The basis for such supporting analyses is very weak at the present stage of the site descriptive modelling, although supporting information is available from projects at the Äspö HRL. Both “old” Äspö data and new data from Simpevarp could be used in future evaluations of site understanding and model confidence, provided that similarities between Äspö and the Simpevarp site can be demonstrated when the new data become available.

5.6.2 Conceptual model with potential alternatives

The conceptual model underlying the present descriptive model is based on a description of solute transport in discretely fractured rock. Specifically, the fractured medium is viewed as consisting of mobile zones, i.e. fractures and fracture zones (deformation zones), where groundwater flow and advective transport take place, and immobile zones in rock mass and fractures where solutes can be retained (temporarily or permanently removed from the mobile water). In the safety assessment framework that provides the basis for identification of retention parameters in the site descriptive models, retention is assumed to take place as a result of diffusion and linear equilibrium sorption. These processes are reversible and are here referred to as retardation processes.

Alternative conceptual models could involve different retention processes and alternative descriptions of the presently considered processes. Furthermore, different conceptualisations of the flow paths (continuum-based, discrete or mixed) could be considered. In the present modelling work, however, neither alternative models for retention/retardation nor alternative descriptions of flow paths have been analysed.

5.6.3 Transport properties of rock domains

As stated in Section 4.10, no site-specific data from laboratory or in situ measurements of retardation parameters are available for the present model version. However, a joint evaluation of site-specific geological information and retardation data obtained at Äspö near the Simpevarp investigation area has been performed. The aim was to relate the Äspö database on retardation parameters to the Simpevarp area, primarily based on geological similarities.

The assessment of Äspö data briefly described in Section 4.10 showed that only the investigations reported by /Byegård et al, 1998, 2001/ met the criteria on laboratory methods and supporting geological and hydrogeochemical information. A comparison was made between the geological characteristics of the samples used in these previous studies and the rock types identified within the Simpevarp area. It was found that retardation parameters are available for two of the rock types at Simpevarp: quartz monzodiorite (Äspö diorite; one of the three main rock types in the area), and fine-grained granite (found in dykes).

In accordance with the strategy for laboratory measurements during the site investigations, formation factors, $F_m = D_e / D_w$ (D_w is the free diffusivity in water), were calculated based on the measured diffusivities of HTO (tritiated water). The diffusion dataset was further constrained by neglecting samples with porosities outside the ranges reported in the petrophysical data from Simpevarp for each the two rock types studied /Mattsson et al, 2003/. The resulting formation factors are $(5.9 \pm 0.8) \times 10^{-5}$ for the quartz monzodiorite and $(8.2 \pm 5.9) \times 10^{-5}$ for the fine-grained granite, are given as mean values ± one standard deviation for each dataset (six F_m values per rock type). The mean values are slightly higher than that underlying the SR 97 database, 4.2×10^{-5} /Ohlsson and Neretnieks, 1997/.

In the strategy for the site descriptive transport modelling, it is proposed that the formation factor is evaluated from diffusion measurements with HTO (and complementary measurements of the electrical resistivity), and then used to calculate the effective diffusivities of individual radionuclides (that is, $D_e = F_m D_w$ with D_w-values for each nuclide). This approach is similar to the one proposed in /Ohlsson and Neretnieks, 1997/. Based on the evaluation of formation factors outlined above, it is concluded that there is not sufficient evidence to assume diffusivities other than those provided in the SR 97 database, or to increase or decrease the uncertainty ranges indicated there. This conclusion is mainly motivated by the fact that only one of the three main rock types within the investigated area is represented in the Äspö data. Further "import" of Äspö data could be possible, primarily for the Ävrö granite, but must be substantiated by additional data.

It can also be noted that the porosities for quartz monzodiorite and fine-grained granite in both the petrophysical dataset and the Äspö data are quite similar to the value that was used in the generic database (0.5%). According to the petrophysical data, one of the main rock types at Simpevarp, the fine-grained dioritoid, has a somewhat lower porosity than the others, 0.3%. Whether this lower porosity corresponds to a lower retardation capacity cannot be judged based on the existing knowledge. However, all the main rock types at Simpevarp have been sampled, and the results of ongoing laboratory measurements will show whether they exhibit (significant) differences in their retardation properties.

Sorption parameters, that is, K_d-values, were also determined during the TRUE project and reported by /Byegård et al, 1998, 2001/. No other sorption data from Äspö that could be used in the description of the Simpevarp area were found in the data assessment performed. Results from batch experiments with sorption of cesium (Cs) and strontium (Sr) on quartz monzodiorite and fine-grained granite are available in the Äspö dataset. These K_d-values are applicable for water compositions consistent with those in the experiments; saline groundwaters with Cl: 5,400–8,350 ppm, Na: 1,735–2,400 ppm, and Ca: 1,310–2,540 ppm.

The Äspö sorption database has been evaluated using the methods proposed by /Widestrand et al, 2003/, which means that the effect of surface sorption was considered (and quantified) and that analogies were used to obtain K_d-values for additional radionuclides. Specifically, the K_d-value for Radium (Ra) was estimated from that of Sr, and the K_d-value for silver (Ag) from that of Cs; the analogies are the same as in /Carbol and Engkvist, 1997/.

A comparison between the resulting Äspö K_d-values and the SR 97 database /Carbol and Engkvist, 1997; data for saline groundwater/ shows that all mean values for sorption on fine-grained granite are approximately one order of magnitude lower than the corresponding values in the generic database. The interpreted mean values are also below the lower limits of the uncertainty intervals in the database. For sorption on quartz monzodiorite, the interpreted mean Äspö K_d-values of Sr (and Ra) are a factor of five lower than those in the SR 97 database, and also outside (below) the uncertainty intervals. The Äspö K_d-values for sorption of Cs (and Ag) on quartz monzodiorite are approximately the same as the corresponding values in the generic database.

A possible conclusion of the above comparison could be that the sorption on site-specific materials is weaker than indicated by the generic database, which means that the retardation capacity of the rock is over-estimated if the database is used as a basis for transport calculations. However, the presently available "site-specific" dataset is quite limited, in terms of the geological materials, water compositions and radionuclides represented. Thus, the results are taken as an indication of the need for further investigations of the sorption on site-specific materials, rather than as definite evidence that a lower sorption capacity should be adopted for the site. For the site descriptive model version Simpevarp 1.1, it is recommended that the SR 97 database is used without modifications.

5.6.4 Transport properties of flow paths

The flow-related transport parameters F and t_w, which characterise advective transport and the conditions for mass transfer along flow paths, are calculated using groundwater flow models. Specifically, two different codes, DarcyTools and ConnectFlow, are used within the site descriptive modelling, c.f. Section 5.4. The groundwater flow modelling performed in support of the Simpevarp 1.1 model, including the calculations of flow-related transport parameters, is described in detail in background reports from the modelling teams /Follin et al, 2004; Hartley et al, 2004/. The present description is focused on the results obtained with DarcyTools, as reported by /Follin et al, 2004/. The reason for focusing on these results is that the DarcyTools team performed an extensive sensitivity study, which is considered as a main contribution to the transport description at the present (early) stage of model development. Thus, this choice does in no way reflect a general preference of the one code over the other.

In a continuum framework, F can be defined as $F = \Sigma\, a_r\, L / q$, where summation is made along the whole flow path, a_r is the flow-wetted surface per unit volume of rock, L is the length of the flow path, and q is the Darcy velocity. This definition is the starting point of the Simpevarp 1.1 continuum calculations with ConnectFlow. Specifically, a_r is calculated for each grid cell based on geometric information in the underlying DFN (Discrete Fracture Network) description. In DarcyTools, F is calculated as $F = \Sigma\, a_w\, t_{w,i}$, where summation again is along the whole flow path, a_w is the flow-wetted surface per unit volume of mobile water, and $t_{w,i}$ is the advective travel time (in each cell; also the other parameters under the summations refer to cell-wise values). Thus, F is defined as an integrated parameter that captures spatial variability along an individual flow path; this variability also implies that different flow paths have different F values. Similarly, the travel time of a flow path, t_w, is calculated by integrating local parameters, as indicated by the second definition of F above.

The method for calculating F and t_w in DarcyTools is described by /Follin et al, 2004/, and in more detail by /Svensson et al, 2004/. The starting point of the flow and transport analysis is a description of the deterministic features (larger fracture zones) and a stochastic DFN (Discrete Fracture Network) description of the fractured medium. The deterministic structures and the DFN are used to calculate the grid cell properties of an equivalent porous medium, in which flow and transport simulations are performed. Thus, the geometric description of fractures and fracture zones is used as a basis for calculating porosities and fracture surface areas in the continuum model in which particle tracking is performed to calculate F and t_w.

In the Simpevarp 1.1 groundwater flow modelling, particles were released at a depth of 500 m below sea level within two “release areas”, within the Laxemar and Simpevarp subares, respectively, see Figure 5-64 and Figure 1-1. These areas were specified in a Task Description (TD) for the modelling, along with a set of parameters and boundary conditions. In the modelling with DarcyTools, the particles were released on a regular grid with a distance of 50 m between adjacent particles. The grid resolution in the flow model was set to 100 m in the horizontal directions in accordance with the TD. The discretisation was 100 m also in the vertical direction, except for in the uppermost part of the model. The particle tracking was performed in steady state flow fields representing the present situation at the site for different model variants (cf. below). Long-term, transient flow simulations were carried out to obtain the flow fields used in particle tracking, see /Follin et al, 2004/ for details.

When evaluating the particle tracking simulations, especially the calculated transport parameters F and t_w, it is important to note that the lower size (length) limit of the DFN was 100 m. Furthermore, particles were released in cells intersected by stochastic and/or deterministic structures only, and the rock mass between the structures was assumed not to contribute to flow-wetted surface, or to flow porosity. This means that structures smaller than 100 m were not considered explicitly in the model, such that particles were released into and transported in a fractured medium consisting of relatively large structures only. As smaller structures realistically can be expected to contribute significantly to the integrated F and t_w values of flow paths, this implies that these parameters are considerably underestimated in the present results. This is due to the fact that only a subset of the structures making up more realistic flow paths are considered in the model, but also to the release of particles at positions that would not be included in a more realistic transport scenario (i.e. in major deterministic deformation zones).

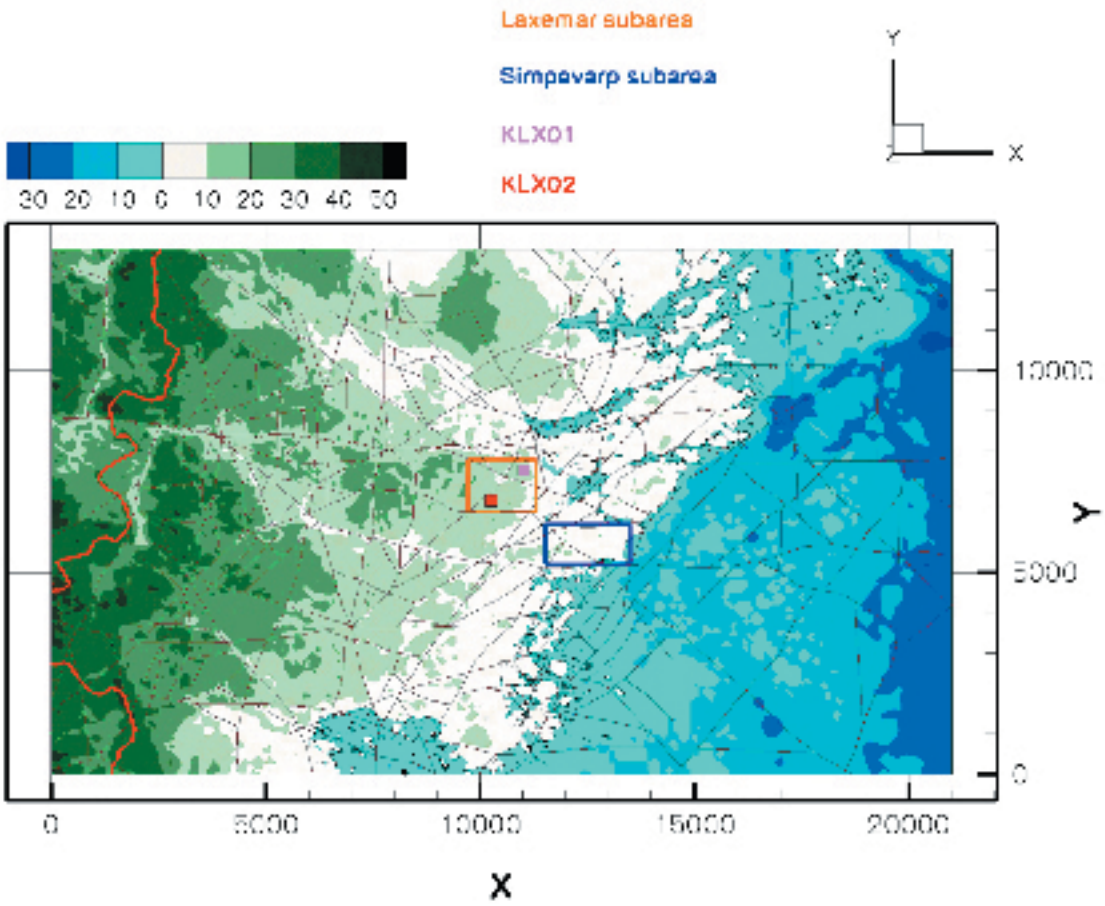

Figure 5-64. *Topographic map with linked lineaments and the two release areas considered in the Simpevarp 1.1 particle tracking simulations (cf. Figure 1-1). From /Follin et al, 2004/.*

The main implication of the model limitations described above is that the transport parameters should not be regarded as quantitative in the sense that they can be used in comparisons with safety criteria. Transport calculations in flow models with finer discretisations are performed by Safety Assessment. The present results can, however, be used for comparing different sensitivity cases, bearing in mind that the values only represent parts of "actual flow paths". Such quantifications are useful for setting the information provided by the visual impressions of the flow paths and the calculated path lengths into a relevant perspective. It should also be noted that other assumptions that affect the transport parameters have been made in the model development. In particular, the geometric surface area of the structures (flow-wetted surface), as calculated for each cell based on the DFN, is used without modification in the F calculation.

Transport parameters were calculated for a "base case" and a number of sensitivity cases, quantifying the effects of various, in some cases highly uncertain, assumptions made in the model development. Flow paths and travel distances (by release location) for the base case are illustrated in Figure 5-65. It can be seen that most of the particles released within the Simpevarp subarea are associated with short travel lengths, whereas the proportion of particles with longer travel lengths appears to be much larger for the release within the Laxemar subarea.

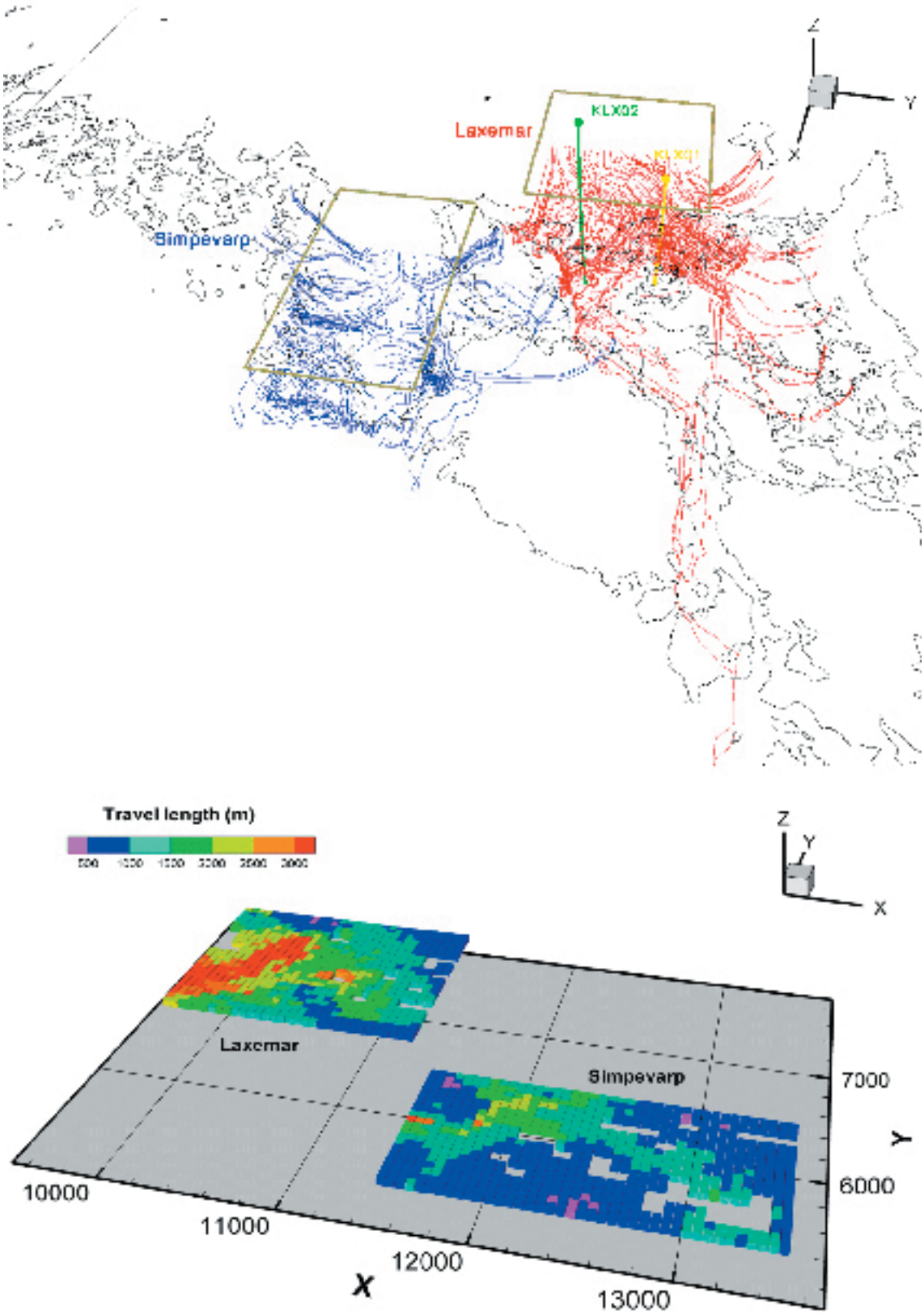

Figure 5-65. *Flow paths (top) and travel lengths (bottom) for particles released within the defined Laxemar and Simpevarp release areas (base case). Note the different orientations of the two illustrations. From /Follin et al, 2004/.*

The base case transport parameters F and t_w for all release positions in the two release areas are illustrated in Figure 5-66. Table 5-47 summarises the 5th, 50th and 95th percentiles from the particle-tracing results. Figure 5-66 indicates that both parameters are highly spatially variable and that the variability appears to follow a similar pattern. Table 5-47 provides a quantification of the variability; e.g. for F the normalised difference of the 95th and 5th percentiles is 19 and 14 for the release areas within the Laxemar and Simpevarp subareas, respectively. A comparison of the two defined release areas show that both F-values and travel times generally are larger in the Simpevarp case than for Laxemar, although the flow paths from the Laxemar release area are longer (on average). The relative difference is about 50% when normalised to the values for the Laxemar release. This should not be taken as a general observation on the differences between these two specific release areas, but illustrates that comparisons of transport conditions related to different release areas cannot be based on path lengths and/or visual impressions of flow paths only.

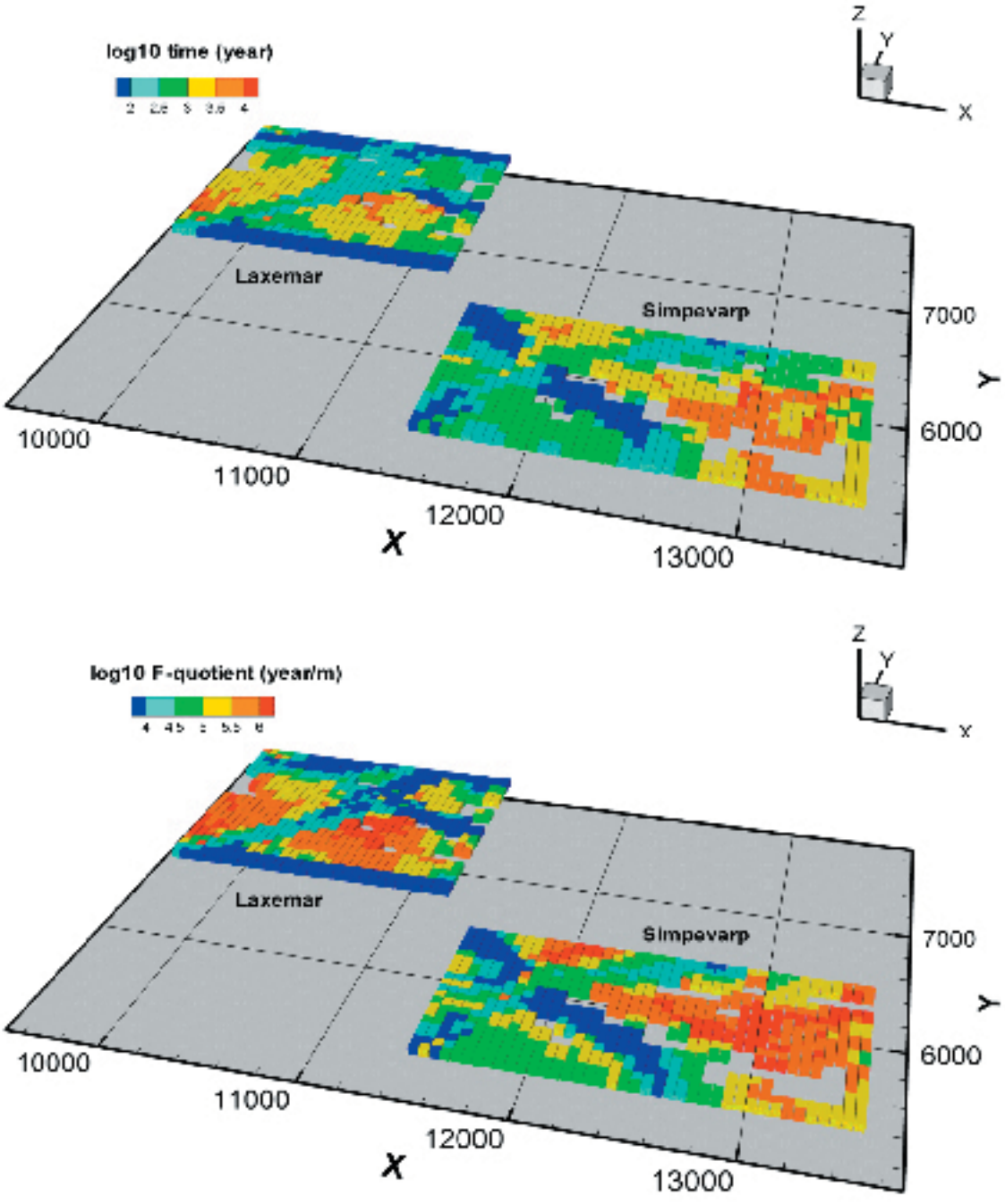

Figure 5-66. *Travel times (top) and F-values (bottom) for particles released within the defined Laxemar and Simpevarp release areas (base case). From /Follin et al, 2004/.*

Table 5-47. Summary of particle tracking results for large-scale flow paths (base case). Release from defined "release areas" within the Simpevarp and Laxemar subareas, c.f. Figure 5-64.

F (y/m)	Laxemar	Simpevarp
$F_{5\%}$	$3.3 \cdot 10^3$	$4.9 \cdot 10^3$
$F_{50\%}$	$6.4 \cdot 10^4$	$1.0 \cdot 10^5$
$F_{95\%}$	$1.2 \cdot 10^6$	$1.4 \cdot 10^6$
$(F_{95\%}–F_{5\%}) / F_{50\%}$	18.7	14.0
t_w (y)	**Laxemar**	**Simpevarp**
$t_{w,5\%}$	50	60
$t_{w,50\%}$	390	560
$t_{w,95\%}$	3,340	5,740
$(t_{w,95\%}–t_{w,5\%}) / t_{w,50\%}$	8.4	10.1

In the sensitivity cases where transport parameters were calculated, the effects of the following parameters and model features were studied:

- *The hydraulic properties of the uppermost rock layer (here: SC1):* In the sensitivity case, the hydraulic conductivity of the superficial rock layer was constant and lower than in the base case, in which fractures and fracture zones were allowed to penetrate also the uppermost layer.
- *The position of the salinity interface (SC2):* In the sensitivity case, the initial condition in the transient flow simulation that produced the present-day flow field for the particle tracking prescribed a more shallow salinity interface than in the base case.
- *The position of the western boundary of the model domain (SC3):* The sensitivity case had the western boundary of the flow model at the regional water divide, instead of further west at the boundary of the regional Simpevarp model domain.
- *The flow porosity of fractures and fracture zones (SC4):* In the sensitivity case, the flow porosity of fractures and fracture zones was reduced to 20% of the value used in the base case.
- *The effect of using a different DFN realisation (SC5):* The whole sequence of flow and particle tracking simulations was repeated for another DFN realisation generated with the same input parameters as the base case.
- *The transmissivity of stochastic fractures/fracture zones (SC6):* Transmissivities of stochastic structures were reduced by one order of magnitude.
- *The transmissivities of deterministic and stochastic fractures/fracture zones (SC7):* Transmissivities of both deterministic and stochastic structures were reduced by one order of magnitude.

For both release areas, the sensitivity case with reduced transmissivities of both deterministic and stochastic structures (SC7) has the largest effect on the transport parameters. The median values of F and t_w in SC7 increase by a factor of 4–10 relative to the base case, with the larger increases observed for the Laxemar release area.

Among the other sensitivity cases studied, SC1 (reduced K in the uppermost rock layer) had the largest effects on F-values and travel times for release within the Laxemar subarea; the median values increase by a factor of 2–3, because the frequency of low values decreases significantly when "fast paths" are eliminated by the introduction of a continuous, low-permeable top layer. Sensitivity cases with relatively large impact on the transport parameters for the Laxemar release included SC4 and SC5 (smaller median F and t_w compared to the base case) and SC6 (larger values). SC2 and SC3 had relatively small effects on the median values of the transport parameters, 20% or less.

For release within the Simpevarp subarea, SC6 (reduced transmissivities of stochastic structures) showed the second largest deviations from the base case; median F and t_w increased by a factor of 1–2 compared to the base case. However, SC1 and SC2 affected the transport parameters almost as much as SC6; F and t_w increase in both SC1 and SC2 for release within the Simpevarp subarea. The additional DFN realisation considered (SC5) resulted in c. 50% larger median F- and t_w-values than those calculated for the base case. The smallest effects, 30% or less, were obtained for sensitivity cases SC3 and SC4, which in both cases result in smaller values of the transport parameters than the base case.

Thus, it can be observed that the qualitative sensitivity effects are not necessarily consistent for the two defined release areas. Calculations performed for the alternative DFN realisation produce smaller values of the transport parameters for release locations within the Laxemar subarea and larger values for particles released within the Simpevarp subarea, as compared to the corresponding values for the base case. Also the comparisons of SC2 and SC3 with the base case showed qualitative differences between the two subareas. In particular, the changed (more shallow) position of the salinity interface in SC2 results in somewhat larger F and t_w for release within the Simpevarp subarea, whereas the effects are relatively small for release within the Laxemar subarea.

5.6.5 Evaluation of uncertainties

For the retardation (diffusion and sorption) parameters, the main uncertainties at the present stage of model development are associated with the fact that no site-specific data are available. The diffusion and sorption parameters that can be "imported" from Äspö provide information on only one of the main rock types at Simpevarp (quartz monzodiorite, or Äspö diorite), and one of the less frequently observed rock types (fine-grained granite). Thus, the conclusion is that there is insufficient site-specific evidence to reduce (or increase) the uncertainties in these parameters, as compared to an analysis based on generic data only.

It should be noted that the available Äspö database will continue to be used in later stages of model development. The Äspö data that has been compiled in connection with the Simpevarp 1.1 modelling work will be useful for parameterisation and uncertainty quantification, as a part of the total dataset that provides input data for the modelling, once the relations between geological materials at Äspö and those at the investigated site are more fully understood.

Spatial variability is an important potential source to uncertainty in diffusion and sorption parameters. In previous investigations of rock samples from Äspö and Laxemar, spatial variability has been observed in the form of differences between different rock materials, as well as variability among samples taken from the same (based on geological classification) materials /Byegård et al, 1998, 2001; Löfgren and Neretnieks, 2003; Xu and Wörman, 1998/. Furthermore, studies at Äspö indicated large differences in retardation properties for materials at different stages of alteration in the vicinity of fractures /Byegård et al, 1998, 2001/. These results show that significant (order of magnitude) spatial variability in retardation parameters can be expected for all these scales/types of variability. However, due to lack of data the significance of spatial variability in retardation parameters for the site-specific transport conditions at Simpevarp has not been evaluated in the present model version.

Obviously, the most important factor for reducing the uncertainties is to measure and evaluate site-specific retardation parameters. The strategy for the sampling programme is to use the first boreholes mainly to collect retardation data on the main rock types, and then perform additional sampling and analysis targeted on specific features and/or materials. The results discussed above emphasise the need for investigating the diffusion properties of the fine-grained dioritoid, and the sorption properties of the site-specific materials in general. Other, more specific issues that have been identified in the initial investigation stage are the potential effects of the commonly observed red-colouring and sealed fractures on the retardation properties of the rock. From a practical modelling perspective, it is important to evaluate if the identified main rock types show distinct differences in transport properties or if they can be treated as a single rock domain in the descriptive modelling of the intact rock.

Uncertainties in flow-related transport parameters (F and t_w) have been quantified in the sensitivity studies summarised above /see Follin et al, 2004 for details/. However, probably more important for the uncertainties in these parameters are the features not represented in the present, large-scale groundwater flow models, i.e. the fractures of sizes smaller than lower limit in the underlying DFN model. Specifically, the DFN model includes fractures/fracture zones in the length interval 100–1,000 m, which implies that fractures smaller than 100 m are not described explicitly in the model; particles are injected into and transported in cells intersected by stochastic and/or deterministic structures only

Generally, it can be expected that relatively large fractions of the total travel times and F-values for flow paths between repository depth and ground surface are associated with the smaller fractures. Therefore, the calculated transport parameters are not considered quantitative in the sense that they could be used for comparisons with safety criteria or other sites. However, the results are considered useful in a relative sense, primarily for comparing uncertainties and for the identification of unfavourable transport conditions on larger scales.

Based on the sensitivity studies reported by /Follin et al, 2004/ it can be concluded that all parameters considered can be associated with large uncertainties in the transport parameters. In particular, the sensitivity cases addressing the properties of the uppermost rock layer and the transmissivities of the stochastic structures show large differences compared to the base case. This emphasises the importance of the surface boundary condition and the uncertainties related to the DFN model of the fractured rock for the identified uncertainties.

5.7 Ecosystems properties description and modelling

5.7.1 Modelling assumptions and input from other models

According to the definition used in this report, the ecosystem starts at the surface of the deep bedrock. This means that any overburden material including Quaternary deposits, together with surface water and the biotic components, are included in the surface ecosystem. The abiotic parts of the ecosystem are described elsewhere in this report; the deposits (overburden including Quarternary deposits) in Section 5.1.2, the hydrology in Section 5.4.2, and the chemistry in Section 5.5. The surface ecosystem is described using a large number of properties which, when combined, will constitute the ecosystem site descriptive model /cf. Löfgren and Lindborg, 2003/. The surface ecosystem is divided into different subsystems based on the presence of system-specific processes and properties, and also on the collection, measurement and calculation of data that may differ between different subsystems. Accordingly, three different subsystems are characterised: (1) the *terrestrial system* which includes all land and wetland areas, (2) the *limnic system*, i.e. lakes and rivers, and (3) the *marine system*, constituted by the sea and brackish waters.

The budgets of organic and inorganic matter will be described within the different subsystems, where matter is recycled between organisms in the food web and the physical environment. Matter may also be accumulated within the subsystems, e.g. as peat, thereby leaving the circulation until some kind of disturbance occurs to release it to circulation again. Moreover, the different subsystems all interact with one another to some degree. For example, the terrestrial environment around a lake acts as a catchment area for rainwater and affects the lake through the runoff of water to the lake. The discharge area in the near-shore marine system is affected by the output from the lake and from the near-shore parts of the terrestrial system. Hydrological processes in the landscape are considered essential in connecting the different subsystems. The landscape is therefore divided into functional units defined by catchment areas that are constructed from surface water divides in the landscape. The flows of matter in the landscape are considered to be hydrologically driven in the present descriptive ecosystem model.

Since many of the ongoing investigations are not yet completed, no budgets of transport of matter have been developed for the version Simpevarp 1.1 of the Site Descriptive Model. Accordingly, no overall ecosystem model will be developed until budgets of matter have been described both within and between the different subsystems.

5.7.2 Biota

Producers

Terrestrial producers – biomass

Tree layer

Biomass of the tree layers in the model area was calculated using information from the local Forestry Management Plan, where data on standing crop (given as m^3sk/ha), were available. The basis for the geometrical resolution was the vegetation map of the area.

Biomass data were not available for all the different vegetation types as given in the vegetation map. Therefore, the vegetation types from the vegetation map were aggregated to five different classes; old (>30 yr) coniferous forests, young (≤30 yr) coniferous forests, deciduous (>70% deciduous trees) forests, no forests and water bodies. The latter two classes have no tree layer. The first three classes were assigned values of biomass (m^3sk/ha), calculated from the local Forestry Management Plan. This value only gives the biomass of the stems (i.e. trunk wood of trees), and therefore the biomass of the bark, pins, needles and roots had to be added. Calculations were made using data from the National Forest Survey /cf. Berggren and Kyläkorpi, 2002/. These calculations showed that the stem weight of old coniferous trees and deciduous trees in this area is 64% of the total above ground weight, and the corresponding value for young coniferous trees is 57%. Hereafter the weight of the root system had to be added. This information was obtained from /Lundmark, 1986/ which showed that the above-ground parts of the trees on average contribute 85% of their total weight.

The resultant values of total tree weight were then converted into dry weight by using the factor 0.42 /Jerling et al, 2001/ and thereafter to carbon content by using the factor 0.5 /Jerling et al, 2001/.

Shrub, field and ground layers

No measurements of the biomass of the model area shrub-, field- and ground layers have been conducted. Therefore, these were calculated using the input data from a study conducted in the Forsmark area /Fridriksson and Öhr, 2003/. In this study, the actual amount of carbon in six different vegetation types was measured; harvested areas, grazing areas, sea shores, wetlands, *Pinus* (Pine) dominated areas and *Picea* (Spruce) dominated areas. For each of these vegetation types, six sample plots were assessed and measured with regards to carbon content. Again, the basis for geometrical resolution was the vegetation map.

The different vegetation types of the vegetation map were aggregated to the six types studied in /Fridriksson and Öhr, 2003/. Subsequently, the average values of biomass dry weight in the different layers was calculated. These weight values were then translated to carbon content using the factor 0.453 in accordance with /Fridriksson and Öhr, 2003/.

For the categories deciduous forest, mixed forest and arable land, no in situ measure-ments of biomass have been conducted. Therefore, the deciduous forest was assigned the same value as grazing area and the mixed forest was assigned the same value as *Picea* forest.

The biomass of the arable land was calculated based on the standard yield figures of barley, which is the main crop cultivated in the model area /Berggren and Kyläkorpi, 2002/. To the standard yield of 287.4 g barley/m^2 /Berggren and Kyläkorpi, 2002/ were added generic values of threshing loss, straw yield and root production /Jerling et al, 2001/. The total figure was then translated to carbon content using the factor 0.453 in accordance with /Fridriksson and Öhr, 2003/.

The categories outcrop rock, water and artificially hardened surfaces were assigned zero values; i.e. no terrestrial biomass was assumed to exist.

Terrestrial producers – production

Tree layer

Production of the tree layer was calculated using data from the National Forest Survey. A previously selected set of 356 sample sites covering a relatively large area including and surrounding the model area /Berggren and Kyläkorpi, 2002/ was used in order to obtain mean values with an acceptable level of statistical certainty.

In the present estimation of production, stem growth (given in m^3sk/ha/yr) was calculated for the same plots as described above. Average values were used for the five different classes; old (>30 yr) coniferous forests, young (≤30 yr) coniferous forests, deciduous (>70% deciduous trees) forests, no forests and water bodies. In addition to stem growth, bark, pin, needle and root growth were included as for biomass calculations described above, assuming that all parts of the trees grow at constsnt rates in direct proportion to each other.

Shrub, field and ground layers

For the six different vegetation types studied in /Fridriksson and Öhr, 2003/, data on dry weight was partitioned into green and non-green categories. In order to arrive at production values, the assumption was made that all green vegetation fractions constitute the yearly production. However, as stated in /Chapin III et al, 2002/, the green biomass only reflects 40% of the total production, so this value was used to increase the green fraction figure. These dry weight values were then translated to carbon content using the factor 0.453 in accordance with /Fridriksson and Öhr, 2003/.

For the categories deciduous forest, mixed forest and arable land, no in situ measurements of biomass have been conducted. Therefore, the deciduous forest was assigned the same value as grazing area and the mixed forest was assigned the same value as Picea forest.

The production of the arable land was assumed to be the same as the standing crop biomass. Thus, the calculations were performed in the same way as described above. The categories bare rock, water and hard surfaces were assigned zero values; i.e. no terrestrial production was taken to occur.

The calculated biomass production rates for the different vegetation types within the separate layers are shown in Table 5-48 and the combined figures for the layers and for the total regional model area are shown in Table 5-49.

Table 5-48. Calculated biomass and production for different vegetation types in the Simpevarp regional model area.

	Vegetation type	Biomass (kgC/m^2)	Production (kgC/m^2/yr)
Tree layer	Old coniferous forest	7.65	0.21
	Young coniferous forest	2.55	0.09
	Deciduous forest	5.91	0.22
	No forest layer	0.00	0.00
	Surface water	0.00	0.00
Other layers	Harvested area	0.69	1.13
	Grazing area	0.19	0.35
	Sea shore	0.25	0.25
	Wetlands	0.57	0.61
	Pinus forest	0.73	0.73
	Picea forest	0.59	1.04
	Arable land	0.27	0.27
	Mixed forest	0.59	1.04
	Deciduous forest	0.19	0.35
	Rocky area	0.00	0.00
	Surface water	0.00	0.00
	Hard surface area	0.00	0.00

Table 5-49. Calculated biomass and production within vegetation layers and in total for the terrestrial vegetation in the Simpevarp regional model area. Mean values are based on the total land area in the regional model area.

	Total biomass (kg C)	Total production (kg C/yr)	Av. biomass (kg C/m^2)	Av. production (kg C/m^2/yr)
Tree layer	8.21 E8	2.41 E7	5.115	0.150
Other layers	7.96 E7	1.07 E8	0.496	0.669
Total	9.01 E8	1.32 E8	5.611	0.819

The calculated values for biomass and production per vegetation type were used to produce biomass and production maps for the tree layer and for the shrub, field and ground layers in the Simpevarp regional model area. These maps were finally converted to 10-metre grids (Figure 5-67).

Aquatic producers – limnic

Microphytobenthos

No new site-specific data were available for the Site Descriptive Model version Simpevarp 1.1.

Plankton

No new site-specific data were available for the Site Descriptive Model version Simpevarp 1.1.

Macrophytes

No new site-specific data were available for the Site Descriptive Model version Simpevarp 1.1.

Aquatic producers – marine

Microphytobenthos

No site-specific data were available for the Site Descriptive Model version Simpevarp 1.1.

Plankton

Chlorophyll A, as a measure of production, has been measured for the period 2002–2003. Mean chlorophyll A concentrations were just over 1 µg/l at the exposed coastal sites and 3,7 and 4,4 µg/l in the two sheltered inner sites, north and south of the island of Äspö. Peak concentrations (approximately 2 and 4 µg/l at the exposed sites and 8 and 10 µg/l in the sheltered sites) are found in April to May and in August (exposed coastal sites) and in October (exposed coastal site) respectively.

No new site-specific data concerning biomass and species composition were available for the Site Descriptive Model version Simpevarp 1.1.

Macrophytes

The macrophyte community was investigated and mapped during 2002 and showed four dominant communities:

- *Chara* dominated, covering a large part of the soft bottoms in the sheltered inner coastal waters, especially in the northern part (around Äspö) of the area.
- *Fucus vesiculosus,* covering shallow hard substrate, especially in wave-exposed areas.
- *Potamogeton sp*. and *Potamogeton/Zostera* community, covering most vegetated soft bottoms in the south part of the area.
- Red algae community, covering shallow and deeper hard substrate bottoms.

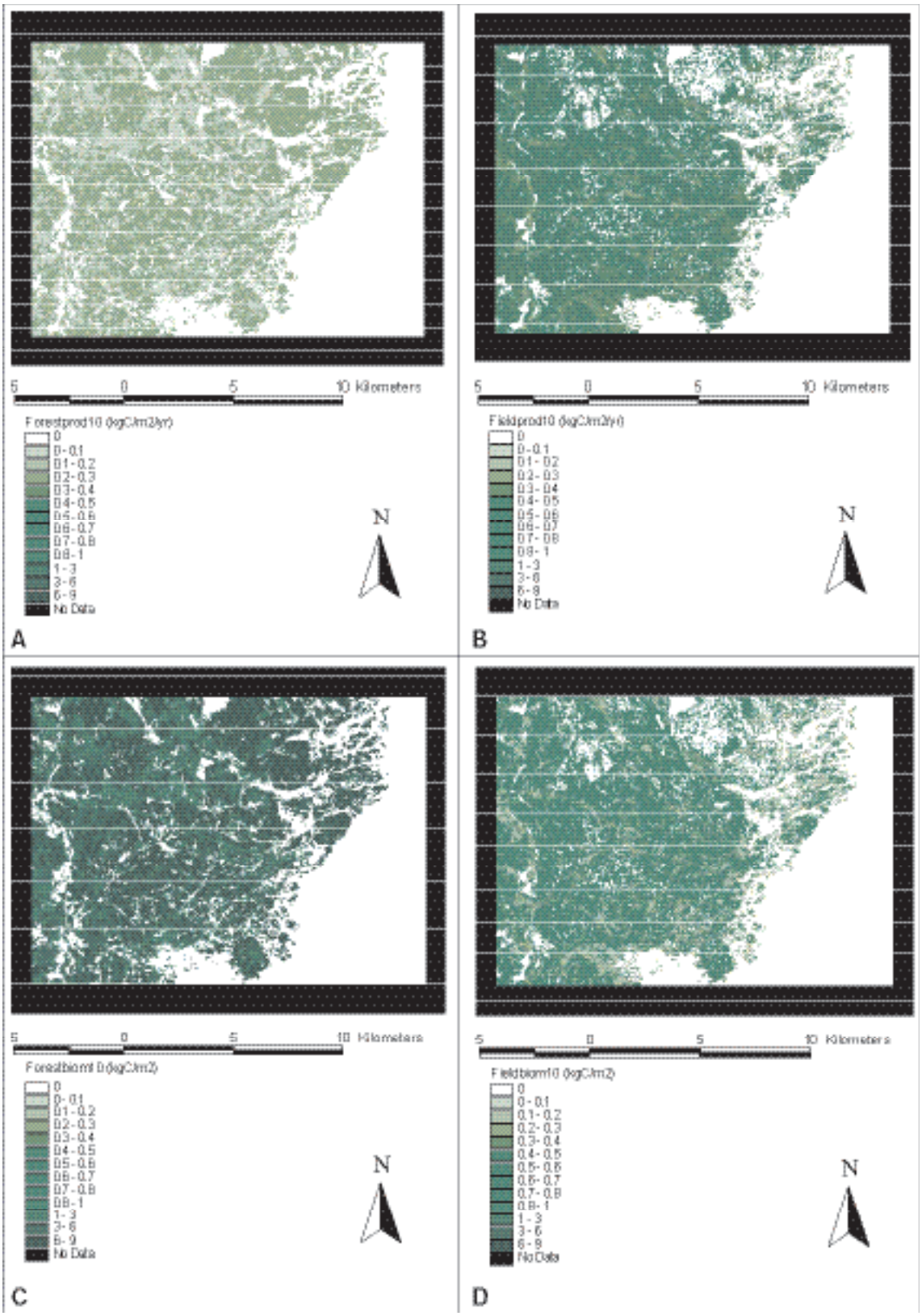

Figure 5-67. *Grid maps illustrating a) tree layer production, b) shrub, field and ground layer production, c) tree layer biomass, and d) shrub, field and ground layer biomass, in the Simpevarp regional model area.*

The *Fucus* community (*F. vesiculosus* and undergrowth) contribute with approximately 1/3 of the producer biomass in the benthic community; 550 ton calculated from an average biomass of 540 g dw/m^2 (including undergrowth), c.f. Figure 5-68 and Table 5-50. The *Chara* community and Red algae contributes with a total of 250 and 300 metric tonnes primary producing biomass respectively in the area (300 and 80 g dw/m^2 respectively). /Fredriksson and Tobiasson, 2003/

Consumers

Terrestrial consumers

No site-specific biomass data for terrestrial consumers, i.e. mammals or birds, are available for the Site Descriptive Model version Simpevarp 1.1. However, data on population abundances for a major part of the birds and mammals in the Simpevarp regional model area were collected during 2002 and 2003 /Cederlund et al, 2003; Green, 2003a/, but investigations are not completed and quantitative analyses of the results remain to be done. Moreover, a significant part of the terrestrial biomass for consumers in the Simpevarp region is probably domestic animals /Berggren and Kyläkorpi, 2002/ (cf. humans and land use, Section 5.7.3).

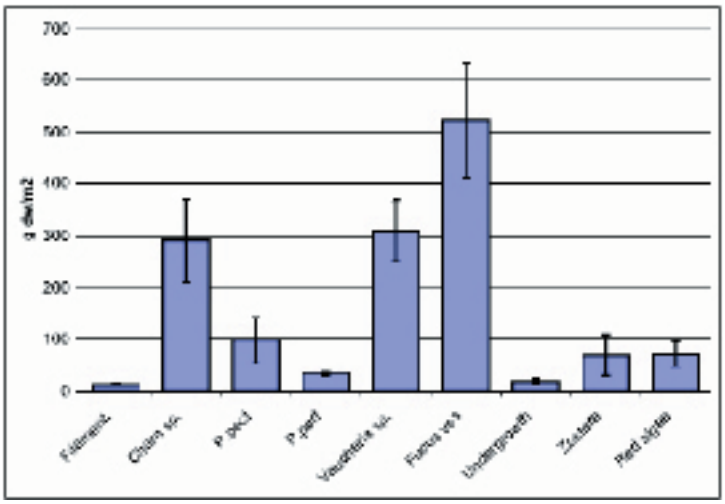

Figure 5-68. *Biomass (average +/– SE, g dw/m^2) for different benthic vegetation communities.*

Table 5-50. Area (m^2), mean cover (%) and biomass of vegetation communities in the coastal parts of the Simpvarp area.

Community	Area m^2	Cover % M +/– SE		Biomass metric ton dw
Filament. Algae	84,735	57	6	3
Chara sp.	1,326,117	57	2	315
Potamogeton pectinatus	1,947,944	49	2	180
Potamogeton perfoliatus	266,999	13	2	2
Vaucheria sp.	302,674	82	2	79
Potamogeton pectinatus/Zostera marina	763,358	52	3	65
Fucus sp. w. under growth	1,026,738	62	1	548
Red algae	5,868,305	30	1	268

No site-specific production or respiration measurements have been made.

Table 5-51. Estimated abundances of mammal species in the Simpevarp regional model area /Cederlund et al, 2003/.

Species	Animals per km²
Badger	Observed
Beaver	No obs.
European / Mountain hare	0.40
Fallow deer	No obs.
Fox	Observed
Lynx	Observed
Marten	Observed
Mink	Observed
Moose	0.6
Otter	No obs.
Red deer	0.03.
Roe deer	4.9
Wild Boar	0.3
Wolf	No obs.

Mammals

Not all of the selected species densities were found in the regional model area, but may be found in future surveys. The species are presented in Table 5-51, but species observed only along transects are denoted as observed . The most common mammal species was roe deer (49 deer/10 km^2) /Cederlund et al, 2004/. Moose were also fairly common (0.6 moose/km^2), but unevenly distributed, which is normal for this part of Sweden due to hunting pressure, snow depth and distribution of food. European and mountain hare were fairly low in abundance (4.0 hare/km^2), compared to other regions.

Birds

In total, 112 species were found in the regional model area, and 22 of these are noted in the Red List as endangered bird species in Sweden. Some 99% of the documented individuals (totally 4,807) were birds associated with land, while only c. 1% were birds associated with marine environments. The most common species on land were Willow Warbler and Chaffinch, and the most common species at sea were Herring Gull and Eider. A major part of the nesting species were small birds, associated with the open or semi-open landscape (Table 5-52). The number of nesting bird species in the outer archipelago was in total 703 pairs and 27 species, e.g. Herring Gull, Arctic Tern and Sea Gull, and in the inner archipelago in total 50 pairs and 11 species nested, e.g. Eider, Arctic Tern and Red-breasted Merganser.

Since no quantitative data were available for the Site Descriptive Model version Simpevarp 1.1 the biomass for each species has not been calculated. It is important to notice that the most common species (in terms of number) are quite small, and a calculation of total biomass for each species might give quite a different picture from the relative abundance estimates based on numbers. For detailed information on each species found in the Simpevarp area, see /Green, 2003a/.

Aquatic consumers – limnic

Invertebrates

No new site-specific data were available for the Site Descriptive Model version Simepvarp 1.1.

Table 5-52. The ten most common nesting species in the Simpevarp regional area, presented as the total number of birds registered and the number of birds per km² during transect surveys /Green, 2003a/.

Species English (Swedish)	Latin	Total number	Abundance (n/km)
Willow Warbler (Lövsångare)	*Phylloscopus trochilus*	765	7.15
Chaffinch (Bofink)	*Fringilla coelebs*	760	7.10
Blackbird (Koltrast)	*Turdus merula*	240	2.24
Robin (Rödhake)	*Erithacus rubecula*	238	2.22
Song Thrush (Taltrast)	*Turdus philomelos*	202	1.89
Tree Pipit (Trädpiplärka)	*Anthus trivialis*	183	1.71
Woodpegeon (Ringduva)	*Columba palumbus*	174	1.63
Great Tit (Talgoxe)	*Parus major*	166	1.55
Swift (Tornseglare)	*Apus apus*	119	1.11
Parrot Crossbill (Korsnäbb)	*Loxia pytyopsittacus*	116	1.08

Fish

No new site-specific data were available for the Site Descriptive Model version Simpevarp 1.1.

Aquatic consumers – marine

Invertebrates

The soft bottom community was characterised through sampling at 40 stations. The water depth varied from 1.3 m to 39 m. Most stations, however, were in the depth range of 5–15 m. All stations were associated with living benthic fauna. Three area subdivisions were distinguished, northern inner, southern inner and offshore. The northern inner area had a low total biomass not exceeding 3 g dw/m², whereas the southern inner and the offshore areas averaged 19 and 16 g dw/m², respectively. Larvae of the taxa Chironomidae (primarily omnivores) had the highest abundance and was the most wide-spread in the inner stations, followed by the detritivore *Macoma baltica. M. baltica* (measured as dry weight including shell) dominated the biomass in all areas. In total, *M. baltica* was the largest contributor (64%) to the benthic fauna biomass, followed by molluscs, primarily *Cerastoderma sp.* and *Mytilus edulis*. The most abundant taxa Chironomidae contributed only 5% of the biomass.

Large differences in biomass density could be seen depending on the sampled vegetation community. The Potamogeton/Zostera community had up to 10 times more of the benthic fauna biomass compared to the *Vaucheria* and *Chara* communities. This pattern coincides with the domination of *Vaucheria* and *Chara* communities with low fauna biomass in the northern area /Fredriksson and Tobiasson, 2004/.

In Figure 5-69 the mean biomass densities of the different trophic (functional) groups are presented.

The hard substrate fauna associated with vegetation communities (fauna attached to the substrate and the vegetation within the community) has been investigated. This associated fauna was dominated by different mollusc species. The *Fucus* and Red algae communities had most associated fauna, 3–4 g dw fauna/g dw vegetation, clearly dominated by the filter feeder *Mytilus edulis*. The associated fauna also included herbivores such as *Theodoxus fluviatilis* and other filter feeders such as *Cerastoderma hauniense*. The biomass of the associated fauna in vegetation communities ranged from 280 g dw/m² in Red algae to 120 g dw/m² in Fucus incl. undergrowth and 24 and 1 g dw/m² in *Potamogeton pectinatus* and *P. perfoliatus* communities, respectively (recalculated from data in /Fredriksson and Tobiasson, 2003/).

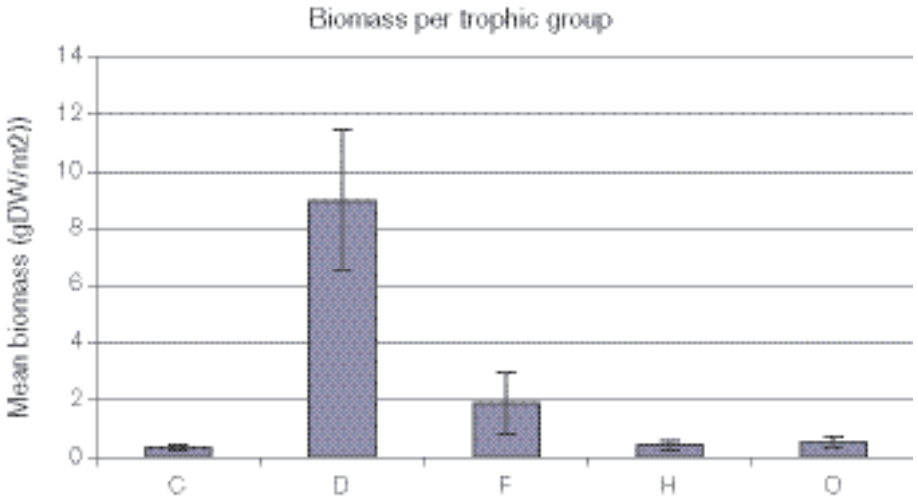

Figure 5-69. *Biomass of C=Carnivores, D=Detritivores, F=Filter feeders, H=Herbivores and O=Omnivores in the investigated area.*

Fish

Population estimates and therefore biomass of fish species do not exist for the region. However, many different sampling programmes (specified in /Lingman and Franzén, 2003/ have been, and are being, performed. Estimated ranking of the relative fish population sizes in coastal waters and inner coastal waters are presented in Table 5-53. A total of 28 and 25 limnic plus marine fish species have been caught by the National Board of Fisheries in the coastal and inner areas, respectively, during the period 1994–2003 /Lingman and Franzén, 2003/.

Mammals

The grey seal colony, approximately 20 km north of Simpevarp, contained 35 (max recorded) individuals in 2002, which was less than in the year 2000 (70 individuals), but more than observed the year 2001 (18 individuals) /Helander et al, 2003/. There are no data on seal activity in the regional modelling area.

Table 5-53. Ranking of fish populations in coastal waters off the Simpevarp area. The ranking is an approximate estimate based on catches from scientific fishing (several different methods) and from estimates of the probabilities of specific species being caught.

	Coastal area	Swedish	Inner (sheltered) area	Swedish
1	*Clupea harengus*	Strömming	*Rutilus rutilus*	Mört
2	*Sprattus sprattus*	Skarpsill	*Perca fluviatilis*	Abborre
3	*Rutilus rutilus*	Mört	*Blicca bjoerkna*	Björkna
4	*Gasterosteus aculeatus*	Storspigg	*Leuciscus idus*	Id
5	*Platichtys flesus*	Skrubbskädda	*Scardinius erythrophthalmus*	Sarv
6	*Gadus morhua*	Torsk	*Alburnus alburnus*	Löja
7	*Perca fluviatilis*	Abborre	*Esox lucius*	Gädda
8			*Gymnocephalus cernuus*	Gärs
9			*Anguilla anguilla*	Ål

5.7.3 Humans and land use

Input data sources and calculated numbers for the variables used to describe humans and land use in Simpevarp regional model area are shown in Appendix 4 on humans and land use. Absolute numbers and calculated numbers per km^2 are for the parish of Misterhult, since many of the data was available on the parish level.

The assessment of the data acquired can be summarised as follows:

- the parish has a low desnisty of population and the number of inhabitants has diminished slowly during the 1990s,
- the main employment sector is within electricity production. There is a clear net influx of commuting individuals to the region due the dominant employer (the OKG Power Company that operates the Oskarshamn nuclear power plant),
- mining (decoration stone) and manufacturing are the main employment sector among the inhabitants of the parish,
- there are proportionately more holiday-houses in the parish than in the Oskarshamn municipality and Kalmar County, which indicates that the region has a proportionally larger holiday population. The number of holiday-houses has increased since 1996,
- the land use is dominated by forestry and the extraction of wood is the only significant outflow of biomass from the area,
- the dominant outdoor activity is hunting; besides this, the coastal area is well used for leisure activities such as hiking, canoeing, fishing and boating; the entire coast is of national interest for outdoor life and nature conservation,
- the agriculture in the area is of limited extent. The arable land comprises 3.5% of the total land area, compared with 11.5% in the county as a whole. A wide spectrum of crops is cultivated, but the major crop is barley. Its significance has grown during the 1990s. The second most important crop, oats, is decreasing in importance.

5.7.4 Development of the ecosystem model

No overall ecosystem model has been produced for the Site Descriptive Model version Simpevarp 1.1.

5.7.5 Evaluation of uncertainties

Data uncertainties and conceptual uncertainties

The site investigation programme concerning surface ecosystems is not designed to produce batches of completed investigations relative to each data freeze and version of the site descriptive model. Consequently, some investigations that have started are only partly completed and are therefore not evaluated for the Site Descriptive Model version Simpevarp 1.1, whereas some other investigations are not evaluated due to lack of complementary data which are required for thorough evaluation and modelling. Consequently, data uncertainty caused by temporal and/or spatial variability, together with lack of data, are, for the present, high for many of the properties used to describe the ecosystem entities, c.f. /Löfgren and Lindborg, 2003/. Table 5-54 provides a subjective estimate of the combined uncertainties for all properties used to describe each specific ecosystem entity. However, the degree of uncertainty differs between the properties used to describe a given ecosystem entity. For some properties, a “high” uncertainty may be sufficient for the purpose of a site descriptive model, whereas it is necessary to attain a “low” uncertainty for other properties (and purposes), c.f. /Lindborg and Kautsky, 2000/ for a discussion on the necessary temporal and spatial resolution for different properties.

Table 5-54. Estimation of data uncertainties (caused by temporal and spatial variability) and conceptual uncertainties, for properties within different ecosystem entities. High/low denotes a subjective and combined evaluation for all properties used to describe the specific ecosystem entity, based on what is judged necessary for a complete Site Descriptive Model.

Ecosystem entity	Data uncertainties Temporal	Spatial	Conceptual uncertainties
Abiotic			
Atmosphere	High	High	Low
Hydrology	High	High	High
Overburden	Not applicable	High	High
Biotic			
Terrestrial			
Producers	High	Low	Low
Consumers	High	High	Low
Human	Low	Low	Low
Limnic			
Producers	High	High	Low
Consumers	High	High	Low
Human	Low	Low	Low
Marine			
Producers	High	High	Low
Consumers	High	High	Low
Human	Low	Low	Low
Historical development	High	High	High

Ecosystem model uncertainties

No overall ecosystem model has been produced for the Simpevarp Site Descriptive Model version Simpevarp 1.1.

6 Overall confidence assessment

The Site Descriptive Modelling involves uncertainties and it is necessary to assess the confidence in the modelling. Based on the integrated strategy report /Andersson, 2003/ procedures (protocols) have been developed for assessing the overall confidence in the modelling. These protocols concern whether all data are considered and understood, uncertainties and potential for alternative interpretations, consistency between disciplines, and consistency with understanding of past evolution as well as comparisons with previous model versions. These protocols have been used in a technical auditing exercise as a part of the overall modelling work. This chapter reports the conclusions reached after this auditing.

6.1 How much uncertainty is acceptable?

A site descriptive model will always contain uncertainties, but a complete understanding of the site is not needed. As set out in the geoscientific programme for investigation and evaluation of sites /SKB, 2000b/ the site investigations should continue until the reliability of the site description has reached such a level that the body of data for safety assessment and repository engineering is sufficient, or until the body of data shows that the rock does not satisfy the requirements. Even if step following the Site Investigation Phase, i.e. the Construction and Detailed Investigation Phase, does not imply radiological hazards, it would still be required that no essential safety issues may remain, which could not be solved by local adaptation of layout and design.

During the Site Investigation there are several planned occasions when Safety Assessment will be able to provide structured feedback as regards the sufficiency of the site investigations. The SR-Can project /SKB, 2003a/ will deliver its first interim report in mid 2004. In late 2004 or early 2005, Preliminary Safety Evaluations /SKB, 2002a/ of the investigated sites will follow. Quantitative feedback from Safety Assessment could thus not be obtained before these studies, but the type of feedback to be obtained can still be assessed in relation to its potential impact on decisions on the site investigation programme. The Safety Assessment planning suggests that only certain site properties are really important for assessing the safety. Generally, these are connected to the requirements already stated in /Andersson et al, 2000/. Consequently, there is a need to ensure that the site modelling is able to produce qualified uncertainty estimates of these properties.

According to current thoughts within Engineering there are essentially three design issues to be addressed during the Site Investigation phase:

Is there enough space?

What is the degree of utilisation (i.e. a subset of the space issue)?

Are critical passages properly assessed?

The overriding issue whether there is enough space for the repository may be divided into determining the generally available space and the degree of utilisation within this generally available space. The factors controlling the generally available space are the regional and local major deformation zones. Deposition tunnels must not be placed closer than a certain respect distance from such zones. Working definitions of respect distances exist, but there is still some refinement work going on regarding what should be appropriate respect distances, see e.g. /SKB, 2002a/.

The repository layout is not only controlled by the regional and local major deformation zones. For example, deposition holes connected to large fractures or high inflows will not be used and the thermal rock properties affect the minimum allowable distances between deposition tunnels and spacings between deposition holes. During site investigations, this is handled in the design by estimating a “degree of utilisation” for the deposition panels already adjusted to the regional and local major deformation zones. Final selection of deposition holes and tunnels will be made locally, underground, during the construction and detailed investigation phase. Distribution of inflow of

groundwater to the deposition tunnels is an important aspect of the degree of utilisation. Apart from water, other factors affect the degree of utilisation. These include thermal conductivity and rock mechanics properties affecting bedrock stability and the potential for rock bursts.

For the engineering planning and selection of the surface access point it is necessary to identify and characterise potentially difficult passages (i.e. deformation zones) in the rock. However, the information needed would be quite detailed, which means that the overall site description will be used to identify potential access locations. At these locations there will be a need to drill some additional exploration boreholes in order to assess the actual critical passages. However, there is no need to assess critical passages over the entire model domain.

6.2 Are all data considered and understood?

The method of interpretation is key to the confidence assessment. A similar and unbiased treatment of all the different data and interpretations that explain several different sets of observations both serve to enhance confidence.

6.2.1 Auditing protocol

A protocol has been developed for checking the use of data sources. It concerns:

- Data that have been used for the current model version (by refering to tables in Chapter 2).
- Available data that have not been used and the reasons for their omission (e.g. not relevant, poor quality, lack of time, …).
- If applicable – What would have been the impact of considering the data that were not used?
- The types of data and interpretation, indicating how accuracy is established for these, e.g. by specified procedure, QA, etc.
- Estimating the potential for inaccuracy and the significance of the inaccuracy, by using the terms ‘high’, ‘medium’, ‘low’ and ‘none’ to describe these.
- If biased data are being produced, can these be corrected?
- To what extent are interpretations supported by more than one observation or set of observations.

Table 6-1 lists the answers to these questions for the bedrock and Table 6-2 for the near-surface descriptions.

Table 6-1. Protocol for use of available data and potential biases in the bedrock description.

Question	Geology	Rock Mechanics and Thermal	Hydrogeology	Hydrogeochemistry	Transport
Which data have been used for the current model version (refer to tables in Chapter 2 of the report).	See Table 2-1. Note, also previous models of Äspö and Ävrö have been used as input. (Also data from the rock caverns on the Simpevarp peninsula).	See Table 2-2	Listed in table 2-3: SKB P-03-70: Difference flow logging in KSH01A. SKB P-03-113: Wireline tests in KSH01A. SKB P-03-114: Hydraulic tests in HSH01, HSH02, HSH03. SKB P-03-56: Hydraulic tests and water sampling in HSH03. SKB reports TR-97-06, TR-02-19, R-98-55, Hydraulic tests in areas Äspö, Ävrö, Hålö, Simpevarp, Mjälen and Laxemar areas. Previous made evaluations compared to new data.	Listed in Table 2-4. KSH01A – Complete chemical characterization (class 4 and 5), sampling during drilling, uranine analyses. KSH02 – sampling during pump tests, during drilling, uranine analyses. Percussion drilled boreholes HSH02 and 03 – Class 3 + isotopes. HSH02 and 03 – Class 3 + isotopes. Environmental monitoring boreholes SSM0001, 0002, 0005 – Class 3+isotopes. Precipitation – Class 3+isotopes. Surface water sampling – Class 3-5 + biosupplements. Other available data: Äspö site data and data from Laxemar and Ävrö, Nordic site data.	Listed in Table 2-5. Generic data (SR-97). Selected Äspö data. Geological data (main rock types and porosity data). Flow related transport parameters from the hydrogeological modelling. (No sorption or diffusion site data available for S1.1).
If available data have not been used –what is the reason for their omission (e.g. not relevant, poor quality, lack of time, …).	No raw data from CLAB were used (such as fracture statistics). Reasons for non-inclusion are: shallow boreholes, different format for representation, judged to be somewhat poorer quality. No raw data from Äspö. No old raw data from Ävrö. (Time available did not allow full consideration). However, the modelling has used models developed for Ävrö, Äspö and CLAB, as a starting point and used the new data from the site investigation to assess the information in these models. Vibro seismic data (a type of reflection seismic data) were not used due to poor quality. "Traditional" method using explosive source will be used in the future.	P-wave velocity, transverse to axis of drill core, KSH01 No established approach for how to use such data for estimation of the selected parameters of the description.	Old data from Åspö, Hålö, Ävrö, Mjälen and CLAB have been just been used for limited comparison due to lack of time. Some of the available data are most likely relevant.	Äspö site data: Used for comparison and for conceptual modelling. Nordic site data, see Chapter 4: Used for comparison and for conceptual modelling. Many observations excluded from modelling due to not being reported at the time of data freeze. Data with a higher than ±10% difference in charge balance were regarded as uncertain.	Some old Äspö data – excluded due to methodological inconsistencies – or lack of supporting geological/ hydrochemical information.

Question	Geology	Rock Mechanics and Thermal	Hydrogeology	Hydrogeochemistry	Transport
(If applicable) What would have been the impact of considering the non-used data?	(Considering all data as “virgin” or “raw” would have been an impossibly huge task). Hard to tell, but lineaments on the Simpevarp peninsula are short, i.e. the deterministic deformation zones are not affected much by the detailed linked lineament interpretation (i.e. the indication is that there are no/few large deformation zones in the Simpevarp peninsula). Reflection seismic on the peninsula would potentially have revealed horizontal features, if they exist. This lack of information in S1.1 will be supplemented by other data in coming model versions.	–	The neglect of CLAB data has minor impact since they cover a depth down to about 50 m below surface. The description of Äspö. Ävrö and Laxemar could have been better, although the hydraulic DFN model could not have been improved due to reasons mentioned early in the report. (it has not been possible to make an integrated hydrogeological and geologic interpretation of the model, hydrogeological implications of the revised deformation zone model or the new DFN-model has not been considered for these old data).	Better description of spatial distribution (more observations).	Small, since it would not give more input on the rock types within the Simpevarp peninsula.
List the data and interpretation types and indicate how accuracy is established for these, e.g. by specified procedure, QA, etc (essentially just refer to tables in chapter 2 and procedures in chapter 4 in the SDM report.	See table 2-1 and referenced P-reports. Chapter 4 (and subsections) addresses uncertainty in data. Important examples of inaccuracy are: • Lack of off-shore lineament information. • fracture mapping procedure was modified during the process, affecting interpretation of open fractures based on mapped aperture values.	The sources for the data are listed in Table 2-2. Available data is presented in section 4.7 and 4.8. For details about data collection and accuracy refer to the individual reports.	The interpretation of hydraulic tests presented in the data reports listed above follows standard QA procedures. The hydraulic tests focus mainly on the transmissivity. These interpretations have been considered “as is”. (Old data, so far not used, are generally of good quality but some tests are of less good quality due to different methodology).	Surface water data: QA established. Measurement errors in the order of (± 5–10% in analyses), see Chapter 4. GW data: QA established. Measurement errors in the order of (± 5–10%), see Chapter 4.	No site specific data. Evaluation of old Äspö data based on comparisons of methods and selection of data judged to be representative for the Simpevarp peninsula conditions.
In the list above, estimate the potential for inaccuracy. Use the terms ‘high’, ‘medium’, ‘low’ and ‘none’ to describe these.	Fracture location and orientation from BIPS logging in boreholes) = low. Geophysical logging in the three percussion boreholes. High. In KSH01A low. Single hole interpretation = low. Fracture openness from Boremap fracture mapping (whether open or not) = high. Bedrock mapping at the surface, including detailed fracture mapping = low. Modal and geochemical analyses = low. Petrophysical analyses and in situ, gamma-ray spectrometry measurements = low.	Stress model: Inaccuracy – High Significance – High Intact rock properties: Inaccuracy – Medium Significance – Medium Rock mass properties: Inaccuracy – High Significance – Medium Thermal properties: Inaccuracy – Medium Significance – Medium	The interpretation of the hydraulic tests is generally considered to be of high quality (low inaccuracy). Possible sources of uncertainty are spatial heterogeneity and different kinds of drilling disturbances.	Low potential for inaccuracy, low significance of inaccuracy (sensitivity analyses will be performed).	Not relevant (no site specific data).

Question	Geology	Rock Mechanics and Thermal	Hydrogeology	Hydrogeochemistry	Transport
	High-resolution reflection data from Ävrö. Medium (but all data from Ävrö not used – only the resulting model). Airborne geophysical data = low. Topographic data = low.				
If biased data are being produced, can these be corrected for the bias?	Bias: few data from areas covered by the sea. • Location of the sedimentary rock cover is uncertain, but it is evident that this boundary must lie east of the deformation zone ZSMNE024A. • There are far more lineaments and, thereby, inferred deformation zones on land than in the off shore area to the east. This reflects the use of four data types on land in the lineament interpretation and the use of one or, in places, two data sets in the off shore area. This bias will be reduced in model version 1.2, when further processing of the detailed bathymetric data will be available. (Note, topography is judged more important for linemeant interpretation in Simpevarp compared to Forsmark due to the thinner layer of Quaternary deposits). There is a bias introduced by the data gap between lineaments (lower cutoff > 500 m) and outcrop mapping (window < 30 m). A second bias concerns the fracture data from cored boreholes. All these boreholes are steep and borehole KLX01 does not have oriented fractures. Both features discussed above introduce a bias in, especially, the orientation of fractures.	Bias due to poor representativity of samples for mineral analysis, used for thermal model within rock domains, may be corrected if the actual rock type mix is described, c.f. section 5.3.3. Bias in data used for stress model and mechanical property model are mainly due to lack of new data and can not be corrected for at this stage.	Only one deep borehole in Simpevarp peninsula (and that is vertical). The core borehole KSH01A may have a window effect in the borehole transmissive feature statistics (similar to problem with fracture statistics – see geology) due to its vertical orientation. Hence, the structural model of the rock between the fracture zones may be biased. (Important of anisotropy). This effect can be addressed by incorporating more boreholes with other orientations.	Potential sources of bias include contamination from drilling fluid. Such biased data (uneven data coverage and erroneous data) can be corrected for by the use of generic data and back-calculations. However, in S1.1 this was not necessary. Water samples are results of mixing of waters from different fractures. This means that groundwater composition modelling represent averages. Water samples represent water in the conductive fractures (i.e. care is needed if drawing conclusions on water composition in the matrix).	Not relevant (no site specific data).

Question	Geology	Rock Mechanics and Thermal	Hydrogeology	Hydrogeochemistry	Transport
	The emphasis on subhorizontal fractures and the low frequency of fractures with NW strike may be two results of this bias. This problem can be tackled with the help of a Terzaghi orientation correction and will be reduced more significantly when data from inclined boreholes in different orientations are evaluated in later model versions. Mapping of fractures at the surface will produce a bias towards steeply-dipping fractures. Some correction can be applied with the help of a Terzaghi orientation correction. Limited fracture statistics are presently available from the upper 100 m. The representativity of surface fracture mapping for the deep rock is thus harder to test, before more such data at shallow depth are available (such data will be available in version 1.2).				
To what extent are interpretations supported by more than one observation or set of observations? (list all examples or give reference to sections of the SDM report where this is stated).	Lineaments indicated by different data sets (magnetic, EM, VLF, topography). Deformations zones (se Tables section 5.1.4 Rock type classification (Petrography, modal and geochemical composition, petrophysical properties). Fracture data are observed on four outcrops and also at lineament scale.	Thermal conductivity estimated from both mineral content and density. See Section 5.3.2. Uniaxial strength estimated from both old direct lab. tests and from new Schmidthammer tests on cores from KSH01. See Section 4.7.2. Rock mass mechanical classification from both Q and RMR, for Q from both Boremap data and direct Q-mapping of core and outcrops. See Section 5.2.	The location and extent of some fracture zones near Äspö and Hålö have been confirmed at more than one location by hydraulic tests and by observations during excavation of the Äspö HRL.	E.g. redox conditions, process description supported by multiple observations. Interpretation of major components is supported by other measurements such as redox, minor components, gas analyses, isotopes, etc.	No site specific data for S1.1. Only a few observations from Äspö of one of the main rock types present within the Simpevarp subarea.

Table 6-2. Protocol for use of available data and potential biases in the description of the near surface.

Question	Surface Water Chemistry	Hydrology	Quaternary Deposits	Ecosystems (biota)
Which data have been used for the current model version (refer to tables in Chapter 2 of the SDM report).	KSH01A – Complete chemical characterization (class 4 and 5), drilling sampling,uranine analyses. KSH02 – sampling pump tests, drilling, uranine analyses. Percussion drilled parts of HSH02 and 03 – Class 3 + isotopes. HSH02 and 03 – Class 3 + isotopes. SSM0001, 0002, 0005 – Class 3+isotopes. Precipitation – Class 3+isotopes. Surface sampling – Class 3-5 + biosupplements. Other available data: Äspö site data including Laxemar and Ävrö, Nordic site data.	SKB TR-02-03, SKB R-99-70: Summary of precipitation, temperature, wind, humidity and global radiation up to 2000. Regional run-off data. Regional oceanographic data. SKB GIS-database: Ground elevation and bathymetry of the Baltic sea. Topographical information for delineation of run-off areas. Oceanographic data (TR-97-14).	See tables in Chapter 2. Surface based data on QD in the Simpevarp subarea, tentative stratigraphical results from limited number of auger boreholes, air photography, topographical data.	See tables in Chapter 2. Terrestrial vegetation model P-03-83, P-03-80, R-02-10, Accessibility map. Terrestrial fauna model – Bird inventory P-03-31 – Mammal inventory P-04-04, R-02-10. Aquatic vegetation model, limnic – Aquatic vegetation model, marine – P-03-69. Aquatic fauna model, limnic – Aquatic fauna model, marine – P-04-17.
If available data have not been used – what is the reason for their omission (e.g. not relevant, poor quality, lack of time, …).	Äspö site data: Used for comparison and for conceptual model. Nordic site data: Used for comparison and for conceptual model. Many observations excluded from modelling due lack of reported analyses at data freeze.	SKB P-03-04: Explore water courses for suitable point of measuring the run-off. SKB P-03-05: Inventory of private wells 2002. Not used explicitly. Document only for planning. Meteorology/hydrology data from SMHI 2002 – not compiled in P-report. Monthly flow estimations in streams (SNV simple).	Older maps of Quaternary deposits were not used due to poor quality /Svedmark, 1904; Bergman, 1998/ The areas of exposed bedrock are too large on the map from 1998. Geographical accuracy too poor on the map from 1904.	Vegetation inventories – complementary data needed. Selected generic data (R-02-10) – poor quality /not relevant.
(If applicable) What would have been the impact of considering the non-used data?	Better description of spatial processes (more observations).	None	None	Possible validation of vegetation models.

Question	Surface Water Chemistry	Hydrology	Quaternary Deposits	Ecosystems (biota)
List the data and interpretation types and indicate how accuracy is established for these, e.g. by specified procedure, QA, etc (essentially just refer to tables in chapter 2 and procedures in chapter 3 in the SDM report.	Surface water data: QA established (+/– 5–10% in analyses). GW data: QA established (+/– 5–10%).	Meteorology: SMHI standard. Surface hydrology: Catchment areas interpreted from maps (but will be checked in the field), measured run-off outside model area measured according to SMHI standard. Oceanography: Scientific "status" (TR-97-14).	Field classification and sampling according to national standard methods. Calibration between experts.	Terrestrial vegetation model: Vegetation map – not validated yet, but accuracy seems fair (L, L), Vegetation inventory – QA established (L, L). Terrestrial fauna model: Bird inventory – QA established (L, L), Mammal inventory – QA established (L, L). Aquatic vegetation model, limnic – Aquatic vegetation model, marine, – P-03-69 – scientific report status (–, L). Aquatic fauna model, limnic – Aquatic fauna model, marine – P-04-17 (accuracy fair) – scientific report status (–, L).
In the list above, estimate the potential for inaccuracy and the significance of the inaccuracy. Use the terms 'high', 'medium', 'low' and 'none' to describe these.	Low potential for inaccuracy, low significance of inaccuracy (sensitivity analyses will be performed).	Meteorology: All stations outside regional model area: low inaccuracy, medium significance. Surface hydrology: Catchment areas: medium inaccuracy, low-medium significance; runoff: medium/high inaccuracy, high significance. Near surface hydrogeology: High inaccuracy, medium significance (lack of data) ; gw levels: high inaccuracy, high significance (no temporal variation, but old data are to some extent available but not evaluated). Oceanography –	Field classification depends on expert judgments, in most cases low but in certain cases medium potential for inaccuracy (difficult to quantify). The exact delineation made in the field of areas with different Quaternary deposits is sometimes difficult (in such cases medium inaccuracy).	See above (estimations within brackets).

Question	Surface Water Chemistry	Hydrology	Quaternary Deposits	Ecosystems (biota)
If biased data are being produced, can these be corrected for the bias?	Biased data (uneven data coverage and erroneous data) can be corrected by use of generic data and back-calculations.	Meteorology: precipitation data – standard correction for measurement errors. Surface hydrology: regional runoff in relatively large catchments – generic information on variations in small areas, influence of topography, land use etc. Near surface hydrogeology: No hydraulic tests in the contact between bedrock and Quaternary deposits (QD) or in QD, no representation of variation with depth, correction by expert judgment; gw level measurements: concentrated mainly in the Laxemar, Ävrö and Äspö areas. Undisturbed conditions mainly for 50-100 m sections of the upper bedrock, No data for QD. Oceanography: None.	Stratigraphical data are concentrated only on certain kind of deposits and to infrastructure (e.g. roads and gravel pits. More data will be available in version 1.2. Data only from terrestrial parts of the area. Data on off-shore sediments will be available for version L 1.2).	Full coverage of presented data – no bias.
To what extent are interpretations supported by more than one observation or set of observations? (list all examples or give reference to sections of the SDM report where this is stated).	E.g. redox conditions, process description. Interpretation of major components is supported by other measurements such as minor components, gas analyses, isotopes, etc.	Meteorology: Several observation stations outside regional model area. Surface hydrology: Runoff: several observation stations outside regional model area. Near surface hydrogeology: None. Oceanography: None.	Not in this version. The field classifications will be compared with results from laboratory analysis in v 1.2.	Vegetation map is supported by several independent surveys.

6.2.2 Observations

The answers to the auditing protocol on the use of data sources as expressed in Table 6-1 and Table 6-2 suggest the following overall observations.

Use of data

- The database for the modelling is well defined and is listed in the tables of Chapter 2.

Generally all data available at the time of the data freeze 1.1 and as listed in the tables of Chapter 2 have been considered for the modelling. The main exception is that the geological modelling did not consider the substantial amount of old raw data from Äspö, Ävrö and CLAB. However, the modelling has used the old models developed for Ävrö, Äspö and CLAB, as a starting point and used the new data from the site investigation to assess the information in these models. Considering all existing raw data would have been very resource demanding, and since the resulting existing models have been used, the impact on the modelling of the Simpevarp peninsula is likely to be moderate.

Also in the hydrogeological modelling the old data from Åspö, Hålö, Ävrö, Mjälen and CLAB have just been used for limited comparison due to lack of time. Some of the available data are most likely relevant and will need to be reassessed when the hydrogeological model of the site is better integrated with the geological model (i.e. to be done in version 1.2).

There are also some measurements made, which proved to be less useful – or hard to use. In particular, the vibro seismics (a type of reflection seismics data) were not used due to poor quality. "Traditional" methods will be used in the future. Clearly, reflection seismics on the peninsula would potentially have revealed other information, but this lack will be supplemented by other data. There are also some older data relating to the surface which have not been used, as the data was not readily available or were judged to be of minor importance.

Accuracy

Accuracy of field data and interpretation have been established using well-defined procedures as is explained in detail in Chapter 4 of this report. The potential for inaccuracy stemming from the field data is assessed and is in general judged to be a minor source of uncertainty in the resulting model description. An important deviation from this general conclusion is the overall confidence in stress measurements as further explained in Table 6-1. These issues, in particular, need further scrutiny in coming model versions.

Bias

There are biases in the Simpevarp version 1.1 data. Important examples include the following:

- There are few data from areas covered by the sea, which makes the location of the cover sedimentary rock uncertain and results in far more lineaments and, thereby, inferred deformation zones on land than in the sea area to the east. This bias will be reduced in model version 1.2, when further processing of the detailed bathymetric data will be available.
- There is a data gap between lineaments (lower cutoff >500 m) and outcrop mapping (window < 30 m).
- There are different directional biases in the data due to i) steep deep boreholes and ii) the surface data fracture mapping. This bias affects both fracture statistics and the hydrogeological interpretation. Partly directional bias can be handled through bias correction techniques, like Therzagi correction, but would generally require information from bore holes with different orientations and inclinations. Data from such holes will also be available in subsequent data freezes.

- No fracture statistics exists from the first 100 m. The representativity of surface fracture mapping for the deep rock is hard to test before such relatively shallow data become available (such data will be available in version 1.2).
- There is a potential bias in the rock mechanics and thermal models due to poor representativity of samples for mineral analysis. This bias will be significantly reduced when more data becomes available and the uncertainty in the description of the rock type distribution in the rock domains (i.e. the geological model) is reduced. Such improvements are expected in later model versions.
- The single vertical core borehole KSH01A on the Simpevarp peninsula may imply a directional bias in the borehole transmissive feature statistics (similar to problem with fracture statistics – see geology). This effect can be addressed by incorporating more boreholes with other orientations, as will be analysed in later model versions and data freezes.
- For hydrogeochemistry a potential source of bias is the contamination from drilling fluid. Such biased data can be corrected by use of generic data and back calculations. However, for the water samples taken in KSH01A this was not necessary.
- Another hydrogeochemical bias is that water samples are results of mixing of waters from different fractures. This means that groundwater composition modelling represent averages and represent water in the conductive fractures (i.e. care is needed if making conclusions on water composition in the matrix).
- The surface hydrology was measured for relatively large catchments, whereas generic information was used to estimate variations in small areas. The stratigraphic data on Quaternary Deposits were concentrated on some deposits and related to infrastructure locations (e.g. roads and gravel pits). More data will be available in version 1.2.
- It is judged that the ecosystem inventory is without bias.

As can be seen from the list these biases mainly concern how well current measurements represent the site (other types of biases are already corrected for). Consequently, data added in later data freezes and analysed in coming model versions, will alleviate most of these biases.

Multiple evidence

Several interpretations, including composition of rock types, orientation of structures, hydraulic responses, interpretation of major components of the groundwater, or means of exploring near-surface hydrogeology are supported by more than one observation or set of observations. The value of these multiple observations (and sometimes lack thereof) has to be considered in the uncertainty evaluation.

6.2.3 Overall assessment

In general, it appears that most available data have been analysed and treated according to good practices and that inaccuracy and biases are understood and accounted for in the subsequent modelling. The overriding issue affecting confidence in models based on the Simpevarp version 1.1 data freeze is the bias and uncertainty resulting from varying spatial coverage of data and the use of limited unidirectional deep borehole data. These biases will be addressed to a substantial degree in future model versions.

6.3 Uncertainties and potential for alternative interpretations

Small estimated uncertainties and an inability to produce many different alternative interpretations from the same database are indications of confidence – although not strict proofs. A related issue is whether new measurements or other tests could resolve uncertainties or separate between alternatives and thereby enhance confidence.

6.3.1 Auditing protocol

The Site Descriptive Models represent the characterization of a natural rock mass, and hence uncertainty is an inherent aspect of the Model development. There are conceptual uncertainties, and other types of uncertainty: data uncertainty, spatial variation, temporal variation, applicability of database information, measurement error, modelling error, etc. In some cases, unresolved scientific issues are involved.

The uncertainties need to be identified and the cause of uncertainty should be established. An associated issue is to what extent uncertainties are related to the information density (not only boreholes) both laterally and vertically. Specifically, confidence in the description could be high even if there are few measurements if geological understanding is high (e.g. if there is a homogenous and evident geology), but could also be low, even with a 'wealth' of data, if the geological understanding is poor.

There is also the distinction between what is uncertain at an absolute level and what is uncertain in terms of the potential for alternative interpretations? We need to be able to state the potential for alternative explanations and later consider how to conduct diagnostic tests to establish the most likely interpretation?

Thus, a common philosophy is required for addressing uncertainty and the implementation needs to be audited. There is a need to consider how uncertainties can be identified through uncertainty elicitation. A protocol has been developed for checking this. It concerns:

- The main uncertainty areas and the subject items in these areas.
- Whether and how the uncertainties can be expressed numerically.
- Whether uncertainties actually are quantified.
- To what extent uncertainties are related to the information density?
- Whether uncertainty can be addressed by alternative interpretations, if so the lines of reasoning for producing alternatives and a list of (or references to) the alternatives produced.
- If there are measurements or other tests, which could separate between alternatives and enhance confidence.

Table 6-3 lists the answers to these questions for the bedrock and Table 6-4 for the near-surface descriptions.

Table 6-3. Protocol for assessing uncertainty in the bedrock description.

Question	Geology	Rock Mechanics and Thermal	Hydrogeology	Hydrogeochemistry	Transport
List the main uncertainty areas and the subject items in these areas.	**Rock domains** Lithology below the sea and off-shore also outside the Simpevarp peninsula, Äspö and Ävrö (lower quality data in these areas). 3D extension of dioritoid and mixed rock type domains. Proportion of rock types in domains (not evenly distributed at 50–100 m scale and smaller scales, veins, patches, dykes, minor bodies) (There could also be statistical anisotropy in their occurrence). Distribution and volumetric shape of mafic bodies. 3D distribution of "secondary red staining" (hydrothermal alteration). **Deterministic structure model** Existence of deformation zones (only some zones interpreted with high confidence) – are all lineaments really deformation zones? Potentially there are non-included zones (mainly sub-horizontal) (e.g. the Nordenskjöld hypothesis. Extension (length and depth) of deformation zones (e.g. "linked lineaments"). Dip of deformation zones. Termination of zones – against each other. Character and properties – also in the well established (e.g. from Äspö) zones. Strong spatial variation of properties (width, fracturing, also hydraulic properties..) as seen in multiple intercepts. **Stochastic model of features** Fracture set (orientation) identification. Fracture size distribution – interpolation between lineament and mapped outcrop data and for some sets only local information (extrapolation to larger sizes).	I) Lack of stress data and uncertainty in interpretation of stress data. II) Applicability/reliability of empirical approach for estimation of rock mass properties at depth. III) Lack of thermal laboratory tests for rock types from the subarea. *I) is the main concern for stress model, II) for mechanical properties and III) for thermal model.*	The current elevation model is not correct in the vicinity of the shoreline. The error is in the bathymetric data between 0 and –3 masl. (Not a main uncertainty). All assumptions made in the structural model are directly transferred to the hydrogeological model. In particular, there is an uncertainty in the interpretation of lineaments as fracture zones (confidence level) and in the assignment of hydraulic properties at depth (i.e. the upscaling of hydrogeologic data is entirely based on the geologic structures). T-distribution in deformation zones. (Uncertainty and spatial variability within zones). The hydraulic DFN model and resulting connectivity is highly uncertain. e.g. • not based on the S1.1. geological DFN-model, • oneT-distribution assigned to all fracture sets, • correlation between T and size is assumed, • spatial distribution. This "interpretation" for S1.1 gw-modelling is unsatisfactory and the data analysis needs to be strengthened.	Spatial variability in 3D at depth. Temporal (seasonal) variability in surface waters, which ultimately impacts the groundwater in the bedrock (but slow processes and temporal averaging a result). Model uncertainties (e.g. equilibrium calculations, migration and mixing). Identification and selection of real end-member waters. There is a judgemental aspect of the M3 (principal component) analysis. Groundwater composition in the rock matrix.	Spatial variability and correlation between matrix transport properties and flow paths. Distribution of flow related transport parameters (i.e. essentially the F-distribution), due to all the uncertainties in the hydrogeological model and the conceptual model for transport (i.e. how F-distribution is calculated). No site specific data on sorption and diffusion in the matrix are available.

Question	Geology	Rock Mechanics and Thermal	Hydrogeology	Hydrogeochemistry	Transport
	Fracture intensity – now based largely on surface data – representativity for conditions at greater depth. Spatial model. Spatial distribution in different rock domains. 3D distribution of "secondary red staining" (hydrothermal alteration) (association to fracturing).		The groundwater salinity currently known at depth only from a few boreholes. This in turn makes it difficult to test the importance of the hydrogeological initial condition (paleohydrogeology). (There is also uncertainty in assumed conditions after last glaciation – studied by sensitivity analyses).		
With reference to the list above, explain whether the uncertainties can be expressed numerically and how this could be done.	**Rock domains**: Uncertainty in lithology below sea and off-shore the Simpevarp peninsula, Äspö and Ävrö – hard to quantify – If deemed important, data from these areas are needed. 3D extension of dioritoid and mixed type domains: Alternatives in extrapolation can be given. Proportion of rock types in domains. Mean and standard deviation can be estimated in 100 m–50 m scale and larger scale. More sophisticated descriptions may be needed to capture spatial statistics of veins, patches, dykes, minor bodies, and their statistical anisotropy. The need for such more sophisticated descriptions should be assessed by the engineering and safety assessment. (A related question is if Ävrö granite and quartz monzodiorite can be combined to one rock domain for engineering/safety applications). Distribution, volumetric shape of mafic bodies. (see previous point). 3D distribution of "secondary red staining" (hydrothermal alteration).–Difficult to quantify this uncertainty.	I) Can be expressed numerically. As a span ±%. II) Can not be numerically expressed. III) Can not be numerically expressed.	Some uncertainties are difficult to estimate, as an integrated analysis of data was not possible. The uncertainties are in the interpretations as such (i.e. qualitative) and suffer from lack of data or bias in the data available. Some of the settings/assumptions can be tested by means of exploration simulations although there is no obvious answer to compare the output with, e.g. the paleohydrogical problem.	Spatial variability and temporal variability can be estimated by expert judgement. Sensitivity to uncertainties in specific model (e.g. M3) input (e.g. measured water composition) can be calculated. Conceptual uncertainties can be judged qualitatively. Groundwater composition in the rock matrix. (Measurements are planned to be incorporated in future model versions).	Spatial variability and correlation between matrix migration properties (sorption and diffusion) and migration paths – Can be described, but not meaningful before data are available. Distribution of flow related transport parameters (i.e. essentially the F-distribution), due to all the uncertainties in the hydrogeological (DFN) model and conceptual model for migration (how F-distribution is calculated). – Propagate uncertainties in the hydro-model to the transport analysis. The conceptual uncertainties could be explored by testing different alternative descriptions of fracture geometry and modelling approaches.

Question	Geology	Rock Mechanics and Thermal	Hydrogeology	Hydrogeochemistry	Transport
	Deterministic structure model:				
	Existence of deformation zones – are all lineaments really deformation zones? (existence of zones judged – high, medium, low).				
	Potentially non-included zones (mainly sub-horizontal) – Yes, e.g. by alternative model.				
	Extension (length and depth) of deformation zones (e.g. “linked lineaments”) – Yes by indication confidence – or as alternative models.				
	Dip – yes (as an interval or distribution). Estimates evidently improved if there are data from boreholes, seismics, ground geophysics.				
	Termination of zones – against each other. (Estimates of the termination can possibly be obtained from outcrop fracturing) Uncertainty can be possibly be expressed by alternatives.				
	Character and properties – Qualitative description.				
	Stochastic model of fractures				
	Fracture set (orientation) identification. – Fitting a distribution. Fracture size distribution. Fracture intensity – now based largely on surface data – representativity for conditions at greater depth. Spatial model. Spatial distribution in different rock domains. – Fitting (different) distributions, but uncertainty due to censoring and truncation effects can be judged qualitatively). Alternative models.				
	3D distribution of “secondary red staining” (hydrothermal alteration), may affect fracturing. Difficult to quantify this uncertainty.				

Question	Geology	Rock Mechanics and Thermal	Hydrogeology	Hydrogeochemistry	Transport
Are uncertainties actually quantified? If so provide reference to where in the SDM-report this information is stated. (Answer can be combined with answer to previous question.)	**Rock domains** 3D extension of dioritoid and mixed type domains: Alternatives in extrapolation, see section 5.1. Proportion of rock types in domains. No quantified estimates in S1.1. Distribution, volumetric shape of mafic bodies. (see previous point). – No estimates apart from the ones observed on the surface. **Deterministic structure model** Existence of deformation zones (existence of zones judged – high, medium, low), see tables in section 5.1. Potentially non-included zones (mainly sub-horizontal) – No alternatives considered, but no indication suggests extensive such zones. Extension (length and depth) of deformation zones (e.g. “linked lineaments”) – Yes by indication confidence – no alternatives developed. Dip – yes (as an interval or distribution). Termination of zones – against each other. (Estimates of the termination can possibly be obtained from outcrop fracturing) Uncertainty not quantified in 1.1. Character and properties – Qualitative description. **Stochastic model of fractures** Fracture set (orientation) identification. – Fitting a distribution. Fracture size distribution. Fracture intensity. Yes, see Section 5.1. 3D distribution of “secondary red staining” (hydrothermal alteration), may affect fracturing, see section 5.1.	I) Yes, the span is judged (not calculated). See Section 5.2.1. II) Discussed in Section 5.2.2. III) Stated in Section 5.3.6.	See the previous answer. The current uncertainties are not actually quantified, but T and standard deviation in deformation zones provided. Other uncertainties not quantified in version S1.1.	Spatial variability is site specific. Spatial variability cannot be described in S1.1 due to too few observations. Temporal variability – not assessed. Uncertainties related to the models underlying the hydrogeochemical SDM are specified in the GW-chemistry method report (R-02-49), mentioned in Chapter 5.	Uncertainties are not quantified in S1.1. However, variability in F-factor due to heterogeneity (spatial variability) is assessed.

Question	Geology	Rock Mechanics and Thermal	Hydrogeology	Hydrogeochemistry	Transport
To what extent are uncertainties related to the information density? (consider wealth of data in relation to overall "understanding")	Lack of subsurface information that concerns geometry and character/properties of deformation zones (especially along inferred strike) and rock domains. Fracture size information is not available at depth and has to be propagated from surface data.	I) Related to a large extent. But also to related to the uncertainty in the data as such. II) To a minor extent. More related to overall understanding. III) Fully related to lack of laboratory data.	A better spatial spread of boreholes and, in particular, more measurements at depth (including salinity data) will clearly reduce some of the current uncertainties.	Uncertainty in spatial variability is mostly related to a limited number of observation points.	For the flow related parameters – see answer under hydrogeology. For matrix transport properties – yes probably (need to see data first).
5) Can (is) uncertainty (be) addressed by alternative interpretations? If so, what are the lines of reasoning for producing alternatives in your discipline?	**Rock domains** 3D extension of dioritoid and mixed type domains: Alternatives in extrapolation (also done see section 5.1). **Deterministic structure model** Potentially non-included zones (mainly sub-horizontal) – Yes, e.g. by alternative model, Not in version S1.1. Extension (length and depth) of deformation zones (e.g. "linked lineaments"). Alternative model where non-linked, but yet coordinated lineaments are used, could be considered. Also other means of carrying out the coordinated lineament interpretation could potentially be a generator for an alternative. Not in version S1.1. Termination of zones. Uncertainty can be possibly be expressed by alternatives. Not in version S1.1. **Stochastic model of fractures** Fracture set (orientation) identification – Estimating orientation distributions. Fracture size distribution. Fracture intensity – now based largely on surface data – representativity with depth. Alternative models are presented in version S1.1, see section 5.1.	I) Yes. The alternatives of stress models are based on alternative understanding of the structural model in combination with observed stress variation in measurement data. Section 5.2.1. II) Yes, other approaches may be used. III) Not for the tests. The thermal model is dependent heavily on geological model. If there is a alternative lithological model it will mean an alternative thermal model.	Alternatives in the geological model – the alternative based on unlinked lineaments may significantly affect the hydraulic DFN-model, but the changes in deterministic zones are probably less important. The power-law relationship between T and L ($T = a \cdot L^b$) used in the current DFN setup can be tested with other values of a and b or, indeed, no correlation whatsoever.	Alternative models will be constructed and model comparison with hydrogeological models and models based on generic data. Hypotheses for alternative models of the bedrock hydrogeochemistry concern reasons for the present groundwater composition, i.e. as a result of: i) mixing and reactions, ii) only reactions, iii) only mixing or iv) alternative end-members.	Same as for hydrogeology concerning F-factor. However, no alternative interpretations are assessed within version S1.1. There may be possibly be alternatives to the present retention models (e.g. sorption vs. co-precipitation). The need and practicality of such alternatives are currently being explored outside the Site Modelling work.

Question	Geology	Rock Mechanics and Thermal	Hydrogeology	Hydrogeochemistry	Transport
(If applicable) list (or provide reference to) actual alternatives produced.	See above.	I) Alt 1:The whole subarea belongs to the same stress domain. Alt 2: Two different stress domains prevail in the subarea. Section 5.2.1. II) Not produced. See TR-02-01. III) Not produced. See Section 5.3.	No alternatives have been evaluated in version S1.1	Mixing models based on alternative end-members, see Chapter 5.	No alternatives in S1.1
Are there measurements or other tests, which could separate between alternatives and enhance confidence?		I) Yes. Stress measurement data, from relevant points, gives a possibility to select between alternatives. II) Not until excavations may be done at depth. However confidence is already acceptable for relative comparison of parameters in different domains/sites. Section 5.2.2. III) Use of density log. See 5.3.6.	One way to calibrate a numerical model is to match simulations to interference tests. Given the many constraints listed above, it is obvious that there is no point in making a calibration of the S1.1 model. On the other hand there are no interference tests available for the core of the Simpevarp subarea. (A large number of tests are however available for Äspö Island). No major interference tests will be conducted for the S1.2 data freeze. A few minor tests will probably be available. For S1.2 it is important to compare the S1.1 findings between T and L with data from other core boreholes, i.e. KSH02A and KSH03A.	New borehole data and water composition of the rock matrix.	Not relevant for S1.1

Table 6-4. Protocol for assessing uncertainty in the description of the near surface.

Question	Surface water chemistry	Hydrology	Quaternary Deposits	Ecosystems (biota)
List the main uncertainty areas and the subject items in these areas.	Temporal variability in surface waters. Model uncertainties (e.g. equilibrium calculations).	Representativity for the model area of SMHI data collected outside the area. Spatial and temporal variability in precipitation and runoff. Lack of data on hydraulic conductivity in Quaternary deposits (QD).	The present knowledge regarding the total thickness of QD and the individual thickness of different QD is very low. There is no information regarding the spatial and stratigraphical distribution of QD on the bottom of the sea. There are no laboratory analyses of QD verifying the field judgments. There are no data regarding the in situ properties of QD (e.g. porosity).	Biomass and production (flora and fauna).
With reference to the list above, explain whether the uncertainties can be expressed numerically and how this could be done.	Spatial variability and temporal variability can be estimated by expert judgement. Impact of model uncertainties can be bounded /see Smellie et al, 2002/.	Uncertainty in hydraulic properties of QD can only be estimated from generic (literature) data and expert judgment.	Not considered.	More measurements and statistical analyses of data.
Are uncertainties actually quantified? If so provide reference to where in the SDM-report this information is stated. (Answer can be combined with answer to previous question.)	Spatial variability is site specific. Spatial variability cannot be described with the limited sampling points at the data freeze. Temporal variability will be captured later as the monitoring proceeds. Uncertainties related to the models underlying the hydrogeochemical SDM are specified in the GW- chemistry method report (R-02-49).	Variability of hydraulic conductivity of the QD in Sweden is shown, see section 5.4.2.	No	No
To what extent are uncertainties related to the information density? (Consider wealth of data in relation to overall “understanding”.)	The uncertainty is mostly related to the poor information density.	The lack of data is a major source of uncertainty.	Strongly dependent on spatial density. More data will be available in v. 1.2.	Stratified sampling + generic data reduce the need for high information density.
Can (is) uncertainty (be) addressed by alternative interpretations? If so, what are the lines of reasoning for producing alternatives in your discipline?	Alternative models will be constructed and model comparison with hydrogeological models and models based on generic data will be performed.	In future quantitative modelling, different modelling approaches can be used and sensitivity analyses and/or stochastic approaches can be applied to analyse uncertainties and their influence on predictions.	Different interpretations regarding the thickness and stratigraphy of QD in the area.	Not applicable.
(If applicable) list (or provide reference to) actual alternatives produced.	Mixing models based on alternative end-members.	In version Simpevarp 1.1 only conceptual modelling ws performed.	No	N/A
Are there measurements or other tests, which could separate between alternatives and enhance confidence?	New borehole data and water composition of the rock matrix.		More stratigraphical data and investigations of off-shore sediments and/or off shore QD fin V 1.2.	N/A

6.3.2 Main uncertainties

Bedrock geological model

As already identified in chapter 5 and as listed in Table 6-3 there are several uncertainties in the Simpevarp version 1.1 bedrock geological model. For the *rock domains* these uncertainties mainly concern the following:

- Lithology below sea and outside the Simpevarp peninsula, Äspö and Ävrö (lower quality data in these areas).
- Three dimensional extension of dioritoid and mixed type domains.
- Proportion of rock types in domains (not evenly distributed at the 50–100 m scale and below, veins, patches, dykes, minor bodies). There could also be statistical anisotropy in their occurrence.
- Distribution, volumetric shape of mafic bodies.
- Three dimensional extent of "secondary red staining" (hydrothermal alteration).

For the *deterministic deformation zones* these uncertainties mainly concern the following:

- Existence of deformation zones (only some zones are identified with high confidence) – are all lineaments really deformation zones?
- Potentially non-included zones (mainly sub-horizontal) (e.g. the Nordenskjöld hypothesis).
- Extension (length and depth) of deformation zones (e.g. "linked lineaments").
- Dip of deformation zones.
- Termination of zones – against each other.
- Character and properties – even in the well-established (e.g. from Äspö) zones. Strong spatial variation of properties (width, fracturing, also hydraulic properties).

For the stochastic model of fractures and deformation zones the uncertainties mainly concern:

- Fracture set identification.
- Fracture size distribution – interpolation between lineament and mapped outcrop data and for some sets of fractures only local information could be used making extrapolation to larger sizes highly uncertain.
- Fracture intensity – now based largely on surface data – leading to questions of the representativity of these data at depth.
- Spatial model.
- Spatial distribution in different rock domains.

Many of these uncertainties are described by statistical distributions or at least by indication of confidence (for details see Table 6-3). Remaining uncertainties are left unresolved or as input to alternative hypothesis. Generally, much of the uncertainty is related to the information density and will thus be reduced in later model versions.

Rock mechanics and thermal

As already identified in Chapter 5 the main uncertainties in the Simpevarp version 1.1 *rock mechanics* and *thermal* model concern the following:

- Stress distribution at depth.
- Rock mechanics properties of the rock mass.
- Distribution of thermal properties.

The uncertainty in these are evaluated – or at least discussed in Chapter 5. Whereas the uncertainties in stress and thermal properties are mainly due to lack of data (poor information density) and the uncertainty in rock type distribution in the rock domains (see previous subsection) there is

also considerable uncertainty stemming from poor understanding. This is especially true for the uncertainty in rock mechanics properties.

Hydrogeology

As already identified in chapter 5 the main uncertainties in the Simpevarp version 1.1 *hydrogeological* model concern the following:

- The current elevation model is not correct in the vicinity of the shoreline. The error is in the bathymetric data between 0 and –3 masl. (Not a major uncertainty).
- All assumptions made in the structural model are directly transferred to the hydrogeological model. In particular, there is an uncertainty in the interpretation of lineaments as fracture zones (confidence level) and in the assignment of hydraulic properties at depth. (i.e. the upscaling of hydrogeologic data is entirely based on the geologic structures).
- The assigned transmissivity distribution in deformation zones and its spatial variability within the zone are uncertain.
- The hydraulic DFN model and resulting connectivity is highly uncertain. It is not based on the v1.1 geological DFN-model, it assumes that the transmissivity distributions are the same for all fracture sets, it has an assumed correlation between transmissivity and size and an assumed spatial distribution. This “interpretation” is evidently unsatisfactory and the data analysis needs to be strengthened in coming versions.
- The current status concerning the groundwater salinity is known at depth only from a few boreholes. This in turn makes it difficult to test the importance of the initial hydrogeological condition (paleohydrogeology). There is also uncertainty in conditions after the last glaciation. The significance of this could be studied by sensitivity analyses.
- The boundary conditions at the regional scale are uncertain, but could be handled by sensitivity analyses in simulations.

Most of the listed uncertainties are difficult to estimate, as an integrated analysis of data was not possible. The uncertainties are in the interpretations as such (i.e. qualitative) and suffer from lack of data or bias in the data available. Some of the settings/assumptions can be tested by means of exploration simulations, although there is no obvious answer to compare the solutions with, e.g. the paleohydrogical problem. A much more elaborate hydrogeologic analysis is expected for version 1.2. More hydraulic data, especially cross-hole tests and additional support for the geological model to be obtained in later data freezes, would allow a more meaningful quantification of the uncertainties.

Hydrogeochemistry

As already identified in Chapter 5 the main uncertainties in version Simpevarp 1.1 *hydrogeochemical* model concern the following:

- Spatial variability in 3D at depth.
- Temporal (seasonal) variability in surface waters, which ultimately impacts the groundwater in the bedrock (but slow processes and temporal averaging make seasonal variability of limited importance).
- Model uncertainties (e.g. equilibrium calculations, migration and mixing).
- Identification and selection of real end-member waters. There is a judgemental aspect of the M3 (principal components) analysis.
- Groundwater composition in the rock matrix.

Spatial variability and temporal variability can be estimated by expert judgement, but the spatial variability at depth cannot be meaningfully quantified before there are data available from depth. In version Simpevarp 1.1 these uncertainties are left unresolved or as inputs to alternative hypotheses. The geochemical model uncertainties are specified in the methodology report /Smellie at al, 2002/ and mentioned in Chapter 5.

Bedrock transport properties

As already identified in Chapter 5 the main uncertainties in the version Simpevarp 1.1 model of the *bedrock transport properties* concern the following:

- Spatial variability and correlation between matrix migration properties and migration paths.
- Distribution of flow-related transport parameters (i.e. essentially the F-distribution), due to all the uncertainties in the hydrogeological (DFN) model and conceptual model for migration (i.e. how the F-distribution is calculated).
- No site-specific data on sorption and diffusion (in the matrix).

In version Simpevarp 1.1 uncertainties were not quantified numerically. For the flow-related transport parameters, the uncertainties could be evaluated by running different variants. However, variability in F ("transport resistance") due to heterogeneity (spatial variability) is assessed.

Surface and near surface

As already identified in Chapter 5 the main uncertainties in the version Simpevarp 1.1 model of the *surface properties and ecosystems* concern the following:

- Surface Hydrochemistry: Temporal variability of water composition in surface waters and model uncertainties (e.g. equilibrium calculations).
- Hydrology: Representativity for the model area of SMHI data collected outside the area, spatial and temporal variability in precipitation and runoff, and lack of data on hydraulic conductivity in Quaternary deposits.
- The present knowledge regarding the total thickness of the Quaternary deposits and its components is low. There is no information regarding the spatial and stratigraphical distribution on the bottom of the sea. There are no laboratory analyses verifying the field judgments. There are no data regarding the in situ properties of the Quaternary deposits.
- Ecosystems (biota): Biomass and production for both flora and fauna.

The normal variation of hydraulic conductivities of the Quaternary deposits in Sweden is shown, see Section 5.4.3. The other uncertainties are not quantified in Simpevarp version 1.1.

6.3.3 Alternatives

As discussed by /Andersson, 2003/ alternatives may both concern:

- An alternative geometrical framework (i.e. the geometry of deformation zones and rock domains), and
- alternative descriptions (models such as DFN or SC – or parameter values) within the same geometrical framework.

Alternative model generation should be seen as a means for model development in general and as a means of establishing and exploring confidence in system behaviour. At least in early stages, when there is little information, it is evident that there will be several different possible interpretations of the data, but this may not necessitate that all possible alternatives are propagated through the entire analysis to Safety Assessment. Combining all potential alternatives with all permutations leads to an exponential growth of calculation cases, and a structured and motivated approach for omitting alternatives at early stages is a necessity.

In particular, for model version Simpevarp 1.1 it is evident that new data from later data freezes may result in considerable changes in later model versions. Spending efforts in completing various alternative models that would then be eliminated by observations would thus be rather pointless. Instead, it is judged more fruitful to consider those alternative hypotheses that may persist and generate alternatives in later model versions. Nevertheless, a few alternatives have been developed and studied also in version Simpevarp 1.1.

Bedrock geological model

As further explained in Table 6-3, identified hypotheses for alternative models of the bedrock geology concern:

- Alternatives in extrapolation of the extension of dioritoid and mixed type domains.
- Alternatives with non-included zones (mainly sub-horizontal).
- Alternative extension (length and depth) of deformation zones and especially one based on the non-linked, but coordinated lineaments, this would result in more, but shorter, zones.
- Other means of carrying out the coordinated lineament interpretations.
- Uncertainty in termination of zones.
- Alternatives in the deformation zone and fracture statistical model including, alternative distributions for orientation, size, and variation with depth.

Of these hypotheses the following alternatives are presented for the version Simpevarp 1.1 model:

- Some alternatives in the extrapolation of the extension of dioritoid and mixed type domains.
- Some alternatives in the fracture statistical model, see section 5.1.

Due to lack of data it has not been judged meaningful to present alternatives for the other hypotheses. As explained in Table 6-3, there are various possibilities to explore these alternative hypotheses using new data to become available in future data freezes.

Rock mechanics and thermal

As further explained in Table 6-3 identified hypotheses for alternative models of the rock mechanics and thermal models concern:

- Alternatives for the stress model, based on alternative understanding of the structural model in combination with observed variations in measurements of stress.
- The heavy dependence of the thermal model on the geological model, implying that if there is an alternative lithological model it will mean an alternative thermal model.

Of these hypotheses the following alternatives are presented for the version Simpevarp 1.1:

- Alternative stress models where i) the whole subarea belongs to the same stress domain or ii) two different stress domains prevail in the subarea, see section 5.2.1.

Hydrogeological model

As further explained in Table 6-3 identified hypotheses for alternative models of the bedrock hydrogeology concern the following:

Alternatives in the geological model (extent of zones and depth decrease of fracture intensity). The obvious alternative interpretation at this point is to reduce the number of lineaments treated as vertical fracture zone segments. Secondly, the impact of at least one sub-horizontal fracture zone should be tested by means of exploration simulation,

The power-law relationship between T and L ($T = a \cdot L^b$) used in the current DFN setup can be tested with other values of a and b or, indeed, no correlation whatsoever. Assignment of T (or K) based on measured data is a critical conceptual issue that will be explored further,

- T correlated to fracture orientation (and stress field).

However, none of these hypotheses have been explored further in version Simpevarp 1.1, but, as explained Table 6-3, there are various possibilities to explore these alternative hypotheses using new data to be available by future data freezes.

Hydrogeochemical model

As further explained in Table 6-3, identified hypotheses for alternative models of the bedrock hydrogeochemistry concern reasons for the observed groundwater composition, i.e. as a result of:

mixing and reactions,

only reactions,

only mixing, or

alternative end-members.

Mixing models based on alternative end-members are already evaluated in version Simpevarp 1.1, see Chapter 5.There has only been initial testing of the other alternative hypotheses.

Bedrock transport properties

As further explained in Table 6-3, identified hypotheses for alternative models of the transport model concern:

- Alternatives in hydrogeology that would propagate into (potential) alternatives for the flow related migration conditions (F-distribution etc).
- Possible alternatives to the retention models (e.g. sorption vs. co-precipitation); the need and practicality of such alternatives are currently being explored outside the Site Modelling work.

It has not been judged meaningful to further discuss alternative models of the bedrock transport properties in Simepvarp version 1.1.

Surface and near surface

In version Simpevarp1.1 only conceptual modelling of the surface hydrology is performed. In later quantitative modelling, sensitivity analyses and/or stochastic approaches can be applied to analyse uncertainties and their influence on predictions. As regards ecosystems, alternative models are not judged a meaningful approach. The objective of the ecosystem modelling is much more to describe the current-day situation, than to be used for predictive modelling in the future, where it is fully understood that uncertainties will be large.

6.3.4 Overall assessment

Evidently there is much uncertainty in the version 1.1 Site Descriptive Model of the Simpevarp subarea, but main uncertainties have been identified, some have also been quantified and others have been left as input to formulation of alternative hypotheses. However, since a main reason for uncertainty in version Simpevarp 1.1 is the lack of data and poor data density, and as many more data are expected by future data freezes, it has not been judged meaningful to carry the uncertainty quantification or alternative model generation too far. These efforts would soon be outdated, whereas the types of uncertainties and alternative hypotheses identified are judged to be very useful input to the uncertainty and alternative model assessments in coming model versions.

6.4 Consistency between disciplines

Another prerequisite for confidence is consistency (i.e. no conflicts) between the different discipline model interpretations.

6.4.1 Interactions considered

As a first step in assessing the consistency between disciplines the modelling group has documented the interactions considered within the framework of an interaction matrix. Table 6-5 provides an overview of these interactions and Table 6-6 lists them in full.

Table 6-5. Summary of interactions considered in version Simpevarp 1.1. Note, an absence of a yes only indicates that the interaction was not considered – not that there is no interaction. (There is a clockwise interaction convention in the matrix, e.g. influence of geology on rock mechanics is located in Box 1,2, whereas the influence of rock mechanics on geology is located in Box 2,1).

Bedrock Geology	Yes	Yes	Yes	Yes	Yes				
Yes	**Rock Mechanics (in the bedrock)**		Yes		Yes				
		Thermal (in the bedrock)							
Yes	Yes		**Hydrogeology in the bedrock**	Yes	Yes				
			Yes	**Hydrogeo-chemistry in the bedrock**	Yes				
			Yes		**Transport properties in the bedrock**				
				Yes		**Hydro-chemistry (surface and near surface)**			Yes
			Yes			Yes	**Near surface hydrology, climate and meteorology**		Yes
Yes			Yes				Yes	**Quaternary Deposits and topography**	Yes
									Ecosystems

Table 6-6. Interactions considered between disciplines in version Simpevarp 1.1.

Bedrock Geology	Spatial distribution of properties based on lithological (rock) domains. (DFN geometry could potentially be used to infer properties)	Modal analyses Main components of lithological model Generic data from Äspö (density)	Deformation zones from v0 DFN-geometry from TR-02-19 and SDM FM v1.1	Fracture mineralogy Bedrock geochemistry	Identified rock types in rock domain model Petrophysics from surface samples	–	–	–	–
Stress orientations in relation to fracture sets.	**Rock Mechanics (in the bedrock)**	–	Stress orientation expected to affect hydraulic anisotropy field (qualitative discussion in v1.1)	–	Consider stress impact on “intact” rock samples for porosity measurements	–	–	–	–
	–	**Thermal (in the bedrock)**	–	–	–	–	–	–	–
Confirmation and indications of structures in previous models (Äspö/Hålö), also based on hydraulic assessments of data from these sites. S1.1 data not used for this purpose	Water pressure reduces the rock stress to effective stress (“assumed hydrostatic”)	–	**Hydrogeology in the bedrock**	Simulation of past salinity evolution, predicted salinity distribution and possibility to compare predicted and measured	H-model used to calculate flow distribution, flow paths, F-values, tw and discharge areas	–	–	–	–
–	–	–	Hypothesis of palaeo evolution. Present day salinity distribution “calibration target” for simulation	**Hydrogeo-chemistry in the bedrock**	GW composition (Eh, pH, salinity etc) used for selection of associated sorption and diffusion values The actual selection is done in the Safety Analysis	–	–	–	–

–	–	–	Consistency check as regards porosities and mass transfer parameters used in palaeo-simulations	–	**Transport properties in the bedrock**	–	–	–	–
–	–	–	–	Seasonal variation in surface chemical composition used as input for the chemistry models	–	**Hydrochemistry (surface and near surface)**	–	–	Surface water chemistry
–	–	–	GW recharge and discharge Boundary conditions and consistency check (meteorological data)	–	–	Spatial distribution of surface water	**Near surface hydrology, climate and meteorology**	–	Climate
Digital Elevation Model / Interpretation of topographic lineaments Map of outcrops based on field data / air photography	–	–	Distribution of permeability in QD based on generic data for different soil types and the distribution in the QD model Topography is boundary condition	–	–	–	QD map from v0 Generic info on conductivity	**QD and topography**	Digital Elevation Model (incl. bathymetry) Soil types Drainage areas
–	–	–	–	–	–	–	–	–	**Ecosystems**

As can be seen from the tables, many inter-disciplinary interactions have been considered. Examples are given below.

Bedrock geology and rock mechanics

Bedrock Geology on Rock Mechanics: There are several qualitative uses of the bedrock geological model in the rock mechanics model. The assessed spatial distribution of rock mechanics properties is based on the lithological domains, i.e. it is assumed that the properties are constant within each rock domain. The DFN model, together with the description of fracture zones and fractures properties, can be used for assessing rock mass properties as outlined in the rock mechanics methodology report /Andersson et al, 2002a/, although this was not done in version 1.1. The structural model is mainly used for estimating the variability of state of stress. Clearly, there is more potential for couplings. In particular, the structural model can be used for simulating the stress distribution as envisaged in the rock mechanics methodology report /Andersson et al, 2002a/.

Rock Mechanics on Bedrock Geology: There are also qualitative uses of the rock mechanics model in assessing the reasonableness of the bedrock geological model. In particular, by determining whether the overall stress orientations are reasonable in relation to the orientation of the fracture sets. In principle, the rock mechanics property model could also have influenced the definition of which rock types could be combined into single rock domains (i.e. rock types of similar rock mechanics properties). However, in practice, the rock domains were defined without specifically soliciting this feedback.

Bedrock geology and hydrogeology

Bedrock Geology on Hydrogeology: The geometry of deformation zones and fractures (deterministic and stochastic DFN) should be directly transferred to the hydrogeological model. However, the version 1.1 local scale geological model of the Simpevarp subarea was, according to plan, developed too late to allow such direct information transfer. In particular, the hydrogeologic DFN-model was not based on the geologic DFN-model developed for Simpevarp, but was instead based on the DFN-models developed for Forsmark version 1.1 /SKB, 2004/ and the model used in the modelling exercise at Laxemar /Andersson et al, 2002b/. Evidently, a much tighter connection between the geological and the hydrogeological model is expected in version 1.2.

Hydrogeology on Bedrock Geology: A number of the deformation zones taken from existing models of Äspö and Hålö are also confirmed hydraulically. However, no new Simpevarp version 1.1 hydraulic data were used for this purpose.

Rock mechanics and hydrogeology

There has been no explicit inclusion of MH or HM coupling. However, there is a qualitative discussion as to whether the stress orientation may affect the anisotropy of the effective hydraulic conductivity has been provided. Also, it is understood and considered that the water pressure (assumed hydrostatic) reduces the rock stress to effective stress.

Hydrogeology and hydrogeochemistry

The simulation of past salinity evolution makes is possible to compare the hydrogeological model predictions with the predictions made in hydrogeochemistry and thus enhance understanding of the hydrogeochemical evolutionary processes. Conversely, the hydrogeochemical description of the current salinity distribution provides a “calibration target” for simulation (but the salinity distribution in the rock matrix would also be “needed”). Ultimately, the aim is to make the hydrogeology and hydrogeochemistry descriptions mutually consistent.

Impact on transport model

Several disciplines impact on the transport model. The rock domains in the geological model provide rock types for which sorption and diffusion characteristics should be described. Through

calculated flows, the hydrogeological model provides (most of) the flow-related transport conditions (i.e. distribution of F, t_w and discharge areas). The groundwater composition from the hydrogeochemical model sets conditions for selecting appropriate sorption and diffusion values, but the actual selection is done in the Safety Assessment.

Quaternary deposits and bedrock geology

The Digital Elevation Model is input to the interpretation of topographic lineaments.

6.4.2 Overall assessment

It can generally be observed that interdisciplinary interactions are considered in the site descriptive modelling. All disciplines share the geometric framework of the bedrock geological model, but, due to restrictions in data freeze 1.1, the implications of the geological model on e.g. rock mechanics and hydrogeology, havee not been considered in full. The interactions from e.g. rock mechanics and hydrogeology on geology have been quite limited. Much more interdisciplinary interactions are expected in version 1.2. Nevertheless, the "palaeohydrological" simulations demonstrate the aim to make the hydrogeology and hydrogeochemistry descriptions mutually consistent.

In later model versions the auditing may be extended to reviewthe interactions that ought to be considered. Then a more definite assessment regarding interdisciplinary consistency should be possible. Furthermore, more quantitative analyses may be warranted, but this does not imply a need to apply coupled THM codes. Direct THM coupling, see e.g. /Andersson, 2004/, need only be considered in cases in which there is significant change of the THM-state. It is probably sufficient to explore whether the final results (i.e. what is observed today) are qualitatively in agreement with known coupled processes. This does not preclude the need to consider whether THM-couplings need to be modelled in the Safety Assessment context.

6.5 Consistency with understanding of past evolution

For confidence, it is essential that the naturally ongoing processes considered as important can underpin – or at least do not contradict – the model descriptions. The distribution of the groundwater compositions should, for example, be reasonable in relation to rock type distribution, fracture minerals, current and past groundwater flow and other past changes. Such 'paleohydrogeologic' arguments may provide important contributions to confidence, even if they may not be developed into 'proofs'.

Table 6-7 lists how the current model is judged to be consistent with the overall understanding of the past evolution of the sites as outlined in Chapter 3. The answers generally suggest that the model as presented is in agreement with current understanding of the past evolution. The following observations are noted:

- It would be potentially interesting to couple the geologic evolution and the formation of the different fracture sets (the order of formation could be determined) with hydrogeochemical indications (e.g. fracture minerals) of age. Such studies performed at Äspö were rather inconclusive, but they could nevertheless provide some insights into the validity of the conceptual model for groundwater flow and hydrogeochemical development.
- In the data freeze for version Simevarp 1.1 there was no information (either for or against) to be used for assessing potential "neo-tectonic" movements. (Such information may potentially be available in later data freezes). Whether near-surface boulder "caves" and "assemblies" are indications of post glacial-seismic events is assessed in a separate study.
- Groundwater flow and salinity transport simulations cover the period from the melting of the last glaciation, but not alterations before that. Instead, the simulations have explored the impact of various assumptions on initial conditions, properties, events and boundary conditions since the latest deglaciation (approximately 10,000 years ago).

Table 6-7. Consistency with past evolution.

Site Descriptive Model (SDM) Technical Audit: Consistency with past evolution	
Assess consistency as regards crystalline bedrock from c. 1,900 million years to the Quaternary.	Geological model is consistent with the regional geological evolutionary model. There are no new data in Simpevarp 1.1 that would necessitate an update of this evolutionary model. The overall stress model is the same as in version 0 and builds on the tectonic evolutionary model and old stress data. It would be potentially interesting to couple the geologic evolution and the formation of the different fracture sets (the order of formation could be determined) with hydrogeochemical indications (e.g. fracture minerals) of age. Such studies performed at Äspö were rather inconclusive, but could nevertheless provide some insights into the validity of the conceptual model for groundwater flow and hydrogeochemical development.
Assess consistency as regards evolution during the Quaternary period.	**Geology: Seismicity** In 1.1 there is no information (for or against) to be used for assessing potential ”neo-tectonic” movements. (Such information may potentially be available in later data freezes). Whether near surface boulder “caves” and “assemblies” are indications of post glacial seismic events is assessed in a separate study, but not addressed in S1.1. **Bedrock Hydrogeology and Hydrogeochemistry** Groundwater flow and salinity transport simulations cover the period from the melting of the last glaciation, but not alterations before that. Instead, the simulations have explored the impact of various assumptions on initial conditions, properties, events and boundary conditions since the latest deglaciation (approximately 10,000 years ago). In general, analysing the impact of potential changes after the glaciation on the current day groundwater flow and distribution of groundwater composition will affect and support the conceptual GW model. The interaction between the evolution of the surface water composition and the evolution of the groundwater composition is described in terms of processes and the origin of various water types (e.g. meteoric water, glacial melt water, Littorina water, brine. **Ecosystems** Historical development of the surface ecosystems is consistent with the current description of these systems.

6.6 Comparison with previous model versions

Another indication of confidence is to what degree measurement results from later stages of the investigation are conssistent with previous predictions. This is important for discussing the potential benefit of additional measurements. Clearly, if new data compare well with a previous prediction, the need for yet additional data may diminish.

6.6.1 Auditing protocol

A protocol has been developed for checking the consistency of successive model versions. It concerns:

- changes compared with previous model version (i.e. in this case version 0, /SKB, 2002b/),
- whether there were any “surprises” associated with these changes, and
- whether these changes were significant or only concern details.

Table 6-8 lists the answers to these questions.

Table 6-8. Comparison with previous model version.

Site Descriptive Model (SDM) Technical Audit: Previous model version	
List changes compared to previous model version (i.e. version 0).	Additional/updated features: • Geological model based on more sub-surface information and much higher resolution surface data. A new DFN-model has been developed (DFN models existed previously for Äspö). • A first thermal model. • Strength information from Äspö HRL and CLAB. Empirical classification (Q) by depth at KSH01A and outcrop assessment. • Hydrogeological simulations including past evolution. New structure model input. New topography, data from depth (KSH01A). • Hydrogeochemical model based on a more detailed process description and better description of the distribution of water types. • A first crude transport model. • Map of Quaternary deposits (more detail, which also better represents the actual distribution of outcrops). • Vegetation model, both land and sea, has been developed. Changes in the description: • Higher resolution (more details) in the rock domain model. • Deformation zone ZSM0003A0 is removed (improved interpretation). • Deformation zone just east of Ävrö and the Simpevarp peninsula (ZSMNE024A) is upgraded to zone (from lineament in version 0) and dipping west. • DFN-model – some fracture sets occur both at large scale (lineaments) and in detailed mapped fractures (outcrops and borehole). Other sets do not. • In KSH01A there is a depth decrease in hydraulic conductivity – but not represented in the hydrogeological model (as this depth decrease is less pronounced in e.g. Äspö, Ävrö. Better to resolve this in version 1.2, when more data from the Peninsula will be available).
Address whether there were any “surprises” connected to these changes.	No major surprises, but: • Measured fracture frequency in KSH01A is high (see chapter 4) in relation to previous experience from Äspö HRL. (Not necessarily a difference in the rock – could also be connected to fracture-mapping practices). • Relatively low mean hydraulic conductivity in KSH01 compared to previous experience in the area – and in relation to the high fracture frequency. • No Littorina water found.
Address whether changes are significant or only concern details.	Indications of low permeability in KHS01A could be very important. However, the current information is too local to make any far reaching conclusions on the entire Simpevarp Peninsula. Deformation zone just east of Ävrö and the Simpevarp. peninsula (ZSMNE024A) may have large implications. Updated process understanding of the surface water. This has significantly improved the understanding of the hydrogeochemical processes in the near-surface.

6.6.2 Assessment

As can be seen, there are two types of changes in version Simpevarp 1.1 compared to version 0 /SKB, 2002b/. One concerns additional features/content of the model and the other concerns changes in the understanding of the site.

Compared with version 0, there are considerable additional features in version Simpevarp 1.1, especially in the geological description and in the description of the near surface. This is natural, since there has been a considerable increase in data compared with the data available for version 0. In summary, these additions and updates concern:

- The Geological model which is now based on more sub-surface information and much higher resolution surface data.

- A geological DFN-model for the Simpevarp peninsula has been developed (DFN models existed previously for Äspö HRL).
- The Rock Mechanics model, which builds on previous models from Äspö and CLAB, but has incorporated new information through e.g. the empirical classification (Q) by depth at KSH01A and the outcrop assessment.
- Establishement of a first thermal model.
- The hydrogeological description, which is partly based on the new geological (structure) model and the fracture transmissivity distribution which is based on data from depth (borehole KSH01A). Hydrogeological simulations of the groundwater evolution since the last glaciation have been performed and compared with the hydrogeochemical conceptual model.
- The conceptual hydrogeochemical post-glacial model formulated to indicate the possible origin of the groundwater has been updated. It is based on a more detailed process description and better description of the distribution of water types.
- Establishment of a first crude transport model.
- Production of a map of the Quaternary deposits with more detail, which also better represents the actual distribution of outcrops.
- Development of a vegetation model, both of land and sea.

Compared to version 0 the main changes concern:

- Higher resolution (more details) in the rock domain model.
- Deformation zone ZSM0003A0 in version 0, which has been removed (improved interpretation).
- The deformation zone just east of Ävrö and the Simpevarp peninsula (ZSMNE024A) which has been upgraded to a zone (from a lineament in version 0) and is dipping west.
- Specification of the DFN-model – some fracture sets occur both in large scale (lineaments) and in detailed mapped fractures (outcrops and borehole), whereas other sets do not.
- In borehole KSH01A, where there is a depth decrease in hydraulic conductivity, but this is not represented in the hydrogeological model as this depth decrease is less pronounced in e.g. Äspö, Ävrö. It is judged better to resolve this in version 1.2, when more data from the Simpevarp peninsula will be available.

Overall there are no major surprises. It is noted that the measured fracture frequency in KSH01A (see Chapter 4) is high in relation to previous experience from Äspö HRL, but this is not necessarily a difference between these rock volumes – it could also be connected to fracture mapping practices. Also, the mean hydraulic conductivity in KSH01A is relatively low compared to previous experience in the area and in relation to the high fracture frequency. No Littorina water has yet been found.

Indications of low permeability in KHS01A could be a very important finding, but the current information is too local to make any far reaching conclusions on the entire Simpevarp peninsula. The deformation zone just east of Ävrö and the Simpevarp peninsula (ZSMNE024A) may have large implications. The updated process understanding of surface water has significantly improved the understanding of the hydrogeochemical processes in the near-surface.

6.7 Overall assessment

This chapter demonstrates that the overall confidence of the version 1.1 Site Descriptive Model of the Simpevarp subarea has been fully assessed. Clearly, the methodology for confidence assessment will be updated in coming model versions. In summary the confidence assessment gives rise to the following conclusions:

Most available data have been analysed and treated according to good practices. Also inaccuracy and biases are understood and accounted for in the subsequent modelling.

There is much uncertainty in the version 1.1 of the site descriptive model of the Simpevarp subarea, but the main uncertainties have been identified, some are also quantified and others are left as input to alternative hypotheses. These hypotheses, if not resolved, would provide a starting point for formulating alternative models in version 1.2.

Interdisciplinary interactions are considered and cross-discipline understanding of the interactions has been established. However, due to restrictions at data freeze Simpevarp 1.1, the interactions between e.g. rock mechanics and hydrogeology on geology have been quite limited. Many more interdisciplinary interactions are expected in version 1.2.

The model as presented is in general agreement with current understanding of the past evolution of the area.

Compared with version 0 there are additional features in version Simpevarp 1.1, especially in the geological description and in the description of the near surface.

In terms of changes in the understanding of the site there are no big surprises.

The overriding issue affecting confidence in models based on the version Simepvarp 1.1 data freeze is the bias and uncertainty resulting from varying spatial coverage of data and very few and unidirectional deep borehole data. These biases will be reduced in coming model versions.

7 Resulting description of the Simpevarp subarea

7.1 Surface properties and ecosystems

7.1.1 Climate

The average monthly mean temperature in the Simpevarp area varies between –2°C in January–February and 16–17°C July. The winters are slightly milder on the coast than further inland. The vegetative period (daily mean temperature exceeding 5°C) has a duration of about 200 days.

The annual precipitation (measured) amounts to 500–600 mm in the region with a slight tendency to increase inland. The mean annual (corrected) precipitation at the meterorological stations Oskarshamn, Kråkemåla, Målilla and Ölands norra udde are 681 mm, 694 mm, 579 mm, and 507 mm, respectively, for the period 1991–2000. About 20% of the precipitation falls in the form of snow.

The relative humidity is 80–100% in the winter and 70–90% in the summer; high values applicable at night and low at mid day. The annual sunshine are about 1,800 hours on the coast and slightly lower inland. The cloudiness is 60–65%, slightly less in summer and slightly higher in winter. In summer, the cloudiness tends to decrease near the coast compared with inland.

Based on the synoptic observations at the station Ölands norra udde, the mean annual global radiation was calculated at 1,021 kWh/m^2, with mean monthly values varying from 8.5 kWh/m^2 in December to slightly more than 179.5 kWh/m^2 in June /Larsson-McCann et al, 2002/.

The ground is covered by snow about 75 days per year, with an average annual maximum snow depth of approximately 35–40 cm. The conditions on the coast do not differ much from those inland.

Air pressure is usually above 950 and below 1,050 hPa. The greatest air pressure variations are experienced in the winter and there are only small variations from May to August. More details can be found in /Larsson-McCann et al, 2002/.

7.1.2 Hydrology

Overview of hydrological development since last ice age

The hydrological conditions in the Simpevarp area have changed considerably since the last glaciation. One component is the shoreline displacement, shown in Figure 5-38 and illustrated and discussed further in Section 3.3. Figure 5-38 also shows different stages from the time of the Baltic Ice Lake to the present Baltic Sea, each stage with different marine salinities (see Section 3.3) that probably have affected the present spatial distribution of the salinity in the groundwater and thus constitute an important conditioning constraint for the groundwater flow modelling.

Preliminary conceptual model

The Simpevarp area is characterised by low topographic relief with a relatively small-scale topography and relatively shallow Quaternary deposits. Almost the entire area is below 50 m.a.s.l. The small-scale topography means that many small catchments have developed with local, shallow groundwater flow systems. Groundwater levels are probably shallow, usually less than a few metres below ground in recharge areas and < 1 m in discharge areas.

The lakes are considered to be permanent discharge areas. The lakes are few and fairly small within the regional area. The hydraulic contact with the groundwater zone is highly dependent on the hydraulic conductivity of the bottom sediments. The streams are also considered as permanent discharge areas. However, some are dry during parts of the year. The wetlands can either be in direct contact with the groundwater zone and constitute typical discharge areas or be separate systems with tight bottoms and little or no hydraulic contact with the groundwater zone.

The shallow groundwater flow in the Quaternary deposits can be considered to be driven by local variations in the topography. The groundwater recharge from the Quaternary deposits to the bedrock aquifer is probably small, due to the generally higher hydraulic conductivity of the Quaternary deposits than the bedrock. The uppermost metre of the Quaternary deposits is generally much more permeable and porous than deeper-lying deposits.

Catchment areas and run-off

Within the regional scale model area there are several principal catchment areas, see Figure 4-38**.** The catchment areas are based on the interpretation by SMHI and are only to be regarded as preliminary and this map will be updated during 2004. As an example of these preliminary data, the size of the catchment area for the Laxemar stream (No. 23 in Figure 4-38) gives and area of 41 km^2 with an expected run-off 5.4 L/(s·km^2) (approximately 170 mm/year) as an annual mean (MQ). The catchment "Forshultesjön nedre" was chosen by SMHI as a representative for the Simpevarp area with a run-off of 5.7 L/(s·km^2) (approximately 180 mm/year) as an annual mean. The expected long-term average of annual minimum discharge (MLQ, 0.24–0.58 L/(s·km^2)) and the highest maximum flow over a period of 50 years (HHQ50, 59–99 L/(s·km^2)) are about 0.05–0.1 and 10–20 times the MQ, respectively.

Lakes

Kalmar län is relatively rich in lakes and running waters. The county contains c. 2,000 lakes bigger than one hectare, and most of them are situated in the northern part. Many lakes in the northern part of the county are situated in fissure valleys and are therefore elongated and narrow /Lindborg and Schüldt, 1998/. Most of the lakes in the area "Smålands and north Götalands archipelago" are oligotrophic and they have a mean depth of 3.8 m. The Simpevarp regional model area contains less than 10 lakes, most of them relatively small, see Figure 4-38. The only larger lake in the area, Lake Götemaren (2.84 km^2), is situated on the northern border of the regional model area. A brief description of this lake can be found in /Lindborg and Schüldt, 1998/, whereas no data for the other lakes in the area are available for this version of the site descriptive model.

Water chemistry in lakes and streams

No new information on the water chemistry in lakes and streams in the Simpevarp area has been compiled for this version of the site descriptive model.

7.1.3 Oceanography

Physical properties

The area in the northern part of the strait of Kalmarsund is part of the Baltic Sea basin where the hydrography is governed by salinity stratification with two haloclines at 50–60 m and about 70 m /Larsson-McCann et al, 2002/. The temperature in the surface layer has the same seasonal variations that are found generally in the Baltic Sea. A warm surface layer is developed during spring due to the increased solar radiation. The temperature in this layer can exceed 20°C, with a thermocline found at 20–25 m depth by the end of the summer. In the autumn, the temperature stratification breaks down due to increased cooling and wind mixing. Below the primary thermocline, the temperature is stable between 5–6°C all the year round.

In the open waters around Simpevarp, the hydrographical conditions are strongly affected by coastal processes with large variability in the surface temperature. This is due to the local wind conditions resulting in near-shore upwelling. The salinity stratification is weak and the water exchange is good, as observed in measurements of high values of oxygen saturation in the water column. The currents in the near-shore area are weak and dominated by long-shore directions /Larsson-McCann et al, 2002/.

A numerical model study based on representative data on physical driving force data (statistically averaged over approximately 10 years) has been performed for the Äspö area, subdivided into five separate basins, interconnected by four straits and connected to the Baltic coast through three

straits, see /Engqvist, 1997/. The water exchange of the shallow Borholmsfjärden bay, with the comparatively small cross-sectional area of its straits, is dominated by sea-level variations, although baroclinic exchange components (estuarine and intermediary circulation) also contribute. The average transit time (averaged over the basin volume for a full year cycle) is found to be a little over 40 days for exogenous water (i.e. coastal water and freshwater combined). This measure of water exchange is comparable to the combined average of an ensemble comprising 157 similarly analysed basins distributed along the Swedish east and west coasts. The consequences for the transit times of short- and long-term variations in the driving forces were also analysed. The standard deviation (S.D.) of the transit time during an average year (intra-annual variation) is greater than the S.D. between years (interannual variation) for all basins except for the Borholmsfjärden bay for which these two measures are of similar magnitude. The range of the retention times that results from an extreme combination of forcing factor variation between years is found to be greater the farther a particular basin is located from the coast, measured in terms of the minimal number of separating straits.

Water chemistry

As mentioned above, the *hydrography* in the area is governed by salinity stratification with two haloclines at 50–60 m and about 70 m. Between the surface and the primary halocline, the salinity varies between 6–7 psu (practical salinity unit) /Larsson-McCann et al, 2002/. Between the primary and the secondary halocline the salinity varies between 8 and 10 psu, whereas it varies between 11 and13 psu below the secondary halocline.

The *oxygen* conditions in the Baltic Sea vary with depth and season. Above the primary halocline the water is saturated during autumn due to the thermohaline circulation. The uppermost layer, reaching down to 20–30 m, stays oxygen saturated all year. In the deeper layers, the oxygen supply is limited by the strong salinity stratification. Oxygen can only be added by inflow of heavy salt water through the Darsser threshold of the region of the Öresund strait in the south. Between such inflows, the oxygen concentration constantly diminishes in the deep water. This is a result of the biological degradation of organic matter sinking from the surface layer.

7.1.4 Overburden including Quaternary deposits

All known Quaternary deposits, which constitute the bulk of the overburden in the Simpevarp region, were formed during and after the latest glaciation, which declinded subsequent to its peak some 14,000 years ago /Lundqvist and Wohlfarth, 2001/. The whole area is located below the highest coastline and the overburden has partly been eroded and redeposited by waves and streams when the water became shallower, as a consequence of the isostatic land uplift. The Simpevarp subarea, in its present state, is a relatively flat area with a coastline well exposed towards the Baltic Sea. Isostatic land uplift is still an active process and other coastal processes are continuously changing the properties and distribution of the overburden

The areal distribution of Quaternary deposits on the Simpevarp peninsula and on the islands of Ävrö and Hålö is shown in Figure 7-1. A relatively large part of the area comprises exposed bedrock. The highest areas are entirely exposed bedrock. There are probably several reasons for the relatively low coverage of Quaternary deposits. One reason may be that a relatively small amount of glacial till was deposited in the area during the latest ice age. Another reason is the fact that large parts of the investigated area are exposed towards the open Baltic Sea. That has caused, and is still causing, erosion and redeposition of overburden by waves and streams. It must also be kept in mind that the lowest parts of the landscape, in the Simpevarp subarea, are still below sea level. It is likely that large amounts of glacial and postglacial deposits occur in these low areas. Forthcoming investigations will reveal the distribution of overburden in the areas covered by water.

The glacial *striae* indicate a dominant ice movement from N40–50°W in the area. This direction probably reflects ice movement shortly before the latest deglaciation. Some *striae* indicate an older more northerly ice flow direction N30°W.

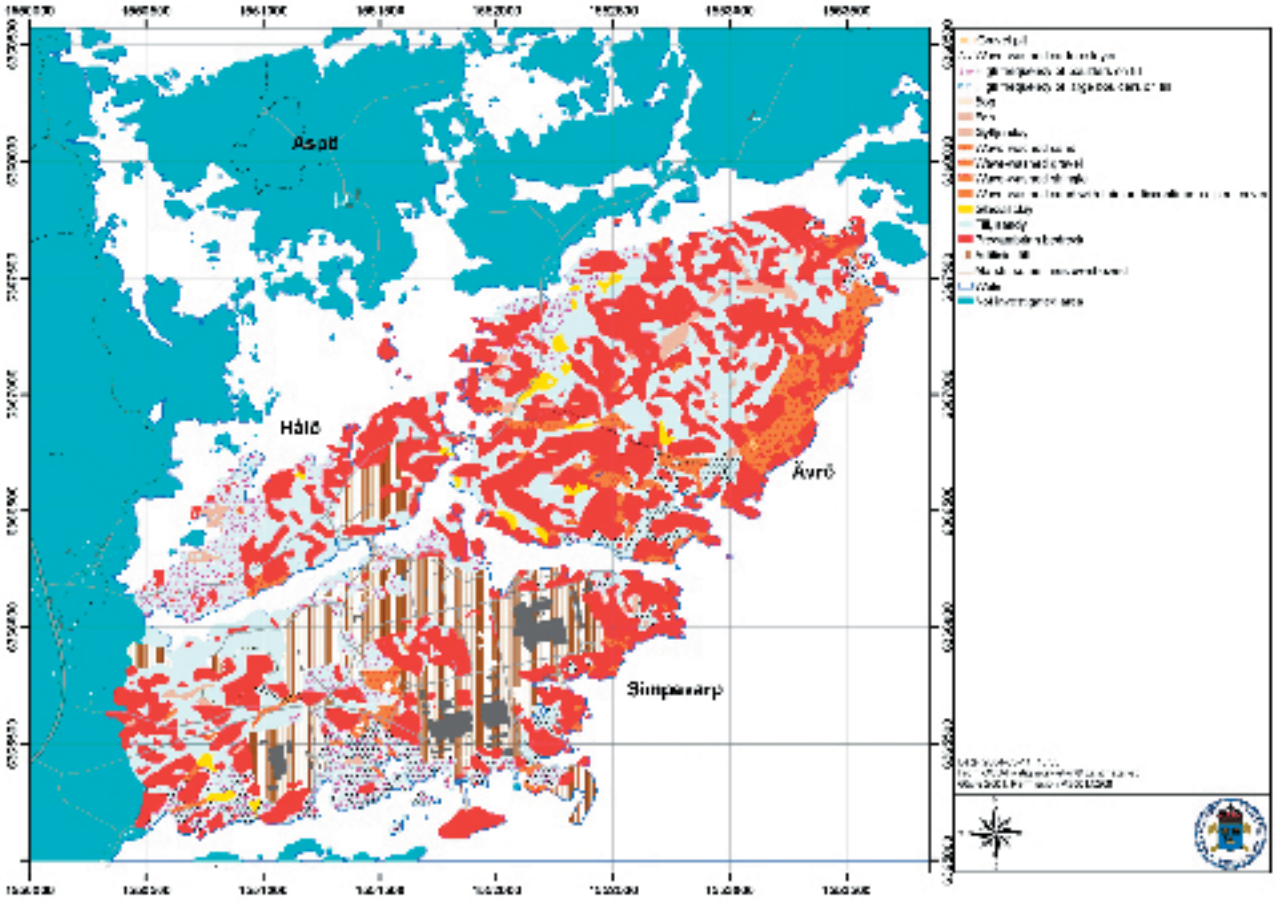

Figure 7-1. *The superficial distribution of Quaternary deposits and bedrock outcrops in the Simpevarp subarea. The map also shows areas with wave-washed surface layers and the superficial boulder frequency of the till. It is noted that the mainland and islands north of Ävrö and Hålö have not been mapped yet.*

The glacial till is the oldest known component of the overburden in the area and was deposited directly by the Quaternary glaciers. It may be assumed, but not concluded, that most of the till was deposited during the latest glaciation and rests directly on the bedrock surface. Till is the dominant Quaternary deposit and covers about 35% of the area (c.f. Table 5-1). The morphology of the till normally reflects the morphology of the bedrock surface. The thickness of the till varies between 0.5 and 3 m. In some areas, e.g. on the western part of the island of Hålö, the till layer may be thicker, which will be substantiated by future drilling and excavations. Most of the till has a sandy matrix, but gravelly till does also occur. Forthcoming grain size analyses will provide a more complete description of till composition.

The melt water from the ice deposited large amounts of sand and gravel (glaciofluvial material), which often formed eskers. No such deposits are, however, known from the Simpevarp subarea. Several eskers are known, further to the east, within the regional model area /Bergman et al, 1998/. These will be a focus for studies during the forthcoming investigations.

Directly after the deglaciation the water depth was c. 100 metres deeper than at present /cf. Agrell, 1976/. The melt water from the receding ice contained large amounts of suspended silt and clay, which were deposited on the deepest parts of the sea floor.

As the water depth decreased, waves and streams eroded and redeposited some of the previously deposited overburden materials. In this way some of the glacial clay was redeposited as postglacial clay, which often can be found in the deeper parts of valleys. These clay deposits often contain organic material, often referred to as gyttja. There is only one such known deposits with postglacial clay (gyttja clay) within the Simpevarp subarea.

Streams and waves have further altered and reworked the glaciofluvial deposits and the till as the water depth in the sea successively decreased. In wave-exposed positions, the fine-grained size fractions have, therefore, often been washed out from the uppermost sequence of the till. The till, at these positions, has a stoney and/or gravelly surface layer. Wave-washed till occurs on southern parts of the Simpevarp peninsula and on the island of Ävrö. These are areas which have been and still are exposed to the Baltic Sea. The material eroded from the till, e.g. sand and gravel, is subsequently deposited at more sheltered localities. Such deposits of sand and gravel often cover the glacial clay within the investigated area (c.f. Table 4-1).

Postglacial clay, which is deposited on the floors of sheltered bays, often contains organic material that originated from algae and other types of vegetation in the area. Such gyttja sediments were found in a core from the Borholmsfjärden bay south of Äspö /Risberg, 2002/. It is therefore likely that the size of the area where clay containing organic material (gyttja sediments) is found will increase when the bays in the Simpevarp subarea, in the future, are lifted above the present sea level.

Peat covers c. 2% of the investigated area and is restricted to some of the more narrow valleys. Peat consists of remnants of dead vegetation which are preserved in areas (often mires) where the prevailing wet conditions preclude the breakdown of the organic material. The mires are divided in two types: bogs and fens. The bogs are poorer in nutrients compared with the fens and are characterised by a coherent cover of *Sphagnum* species. Fen peat is the most common peat type in the Simpevarp subarea. There are, however, a number of small, not raised, bogs on the northern part of the island of Ävrö. The bog peat is often underlain by fen peat and it is possible that some of the present areas covered by fen peat in the future will be covered by bog peat.

Hydrogeology

No tests for determination of hydraulic conductivity of the Quaternary deposits have been made so far, but are planned for the later stages of the initial site investigations. The hydraulic conductivity of Quaternary deposits at Simpevarp therefore has to be based on generic data.

The Quaternary deposits have been treated in a very simplified way in the numerical groundwater simulations, as a layer of constant thickness of 3 m and homogeneous hydraulic properties with e.g K=1.5E–5 m/s (Table 5-33).

7.1.5 Biotic entities and their properties

The description of the biotic components of the ecosystem is divided into the entities primary producers and consumers /cf. Löfgren and Lindborg, 2003/. The entity consumers includes, beside herbivores and predators, also detrivores, such as invertebrates, fungi and bacteria.

Producers

Terrestrial producers

The vegetation map /Boresjö Bronge and Wester, 2003/ for the Simpevarp regional model area is shown in Figure 7-2. The area is situated within the Boreonemoral zone, which contains woodlands south of “Limes Norrlandicus”, the biological Norrland boundary /Sjörs, 1967/. The northern limit of the boreonemoral zone coincides with the limit of oak and the area contains 750–900 species of vascular plants /NMR, 1984/. The region is part of the “Archipelagos of Södermanland and northern Götaland”, a sub-region of the “Coast and archipelagos of the Baltic Sea” /NMR, 1984/. In this part of the archipelago, no birch (*Betula pendula*) occur and the annual temperature and the water deficit during the vegetation period are higher than in the main region /Gustafsson et al, 1995/.

The *categories of coniferous forest* compose 80% of the total forest area and are divided into: pine forest (c. 40%), spruce forest (c. 25%) and mixed forest (c. 15%) /Gustafsson and Ahlén, 1996/. Mixed deciduous forest also occurs, in addition to forests with one dominating species, for example oak (*Quercus robur*). The dominating vegetation type in the coastal area is pine forest on outcrops of bedrock /Gustafsson et al, 1995/.

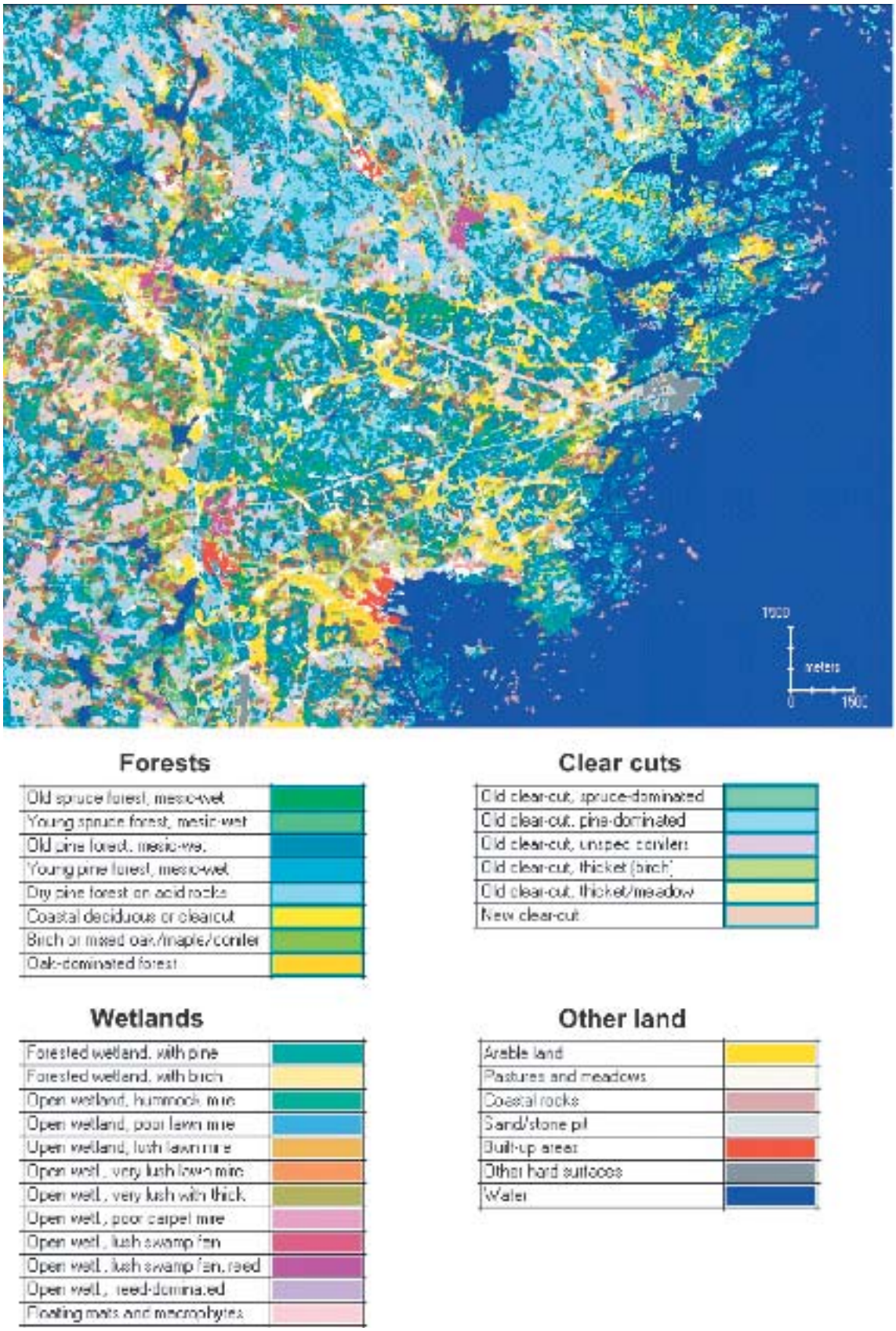

Figure 7-2. *The vegetation/land cover map of the Simpevarp area /from Boresjö Bronge and Wester, 2003/.*

The most common *undergrowth* is the grass type, which is considerably more common in southern Sweden. The beech (*Fagus sylvatica*), which is sensitive to frost in spring, has its northern limit in the Kalmar county /Gustafsson and Ahlén, 1996/.

Limnic producers

No site specific description of limnic producers has been undertaken for Simpevarp 1.1.

Marine producers

The marine/brackish primary producers are found in the free water (pelagic community) and on the soft and hard bottoms (benthic communities).

Species composition, biomass and community dynamics for the *pelagic* producers (planktonic algae and bacteria) are not known at the time of writing. Below is a description of major primary producers of the benthic communities.

On *shallow soft bottoms* the vegetation is dominated by vascular plants. In the bay Borholmsfjärden, surrounding Äspö island, the shallow waters are dominated by dense covers of species of *Chara* and *Najas* – calcium-rich vascular plants, and *Vaucheria* – a green algae. These, and other vascular plants, as species of Potamogeton, are common down to depths of approximately 4–5 m were the macro-vegetation disappears /Fredriksson and Tobiasson, 2003/. South of Simpevarp, the coast is more fragmented and the more exposed soft bottoms are less dominated by Chara and Vaucheria but are grown over with phanerogams such as *Zostera marina*, *Potamogeton spp.* and *Myriophyllum spicatum*. This difference in vegetation communities reflects differences in the fauna in the shallow waters.

On the *shallow hard bottoms*, especially on rock and boulders in wave-exposed areas, the bladder wrack (*Fucus vesiculosus*), one of the few perennial algae, is found. The bladder wrack covers most of the wave-exposed coast at depths of between approximately 1–2 m to 4–7 m depth (depending on water quality and light conditions). Above and within the *Fucus* community different annual algae grow. The bladder wrack forms a substrate for a wide variety of other organisms, thereby creating a community consisting of epiphytic algae (eg. *Ceramium sp*.), molluscs (eg. *Mytilus edulis*), spawning fish (eg. *Herring, stickleback*).

Deeper hard bottoms are inhabited mostly by other filamentous red and brown algae. At depths between 7 and 20 m mostly red algae are found. As this depth interval comprises such a large part of the vegetation-covered bottoms, red algae covers the largest fractions of the local area. Large red algae covered areas are found offshore of the island of Ävrö and off the archipelago south of Simpevarp /Fredriksson and Tobiasson, 2003/.

Consumers

Terrestrial consumers

See Section 5.7.2.

Limnic consumers

No site-specific description of limnic consumers has been undertaken for Simpevarp 1.1.

Marine aquatic consumers

The marine/brackish consumers are found in the free water (pelagic community) and on the soft and hard bottoms (benthic communities).

The *pelagic community* comprises fish, zooplankton and marine mammals. Species composition, biomass and community dynamics for zooplankton are not known at the time of writing. In the sheltered inner areas, eg. north and south of Äspö and in the archipelago south of Simpevarp, the fish community is dominated by the omnivores roach, *Rutilus rutilus*, white bream, *Blicca bjoerkna* and

the carnivore perch, *Perca fluviatilis*, but harbours also approximately 22 other species including the carnivorous pike, *Esox lucius*, and ide, *Leuciscus idus*. The coastal fish community is dominated by the zooplankton-feeding herring, *Clupea harengus*, and its relative sprat *Sprattus sprattus*, but also here the roach and perch are common. Cod, *Gadus morhua*, is an important fish eating species in the coastal system. In total, 28 species have been caught by the National Board of Fisheries between 1994 and 2003 /Lingman and Franzén, 2003/.

The only marine mammal in the area is the grey seal and the nearest colony (35 individuals in 2002) is found 20 km north of Simpevarp. The extent of their presence in the area is not known /Helander et al, 2003/.

The fauna of the *soft bottom communities* have generally low total biomass in the area, probably partly due to the small portion of stable bottom substrates in the offshore areas and the large areas covered by *Vaucheria* and *Chara* vegetation. The offshore soft bottoms are dominated by the filter feeder *Macoma baltica*, with approximately 95% of the biomass. The mean biomass density was 16 g dw/m^2, but most stations had considerably values. In the northern area, very low biomass density was recorded (3 g dw/m^2) and this is probably explained by the dense vegetation which suffocates other organisms. The southern area, the archipelago, has a more homogenous soft bottom community and higher biomass and also more contributors to the total biomass than the other areas, such as the crustaceans *Corophium volutator* and other filter feeders such as the blue mussel *Mytilus edulis* /Fredriksson and Tobiasson, 2004/.

The *hard bottom communities* have been sampled and here much higher biomass densities are found compared with the soft bottom communities. The biomass densities at the hard bottoms in red algae and bladder wrack communities are 10 to 50 times the soft bottom fauna densities /Fredriksson and Tobiasson, 2003/. The deeper hard bottoms (below approximately 10 m) have not yet been investigated.

7.1.6 Humans and land use

See Section 5.7.3 and Appendix 4.

7.1.7 Nature values

During the planning process, a methodology for compiling and assessing areas of environmental and/or cultural concern was developed. This aimed at producing a map showing areas suitable and not suitable for e.g. drilling or other disturbing activities, i.e. an *accessibility map*, but also at documenting site-specific information of environmental and/or cultural interest for an Environmental Impact Assessment.

The basis for this map was an aggregation of spatially defined areas, such as legally protected areas, ecologically sensitive areas, buffered watercourses and buildings, cultural amenities etc. In Table 7-1 some examples of defined areas/points, and how these were spatially delimited, are given. For a full description on the procedure, see /Kyläkorpi, 2004/. After the aggregation of all non-suitable areas into one zone, the remaining area can be considered as potentially available for the various survey activities after a complementary field check.

7.1.8 Overall ecosystem model

No overall ecosystem model has been produced for the Simpevarp Site Descriptive Model version Simpevarp 1.1.

Table 7-1. Examples of natural, cultural and socio-economic values used to produce the accessibility map for the Simpevarp regional model area.

Area of interest	Value	Characteristics	Delimitation
Nature values	Nature reserves	Legally protected	Polygon boundary
	Key biotopes	Ecologically sensitive	Polygon boundary
	Red listed species	Ecologically sensitive / Legally protected	Occurrence buffered 100 m
	Water courses	Ecologically sensitive	Buffered 50 m
	Lakes	Ecologically sensitive	Shoreline buffered 100 m
Cultural values	Ancient monuments	Legally protected	Occurrence buffered 100 m
Socio-economic values	Residental properties	Legally protected / policy reasons	Buildings buffered 100 m
	Wells		Buffered 100 m

7.2 Bedrock – regional scale

7.2.1 Geological description

The rock domain model and the deterministic model of deformation zones has only been constructed for the local scale model domain employed for the Simpevarp descriptive model version 1.1, c.f. Section 7.3.1.

7.2.2 Rock mechanical description

The stress model for the regional scale coincides with the model for the local scale (see Section 7.3.2.

7.2.3 Thermal properties

The model of thermal properties for the regional scale coincides with the model for the local scale (see Section 7.1.1).

7.2.4 Hydrogeological description

Hydraulic properties are described for deformation zones (Hydraulic Conductor Domains, HCD), the rock mass between the HCDs (Hydraulic Rock Domains, HRD) and the geometrical domains of the overburden (Hydraulic Soil Domains, HSD).

Hydraulic properties

Hydraulic Conductor Domains, HCD

The HCDs in the hydrogeological model are based on version 0 of the regional scale structural model, which consist of 171 deformation zone segments. Some of the zones in the regional scale model area, in the vicinity of Äspö Island, are to be considered as high-confidence fracture zones (concerning their existence) and several of them have been hydraulically tested. However, most HCDs have attributed hydraulic properties.

As the groundwater flow modelling that has been performed is to be considered as more or less generic, a simplified approach was employed in the assignment of properties to the HCDs. The geometric mean of the transmissivity of HCDs from the Äspö HRL was $T=1.3 \cdot 10^{-5}$ m^2/s with a standard deviation of $Log_{10}T = 1.55$ /Rhén et al, 1997b/. This geometric mean T was applied to all HCDs in the regional scale model, see Table 5-34.

The hydraulic thickness of the HCDs was based on the geological interpretation of zone thickness made for the regional scale structural model version 0.

There is very limited information concerning storage coefficient and kinematic porosities of the deforamtion zones. In /Rhén et al, 1997b/ and /Rhen and Forsmark, 2001/ these parameters were estimated. Based mainly on results from the Prototype Repository $S=2.5 \cdot 10^{-5}$ was chosen and the kinematic porosities in Table 5-34 are considered a reasonable estimates compared with data reported from other tests conducted at Äspö HRL.

Hydraulic Rock Domains, HRD

No statistics for a hydraulic DFN model were available at the time of the Simpevarp 1.1 groundwater flow modelling. Therefore, the results in this section cannot directly be compared with the geological description in Section 7.3.1.

Approximate statistical values of parameters for the hydraulic DFN model were estimated on the basis of parameters evaluated from boreholes KLX01 and KLX02 (in the Laxemar subarea) and parameters estimated for the Forsmark 1.1 descriptive model.

The working hypothesis embedded in the hydraulic DFN model employed for Simpevarp 1.1 is that it couples an inferred power-law size distribution of fractures (up to the size of local minor fracture zones) to hydraulic properties by assuming that the transmissivity value is dependent on the size through a power-law relationship. In most cases, the hydraulic feature sizes in the simulations were within the range 100–1,000 m. It was minor fracture zones that were simulated rather than small-scale fractures.

The same hydraulic DFN model was assigned to all HRDs and one common size distribution was used for all interpreted fracture sets. The fracture centres were assumed be Poisson distributed in space. Tables 5-38 through 5-42 present the parameter values considered to best describe the rock mass properties.

Boundary and initial conditions

Initial conditions for the salt water distribution and water types at the end of the last glaciation were tested. A best fit of simulated results to available measured data was obtained by employing freshwater conditions, mainly of glacial type, down to 500 m depth, with a linear increase of salinity below that to 10% at depth of 2,100 m. Considering the water types, the Glacial type decreased linearly from 500 m depth reaching a fraction 0 (non-existent) at a depth of 2,100 m, whereas the Brine type increased from fraction 0 at 500 m depth to fraction 1 (only component) at 2,100 m depth. No other water types were assumed as initial conditions. All other water types were imposed from the upper boundary as a function of time, based on the shore-line displacement due to the land uplift.

However, due to uncertainty in modelling parameters of the rock mass and Quaternary deposits the modelling results are associated with uncertainty.

Groundwater flow pattern

Flow distribution

The topography appears to control much of the flow pattern in the upper part of the rock mass and this is visible also in the salinity distribution. At depth, the salinity field decreases the magnitude of the flow rates considerably and hence groundwater fluxes near ground surface are much higher than those at depth. At –1,000 masl, flow rates are very low in magnitude. Near the surface, at –10 masl and –100 masl, the vertical flow component is mainly oriented downwards (recharge). Discharge areas are located in the extreme east, associated with the Baltic Sea and a few onshore discharge areas, the latter mainly located in conjunction with fracture zones.

The results of the groundwater flow simulations undertaken suggest that the Laxemar subarea is predominantly subjected to recharging flow conditions at –500 masl. This is in contrast to the Simpevarp subarea, which is predominantly subjected to discharging flow conditions at the same

depth. However, it should be remembered that these comments are for modelling based on present day boundary conditions.

Flow paths

Based on the present day boundary conditions, the flow paths from release areas located within the Laxemar and Simpevarp subareas at 500 m depth were simulated. It was found that the released particles rapidly reach a HCD and subsequently follow the system of HCDs to discharge points below the Baltic Sea. The discharge points for the Laxemar subarea are mainly around the Äspö island, whereas discharge points for particles released in the Simpevarp subarea are found to the south and east of the sub-area, as expected.

Hydrogeochemistry of the groundwater

The modelling results suggest the possibility that Littorina water may be present near the coast and below the Baltic Sea and furthermore that the water chemistry may be quite heterogeneous. This heterogeneity in distribution is attributed to an underlying heterogeneity in the distribution in hydraulic properties.

7.2.5 Hydrogeochemical description

Groundwater composition

One of the objectives of the Initial Site Investigation (ISI) stage is to produce a preliminary version of the hydrogeochemical descriptive model on a site scale /Smellie et al, 2002/. Visualisation can be based on modelling and also on an approach where expert judgement is schematically illustrated. A model based on the latter approach, and presently available Simpevarp data, is presented in Figure 7-3.

Figure 7-3 is a conceptual visualisation based not only on measured salinity, but on all relevant hydrochemical and isotopic data (although these were very limited), and general geological and hydrogeological considerations. The hydrogeochemical trends described and illustrated in Chapter 4, together with information from the postglacial scenario illustrated in (cf. Figure 3-16 in Section 3.3) and the characteristics and structures of borehole KSH01A, have been used to make a first schematic attempt at integrating a site-specific hydrochemistry with the general hydrogeostructural character of the Simpevarp area. This model will be updated when more detailed local hydrogeological and geological models become available.

Figure 7-3, schematically representing a WNW-SSE profile, including the Laxemar and Simpevarp sub areas, is oriented parallel to one direction of regional structural faulting and perpendicular to another faulting direction trending NE-SW. These latter features, which may be of greater importance, are thought to be sub-vertical in orientation, but due to a lack of information on their respective dips and directions may, in some cases, be at variance with those shown in the figure. At greater depths, the situation remains unclear, but to date there is no evidence of interactions between borehole KSH01A and the adjacent interpreted defoemation zone. For example, borehole KSH01A generally shows low hydraulic conductivities below 300 m, and even more so below 600 m.

Superimposed on this profile, including structures perpendicular to the section, are possible groundwater flow directions, essentially representing flow along fracture planes along the regional WNW-SSE trending structures. Since the intercepted structures are trending NE-SW and are perpendicular to the proposed flow direction, a number of hydraulic compartments may be formed, where possibly each compartment may have distinct hydrodynamic properties which might affect both the distribution of groundwater and its chemistry. There is presently no specific information as to the hydraulic character (i.e. recharge/discharge conditions) associated with these large-scale structures.

The solid blue arrows represent the possible directions of groundwater flow in the bedrock, including a dashed variety indicating weaker, more uncertain flow directions. At Laxemar, with a more elevated topography, meteoric groundwater recharge is indicated in the figure with a penetration

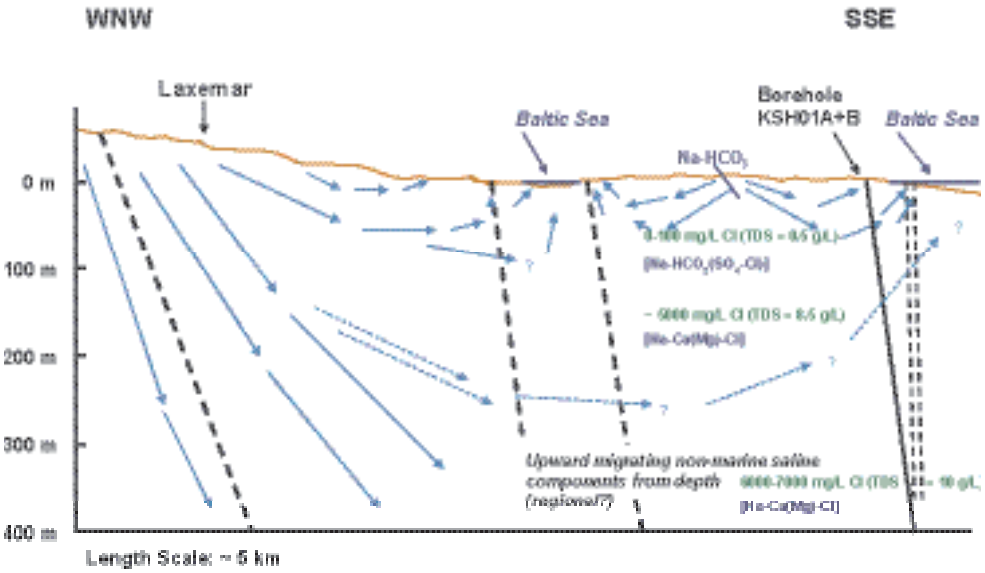

Figure 7-3. *Integrated conceptual visualisation of the Simpevarp area based on hydrochemical and isotopic criteria, and general geological and hydrogeological considerations. Note that the geological structures and groundwater flow directions are not based on measurement but are used only for illustration purposes to fit with present conceptual ideas (for example, when more information is available, the sub-vertical zones may have other dip orientations).*

to at least 400 m, but probably to even greater depths, as indicated by earlier studies /Laaksoharju et al, 1995/. Furthermore, there may be a weak upward discharge towards the Baltic coastline as shown. Local recharge/discharge groundwater circulation, independent of deeper flow pathways, is characteristic along the profile at shallow depths down to around 100 m, with distinctive discharge towards the Baltic coastline.

At still greater depths (> 1,000 m), slowly moving, larger-scale regional flow systems are probably active, with potentially some upward flow towards the coastline. This is suggested in the hydrogeochemical evaluation as being associated with saline waters of a non-marine origin or a non-marine/marine mixing origin.

Available groundwater compositions are shown in green in the near vicinity of borehole KSH01A. These indicate essentially fresh water (0–100 mg/L Cl; ~0.5 g/L TDS) down to around 100 m, with a sharp increase to approximately 5,000 mg/L Cl (~8.5 g/L TDS) at around 150 m and to 6,000–7,000 mg/L Cl (~10 g/L TDS) at about 400 m. This abrupt increase in salinity at around 150 m suggests the presence of two distinct hydrodynamic and hydrochemical regimes which is clearly reflected in the hydrogeochemical evaluation. In addition, this distinction may suggest the influence of the presence of subhorizontal structural features at this interface, or alternatively the opening of isolated ‘pockets’ of saline-glacial meltwater mixtures. Such a glacial melt water component extends to at least 250 m depth and, apart from being preserved in ‘pockets’, it may also have its origin from the closely located NE-SW structures which could have facilitated deep recharge of glacial melt water during glacial advance and retreat. A further possibility may be an origin from sources further inland.

The palaeoevolution of the Simpevarp area implies that a Littorina Sea component should be present in the groundwaters; this, however, has not been established by the hydrogeochemical evaluation to date. Either: a) no Littorina Sea component has been introduced, b) it has subsequently been flushed out, or c) it has not been seen yet because of the limited number of boreholes. A combination of (b) and (c) is probably the case. In the vicinity of KSH01A it would seem likely that any penetration of Littorina Sea water would be restricted hydrogeologically to the upper 100–150 m, and therefore easily flushed out during land uplift and displacement of the Baltic Sea shoreline. Limited penetration of Littorina Sea water to greater depths probably has occurred, especially along the sub-vertical fractures/fracture zones and evidence of existing pockets and/or lenses may still be discovered by subsequent investigations.

Processes and boundary conditions

The mixing processes, schematically visualised in Figure 7-3, are the result of: a) present-day meteoric recharge/discharge hydraulic gradients of local extent with potentially a more saline discharge contribution from depth, b) the forced introduction of glacial melt water to unknown depths during glacial advance/retreat, c) density-induced turnover inflicted by saline waters introduced during marine transgressions (e.g. Littorina Sea) since the last glaciation, and d) possibly some limited recent introduction of brackish water when the Baltic Sea covered the Simpevarp area. The higher topography to the west of the Simpevarp area towards Laxemar has resulted in local induced hydrogeological gradients which have partially flushed out old water types (e.g. potentially the Littorina Sea component), at least in the upper 100–150 m of the bedrock in the vicinity of the KSH01A borehole location, and possibly even at greater depths depending on the local hydrodynamics. The highest degree of preservation of the more saline, denser Littorina Sea, Littorina Sea/glacial water and possibly some brackish Baltic Sea mixtures may be be expected as pockets and lenses in the bedrock in association with the interpreted subvertical structures which are hydraulically active. Some preservation along possible subhorizontal hydraulic structures cannot be ruled out.

The structural pattern of the area, i.e. apparently dominated by vertical and subvertical fracture zones, presumed hydraulically active to a variable degree, may have produced a series of distinct hydraulic (and therefore hydrochemical) 'compartments' contributing to the heterogeneity of the hydrochemical systems.

7.2.6 Transport properties

In the present model version, only transport properties relevant to the local model are addressed. The description of the local model properties is presented in Section 7.3.6.

7.3 Bedrock – local scale

7.3.1 Geological description

Lithological model

A three-dimensional lithological model, which consists of seventeen rock domains, is presented for the local-scale model area employed for the Simpevarp 1.1 description. The modelled rock domains have been distinguished on the basis of their composition, grain size and texture.

Igneous rocks that belong to the c. 1,800 Ma generation of the Transscandinavian Igneous Belt (see Section 3.1) predominate in the Simpevarp local scale model area. The dominating rock types display a gradational compositional variation between dioritoid and granite. Mean values of recalculated quartz content that are used in the QAPF-diagrams, c.f. Section 4.2.2, vary between approximately 11 and 20%. Thus, the true quartz content is lower since only the relative proportions of quartz, alkali feldspar and plagioclase are represented in the QAPF-diagram.; other minerals are not accounted for in this diagram. The fine-grained dioritoid that dominates in the southern part of the Simpevarp peninsula has a quartz content that is <5% locally. The uranium content is low, except for some pegmatites that display a slightly higher content.

Information concerning the properties of all the seventeen rock domains, in accordance with the procedures outlined in section 5.1.2, is summarised in tables, one for each rock domain (Appendix 5). However, the properties of two of the rock domains, RSMA01 (Ävrö granite) that dominates and form the "matrix" of the three-dimensional lithological model, and RSMC01 (mixture of Ävrö granite and quartz monzodiorite) that is penetrated by the cored borehole KSH01, are illustrated in Table 7-2 and Table 7-3, respectively. All rock codes according to SKB´s nomenclature are listed in Appendix 5. The character of the rock types of the rock domains in the Simpevarp local scale model domain, i.e. composition, grain size, texture, age and physical properties as well as the uranium content, are presented in Table 7-4, Table 7-5 and Table 7-6.

Table 7-2 . Properties of rock domain RSMA01 (Ävrö granite).

RSMA01					
Property	**Character**	**Quantitative estimate**	**Confidence**	**Basis for interpretation**	**Comments**
Volume (m^3)					
Rock type, dominant	501044		High	See confidence table	
Rock type, subordinate	511058, 501061, 501033, 501058, 505102		High	See confidence table	
Degree of inhomogeneity	Medium		High	See confidence table	
Low temperature alteration	Inhomogeneous hydrothermal alteration (secondary red staining)		High	See confidence table	Confidence based on outcrop database
Low-grade ductile deformation	Isotropic to weakly foliated; scatttered mesoscopic, ductile shear zones		High	See confidence table	

Table 7-3. Properties of rock domain RSMC01 (mixture of Ävrö granite and quartz monzodiorite).

RSMC01					
Property	**Character**	**Quantitative estimate**	**Confidence**	**Basis for interpretation**	**Comments**
Volume (m^3)					
Rock type, dominant	Mixture of 501036 and 501044	 51.5% 34,1%	High	See confidence table	Quantitative estimate based on occurrence in KSH01A
Rock type, subordinate	501030 511058 501058 505102 501061 501033	6.5% 4.2% 2.0% 1.2% 0.3% 0.2%	High	See confidence table	Quantitative estimate based on occurrence in KSH01A
Degree of inhomogeneity	High		High	See confidence table	In particular, the degree of inhomogeneity is high in the northeastern part
Low temperature alteration	Inhomogeneous hydrothermal alteration (secondary red staining)		High	See confidence table	Confidence based on KSH01 and outcrop database
Low-grade ductile deformation	Isotropic to weakly foliated; scatttered mesoscopic, ductile shear zones		High	See confidence table	Confidence based on KSH01 and outcrop database

Table 7-4. Composition, grain size, texture and age of different rock types in the Simpevarp local model area.

Code (SKB)	Composition								Grain size / Texture	Age
	Name	Quartz (%) in QAPF plot		Alkali feldspar (%) in QAPF plot		Plagioclase (%) in QAPF plot		N (No. of obs.)	Class (SGU)	Million years
		Mean	Std	Mean	Std	Mean	Std			
511058	Granite, fine- to medium-grained	33.8	3.0	41.5	2.7	24.7	3.8	4	Fine- to medium-grained / equigranular	c. 1,808–1,794
501061	Pegmatite	No data							Very coarse-grained / unequigranular	c. 1,800
501058	Granite	27.5	3.0	34.2	0.4	38.4	3.4	2	Medium- to coarse-grained / equigranular	c. 1,800
501044	Ävrö granite (granite to quartz monzodiorite)	19.9	6.7	21.5	8.3	58.6	12.9	18	Medium-grained / unequigranular to porphyritic	1,800+/–4
501036	Quartz monzodiorite (quartz monzonite to monzodiorite)	16.7	1.7	20.9	1.6	62.4	3.3	3	Medium-grained / equigranular	1,802+/–4
501033	Diorite to gabbro	6.1	3.6	1.2	0.8	92.8	4.3	4	Medium-grained / equigranular	c. 1,800
501030	Fine-grained dioritoid (intermediate magmatic rock)	11.2	7.2	18.0	8.9	70.8	13.6	13	Fine-grained / unequigranular	c. 1,800
505102	Fine-grained diorite to gabbro (mafic rock, fine-grained)	11.3	2.6	1.6	1.6	87.2	4.1	2	Fine-grained / equigranular	c. 1,800

Table 7-5. Physical properties of different rock types (surface samples) in the Simpevarp local model area.

Code (SKB)	Composition	Physical properties								
	Name	Density (kg/m³)		Porosity (%)		Magnetic susceptibility (SI units)		Electrical resistivity in fresh water (ohmm)		N (No. of obs.)
		Mean	Std	Mean	Std	Mean values logarithmic scale	Standard deviation (log)	Mean values logarithmic scale	Standard deviation (log)	
511058	Granite, fine- to medium-grained	No data								
501061	Pegmatite	No data								
501058	Granite	No data								
501044	Ävrö granite (granite to quartz monzodiorite)	2,681	16	0.57	0.12	3.12	0.16	4.16	0.18	5
501036	Quartz monzodiorite (quartz monzonite to monzodiorite)	No data								
501033	Diorite to gabbro	No data								
501030	Fine-grained dioritoid (intermediate magmatic rock)	2,803	52	0.29	0.11	3.22	0.84	4.58	0.41	5
505102	Fine-grained diorite to gabbro (mafic rock, fine-grained)	No data								

Table 7-6. Uranium contents of different rock types in the Simpevarp local model area, based on in situ, gamma-ray spectrometric measurements (without brackets) of natural exposures and geochemical analyses of bedrock samples (brackets).

Code (SKB)	Composition	Content of uranium				
	Name	Gamma-ray spectrometric and geochemical measurements of U				N (No. of obs.)
		Mean U (ppm). Gamma-ray spec./(geochemical)	Standard deviation (Std)	Mean total gamma radiation. Natural exposure (µR/h)	Std	
511058	Granite, fine- to medium-grained	6.1 (3.0)	2.3 (–)	26.4	6.0	20 (1)
501061	Pegmatite	9.8	7.4	21.0	6.6	3
501058	Granite	(2.65)	(–)	No data		(1)
501044	Ävrö granite (granite to quartz monzodiorite)	4.9 (4.1)	2.2 (2.0)	9.5	1.4	25 (14)
501036	Quartz monzodiorite (quartz monzonite to monzodiorite)	No data (1.89)	No data (0.29)	No data		(2)
101033	Diorite to gabbro	No data (1.56)	No data (–)	No data		(1)
501030	Fine-grained dioritoid (intermediate magmatic rock)	3.7 (3.5)	1.8(1.2)	11.0	3.3	14 (10)
505102	Fine-grained diorite to gabbro (mafic rock, fine-grained)	No data (2.9)	No data (1.9)	No data		(2)

The three-dimensional lithological model of the Simpevarp local scale model domain is displayed in Figure 7-4. The modelled three-dimensional geometry of the rock domains is dominated by 1) porphyritic granite to quartz monzodiorite (Ävrö granite; RSMA01), 2) fine-grained dioritoid (RSMB01–04) and 3) a mixture of porphyritic granite to quartz monzodiorite (Ävrö granite) and quartz monzodiorite (RSMC01) as presented in Figure 7-5, Figure 7-6 and Figure 7-7, respectively. With the exception of occurrence of mesoscopic, low-grade, ductile to brittle-ductile shear zones and a locally developed weak foliation, all rock types in the rock domains are more or less structurally well preserved.

As can be seen in Figure 7-4 and Figure 7-5, the rock domain RSMA01 dominates and constitutes the main “matrix” of the local scale model volume.

The eastward protuberance at depth of the rock domain RSMB01 is based on the documented occurrence of fine-grained dioritoid between approximately 322 and 631 metres in the cored borehole KSH01A (c.f. Figure 7-6, Figure 7-7 and Section 4.4).

The degree of inhomogeneity in the rock domains is related to the frequency of subordinate rock types. Of these, the fine- to medium-grained granite, and to some extent also pegmatite, are the most important ones. They are treated qualitatively and are judged to be more or less homogeneously distributed within the entire local scale model volume, i.e. they occur in more or less the same amounts in each rock domain, though there might be local internal variations.

The remaining subordinate rock types occurr much less frequently. Locally, inclusions or minor bodies of diorite to gabbro and enclaves of intermediate to basic composition, are characteristic in the Ävrö granite in rock domain RSMA01.

The red staining (hydrothermal alteration) which is a ubiquitous characteristic in conjunction with fracturing throughout the local model area is considered to be homogeneously distributed in the local scale model volume.

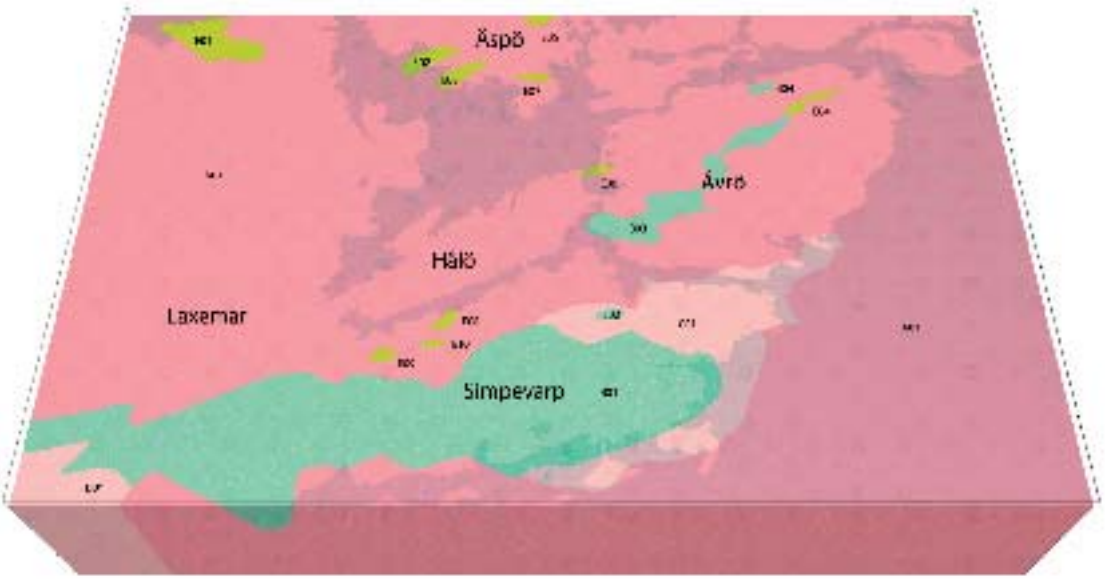

Figure 7-4. *Rock domain model for the Simpevarp 1.1 local scale model domain viewed from the south. The dominant rock type in each domain is illustrated with the help of different colours (see the rock domain map at the surface in Figure 5-1).*

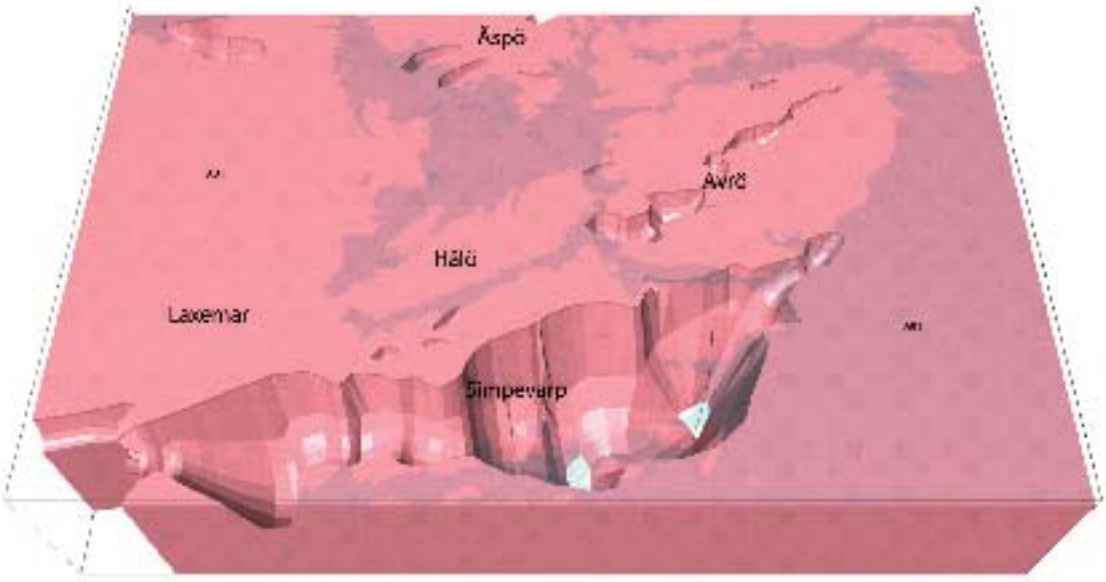

Figure 7-5. *The dominating rock domain RSMA01, which is composed of the porhyritic granite to quartz monzodiorite. View from the south.*

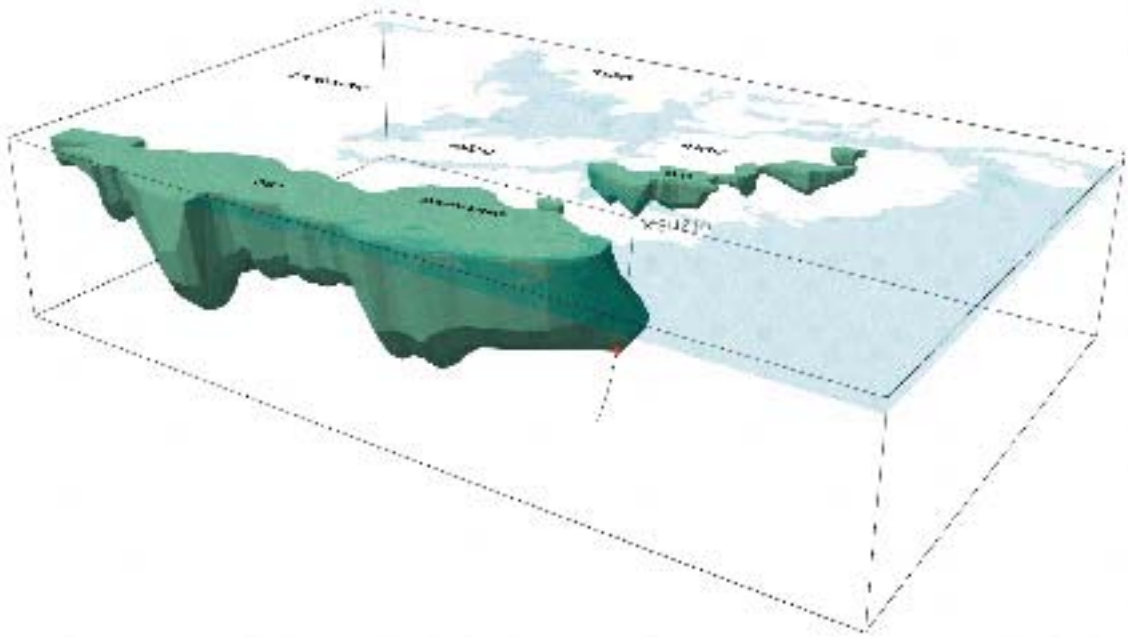

Figure 7-6. *Rock domains RSMB01–04 which are dominated by fine-grained dioritoid. Note the position of the cored borehole KSH01 (c.f. Figure 7-7.). View from the southeast.*

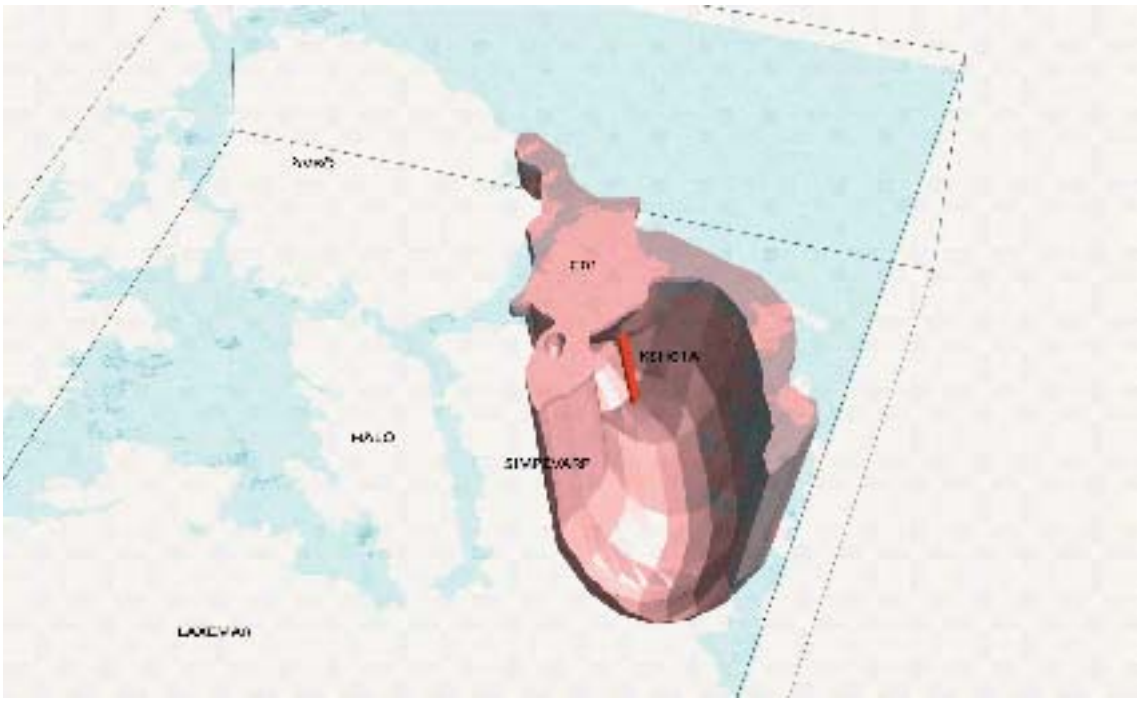

Figure 7-7. *Rock domain RSMC01 which is characterised by a mixture of porphyritic granite to quartz monzodiorite and quartz monzodiorite. Note the section in the cored borehole KSH01, in which the fine-grained dioritoid is the dominating rock (c.f. Figure 7-6). View from the westsouthwest.*

There are no site investigation data available in the western part of the local scale model area west of the Simpevarp subarea. In this area, the compilation of the bedrock at the surface, completed in conjunction with the SDM version 0 /SKB, 2002b/, has formed the basis for the Simpevarp 1.1 three-dimensional rock domain model.

The variation in the quality of the surface geological data and the restricted subsurface information are the two most important factors that govern the uncertainties associated with the modelling of the seventeen rock domains. However, this uncertainty will to a great extent also remain in the descriptive modelling of the local model area for the Simevarp 1.2 descriptive model. Based on available information, a judgement concerning the confidence of the occurrence and geometry of individual rock domains was presented earlier (Section 5.1.3). To summarise, the confidence of occurrence and geometry of the rock domains at the surface is judged to be medium to high in the part of the local model area that is covered by the bedrock map of the Simpevarp subarea, whereas it is judged to be low to medium outside the Simpevarp subarea. Due to the lack of subsurface information, the confidence of occurrence and geometry at depth is medium to low for most rock domains, except for the dominating rock domain RSMA01 which forms the matrix in the local scale model volume. However, the geometrical relationships between rock domain RSMA01 and the other rock domains, in particular the major rock domains, are highly uncertain.

One alternative to the developed “base case” lithological model has been constructed. In the alternative rock domain model, the contacts between rock domain RSMA01 and the rock domains RSMB01, RSMB03, RSMC01 and RSMD01 have been modelled with vertical contacts to the bottom of the local model volume (c.f. Figure 7-8 and Figure 7-9), while the minor rock domains are retained with a modelled depth extent that equals their widths at the surface.

Figure 7-8. *Alternative modelling of rock domain RSMA01. Note the vertical contacts between this rock domain and the other major rock domains. View from the south.*

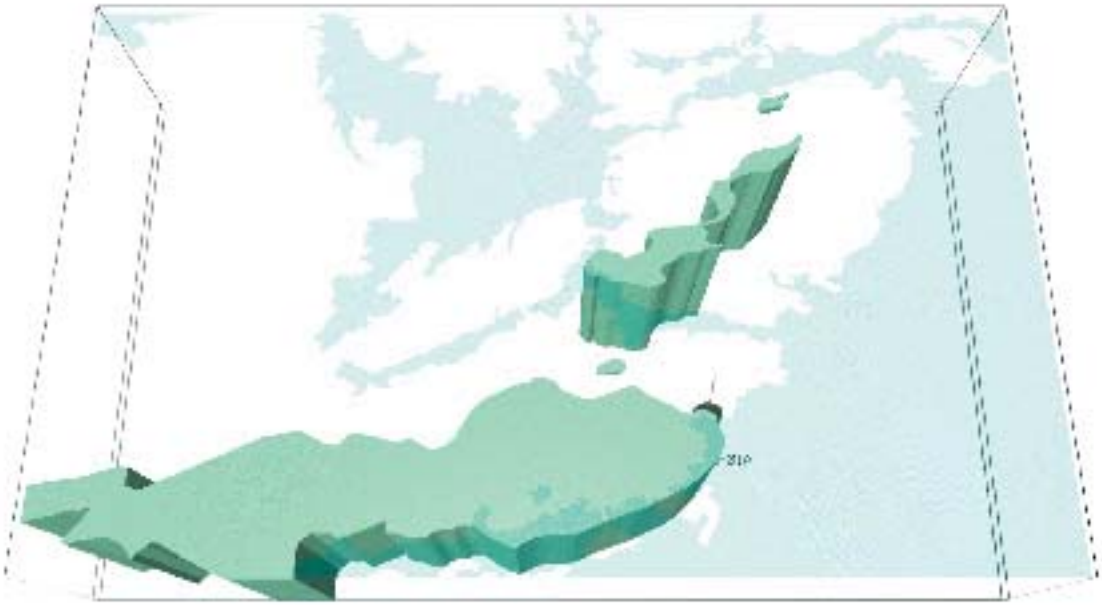

Figure 7-9. *Alternative modelling of rock domains RSMB01 and RSMB03. Note the vertical contacts of the two major rock domains. View from the south.*

Deterministic model of deformation zones

The Simpevarp 1.1 SDM includes a base case three-dimensional model of deformation zones in the local scale model. The zones so far recognised are interpreted with variable confidence. Only zones with a length of 1 km or more are addressed in the deterministic structural model. Older existing structural models, a variety of new surface and sub-surface data, and the interpreted so-called "linked lineaments", c.f. Section 4.2.3, have been used in the modelling procedure.

Deterministic model of interpreted deformation zones

A total of 63 interpreted deformation zones are included in the local scale model volume. Several of the zones have been modelled in segments, due to either geological reasons or due to confidence assessments inherent in the associated linked lineaments. For this reason, there are 74 underlying zone segments. Fourteen deformation zones, for which there are supporting geological and geophysical data, are judged to have a high level of confidence for their occurrence. However, the majority of deformation zones in the structural models (the remaining 49 zones) are based solely on the interpretation of linked lineaments. The confidence of occurrence of these zones is judged to vary from medium to very low.

The possible deformation zones with assigned medium confidence (N=39) are based on well-defined lineaments identified, to a large extent, with the help of the airborne, magnetic and topographic data. The remaining possible deformation zones, which are based solely on the interpretation of linked lineaments (N=10), are presented with a low to very low level of confidence for their occurrence. The lowest level of confidence is associated with the possible zones that are based on linked lineaments derived solely from electromagnetic or topographic data. This judgement is governed by the uncertainty concerning whether the lineament represents a geological feature in the crystalline bedrock or only a feature in the Quaternary overburden.

Detailed information concerning the properties of the deformation zones, in accordance with the procedures outlined in section 5.1.4, are summarised in a series of tables (Appendix 2). A sample property sheet for one of the fourteen high-confidence zones is illustrated in Table 7-7.

Table 7-7. Properties of fracture zone ZSMNE005A (Äspö shear zone). Empty fields reflect no data available or not yet estimated.

ZSMNE005A (Äspö shear zone)					
Property	**Quantitative estimate**	**Span**	**Confidence level**	**Basis for interpretation**	**Comments**
Position		+/–50 m		Linked lineaments, v0	
Orientation (strike/dip)	40/80	dip 70–90NW ductile sinistral; 60–90SE brittle dextral		Linked lineaments	Ref: NEHQ3, EW1b Geomod; ZSM0005A0, ZSM0004A0 v0; ZLXNE01 Lax'
Width	40	Ductile 10–40 m Brittle 70–200 m		v0	
Length	5,100 m			Linked lineaments	
Ductile deformation	Mylonitic			Field data, Äspö data	
Brittle deformation	Cataclastic			Field data, ground geophysics, Äspö data	
Alteration					
Fracture orientation					
Fracture frequency					
Fracture filling					

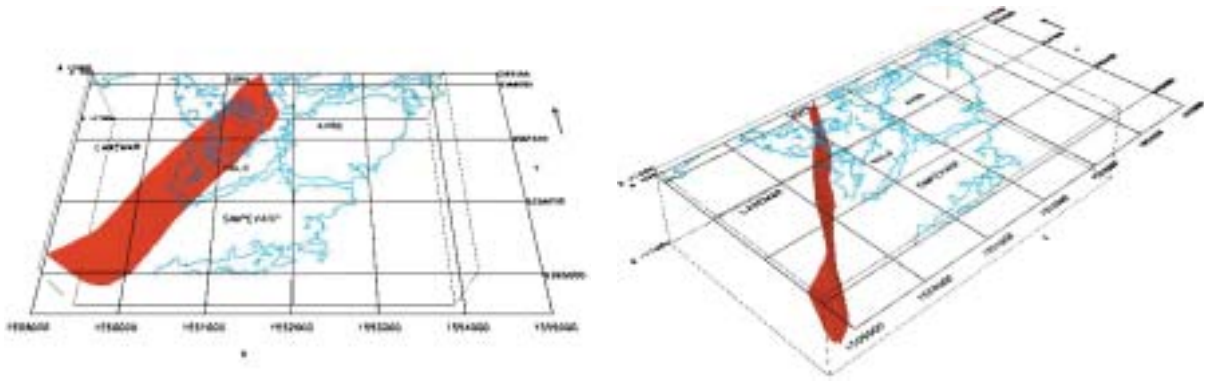

The structural model for the fourteen high confidence deformation zones is presented in Figure 7-10. The zones are supported by a variety of geological and geophysical information and their locations are to a lesser extent governed by the interpretation of linked lineaments. Two important types of deformation zones are present within this group:

- Important Regional major deformation zones with northeasterly strike, confirmed already in model version 0 or in other previous models established in the Simpevarp area.
- Local major fracture zones, which have been confirmed already in model version 0 or in other previous models in the Simpevarp area.

Smaller zones and larger fractures, with a surface extent of less than 1 km have not been included deterministically in the model, but are handled in a statistical way through DFN models.

The Mederhult zone and the Äspö shear zone, are the two most well known regional deformation zones in the Simpevarp subarea. Low-grade mesoscopic, ductile to brittle-ductile deformation are present along both these zones. Their interpreted lengths suggest that both extend to the base of the *local scale* model volume. Kinematically, the Äspö shear zone is characterised by sinistral strike-slip

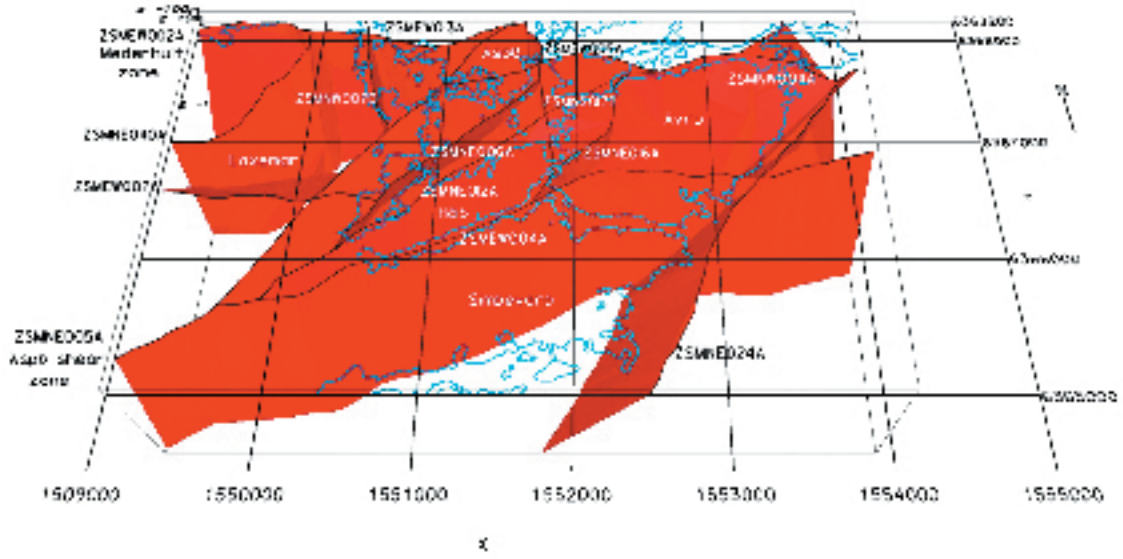

Figure 7-10. *Simpevarp 1.1 local scale structural model, showing fourteen interpreted deformation zones supported by geological and geophysical data and judged to have a high confidence of occurrence. This figure should be compared with Figure 4-8 in the SDM version 0 /SKB, 2002b/.*

component of movement. There are also other, smaller ductile high strain zones in the Simpevarp subarea, usually NE-SW and ENE-WSW striking decimetre wide vertical zones or alternatively with moderate dips /Bergman et al, 2000/. Based on their structural and tectonic similarities, as well as their spatial interrelations, these structures are likely to be related to the Äspö shear zone.

The detailed tectonic evolution of the deformation zones in the model is not well established, and hence little is known about the mutual terminations of the individual zones. The interpreted linked lineaments have been used as a guide where evidence is lacking.

The fourteen deformation zones with high confidence are complemented with 49 possible deformation zones that are based solely on the interpretation of linked lineaments. These possible zones are considered to show medium to very low confidence of occurrence. The zones with medium confidence are based, at least in part, on distinct, low-magnetic or topographic lineaments. All the zones in the Simpevarp 1.1 local scale structural model showing high and medium confidence of occurrence are shown in Figure 7-11. All the inferred deformation zones in the base structural model, irrespective of the judgement of confidence of occurrence, are shown in Figure 7-12.

Zones with a medium confidence of occurrence are present in all directions, with a preference towards NE and EW. Several of these deformation zones were identified already in the SDM version 0 /SKB, 2002b/. The occurrence of distinctive fracture orientation sets striking NE and EW (c.f. Section 4.4) provides support for the inference that at least linked lineaments with these orientations represent deformation zones

Besides the question marks concerning the occurrence of these interpreted deformation zones, a key uncertainty concerns their dip. In the absence of data, all medium and low confidence zones have been modelled with a vertical dip.

The along-strike continuity of nearly all the interpreted vertical or steeply dipping deformation zones, irrespective of their confidence of occurrence, is governed by the interpretation of the length of the linked lineament that is related to the deformation zone. It is considered probable that the number of smaller segments that are present along an individual interpreted deformation zone have been underestimated. Such segments may be related to shorter zones arranged, for example, in an *en echelon* manner along the main zone direction. It is difficult to resolve the individual breaks between such segments, bearing in mind the uncertainty inherent in the location of the lineaments. It is con-

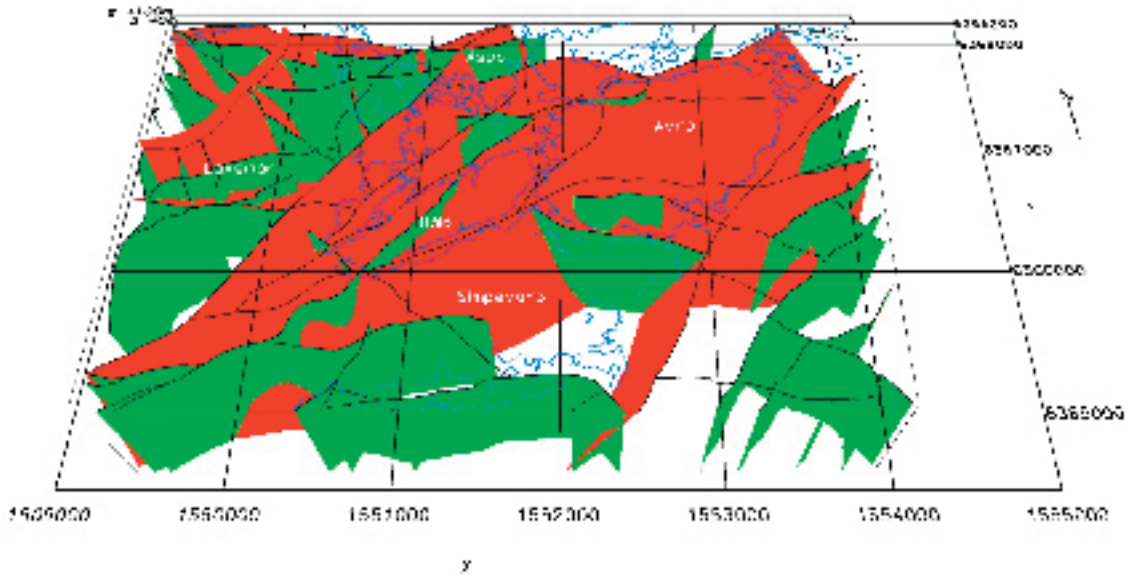

Figure 7-11. *Simepvarp 1.1 local scale model of interpreted deformation zones with both high (red) and medium (green) confidence of occurrence.*

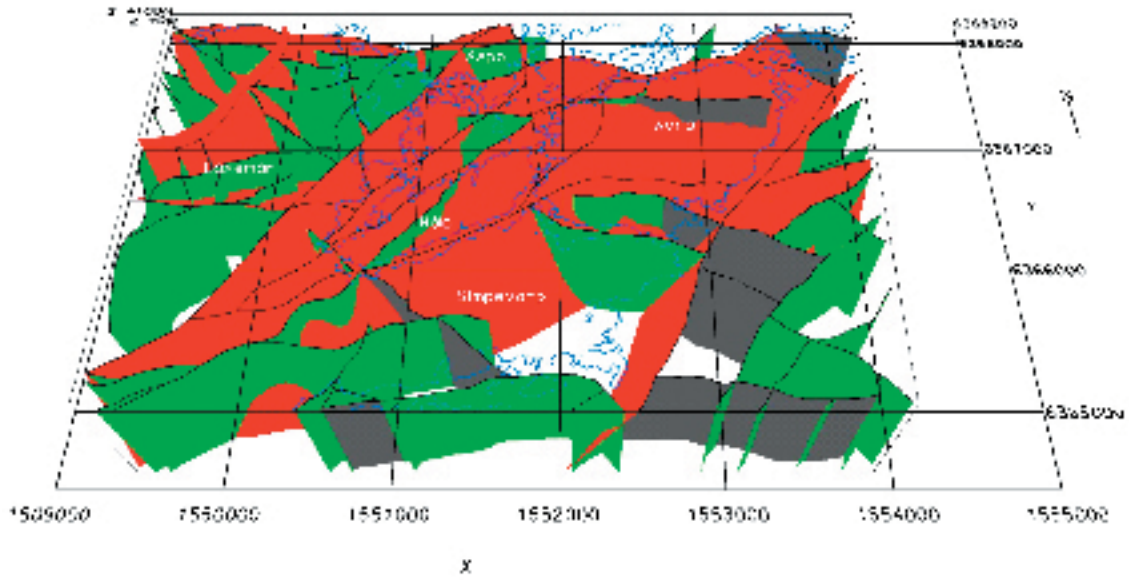

Figure 7-12. *Simpevarp 1.1 local scale structural model of all interpreted deformation zones. Red identifies zones with a high confidence of occurrence. Green shows the zones with medium confidence of occurrence and grey indicates zones with low or very low confidence of occurrence. The zones within interpreted medium or lower confidence of occurrence are based solely on the interpretation of linked lineaments and have been modelled with vertical or steep dips.*

sidered likely that many of the deformation zones are far less continuous in their strike direction than is shown in the Simpevarp 1.1 local scale structural model of deformation zones. The recognition of separated segments along the same zone may have important implications for i.a. the establishment of so-called respect distances associated with the interpreted deformation zones.

Alternative structural model

No alternative structural model of interpreted deformation zones has been produced for Simpevarp 1.1 SDM. However, it is anticipated that alternative models will be devised for model version Simepvarp 1.2. Key issues, such as the existence of sub-horizontal zones on the Simpevarp peninsula or the extent and persistence of zone ZSMNE024A (parallel to the coastline of Simpevarp and Ävrö) can be targets for alternative model development in the future.

Finally, it should be stated that considerably more work is required to relate more closely the different sets of fracture orientations (see Section 4.6), the different groups of mineral fracture fillings, kinematic data along the various deformation zones and the geological evolutionary model (see Section 3.1). In this way, a better understanding of the timing of brittle deformation in the Simpevarp area may be achieved.

Stochastic DFN model – local scale

There are two groups of fracture sets: Group 1, consisting of three subvertical sets trending NNE-NE, EW-WNW and NW-NNW, which are related to present-day lineament orientations; and Group 2, consisting of three subvertical orientations and one subhorizontal set unrelated to current lineament orientations. The Group 1 sets show evidence of being the earliest formed fractures in the outcrops, whereas the Group 2 fractures appear to have formed after Group 1. The orientations of the Group 1 sets vary somewhat according to the local orientation of nearby lineaments, and are given in Table 7-8.

The orientations of the Group 2 fracture sets appear relatively consistent throughout the four outcrop data sets and independent of the local lineament orientations and are presented in Table 7-9.

Table 7-8. Summary of orientation parameters for Group 1 fracture sets. The relative percent values reflect the amount of fractures belonging to each set. Values are given both for the relation in group 1 and both groups together.

Lineament-Related Fracture Set Identifier	Mean pole Trend/plunge/dispersion	Model	Relative % of Group 1	Relative % of group 1 and group 2
NNE-NE	118.0/1.9/17.3	Fisher	32.06%	18.25%
EW-WNW	17.1/7.3/11.2	Fisher	29.97%	17.06%
NW-NNW	73.1/4.7/13.7	Fisher	37.97%	21.62%

Table 7-9. Summary of orientation parameters for Group 2 fracture sets. The relative percent values reflect the amount of fractures belonging to each set. Values are given both for the relation in group 2 and both groups together.

Set Name BG (group 2 sets)	MeanPole Trend/ Plunge/Dispersion	Model	K-S	Relative % of group 2	Relative % of group 1 and group 2	Comments
BGNE	326.3/5.5 K1:17.65 K2:18.14	Bivariate Fisher	0.041/45.4%	41.5%	17.87%	Univariate Fisher also significant at 43.9% (K=16.9)
BGNS	96.8/3.8/20.32	Fisher	not significant	34.4%	14.84%	
BGNW	22.1/2.4 K1:5.36 K2: 6.66	Bivariate Fisher	0.051/61.3%	15.0%	6.45%	Weakly-developed set; Bivariate normal also significant at 18.8%
BGHZ	123.0/55.3 K1:83.58 K2:15.97 K12=–0.05	Bivariate Normal	0.072/24.2%	9.1%	3.91%	Bivariate Bingham also signifnicant at 6.2%

The size model for each set was estimated differently. Group 1 fractures were considered to be part of a "super population" of fractures that included the lineaments. The size distribution was fit to each Group 1 set by area- and mass-dimension renormalisation of the trace length frequency data in which outcrop trace length data and lineament trace length data were combined. All of these data sets are described by Power Law functional relations as summarised in Table 7-10.

The size model for the Group 2 sets was estimated by fitting a fracture radius distribution directly to the measured outcrop trace length data, c.f. Table 7-11. All of these size models are best fit by lognormal distributions. However, an alternative size model (powerlaw) is given. The size distribution for the Group 2 horizontal set is very poorly constrained due to small amounts of data and severe bias.

Table 7-10. Summary of fracture size parameters for Group 1 fracture sets. The parameters k_r and X_{r0} refer to the radius distribution and X_{t0} to the minimum trace length, respectively. The corresponding trace length exponent, k_t, can be obtained by k_r–1. Estimates are given both for intensity-scaling (mass) and euclidian (euc) renormalisation respectively as well as a span (upper, median, lower).

SET	Size model preferred	Powerlaw (radius distribution)		
		Upper $k_r/X_{t0}/X_{r0}$ (mass) (euc)	Median $k_r/X_{t0}/X_{r0}$ (mass) (euc)	Lower $k_r/X_{t0}/X_{r0}$ (mass) (euc)
NNE-NE	Powerlaw	2.68/0.6/0.38 2.85/0.43/0.27	2.58/0.36/0.23 2.82/0.31/0.20	2.50/0.20/0.13 2.69/0.15/0.10
EW-WNW	Powerlaw	2.93/0.63/0.40 2.99/0.71/0.45	2.80/0.36/0.23 2.82/0.32/0.20	2.67/0.18/0.11 2.78/0.21/0.13
NW-NNW	Powerlaw	2.97/0.75/0.48 3.02/0.54/0.35	2.87/0.49/0.31 2.91/0.35/0.22	2.62/0.13/0.08 2.83/0.14/0.10

Table 7-11. Fracture size parameters for Group 2 fracture sets. Lognormal size models are preferred, but also powerlaw models are given as alternative models. The parameters k_r and X_{r0} refer to the radius distribution and X_{t0} to the minimum trace length. The corresponding trace length exponent, k_t, can be obtained by k_r–1. Estimates are given both for intensity-scaling (mass) and euclidian (euc) renormalization respectively as well as a span (upper, median, lower).

SET	Size model preferred, (alternative)	Lognormal (radius distribution)			Powerlaw (radius distribution)		
		Arithmetic space Mean [(1/n) Σx_i] (meter)/ Standard deviation	Log^{10} space Mean [(1/n) $\Sigma \log^{10} x_i$]/ Standard deviation	LN space Mean [(1/n) $\Sigma \ln x_i$]/ Standard deviation	Upper $k_r/X_{t0}/X_{r0}$ (mass) (euc)	Median $k_r/X_{t0}/X_{r0}$ (mass) (euc)	Lower $k_r/X_{t0}/X_{r0}$ (mass) (euc)
BGNE	Lognormal (Powerlaw)	0.48/0.55	–0.50/ 0.60	–1.15/ 0.92	2.86/0.87/0.55 3.07/0.82/0.51	2.77/0.56/0.35 3.00/0.57/0.36	2.61/0.27/0.17 2.78/0.18/0.11
BGNS	Lognormal (Powerlaw)	0.67/0.82	–0.37/0.63	–0.86/0.96	2.93/0.94/0.60 2.99/0.56/0.36	2.77/0.56/0.35 2.95/0.46/0.29	2.72/0.44/0.28 2.95/0.36/0.23
BGNW	Lognormal (Powerlaw)	0.45/1.00	–0.73/0.88	–1.69/1.33	3.05/1.09/0.69 3.14/0.86/0.55	2.82/0.44/0.28 2.94/0.38/0.24	2.80/0.36/0.23 2.89/0.28/0.18
SubH	Lognormal	0.57/1.86	–0.78/1.03	–1.79/1.57			

Intensity is a function of rock type and possibly also alteration. However, alteration may be an effect of fracturing and is not included in the proposed model values. Specific intensity values for altered rock can be found in the analysis section for DFN parameters in Chapter 5 Depending on the purpose of the model, the intensity of both the Group 1 and Group 2 sets can be specified as a function of rock domain or rock type. A summary of intensity estimates is presented in Table 7-12.

Table 7-12. Summary of best estimates of fracture intensity, P_{32}, as a function of rock type and rock domain.

Rock Class	Key to rock domains Including comments	Boreholes (open and partly open fractures)	Outcrop (All)	Outcrop (Open fractures)
Granite to quartz monzodiorite, generally porphyritic (Ävrö granite)	A01 Estimated to be >90% Ävrö granite	0.41	2.93	0.62
Fine-grained dioritoid (Metavolcanite, volcanite)	B01 94.2% Fine-grained dioritoid	3.67	4.86	0.69
quartz monzodiorite, equigranular	C01 is a mix between Ävrö granite (51.5%) and quartz monzodiorite (34.1%) and other subordinate rock types (14.4%). KSH01 is dominated by C01 with a section of B01	1.36	3.27	0.93

Table 7-12 shows results for open and all fractures in outcrop as well as for open (including partly open) fractures based on aperture measurements in the boreholes. The agreement between borehole and outcrop open fractures is quite good for the *granite to quartz monzodiorite* group (Rock domain A), as well as the *quartz monzonite to monzodiorite* group (Rock domain C). The outcrop intensity for the *fine-grained dioritoid/metavolcanic* group (Rock domain B) is much lower than the borehole counterpart, possibly due to the lack of alteration zones in the outcrops as compared to the boreholes in this lithology.

7.3.2 Rock mechanical description

In situ stress conditions

Table 7-13 and Table 7-14 the stress estimates are presented for the Simpevarp subarea, which are also assumed applicable to the whole Simpevarp region. The mean principal stress magnitudes are estimated to lie in a span that increases with depth. The span is wider at large depths reflecting the inherent larger uncertainty. Inside the rock mass (including naturally occurring fractures) between major deformation zones the spatial variation of the stress is expected to be less than in the immediate vicinity of the deformation zones. With spatial variation is here implied the local variation (from data point to data point, < 1 m^3 scale) at the same depth. The mean stress values are applicable to a rock volume of 30x30x30 m size.

Table 7-13. Model for in situ stress magnitudes in the Simpevarp subarea.

Parameter	σ_1	σ_2	σ_3
Mean stress magnitude, z = depth below ground surface	0.066·z+3 MPa	0.027·z MPa	0.022·z+1 MPa
Uncertainty, 0–500 m	±25%	±25%	±25%
Uncertainty, 500–1,100 m	±40%	±25%	±40%
Spatial variation in rock domains	±15%	±15%	±15%
Spatial variation in or close to deformation zones	±50%	±50%	±50%

Table 7-14. Predicted in situ stress orientations in the Simpevarp subarea.

Parameter	σ_1, trend	σ_1, dip	σ_2, trend	σ_2, dip	σ_3, trend	σ_3, dip
Mean stress orientation	132°	0°	90° **	90°	42°	0°
Uncertainty	±15°	±10°	±90°	±15–45° *	±15°	±15–45° *
Spatial variation, rock domains	±15°	±15°	±15°	±15°	±15°	±15°
Spatial variation inside or close to deformation zones	±25°	±30°	±25°	±30°	±25°	±30°

*At some level σ_2 and σ_3 may have similar magnitude and the dip can then be in any dierction. The tree principal stresses are in each point oriented perpendicular to each other.

** Since the direction is expected to be subvertical, i.e. the dip 90, the trend of the tensor may therfore be in any direction.

Mechanical properties

The rock quality class, as used for assessing repository constructability, is either “very good rock” or “good rock”. This is also supported by the fact that underground constructions have been built without problems in the area. In the larger deformation zones, the rock mass may however be “poor”.

The Simpevarp subarea consists mainly of three rock types, c.f. Section 7.3.1, and for these rock types some intact rock (matrix) mechanical property parameters have been estimated. The estimates are given in Table 7-15 as a span for each parameter. Almost all rock samples from the individual rock type are expected to have properties falling inside the given span. Parameter values in the middle of the span are more probable. The reasoning behind the selected spans is given in Section 5.2.

Table 7-15. Predicted rock mechanical properties for intact rock (matrix) for the main types (i.e. small pieces of rock without any fractures) in the Simpevarp subarea.

Parameter for intact rock (drill core scale)	Quartz- monzodiorite	Finegrained dioritoid	Ävrö granite
Uniaxial compressive strength	75–300 MPa	95–280 MPa	75–300 MPa
Deformation Modulus	40–90 GPa	70–100 GPa	40–90 GPa
Poisson’s ratio	0.18–0.28	0.20–0.30	0.18–0.28
Tensile strength	10–20 MPa	10–20 MPa	10–20 MPa

The properties of the rock mass, i.e. considering the rock at a larger scale with intact rock and naturally occurring fractures included, may be characterised with a selection of parameters as given in Table 7-16. The estimates are given as a span for each parameter. This span is judged to cover the possible values for the mean of the parameter at a support scale of 30 m scale. The most probable values are found in the middle of the given span. The reasoning behind the selected span for each parameter is given in Chapter 5.2.

For the deformation modulus it should be noted that the parameter refers to the modulus if the rock mass volume is compressed with low confinement. For a rock mass at larger depth one would have higher confinement and the deformation modulus under these conditions should be adjusted for the change in stress, i.e. the same rock mass may behave differently at small and large depths. The deformation modulus in Table 7-16 is given for a low degree of confinement, in the order of 0–5 MPa. The increase in modulus due to stress increase is roughly estimated to be in the order of 10 GPa per 5 MPa increase in confining stress /Hakami et al, 2002/ and /Barton, 2003/.

Table 7-16. Predicted rock mechanical properties for the rock mass (including naturally occurring fractures) in the Simpevarp local model area. The area is divided into different rock domains according to the geological model in Section 7.2.

Parameter for the rock mass (30x30x30 m scale)[5]	Rock Domain A Ävrö granite dominating Min–Max	Rock Domain B Finegrained dioritoid dominating	Rock Domain C Mix of Ävrö granite and quartz monzo-diorite	Rock Domain D Quartz-monzodiorite dominating	Rock mass Inside Deformation Zones[4] [5]
Uniaxial compressive strength[1]	5–55 MPa	5–35 MPa	5–55 MPa	5–35 MPa	1–15 MPa
Friction angle[2]	20–40°	20–40°	20–40°	20–40°	10–35°
Cohesion[2]	10–30 MPa	5–25 MPa	10–30 MPa	5–25 MPa	0–20 MPa
Deformation Modulus[3]	25–55 GPa	15–40 GPa	15–55 GPa	15–40 GPa	1–10 GPa
Poisson's ratio	0.05–0.25	0.05–0.20	0.05–0.25	0.05–0.20	0.05–0.20

[1] This description parameter is not a standard parameter, it refers to the strength of a block of 30 m size with low confinement at boundaries. The conditions inside the block is not really uniaxial.

[2] Linear model between 10 and 20 MPa confining stress.

[3] For low confining stress, 5 MPa and lower. For higher stress the modulus should be adjusted, See text.

[4] This is meant to refer to the larger deterrministically determined deformation zones included in the deformation zone model.

[5] The properties of rock mass inside minor deformation zones (or effects on rock mass blocks from minor zones) are also included in the parameter span for the rock domains. Minor zonez are the zones that are not part of the deterministic zone model.

7.3.3 Thermal properties

Thermal properties

The thermal properties vary in the rock mass due to variable lithological (and inherently mineralogical) conditions. The estimation of the thermal properties is therefore described following the geological division introduced where the bedrock is divided into different rock domains, c.f. Section 7.3.1 for the division and associated labels. For each domain, a number is given for the thermal conductivity, a span for the specific heat capacity and the thermal expansion coefficient (Table 7-17). The spans for the parameter values cover the expected values for the mean of the parameter at a support scale of 1 m, i.e. equivalent to the scale of a deposition hole. Thus, values outside the given span are to be expected for single core samples but not for the mean of several samples spread in a block of a metre scale.

The rock domain B, where the fine-grained dioritoid is dominant, has a slightly lower thermal conductivity compared with the other units, but the mean conductivity for all domains in the Simpevarp subarea seems to be fairly low, 2.7 W/mK or lower. A higher conductivity is advantageous because the heat will be spread out more effectively in the rock and the maximum temperature at the deposition hole wall will be reduced, comparatively. There are no differences amongst the rock units with regard to expected values for specific heat capacity and thermal expansion coefficient at this stage. The reasoning behind the selection of spans of parameter values is given in Section 5.3.

Table 7-17. Predicted thermal properties for the rock mass in the Simpevarp subarea. The rock of the local model volume is divided into different rock domains according to the geological model, c.f. Section 7.2. 0

Rock Domain (See Figure 7-4)	Model distribution for Thermal conductivity Scale 1x1 m [W/m·K] Function type	Mean value	Standard deviation
A Dominated by grainte to quartz monzodiorite (Ävrö granite)	Normal	2.673	0.2528
B Dominated by Finegrained dioritoid	Lognormal	0.8024 (= ln2.231)	0.08294
C Dominated by a mixture of quartz monzodiorite and Ävrö granite	Lognormal	0.9168 (= ln2.501)	0.09140
D Dominated by quartz monzodiorite	Normal	2.384	0.1040

In situ temperature

In the bedrock at the Simpevarp subarea the temperature increases from about 9–9.5°C at a depth of 100 m to about 15.5–16°C at 600 m and about 21–22°C at the depth 950 m. The temperature gradient increases with depth in the two boreholes studied, from about 13°C/km at the depth 200 m to about 15.5°C/km at 900 m. The change in the temperature gradient may be explained either by changes in thermal conductivity with depth, climatic changes in the past, or perturbation by drilling and water flow.

7.3.4 Hydrogeological description

No description was made for the local scale model domain.

7.3.5 Hydrogeochemical description

Groundwater composition

Detailed evaluation of the groundwater observations indicates the following characteristics.

Descriptive observations

- Except for sea waters, most surface waters and some groundwaters sampled from percussion boreholes are fresh, non-saline waters according to the classification used for Äspö groundwaters. The rest of the groundwaters are brackish (Cl <5,000 mg/L), with the exception of three samples from KSH01A (at 253 m and 439 m depth) which are saline. Most surface waters are of Ca-HCO_3 or Na-Ca-HCO_3 type and naturally the sea water is of Na-Cl type. The deeper groundwaters are mainly of Na-Ca-Cl type.
- The surface waters are dilute, usually with very short residence times (high tritium and ^{14}C). However, the $\delta^{18}O$ values are relatively homogeneous when compared with those expected for surface waters, which may reflect a more evolved surface/subsurface water system down to the overburden/bedrock interface.
- Saline water with Cl contents around 3,000–6,500 mg/L and $\delta^{18}O$ values between –11 and –14‰ indicate mixtures between cold climate meteoric water and saline water. Based on present data a marine signature (Littorina?) of the saline component is not significant in the Simpevarp samples in contrast to the Forsmark samples. The saline component in the Simpevarp groundwater is modified by water-rock interactions and shows similarities to an old, non-marine/marine saline water of brine type.

- $\delta^{36}Cl$, $\delta^{37}Cl$ and ^{14}C analyses, when available, can add significant information concerning the origin of the Simpevarp (and Forsmark) saline waters.
- The presence of groundwater with major components of deep saline and glacial melt water at relatively shallow depths (150 to 260 m) suggests either very stagnant conditions in general or the presence of isolated pockets of very old groundwater.
- Ion exchange reactions have modified the groundwaters (e.g. in respect of Mg, Na and Ca concentrations).
- Some evidence of decreased sulphate content coupled with higher $\delta^{34}S$ values suggests the activity of sulphate-reducing bacteria (based on very few analyses).
- The isotope ratios of the Lake Water and Stream Water show some puzzling values, but probably indicate mixing of different sources (e.g. including surface water and near-surface water mixing).

Modelled observations

- *Fresh, non-saline groundwaters*. Their chemistry is manly controlled by water-rock interaction processes. The identified heterogeneous reactions are: a) organic matter decomposition, b) dissolution of calcite, plagioclase, biotite and gypsum (or sulphides), and c) Na-Ca exchange and precipitation of some phyllosilicates, all of them with very low mass transfers. The Cl (132 mg/L) end members in this group show a small contribution from mixing with a marine end member.
- *Saline groundwaters*. Their chemistry is mainly controlled by the mixing of multiple end members. The mixing proportions obtained using PHREEQC indicate that the Glacial end member is generally the most abundant and shows up to a 20% variation in mixing proportion (30–50%) depending on the meteoric end member that the model includes. The use of two meteoric end members increases the variability of their mixing ratios, but the lumped contribution remains similar, in the order of 30–40%. A marine end member (Littorina or Sea Sediment) appears in all models, although always in low proportions, especially Littorina (< 10%). Taking into account all the uncertainties, the actual presence of a marine end member cannot be demonstrated. The mixing proportions obtained by M3 modelling indicate that the saline waters are dominated by mixing with the Glacial end member (37–54%), a Meteoric water input of 9–22%, a smaller contribution from a Littorina Sea or Sea Sediment end member (9–11%) and a equally small proportion of Brine end member (around 9–11%). The model uncertainty of the mixing models is generally ±0.1 mixing units and the detection limit is 0.1 unit. This means that the occurrence of a water type with a calculated mixing proportion of ≤20% may not be significant and the occurrence in the rock may still be uncertain. The interpretation is therefore that the saline water samples are affected by glacial and meteoric water but the input of e.g. Littorina Sea water is not significant. The model results generally agree, therefore, with what was obtained in the exploratory analysis. This apparently complex mixing system agrees with the models presented by /Laaksoharju, 1999/, /Puigdomenech, 2001/ and /Luukkonen, 2001/ for Äspö at similar depths.
- The heterogeneous reactions identified during mixing processes include organic matter decomposition, dissolution of plagioclase, biotite and Fe-chlorite (or $Fe(OH)_3$), precipitation of calcite, illite and SiO_2 phases (or phyllosilicates), the possible actuation of bacterial sulphate reduction processes with the simultaneous precipitation of iron sulphides, and, finally, the ionic exchange between Na and Ca.

Processes and boundary conditions

Based on measured salinity distributions and modelling results, the major processes affecting the local chemistry at Simpevarp are summarised in Figure 7-13 is based on model calculations integrating the inverse modelling in PHREEQC to explain the evolutionary reaction paths and mixing proportions of the Simpevarp groundwaters, with the M3 mixing modelling approach used to select appropriate groundwater end members. The modelling is preliminary and will be updated when more samples become available.

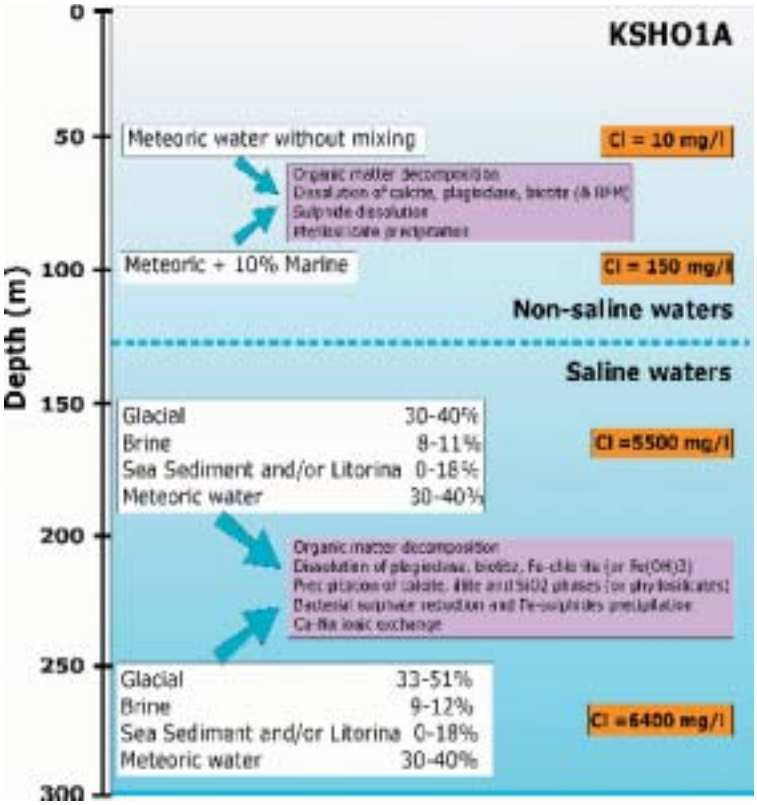

Figure 7-13. *Integrated conceptual visualisation of the local hydrochemistry in the Simpevarp subarea is based on integration of: 1) Salinity distributions based on measured Cl concentrations 2) Modelled evaluation paths of the non-saline and saline groundwater. For each sample, the mixing proportions and the main heterogeneous reaction processes are indicated. Mixing calculations were based on inverse modelling in PHREEQC, but used M3 mixing models and expert judgment for selecting appropriate end members. The mixing modelling results are significant only for water proportions >20%.*

The present model-based state of hydrogeochemical knowledge of the Simpevarp groundwater water system is that the main water-rock interaction processes that affects the chemistry are: (i) decomposition of organic matter, (ii) calcite, plagioclase, biotite and sulphide dissolution, (iii) Na-Ca ion exchange, and (iv) phyllosilicate precipitation. The generic reaction model in Figure 7-13 will be refined when more data concerning the mineralogy of the system and its hydrological functioning become available.

The interpretation of the mixing modelling indicates that three water types dominate. The meteoric type of water at the surface shows typical seasonal variations in its composition. Closer to the coast an influence of marine water is detected. At greater depth the saline water has been affected by mainly glacial water.

The modelling indicated that water-rock interaction processes in the saline groundwaters are assumed to be much less important than in the fresh waters and secondary to the mixing process. The reason is: a) the modelling does not take into account the reactions forming the end-members, b) the groundwater at depth is generally in equlibrium with most of the minerals and c) the temperature of the groundwater is low. These circumstance allows for the calculation of the mixing proportions even without a precise knowledge of the detailed mineralogy of the system. However, the influence of sulphate-reducing processes on the final mixing proportions has not been evaluated rigorously enough, and it is therefore likely that further detailed studies will produce a refinement of the generic reaction model used in the present calculations.

The results from the redox modelling suggest that the redox state of the brackish waters from depth interval (centred at 161.7 m and 253.5 m) in borehole KSH01A could be buffered by the presence of iron oxides and hydroxides and by redox reactions among phyllosilicates, the latter which is possible from a mineralogical point of view. On the other hand, the good match between the sulphur redox-pair and measured Eh values points to sulphide minerals as redox buffers. This buffering action, together with the presence of dissolved sulphides, suggests the development of an anoxic-sulphidic state mediated by sulphate-reducing bacteria (SRB). Typical precipitation of sulphide minerals associated with this environment is suggested by the equilibrium between the waters and several monosulphide phases, as deduced from speciation-solubility calculations: Pyrite is a relatively common fracture phase and is present in small amounts in the fracture systems sampled for groundwater.

The modelling indicates also that the groundwater composition at shallow depth, i.e. far from repository depth, is such that the representative sample from KSH01A:245–261.5 m can meet the SKB chemical stability criteria (Table 7-18) for Eh, pH, TDS and Ca+Mg, see /Anderson et al, 2000/.

Table 7-18. The hydrochemical stability criteria defined by SKB are valid for the analysed values of the represenative sample in borehole KSH01A, L=245–261.5 m.

	Eh mV	pH (units)	TDS (g/L)	DOC (mg/L)	Colloids* (mg/L)	Ca+Mg (mg/L)
Criterion	<0	6–10	<100	<20	<0.5	>4
KSH01A:245–261 m	–210	7.4	10.7	NA	NA	1,223.5

NA = Not analysed.

In conclusion, the very different modelling approaches used in this first attempt to construct a Hydrogeochemical Site Descriptive Model (v. 1.1) of the Simpevarp area have produced hydrochemical models that agree fairly well. With additional hydrogeochemical, geological and hydrogeological data linked to model development there are good possibilities of further quantifying the groundwater system and meeting the required modelling objectives.

7.3.6 Transport properties

The site descriptive transport modelling presents two types of transport parameters: retardation parameters associated with geological units (rock mass and structural units), and flow-related parameters associated with flow paths. The retardation parameters include the porosity, θ_m, the effective diffusivity, D_e, and the linear equilibrium sorption coefficient, K_d, whereas the flow-related parameters considered in the present model are the F parameter (or "transport resistance"), and the advective (water) travel time, t_w. The Simpevarp 1.1 modelling of transport properties is described in Section 5.6.

No site-specific data from laboratory or *in situ* measurements of retardation parameters are available for the present model version. However, a joint evaluation of site-specific geological information on intact rock and retardation data obtained at Äspö HRL near the Simpevarp investigation area has been performed, with the aim of relating the database from previous investigations the Äspö HRL to rocks characterised in the Simpevarp area. Specifically, the evaluation was primarily focused on geological similarities, that is, on the compilation of retardation data for the main rock types identified in the geological model of the Simpevarp area. Furthermore, it was required that the laboratory methods used to produce the Äspö data were consistent with those employed in the site investigation programme.

The compilation and evaluation of Äspö HRL data showed that diffusion and sorption parameters are available for two of the rock types at Simpevarp: quartz monzodiorite, one of the three main rock types in the area, and fine-grained granite (found in dykes). Further "import" of Äspö data could be possible, primarily for parameterisation of the Ävrö granite, but must be substantiated by additional data. Sorption data on cesium (Cs) and strontium (Sr) are available in the Äspö dataset; these K_d-values are applicable for saline water compositions consistent with those in the experiments.

Formation factors, $F_m = D_e / D_w$ (D_w is the free diffusivity in water), were calculated based on the measured diffusivities of HTO (tritiated water). The diffusion dataset was further constrained by neglecting samples with porosities outside the ranges reported in the petrophysical data from the site. The Äspö sorption dataset was evaluated using the methods proposed by /Widestrand et al, 2003/. Comparisons of the resulting parameter values with generic databases, /Ohlsson and Neretnieks, 1997/ for diffusion and /Carbol and Engkvist, 1997/ for sorption, indicated slightly higher diffusivities and lower or similar sorption capacities for the Äspö dataset, as compared to the generic databases.

Concerning the retardation parameters, the main conclusion at the present stage of model development is that there is not sufficient site-specific evidence to support the use parameter values other than those in generic databases in transport calculations for Simpevarp. This conclusion is primarily based on the fact that only one of the three main rock types within the investigated area, quartz monzodiorite, is represented in the "site-specific" database; this rock type covers (as main rock type) a relatively small part of the model area (rock domains C01, where it is only one of the main rock types, and D01). Furthermore, the available sorption dataset is quite limited in terms of the combinations of water compositions and radionuclides represented.

The most important factor for reducing the uncertainties associated with the retardation parameters is obviously to measure and evaluate site-specific parameters. This will provide data on materials not represented in the present database, but will possibly also support further use of Äspö data in future model versions. Furthermore, geological and hydrogeochemical data (fracture mineralogy and trace elements) will be used for assessing site understanding and model confidence, in accordance with the proposed modelling strategy /Berglund and Selroos, 2003/.

Flow-related transport parameters (F and t_w) were calculated by particle tracking in large-scale groundwater flow models. Specifically, particles were released on a regular grid in two release areas at a depth of 500 m below sea level located within the Laxemar and Simpevarp subareas, respectively. Both release areas are contained within the Simpevarp 1.1 local model area. An evaluation of simulation results obtained with DarcyTools /Follin et al, 2004/ has been performed. The available results include transport parameters for a "base case" and a number of sensitivity cases, quantifying the effects of, primarily, boundary conditions and hydraulic properties on the transport parameters. The results for the base case show that F and t_w are highly spatially variable and that the variability follows a similar pattern (i.e. the two parameters are correlated). It can also be observed that F-values and travel times are larger for the Simpevarp subarea than for the Laxemar subarea, although the flow paths from the Laxemar release area are longer (on average). This should not be taken as a general observation on the transport conditions associated with these specific release areas, but illustrates that comparisons of transport conditions related to different release areas cannot be based on path lengths and/or visual impressions of flow paths only.

The base case indicates that spatial variability is an important source to uncertainty. Other uncertainties were quantified in the sensitivity analysis. Essentially, all sensitivity cases indicate high uncertainties in the transport parameters. In particular, the cases addressing the properties of the uppermost rock layer and the transmissivities of the deterministic and stochastic structures show the largest differences compared to the base case. The results emphasise the importance of, inparticular, the deterministic structures, but also the interactions with the surface system and the uncertainties related to the stochastic DFN (Discrete Fracture Network) description are important sources of uncertainty in the transport description.

Probably even more important for the quantification of transport parameters and the associated uncertainties are the features not represented in the present regional scale groundwater flow models. In particular, fractures and deformation zones of sizes smaller than 100 m are not described explicitly in the present regional scale models. Since these features can be expected to contribute significantly to the integrated F- and t_w-values for flow paths from repository depth, the calculated transport parameters should not be considered quantitative in the sense that they are used for comparisons between different release areas, or sites, or with safety criteria. Thus, the main result of the present analysis of flow paths and flow-related transport parameters is an improved understanding of some of the main factors affecting advection and retention within the "subset" of structures included in the flow models.

8 Conclusions

This chapter provides a comparison with previous model versions and highlights the important steps taken with regard to understanding of the Simpevarp site. Furthermore, an assessment is given of the overall confidence of the model description. In light of the discussion of uncertainty in Chapter 6, an account is provided of the overall understanding of the site. This discussion is followed by a review of the important steps to be taken in the subsequent modelling to improve the model and reduce uncertainty. Finally, the implications for the ongoing site investigations are discussed. This latter part addresses what additional data or measurements are required to improve the model and reduce existing uncertainty.

8.1 Overall changes since the previous model version

The current step from the version 0 model naturally constitutes a definite step from a tentative description on a regional scale to a description which has a more profound local focus on the Simpevarp subarea. This shift is true for most disciplines, and particularly so with regards to the surface-based geological description (lithology, deformation zones). The one exception is the description of surface ecology where the database and the associated model/description are still essentially regional in character. However, with regards to the description of the subsurface, the amount of new information is modest and is essentially limited to information from one new (KSH01A/B) and two existing (KLX01 and KLX02) cored boreholes and three new percussion-drilled boreholes. Furthermore, the amount of information from the boreholes is not evenly distributed amongst the disciplines. There is a marked overweight on geological and hydrogeochemical information with a more limited data and scooping modelling studies in hydrogeology. Overall, the information at depth for Simpevarp 1.1, is not very different from the version 0 model of the Simpevarp area.

Despite this, a series of important steps have been taken compared to the version 0 model. These are set out below.

- A detailed lithological model covering the local model area has been devised which identifies three principal rock domains. The lithological model of the regional model area corresponds to the version 0 model.
- A model of deformation zones covering the local model area has been constructed using available new data and existing information from previous work. The model of deformation zones in the regional model area essentially corresponds to that developed for version 0.
- A model of discrete features (DFN) has been devised for the local model area based on detailed fracture mapping on four outcrops and data from three cored boreholes and three percussion-drilled boreholes.
- The developed hydrogeological description is conceptually focused mainly on the description of the evolution of the distribution of salinity in the groundwater as a function of the shoreline displacement with time. Because of the planned delay in the data freeze for the local scale lithological model and deformation zone model, a volumetric local scale description of the hydrogeology has not been developed.
- The conceptual model of hydrogeochemical development, including assessment of origin of different waters, has been updated. A Simpevarp 1.1 descriptive model of the Simpevarp subarea has been developed including descriptions of the distribution of salinity, mixing and a more detailed description of major reactions/processes down to a vertical depth of approximately 300 m.
- A model of mechanical properties (modulus, strength etc.) has been developed based on an empirical model (Q and RMR). Strength information from Äspö HRL and CLAB was utilised. The model of rock stresses basically corresponds to the version 0 model.

- A first descriptive model of thermal properties has been devised. A description of thermal properties was not included in version 0. A characteristic of the rocks of the Simpevarp local scale model area is a comparatively low thermal conductivity.
- A first attempt on a description of the transport properties of the rock has been made. Transport properties were not included in the version 0 model. However, although some data can be imported from Äspö HRL, it is concluded that the parameterisation of the present model with diffusion and sorption parameters should be based on existing generic databases. In addition, calculations of flow-related transport parameters have provided indications on some of the main uncertainties related to radionuclide transport from repository depth.
- The surface ecological model essentially describes the situation in the regional area. New elements in the local scale description are an established map of the Quaternary deposits (with spatial distribution of outcrop rock), a description of biotic entities and their properties, human activities and natural values.

Among the more marked changes in the present description compared to the version 0 model and description are the following.

- The geological model is based primarily on surface data of much higher resolution and in part on new sub-surface information.
- Attribution of properties and estimates of the confidence of existence have been made for a total of 63 interpreted deformation zones in the local scale model domain.
- Deformation zone ZSM0003A0 in the version 0 model has been removed (as a result of improved interpretation).
- The off-shore lineament trending north-south immediately east of Ävrö and the Simpevarp peninsula has been upgraded to a deformation zone (ZSMNE024A) with a dip towards the west. Considered only as a lineamt in the version 0 model.
- A comparatively low overall thermal conductivity is noted. This is caused by the generally low quartz content in the bedrock. The rock domains dominated by fine-grained dioritoid show the lowest heat conductance in the Simpevarp subarea.
- A high frequency of sealed fractures (fractures with a hard lithified infilling) has been noted.
- A Geological DFN model has been developed which also explores the geological and structural controls on the evaluated parameters. Geological DFN and hydrogeological DFN models were also developed as part of previous Äspö HRL work.
- A first step has been taken through hydrogeological modelling to explore the palaeoevolution in the Simpevarp area. Specifically, the evolution of the salinity distribution caused by the post-glacial sea shore displacement has been studied.
- A decreasing hydraulic conductivity with depth is observed in borehole KSH01A. This depth dependence is not represented in the regional scale hydrogeological model, and it is not as pronounced on Ävrö and Äspö. This will be followed up in Simpevarp 1.2.

A hydrogeological descriptive model has only been developed at the regional scale. No hydrogeological descriptive model was developed in the local scale. This stems from the fact that the local scale geological model was developed following a planned delayed data freeze for the bedrock map and the linked lineament map of the Simpevarp subarea, c.f. Chapter 2. This constitutes an important deviation from the strategy document for hydrogeological descriptive modelling.

8.2 Overall understanding of the site

The overall understanding of the Simpevarp subarea is addressed and discussed in Chapter 6 dealing with confidence assessment. The following section explores further the conclusion made there.

8.2.1 General

As discussed in detail in Section 6.2 there is much uncertainty in the Simpevarp 1.1 Site Descriptive Model. However, the main uncertainties are identified, and in some cases even quantified, whereas others are left as input to alternative hypotheses. A major reason for uncertainty in Simpevarp 1.1 is the lack of data and poor data density, and, as many more data are expected in subsequent data freezes, it was not considered meaningful to carry the uncertainty quantification or the alternative model generation too far. Such efforts would soon be outdated. However, the types of uncertainties and alternative hypotheses identified are judged to likely serve as highly useful inputs to the uncertainty assessment and alternative model assessment in subsequent model versions.

A large number of interdisciplinary interactions have been considered and good start on cross-discipline understanding of possible interactions has been established. The current site descriptive model incorporates a direct consistency in geometry between the geological, rock mechanics, thermal and bedrock hydrogeological models. No attempts have been made, mainly due to lack of data at depth in the bedrock, to quantitatively explore implications from e.g. rock mechanics, hydrogeological or hydrogeochemical measurements on the geological description (lithology and deformation zones). Such evaluations are, however, expected in subsequent model versions. Of particular interest in this context will be evidence of hydraulic connections from drilling and or cross-hole interference tests that could potentially help assess the hydraulic properties and connectivity (extent) of interpreted deformation zones.

The current site descriptive model is in general agreement with current understanding of the past evolution, c.f. Chapter 3. However, one constraint in this context is the fact that the local scale hydrogeochemical understanding of the site is restricted to the processes taking place at the surface and down to an approximate depth of 300 m. Despite the fact that the model is restricted depth-wise, the confidence in the hydrogeochemical description is considered high, because a number of independent model approaches have been utilised in the work. The origin and the post-glacial evolution of the water are fairly well understood. The confidence concerning the spatial variation is low due to the small number of observations at depth. The ongoing sampling programme is expected to provide more data at depth, better overall spatial information, and will increase confidence.

Compared to version 0 there are a considerable amount of additional features underlying Simpevarp 1.1, especially in the local scale geological model.

There are no real big surprises in the Simpevarp 1.1 model. However, the fracture frequency in borehole KSH01A (open and sealed) is high compared to conditions experienced at Äspö HRL. Whether this is a characteristic of the bedrock or due to differences in the mapping procedure will be explored further. Furthermore, the hydraulic conductivity in KSH01A is surprisingly low, despite the noted high fracture frequency, and in comparison to results from exiting boreholes in the area.

The overriding factors affecting confidence in the Simpevarp 1.1 is the bias and uncertainty resulting from a small number of unidirectional deep boreholes and an inherent varying spatial coverage of data.

8.2.2 Advance on important site-specific questions

In the execution programme for the Simpevarp area /SKB, 2002b/ a number of important site specific questions were formulated. They concerned *"Size and locations of rock volumes with suitable properties, location and importance (particularly in terms of permeability) of fine-grained granite bodies and fracture zones, high rock stresses, thermal conductance of the bedrock, rock mechanics properties of rock mass, and ore potential"*.

Based on the outcome of the Simpevarp 1.1 modelling the following advances can be reported.

- "Size and locations of rock volumes with suitable properties (Simpevarp peninsula)": Possible volume-delineating deformation zones have been interpreted with uncertainty associated with their existence (and geometry). Only very limited new information is available on material properties of the rock mass at depth.

- "Location and importance (particularly in terms of permeability) of fine-grained granite and fracture zones": Fine-grained granite and pegmatite veins and dikes exist throughout the investigated subarea. No new information is available on material properties of the deformation zones bounding potential repository rock volumes.
- Information on "High rock stresses" is at this stage primarily based on import of data from the Äspö HRL, implying a bias towards the stress situation experienced at Äspö.
- The "rock mechanics properties of the rock mass" are inferred indirectly using empirical relationships based on the Q and RMR indices.
- The "thermal conductance" of the bedrock is found to be low (based on indirect assessment using density logs and mineralogical content). The rock domains with the lowest thermal conductance are dominated by the fine-grained dioritoid.
- The "ore potential" of the Simpevarp area has not been addressed yet, but a similar study to that carried out for the Forsmark region /Lindroos et al, 2004/ is under way and will be reported as part of the Simpevarp 1.2 model.

In conclusion, the remaining site-specific issues following the Simpevarp 1.1 modelling are associated with rock stresses, thermal, mechanics and hydrogeochemical properties of the rock at depth. In addition, to verify and assess the properties of important interpreted deformation zones, some of which are repository volume-delineating zones, require more attention. Furthermore, the issue of the ore potential in the area remains to be settled.

Auxiliary issues which are to regarded as means to address and resolve the remaining issues above are; the establishment of a hydrogeological DFN model, inclusion of an interface between surface and subsurface systems (surface hydrology/near surface hydrogeology), and the further integration/comparison of hydrogeochemical and hydrogeological data, models and understanding.

8.3 Implications for further modelling

The Simpevarp 1.1 model version is presently subject to update using data available at the data freeze of April 1 2004. In preparation for the Simpevarp 1.2 modelling, experience has been assembled regarding issues of technical/scientific and procedural nature to be considered in the upcoming work. Experience which forms the basis for these considerations has been assembled during the modelling work and has to some extent also been discussed during project meetings.

8.3.1 Technical aspects and scope of the Simpevarp 1.2 modelling

The needs expressed by Safety Assessment and Repository Engineering define the requirements for resolution and accuracy within the regional and local scale model volumes. Expressed needs for high resolution and low uncertainty may call for a reduced local scale model domain with a focus on the area where information is available.

On the other hand, the data underlying Simpevarp 1.1 model do not have the coverage to allow such focusing. Furthermore, the modelling work in the Simpevarp area includes a subsequent modelling effort also on the Laxemar area. In fact the Simpevarp 1.2 modelling incorporates a version 1.1 modelling effort on the Laxemar subarea. The Laxemar 1.2 modelling follows in direct succession to the Simpevarp 1.2 model version. In order to satisfy a coordinated effort on the two adjacent Simpevarp and Laxemar subareas, the local scale modelling area will in fact be increased in size to include the two. This step will enable an iterative and interactive inclusion of data from both subareas in the process of building the Laxemar 1.2 model, which in essence will provide the concluding model of the Simpevarp area as part of the initial site investigations. When taking the step to the complete site investigation phase, a decision will be taken whether to retain or reduce the size of the local scale model domain.

The data freeze of Simpevarp 1.2 (April 1, 2004) will include data from several deep core drilled boreholes, some from new boreholes and some from existing boreholes in the two subareas. The data include results from various types of loggings and tests (geological, geophysical, hydrogeological and hydrogeochemical). It is expected that these new data will help unravel some of the site-specific issues outlined above. Apart from improving the site-descriptive model, the new data also provide a number of modelling challenges and foreseen interactions between disciplines.

- For the Simpevarp 1.1 geological modelling, essentially no feedback from other disciplines was worked into the modelling, primarily because of the planned delayed data freeze for Geology. For Simpevarp 1.2, the geological modelling needs to consider input mainly from hydrogeology (possible indications of connectivity of deformation zones) and rock mechanics (hypotheses regarding the observed stress situation in the Simpevarp area).
- Modelling of the rock stress development and observed stress levels with due consideration of the geological model (rock domains and deformation zones) may help to better understand the rock stress distribution.
- With due respect to limited numbers and distances, it is expected that hydraulic interference tests and possibly also pressure interference during drilling may be explored in developed hydrogeological models to better assess how the investigated site works hydraulically.
- An objective for the Simpevarp 1.2 modelling is to better define and describe the (hydraulic and chemical) interface between the surface system and the deeper bedrock system.
- A three-dimensional hydrogeochemical description should be produced down to potential repository depths. Jointly with the above “surface interface” a three-dimensional hydrogeochemical description paves the way for further integration between hydrogeological and hydrogeochemical modelling.

One requirement for the version 1.2 modelling is that more attention should be paid to model alternatives. However, such developments have to be made with a close attention to what is important for the principal consumers of the site descriptive models, i.e. Safety Assessment and Repository Engineering. Furthermore, it is foreseen that only one (or two) alternatives can be propagated all the way from geology (geometry) through hydrogeology (property assignment) to assessment of groundwater flow and transport. It is expected that the following possible alternatives will be addressed, individually or in combination:

- Various assumptions regarding distributions of hydraulic material properties, in particular regarding fracture length distributions and the correlation between fracture transmissivity and fracture size (length) and fracture orientation (anisotropy).
- Assumptions regarding existence, geometry (dip, lateral and vertical extent) and (hydraulic) properties of interpreted deformation zones. One component is the so-called “linked lineament map” and underlying assumptions regarding linkage of individual lineament segments.

The use of independent modelling approaches within the hydrogeochemical, and to some extent also within the hydrogeological modelling provides opportunities to compare outcomes and use noted discrepancies to guide future modelling work. This work has to be carried out in an atmosphere of “balanced competition” working towards one common goal.

8.3.2 Modelling procedures and organisation of work

A great deal of experience has been gained on modelling procedures and organisation of work. It is noted that interdisciplinary modelling is a continuous learning process, and this process will continue throughout the site descriptive modelling. Most of the participants joined the modelling of the Simpevarp area with different experiences of interdisciplinary modelling. These range from modelling work related to Äspö HRL (Äspö site modelling, TRUE Programme, Prototype, Äspö Task Force on modelling of groundwater flow and solute transport etc.), the version 0 modelling work on Forsmark and Simpevarp, the model test on Laxemar, or the version 1.1 modelling of Forsmark. Many of the strategy documents developed had these experiences as raw models for the developed strategies.

Most of listed work above involved modelling on single spatial scales, or addressed multiple scales with relatively loose coupling. Perhaps the most important experience from the presently ongoing modelling work is that the unification of scales (e.g. in devising “universal” fracture length distributions and expressions that link fracture transmissivity with fracture size) is non-trivial. This realisation has posed conceptual issues that will be pursued in continued modelling process. In addition, the following issues related to the modelling work were highlighted for consideration and improvement in future modelling steps:

- Capture and evaluation of primary data, as reported in Chapters 2 and 4 of the current report, are highly resource-demanding efforts. Procedures have been updated as a consequence of the Simpevarp 1.1 modelling which is expected to make this step less cumbersome in future modelling. However, the amount of data will successively grow. This calls for expedient procedures (including mature and usable data table formats) and resources to make the data readily available to site modelling at the time of the data freeze, and in some instances even prior to this set date. Ideally, the primary data as stored in the SICADA database are accompanied by a primary data report which account for the collection and basic evaluation of the data.
- Information exchange with the on-site investigations has been continuous during the Simpevarp 1.1 modelling. This has been realised by attendance at the Simpevarp site modelling project meetings by representatives of the site investigations. During the later part of the Simevarp 1.1 modelling, representatives of the site modelling team have been present at planning meetings organised by the site.

One drawback with the data freeze concept is that unlike the modelling team, the site continues to work in a successively evolving model where new data successively are fed in. In the case of Simpevarp 1.1, the dialogue with the site was complicated further by the fact that important parts of the geological data freeze were subject to a planned delay of almost six months, c.f. Section 8.4.1. It is still firmly believed that the concept of well-defined data freezes, in terms of time and content, is required to allow the necessary traceability and consistency (between disciplines) in the ongoing staged modelling. It is noticed that the “gap” between the model worked on by the site and the site descriptive modelling team successively will be diminished. A challenge is to maintain the highly necessary dynamic interaction with the site without working in a bias resulting from being exposed to new facts and insight, coming subsequent to the data freeze. The latter should not be overemphasised, because the “learning curve” is expected to level off dramatically towards the end of the initial site investigations. It should, however, be remembered that the latter is not necessarily true for the disciplines that obtain their primary site data late, e.g. transport properties.

The upcoming model versions will require further integration between disciplines. Given the sequential nature of the work where geology provides the geometrical skeleton to all disciplines, and e.g. hydrogeology provides results underlying estimation of flow-related transport properties, there is a high demand to adhere to set up plans and milestones to keep the overall schedule. Furthermore, the version 1.2 modelling implies a more direct interplay with Repository Engineering and Safety Assessment in that well specified deliveries have been defined for the course of the 1.2 modelling work.

Review comments on the report structure used for the v1.1 reporting already received on the Forsmark 1.1 report have resulted in a revision of the report disposition for the version 1.2 reporting. The primary change to structure and style is that individual chapters will be devised for all disciplines dealing with the bedrock system. A separate chapter will describe the surface system and the interface to the bedrock system. In addition, the possibility to divide the report in separate volumes will be explored, as will the possibility to develop supporting documents (reports) that would allow for less detail in the main report. It is acknowledged that there is a subtle balance between allowing the main report to be sufficiently self-contained and at the same time providing a report that is not prohibitively voluminous.

8.4 Implications for the ongoing investigation programme

One of the objectives of the version 1.1 site modelling of the Simpevarp area is to provide recommendations on continued field investigations during the initial site investigations. The interplay between the site modelling project and the site investigations is complicated by the fact that two adjacent subareas are being investigated in parallel. The start up of the investigations at Laxemar commenced towards the end of 2003. In addition, the geological modelling for Simepvarp 1.1 was subject to a planned delay until mid December 2003. Effectively, the site modelling project was thus faced with the task of responding to issues and providing feedback on Simpevarp and Laxemar based on the existing version 0 model.

An account of the recommendations arising from the work with the Simpevarp 1.1 model is provded in the ensuing sections and is divided into recommendations and/or feedback provided to the site investigation organisation at Simpevarp during the course of the modelling work, and recommendations arising from identified uncertainties in the model Simpevarp 1.1.

8.4.1 Recommendations/feedback given during the modelling work

During the work with Simpevarp 1.1, the project group has had an information exchange with the site investigation team regarding the site investigation programme. These questions have ranged from more profound ones (location of drilling platforms, location of boreholes and their geometries) to details regarding e.g. sampling procedures and methods. Comments and feedback have been given to draft versions of planning documents and decision papers on specific boreholes produced by the site investigation team. Recommendations and feedback from the hydrogeochemical modelling work have been provided in various documents. Overall, the feedback to the site investigation team has been given in an “informal” manner via electronic mail, telephone and during meetings, ans has not necessarily been fully documented. An electronic log has therefore been devised in an attempt to keep track of some of this “informal” exchange of information.

Recommendations concerning drilling of new boreholes

Mid 2003 a draft document was produced by the site investigation team that outlined the plans for drilling deep cored boreholes in the Simpevarp and Laxemar subareas /SKB, 2003c,/. This document broadly identified the locations and geometries of; borehole KSH03 on the eastern shore of the Simpevarp peninsula, the borehole KAV04 on Ävrö and the drilling platforms for boreholes KLX03 and KLX04 in the western part of the Laxemar area. The modelling team provided feedback on geometries and the relative order of the KLX03 and KLX04 boreholes. In addition, the modelling team was involved in the siting and orientation of the planned borehole KBH03 on the Hålö island (later postponed). Finally, the modelling team provided recommendations on the usage of existing drilling platforms and location of future drilling platforms in the Laxemar subarea. None of these recommendations were documented in dedicated decision documents, but rather in electronic mail correspondence in response to draft reports or decision documents drawn up by the site investigation team.

During the first quarter of 2004 the modelling team also provided feedback on a document concering detailed plans for drilling short percussion boreholes with the purpose of verifying interpreted deformation zones in the Simpevarp subarea (boreholes HAV11–HAV14, HSH04–HSH06).

Feedback to the hydrogeochemical site investigation programme

The analyses of hydrogeochemical primary data and subsequent modelling work have been carried out by a group of experts, the so-called Hydrogeochemical Analysis Group (HAG). During the course of their work this group has provided continuous feed-back to the hydrogeochemical site investigation programme through the activity leader for hydrogeochemistry at Simpevarp. The provided feed-back and the response obtained have been documented by the representative for hydrogeochemistry in the modelling project, c.f. Table 8-1.

Table 8-1. Hydrogeochmical feed-back from the modelling project (HAG) to site investigation and the response from the site investigation.

Feed-back	Response
All samples should have x, y, z coordinates in order to be useful in the visualisation work. The z coordinates were not available for the surface samples (sea, lake, streams, soil tubes). Therefore, the z coordinate was estimated from a grid-map with an error bar +/–10m /Henrik Stridsman, pers. comm., 2003/. A reference level should be used for future sampling so that the z-coordinate can be calculated in the field during the sampling. The tube sampling in boreholes with low hydrogeological conductivity is of limited use for accurately reflecting variations in the formation groundwaters. However, the information may be useful for reflecting the disturbances in the open borehole.	A more precise Z-coordinate determination will be available in the future by using high precision GPS.
For the Forsmark study emphasis was put on the need for more background information in order to evaluate sample representativeness. For example: a) at which stage during the Chemac monitoring of pH, Eh, O_2 and Temp. is it decided to take samples and why?, b) when there are time constraints and it is not possible to wait for chemical stability – sampling should be planned to cover the complete sampling period, rather than choosing just one time interval. This will give a spread of sampling which should also show up time variations which can be important, c) SICADA only indicates the 'Start' and 'Completion' dates of the sampling. It is necessary to know the actual day of sampling for proper evaluation, and d) information concerning drilling/sampling protocols (e.g. pump stops; other pauses etc.) and the sequences of events carried out in the boreholes are needed. Information relating to these points generally was made available for the Simpevarp evaluation which greatly improved the potential for establishing the representativeness of the borehole groundwater samples. Additional information for point (d) would be appreciated in the future.	a) This will be better documented in the future Chemical Characterisation program. b) In the future the sampling will have a better distribution during the pumping period of each section regardless of flushing water content. c) This information is already in SICADA, and it is only a question of how the data are sorted. d) Every sub-activity (eg. Start and stop of pumping, calibrations, signal failure) of the borehole are documented in the Daily-Log, and this information is available in SICADA. If there is need for additional information the responsible personnel can record such information in separate tables.
The CHEMAC data are always very useful but the technology should be improved in order to avoid the many technical problems during field measurements.	Improvements have already been made during autumn 2003.
Analytical questions have been taken up with the site and moves are being made for improvement (e.g. Br data quality; U-series data). Also proper presentation of some data to the required precision (e.g. Sr isotope ratios; ^{11}B etc.) have been improved in the SICADA data base.	
The flushing/drilling waters should be allocated Class 5 status which is useful to track contamination especially using trace elements and isotopic signatures which may be quite sensitive. Required would be: a) sampling at the point of removal from the source percussion borehole, and b) sampling prior to injection into the cored borehole. This should be checked on a monthly basis during the drilling period.	A change in the analytical quality for flushwater is a cost issue (three times the amount of samples and three times higher cost for each sample). There are no plans to change these routines but archived samples for Class 5 can be collected for later analysis.
Some data such as REEs are always below detection limits with the result that all granitic waters will show the same range of REE contents. Can other analytical techniques or laboratories be used so this information can be used in models? The same is valid for S^{2-}, for example, since it seems that the SO_4^{2-} / S^{2-} redox pair is crucial for the redox control of these systems, could the analysis of S^{2-} not be improved in order to obtain a greater amount of groundwater data?	This issue will be further investigated. New ICP-MS equipment with very high precision (detection limits in the area of 0,1 ppt for U and Th) is now available. This instrument can also be used for specific analyses requiring low detection limits and to be used for control analysis.

DIS (Drilling Impact Study) should be made during drilling in order to identify the degree of contamination and guide the sampling strategy. The drilling data should be available earlier concerning: a) the drilling water volume pumped in and out from the borehole, b) the uranine concentration in the drilling water pumped in and out from the borehole, and c) the water pressure and drawdown along the borehole. The equipment should be more reliable, for example: a) the water pressure during drilling could not be measured properly due to a sensor failure, and b) the quality is poor for the drilling water pumped into the borehole, showing plateaus with no inflow. During the "plateau period" drilling was still conducted and water was pumped into the borehole. The error is explained by a sensor problem.

Our general opinion is that it is difficult to use the data collected during drilling (DMS-data) for modelling or for sample guidance due to large uncertainties. If there is a need for a DIS-evaluation associated with the modelling of the data, a proposed methodology must be prepared in which it is stated exactly what information/data is needed and at what frequency.

Log of "informal feedback"

An attempt has been made to organise the "informal" information exchange between the modelling project and the site investigation team. In order to exemplify the type of feedback given, an extract is provided in Table 8-2. It is noted that this list primarily includes the type of feedback provided/funnelled through the project manager. Hence, the provided list is not claimed to include all information exchanges of informal nature during the work on Simepvarp 1.1.

Table 8-2. Example of items related to feed-back to site investigation extracted from log for "informal" information exchange during the Simpevarp 1.1 work between the modelling project and site investigations (original log-file is in Swedish).

ID	Specification	When?	Follow up?
16	Request for discussion of nomenclature related to the area notations used for the Simpevarp and Laxemar subareas and their surroundings.	February 2003	Yes (see ID31)
21	Project group provide comments SKBs memo on selection of geologically interesting area (Email to cPOU, 2004-02-18).	February 2003	
27	Project group provide comments on Simpevarp 1.1 delivery of primary data (E-mail to uPOU, 2004-03-17).	March 2003	
28	Project group provide joint proposal regarding geometry of new borehole in the Laxemar subarea (E-mail to uPOU, 2003-03-18).	March 2003	
31	Proposal from PL to uPOU regarding nomenclature related to areal notations for Simpevarp and Laxemar subareas.	March 2003	
43	Telephone meeting on division of work between the site and the modelling project regarding characterisation of Quarternary and soils in the Simpevarp subarea.	May 2003	
83	OK to POU on location and geometry of cored borehole KBH03.	November 2003	
84	Feedback to POU on possible alternate geometry of KBH03.	December 2003	
85	Comment on proposed percussion borehole program for lineament verification in the Simpevarp subarea.	March 2004	
86	List of prioritised primary data related to S1.2 delivered to POU.	March 2004	
87	Comments on tentative positioning of KLX05, KLX06 and KLX07 provided to POU in conjunction wuth POU Planning meeting #35.	March 2004	

8.4.2 Recommendations based on uncertainties in the site descriptive model Simpevarp 1.1

The site-specific issues of critical nature raised in FUD-K /SKB, 2001c/ and subsequently in the planning of the site investigations in Simpevarp /SKB, 2002c/ are essentially still valid, c.f. Section 8.2.2. Model version Simpevarp 1.1 provides some increase in understanding of the geological features of the site, but high uncertainties in the site description still prevail. Furthermore, given the planned delay of important parts of the geological data freeze (bedrock map and linked lineament

map, implies that the geological model has not propagated in full into the modelling work of some disciplines. This is particularly true for the hydrogeological and hydrogeochemical modelling, and to some extent for the rock mechanics modelling.

The main noted uncertainties are listed and discussed in Section 6.3, where also the main reason for the noted uncertainties is the lack of data at depth in the bedrock combined with a poor data density. Using these uncertainties as a starting point, the project group has made an effort to assess whether the identified uncertainties will be reduced by additional data, and if so, how those data should/can be obtained.

The assessment was carried out by filling in the table with the following information:

- A specification of the uncertainty in the Simpevarp 1.1 model and the underlying cause for this uncertainty, i.e. a copy for reference of the information already provided in Section 6.3.
- An assessment as to how much of this uncertainty that can be reduced by additional data that will become available fro model version Simpevarp 1.2 (and subsequently from model version Laxemar 1.2 which follows in close succession).
- An assessment of how much of the uncertainties remaining in model Laxemar 1.2 can be reduced by site investigation data provided during the complete site investigation phase, and how this in practice can be achieved.

The results of the assessments are shown in Table 8-3 and are summarised below. No specific recommendations are given in Table 8-3 on elements in site investigations that will reduce uncertainties in the description of transport properties of the bedrock. The reason for this is that no site-specific transport data are available for Simpevarp 1.1. Some data will become available for Simpevarp 1.2 and will be evaluated according to the strategy document for laboratory measurements of transport properties in the rock /Widestrand et al., 2003/ It is therefore premature at this stage to make suggestions for additional measurements prior to obtaining the imminent results from the initiated strategy.

Location of new boreholes

For obvious reasons, a continued drilling programme and new borehole information (during and after completion of drilling) will contribute to an improved description of the bedrock. In the case of the Simpevarp area, the completion of two new core-drilled boreholes on the Simpevarp peninsula and Ävrö, respectively essentially concludes the drilling programme in the Simpevarp subarea. These boreholes and associated characterisation will be supplemented by complementary characterisation in boreholes KAV01, KLX01 and KLX02, all of which are located inside the local scale model area used in the Simpevarp 1.1 modelling. In addition to these boreholes, two more boreholes are being drilled in the Laxemar subarea furnishing data for the Laxemar 1.2 modelling. As described earlier in this chapter, the local scale model domain employed for Simpevarp 1.2 will be enlarged to also include the Laxemar subarea in its entirety. It is envisioned that the results of the Simpevarp 1.2 modelling can be used to pinpoint a smaller prioritised area for further analysis. Following Laxemar 1.2, it cannot be ruled out that such a prioritised area could be made up of parts of the two subareas in combination.

Although borehole KLX02 provides existing data and access to depths down to some 1,700 metres, the need of additional reference boreholes, upstream and downstream to the Simepvarp subarea, cannot be ruled out.

Heterogeneity of lithological domains

The heterogeneity of the interpreted lithological domains (and underlying rock units) and the locations of lithological boundaries, both at the surface and at depth, may have implications for the layout and construction of a geological repository, primarily through the distribution of rocks of variable thermal properties. It is not expected that the planned drilling prior to Simpevarp 1.2 will shed more light on this issue. Gravity measurements may provide some insight if the density contrast between the rock units is is high enough to allow conclusive interpretation.

Occurrence, geometry and properties of deformation zones

The occurrence and geometry of interpreted deformation zones are both associated with high uncertainties. This is also true for subhorizontal zones, although such zones of significant nature neither have been seen in available boreholes, nor in the underground openings of the Äspö HRL. Despite the fact that the boreholes drilled are all near vertical and should be optimal for identifying horizontal structures, their existence cannot be ruled out. This is particularly true for subhorizontal structures of minor extent. Suggested field activities in order to reduce uncertainties related to deformation zones are:

- Field investigations of selected lineaments in order to confirm their occurrence, geometry and properties (reflection and refraction seismic surveys, targeted percussion drilling on selected lineaments (interpreted deformation zones).
- Cross-hole hydraulic interference tests between boreholes (where applicable, and possibly supplemented by injections of solute tracers) may provide information on the occurrence and connectivity (continuity) of interpreted deformation zones.

Fracture mapping, fracture statistics and DFN modelling

The geological DFN model developed for Simpevarp 1.1 is firmly related to geology. This includes supporting analysis of the representativity of surface fracture mapping for conditions at depth, and relationships between fracture sets and interpreted lineaments and mineralogy and alteration, c.f. Section 5.1.6. Notwithstanding these findings there is a need for confirmatory results using short cored boreholes in variable directions.

Rock stress distribution – rock mechanics properties

The uncertainty in rock stress magnitudes and distribution at depth will most likely be reduced significantly by measurements performed for data freeze Simpevarp 1.2. Similarly, measurements of mechanical properties on site-specific rock materials will be become available for Simpevarp 1.2.

Transmissivity distribution – hydraulic tests

The uncertainty in geometry of water-bearing structures and transmissivity distribution in zones and fractures will be reduced by improved understanding of the geological model of deformation zones and by joint interpretation of new information from additional boreholes and hydraulic tests. Such data will become available for Simpevarp 1.2. However, addressing of key conceptual issues – like the transmissivity/fracture size relation – calls for a targeted focus on cross-hole interference tests. Given the potential lack of suitable sink-source pairs of boreholes, there may be a need to consider import of existing data/results from e.g. Äspö HRL. It is however noted that any inference of fracture/structure size and subsequent coupling to a transmissivity value is associated with uncertainty.

Groundwater composition – pore water in intact rock matrix

The conceptual understanding of hydrogeology and hydrogeochemistry, individually or jointly, is associated with uncertainties concerning the past evolution. There is a general need to obtain chemical data from depth – and more such data are expected in the data freeze Simpevarp 1.2.

In addition, information on the composition of the rock matrix water and the intact rock matrix porosity will provide valuable input to this understanding of the past, as well as the present hydrogeological and hydrogeochemical conditions at the site. Measurements of these entities are therefore recommended. Pilot work on matrix fluid chemistry has been conducted by /Smellie at al, 2003/.

Surface system

Table 8-3 shows that much of the current uncertainty in the surface system properties and processes description stems from lack of data. This uncertainty is expected to be partly resolved through the data that will become available by the data freeze for Simpevarp 1.2. However, the available time series of hydrological data will be short also in the Simpevarp 1.2 modelling. Prolongation of the

monitoring programmes for e.g. meteorology, hydrology (water levels, runoff etc.), hydrogeochemistry and ecosystems will result in longer time series, which will help reduce uncertainties in future models.

There exists a need for further characterisation of the overburden and the Quaternary deposits. The understanding of the thickness (and inherently the depth to the bedrock surface) is only known at a limited number of localities in the subarea. Hence the understanding of the spatial variability of the latter two entities needs improvement. Integration of data from marine geological surveys, mapping of coastal bays and results from new drillings in the Quaternary deposits should eventually produce a continuous map of the overburden from the present day land areas to the offshore sea floor. Furthermore, the hydraulic properties of the Quarternary deposits are at present deduced from empirical relationships applied in a generalised manner to the available types of deposits. There is therefore a need for direct measurements of the hydraulic properties of the Quaternary deposits.

Table 8-3. Uncertainties in the site descriptive model version Simpevarp 1.1 and field data/ activities that can reduce these uncertainties.

Discipline	Model version S1.1		Will S1.2 data reduce this uncertainty?		Can remaining uncertainty in SDM S1.2 be reduced by more field data? Laxemar 1.2 and beyond?	
	Uncertainty	Cause	Much/To some extent/ Little	How	Much/To some extent/Little	How
Geology – rock domain model	Mainland lithology.	Limited subsurface data.	To some extent.	Observations in additional cored boreholes.	To some extent.	Observations in additional cored boreholes. Modelling of geophysical data.
	Offshore lithology (lower quality data in these areas).	No data.	Little.		Little.	
	3D extension of dioritoid and mixed rock type domains.	Little or no data.	To some extent.		To some extent.	Additional boreholes.
	Heterogeneity – Proportion of rock types in domains, veins, patches, dykes, minor bodies, frequency of minor deformation zones) (Statistical anisotropy ?).	Limited data.	Little.	Observations in additional cored boreholes.	Much / To some extent.	Specified field investigation at a limited number of outcrops in key rock domains. Observations in additional cored boreholes.
Geology – structural model	Existence of deformation zones (only some interpreted with high confidence) – are all lineaments really deformation zones?		To some extent.	Additional refraction seismic survey data and percussion drillings from Ävrö.	To some extent in the local model area.	Observations in additional cored boreholes. New reflection seismic data.
	Potentially there are non-included zones (mainly subhorizontal) (e.g. the Nordenskjöld hypothesis.		Little.	Drilling. Field investigation of selected lineaments by stripping away the Quaternary cover. Ground geophysics. Hydrogeological interference tests between boreholes.	To some extent in the candidate area.	

	Continuity along strike and at depth, dip and termination.	Very few surface and sub-surface observations.	To some extent in the local scale model area.	Drilling activity. Field investigation of selected lineaments by stripping away the Quaternary cover. Ground geophysics. Interference tests between boreholes.	To some extent in the local model area.	Observations in additional cored boreholes. New reflection seismic data.
	Character and properties – also in the well established (e.g. from Äspö) zones. Strong spatial variation of properties (width, fracturing, also hydraulic properties) as seen in multiple intercepts.	Very few sub-surface observations.	To some extent in the local scale model area.	Additional boreholes. Interference tests between boreholes.	To some extent.	Additional boreholes. Field investigation of selected lineaments by stripping away the Quaternary cover. Ground geophysics. Interference tests between boreholes.
Geology – DFN model	Fracture set (orientation) identification.		To some extent.	More information regarding sub-horizontal fracture orientations and intensity in new boreholes.		
	Fracture size distribution – interpolation between lineament and mapped outcrop data and for some sets only local information (extrapolation to larger sizes).		To some extent.	Availability of more fracture data from tunnels and openings at Äspö HRL.		
	Fracture intensity – now based largely on surface data – representativity for conditions at greater depth!?		To some extent.		To some extent.	
	Assumption of fracture intensity coupled to ductile deformation and lineaments. Spatial model. Spatial distribution in different rock domains. 3D distribution of “secondary red staining” (hydrothermal alteration).		To some extent.		To some extent.	
Bedrock in situ stress state	Rock stress magnitudes and distribution within the model area.	Lack of stress data and uncertainty in interpretation of stress data.	Much.	More site specific data available. Deformation zone model may support stress modelling.	Much/To some extent.	Further stress measurement.

Bedrock mechanical properties	Applicability/reliability of empirical approach for estimation of rock mass properties.	Inherent uncertainty in empirism. Uncertainty in lithological model.	Much.		Little.	
	Mechanical properties on rock mass scale – spatial variability.	No direct measurements. Model based on observed fracture statistics from one borehole.	Much/To some extent.	More boreholes + labdata+ numerical modelling of rock mass properties.	To some extent.	More data + Further modelling.
	Mechanical properties – deformation zones.	No direct observations.	Much (If observed in boreholes)/ To some extent.	Furher investigations, study of old data from Äspö HRL.	Much/To some extent.	Further geological and geophysical investigations.
Bedrock thermal properties	Thermal conductivity – rock type.	No measurements.	Much/To some extent.	Additional lab data + Äspö data+ modelling.	To some extent	Additional measurements.
	Thermal properties – spatial variability.	No direct measurements. Model based on rock domain model. Possibly also insufficient information on the variation of lithology in 3D (limited data from deep boreholes).	Much/To some extent	More measurements, potential correlation between density and thermal conductivity for all rock types.	Much/To some extent.	Additional bore hole information and measurements in relevant scale.
	Thermal expansion.	No direct measurements.	Much/To some extent.	Additional lab data+ modelling.	To some extent.	Additional lab data+ modelling.
Bedrock hydrogeology	Geometry of waterbearing structures.	Uncertainties in geological structural model.	To some extent.	Response tests during drilling.	Much.	Focus on hydraulic interference testing.
	Transmissivity distribution in zones (spatial variability).	Few intercepts implies few site data.	Little.	Response tests during drilling.	To some extent.	Additional boreholes and hydrotests.
	Fracture transmissivity distribution.	Few site data.	Much.	Additional boreholes and hydrotests (difference flow logging).	Much.	Additional boreholes and hydrotests (difference flow logging).
	Digital elevation model in the vicinity of the shoreline.	Few site data.	To some extent.	Possibly boosted by geostatistical analysis.	Much.	
	Hydraulic DFN model.	Not based on S1.1 geological DFN. One T-distribution assigned to all fracture sets.	Much	Application of updated strategy for DFN Hydro based on v1.1 models.	To some extent/ Much.	Additional boreholes. Improved geological basis and statistics.

Paleo-hydro-geology	Present day salinity conditions.	Few site data. Few data at depth.	To some extent.	Additional boreholes and hydro-geochemical analysis.	Much.	Additional boreholes and hydro-geochemical analysis.
	Regional scale boundary conditions.	Current size of the model domain does not coincide with natu-ral physical boundaries.	To some extent.	Exploration numerical simulation.	Little.	
Hydrogeo-chemistry	Spatial variability in 3D at depth.	Few site data.	Much, but remaining uncertainty.	Additional borehole data from KSH02, KSH03 and KAV04.	To some extent. Confirmation aspects. Details of resolution aspects will not be resolved.	Boreholes in regional model volume. Long-term hydro monitoring. Detailed analy-ses of fracture minerals. Microbes.
	Temporal (seasonal) variability in surface waters, which ultimately impacts the groundwater in the bedrock. Temporal averaging follows from processes being slow.	Few site data.	To some extent.	Additional data.	To some extent.	Additional data.
	Model uncertainties (e.g. equilibrium calculations, migration and mixing).	Few site data.	To some extent.	Test of models on new data.		
	Identification and selection of real end-member waters. There is a judgemental aspect of the M3 (principal compo-nents) analysis.	Few site data. Few data at depth.	To some extent/Much.	New boreholes. New in situ data.		
	Groundwater composition in the rock matrix.	No site data.	To some extent.	Targeted laboratory data. Import of results from Äspö HRL.		
Transport properties	Spatial variability and correlation between matrix transport properties and flow paths.	Lack of data.	Little.			
	Distribution of flow-related transport parameters (i.e. essentially the F-distribution), due to all the uncertainties in the hydrogeologi-cal model and the conceptual model for transport.	Hydrogeological model avail-able only at a regional scale (resolution). Conceptual uncertainties. Lack of data.	Little/To some extent.			
	No site-specific data on sorption and diffu-sion in the matrix are available.	Lack of data.	Little.	Site-specific laboratory measure-ments.		

Surface system – Quaternary deposits	Terrestrial – composition, spatial distribution, depth and thickness of individual strata.	Few sampling locations (drillings).	Much.	QD-mapping of Laxemar area and central part of main catchment areas. Stratigraphic data from trenches and additional boreholes.	To some extent.	Continued investigations. Geological characteristics of discharge areas.
	Aquatic/Marine : No information about the offshore spatial and stratigraphic distribution of deposits. Similar situation for shallow bays.	Marine geological data not accessed. No data available for shallow bays.	To some extent/Much.	New soundings in shallow bays. Marine geological data being accessed.	To some extent.	Continued investigations.
	No laboratory analyses of QD to verify/support the judgements in the field.	Samples have not been analysed.	To some extent.	New samples.	Little.	
	No data regarding in situ properties of the QD (e.g. porosity)	No in situ tests	To some extent.	Slug tests (hydraulic conductivity).		
Surface system – Surface hydrology, near-surface hydrogeology	Meteorology – spatial variability in precipitation etc.	Representativity of SMHI data – all stations outside regional model area.	Little.	Short time series. from one existing ststion. New data from one new station in the Simpevarp area.	Much.	Longer time series from the two targeted meteorological stations in the area.
	Spatial variability in runoff.	Run-off measured outside regional model area. Variation in vegetation, topography, geology etc. not considered.	Little.	Short time series from one runoff station within the area.	Much.	
	No data on hydraulic conductivity in Quaternary deposits.	No in situ data. Only empirical inference.				
Surface system – Chemistry	Temporal and spatial variation in water composition of surface waters.		Much.		To some extent.	Continued measurements .
	Uncertainty in model (e.g. equilibrium. calculations)					
Ecosystems – biotic	Biomass and production (flora and fauna).	No data available.	To some extent.	Laboratory analyses will become available.	To some extent.	Continued investigations.

References

Aaltonen J, Gustafsson C, Nilsson P, 2003. Oskarshamn site investigation – RAMAC and BIPS logging and deviation measurements in boreholes KSH01A, KSH01B and the upper part of KSH02. SKB P-03-73. Svensk Kärnbränslehantering AB.

Agrell H, 1976. The highest coastline in south-eastern Sweden. Boreas 5, 143–154.

Alm E, Sundblad K, 2002. Fluorite-calcite-galena-bearing fractures in the counties of Kalmar and Blekinge, Sweden. SKB R-02-42. Svensk Kärnbränslehantering AB.

Amadei B, Stephansson O, 1997. Rock stress and its measurement. Chapman & Hall, London, 490 p.

Analyse-It Software Ltd, 2003. Version 1.71 (Dec. 11, 2003). Analyse-It Software, Ltd. PO Box 77, Leeds, LS12 5XA, England, UK, http://www.analyse-it.com/ .

Andersson J, Ström A, Svemar C, Almén K-E, Ericsson L O, 2000. What requirements does the KBS-3 repository make on the host rock? Geoscientific suitability indicators and criteria for siting and site evaluation. SKB TR 00-12, Svensk kärnbränslehantering AB.

Andersson J, Christiansson R, Munier R, 2001. Djupförvarsteknik: Hantering av osäkerheter vid platsbeskrivande modeller. Tech. Doc. (TD-01-40), SKB, Stockholm, Sweden.

Andersson J, Christiansson R, Hudson J, 2002a. Site Investigations Strategy for Rock Mechanics Site Descriptive Model. SKB TR-02-01, Svensk Kärnbränslehantering AB.

Andersson J, Berglund J, Follin S, Hakami E, Halvarson J, Hermanson J, Laaksoharju M, Rhén I, Wahlgren C-H, 2002b. Testing the methodology for site descriptive modelling. Application for the Laxemar area, SKB TR-02-19, Svensk Kärnbränslehantering AB.

Andersson P, Byegård J, Dershowitz B, Doe T, Hermanson J, Meier P, Tullborg E-L, Winberg A, 2002c. TRUE Block Scale Project. Final report. 1. Characterisation and model development. SKB TR-02-13. Svensk Kärnbränslehantering AB.

Andersson J, 2003. Site descriptive modelling – strategy for integrated evaluation. SKB R-03-05. Svensk Kärnbränslehantering AB.

Andersson J (ed), 2004. T-H-M in Safety Assessments. Findings of DECOVALEX III, SKI Report (in progress).

Andrén T, Björck J, Johnsen S, 1999. Correlation of the Swedish glacial varves with the Greenland (GRIP) oxygen isotope stratigraphy. Journal of Quaternary Science 14, 361–371.

Ask H, 2003. Oskarshamn site investigation. Installation of four monitoring wells, SSM000001, SSM000002, SSM000004 and SSM000005 in the Simpevarp subarea. SKB P-03-80. Svensk Kärnbränslehantering AB.

Ask H, Morosini M, Samuelsson L-E, Stridsman H, 2003. Oskarshamn site investigation – Drilling of cored borehole KSH01. SKB P-03-113. Svensk Kärnbränslehantering AB.

Ask H, Samuelsson L-E, 2004. Oskarshamn site investigation – Drilling of three flushing water wells, HSH01, HSH02 and HSH03. SKB P-03-114. Svensk Kärnbränslehantering AB.

Ask H, Morosini M, Samuelsson L-E, Stridsman H, 2004. Oskarshamn site investigation – Drilling of cored borehole KSH02. SKB P-04-XX (in prep). Svensk Kärnbränslehantering AB.

Banwart S A, 1999. Reduction of iron (III) minerals by natural organic matter in groundwater. Geochim. Cosmochim. Acta, 63, 2919–2928.

Barton N, 2003. Oskarshamn site investigation – Q-logging of KSH01A and 01B core. SKB P-03-74. Svensk Kärnbränslehantering AB.

Barton, N. Simpevarp site characterisation. Q-logging of surface exposures. Svensk Kärnbränslehantering AB (in prep).

Bein A, Arad A, 1992. Formation of saline groundwaters in the Baltic region through freezing of seawater during glacial periods. Journal of Hydrology, 140, Elsevier Science B.V. pp. 75–87.

Berggren J, Kyläkorpi L, 2002. Ekosystemen i Simpevarpsområdet – Sammanställning av befintlig information. SKB R-02-10. Svensk Kärnbränslehantering AB.

Berglund B E, Digerfeldt G, Engelmark R, Gaillard M-J, Karlsson S, Miller U, Risberg J, 1996. Sweden. In B E Berglund, HJ B Birks, M Ralska-Jasiewiczowa and H E Wright (eds): Palaeoecological events during the last 15,000 years. Regional synthesis of palaeoecological studies of lakes and mires in Europe, p 233–280. John Wiley & Sons Ltd.

Berglund J, Curtis P, Eliasson T, Olsson T, Starzec P, Tullborg E-L, 2003. Äspö Hard Rock Laboratory – Update of the geological model 2002. SKB IPR-03-34 (in press). Svensk Kärnbränslehantering AB.

Berglund S, Selroos J-O, 2003. Transport properties site decsriptive model – Guidelines for evaluation and modelling. SKB R-03-09, Svensk Kärnbränslehantering AB.

Berglund J, Curtis P, Eliasson T, Ohlsson T, Starzec P, Tullborg E-L, 2003. Äspö Hard Rock Laboratory – Update of the geological model 2002. SKB IPR-03-34. Svensk Kärnbränslehantering AB.

Bergman T, Isaksson H, Johansson R, Lindén A H, Lindgren J, Lindroos H, Rudmark L, Wahlgren C-H, 1998. Förstudie Oskarshamn. Jordarter, bergarter och deformationszoner. SKB R-98-56.

Bergman T, Follin S, Isaksson H, Johansson R, Lindén A H, Lindroos H, Rudmark L, Stanfors R, Wahlgren C-H, 1999. Förstudie Oskarshamn. Erfarenheter från geovetenskapliga undersökningar i nordöstra delen av kommunen. SKB Rapport R-99-04.

Bergman T, Isaksson H, Rudmark L, Stanfors R, Wahlgren C-H, Johansson R, 2000. Förstudie Oskarshamn. Kompletterande geologiska studier. SKB R-00-45. Svensk Kärnbränslehantering AB.

Berman R G, Brown H, 1985. Heat capacity of minerals in the system Na2O-K2O-CaO-MgO-FeO-Fe2O3-Al2O3-SiO2-TiO2-H2O-CO2: representation, estimation, and high temperature extrapolation. Contrib. Mineral Petrol., 89, p 163–183.

Beunk F F, Page L M, 2001. Structural evolution of the accretional continental margin of the Paleoproterozoic Svecofennian orogen in southern Sweden. Tectonophysics 339, 67-92.

BFS, 1990. Nybyggnadsregler ändringar. Boverkets författningssamling. BFS 1990:28, Nr. 2, Stockholm, ISBN 91-38-12510-2.

Björck S, 1995. A review of the history of the Baltic Sea, 13.0–8.0 ka BP. Quaternary International 27, 19–40.

Björck S, Kromer B, Johnsen S, Bennike O, Hammarlund D, Lemdahl G, Possnert G, Lander Rasmussen T, Wohlfarth B, Hammer C H, Spurk M, 1996. Synchronized Terrestrial-atmospheric deglacial records around the North Atlantic. Science 274, 1155–1160.

Björck J, 1999. The Alleröd-younger Dryas pollen zone in an 800-years varve chronology from southeastern Sweden. GFF 121, 287–292.

Boresjö Bronge L, Wester K, 2003. Vegetation mapping with satellite data of the Forsmark, Tierp and Oskarshamn regions. SKB P-03-83, Svensk Kärnbränslehantering AB.

Borgiel M, 2003. Makroskopiska organismers förekomst i sedimentprov. En översiktlig art-bestämning av makroskopiska organismer. SKB P-03-67, Svensk Kärnbränslehantering AB.

Bossart P, Hermanson J, Mazurek M, 2001. Analysis of fracture networks based on the integration of structural and hydrogeological observations at different scales. SKB TR-01-21. Svensk Kärnbränslehantering AB.

Bratt P (ed), 1998. Forntid i ny dager – Arkeologi i Stockholmstrakten, Raster Förlag, Stockholm (in Swedish).

Bruno J, Cera E, Grivé M, Rollin C, Ahonen L, Kaija J, Blomqvist R, El Aamrani F Z, Casas I, de Pablo J, 1999. Redox Processes in the Palmottu uranium deposit. Redox measurements and redox controls in the Palmottu system. Draft. Informe 64023. ENRESA, 76 p.

Brydsten L, 1999. Shore line displacement in Öregrundsgrepen.
SKB TR-99-16, Swedish Nuclear Fuel and Waste Management Co, Stockholm.

Brydsten L, 2004a. Method for construction of digital elevation models for site investigation program in Forsmark and Simpevarp. SKB P-04-03, Svensk kärnbränslehantering AB

Brydsten L, 2004b. Shore displacement simulation. Excerpt from PowerPoint presentation available on SKB server (G-disk).

Byegård J, Johansson H, Skålberg M, Tullborg E-L, 1998. The interaction of sorbing and non-sorbing tracers with different Äspö rock types – Sorption and diffusion experiments in the laboratory scale. SKB TR 98-18, Svensk Kärnbränslehantering AB.

Byegård J, Widestrand H, Skålberg M, Tullborg E-L, Siitari-Kauppi M, 2001. Complementary investigation of diffusivity, porosity and sorptivity of Feature A-site specific geological material. SKB ICR-01-04. Svensk Kärnbränslehantering AB.

Bödvarsson R, 2003. Swedish National Seismic Network (SNSN). A short report on recorded earthquakes during the fourth quarter of the year 2002. SKB P-03-02. Svensk Kärnbränslehantering AB.

Carbol P, Engkvist I, 1997. Compilation of radionuclide sorption coefficients for performance assessment. SKB R-97-13, Svensk Kärnbränslehantering AB.

Carlsson L, Gustafson G, 1997. Provpumpning som geohydrologisk undersökningsmetodik (ver 2.1), Chalmers Tekniska Högskola, Geologiska institutionen, Publ C62 (In Swedish)

Cederlund G, Hammarström A, Wallin K, 2003. Surveys of mammal populations in the areas adjacent to Forsmark and Tierp. SKB P-03-18. Svensk Kärnbränslehantering AB.

Cederlund G, Hammarström A, Wallin K, 2004. Surveys of mammal populations in the areas adjecent to Simpevarp. SKB P-report, In press.

Chapin III F S, Matson P A, Mooney H A, 2002. Principles of Terrestrial Ecosystem Ecology. Springer Verlag New York, Inc. ISBN 0-387-95439-2.

Chryssanthakis P, 2003. Borehole: KSH01A. Results of tilt testing. Oskarshamn site investigation. P-03-107, Svensk Kärnbränslehantering AB.

Cousins S A O, 2001. Plant species diversity patterns in a Swedish rural landscape. Effects of the past and consequences for the future. Doctoral thesis, No. 17. Department of Physical Geography and Quaternary Geology, Stockholm University.

Cramer J, Smellie J (eds), 1994. Final report of the AECL/SKB Cigar Lake Analog Study. SKB Technical Report 94-04. Swedish Nuclear Fuel and Waste Management Co, Stockholm, 391 p.

Curtis P, Elfström M, Stanfors R, 2003a. Oskarshamn site investigation – Compilation of structural geological data covering the Simpevarp peninsula, Ävrö and Hålö. SKB P-03-07. Svensk Kärnbränslehantering AB.

Curtis P, Elfström M, Stanfors R, 2003b. Oskarshamn site investigation. Visualization of structural geological data covering the Simpevarp peninsula, Ävrö and Hålö. SKB P-03-86. Svensk Kärnbränslehantering AB.

Debon F, Le Fort P, 1983. A chemical-mineralogical classification of common plutonic rocks and associations. Transactions of Royal Society of Edinburgh, Earth Sciences 73, 135–149.

Dershowitz W, Winberg A, Hermanson J, Byegård J, Tullborg E-L, Andersson P, Mazurek M, 2003. Äspö Hard Rock Laboratory. Äspö Task Force on modelling of groundwater flow and transport of solutes – Task 6C – A semi-synthetic model of block scale conductive structures at the Äspö HRL. SKB IPR-03-13. Svensk Kärnbränslehantering AB.

Deutsch W J, Jenne E A, Krupka K M, 1982. Solubility equilibria in basalt aquifers: The Columbia Plateau, Eastern Washington, U.S.A. Chemical Geology, 36, 15–34.

Dingman S L, 2002. Physical hydrology (second ed), Prentice-Hall, New Jersey

Domenico P A, Schwartz F W, 1998. Physical and chemical hydrogeology (second ed.), John Wiley & Sons Inc, New York.

Drake H, Tullborg E-L, (in manuscript). Fracture mineralogy – results from XRD, microscopy, SEM/EDS and stable isotopes analyses. SKB P-report (in prep).

Edenmo R, 2001. Stenåldersboplatsen Lilla Mark under 4 000 år. Bosättningsmönster, utbytessystem och neolitisering i östra Småland. In: Projekt uppdragsarkeologi Övre Grundsjön, Vojmsjön och Lilla Mark. Rapport över arkeologiska undersökningar. Rapport 2001:1.

Ekman M, 1996. A consistent map of the postglacial uplift of Fennoscandia. Terra-Nova 8/2, 158–165.

Engdahl A, Ericsson U, 2003. Fish sampling in connection with geophysical measurements at Simpevarp 2003. SKB P-04-19, Svensk Kärnbränslehantering AB.

Engqvist A, 1997. Water exchange estimates derived from forcing for the hydraulically coupled basins surrounding Äspö island and adjacent coastal water. SKB TR-97-14, Svensk Kärnbränslehantering AB.

Engqvist A, Andrejev O, 1999. Water exchange of Öregrundsgrepen. A baroclinic 3D-model study. SKB TR-99-11, Svensk Kärnbränslehantering AB.

Ericsson U, Engdahl A, 2004. Surface water sampling at Simpevarp 2002–2003. SKB P-04-13, Svensk Kärnbränslehantering AB.

Espeby B, 1989. Water flow in a forested till slope – field studies and physically based modelling. Dept. of Land and Water Resources, Rep. Trita-Kut No. 1052, Royal Inst.of Technology, Stockholm.

Fairbanks R, 1989. A 17,000-year glacio-eustatic sea level record: influence of glacial melting rates on the Younger Dryas event and deep-ocean circulation. Nature 342, 637–642.

Follin S, Årebäck M, Axelsson C-A, Stigsson M, Jacks G, 1998. Förstudie Oskarshamn, Grundvattnets långsiktiga förändringar. SKB R-98-55, Svensk Kärnbränslehantering AB.

Follin S, Svensson U, 2003. On the role of mesh discretisation and salinity for the occurrence of local flow cells. Results from a regional scale groundwater flow model of Östra Götaland, SKB R-03-23, Swedish Nuclear Fuel and Waste Management Co, Stockholm.

Follin S, Stigsson M, Svensson U, 2004 (in press). Variable-density groundwater flow simulations and particle tracking in support of the Preliminary Site Description for the Simpevarp area (version 1.1), SKB R-04-65. Svensk Kärnbränslehantering AB.

Frape S K, 2003. Pers. comm.

Fredén C, 2002. Berg och Jord, Sveriges Nationalatlas. 208 pp (in Swedish).

Fredriksson A, Hässler L, Söderberg L, 2001. Extension of CLAB – Numerical modelling, deformation measurements and comparison of forecast with outcome. Proceedings of the ISRM Reg Symp EUROCK 2001 , Espoo, Finland 4–7, June 2001.

Fredriksson R, Tobiasson S, 2003. Simpevarp site investigation. Inventory of macrophyte communities at Simpevarp nuclear power plant. Area of distribution and biomass determination. SKB P-03-69. Svensk Kärnbränslehantering AB.

Fredriksson R, Tobiasson S, 2004. Inventory of the soft-bottom macrozoobenthos community in the area around Simpevarp nuclear power plant. SKB P-04-17, Svensk Kärnbränslehantering AB.

Freeze R A, Cherry J A, 1979. Groundwater, Prentice-Hall, New Jersey

Fridriksson G, Öhr J, 2003. Forsmark site investigation. Assessment of plant biomass of the ground, field and shrub layers of the Forsmark area. SKB P-03-90, Svensk Kärnbränslehantering AB.

Garcia Ambrosiani K, 1990. Macrofossils from the till-covered sediments at Öje, central Sweden. In: Late Quaternary Stratigraphy in the Nordic Countries 150,000–15,000 B.P. (Andersen B.G. and Königsson L.-K. Eds). Striae 34, 1–10.

Garrels R M, 1984. Montmorillonite/illite stability diagrams. Clays and Clay Minerals, 32, 161–166.

Glynn P D, Voss C I, 1999. Geochemical characterization of Simpevarp ground waters near Äspö Hard Rock Laboratory. SITE-94 SKI Report 96:29, 210 p.

Green M, 2003a. Platsundersökning Simpevarp. Fågelundersökningar inom SKB:s platsundersökningar 2002. SKB P-03-31. Svensk Kärnbränslehantering AB.

Green M, 2003b. Site investigations Simpevarp Bird surveys in Simpevarp 2003. SKB P-04-21, Svensk Kärnbränslehantering AB.

Gregersen S, Korhonen H, Husebye E S, 1991. Fennoscandian dynamics: Present-day earthquake activity. Tectonophysics 189, 333–344.

Gregersen S, 1992. Crustal stress regime in Fennoscandia from focal mechanisms. Journal of Geophysical Research 97, B8, 11821–1827.

Grenthe I, Stumm W, Laaksoharju M, Nilson A C, Wikberg P, 1992. Redox potentials and redox reactions in deep groundwater systems. Chem. Geol. 98, 131–150.

Grimaud D, Beaucaire C, Michard G, 1990. Modeling of the evolution of ground waters in a granite system at low temperature: the Stripa ground waters, Sweden. Applied Geochemistry, 5, 515–525.

Gurban I, Laaksoharju M, 2002. Drilling Impact Study (DIS); Evaluation of the influences of drilling, in special on the changes on groundwater parameters. SKB report in progress.

Gustafsson G, Stanfors R, Wikberg P, 1989. Swedish Hard Rock Laboratory. First evaluation of 1988 year pre-investigations and description of the target area, the island of Äspö. SKB TR 89-16.

Gustafsson S, 1991. Transient plane source techniques for thermal conductivity and thermal diffusivity of solid materials. Rev. Sci. Instrum. 62, p 797–804. American Institute of Physics, USA.

Gustafsson R, Eriksson B, Nilsson L 1995. Odlingslandskapet i Kalmar län – Bevarandeprogram. Oskarshamns kommun. Länsstyrelsen i Kalmar län informerar. Meddelande 95:16, Länsstyrelsen i Kalmar Län.

Gustafsson L, Ahlén I (eds), 1996. Geography of Plants and Animals. National Atlas of Sweden.

Hakami E, Hakami H, Cosgrove J, 2002. Strategy for a Rock Mechanics Site Descriptive Model. Development and testing of an approach to modelling the state of stress. SKB R-02-03. Svensk Kärnbränslehantering AB.

Hartley L J, Holton D, 2003. ConnectFlow (Release 2.0) Technical Summary Document. SERCO/ERRA-C/TSD02V1.

Hartley L J, Hoch A R, Cliffe K A C, Jackson C P, Holton D, 2003a. NAMMU (Release 7.2) Technical Summary Document. SERCO/ERRA-NM/TSD02V1.

Hartley L J, Holton D, Hoch A R, 2003b. NAPSAC (Release 4.4) Technical Summary Document. SERCO/ERRA-N/TSD02V1.

Hartley L, Gylling B, Marsic N, Holmén J, Worth D, 2004 (in prep). Preliminary Site Description: Groundwater flow simulations Oskarshamn area (version 1.1) modelled with ConnectFlow, SKB R-04-63. Svensk Kärnbränslehantering AB.

Haveman S A, Pedersen K, Ruotsalainen P, 1998. Geomicrobial investigations of groundwaters from Olkilouto, Hästholmen, Kivetty and Romuvaara, Finland. POSIVA Report 98-09, Helsinki, Finland, 40 p.

Helander B, Karlsson O, Lundberg T, 2003. Inventering av gråsäl vid Svenska Östersjökusten 2002,. Sälinformation 2003:1.

Helgeson H C, 1969. Thermodynamics of hydrothermal systems at elevated temperatures. Am. J. Sci. 267, 729–804.

Helgeson H C, Delany J M, Nesbitt H W, Bird D K, 1978. Summary and critique of thermodynamic properties of rock forming minerals. Am. J. Sci. 278-A.

Hermanson J, Hansen L, Wikholm M, Cronquist T, Leiner P, Vestgård J, Sandahl K-A, 2004. Detailed fracture mapping of four outcrops at the Simpevarp peninsula and Ävrö. SKB P-04-35. Svensk Kärnbränslehantering AB.

Hoch A R, Hartley L J, 2003. NAMMU (Release 7.2) Verification Document. SERCO/ERRA-NM/VD02V2

Hoch A R, Hartley L J, Holton D, 2003. NAPSAC (Release 4.3) Verification Document. SERCO/ERRA-NM/VD02V1

Holmén J G, Stigsson M, Marsic N, Gylling B, 2003. Modelling of groundwater flow and flow paths for a large regional domain in northeast Uppland. A three-dimensional, mathematical modelling of groundwater flows and flow paths on super-regional scale, for different complexity levels of the flow domain, SKB R-03-24, Svensk Kärnbränslehantering AB.

Horai K, Simmons G, 1969. Thermal conductivity of rock-forming minerals. Earth Planet. Sci. Lett. 6, p 359–368.

Horai K, 1971. Thermal conductivity of rock-forming minerals. J. Geophys. Res. 76, p 1278–1308.

Hättestrand C, Stroeven A, 2002. A preglacial landscape in the centre of Fennoscandian glaciation: geomorphological evidence of minimal Quaternary glacial erosion. Geomorphology 44, 127–143.

Jacobsson O, 1978. Skog för framtid. SOU 1978:7, bilaga 1 pp 200–205 (in Swedish).

Jerling L, Isæus M, Lanneck J, Lindborg T, Schüldt R, 2001. The terrestrial biosphere in the SFR region. SKB R-01-09, Svensk Kärnbränslehantering AB.

Johansson P-O, 1986. Diurnal groundwater level fluctuations in sandy till – a model analysis. J. of Hydrology, 87, 125–134.

Johansson P-O, 1987a. Estimation of groundwater recharge in sandy till with two different methods using groundwater level fluctuations. J. of Hydrology, 90, 183–198.

Johansson P-O, 1987b. Spring discharge and aquifer characteristics in a sandy till area in south-eastern Sweden. Nordic Hydrol. 18, 203–220.

Johansson L, Johansson Å, 1990. Isotope geochemistry and age relationships of mafic intrusions along the Protogine Zone, southern Sweden. Precambrian Research 48, 395–414.

Knutsson G, Morfeldt C-O, 2002. Grundvatten, teori & tillämpning, AB Svensk Byggtjänst, Stockholm (In Swedish).

Koistinen T, Stephens M B, Bogatchev V, Nordgulen O, Wennerström M, Korhonen J, 2001. Geological map of the Fennoscandian Shield, scale 1:2 000 000. Geological Surveys of Finland, Norway and Sweden and the North-West Department of Natural Resources of Russia.

Kornfält K-A, Wikman H, 1987. Description of the map of solid rocks around Simpevarp. SKB PR 25-87-02.

Kornfält K-A, Persson P-O, Wikman H, 1997. Granitoids from the Äspö area, southeastern Sweden – geochemical and geochronological data. GFF 119, 109–114.

Kresten P, Chyssler J, 1976. The Götemar massif in south-eastern Sweden: A reconnaissance survey. Geologiska Föreningens i Stockholm Förhandlingar 98, 155–161.

Kristiansson J, 1986. The ice recession in the south-easten part of Sweden. University of Stockholm. Department of Quaternary Research 7, 132 pp.

Kyläkorpi L, 2004. Nature Values and site accessibility maps of Forsmark and Simpevarp. SKB R-04-12 (in press.) Svensk Kärnbränslehantering AB.

Laaksoharju M, Smellie J, Nilsson A-C, Skårman C, 1995. Groundwater sampling and chemical characterisation of the Laxemar deep borehole KLX02. SKB TR 95-05. Svensk Kärnbränslehantering AB.

Laaksoharju M, Wallin B (eds), 1997. Evolution of the groundwater chemistry at the Äspö Hard Rock Laboratory. Proceedings of the second Äspö International Geochemistry Workshop, June 6–7, 1995. SKB International Co-operation Report ISRN SKB-ICR-91/04-SE. ISSN 1104-3210 Stockholm, Sweden.

Laaksoharju M, 1999. Groundwater Characterisation and Modelling: Problems, Facts and Possibilities. Dissertation TRITA-AMI-PHD 1031; ISSN 1400-1284; ISRN KTH/AMI/PHD 1031-SE; ISBN 91-7170-. Royal Institute of Technology, Stockholm, Sweden. Also as SKB TR-99-42, SKB, Stockholm.

Laaksoharju M, Gurban I, Andersson C, 1999a. Indications of the origin and evolution of the groundwater at Palmottu. The Palmottu NaturalAnalogue Project. SKB Technical Report TR 99-03, Stockholm, Sweden.

Laaksoharju M, Skårman C, Skårman E, 1999b. Multivariate Mixing and Mass-balance (M3) calculations, a new tool for decoding hydrogeochemical information. Applied Geochemistry Vol. 14, #7, 1999, Elsevier Science Ltd. pp 861–871.

Laaksoharju M (ed), Gimeno M, Smellie J, Tullborg E-L, Gurban I, Auqué L, Gómez J, 2004a. Hydrogeochemical evaluation of the Forsmark site, model version 1.1. SKB R-04-05.

Laaksoharju M (ed), Smellie J, Gimeno M, Auqué L, Gómez J, Tullborg E-L, Gurban I, 2004b. Hydrogeochemical evaluation of the Simpevarp area, model version 1.1. SKB R-04-16. Svensk Kärnbränslehantering AB.

Lagerbäck R, Robertsson A-M, 1988. Kettle holes – stratigraphical archives for Weichselian geology and palaeoenvironment in northernmost Sweden. Boreas 17, 439–468.

Landström O, Tullborg E-L, 1995. Interactions of trace elements with fracture filling minerals from the Äspö Hars Rock laboratory. SKB Technical Report TR 95-13. ISSN 0284-3757. 65 pp.

Landström O, Tullborg E-L, Eriksson G, Sandell Y, 2001. Effects of glacial/post-glacial weathering compared with hydrothermal alteration – implications for matrix diffusion. SKB report R-01-37. ISSN 1402-3091.

La Pointe P, Burago A, Lee K, Dershowitz B, 1992. geoFractal: Geostatistical and Fractal Analysis for Spatial Data, Version 1.0.

La Pointe P R, 2001. Scaling analysis of natural fracture systems in support of fluid modeling and seismic risk assessment [abstr.]. Annual Meeting, American Geophysical Union, December 14, 2001, San Francisco, CA.

La Pointe P R, 2002. Derivation of parent fracture population statistics from trace length measurements for fractal fracture populations. International Journal of Rock Mechanics and Mining Sciences, Vol. 39, 381–388.

Larson S Å, Tullborg E-L, 1993. Tectonic regimes in the Baltic Shield during the last 1200 Ma – A review. SKB TR 94-05.

Larson S Å, Tullborg E-L, Cederbom C, Stiberg J-A, 1999. Sveconorwegian and Caledonian foreland basins in the Baltic Shield revealed by fission-track thermochronology. Terra Nova 11, 210–215.

Larsson-McCann S, Karlsson A, Nord M, Sjögren J, Johansson L, Ivarsson M, Kindell S, 2002. Meteorological, hydrological and oceanographical information and data for the site investigation program in the community of Oskarshamn. SKB TR-02-03, Svensk Kärnbränslehantering AB.

LeMaitre R W (Editor), 2002. A classification of igneous rocks and glossary of terms: Recommendations of the International Union of Geological Sciences, Subcommission on the Systematics of Igneous Rocks, 2nd edition, Blackwell, Oxford.

Lidmar-Bergström K, 1991. Phanerozoic tectonics in southern Sweden. Zeitschrift für Geomorphologie N.F. 82, 1–16.

Lidmar-Bergström K, Olsson S, Olvmo M, 1997. Paleosurfaces and associated saprolites in southern Sweden. Geological Society 120, 95–124.

Lindborg T, Schüldt R, 1998. The biosphere at Aberg, Bberg and Ceberg. SKB TR-98-20, Svensk Kärnbränslehantering AB.

Lindborg T, Kautsky U, 2000. Variabler i olika ekosystem, tänkbara att beskriva vid platsundersökning för ett djupförvar. SKB R-00-19, Svensk Kärnbränslehantering AB (in Swedish).

Lindell S, Ambjörn C, Juhlin B, Larsson-McCann S, Lindquist K, 1999. Available climatological and oceanographical data for site investigation program. SKB R-99-70, Svensk Kärnbränslehantering AB.

Lindroos H, Isaksson H, Thunehed H, 2004. The potential for ore and industrial minerals in the Forsmark area. SKB R-04-18. Svensk Kärnbränslehantering AB.

Lindström G, Rodhe A, 1986. Modelling water exchange and transit times in till basins using oxygen-18. Nordic Hydrol. 17, 325–334.

Lingman A, Franzén F, 2003. Litteratursammanställning avseende resultat från den biologiska recipientkontrollen, samt undersökningar gällande fiskpopulationer vid Oskarshamnsverket 1962–2002, SKB P-04-18.

Ludvigson J-E, Levén J, Jönsson S, 2003. Oskarshamn site investigation. Hydraulic tests and flow logging in borehole HSH03. SKB P-03-56. Svensk Kärnbränslehantering AB.

Lundin L, 1982. Soil and groundwater in moraine and the influence of the soil type on the runoff. Dept. of Phys. Geogr. Rep. No. 56. Univ. of Uppsala.

Lundmark J-E, 1986. Skogsmarkers ekologi – Ståndortsanpassat skogsbruk. Del 1 – Grunder. Skogsstyrelsen Förlag, Jönköping. ISBN 91-85748-50-1 (in Swedish).

Lundqvist J, 1985. Deep-weathering in Sweden. Fennia 163, 287–292.

Lundqvist J, 1992. Glacial stratigraphy in Sweden. Geological Survey of Finland Special paper 15. 43–59.

Lundqvist J, Wohlfarth B, 2001. Timing and east-west correlation of south Swedish ice marginal lines during the Late Weichselian. Quaternary Science Reviews 20, 1127–1148.

Lundqvist L, 2004. Inledande kulturhistoriska studier i Simpevarpsområdet. R 04-07 (in press), Svensk Kärnbränslehantering AB.

Luukkonen A, 2001. Groundwaters mixing and geochemical reactions. An inverse-modelling approach. In: A. Luukkonen and E. Kattilakoski (eds.), Äspö hard-rock laboratory. Groundwater flow, mixing and geochemical reactions at Äspö HRL. Task 5. Äspö Task Force on groundwater flow and transport of solutes. SKB IPR-02-041.

Lärke A, Hillgren R, 2003. Rekognoscering av mätplatser för ythydrologiska mätningar i Simpevarpsområdet, SKB P-03-04. Svensk Kärnbränslehantering AB.

Löfgren A, Lindborg T, 2003. A descriptive ecosystem model – a strategy for model development during site investigations. SKB R-03-06. Svensk Kärnbränslehantering AB.

Löfgren M, Neretnieks I, 2003. Formation factor logging by electrical methods. Comparison of formation factor logs obtained in situ and in the laboratory. J. Contam. Hydrol. 61: 107–115.

Maddock R H, Hailwood E A, Rhodes E J, Muir Wood R, 1993. Direct fault dating trials at the Äspö Hard Rock Laboratory. SKB TR 93-24.

Mansfeld J, 1996. Geological, geochemical and geochronological evidence for a new Paleoproterozoic terrane in southeastern Sweden. Precambrian Research 77, 91–103.

Markström I, Stanfors R, Juhlin C, 2001. Äspölaboratoriet – RVS-modellering, Ävrö – Slutrapport. SKB R-01-06. Svensk Kärnbränslehantering AB.

Mattsson H, Triumf C-A, Wahlgren C-H, 2002. Prediktering av förekomst av finkorniga granitgångar i Simpevarpsområdet. SKB P-02-05. Svensk Kärnbränslehantering AB.

Mattsson H, Thunehed H, Triumf C-A, 2003. Oskarshamn site investigation – Compilation of petrophysical data from rock samples and in situ gamma-ray spectrometry measurements. SKB P-03-97, Svensk Kärnbränslehantering AB.

Mattsson H, Thunehed H, 2004. Interpretation of geophysical borehole data from KSH01A, KSH01B, KSH02 (0–100 m), HSH01, HSH02 and HSH03, and compilation of petrophysical data from KSH01A and KSH01B. SKB P-04-28.

Mazurek M, Bossart P, Eliasson T, 1997. Classification and characterization of water-conducting features at Äspö: Results of investigations on the outcrop scale. SKB International Cooperation Report ICR 97-01.

Microsoft Corporation, 2000. Excel 2002.

Middlemost E A K, 1994. Naming materials in the magma/igneous rock system. Earth-Science Reviews 37, 215–224.

Miliander S, Punakivi M, Kyläkorpi L, Rydgren B, 2004. Simpevarp site description: Human population and human activities. SKB R-04-11.

Milnes A G, Gee D G, 1992. Bedrock stability in southeastern Sweden. Evidence from fracturing in the ordovician limestones of northern Öland. SKB TR 92-23.

Milnes A G, Gee D G, Lund C-E, 1998. Crustal structure and regional tectonics of SE Sweden and the Baltic Sea. SKB TR 98-21.

Moberg M, Hector I, Ingevald K, 1995. Utbyggnad av lagringskapacitet. CLAB, Simpevarp – Berggrundundersökning 1979, Material sammanställt av Larsson H, Rapport 95-3450-07, Svensk kärnbränslehantering AB (in Swedish).

Morén L, Påsse T, 2001. Climate and shoreline in Sweden during Weichsel and the next 150,000 years. SKB TR-01-19, 67 pp.

Morosini M, Hultgren H 2003. Inventering av privata brunnar i Simpevarpsområdet, 2001–2002. SKB P-03-05. Svensk Kärnbränslehantering AB.

Muir-Wood R, 1993. A review of the seismotectonics of Sweden. SKB TR 93-13.

Munier R, 1989. Brittle tectonics on Äspö, SE Sweden. SKB PR 25-89-15.

Munier R, 1993. Segmentation, fragmentation and jostling of the Baltic shield with time. Thesis, Acta Universitatus Upsaliensis 37.

Munier R, 1995. Studies of geological structures at Äspö. Comprehensive summary of results. SKB PR 25-95-21.

Munier R, Hermanson J, 2001. Metodik för geometrisk modellering. Presentation och administration av platsbeskrivande modeller. SKB R-01-15. Svensk Kärnbränslehantering AB.

Munier R, Stenberg L, Stanfors R, Milnes A G, Hermanson J, Triumf C-A, 2003. Geological Site Descriptive Model. A strategy for the model development during site investigations. SKB R-03-07. Svensk Kärnbränslehantering AB.

Müller B, Zoback M L, Fuchs K, Mastin L, Gregersen S, Pavoni N, Stephansson O, Ljunggren C, 1992. Regional Patterns of Tectonic Stress in Europe. Journal of Geophysical Research, 97, No. B8, 11, 783–803.

Mörner N-A, 1989. Postglacial faults and fractures on Äspö. SKB PR 25-89-24.

Nielsen U T, Ringgaard J, 2003. Simpevarp site investigation. Geophysical borehole logging in borehole KSH01A, KSH01B and part of KSH02. SKB P-03-16. Svensk Kärnbränslehantering AB.

Nilsson P, Gustafsson C, 2003. Simpevarp site investigation – Geophysical, radar and BIPS logging in borehole KSH01A, HSH01, HSH02 and HSH03. SKB P-03-15. Svensk Kärnbränslehantering AB.

NMR, 1984. Naturgeografisk regionindelning av Norden. Nordiska ministerrådet.

Nordstrom D K, Andrews J N, Carlsson L, Fontes J-Ch, Fritz P, Moser H, Olsson T, 1985. Hydrogeological and hydrogeochemical investigations in boreholes – final report of the Phase I geochemical investigations of the Stripa groundwaters. SKB Tech. Rep. (TR-85-06), Svensk Kärnbränslehantering AB.

Nordstrom D K, Puigdomenech I, 1989. Redox chemistry of deep ground water in Sweden. SKB TR-86-03. Svensk Kärnbränslehantering AB.

Näslund J O, Rodhe L, Fastook J L, Holmlund P, 2003. New ways of studying ice sheet flow directions and glacial erosion by computer modelling-examples from Fennoscandia. Quaternary Sciences Reviews 22, 245–258.

Ohlsson Y, Neretnieks I, 1997. Diffusion data in granite – Recommended values. SKB TR-97-20, Svensk Kärnbränslehantering AB.

Olsen L, Mejdahl V, Selvik S, 1996. Middle and Late Pleistocene stratigraphy, Finnmak, north Norway. NGU Bulletin 429, 111 p.

Parkhurst D L, Appelo C A J, 1999. User's Guide to PHREEQC (Version 2), a computer program for speciation, batch-reaction, one-dimensional transport, and inverse geochemical calculations. U.S. Geological Survey Water-Resources Investigations Report 99-4259, 312 p.

Pitkänen P, Luukkonen A, Ruotsalainen P, Leino-Forsman H, Vuorinen U, 1998. Geochemical modelling of groundwater evolution and residence time at the Kivetty site. POSIVA Report 98-07, Helsinki, Finland, 139 p.

Pitkänen P, Luukkonen A, Ruotsalainen P, Leino-Forsman H, Vuorinen U, 1999. Geochemical modelling of groundwater evolution and residence time at the Olkilouto site. POSIVA Report 98-10, Helsinki, Finland, 184 p.

Puigdomenech I (ed), 2001. Hydrochemical stability of groundwaters sourrunding a spent nuclear fuel repository in a 100,000 year perspective. (Technical Report SKB TR 01-28), Svensk Kärnbränslehantering AB, 83 p.

Påsse T, 1996. A mathematical model of shore displacement in Fennoscandia. SKB TR-96-24, Svensk Kärnbränslehantering AB.

Påsse T, 1997. A mathematical model of past, present and future shore level displacement in Fennoscandia. SKB TR 97-28, 55 pp.

Påsse T, 2001. An empirical model of glacio-isostatic movments and shore-level displacement in Fennoscandia. SKB R-01-41, 59 pp.

Påsse T, 2003. Pers. comm.

Rhén I, Bäckblom G, Gustafsson G, Stanfors R, Wikberg P, 1997a. Äspö HRL – Geoscientific evaluation 1997/2. Results from pre-investigations and detailed characterization. SKB TR-97-03. Svensk Kärnbränslehantering AB.

Rhén I, Gustafsson G, Wikberg P, 1997b. Äspö HRL – Geoscientific evaluation 1997/5. Models based on site characterization 1986–1995. SKB TR-97-03. Svensk Kärnbränslehantering AB.

Rhén I, Forsmark T, 2001. Äspö Hard Rock Laboratory, Prototype repository, Hydrogeology, Summary report of investigations before the operation phase. SKB IPR-01-65, Svensk Kärnbränslehantering AB.

Rhén I, Smellie J (eds), 2003. Task force on modelling of groundwater flow and transport of solutes. Task 5 summary report. SKB TR-03-01. Svensk Kärnbränslehantering AB.

Rhén I, Follin S, Hermanson J, 2003. Hydrological Site Descriptive Model – a strategy for its development during site investigations. SKB R-03-08. Svensk Kärnbränslehantering AB.

Ringberg B, Hang T, Kristiansson J, 2002. Local clay-varve chronology in the Karlskrona-Hultsfred region, southeast Sweden. GFF 124, 79–86

Risberg J, 2002. Holocene sediment accumulation in the Äspö area. SKB R-02-47. 37 pp.

Robertsson A-M, Svedlund J-O, Andrén T, Sundh M, 1997. Pleistocene stratigraphy in the Dellen region, central Sweden. Boreas 26, 237–260.

Rockscience, 1989. DIPS, Version 5.103 June 9, 2004. Rocscience Inc., 31 Balsam Avenue, Toronto, Ontario M4E 3B5, http://www.rocscience.com/.

Rodhe A, 1987a. Depositional environment and lithostratigraphy of the middle Proterozoic Almesåkra Group, southern Sweden. Sveriges geologiska undersökning Ca 69.

Rodhe A, 1987b. The origin of streamwater traced by oxygen-18. Dept. of Phys. Geogr. Rep. Series A No. 41, Univ. of Uppsala.

Rouhiainen P, Pöllänen J, 2003. Oskarshamn site investigation – Difference flow measurements in borehole KSH01A at Simpevarp. P-03-70. Svensk Kärnbränslehantering AB.

Rydström H, Gereben L, 1989. Regional geological study. Seismic refraction survey. SKB PR 25-89-23, Svensk Kärnbränslehantering AB.

Rønning H J S, Kihle O, Mogaard J O, Walker P, 2003. Simpevarp site investigation – Helicopter borne geophysics at Simpevarp, Oskarshamn, Sweden. SKB P-03-25. Svensk Kärnbränslehantering AB.

Röshoff K, Cosgrove J, 2002. Sedimentary dykes in the Oskarshamn-Västervik area. A study of the mechanism of formation. SKB R-02-37. Svensk Kärnbränslehantering AB.

Röshoff K, Lanaro F, Jing L, 2002. Strategy for a rock mechanics Site descriptive model – Development and testing of the empirical approach. SKB R-02-01.

Schackelton N J, Berger A, Peltier W R, 1990. An alternative astronomical calibration of the lower Pleistocene timescale based on ODP Site 677. Transactions of the Royal Society of Edinburgh: Earth Sciences 81, 251–261.

Shackelton N J, 1997. The deep-sea sediment record and the Pliocene-Pleistocene boundary. Quaternary International 40, 33–35.

Šibrava V, 1992. Should the Pliocene-Pleistocene boundary be lowered? Sveriges Geologiska Undersökning, Ca 81, 327–332.

Sjöberg J, 2004. Oskarshamn site investigation – Overcoring rock stress measurements in borehole KSH02. SKB P-04-23. Svensk Kärnbränslehantering AB.

Sjörs H, 1967. Nordisk växtgeografi. 2:a upplagan. Stockholm. (in Swedish).

SKB, 1990. Granskning av Nils-Axels Mörners arbete avseende postglaciala strukturer på Äspö. SKB AR 90-18 (in Swedish).

SKB, 2000a. Förstudie Oskarshamn – Slutrapport. Svensk Kärnbränslehantering AB (in Swedish).

SKB, 2000b. Geoscientific programme for investigation and evaluation of sites for the deep repository. SKB TR-00-20. Svensk Kärnbränslehantering AB.

SKB, 2001a. Site investigations – Investigation methods and general execution programme. SKB TR-01-29. Svensk Kärnbränslehantering AB.

SKB, 2001b. Geovetenskapligt program för platsundersökning vid Simpevarp SKB R-01-44. Svensk Kärnbränslehantering AB.

SKB, 2001c. Integrated account of method, site selection and programme prior to the site investigation phase. Svensk Kärnbränslehantering AB.

SKB, 2002a. Preliminary safety evaluation, based on initial site investigation data. Planning document, SKB TR 02-28, Svensk Kärnbränslehantering AB.

SKB, 2002b. Simpevarp – site descriptive model version 0. SKB R-02-35, Svensk Kärnbränslehantering AB.

SKB, 2002c. Execution programme for the initial site investigations at Simpevarp. SKB P-02-06. Svensk Kärnbränslehantering AB.

SKB, 2003a. Planning report for the safety assessment SR-Can, SKB TR-03-08, Svensk Kärnbränslehantering AB.

SKB, 2003b. Prioritering av områden för platsundersökningen i Oskarshamn. SKB R-03-12. Svensk Kärnbränslehantering AB.

SKB, 2003c. Planering för fortsatt kärnborrning, våren 2003. Platsundersökning Oskarshamn. SKB P-03-61. Svensk Kärnbränslehantering AB

SKB, 2004. Preliminary site description, Forsmark area – version 1.1. SKB R-04-15, Svensk Kärnbränslehantering AB.

SKB GIS, 2004. (Map generated from SKB GIS database for this report). Svensk Kärnbränslehantering AB.

Slunga R, Norrman P, Glans A-C, 1984. Baltic shield seismicity, the results of a regional network. Geophysical research letters 11, 1247–1250.

Slunga R, 1989. Analysis of the earthquake mechanisms in the Norrbotten area. In Bäckblom and Stanfors (Eds.), Interdisciplinary study of post-glacial faulting in the Lansjärv area northern Sweden. 1986–1988. SKB TR 89-31.

Slunga R, Nordgren L, 1990. Earthquake measurements in southern Sweden APR 1 1987–NOV 30 1988. SKB AR 90-19.

Smellie J A T, Wikberg P, 1991. Hydrochemical investigations at Finnsjön, Sweden. J. Hydrol. 126, 129–158.

Smellie J, Laaksoharju M, 1992. The Äspö hard rock laboratory: final evaluation of the hydrogeochemical pre-investigations in relation to existing geologic and hydraulic conditions. SKB Technical Report TR 92-31, Swedish Nuclear Fuel and Waste Management Co, Stockholm, Sweden, 239 p.

Smellie J, Laaksoharju M, Tullborg E-L, 2002. Hydrogeochemical site descriptive model – a strategy for the model development during site investigations. SKB R-02-49. Svensk Kärnbränslehantering AB.

Smellie J A T, Waber H N, Frape S K, 2003. Matrix fluid experiment. Final report, June 1998 – March 2003. SKB TR-03-18. Svensk Kärnbränslehantering AB.

Snellman M, Pitkänen P, Luukkonen A, Ruotsalainen P, Leino-Forsman H, Vuorinen U, 1998. Summary of recent observations from Hästholmen groundwater studies. POSIVA Working Report 98-44, Helsinki, Finland, 71 p.

Stanfors R, Erlström M, 1995. SKB Palaeohydrogeological programme. Extended geological models of the Äspö area. SKB AR 95-20, Svensk Kärnbränslehantering AB.

Stanfors R, Erlström M, Markström I, 1997. Äspö HRL – Geoscientific evaluation 1997/1. Overview of site characterization 1986-1995. SKB TR-97-02, Svensk Kärnbränslehantering AB.

Statgraphics, 1998. Statgraphics Professional edition, Manugistics Inc (Software manual).

Staub I, Janson T, Fredriksson A, 2003. Äspö Hard Rock Laboratory. Äspö Pillar Stability Experiment. Geology and properties of the rock mass around the experiment volume. SKB. IPR-03-02.

Staub I, Andersson C, Magnor B, 2004. Äspö Hard Rock Laboratory – Äspö Pillar Stability Experiment, Geology and mechanical properties of the rock mass in TASQ. SKB R-04-01. Svensk Kärnbränslehantering AB.

Stenberg L, Sehlstedt S, 1989. Geophysical profile measurements on interpreted regional aeromagnetic lineaments in the Simpevarp area. SKB PR 25-89-13, Svensk Kärnbränslehantering AB.

Stephansson O, Dahlström L-O, Bergström K, Sarkka P, Vitinen A, Myrvang A, Fjeld O, Hansen T H, 1987. Fennoscandian Rock Stress Database – FRSDB. Research report TULEA 1987:06, Luleå University of Technology, Luleå.

Stephens M B, Wahlgren C-H, Weihed P, 1994. Geological Map of Sweden, scale 1:3 000 000. SGU series Ba 52, Sveriges Geologiska Undersökning.

Stephens M B, Wahlgren C-H, 1996. Post-1.85 Ga tectonic evolution of the Svecokarelian orogen with special reference to central and SE Sweden. GFF 118, Jubilee Issue, A26–27.

Stigsson M, Follin S, Andersson J, 1999. On the simulation of variable density flow at SFR, Sweden, SKB R-99-08.

Streckeisen A, 1976. To each plutonic rock its proper name. Earth Science Reviews 12, 1–33.

Streckeisen A, 1978. IUGS Subcommision on the Systematics of Igneous Rocks. Classification and Nomenclature of Volcanic Rocks, Lamprophyres, Carbonatites and Melilitic Rocks. Recommendations and suggestions. Neues Jahrbuch für Mineralogie Abhandlungen 143, 1–14.

Stridsman H, 2003. Pers. comm.

Sultan L, Claesson S, Plink-Björklund P, Björklund L, 2004. Proterozoic and Archaean detrital zircon ages from the Palaeoproterozoic Västervik Basin, southern Fennoscandian Shield. GFF 126, 39.

Sundberg J, 1988. Thermal properties of soils and rocks, Publ. A 57 Dissertation, Doctoral thesis, Geologiska institutionen, Chalmers University of Technology and University of Göteborg.

Sundberg J, 2002. Determination of thermal properties at Äspö HRL, Comparison and evaluation of methods and methodologies for borehole KA 2599 G01, SKB R-02-27.

Sundberg J, 2003a. Thermal Site Descriptive Model, A Strategy for the Model Development during Site Investigations, SKB R-03-10, Svensk Kärnbränslehantering AB.

Sundberg J, 2003b. Thermal Properties at Äspö HRL, Analysis of Distribution and Scale Factors, SKB R-03-17, Svensk Kärnbränslehantering AB.

Svedmark E, 1904. Beskrifning till kartbladet Oskasrhamn. SGU Ac 5, 85 pp.

Svensson N-O, 1989. Late Weichselian and early Holocene shore displacement in the central Baltic, based on stratigraphical and morphological records from eastern Småland and Gotland, Sweden. LUNDQUA 25, 181 pp.

Svensson U, 1996. SKB Palaeohydrogeological programme. Regional groundwater flow due to advancing and retreating glacier-scoping calculations. In: SKB Project Report U 96-35, Stockholm, Sweden.

Svensson U, Laaksoharju M, Gurban I, 2002. Impact of the tunnel construction on the ground-water chemistry at Äspö. SKB report in progress.

Svensson U, 2004. DarcyTools, Vesrion 2.1. Verification and validation. SKB R-04-21, Svensk Kärnbränslehantering AB.

Svensson U, Ferry M, 2004. DarcyTools, Version 2.1. User's guide. SKB R-04-20, Svensk Kärnbränslehantering AB.

Svensson U, Kuylenstierna H-O, Ferry M, 2004. DarcyTools, Version 2.1. Concepts, methods, equations and demo simulations. SKB R-04-19, Svensk Kärnbränslehantering AB.

Söderlund P, Juez-Larre J, Dunai T, Page L, in prep. Apatite (U-Th)-He-dating of drill-core samples from Oskarshamn, southeast Sweden.

Söderlund U, Patchett P J, Isachsen C, Vervoort J, Bylund G, 2004. Baddeleyite U-Pb dates and Hf-Nd isotope compositions of mafic dyke swarms in Sweden and Finland. GFF 126, 38.

Talbot C, Munier R, 1989. Faults and fracture zones in Äspö. SKB PR 25-89-11.

Talbot C, Ramberg H, 1990. Some clarification of the tectonics of Äspö and its surroundings. SKB PR 25-90-15.

Tirén S A, Beckholmen M, Isaksson H, 1987. Structural analysis of digital terrain models, Simpevarp area, southeastern Sweden. Method study EBBA II. SKB PR 25-87-21.

Tobiasson S, 2003. Tolkning av undervattensfilm från Forsmark och Simpevarp. SKB P-03-68. Svensk Kärnbränslehantering AB.

Triumf C-A, 2003. Oskarshamn site investigation – Identification of lineaments in the Simpevarp area by the interpretation of topographical data. SKB P-03-99. Svensk Kärnbränslehantering AB.

Triumf C-A, Thunehed H, Kero L, Persson L, 2003. Oskarshamn site investigation. Interpretation of airborne geophysical survey data. Helicopter borne survey data of gamma ray spectrometry, magnetics and EM from 2002 and fixed wing airborne survey data of the VLF-field from 1986. SKB P-03-100. Svensk Kärnbränslehantering AB.

Triumf C-A, 2004. Oskarshamn site investigation. Joint interpretation of lineaments in the eastern part of the site descriptive model area. SKB P-04-37. Svensk Kärnbränslehantering AB.

Tullborg E-L, Larson S Å, 1984. $\delta^{18}O$ and $\delta^{13}C$ for limestones, calcite fissure infillings and calcite precipitates from Sweden. Geologiska föreningens i Stockholm förhandlingar 106(2).

Tullborg E-L, Larson S Å, Björklund L, Samuelsson L, Stigh J, 1995. Thermal evidence of Caledonide foreland, molasse sedimentation in Fennoscandia. SKB Technical Report TR-95-18.

Tullborg E-L, Larson S Å, Stiberg J-A, 1996. Subsidence and uplift of the present land surface in the southeastern part of the Fennoscandian Shield. GFF 118, 126–128.

Ukkonen P, Lunkka J P, Jungner H, Donner J, 1999. New radiocarbon dates from Finnish mammoths indicating large ice-free areas in Fennoscandia during the Middle Weichselian. Journal of Quaternary Science 14, 711–714.

Wacker P, 2003. Oskarshamn site investigation. Hydrochemical logging in KSH01A. SKB P-03-87.

Wacker P, 2003. Pers. comm..

Wahlgren C-H, Persson L, Danielsson P, Berglund J, Triumf C-A, Mattsson H, Thunehed H, 2003. Geologiskt underlag för val av prioriterad plats inom området väster om Simpevarp. Delrapport 1–4. SKB P-03-06. Svensk Kärnbränslehantering AB.

Wahlgren C-H, Ahl M, Sandahl K-A, Berglund J, Petersson J, Ekström M, Persson P-O, 2004. Oskarshamn site investigation. Bedrock mapping 2003 – Simpevarp subarea. Final P-report to be submitted (preliminary report used).

Welinder S, Pedersen E A, Widgren M, 1998. Det svenska jordbrukets historia: Jordbrukets första femtusen år. Natur och Kultur/LTs förlag, Borås (in Swedish).

Westman P, Wastegård S, Schoning K, Gustafsson B, 1999. Salinity change in the Baltic Sea during the last 8,500 years: evidence causes and models. SKB TR 99-38. 52 pp.

Wetzel, 2001. Limnology: Lake and River Ecosystems. 3rd Edition, Academic Press, San Diego. 1006 pp.

Widestrand H, Byegård J, Ohlsson Y, Tullborg E-L, 2003. Strategy for the use of laboratory methods in the site investigations programme for the transport properties of the rock. SKB R-03-20, Svensk Kärnbränslehantering AB.

Wikberg P, 1998. Äspö Task Force on modelling of groundwater flow and transport of solutes. SKB progress report HRL-98-07.

Wiklund S, 2002. Digitala ortofoton och höjdmodeller. Redovisning av metodik för platsundersökningsområdena Oskarshamn och Forsmark samt förstudieområdet Tierp Norra. SKB P-02-02. Svensk Kärnbränslehantering AB.

Wikman H, Kornfält K-A, 1995. Updating of a lithological model of the bedrock of the Äspö area. SKB PR 25-95-04.

Winberg A, Andersson P, Hermansson J, Byegård J, Cvetkovic V, Birgersson L, 2000. Äspö Hard Rock Laboratory. Final report of the first stage of the Tracer Retention Understanding Experiments, SKB TR-00-07. Svensk Kärnbränslehantering AB. ISSN 1404-0344.

Wu P, Johnston P, Lambeck K, 1999. Postglacial rebound and fault instability in Fennoscandia. Geophysical Journal International 139, 657–670.

Xu S, Wörman A, 1998. Statistical patterns of geochemistry in crystalline rock and effect of sorption kinetics on radionuclide migration. SKI Technical Report 98:41. Statens kärnkraftsinspektion.

Åberg G, 1978. Precambrian geochronology of south-eastern Sweden. Geologiska Föreningens i Stockholm Förhandlingar 100, 125–154.

Åhäll K-I, 2001. Åldersbestämning av svårdaterade bergarter i sydöstra Sverige. SKB R-01-60. Svensk Kärnbränslehantering AB (in Swedish).

Åhäll K-I, Connelly J, Brewer T, 2002. Transitioning from Svecofennian to Transscandinavian Igneous Belt (TIB) magmatism in SE Sweden: Implications from the 1.82 Ga Eksjö tonalite. GFF 124, 217–224.

Åkesson U, 2003. Äspö Hard Rock Laboratory (HRL) KQ0064G01 and KQ0064G05. Coefficient of thermal expansion of rock – using an extensometer. Determination of density and porosity. Report to SKB October 2003.

Appendix 1

Rock type occurrence statistics in the rock domains based on the outcrop database from the bedrock mapping of the Simpevarp subarea

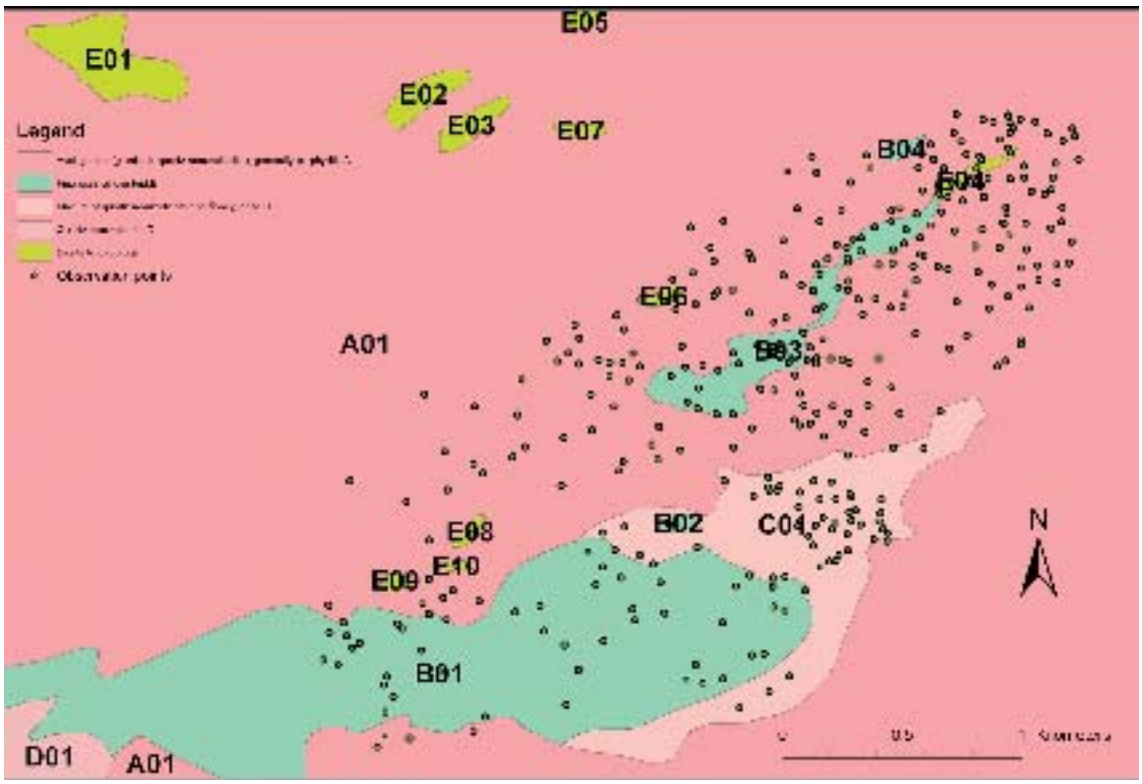

Figure A1-1. *Observation points from the bedrock mapping of the Simpevarp subarea, shown on the top surface of the 3D rock domain model.*

The outcrop observations are extracted from the outcrop database that was compiled during the bedrock mapping of the Simpevarp subarea during 2003. The registered rock type nomenclature in the database has been transferred to the nomenclature decided by SKB for the site investigation at Oskarshamn (Table A1-1).

A01 contains 216 observation points

1) Number of observation points where each rock type is dominant.

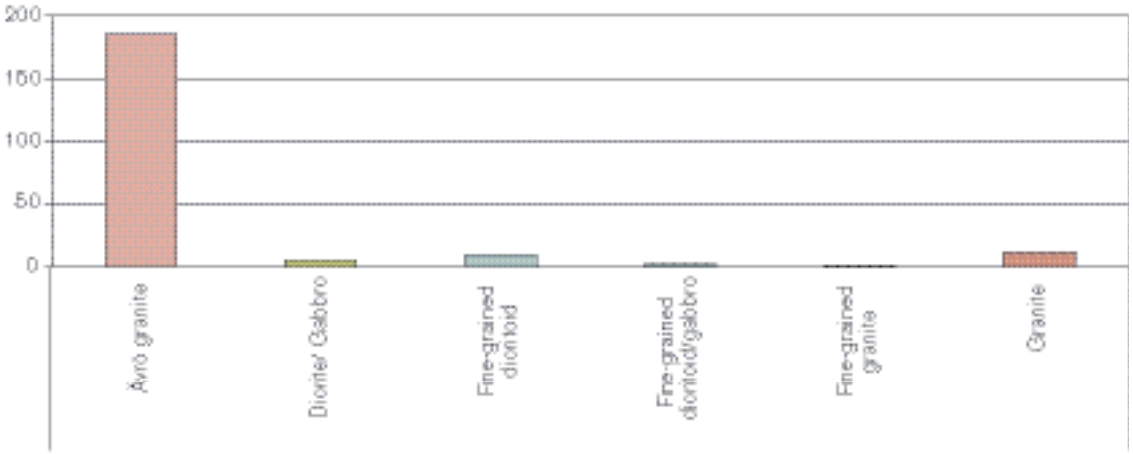

2) Number of observation points with only one rock type present.

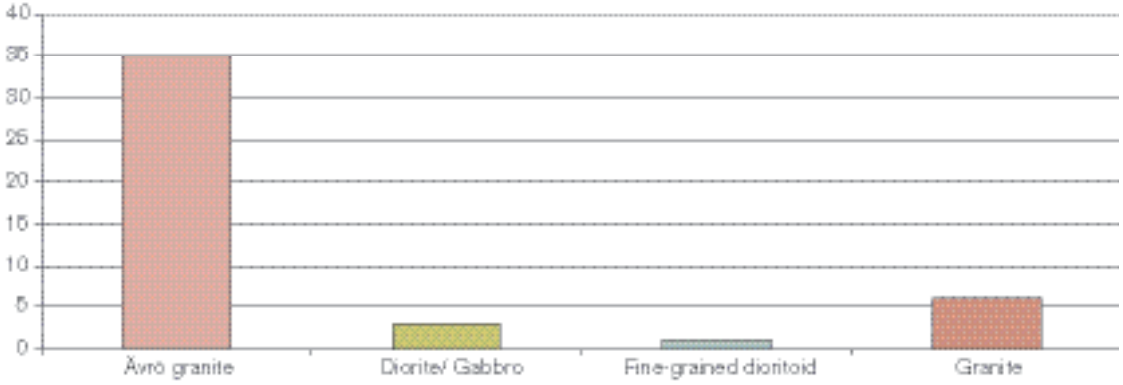

3) Number of occurrences of each rock type, of any order.

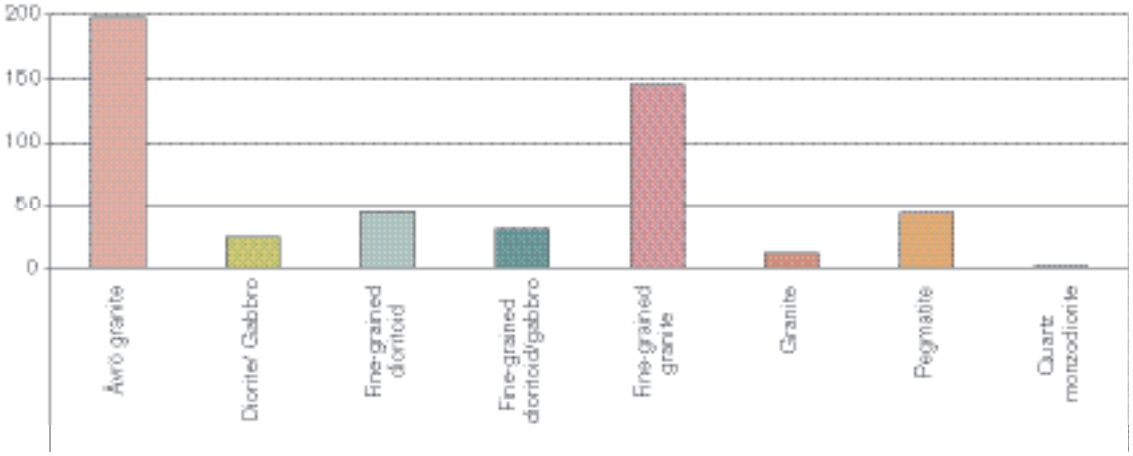

B01 contains 46 observation points

1) Number of observation points where each rock type is dominant.

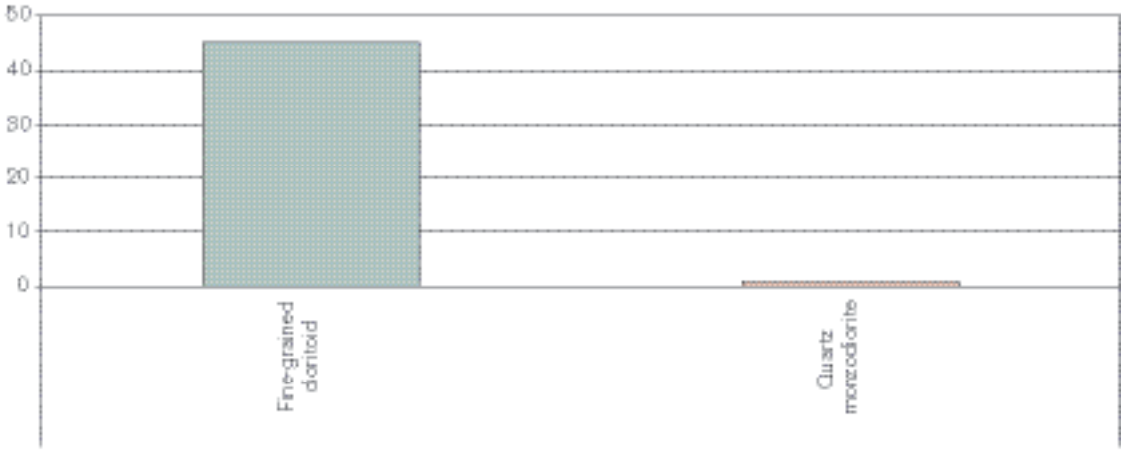

2) At two observation points only fine-grained dioritoid has been observed.

3) Number of occurrences of each rock type, of any order.

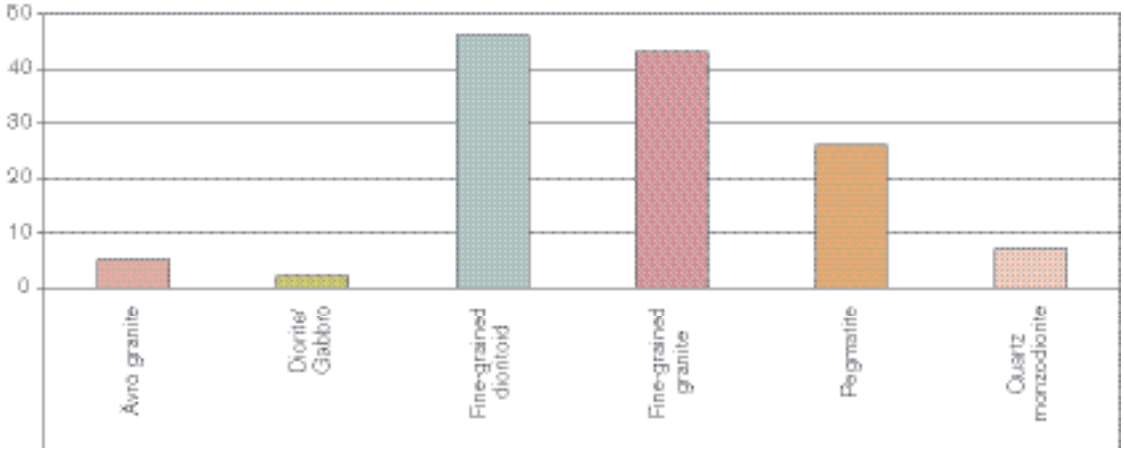

B02 contains only one observation point

The first- and second-order rock type is fine-grained dioritoid. Pegmatite has been observed as well.

B03 contains 27 observation points

1) Number of observation points where each rock type is dominant.

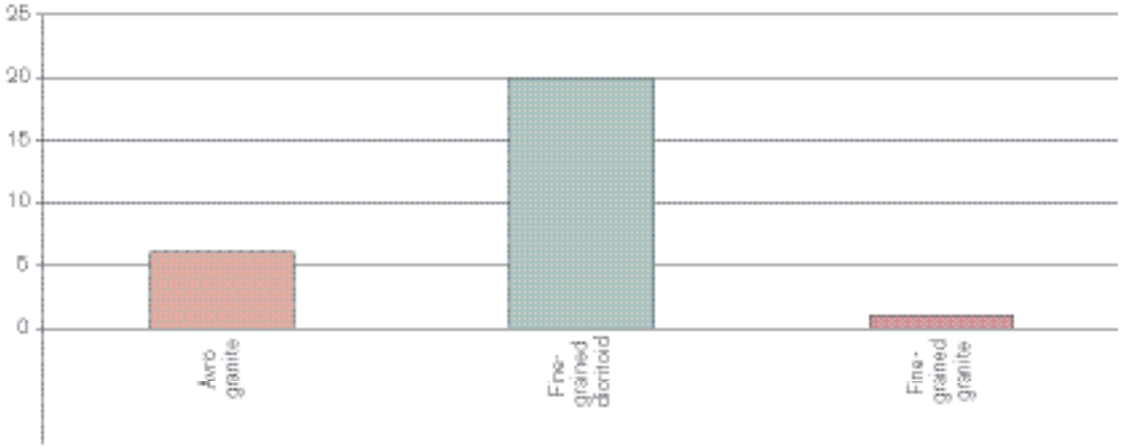

2) At four observation points only fine-grained dioritoid has been observed.

3) Number of occurrences of each rock type, of any order.

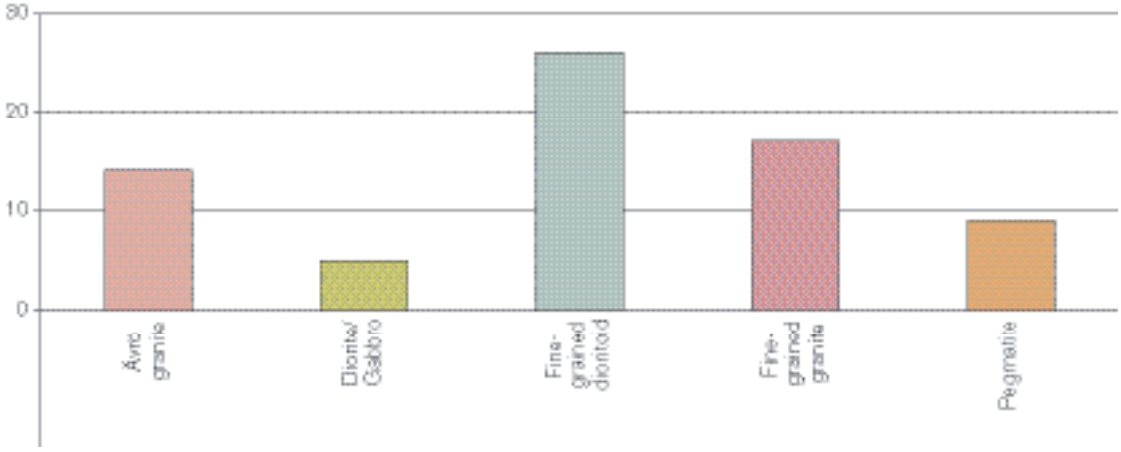

B04 contains no observation points

C01 contains 52 observation points

1) Number of observation points where each rock type is dominant.

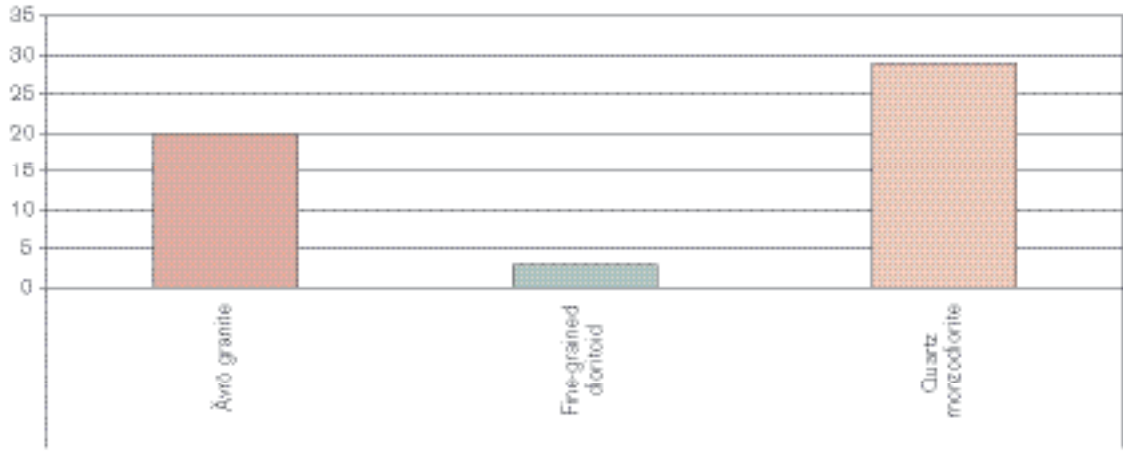

2) Number of observation points with only one rock type present.

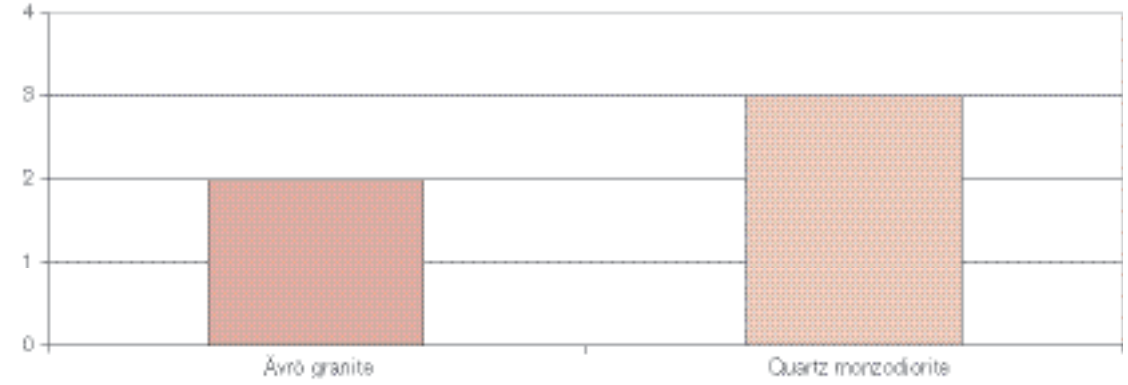

3) Number of occurrences of each rock type, of any order.

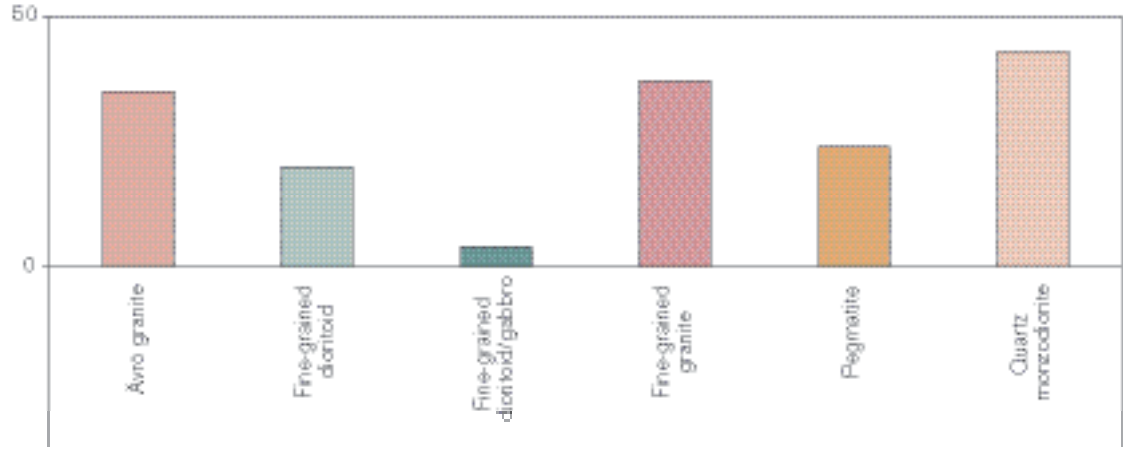

E01–E03 contain no observation points

E04 contains 8 observation points

1) Number of observation points where each rock type is dominating.

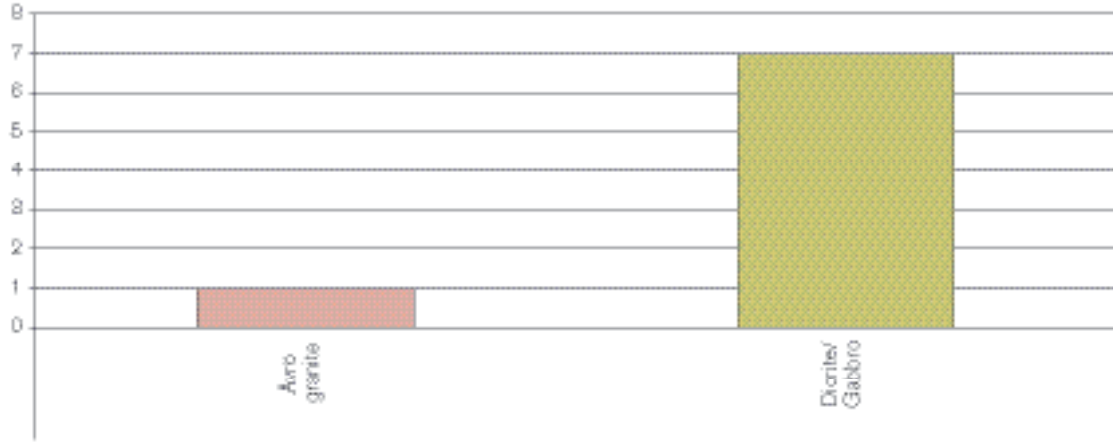

2) At one of the observation points only diorite to gabbro has been observed.

3) Number of occurrences of each rock type, of any order.

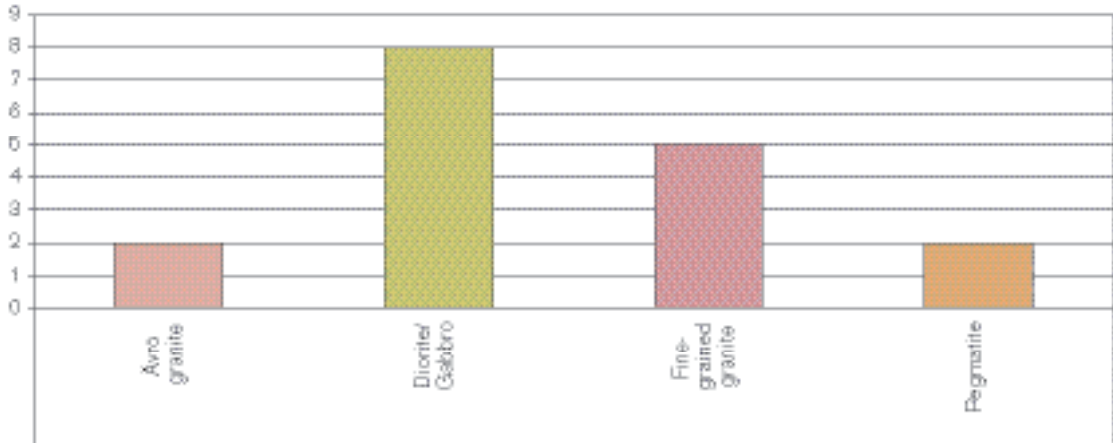

E05 contains no observation points

E06 contains only one observation point

The dominating rock type is diorite/gabbro. The secondary rock type is fine-grained granite. Pegmatite has been observed as well.

E07 and E08 contain no observation points

E08 contains only one observation point

Only diorite to gabbro has been observed at the observation point.

E09 contains only one observation point

The dominating rock type is diorite. The secondary rock type is granite. Pegmatite has been observed as well.

E10 contains only one observation point

Only diorite has been observed at the observation point.

Table A1-1. Translation key from nomenclature in the outcrop database (SGU) to SKB nomenclature. The key is custom made for this analysis and site. It is not for general use.

SGU Code	Comment	SGU Rock type (swedish names)	SKB Code	SKB Rock type
300		Basic rock	505102	Fine-grained diorite/gabbro
1033		Diorite	501033	Diorite/ Gabbro
1020		Gabbroid		
1022		Gabbro		
1036		Monzodiorite		
1038		Quartz diorite		
11146		Monzogranite	501058	Granite
1058		Granite	501058	Granite
1058 to 1098 1058 to 1061		Granite to pegmatitic granite Granite to pegmatite	511058	Fine-grained granite
1058	Remaining obs. of order less than 1	Granite	511058	Fine-grained granite
1058 to 1056 and 1058 to 1046		Granite to granodiorite and granite to quartz monzonite	501044	Ävrö granite
200		Intermediate rock	501030	Fine-grained dioritoid
1058 to 1037		Granite to quartz monzodiorite	501044	Ävrö granite
11146 to 1037		Monzogranite to quartz monzodiorite	501044	Ävrö granite
1046		Quartz monzonite	501044	Ävrö granite
1045		Monzonite		
1037		Quartz monzodiorite	501036	Quartz monzodiorite
1061		Pegmatite	501061	Pegmatite
1098		Pegmatitic granite		

8003 and 8004 = No SKB code exists. The data have been excluded, since there are very few observations of these rock types.

Appendix 2

Deformation zones – basis for interpretation and confidence

This appendix presents tables of confidence in occurrence for interpreted deformation zones included in the Simpevarp local scale model version 1.1.

Table A2-1. Confidence of zone occurrence of 14 confidence zones.

Zone ID	Basis for interpretation	Confidence	Comments
ZSMEW002A (Mederhult zone)	Linked lineaments, VLF, seismic refraction. Ground geology.	High	Position on surface: combination of a short section of XSM013A0 with v0 (Version 0, ref: R-02-35) ZSM0002A0.
ZSMEW004A	Airborne geophysics (magnetic 100% along the length, low uncertainty), tunnel. v0.	High	Position on surface and Äspö tunnel. Based on XSM0010A0, B0 & XSM0016A0. Ref: v0.
ZSMEW007A	Airborne geophysics (magnetic 100% along the length, electrical data, low uncertainty), topography, borehole.	High	Ref: ZLEW02 alternative Laxemar model TR-02-19.
ZSMEW009A (EW3)	Topography, ground geology, tunnel, borehole.	High	Ref: EW3 Geomod model.
ZSMEW013A	Airborne geophysics (magnetic 100% along the length, electrical data, low uncertainty), topography, borehole.	High	Ref: ZLXNW04 alternative Laxemar model.
ZSMNE005A (Äspö shear zone)	Airborne geophysics (magnetic 100% along the length, low to medium uncertainty), Ground geology, ground geophysics, borehole, Äspö data.	High	'Äspö shear zone' Ref: NEHQ3, EW1b Geomod model. Ref: ZSM0005A0, ZSM0004A0 v0. Ref: ZLXNE01 alternative Laxemar model.
ZSMNE006A (NE1)	Airborne geophysics (magnetic 100% along the length, low to medium uncertainty), tunnel, boreholes, Äspö data.	High	Ref: NE1 Geomod model. Ref: ZSM0006A0 v0. Ref: ZLXNE06 alternative Laxemar model.
ZSMNE012A (NE4)	Airborne geophysics (magnetic 100% along the length, low to medium uncertainty), tunnel, borehole.	High	Linked lineaments XSM0012A0, (part of B0), A1, A3 & B1. Ref: NE4, Äspö 96, TR97-06. Ref: Z15 Ävrö model, R-01-06.
ZSMNE016A	Airborne geophysics, topography, tunnel.	High	Only N section of lineament XSM0016A0. Ref: ZSM0004A0/B0 v0.
ZSMNE024A	Airborne geophysics (magnetic 91% along the length) tunnel.	High	Ref: OKG 3 intake tunnel. Ref: Z13 Ävrö model.
ZSMNE040A	Airborne geophysics (magnetic 60% along the length), boreholes.	High	Ref: ZSM0003A0 v0. Ref: ZLXNE04 (part ZLXNE03) alternative Laxemar model.
ZSMNS017A ZSMNS017B	Topography, borehole and tunnel evidence.	High	Ref: Geomod model, NNW4.
ZSMNW004A	Airborne geophysics (magnetic 100% along the length, low to medium uncertainty) ground geophysics, boreholes, topography.	High	Ref: Z14 Ävrö model.
ZSMNW007B	Airborne geophysics (magnetic >70% along the length, medium uncertainty), topography.	High	Ref: ZSM0007A0 v0. Ref: ZLXNS01 alternative Laxemar model.

Table A2-2. Confidence of zone occurrence (EW set).

Potential Zone	Basis for interpretation	Confidence level	Comments
EW set of possible deformation zones ZSMEW006A ZSMEW013B ZSMEW013C ZSMEW014A ZSMEW014B ZSMEW023A ZSMEW028A ZSMEW038B ZSMEW039A ZSMEW039B ZSMEW042A ZSMEW052A	Airborne geophysics (magnetic ≥70% along the length ± electrical, low to medium uncertainty), ± topography.	Medium	
ZSMEW026A ZSMEW027A ZSMEW038A	Airborne geophysics (magnetic <70% along the length ± electrical, medium to high uncertainty), ± topography.	Low	
ZSMEW023B	Topography	Very low	

Table A2-3. Confidence of zone occurrence (NE set).

Potential Zone	Basis for interpretation	Confidence level	Comments
NE set of possible deformation zones ZSMNE008A ZSMNE011A ZSMNE012D ZSMNE018A ZSMNE019A ZSMNE020A ZSMNE021A ZSMNE022A ZSMNE029A ZSMNE031A ZSMNE032A ZSMNE033A ZSMNE033B ZSMNE034A ZSMNE036A ZSMNE041A ZSMNE044A ZSMNE044B ZSMNE044C ZSMNE045A ZSMNE050A	Airborne geophysics (magnetic ≥70% along the length ± electrical, low to medium uncertainty), ± topography.	Medium	ZSMNE018A, an interpreted splay of this zone has been identified by ground geophysics Ref: P-03-66.
ZSMNE043A	Topography	Very low	

Table A2-4. Confidence of zone occurrence (NS set).

Potential Zone	Basis for interpretation	Confidence level	Comments
NS set of possible deformation zones ZSMNS037A ZSMNS046A ZSMNS049C	Airborne geophysics (magnetic ≥70% along the length ± electrical, low to medium uncertainty), ± topography.	Medium	
ZSMNS001A	Topography (ref: Laxemar model)	Very Low	XSM0003A1 outside the local domain, ZLXNS04 Lax' within the domain volume present at depth- not on surface.

Table A2-5. Confidence of zone occurrence (NW set).

Potential Zone	Basis for interpretation	Confidence level	Comments
NW set of possible deformation zones ZSMNW025A ZSMNW025D ZSMNW030A ZSMNW035A ZSMNW035D ZSMNW047A ZSMNW048A ZSMNW048B ZSMNW049A ZSMNW051A ZSMNW051B	Airborne geophysics (magnetic ≥70% along the length ± electrical, low to medium uncertainty), ± topography.	Medium	ZSMNW047A confidence based on Laxemar model. Partial coincidence with ZLXNS03 and ZLXNW01.
ZSMNW028B ZSMNW035B ZSMNW035C ZSMNW049B	Airborne geophysics (magnetic <70% along the length ± electrical, medium to high uncertainty), ± topography.	Low	
ZSMNW007A ZSMNW025C	Topography	Very low	

Table A2-6. Tabulations of properties of interpreted deformation zones.

ZSMEW002A (Mederhult zone)

Property	Quantitative estimate	Span	Confidence level	Basis for interpretation	Comments
Position		± 50 m	High	Linked lineaments	Position on surface. Combination of a short section of XSM013A0 with v0 ZSM0002A0
Orientation (strike/dip)	76/55	± 15/ ±15	Medium	Linked lineaments, VLF, seismic refraction	Strike based on model version 0, dip based on Laxemar model
Width	20 m	+50 m	low	VLF	From model version 0
Length[1]	30 km	± 10 km	low	Linked lineaments, model version 0	Extension outside local scale model domain based on model version 0
Ductile deformation	Likely, but no evidence				
Brittle deformation	Yes			Ground geology	From model version 0
Alteration					
Fracture orientation					
Fracture frequency					
Fracture filling					

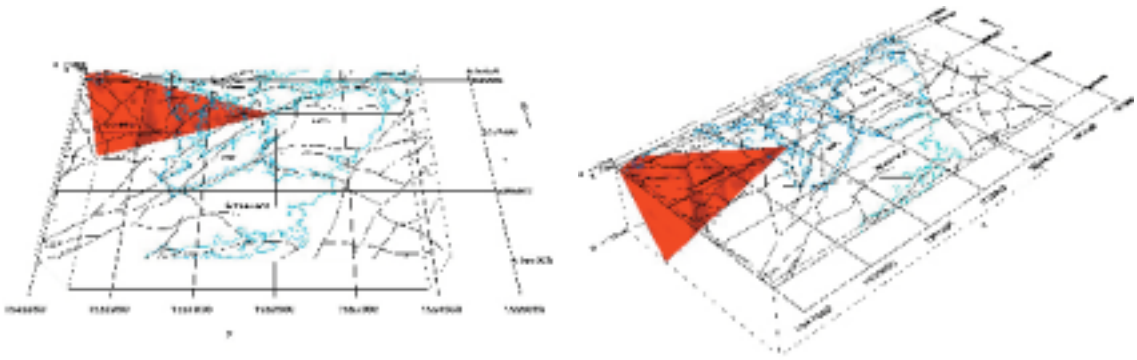

[1]Concerns total length. Extends outside both local scale and local scale model domain.

ZSMEW004A

Property	Quantitative estimate	Span	Confidence level	Basis for interpretation	Comments
Position		± 50 m	medium	Linked lineaments, tunnel (Äspö TASA ch.318 m)	Position on surface and Äspö tunnel. Based on XSM0010A0, B0 & XSM0016A0
Orientation (strike/dip)	74/70	± 15/ ±15	high	Linked lineaments, Äspö TASA ch.318 m	Dip from model version 0, ZSM0004A0. Dip in tunnel =75°
Width	50 m	± 20 m	medium	v0=50 m	Äspö TASA ch.318 m =30 m
Length[1]	c.6 km	± 5 km	low	Linked lineaments, model version 0. Unknown extension eastward.	Based on XSM0010A0, B0 & XSM0016A0
Ductile deformation					
Brittle deformation	Yes			Äspö TASA 0/318 m	
Alteration					
Water	5 l/min inflow to tunnel		High	Äspö TASA 0/318 m	
Fracture orientation	Not yet assessed			Äspö TASA 0/318 m	
Fracture frequency	Not yet assessed			Äspö TASA 0/318 m	
Fracture filling	Chl,Ca,Cy,Fe, Qz		High	Äspö TASA 0/318 m	

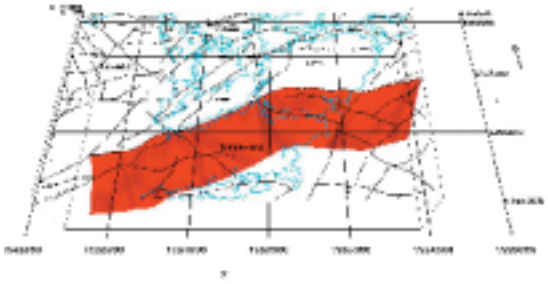

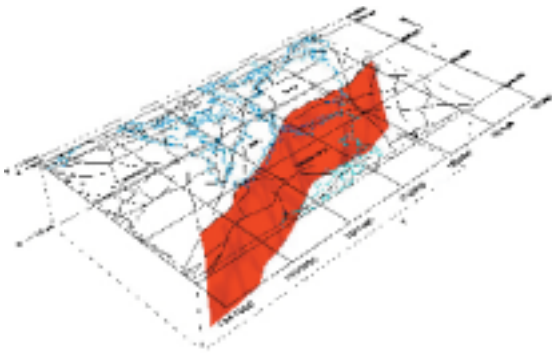

[1]Concerns total length. Extends outside local scale model domain.

ZSMEW007A

Property	Quantitative estimate	Span	Confidence level	Basis for interpretation	Comments
Position		± 50 m	medium	Linked lineaments	Position on surface
Orientation (strike/dip)	264/53	± 20/± ?	Medium in strike, low in dip	Dip from seismic reflector and KLX02 (340 m),	ZLEW02 alt' Lax' mod'
Width	2 m	1–10 m	medium		ZLEW02 alt' Lax' mod', based on one observation
Length[1]	4,900 m		medium	Linked lineaments	
Ductile deformation					
Brittle deformation	Cataclastic		High	Crush zone and fracture zone in KLX02 (340 m)	Based on one observation
Alteration	ca. 50% medium strong oxidation		High	Altered section in KLX02 (340 m)	Based on one observation
Water					
Fracture orientation	Not yet assessed				
Fracture frequency	24.3 fractures per metre		High	Crush zone and fracture zone in KLX02 (340 m)	Based on one observation
Fracture filling	Not yet assessed				

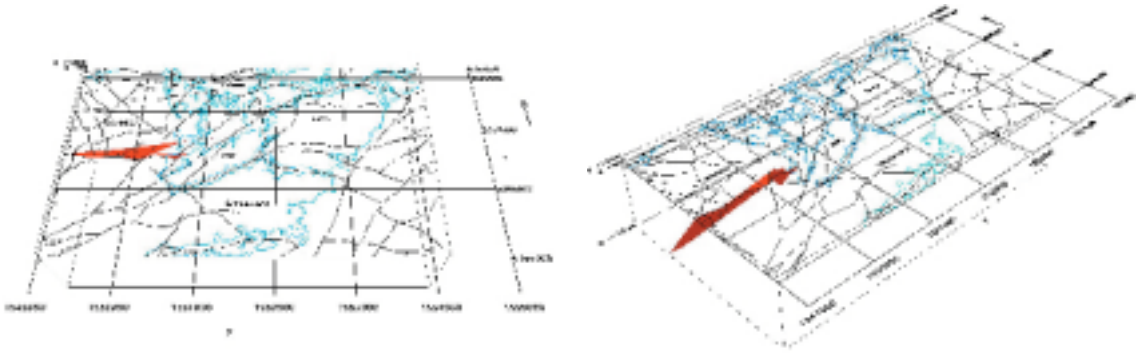

[1]Concerns total length. Extends outside local scale model domain.

ZSMEW009A (EW3)

Property	Quantitative estimate	Span	Confidence level	Basis for interpretation	Comments
Position		± 50 m	medium	Linked lineaments	Position in tunnel, borehole, Geomod
Orientation (strike/dip)	85/76	± 15/± 15	High	Tunnel, topography, borehole, magnetics, surface mapping (trench)	EW3 Geomod. Dip from TASA 1,407 m, Trench point X=6367638, Y=1551412, Z=2
Width	12 m		High	Äspö TASA 1/407 m	EW3 Geomod
Length[1]	1.8 km		Medium	Linked lineaments	
Ductile deformation					
Brittle deformation	Yes		High	Äspö TASA 1/407 m	
Alteration	1.5–2 m central clay zone		High	Äspö TASA 1/407 m	EW3 Geomod
Water	90 litres/min		High	Äspö TASA 1/407 m	90 litres/min
Fracture orientation	Not yet assessed				
Fracture frequency	10 m^{-1}		High	Borehole KAS06 (66 m)	'mean' value but ignores sections of crushed core.
Fracture filling	Chl, Cy, Ca, Fl		High	Borehole KAS06 (66 m)	mapped as mylonitic

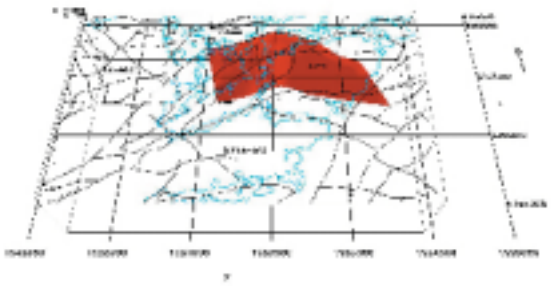

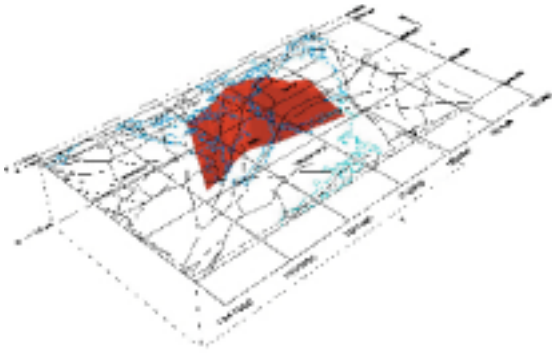

[1] Concerns total length. Extends outside local scale model domain.

ZSMEW013A

Property	Quantitative estimate	Span	Confidence level	Basis for interpretation	Comments
Position		± 50 m	Medium	Linked lineaments, ZLXNW04,	Position on surface, XSM0013A0, modified to terminate against ZSMEW002A in W, comb' wih XSM0014A0 in E.
Orientation (strike/dip)	270/90	± 15/± 15	medium strike, low dip	Linked lineaments, borehole HLX02	HLX02 penetrates a zone ''related'' to the lineament (Lax' mod')
Width					
Length[1]	c.3 km		low	Linked lineaments	XSM0013A0, modified to terminate against ZSMEW002A in W, comb' wih XSM0014A0 in E.
Ductile deformation					
Brittle deformation	Cataclastic		medium	Topography, HLX02	
Alteration					
Fracture orientation					
Fracture frequency					
Fracture filling					

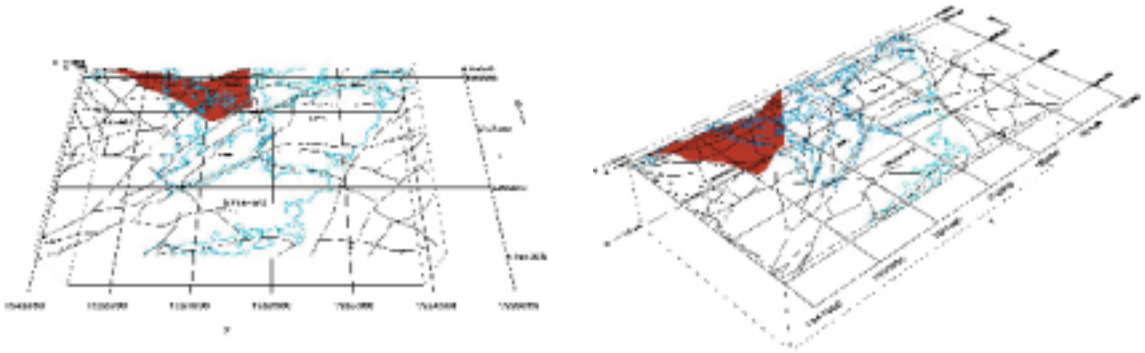

[1]Concerns total length. Extends outside local scale model domain.

ZSMNE005A (Äspö shear zone)

Property	Quantitative estimate	Span	Confidence level	Basis for interpretation	Comments
Position		+/–50 m	medium	Linked lineaments, v0	
Orientation (strike/dip)	40/80	dip 70–90NW ductile sinistral; 60–90SE brittle dextral	high	Linked lineaments	Ref: NEHQ3, EW1b Geomod; ZSM0005A0, ZSM0004A0 v0; ZLXNE01 Lax'
Width	40	Ductile 10–40 m Brittle 70–200 m	high	v0	
Length[1]	10 km (5,100 m in model)		low	Linked lineaments	
Ductile deformation	Mylonitic		high	Field data, Äspö data	
Brittle deformation	Cataclastic		high	Field data, ground geophysics, Äspö data	
Alteration	Not yet assessed				
Fracture orientation	Not yet assessed				
Fracture frequency	Not yet assessed				
Fracture filling	Not yet assessed				

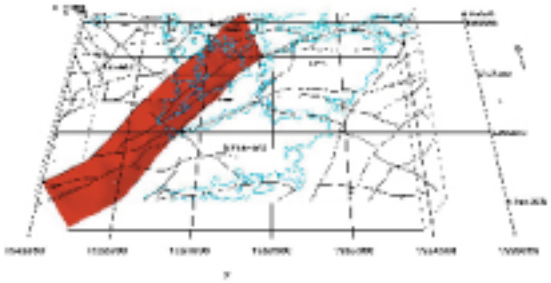

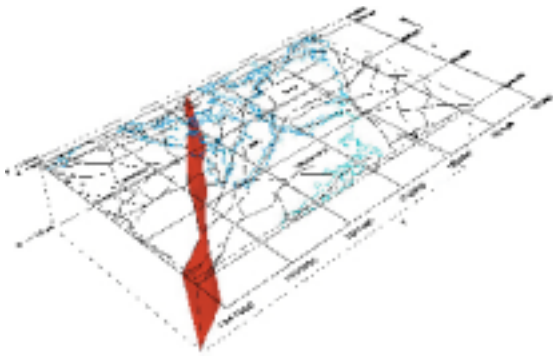

[1]Concerns total length. Extends outside local scale model domain.

ZSMNE006A (NE1)

Property	Quantitative estimate	Span	Confidence level	Basis for interpretation	Comments
Position		+/–50 m	medium	Linked lineaments	Ref: NE1 Geomod, ZSM0006A0 v0, ZLXNE06 Lax'
Orientation (strike/dip)	224/65	+/–15 / +/–15	medium	Strike- linked lineaments, dip- Geomod NE1	KA1061 203 m, KA1131B 188 m, KAS07 550 m, KAS08 569 m, KAS09 81 m, KAS11 188 m, KAS14 71 m, KBH02 687 m, KAS02 860 m,
Width	28 m		high	Äspö TASA 1/290 m (northernmost branch)	Complex zone with 3 branches total 60 m
Length[1]	1,950 m	+/–5 km	low	Linked lineaments	
Ductile deformation					
Brittle deformation	Yes		high	Äspö TASA 1/290 m	
Alteration	1 m wide, central, completely clay altered		high	Äspö TASA 1/290 m	5–8 m wide partially clay altered
Water	2,000 l/min		high	Äspö TASA 1/290 m	
Fracture orientation	Not yet assessed				
Fracture frequency	Not yet assessed				
Fracture filling	Chl,Cy,Ca,Fl, Fe,Ep,Qz,My		high	Äspö TASA 1/290 m	

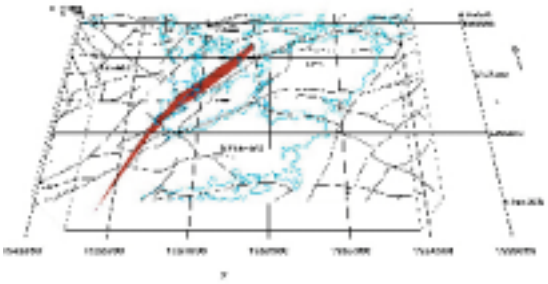

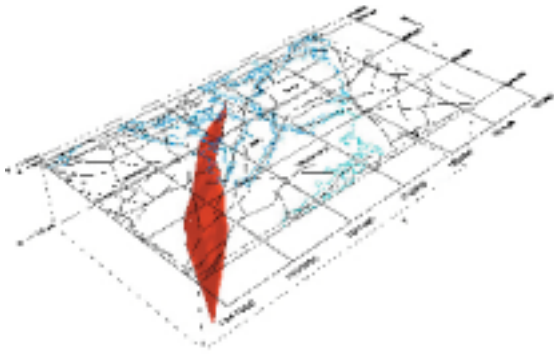

[1]Concerns total length. Extends outside local scale model domain.

ZSMNE012A (NE4)

Property	Quantitative estimate	Span	Confidence level	Basis for interpretation	Comments
Position		+/–50 m	medium	Linked lineaments	Linked lineaments XSM0012A0, (part of B0), A1, A3 & B1.
Orientation (strike/dip)	58/50	+/–15 / +/–15	high	Strike from linked lineaments, dip from Äspö tunnel TASA 0/827 m, additional intersection points in boreholes KAV01 L=413 m, KAV03 L=190 m, HAV07 L=98 m, plus 6 points from 3 interpreted reflectors (all Z15 Ävrö model)	
Width	41 m		high	Äspö TASA 0/827 m	NE4
Length[1]	2 km	+/–1 km	low		Linked lineaments XSM0012A0, (part of B0), A1, A3 & B1.
Ductile deformation					
Brittle deformation	Yes		high	Äspö TASA 0/827 m, KAV01 L=413 m, Z15 (Ävrö)	
Alteration	Clay		high	KAV01 L=413 m, Z15 (Ävrö)	
Water	60 l/min		high	Äspö TASA 0/827 m	
Fracture orientation	Not yet assessed				
Fracture frequency	Not yet assessed				
Fracture filling	Chl,Cy,Ep		high	Äspö TASA 0/827 m	

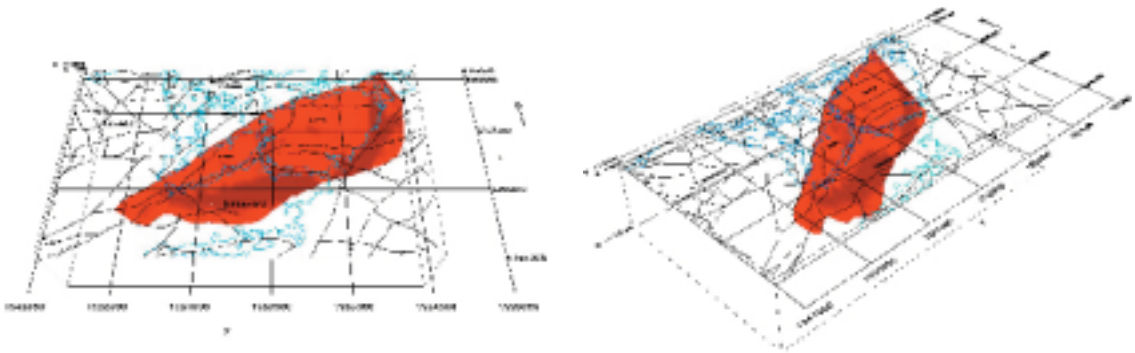

[1]Concerns total length. Extends outside local scale model domain.

ZSMNE016A

Property	Quantitative estimate	Span	Confidence level	Basis for interpretation	Comments
Position		+/–50 m	medium	Modified linked lineaments	Only N section of lineament XSM0016A0. Partial coincidence with v0. ZSM0004B0
Orientation (strike/dip)	30/90	+/–15 / +/–15	medium	Modified linked lineaments. Äspö TASA ch.359 m	Only N section of lineament XSM0016A0
Width	12.6 m		high	Äspö TASA ch.359 m	
Length[1]	1.470 m		medium	Modified linked lineaments	
Ductile deformation					
Brittle deformation	Yes		high	Äspö TASA ch.359 m	
Alteration					
Water	0.5 l/min		high	Äspö TASA ch.359 m	
Fracture orientation					
Fracture frequency					
Fracture filling	Chl,Cy,Ca,Fe		high		

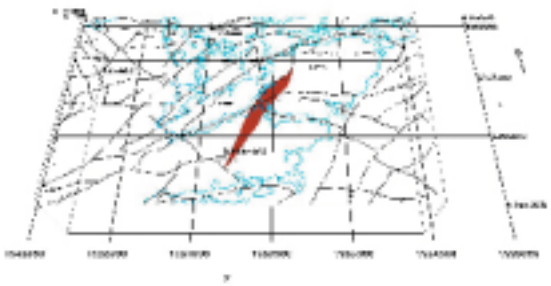

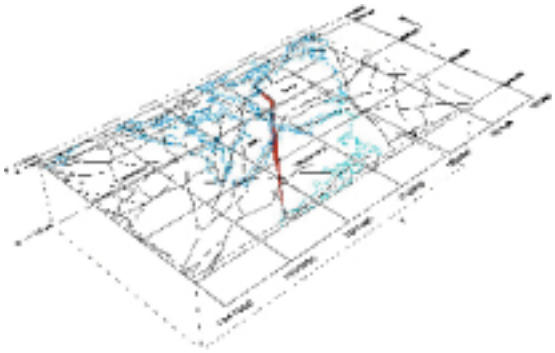

[1]Concerns total length. Extends outside local scale model domain.

ZSMNE024A

Property	Quantitative estimate	Span	Confidence level	Basis for interpretation	Comments
Position		+/–50 m	medium	Linked lineaments	
Orientation (strike/dip)	211/60	+/–15 / +/–15	high	Linked lineaments, OKG-III cooling water intake tunnel –25 to 150 m, incl. 6 points from 4 seismic reflectors from Z13 (Ävrö)	Complex zone
Width	100 m		high	Ävrö Z13 (seismic)	Summed up width of individual branches is 20 m as mapped within a 175 m stretch of OKG-III cooling water intake tunnel. Widest individual branch is 10 m. Associated with aplites.
Length[1]	7.8 km	+10 km	low	Linked lineaments	
Ductile deformation					
Brittle deformation	Yes		high	OKG-III cooling water intake tunnel –25 to 150 m	
Alteration	Clay, weathering		high	OKG-III cooling water intake tunnel –25 to 150 m	test result exists, OKG-III cooling water intake tunnel –25 to 150 m
Water					Moderately water bearing
Fracture orientation					
Fracture frequency					
Fracture filling	Chl, Ca, limonite		high		OKG-III cooling water intake tunnel –25 to 150 m

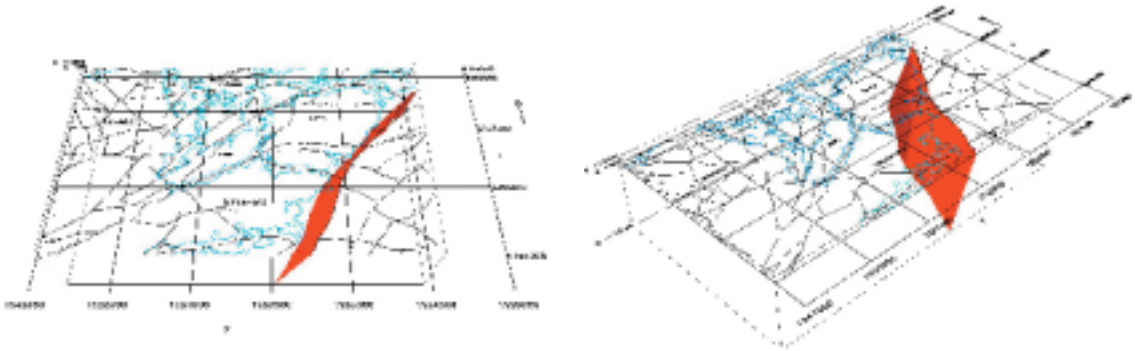

[1]Concerns total length. Extends outside local scale model domain.

ZSMNE040A

Property	Quantitative estimate	Span	Confidence level	Basis for interpretation	Comments
Position		+/–50 m	medium	Linked lineaments	
Orientation (strike/dip)	45/63	+/–15 / +/–15	High	Linked lineaments. Dip based on KLX01 (L=421 m) and KLX02 (L=1,040 m)	Linked lineaments, ZSM0003A0 in v0, ZLXNE04 and part of ZLXNE03, Laxemar model
Width	15 m	1–30 m	High	KLX01 (L=421 m) and KLX02 (1,040 m)	ZLXNE03 and ZLXNE04 Laxemar model
Length[1]	1,580 m		Low	Linked lineaments	
Ductile deformation					
Brittle deformation	Cataclastic		High	HLX04, KLX01 (L=421 m) and KLX02 (L=1,040 m)	ZLXNE03 and ZLXNE04 Laxemar model
Alteration	Oxidation		High	KLX01 (L=421 m)	ZLXNE04 Laxemar model
Fracture orientation	NNE		High	KLX01 (L=421 m)	ZLXNE04 Laxemar model
Fracture frequency	14 per m		High	KLX01 (L=421 m) and KLX02 (L=1,040 m)	ZLXNE03 and ZLXNE04 Laxemar model
Fracture filling	Ca, Chl, Ep, Fe		high	KLX01 (L=421 m) and KLX02 (L=1,040 m)	ZLXNE03 and ZLXNE04 Laxemar model

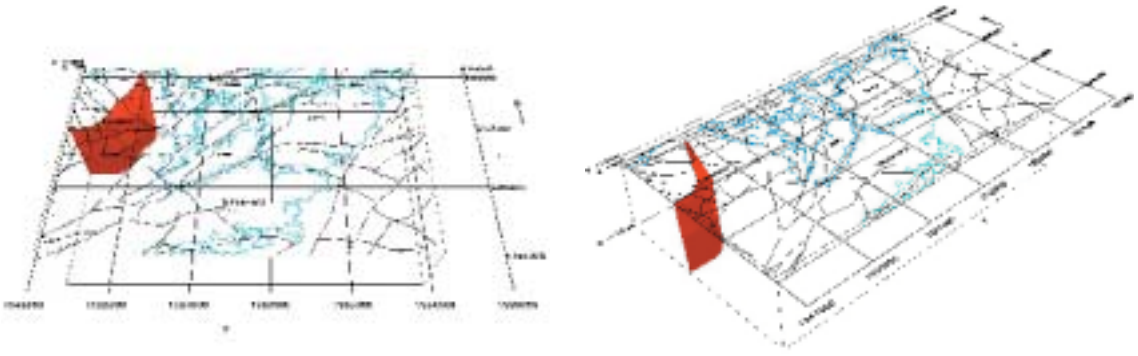

[1]Concerns total length. Extends outside local model domain.

ZSMNS017A and B

Property	Quantitative estimate	Span	Confidence level	Basis for interpretation	Comments
Position		+/–50 m	Medium	Linked lineaments	
Orientation (strike/dip)	176/90	+/–15 / +/–15	High	Äspö TASA 1/876 m, 1/979 m and 3/083 m	One of a number of parallel steep structures present in this area, ref: NNW4 Geomod.
Width	5 m	0.5–10 m	High	Äspö TASA 1/876 m, 1/979 m and 3/083 m	
Length[1]	1,575 m		Low	Linked lineaments	
Ductile deformation					
Brittle deformation	Cataclastic		High	KA2048B, L=35 m	
Alteration	Weak to medium		High	Äspö TASA 1/876 m, 1/979 m and 3/083 m	
Water	102 l/min,	100–500 /minl	High	TASA 1/876 m	One of a number of parallel steep structures present in this area, ref: NNW4 Geomod
Fracture orientation					
Fracture frequency	8 fractures per m and crushed core ca 1 m total		High	KA2048B, L=35 m	
Fracture filling	Clay, Chl, Ca, Ep, Cy		high	Äspö TASA 1/876 m, 1/979 m and 3/083 m	

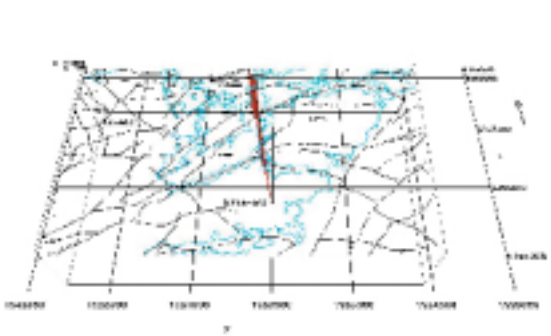

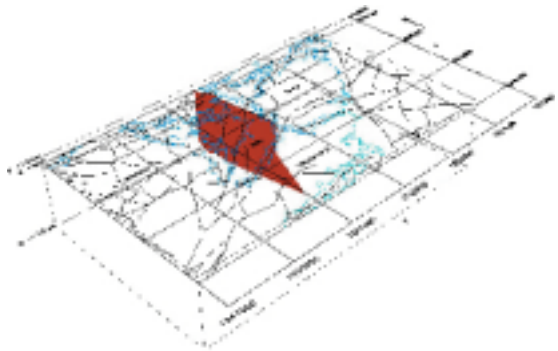

[1]Concerns total length. Extends outside local scale model domain.

ZSMNW004A

Property	Quantitative estimate	Span	Confidence level	Basis for interpretation	Comments
Position		+/–50 m	Medium	Linked lineaments	
Orientation (strike/dip)	108/49	+/–15 / +/–15	Medium	Linked lineaments, seismic reflectors from Z14 version 2 (Ävro model)	
Width	50 m	+/–20 m	Medium	Z14 version 2 (Ävro model)	
Length[1]	940 m		Low	Linked lineaments	
Ductile deformation					
Brittle deformation					
Alteration					
Fracture orientation					
Fracture frequency					
Fracture filling					

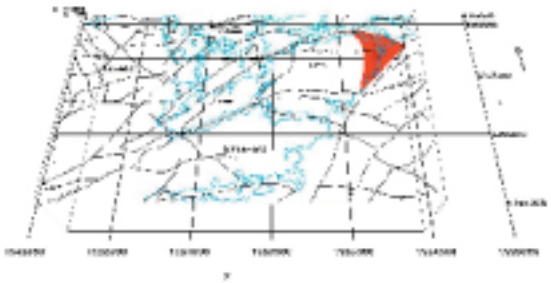

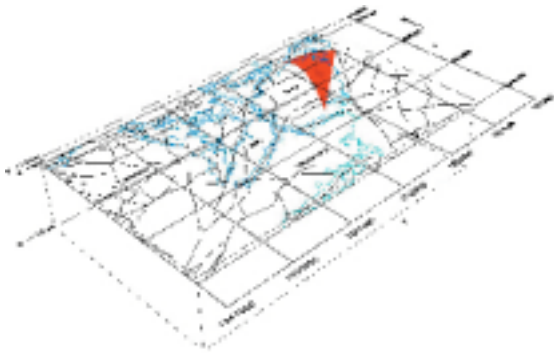

[1]Concerns total length. Extends outside local scale model domain.

ZSMNW007B

Property	Quantitative estimate	Span	Confidence level	Basis for interpretation	Comments
Position		+/–50 m	Medium	Linked lineaments	
Orientation (strike/dip)	165/90	+/–15 / +/–15	Medium	Linked lineaments, ZSM0007A0 v0, ZLXNS01 (Laxemar)	
Width	50 m	+/–20 m	Medium	ZSM0007A0 v0 (topoography, ground geophysics), ZLXNS01 (Laxemar)	
Length[1]	1,735 m		Low	Linked lineaments	
Ductile deformation					
Brittle deformation	yes		low	v0 (topoography, ground geophysics)	
Alteration					
Fracture orientation					
Fracture frequency					
Fracture filling					

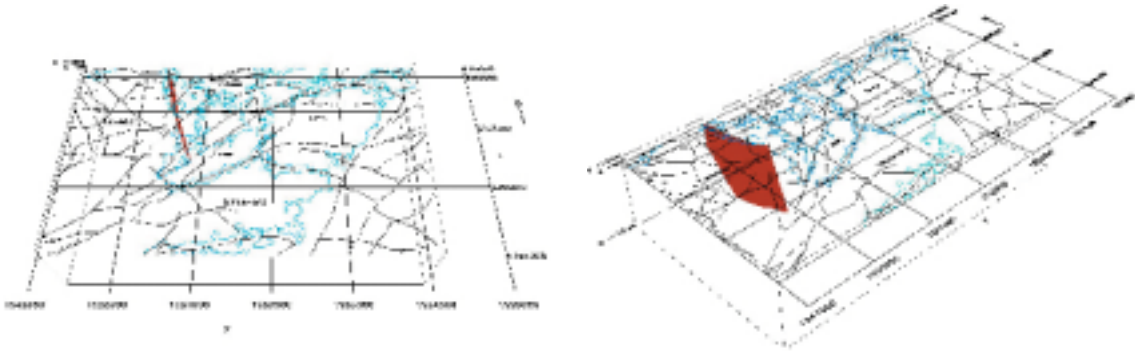

[1]Concerns total length. Extends outside local scale model domain.

EW set of possible deformation zones- Medium Confidence level

ZSMEW006A

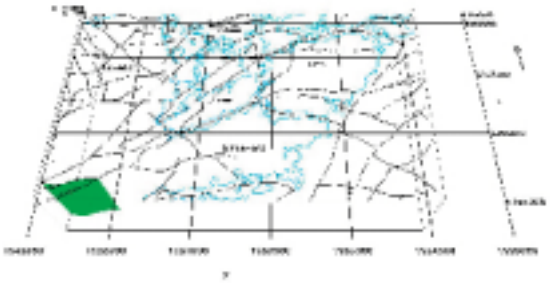

ZSMEW014B

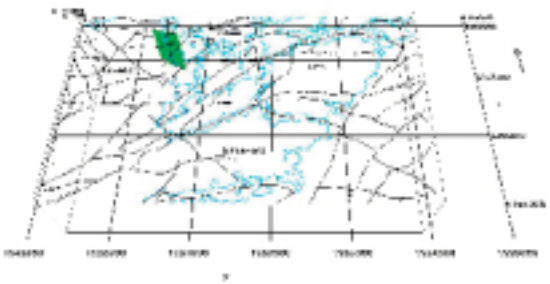

ZSMEW013B

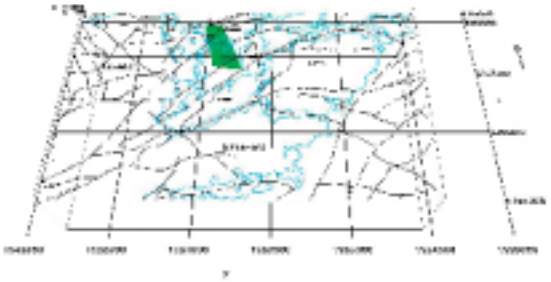

ZSMEW023A

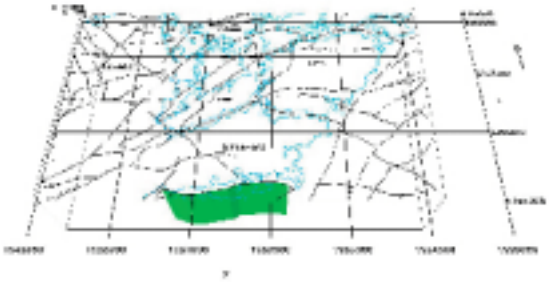

ZSMEW013C

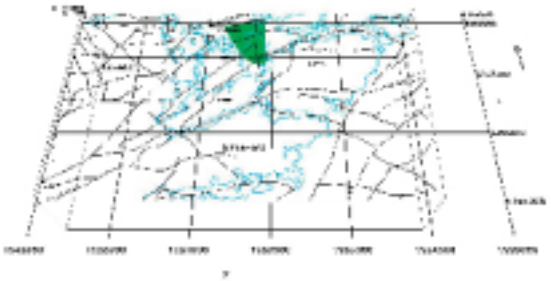

ZSMEW028A

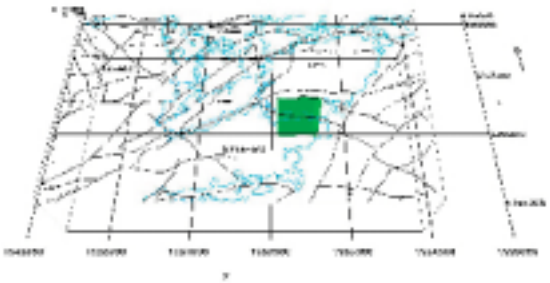

ZSMEW014A

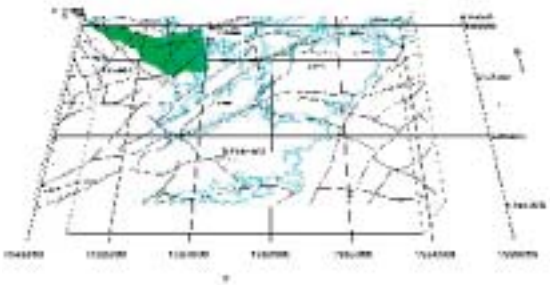

ZSMEW038B

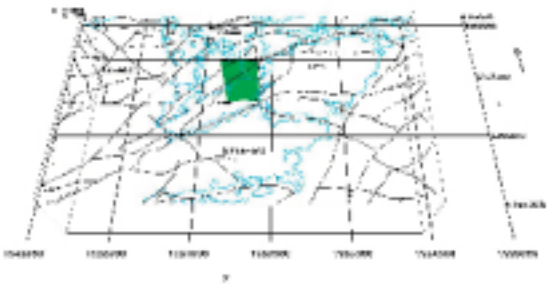

EW set of possible deformation zones- Medium Confidence level cont'd

ZSMEW039A

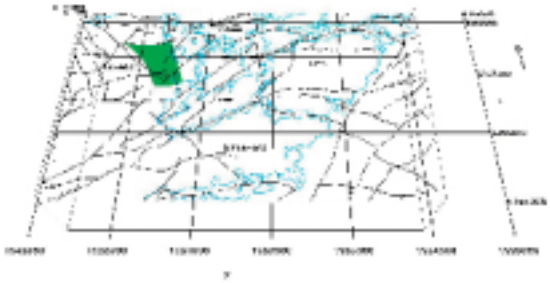

ZSMEW042A

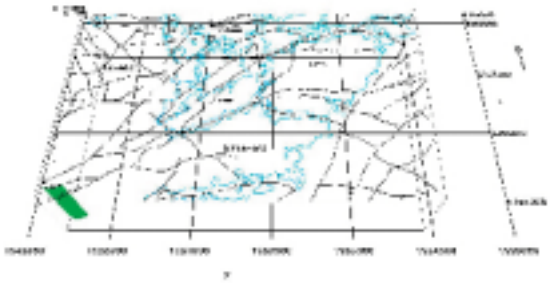

ZSMEW039B

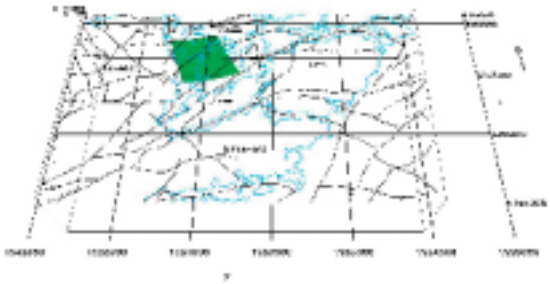

ZSMEW052A

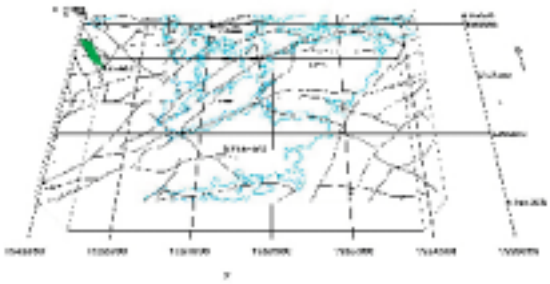

EW set of possible deformation zones- Low to very low Confidence level

ZSMEW026A

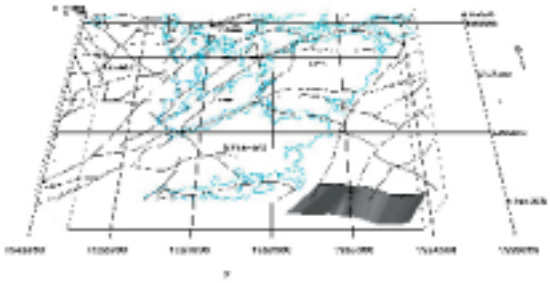

ZSMEW038A

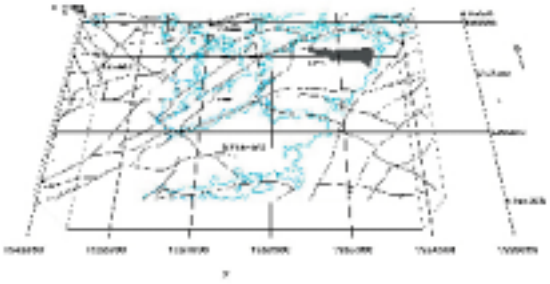

ZSMEW027A

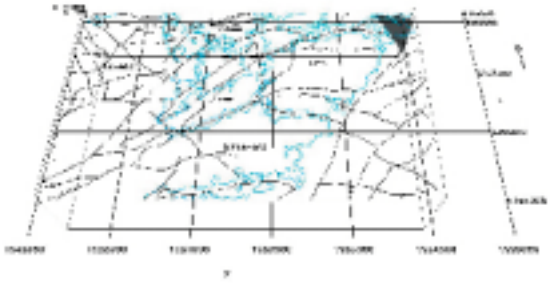

ZSMEW023B

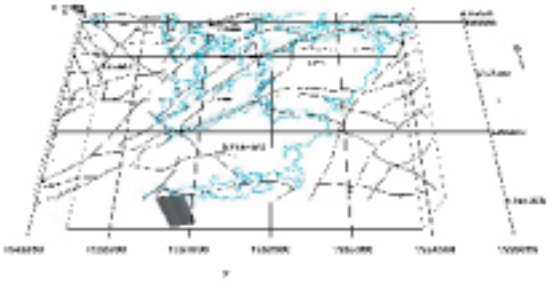

NE set of possible deformation zones- Medium Confidence level

ZSMNE008A

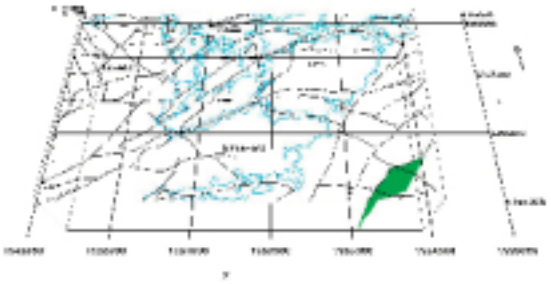

ZSMNE019A

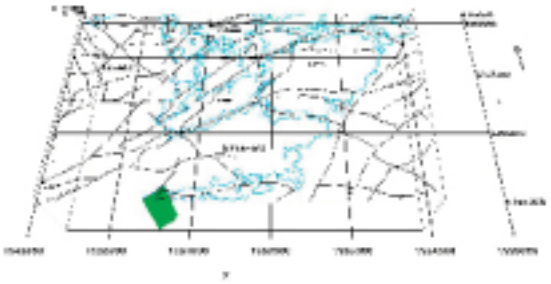

ZSMNE011A

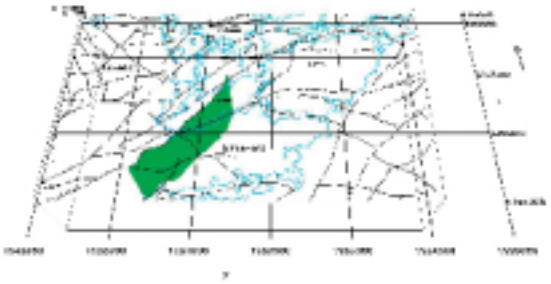

ZSMNE020A

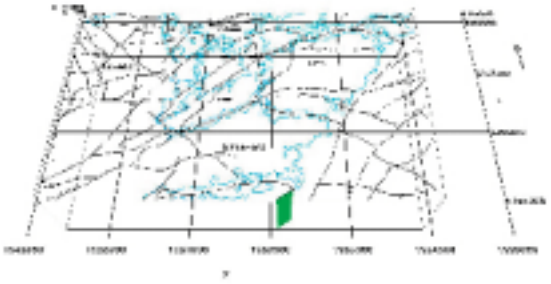

ZSMNE012D

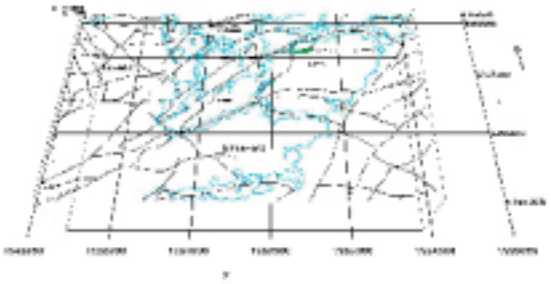

ZSMNE021A

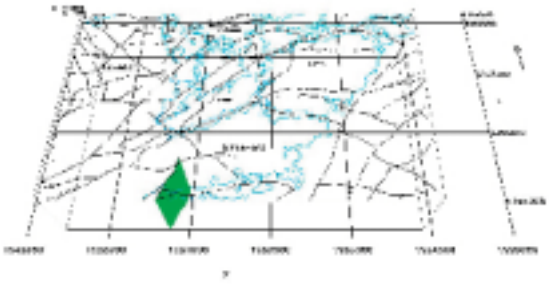

ZSMNE018A

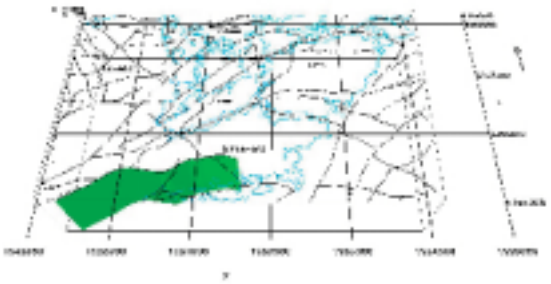

ZSMNE022A

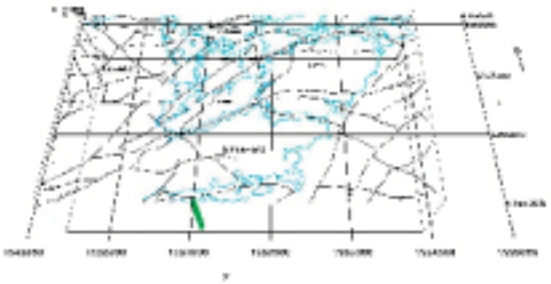

NE set of possible deformation zones- Medium Confidence level cont'd

ZSMNE029A

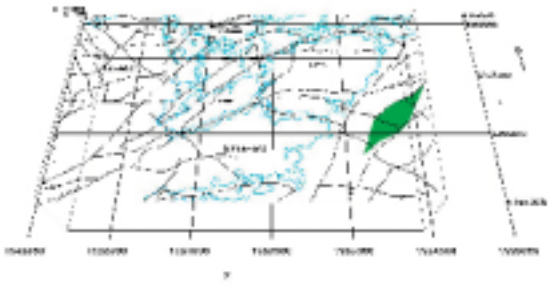

ZSMNE031A

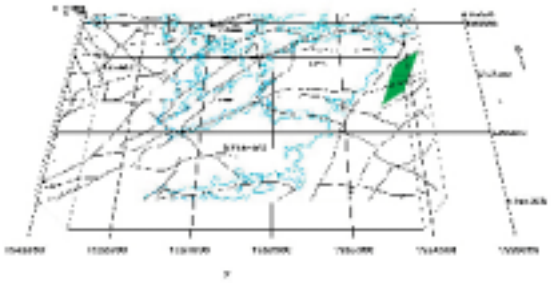

ZSMNE032A

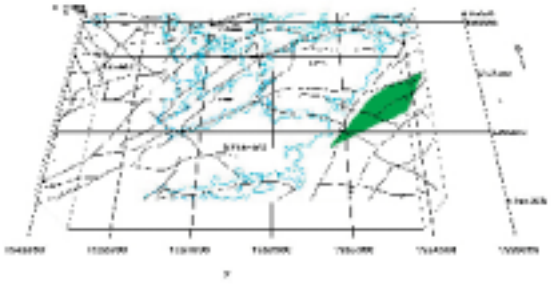

ZSMNE033A

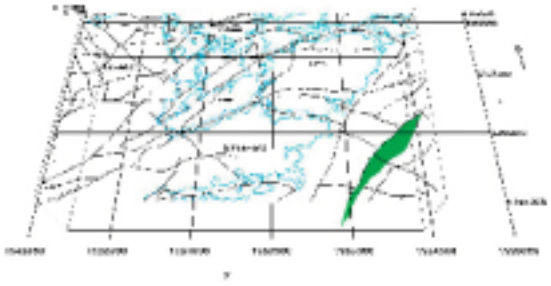

ZSMNE033B

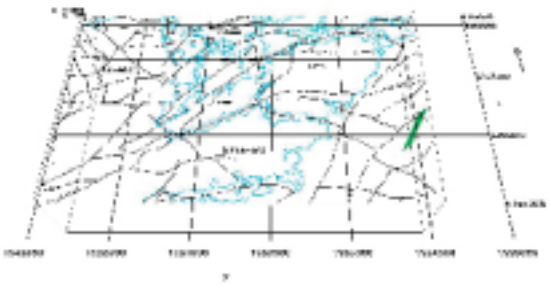

ZSMNE034A

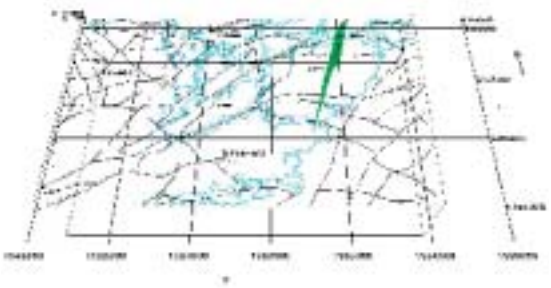

ZSMNE036A

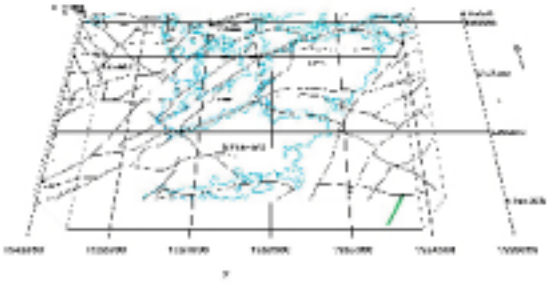

ZSMNE041A

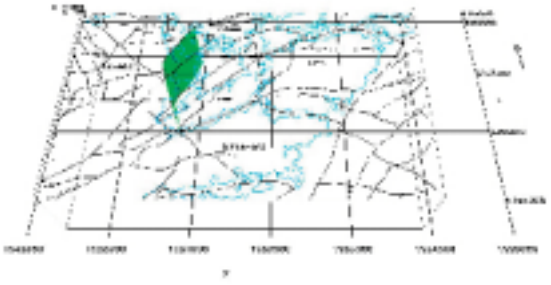

NE set of possible deformation zones- Medium Confidence level cont'd

ZSMNE044A

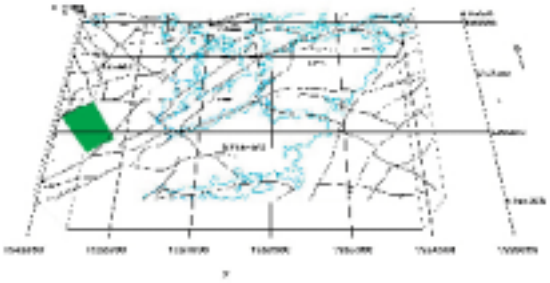

ZSMNE045A

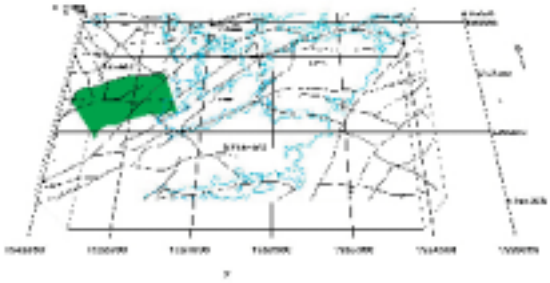

ZSMNE044B

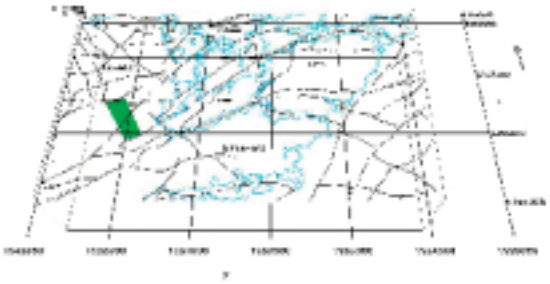

ZSMNE050A

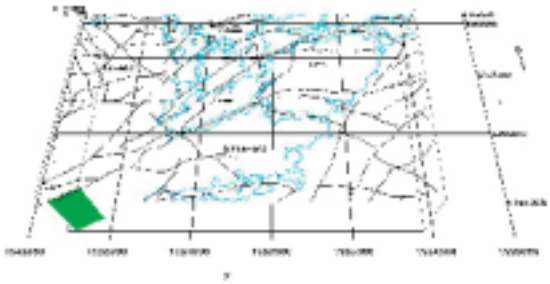

ZSMNE044C

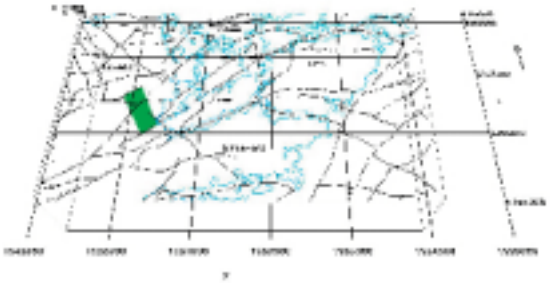

NE set of possible deformation zones- Low to very low Confidence level

ZSMNE043A

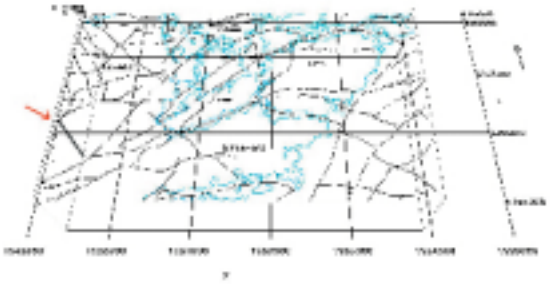

NS set of possible deformation zones- Medium Confidence level

ZSMNS037A

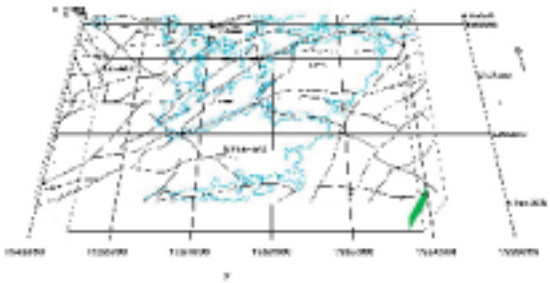

ZSMNS049C

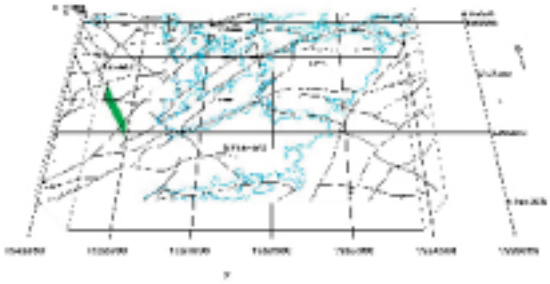

ZSMNS046A

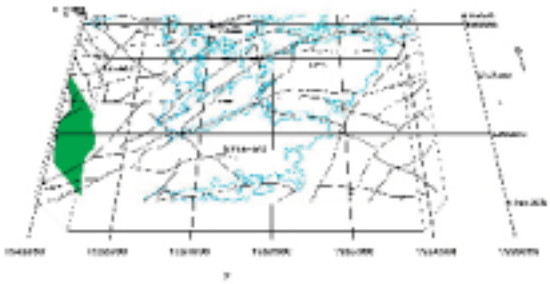

NS set of possible deformation zones- Low to very low Confidence level

ZSMNS001A

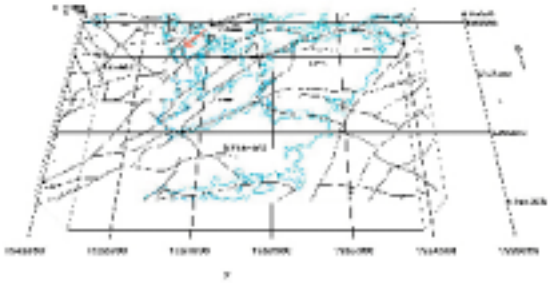

NW set of possible deformation zones- Medium Confidence level

ZSMNW025A

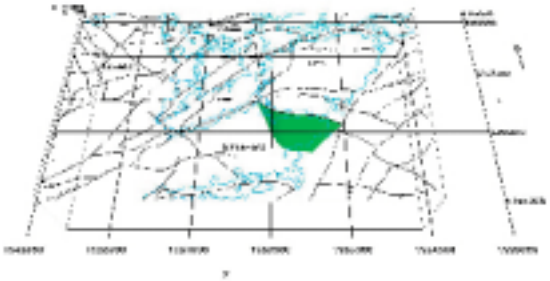

ZSMNW025D

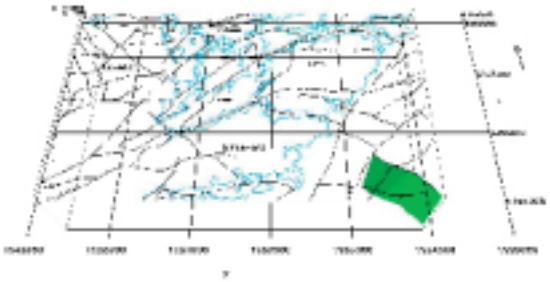

ZSMNW030A

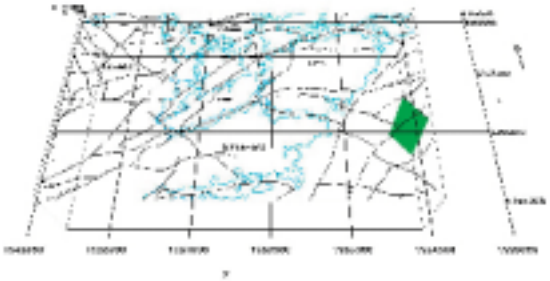

ZSMNW035A

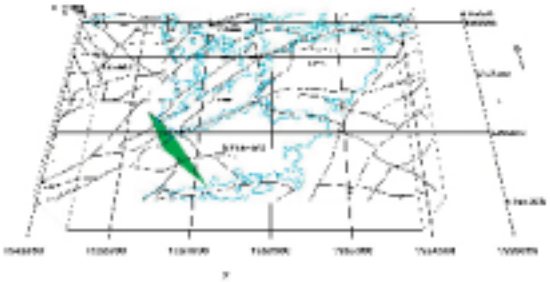

ZSMNW035D

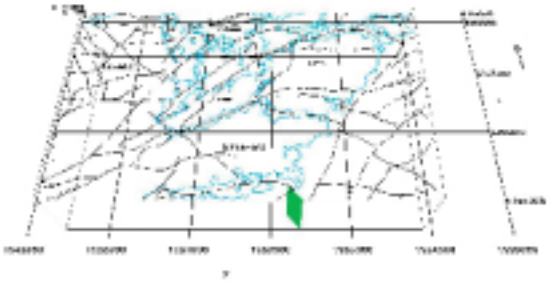

ZSMNW047A

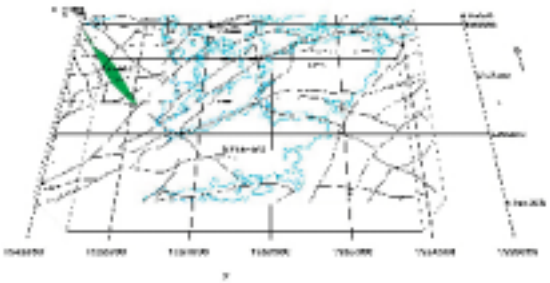

ZSMNW048A

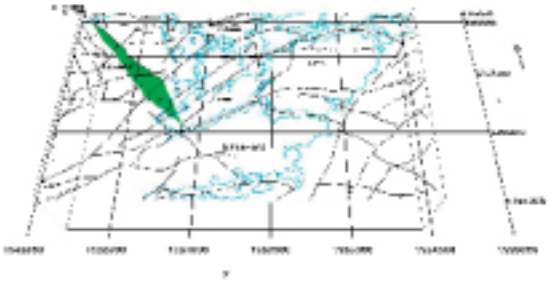

ZSMNW048B

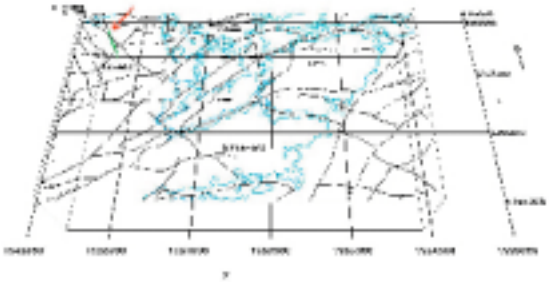

NW set of possible deformation zones- Medium Confidence level cont'd

ZSMNW049A

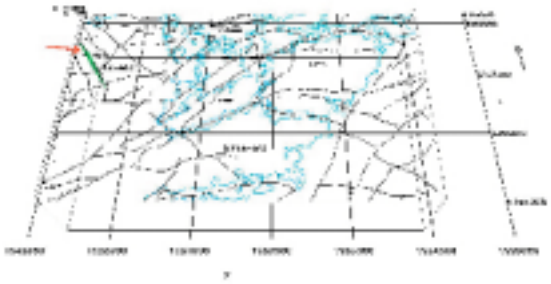

ZSMNW051B

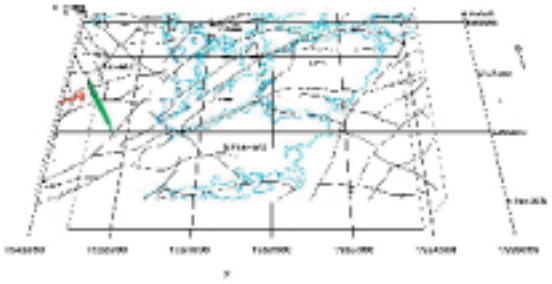

ZSMNW051A

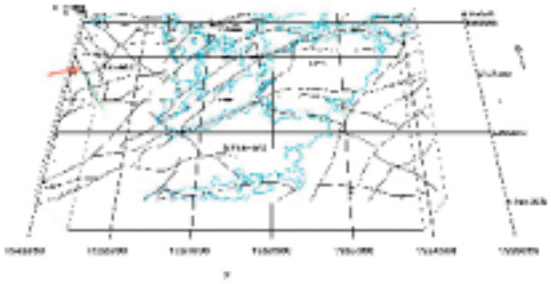

NW set of possible deformation zones- Low to very low Confidence level

ZSMNW028B

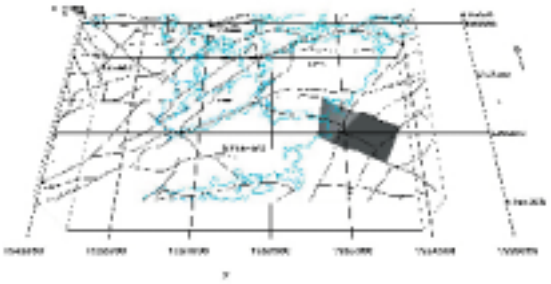

ZSMNW049B

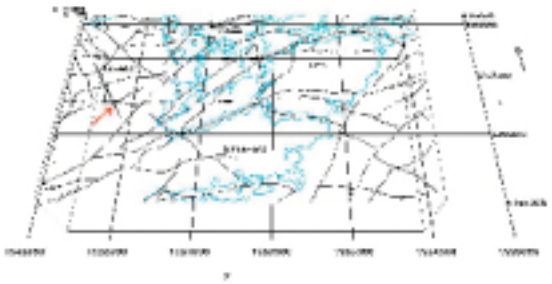

ZSMNW035B

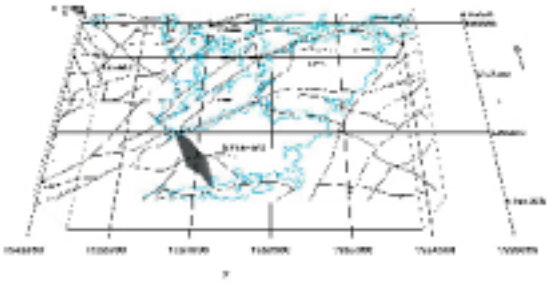

ZSMNW007A

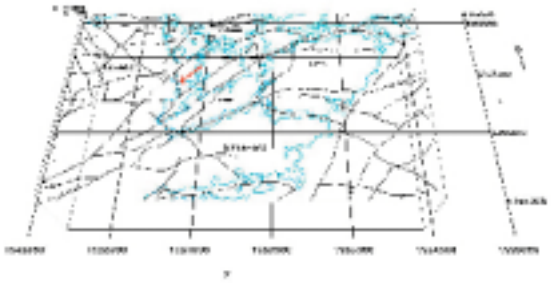

ZSMNW035C

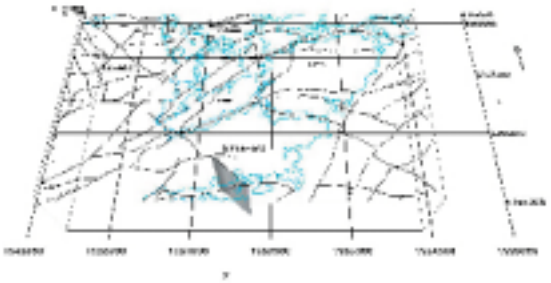

ZSMNW025C

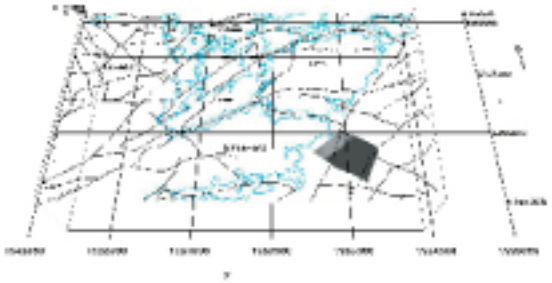

Appendix 3

A3.1 Methodology for fracture data analysis for development of the local scale DFN model

A3.1.1 Analysis of the fracturing in local data sets

The workflow for analysing the individual borehole, outcrop and lineament data sets (Figure 1-1) is best presented within its context for achieving the overall characterization objectives. This is because the data are primarily being analyzed to determine regional controls on fracture pattern geometry, in particular, to develop a predictive algorithm to specify fracture intensity, orientation and size throughout the spatial and depth extent of the Simpevarp regional domain. The workflow diagram begins with the analysis of data sets for each individual borehole, outcrop trace map or lineament data set. These individual data sets are described as "local" in the sense that it is not initially known whether the fracture controls and geometry determined for each individual set are found elsewhere; they may not have any "regional" consistency. The results from the analyses for each borehole or outcrop are assumed to initially only represent the fracturing in the rock in the immediate proximity of the outcrop or borehole, unless comparative analysis later demonstrates that fracture orientations, geological controls on intensity, etc exhibit regional consistency. The term, local fracture set should not be confused with the local DFN model, which is the fracture model of the Simpevarp region. The local DFN model is independent of whether it is composed of local fracture sets where individual borehole or outcrop data sets show little spatial consistency, regional sets, which show great spatial consistency, or some combination of regional and local sets.

The flowchart shows the components of the analysis of the local data sets. Any box that can be traced to an original input data source without connection to another data source is part of the local fracture data set analyses. For example, the chart shows that calculating the mass dimension of the trace intensity is part of the local data analysis for the outcrop trace data, but the derivation of the regional size model for lineament-related sets is not, as it relies upon the joint analysis of both the lineament and outcrop trace data sets, and whether the outcome of these analyses suggest that lineaments and smaller-scale fracturing ought to be combined. In contrast, the stages in determining the possible regional controls on fracturing are based on the borehole data, as these data sets contain the most detailed geological information. Any controls identified in the borehole data set are then extended to the outcrop data to see if the controls appear to persist for these data sets as well. All of the analyses eventually flow towards the conceptual basis and parameters values for the local stochastic DFN model. This model consists of all of the pink-shaded output data sets and relations.

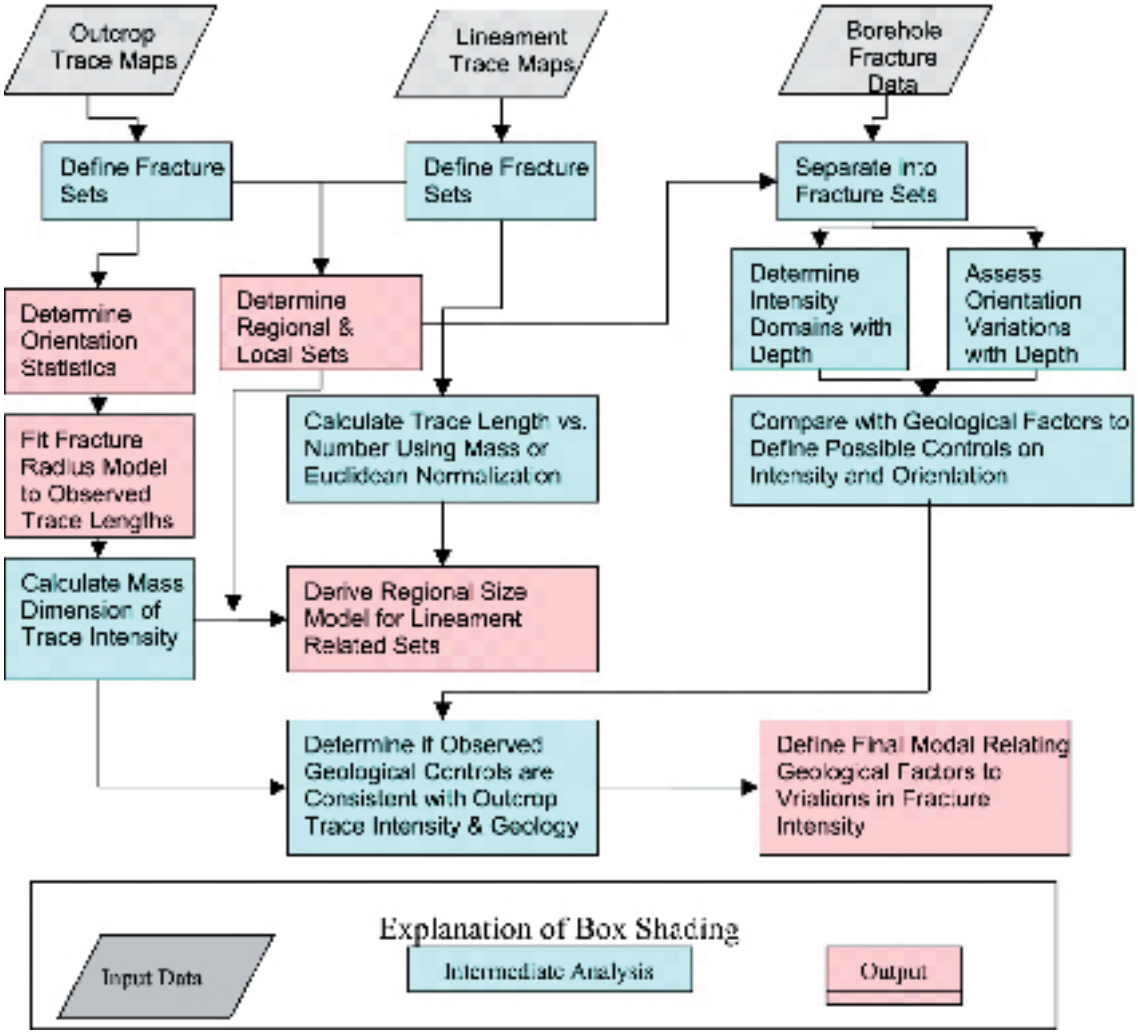

Figur A3-1. *Flow chart which illustrates the varios steps in the geological DFN modelling process.*

A3.1.1.1 Outcrops

The first step, as shown in the chart (Figure A3-1) was to identify statistically homogeneous sub-populations for each of the four outcrops independently of any other outcrop, borehole or lineament data set. The first step of this analysis was to plot stereoplots of the fracture data, expressed as poles to the fracture planes, and to identify visually distinct clusters of orientations. At the same time, plots of the trace pattern were visually evaluated to determine if there might be other, less prominent sets that were visually obscured in the stereoplots due to the greater number of fractures in some sets. Stereoplots were constructed using DIPS© Version 5.0 /Rocscience, 1989/, whereas the trace plots were generated using GeoFractal© Version 1.2 /La Pointe et al, 1992/. An example of the analysis workflow follows.

Figure A3-2 shows the fracture traces measured for outcrop ASM000025, along with the stereoplot of fracture poles superimposed for reference in the upper right-hand corner. The stereoplot shows two dominant, nearly vertical fracture sets: one striking north-northeast and the other striking west-northwest. However, the fracture trace pattern appears visually to contain more than two orientation sets.

For example, the north-northeast set in the stereoplot looks to range in orientation from 340° to 60°, yet the traces in that same strike range appear to consist of at least two sets.

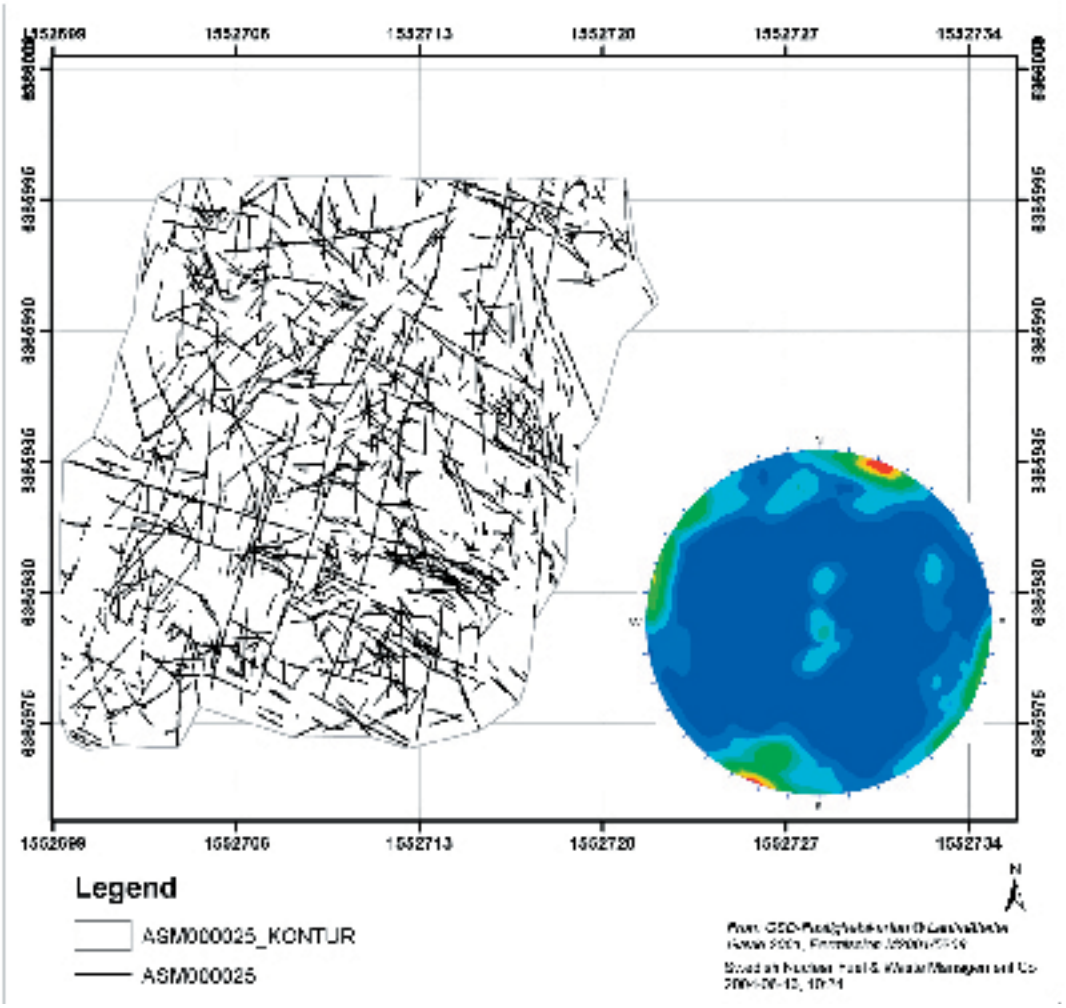

Figure A3-2. *Composite stereoplot of fracture poles and fracture traces for outcrop ASM000025.*

The visual display of the fracture pattern suggested a further subdivision into a north-south set, ranging from 340° to 10°, a north-northeast set, ranging from 10° to 30°, and a northeast set ranging from 30° to 60°.

When this subdivision is made, the resulting trace sets look geologically more reasonable (Figure A3-3 and Figure A3-4).

The next step in the analysis of the outcrop trace data was to fit an orientation model to each identified set. This was done using the ISIS algorithm in FracMan Version 2.604 /Dershowitz et al, 2003/. Next, the FracSize algorithm in FracMan™ Version 2.604 was used to fit a fracture radius model to each of these sets using the orientation model derived from the ISIS analysis.

The final step in the analysis of outcrop fracturing was to compute the mass dimension, D_m, of the fracture trace intensity. Knowledge of this parameter is important because (1) it provides evidence as to whether a Poissonian, Fractal or other type of model best describes the spatial pattern of fractures in an identified fracture trace set; and (2) it provides the basis for selecting the type of area renormalization appropriate for defining regional size models of any lineament-related fracture set.

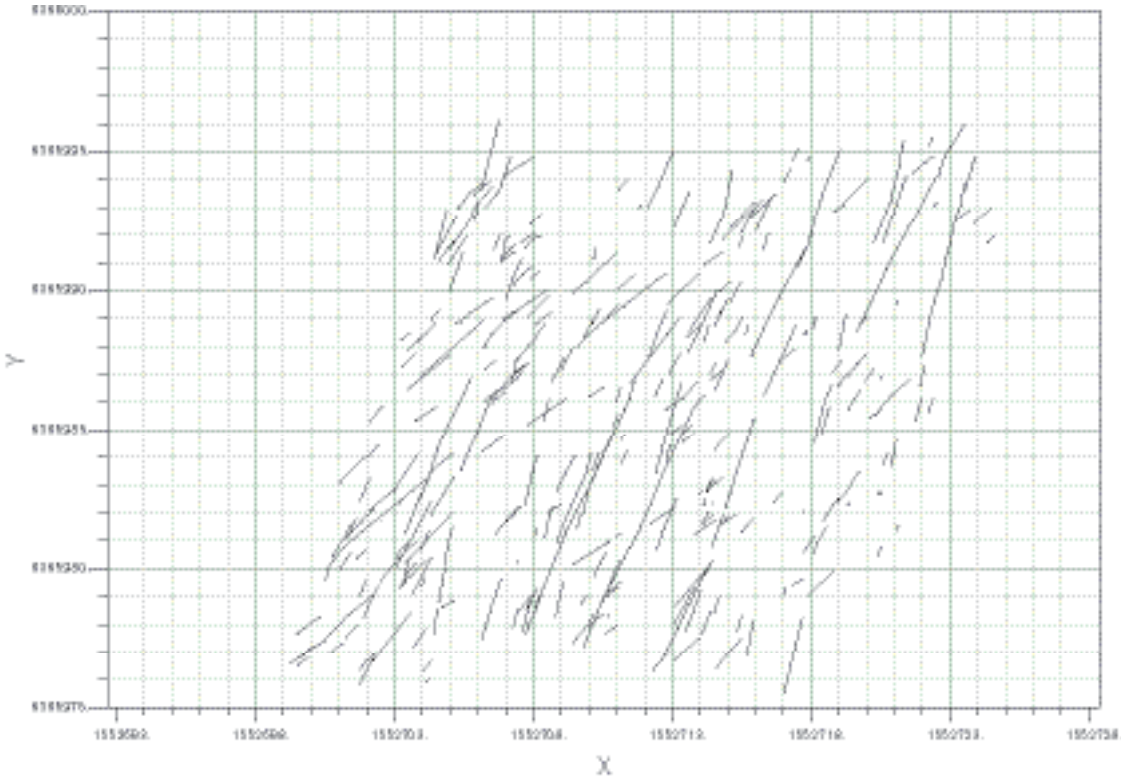

Figure A3-3. *Example of refining set definitions from stereoplots by means of trace maps (ASM000025)*

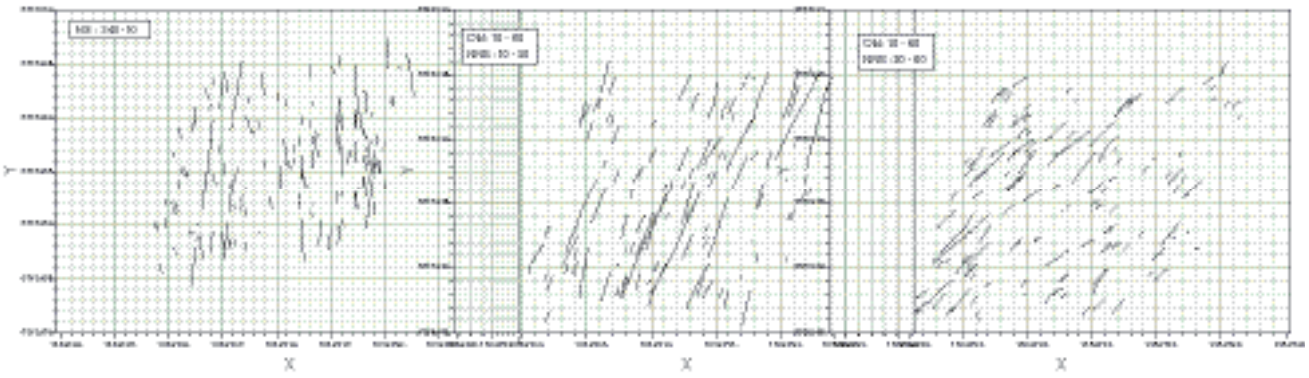

Figure A3-4. *Visual re-definition of northeast set initially defined in stereoplot into three local fracture sets (ASM000025).*

The computation of the mass dimension can take several distinct forms, such as the scaling properties of fracture center points or random points selected along the fracture trace, of the number of traces (P_{20}) themselves, or of P_{21} (fracture trace length per unit area). All are useful for particular purposes. For size-scaling analysis, the desired parameter is how the number of fractures changes with scale.

The calculation is based upon

$$N(r) = \rho * r^{D_m}$$ Equation A3-1

where ρ is a constant, termed the prefactor,

r is the radius of a circle,

D_m is the Mass Fractal dimension, and

N(r) is the number of fracture traces (partial or entire) contained within the circle of radius r.

The procedure for calculating the mass dimension is illustrated in Figure A3-5. It is important to make this calculation on individual sets rather than all of the traces at once, as each set may have different scaling properties.

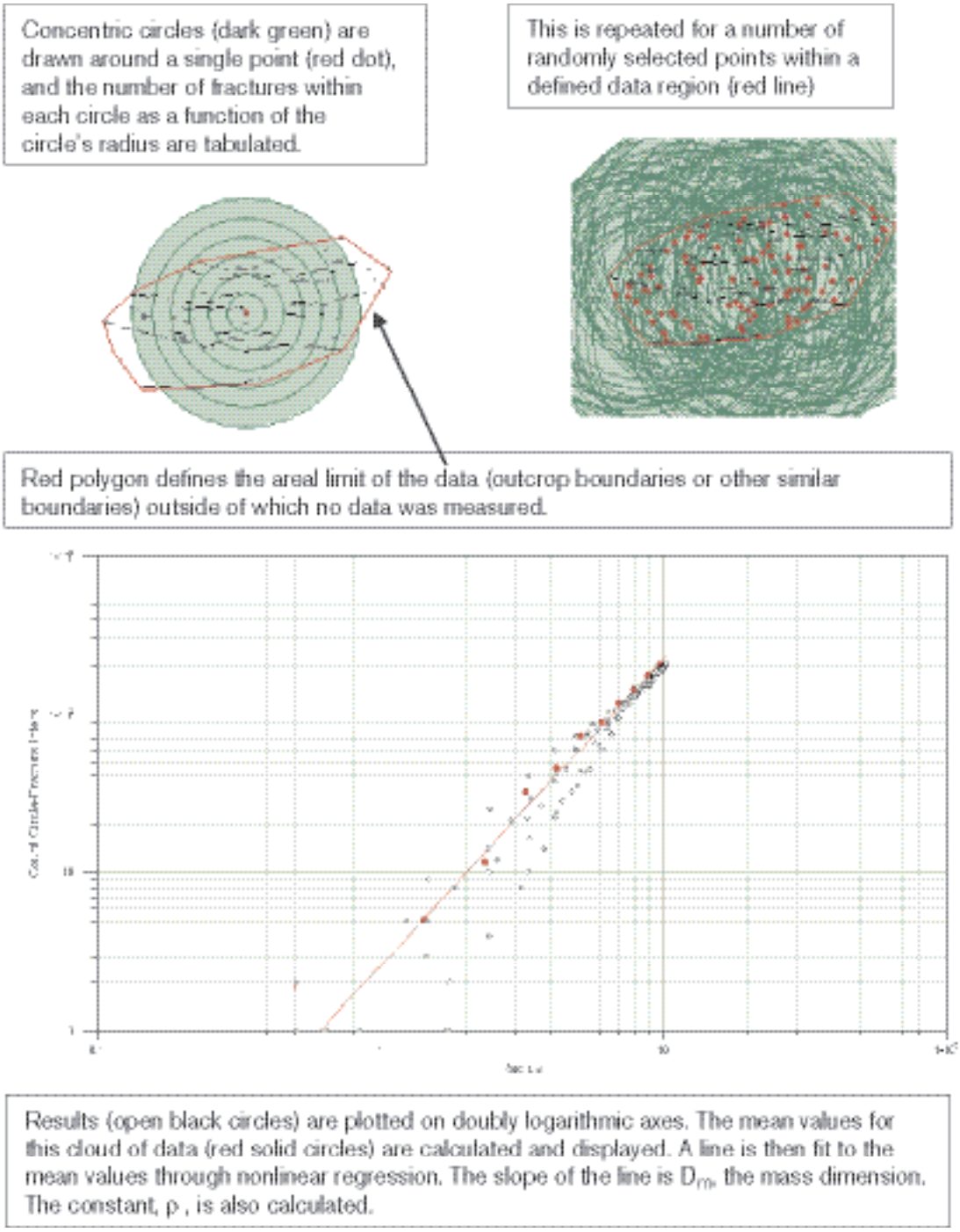

Figure A3-5. *Workflow for calculating the mass dimension from maps of fracture traces.*

A3.1.2 Lineaments

The workflow for analyzing lineament data follows a subset of the same steps used in the analysis of the outcrop trace data.

The first analysis is to determine what fracture sets in terms of strike orientation are present in the data. This was done by computing the rosette for all of the linked lineaments, as well as just for those lineaments belonging to the regional and to the local major subgroups (Figure A3-6).

The analyses were carried out on the lineament trace segments, the linked lineaments, and also trace length-weighted segments to assess whether the different treatment of the lineament data might lead to different results. In the lineament trace segment alternative, the orientation of each piecewise-linear portion of the lineament trace was treated as a single data point; a linked lineament consisting of three connected linear segments provided three data points for strike orientation. In the linked-lineament alternative, segments that had been judged to all be part of the same lineament were averaged and treated as a single data point on orientation. In the third alternative, each piecewise linear trace segment had its orientation value weighted by the segment trace length. This latter alternative helps adjust for the relative importance of a single, but very long, trace segment in comparison with two or three much shorter segments.

Once the sets for the Regional and Local Major lineament groups was determined, the trace length data for the linked lineament total length were compiled. These data were used together with outcrop data discussed in Section 1.4 for estimating a regional fracture size model for any fracture sets thought to be expressed in both the outcrop and lineament data sets.

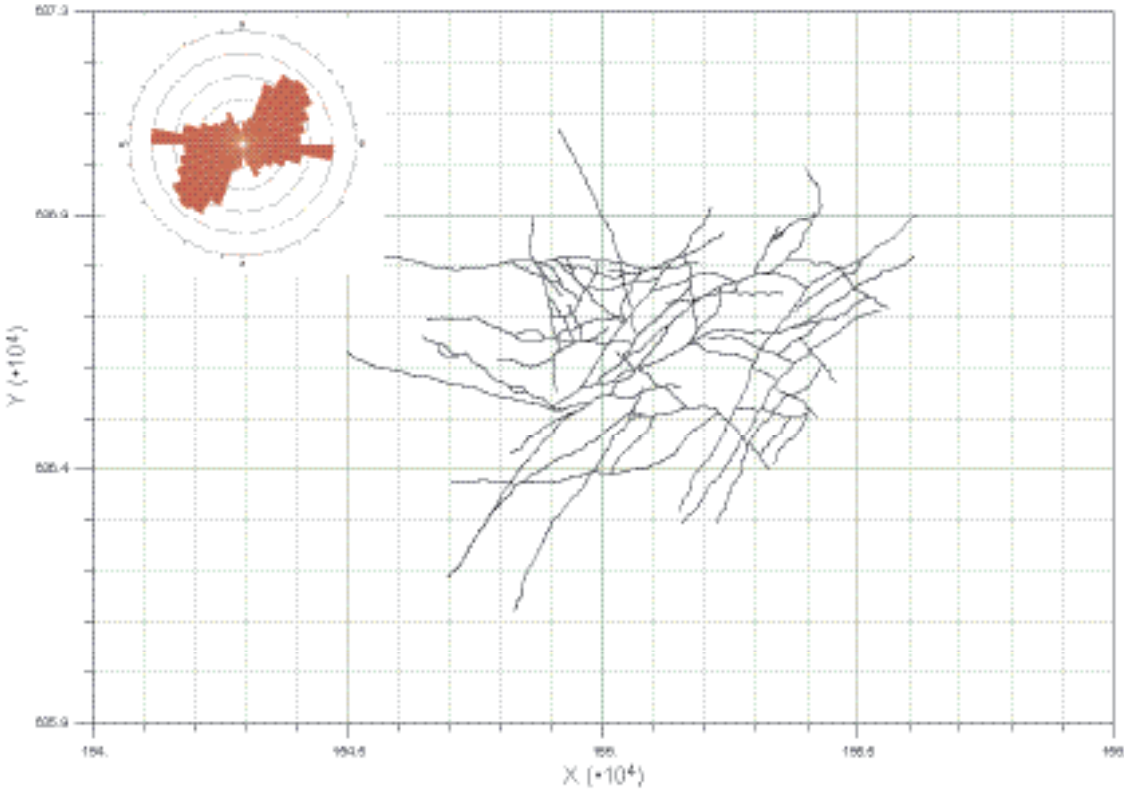

Figure A3-6. *Map of regional and local major lineaments, with rosette of trace azimuths superimposed. Definition of regional and local major lineaments is presented in Chapter 4.*

A3.1.3 Boreholes

No analyses to determine what sets might be present were carried out on the borehole data because these near-vertical boreholes severely under-represent the subvertical sets, and the corrections that can be applied to compensate increase the uncertainty substantially. As a result, the outcrop orientations were used in preference to the borehole data for set identification, as the bias correction for the outcrops produces much smaller uncertainty.

The primary uses of the borehole fracture data were to:

1. Determine whether surface stress-relief effects might have produced different fracture statistics in outcrops than at the repository depths.
2. Identify what geological factors might correlate with fracture intensity changes.
3. Determine whether and how intensity might change as a function of depth.
4. Establish parameter values for intensity and orientation for any subhorizontal fracture sets found ito be present.

Objectives 1 and 3 were addressed through Cumulative Fracture Intensity (CFI) plots (Figure A3-7). These plots are constructed by sorting the fracture data by measured depth, starting either at the top or the bottom of the borehole. The depth value is the ordinate in the CFI plot. Next, the fractures are numbered from 1 to n, where n is the total number of fractures that are to be plotted. These numbers are divided by n, such that the 1st fracture has the abscissa value of 1/n, the 2nd fracture has the value 2/n, continuing to the last fracture, which has the value of n/n or 1.

In the CFI plot, portions of the line that have constant slope indicate where the fracture intensity has a constant value. Shallow slopes indicate higher intensity, whereas steeper slopes indicate lower intensity. The range of depth values over which the line maintains constant slope indicate domains of constant fracture intensity. Surface stress-relief effects leading to a higher fracture intensity, for example, would manifest as a domain extending down from the surface possibly a few tens of meters, with a slope much shallower than found below in rock of similar geological character.

The intensity domains can also be compared to mapped geological factors such as lithology, alteration, mineral infilling and other variables to see if zones of consistently higher or lower intensity correspond to specific geological characteristics (Objective 2).

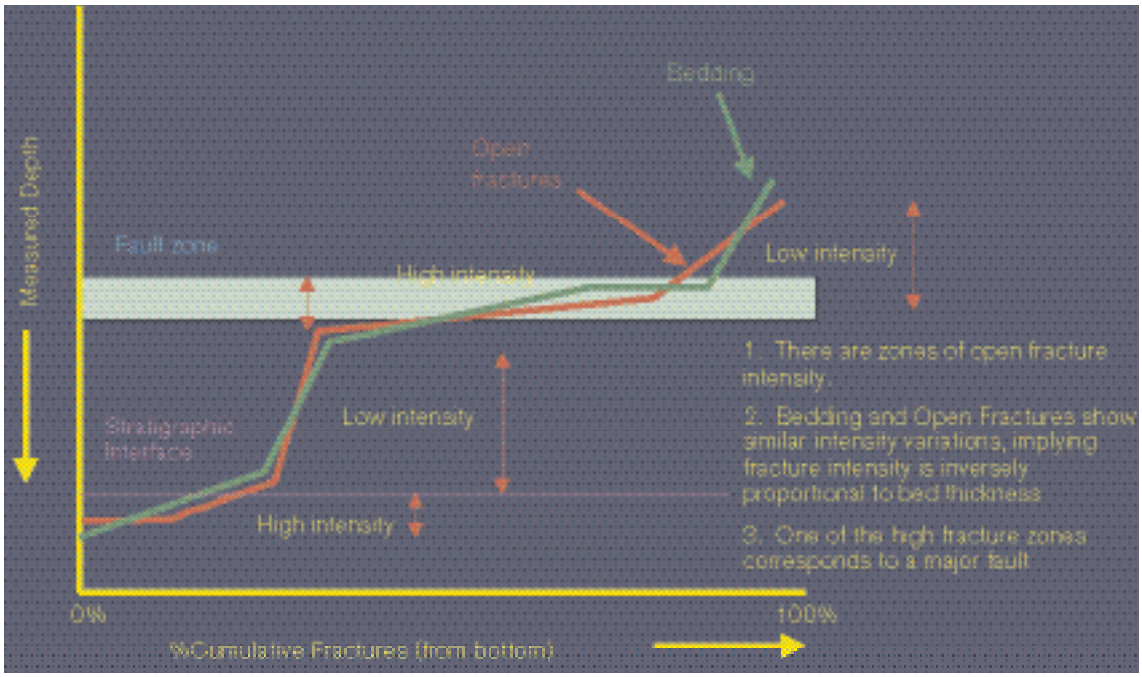

Figure A3-7. *Hypothetical Cumulative Fracture Intensity (CFI) plot.*

The fracture frequency analysis was carried out in two steps: superimposition of the CFI plots on graphical displays of geological variables to formulate testable hypotheses regarding possible geological controls; and statistical testing and analysis to refute or buttress the hypotheses. The statistical tests employed standard parametric and non-parametric tests of confidence intervals about the mean and median, tests to examine the similarities of means and medians among groups, and linear regression. CFI plots were constructed using Excel2000©/MicroSoft Corporation, 2000/ Statistical analyses were carried out using the Excel Add-In Analyse-It© Version 1.71 /Analyse-It Software Ltd, 2003/.

Additional analyses to complete Objectives 1–3 involved constructing depth vs. orientation plots to see if orientations remained constant throughout, or whether there are zones with distinct orientations, such as the absence of a set or the addition of a new set. Depth vs. orientation plots were constructed using Excel2000©.

Objective 4 was achieved by separating out the subhorizontal fracturing, and then determining values for intensity and orientation. Horizontal fracture intensity domains were identified through CFI plots, whereas orientation statistics were generated using the ISIS module of FracMan™ Version 2.604 /Dershowitz et al, 2003/.

A3.1.4 Assessment of regional geological controls on fracturing and specification of the regional site model

As previously described, the development of the Simpevarp site model is built upon the analyses of individual local data sets from boreholes and outcrops together with regional lineament patterns. A critical question is how consistent the results are among the local data sets. For example, are the controls on fracture intensity identified in one borehole consistent with the controls identified in other boreholes and at outcrop? Do the fracture sets defined at each outcrop appear at all other outcrops, or do some outcrops have unique sets? Are any of these sets found at outcrop related to the sets identified in the lineament data? If so, is there further evidence that the outcrop and lineament data sets are size-limited subsets of single parent fracture populations whose sizes span the range from outcrop to lineament?

Once these and related questions are satisfactorily resolved, it is possible to aggregate the local data in ways that are consistent with the resolution, and summarize or re-analyze these aggregated groups of data to derive the regional site-scale fracture model parameters.

A3.1.4.1 Similarity of sets in outcrop

The assessment of whether the same sets are present in outcrop relies upon the qualitative evaluation of several factors, as outlined below (Figure A3-8):

The primary observations to decide whether any sets identified in individual outcrops form part of a regional set are whether the orientations are similar AND the sets are in the same approximate chronological order; or if their orientations differ, do they still occupy about the same place in the chronological order AND can the difference in orientation be explained by changes in the lineament geometry? The rationale for this decision tree is that similarity in orientation may be insufficient given the large number of sets in each outcrop. Adding the additional constraint that the set order in the relative chronology should be approximately the same helps to provide confidence that the sets in each outcrop are actually part of a regional set. On the other hand, it may be that the stress pattern has rotated slightly, so that the fracturing that was developing at a particular time has somewhat different orientations in different outcrops. If this were the case, then it would be expected that the relative set chronology would be very similar, and that the orientations would reflect the difference in the orientations of the lineament pattern near the outcrop.

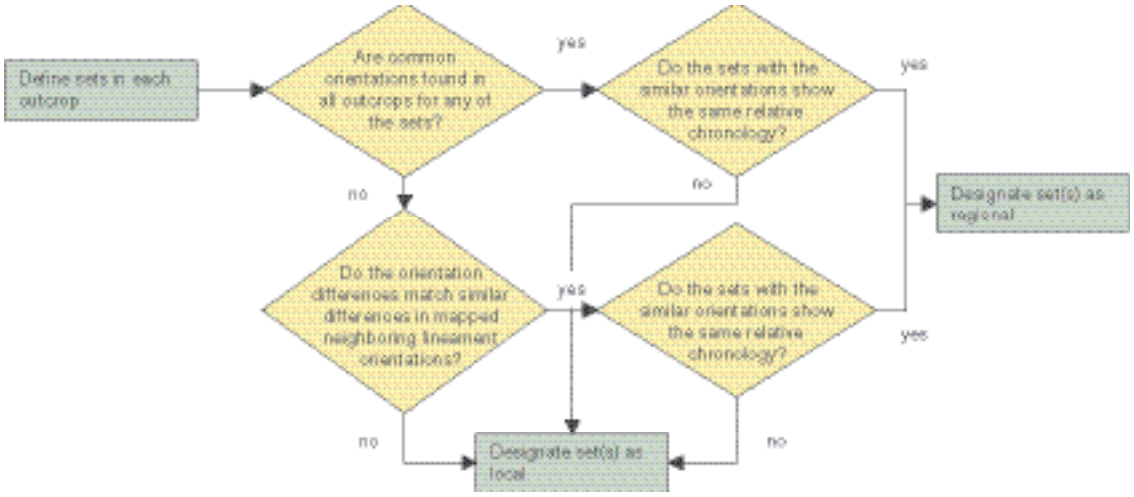

Figure A3-8. *Decision tree for identifying sets identified in separate outcrops as belonging to a regional fracture set.*

A3.1.4.2 Relation to lineaments

Figure 1-8 allows account to be taken of the possibility that lineament pattern geometry may change spatially within the local model domain under study. If fractures found in outcrop were formed at the same time and in response to the same stress system that formed the lineaments, then it would be expected that one or more outcrop regional sets would correspond to lineaments. When fractures at outcrop were among the earliest formed, and are possible old, as can be implied if they are filled with minerals thought to be formed early in the history such as epidote /Munier, 1989/, then it is likely that the regional outcrop set and the corresponding lineament set are samples from a single fracture population that spans a size range from at least as small as fractures seen at outcrop, to at least as large as lineaments. These sets are termed “lineament-related sets” (Figure A3-9).

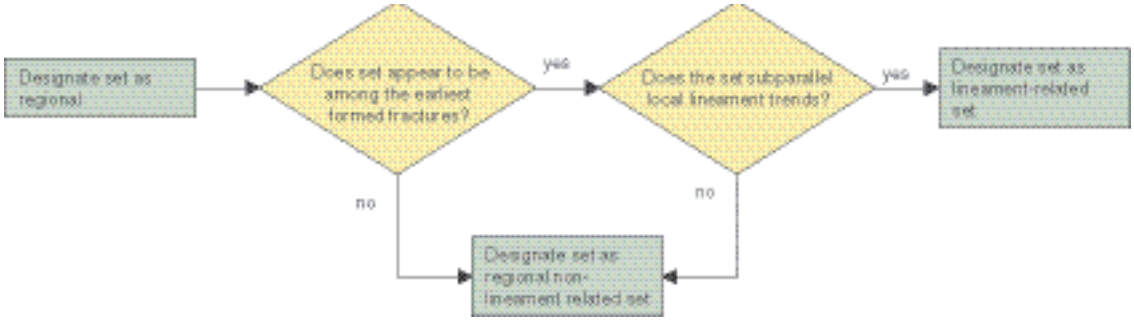

Figure A3-9. *Decision tree for identifying lineament-related sets.*

A3.1.5 Size analysis of lineament-related fracture sets

The methodology for analyzing the size of lineament-related fracture sets has been presented by /La Pointe, 2001/ and consists of a two-stage process. The first stage is to determine how fracture intensity for an individual fracture set scales with area. The second stage is to use this information to interpret fracture trace data acquired over regions of different area.

The goal of this analysis is to relate the number of fractures in a given interval of trace length measured over an area, A_i, to the number of fractures in the same size class measured over an area, A_j, of a different size. A simple way of resolving this issue is to assume that the number of fractures in a particular size class scales with area; if the area is doubled, the numbers of fractures are doubled. When the number scales linearly with area, as in this example, the scaling is termed Euclidean.

However, it is not necessary that fracture intensity should scale according to a simple Euclidean rule. In fact, fracture intensity could scale according to fractal or other non-Euclidean functions, as has been shown previously for many regions in Sweden and in Finland /La Pointe, 2002/. In these cases, Euclidean scaling will produce errors when data measured over different sized regions are combined.

The calculation of the fractal mass dimension is used to determine whether Euclidean, Fractal or some other function best characterizes the scaling behavior of each individual lineament-related fracture set. The mass dimension exponent can vary from 2.0, which indicates Euclidean scaling, to lower values that imply that the traces scale in a fractal manner.

The procedure is to calculate and plot the cloud of mass dimension data points, as in Figure A3-5, and then compute a nonlinear least-squares fit of Equation A3-4 to the locus of the mean and test for statistical significance. If the regression is found significant at the $\alpha = 0.05$ level, then the regression is deemed significant and the scaling is treated as fractal. The calculations are always performed on the data set with the least censoring on the small trace end of the distribution, as censoring produces an underestimation of the number of fractures per unit area. For this reason, the mass dimensions were always calculated on the outcrop trace data rather than the lineament data.

The second stage is to use these results to combine data obtained over regions of very different area. The process is as follows:

Let the “o” subscript denote outcrop, and the “l” subscript denote lineament. Furthermore, let the variable “A” denote the area of the outcrop or lineament map, and “R” denote the radius of an imaginary circle that would have the same area as “A”. Also, let “x” represent the trace length of a fracture. Then, from Equation A3-1, it is possible to calculate the number of fracture traces that would be expected in the lineament map area based on what was measured in the outcrop area. At the lineament scale::

$$A_j = \pi R_j^2$$

$$\text{so } R_j = \sqrt{\frac{A_j}{\pi}}$$

$$\text{and } N(R_j) = \rho R_j^{D_0}$$

Equation A3-2

Equation A3-3 makes it possible to compensate for the difference in area by computing a normalization factor that is the ratio of the number of fracture traces measured in outcrop to the number estimated in Equation A3-2:

$$NF = N(R_o) / N(R_l)$$

Equation A3-3

This equation also describes how many fractures would be expected in an area of any size, for example, a reference area of 1 square metre.

It is easiest when comparing multiple data sets to reference all of them to an easily converted reference scale like the number of fractures per square metre. In this case, Equation A3-3 becomes:

$$NF_i = N(R_i) / N(\sqrt{\frac{1}{\pi}})$$

Equation A3-4

where NF_i is the correction factor for converting the number of fractures actually measured in a domain, *i*, to the reference domain,

$N(R_i)$ is the number of fracture traces measured in domain *i*, and

$N(1/\pi)$ is the number of fractures in an area of 1 m^2 estimated from Equation A3-2.

To construct the plot, the trace lengths actually measured in the domain are ordered from shortest to longest. Each trace is numbered according to its cumulative frequency. If k_i fracture traces were measured in domain *I*, then the shortest trace has the cumulative frequency value of k_i, and the next longest has the value of $k_i–1$, and so on such that the longest trace measured has the value of *1*. Next, these cumulative frequency numbers are each multiplied by NF_i. The values are plotted with the normalized cumulative frequency value on the ordinate (Y-axis), and the trace length value on the abscissa (X-axis) as shown in Figure A3-10.

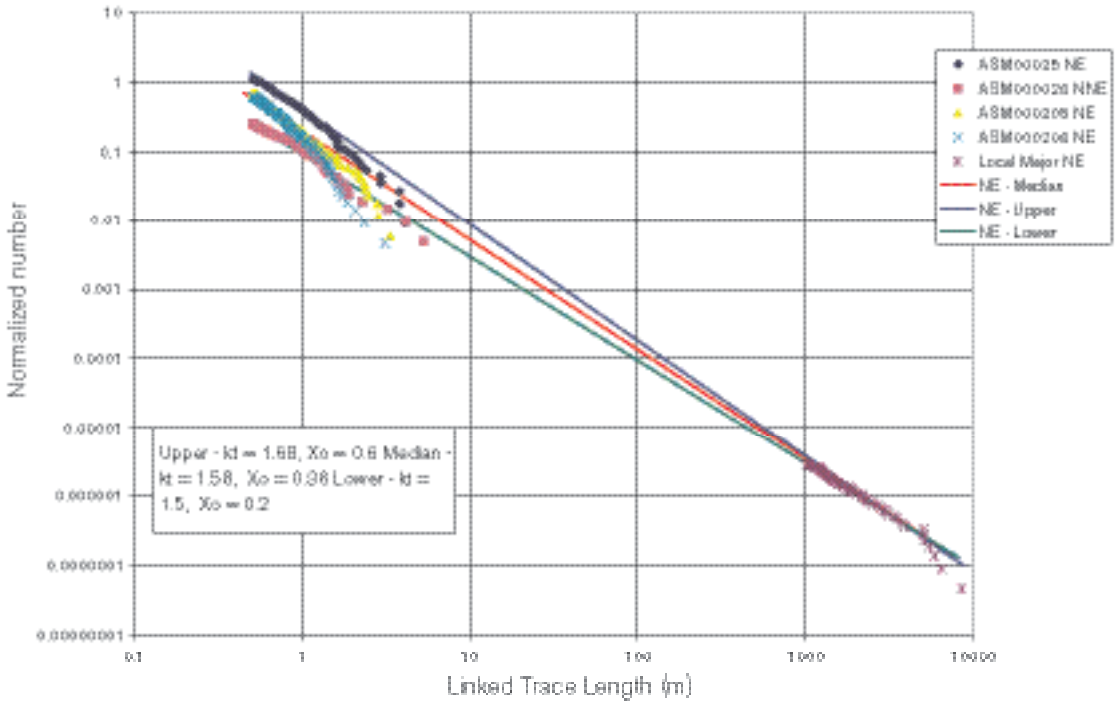

Figure A3-10. *Example of trace length model estimation plot resulting from fractal mass dimension normalization of fracture intensity with area. Plot shown is for the NE lineament-related regional fracture set.*

This graph shows the results of normalization of 6 outcrop sets, the lineament set, and a model fitted to the composite data.

The equation of the red line shown on the figure is also in a power law form. The complementary cumulative probability density (CCDF) function, which is quantified by this line, has the functional form:

$$Prob(x \geq x_0) = \left(\frac{x_0}{x} \right)^{k_t}$$

Equation A3-5

where x_0 is the minimum trace length,

x is any trace length greater than or equal to x_0,

k_t is the Trace Length Dimension, and

$Prob(x \geq x_0)$ is the probability that x is greater than or equal to x_0.

The parameter k_t is the slope of the red line on Figure A3-8, while the parameter x_0 is calculated from the intercept of the line.

Note that the parameter k_t is not the same as the mass fractal dimension, D_m! They are, in fact, independent parameters.

Finally, it is necessary to estimate the fracture *radius* distribution of the fracture population in the rock volume. This can be done following /La Pointe, 2002/.

In effect, the necessary values can be calculated from the trace length parameter values according to:

$$k_r(radius) = k_t(traces) + 1.0$$
$$x_0(radius) = x_0(traces) * \frac{2}{\pi}$$

Equation A3-6

A3.1.6 Regional consistency of geological controls on fracture intensity

The regional consistency of geological controls are evaluated by testing the observations made in the boreholes, primarily KSH01A, against the observed open fracture intensity variations in the outcrops. If the same relations are found, then the confidence that the geological controls on fracture intensity are regional is increased.

A3.1.6.1 Chronology of sets

The chronology of fracture sets is based upon three semi-quantitative parameters:

- Whether one set consistently terminates against another set.
- Whether a set that appears to be earlier based on terminations has long traces, or a set that appears to be younger has short traces.
- Whether a set that appears to be earlier based on terminations has more uniformly or periodically distributed traces, or a set that appears to be younger exhibits spatially restricted traces.

These three observational criteria are used to classify fracture sets as early or late (or somewhere in between) in their relative formation chronology (Figure A3-11 and Figure A3-12).

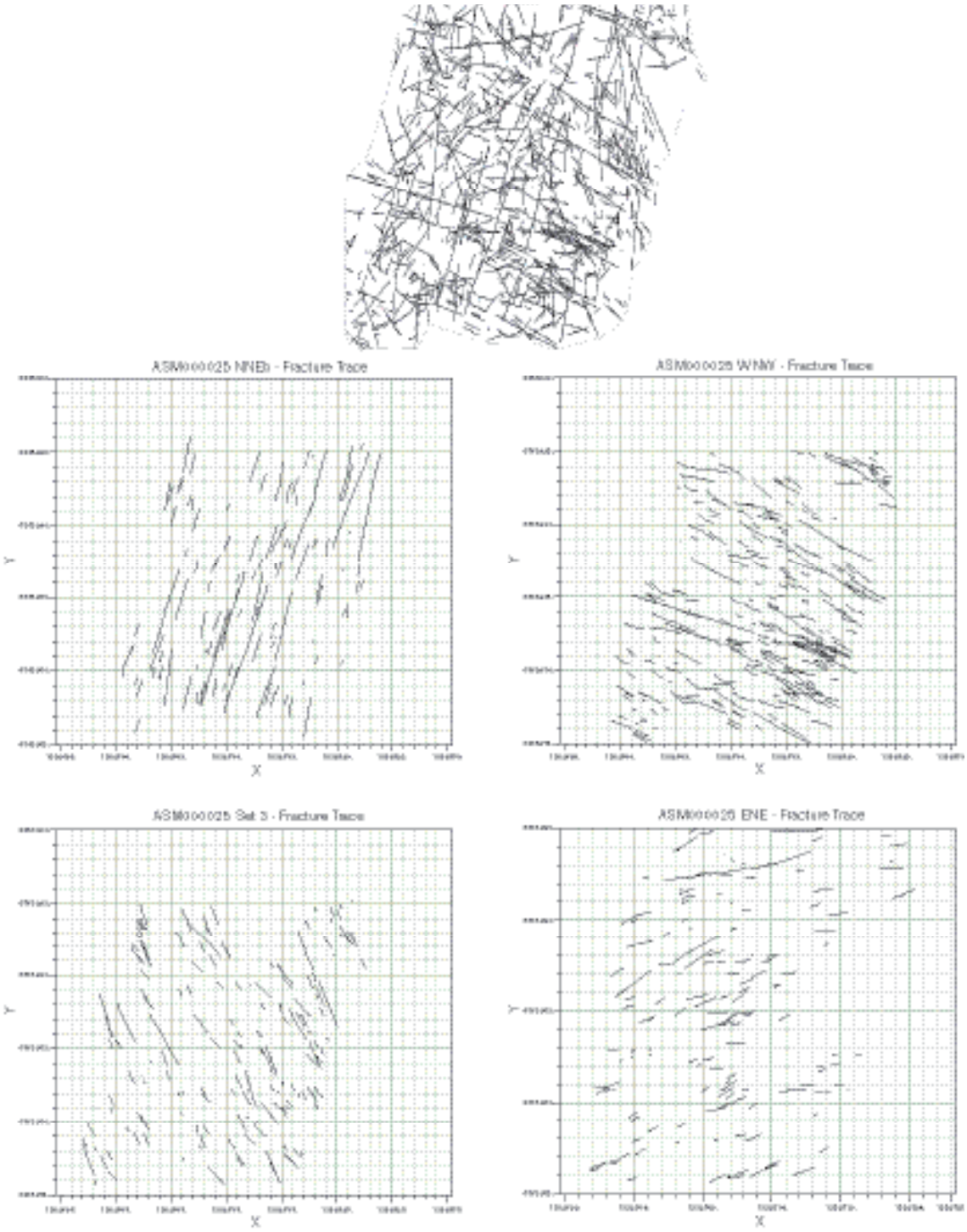

Figure A3-11. *Methodology for assigning chronology to identified outcrop fracture sets.*

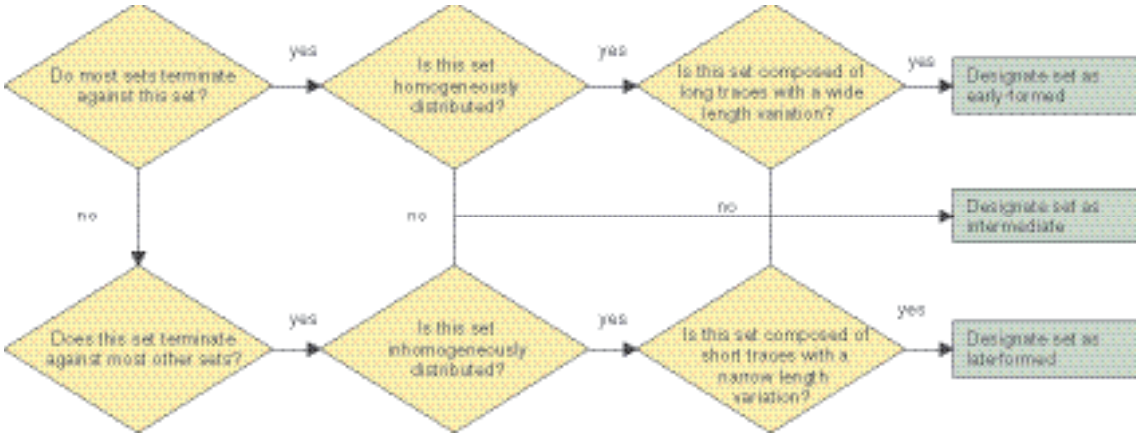

Figure A3-12. *Decision tree for identifying set chronology.*

Figure A3-11 shows an interpretation for outcrop ASM000025. The oldest sets (shown as the topmost two inset diagrams) have long traces that are homogeneously scattered over the outcrop. The WNW set, however, shows some indications of banding caused by its terminations against the NNE set. The sets shown in the two bottom most inset diagrams have shorter traces and show pronounced terminations against other sets, leading to much more of a banded appearance. They are also not as pervasively distributed across the outcrop. As a consequence, the NNE set is interpreted to be the oldest formed, followed by the WNW, and then followed by the remaining two sets whose relative chronology is harder to distinguish.

A3.1.6.2 Consistency of site model with tectonic and geological history

Confidence is improved in the regional site model if the conclusions made are consistent with what is known concerning the tectonic and magmatic history of the region. For example, sets identified as regional lineament-related should show orientations that are as would be expected from the tectonic stresses that the rock has experienced in the past. Also, fracture sets identified as old should show mineral fillings indicative of a time when the rock was much hotter and under greater pressure. In this respect, epidote-filled fractures should be among the very oldest, as epidote probably was mobile not much later than about 1.4 Ga ago /Munier, 1989/.

A3.1.7 Quantification and propagation of uncertainty

Uncertainty in the model derives from several sources, including the uncertainty inherent in the data variability among the various outcrops and boreholes, as well as in the conceptual model in which the data is used.

The uncertainty in fracture orientation has been quantified by calculating the orientation dispersion for each set at each of the four outcrops. Since there are many alternative ways to aggregate the data at each outcrop, for example, by weighting by area or by fracture intensity, it is left to the modellers to decide the best way to propagate the uncertainty for their own purposes.

The uncertainty in size is quantified in two different ways. For local fracture sets, the size model for the parent fracture radius distributions are based on aggregating all of the outcrop data for that set, and estimating a model for the distribution of fracture radii. For the lineament-related sets, three values are given: two bounding cases and a ”best estimate”. Because of artefacts having to do with censoring of trace length data, the trace length model fit to the normalised data is done visually rather than through non-linear regression. The ”best estimate” is the best visual fit through all of the outcrop and lineament data. The two bounding cases are lines that approximate the shallowest and steepest lines that could be fit through the data. These represent the span of possible size variation given the existing data. As in the case of orientations, it is up to the user of these data to decide which parameter values to select.

The intensity of fracturing is specified as a function of the geological factors in terms of the mean and standard deviation of P_{32}. The user of this information should decide whether a mean value suffices, or whether something more complex, such as a Monte Carlo sample from the distribution, is appropriate for the intended usage.

A3.1.7.1 Validation

It is not possible to validate this model given the existing data, as it is based on all existing data. Although it would have been beneficial from the standpoint of validation to withhold some of the data, there were not enough data to do this and still develop a reasonable model for such parameters as intensity, orientation and size. It will be appropriate to validate the present model against new data when these are obtained.

A3.2 Geometrical DFN modelling – a complement to section 5.1.6 in the main report

This section of Appendix 4 presents a number of plots and tables that were used in the analysis of data, but were left out of the main report. These plots are not necessary for understanding the process of the geometrical modelling described in the main report, but are presented here for completeness and for readers who wish to go deeper into the geological DFN analysis. References to each step in the analysis process is made in the main report for easy access to diagrams and tables.

A3.2.1 Identification of fracture sets

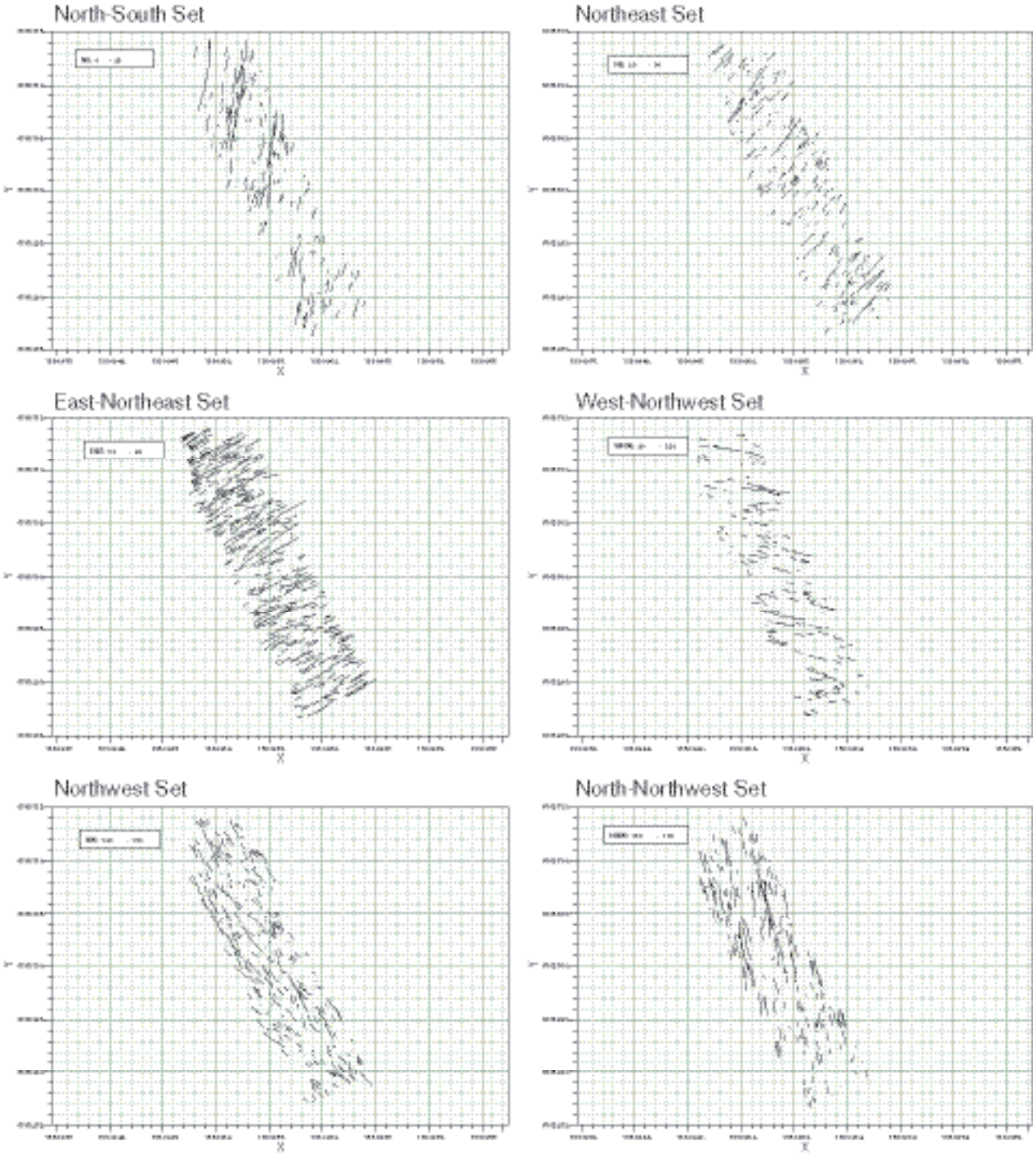

Figure A3-13. *Trace sets in ASM000205.*

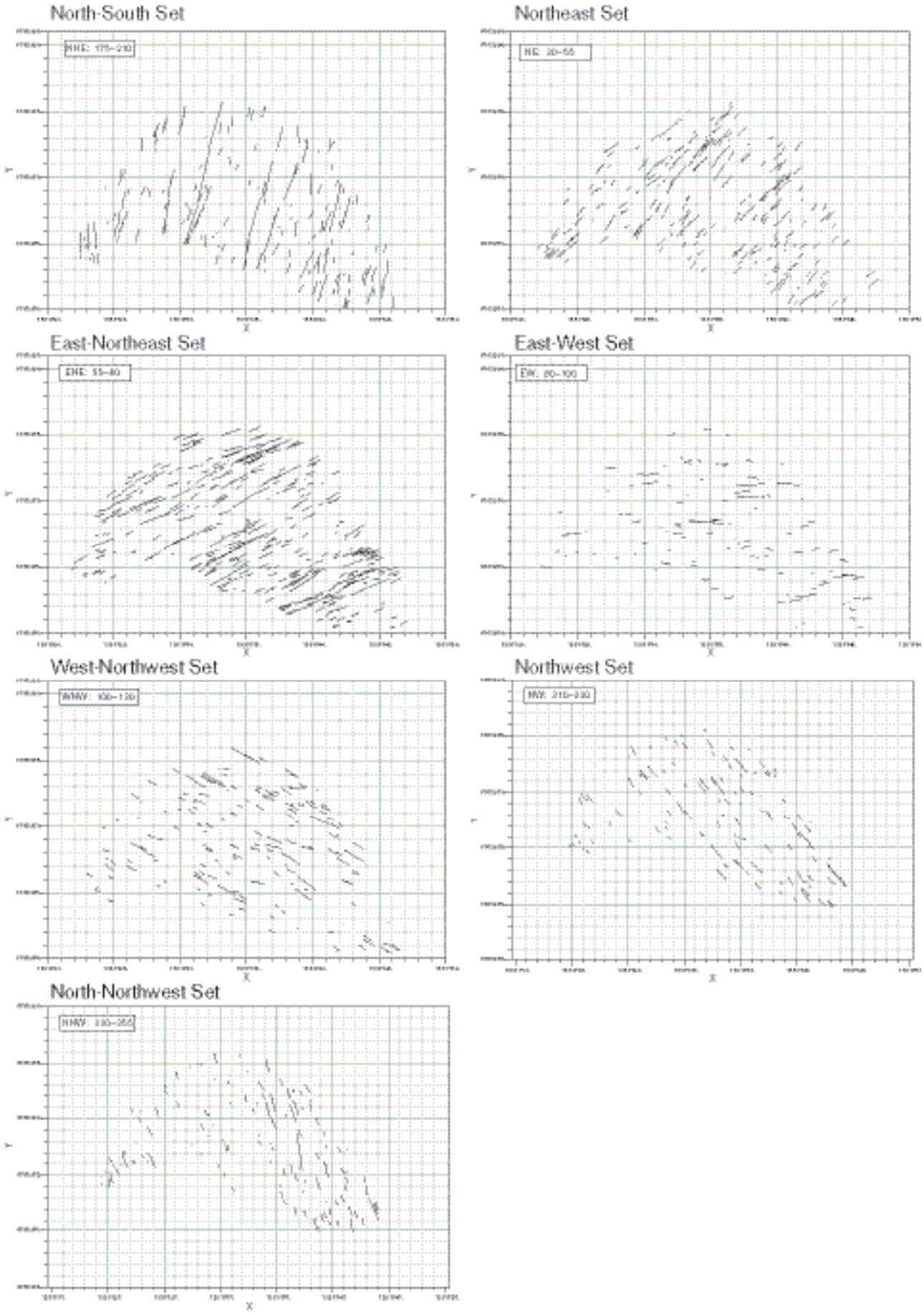

Figure A3-14. *Trace sets in ASM000206.*

A3.2.2 Fracture size estimation

A3.2.2.1 Mass dimension analyses

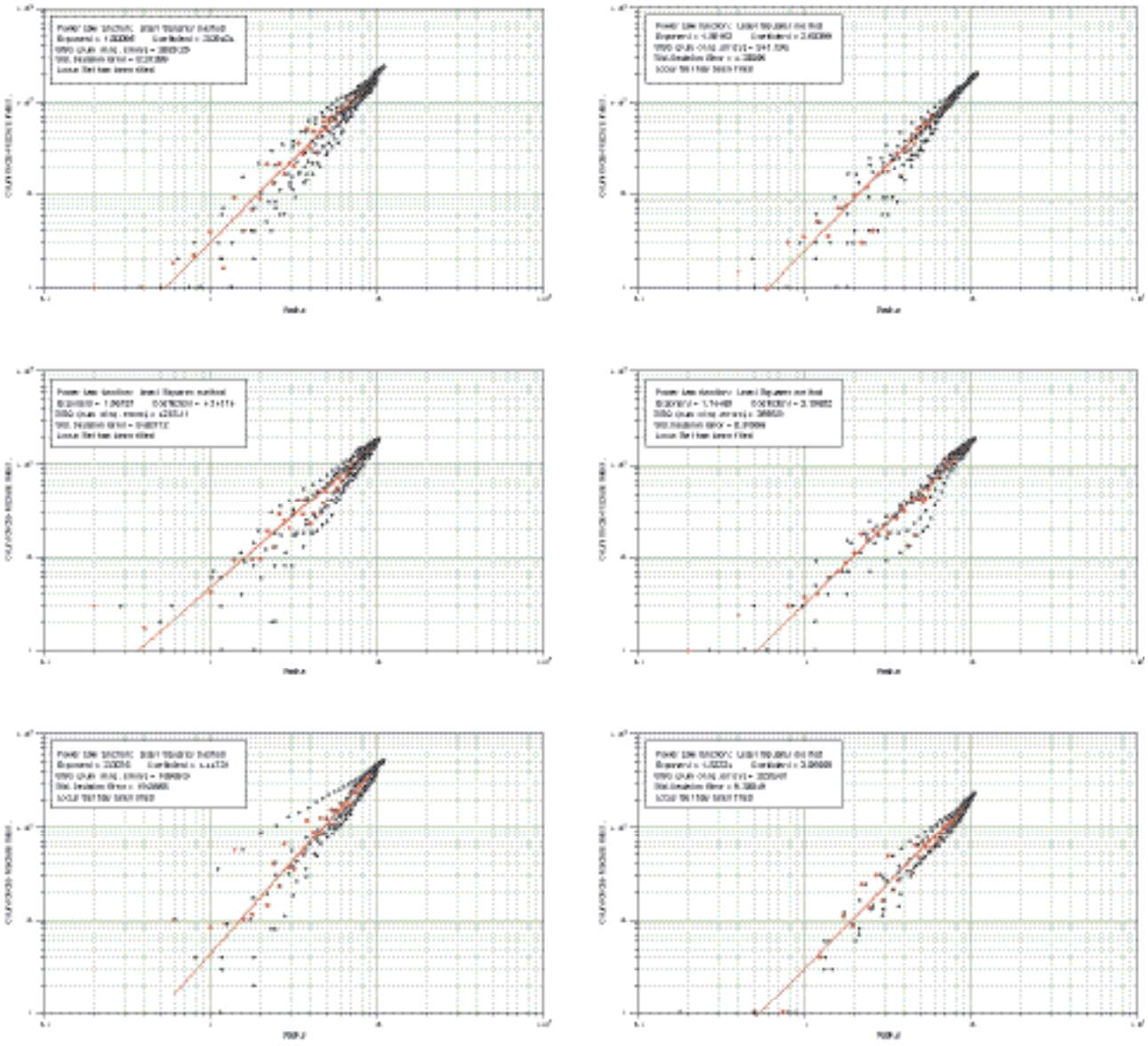

Figure A3-15. *Mass dimension calculations for individual fracture sets identified in outcrop ASM000025.*

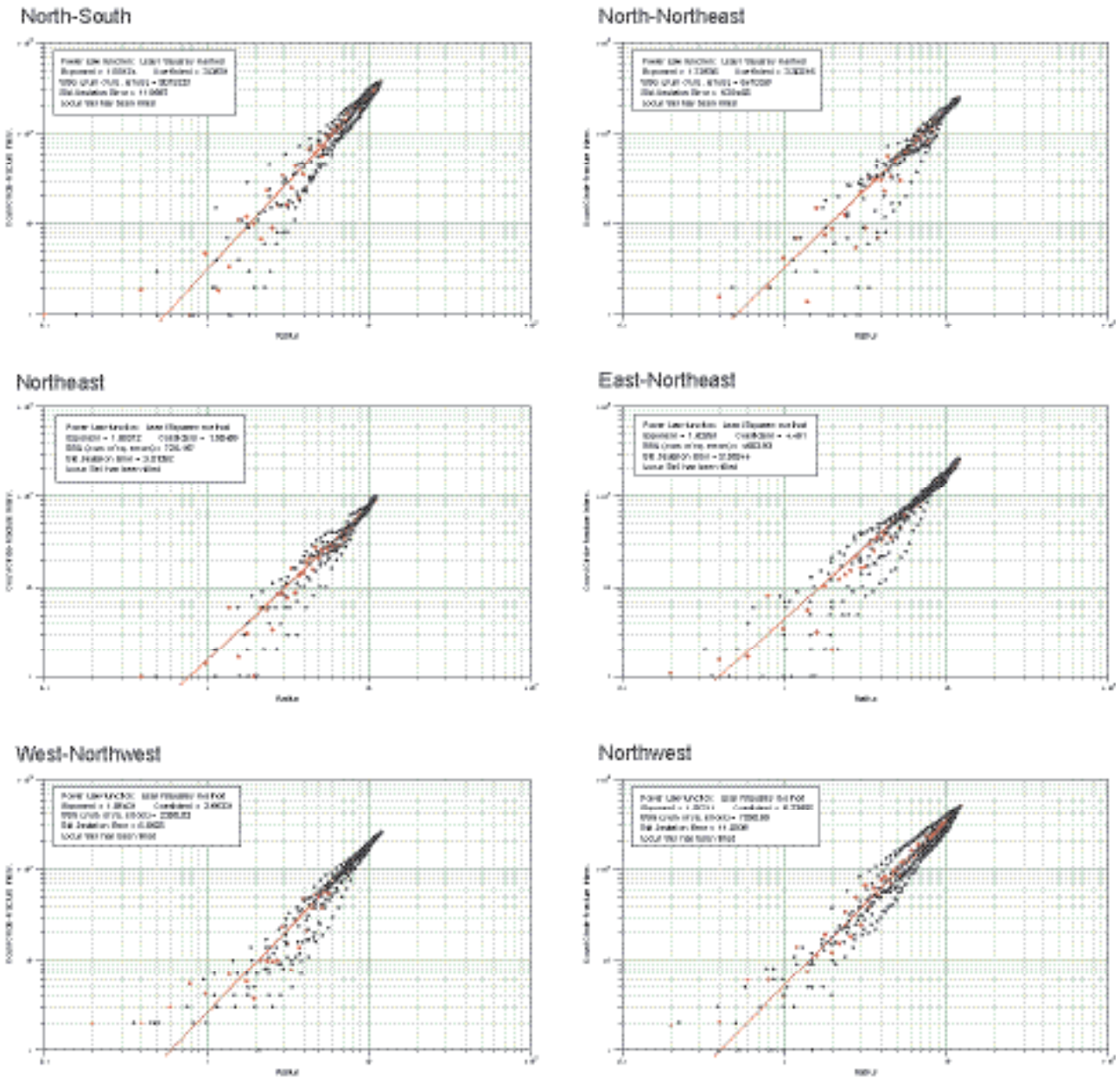

Figure A3-16. *Mass dimension calculations for individual fracture sets identified in outcrop ASM000026.*

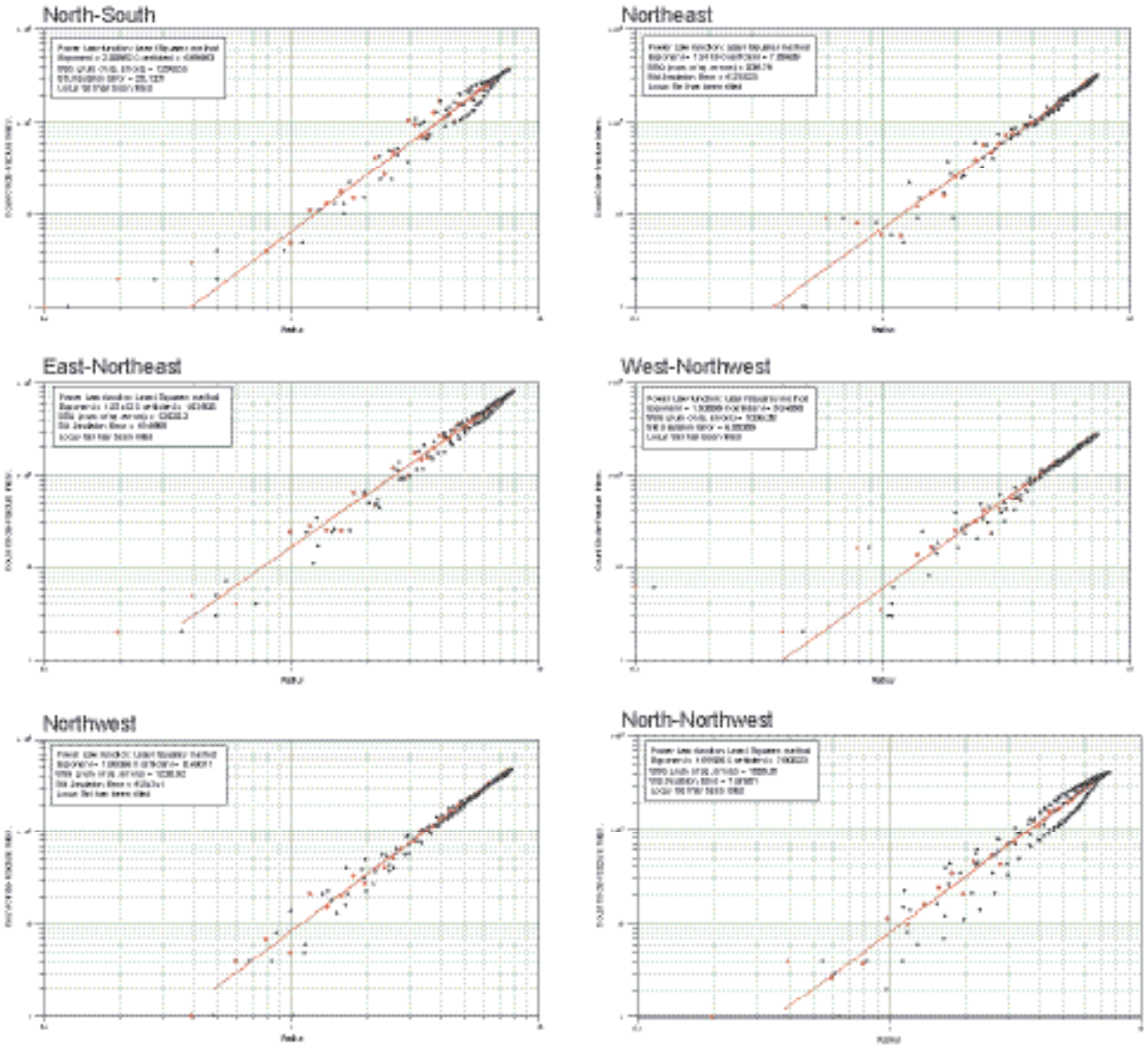

Figure A3-17. *Mass dimension calculations for individual fracture sets identified in outcrop ASM000205.*

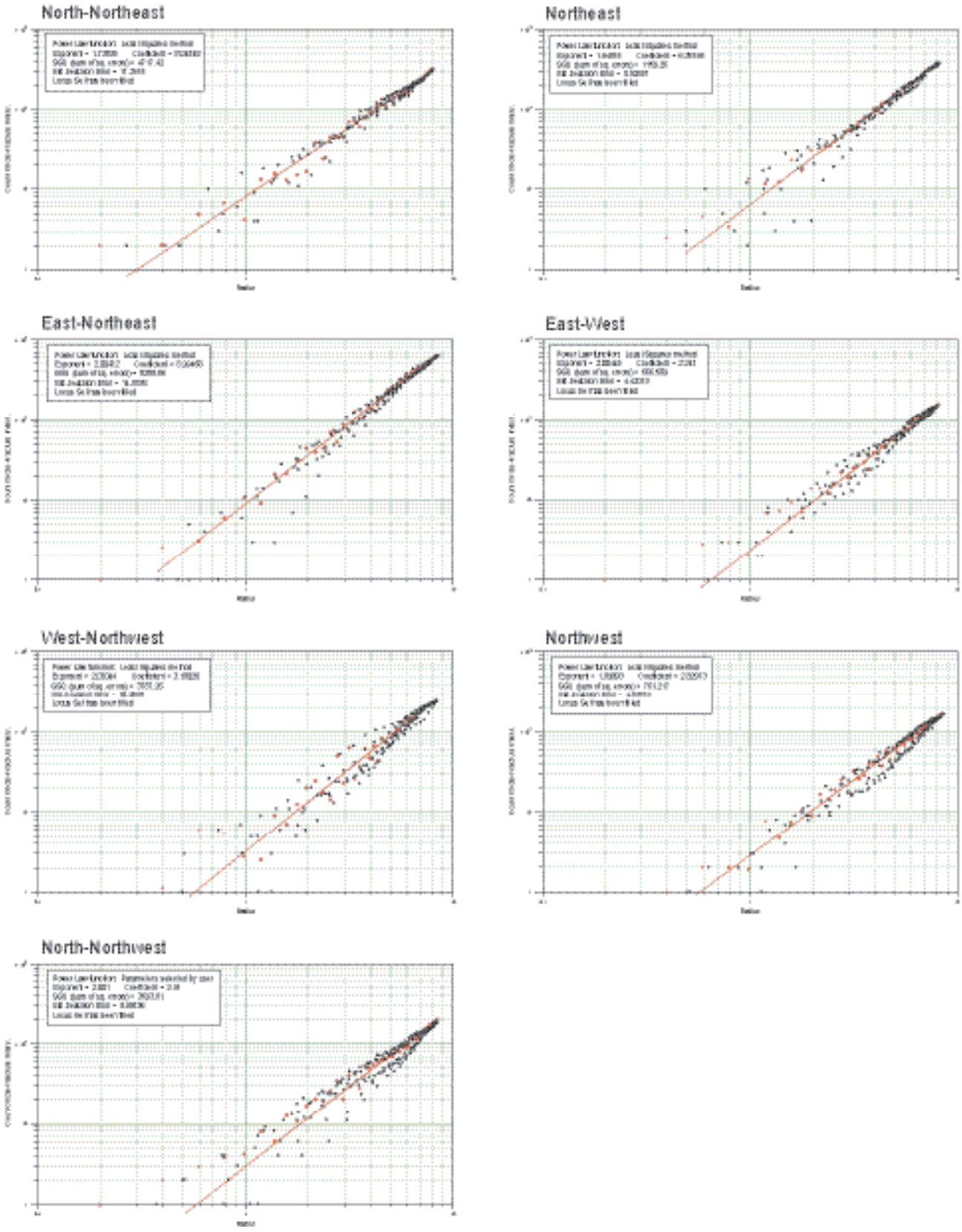

Figure A3-18. *Mass dimension calculations for individual fracture sets identified in outcrop ASM000206.*

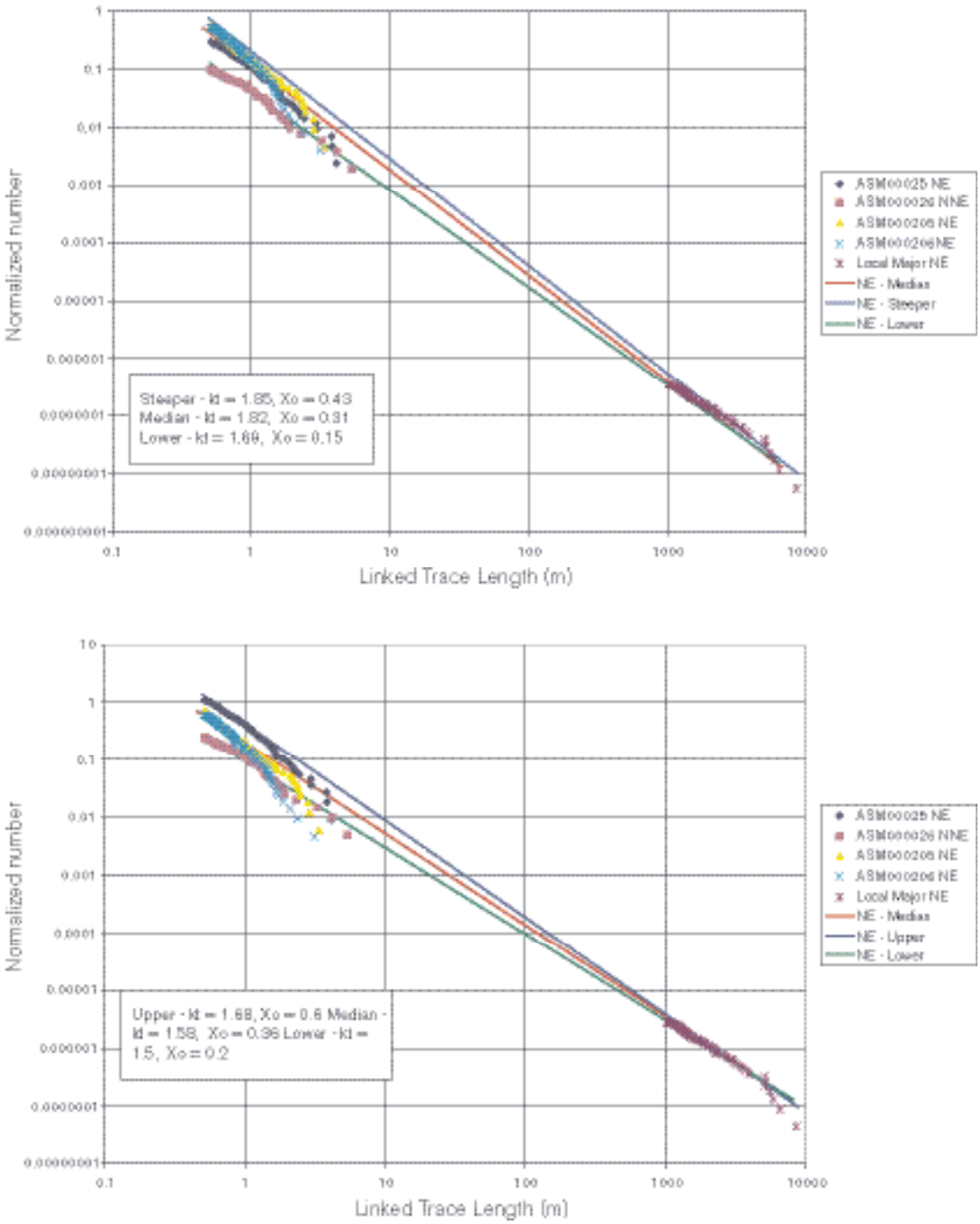

Figure A3-19. *Fracture size calculation for the northeast lineament-related fracture set. Euclidean analysis is shown on top; mass dimension renormalisation is shown at bottom.*

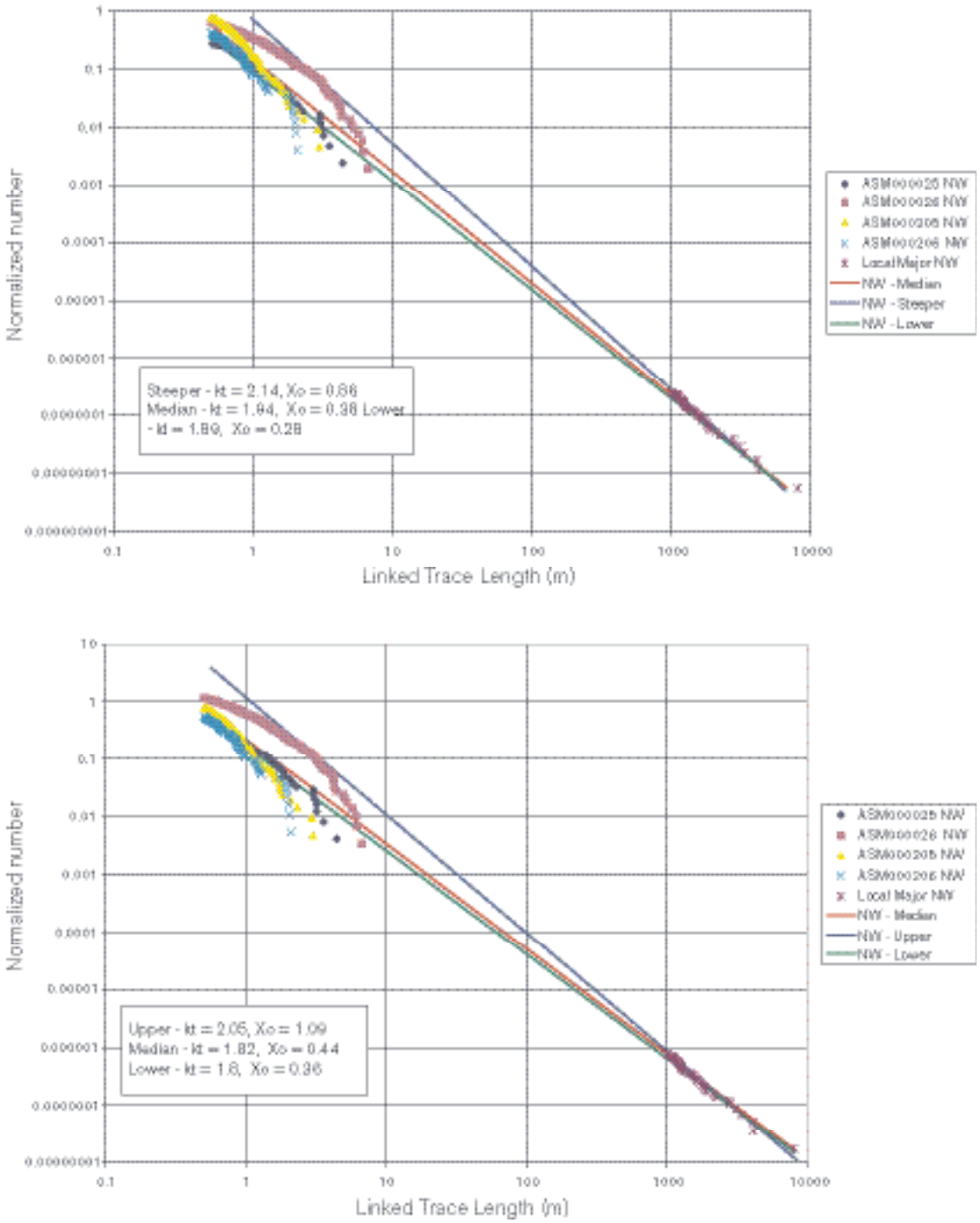

Figure A3-20. *Fracture size calculation for the northwest lineament-related fracture set. Euclidean analysis is shown on top; mass dimension renormalisation is shown at bottom.*

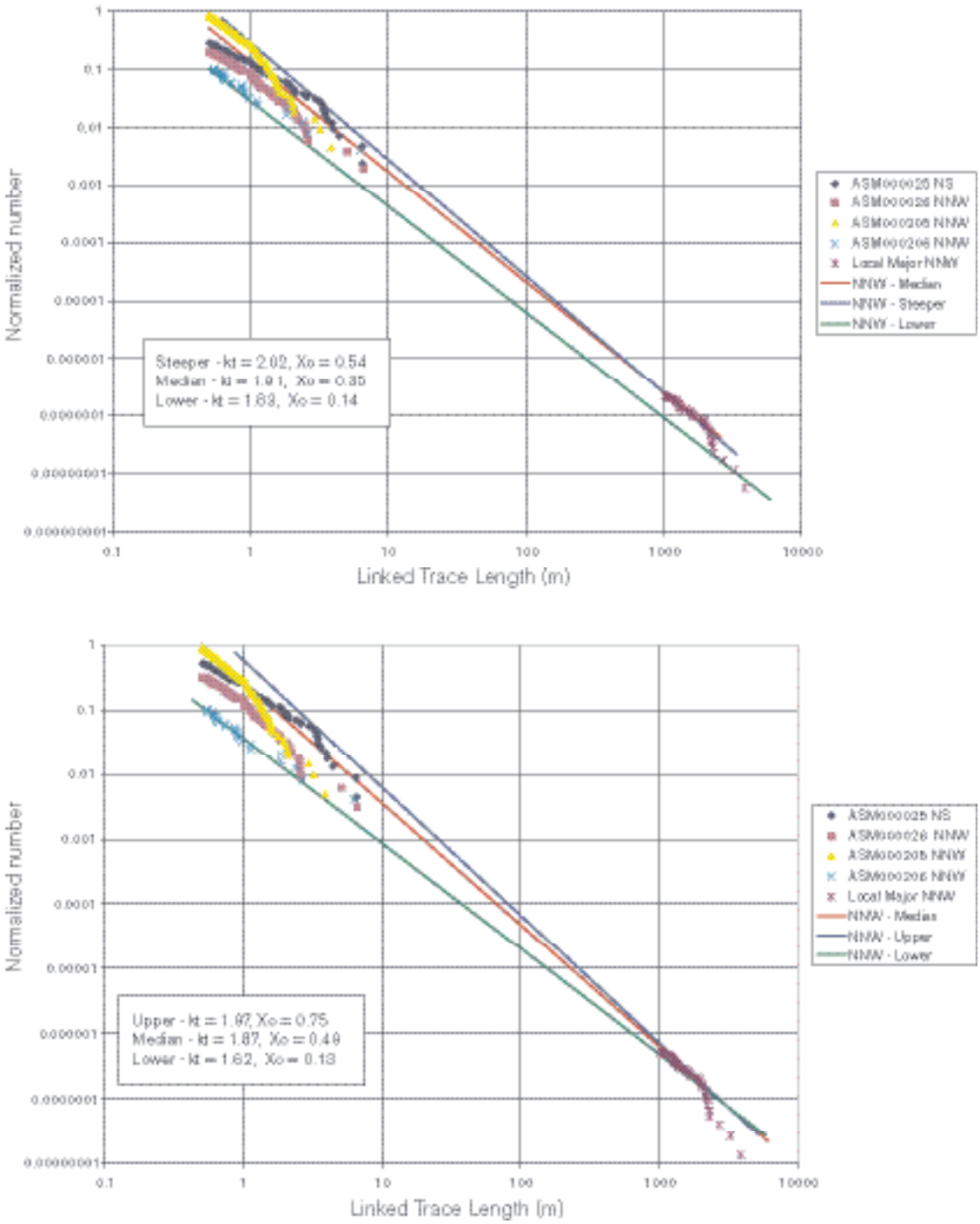

Figure A3-21. *Fracture size calculation for the west-northwest lineament-related fracture set. Euclidean analysis is shown on top; mass dimension renormalisation is shown at bottom.*

A3.2.3 Fracture intensity analysis

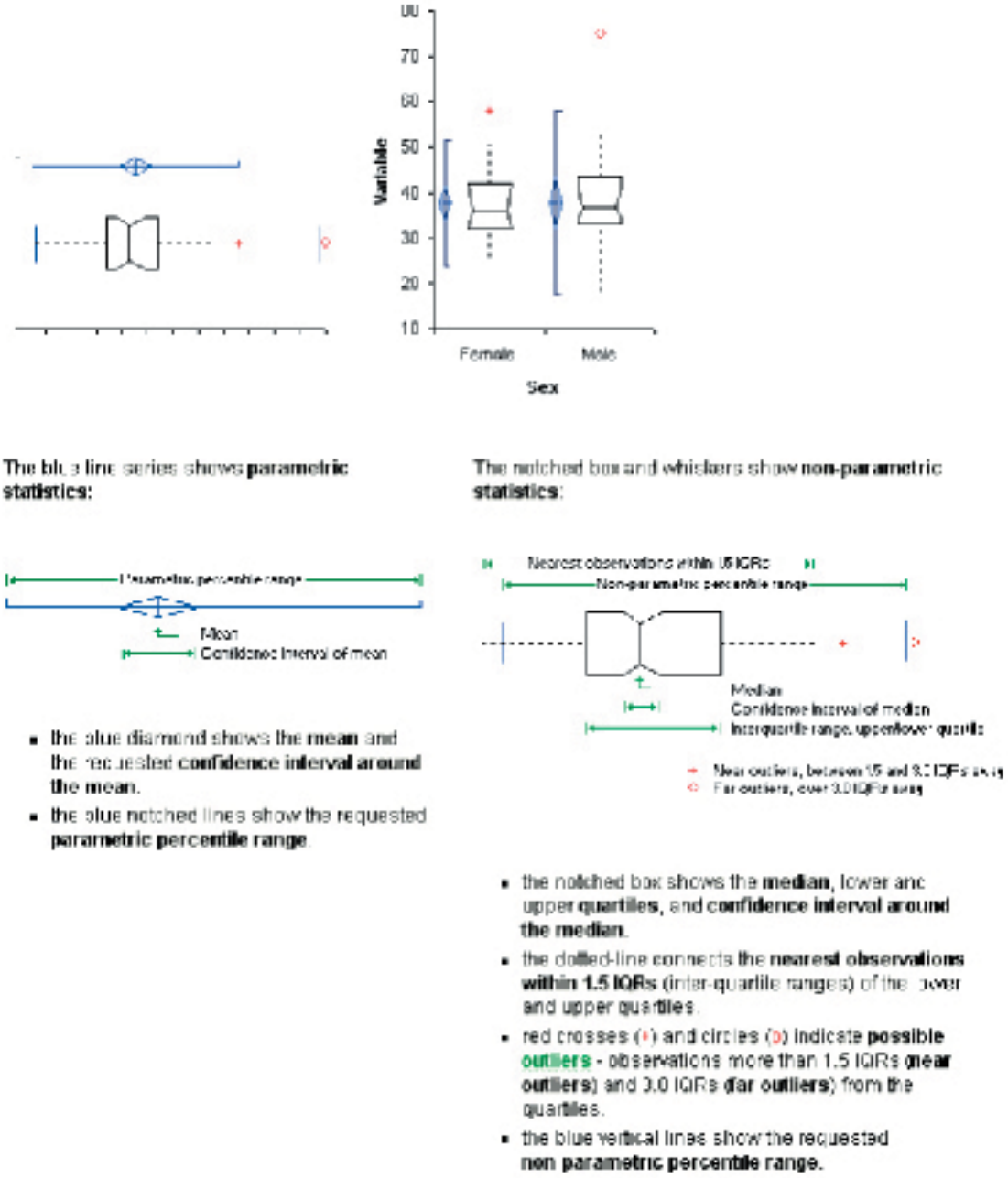

Figure A3-22. *Explanation of how box-plots graphically show the central location and scatter/ dispersion of the observations of data.*

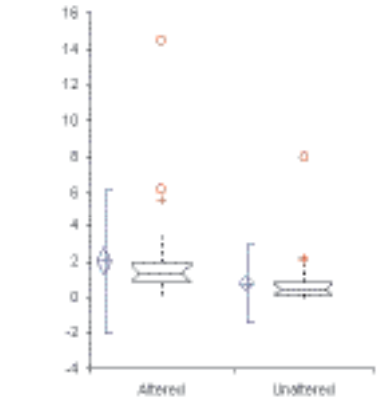

Fracture Frequency by Alteration	n	Mean	SD	SE	95% CI of Mean	Median	IQR	95% CI of Median
Altered	40	2.043	2.4617	0.3892	1.255 to 2.830	1.400	1.196	0.886 to 1.772
Unaltered	38	0.793	1.3310	0.2159	0.355 to 1.230	0.384	0.679	0.217 to 0.762

Figure A3-23. *Descriptive statistics for intensity as a function of alteration, borehole KSH01A.*

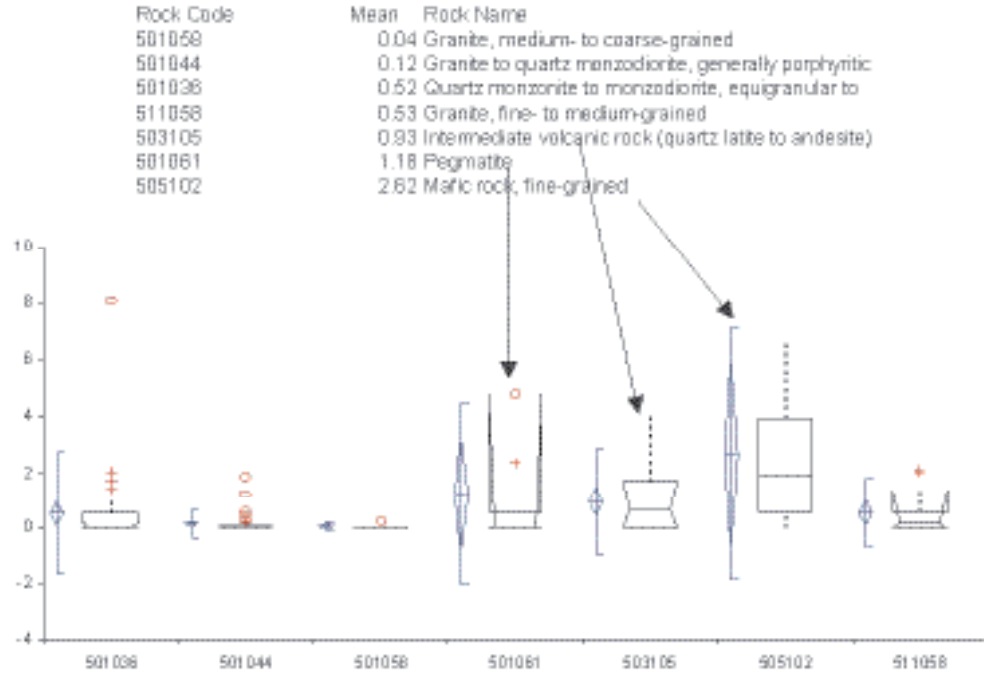

Open Fracture Frequency by Rock Type Code	n	Mean	SD	SE	95% CI of Mean
501036	42	0.522	1.3292	0.2051	0.108 to 0.936
501044	55	0.122	0.3156	0.0426	0.037 to 0.207
501058	5	0.042	0.0944	0.0422	-0.075 to 0.160
501061	6	1.181	1.9865	0.8106	-0.902 to 3.265
503105	21	0.932	1.1366	0.2480	0.414 to 1.449
505102	5	2.622	2.7180	1.2155	-0.753 to 5.997
511058	14	0.526	0.7488	0.2001	0.094 to 0.959

Figure A3-24. *Descriptive statistics for borehole KSH01A regarding fracture intensity and rock type.*

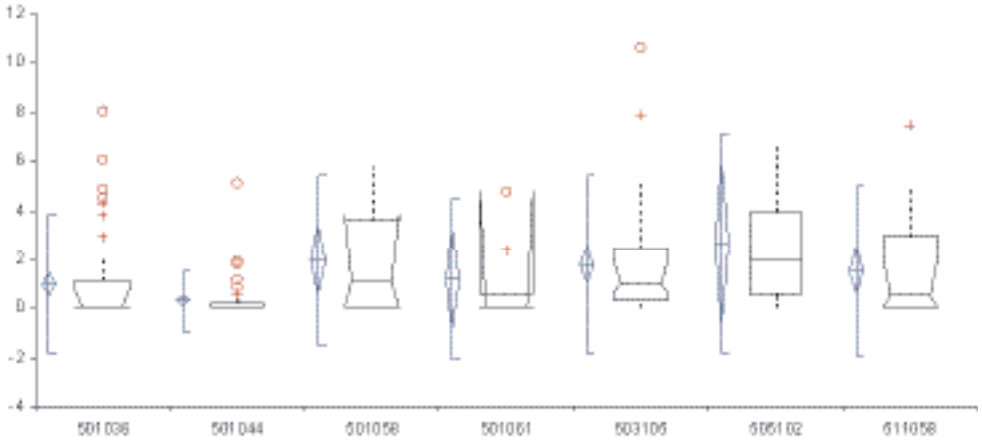

Rock Code	n	Mean	SD	Description
501044	81	0.39	0.79	Granite to quartz monzodiorite, generally porphyri
501036	55	0.97	1.71	Quartz monzonite to monzodiorite, equigranular to
501061	8	1.18	1.99	Pegmatite
511058	20	1.54	2.11	Granite, fine- to medium-grained
503105	38	1.76	2.22	Intermediate volcanic rock (quartz latite to andes
501058	11	1.94	2.10	Granite, medium- to coarse-grained
505102	5	2.62	2.72	Mafic rock, fine-grained

Figure A3-25. *Descriptive statistics for all analysed boreholes regarding fracture intensity and rock type. Yellow-shaded lithologies are found in both boreholes and outcrops*

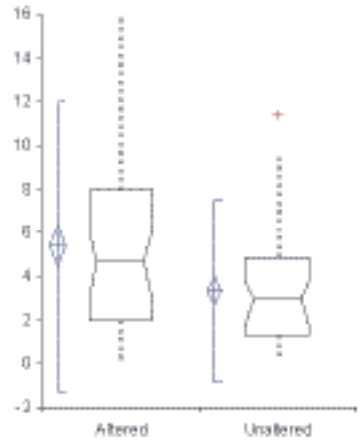

FF by Class	n	Mean	SD	SE	95% CI of Mean	Median	IQR	95% CI of Median
Altered	72	5.400	4.0282	0.4747	4.453 to 6.347	4.854	6.010	2.941 to 6.061
Unaltered	73	3.339	2.9347	0.2967	2.747 to 3.930	2.999	3.537	1.743 to 3.710

Figure A3-26. *Descriptive statistics for intensity as a function of alteration, borehole KLX02.*

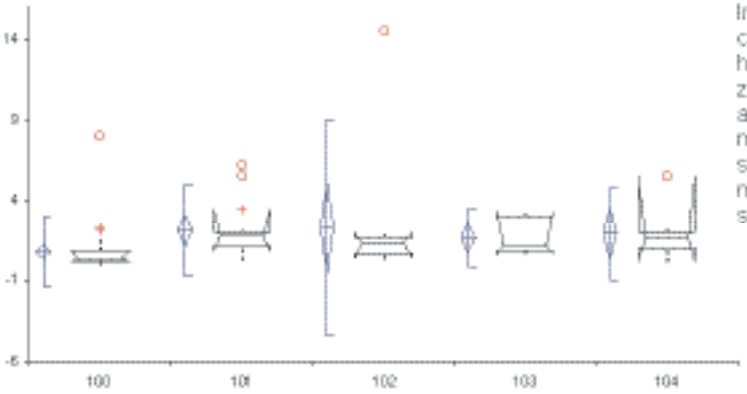

In the KSH01a data, all alteration classes show statistically significant higher intensity than unaltered zones. All mean values for the four alteration classes are within their mutual 95% confidence intervals, suggesting that the apparent lack of monotonicity may not be statistically significant.

Interval Fracture Frequency by Alteration Degree	n	Mean	SD	SE	95% CI of Mean	Median	IQR	95% CI of Median
100	38	0.763	1.3218	0.2319	0.385 to 1.239	0.394	0.870	0.317 to 0.752
101	14	2.130	1.7658	0.4781	1.114 to 3.148	1.710	0.840	0.800 to 3.429
102	11	2.308	4.8901	1.2312	-0.448 to 5.048	1.215	0.854	0.469 to 1.857
103	8	1.656	1.3093	0.3902	0.725 to 2.583	1.895	2.161	0.851 to 3.226
104	7	1.907	1.7038	0.6582	0.284 to 3.519	1.581	0.831	0.210 to 5.956

Figure A3-27. *Descriptive statistics for intensity as a function of alteration degree, borehole KSH01A.*

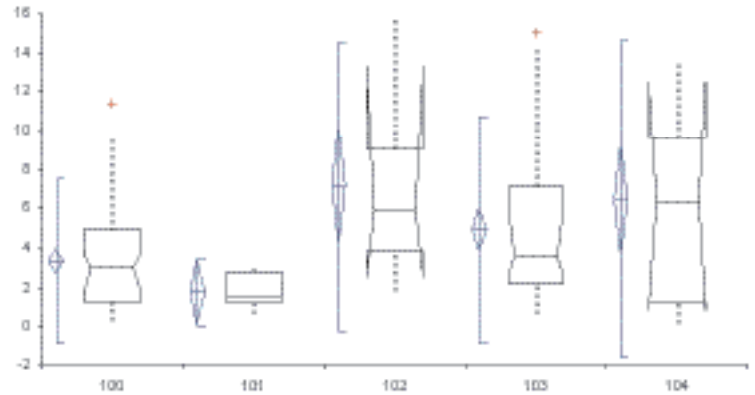

Alteration zones do show higher intensity, but there is not a monotonic progression with alteration degree. Essentially, if the rock has alteration equal to weak or more (classes 102, 103 & 104), it has a statistically significant ly higher fracture intensity. Oddly, faint alteration (class 101) has the lowest intensity, although this may be due to small sample size effects.

FF by Alteration Type - R2	n	Mean	SD	SE	95% CI of Mean	Median	IQR	95% CI of Median
100	75	3.392	2.8534	0.3297	2.747 to 3.950	2.999	3.697	1.748 to 3.710
101	4	1.358	1.0200	0.5101	0.135 to 2.582	1.575	1.546	- to -
102	11	7.193	4.4702	1.3478	4.195 to 10.191	5.982	5.210	2.494 to 13.333
103	40	4.699	3.5106	0.5554	3.655 to 6.020	3.517	4.947	2.621 to 6.090
104	19	6.465	4.9339	1.2195	3.867 to 9.304	6.332	6.346	0.928 to 12.600

Figure A3-28. *Descriptive statistics for intensity as a function of alteration degree, borehole KLX02.*

Table A3-1. Kruskal-Wallis statistics for testing whether the medians of various classifications of alteration type are similar or different.

n	145	

FF by Class	n	Rank sum	Mean rank
Altered	72	6062.0	84.19
Unaltered	73	4523.0	61.96

Kruskal-Wallis statistic	10.16	
p	0.0014	(chisqr approximation, corrected for ties)
n	78	

e Frequency by Alteration Degree	n	Rank sum	Mean rank
100	38	1036.5	27.28
101	14	766.5	54.75
102	11	509.0	46.27
103	8	409.0	51.13
104	7	360.0	51.43

Kruskal-Wallis statistic	22.43	
p	0.0002	(chisqr approximation, corrected for ties)
n	78	

Fracture Frequency by Alteration	n	Rank sum	Mean rank
Altered	40	2044.5	51.11
Unaltered	38	1036.5	27.28

Kruskal-Wallis statistic	21.56	
p	<0.0001	(chisqr approximation, corrected for ties)
n	145	

FF by Alteration Type - R2	n	Rank sum	Mean rank
100	73	4523.0	61.96
101	4	149.0	37.25
102	11	1147.0	104.27
103	43	3542.0	82.37
104	14	1224.0	87.43

Kruskal-Wallis statistic	17.83	
p	0.0013	(chisqr approximation, corrected for ties)

Table A3-2. Two-way contingency table for fracture roughness vs. aperture, open fractures only.

		Roughness			
		Irregular	Planar	Stepped	Undulating
Aperture	0.5	1.52%	93.40%	0.51%	4.57%
	1	4.20%	84.03%	3.36%	8.40%
	2	2.33%	81.40%	6.98%	9.30%
	3	10.00%	80.00%	10.00%	
	4				
	5				
Marginal Probability		3.06%	87.55%	2.65%	6.73%

Table A3-3. Two-way contingency table for fracture mineral filling vs. aperture, open fractures only.

		Aperture					
		0.5	1	2	3	4	5
MIN1	Calcite	33.94%	56.97%	7.27%	1.21%		0.61%
	Chlorite	50.00%	37.93%	10.34%	1.15%	0.57%	
	Clay Minerals		80.00%		20.00%		
	Epidote	40.91%	48.48%	9.09%	1.52%		
	Goethite	50.00%	50.00%				
	Hematite	32.08%	47.17%	13.21%	7.55%		
	Laumontite						
	Oxidized Walls						
	Prehnite						
	Quartz	63.64%	36.36%				
	X3						
Marginal Probablity		40.20%	48.57%	8.78%	2.04%	0.20%	0.20%

Appendix 4

Humans and land use

Input data sources and calculated figures for the variables used to describe humans and land use in the Simpevarp regional model area. Absolute numbers and calculated numbers per km^2 are for the Misterhult parish, since manyof the data was available on the parish level.

Humans

Table A4-1. Variable group – Demography.

Variable	Time series	Data source	Method	Results No.		No. per km^2
Total population	1993–2002	Statistics Sweden	The latest statistical figure concerning the total population in Forsmark parish is for 2002 Mean value for 1993–2002	2,709 2,879		6.6 7.1
Age structure	1993–2002	Statistics Sweden	The distribution over the five age classes was calculated for 2002	0–15 y 16–24 y 25–44 y 45– 64 y ≥ 65 y	17.0% 8.1% 19.4% 32.8% 22.7%	
Excess of births over deaths	1993–2002	Statistics Sweden	The latest birth figure is from 2002 Mean value for 1993–2002 The latest death figure is from 2002 Mean value for 1993–2002 The excess of births over deaths for 2002 Mean excess value for 1993–2002	31 23 29 36 2 –13		
Net-migration	1993–2002	Statistics Sweden	The latest figure concerning in-migration from 2002 Mean value for 1993–2002 The latest out-migration figure from 2002 Mean value for 1993–2002 Net-migration value for 2002	116 176 148 186 –32		
Ill-health number	1998–2002	Statistics Sweden	Mean net-migration value for 1993–2002 The latest figure for the ill-health number from 2002 Mean value for 1998–2002 The latest figure over the men ill-health number from 2002 Mean value for 1998–2002 The latest figure over the women ill-health number from 2002. Mean value for 1998–2002	–10 49.1 42.1 38.8 32.3 60.0 52.4		

Table A4-2. Variable group – Properties and buildings.

Variable	Time series	Data source	Method	Results No.		No. per km²
Type of properties	1996 and 2002	Statistics Sweden	The actual number of properties was obtained from Statistics Sweden for 2002 and 1996. The number was calculated as a percentage			
			Number of farms in 2002 (1996)			
			Number of one- or two dwelling buildings in 2002 (1996)	388 (237)	17.3%	
			Number of holiday-houses in 2002 (1996)	1,012 (998)	45.1%	
			Number of multi-dwelling buildings in 2002 (1996)	707 (668)	31.5%	
			Number of “other” buildings in 2002 (1996)	38 (34)	1.7%	
				101 (113)	4.5%	
Building permits	1996–2002	Statistics Sweden	The latest figure for the number of building permits for dwellings from 2002	3		
			Mean value for 1996–2002	4		
			The latest figure over the number of building permits for business premises from 2002	5		
			Mean value for 1996–2002	7		
Completed dwellings	1993–2002	Statistics Sweden	The latest figure for completed dwellings in one- two or multi dwelling buildings from 2002	0		
			Mean value for 1993–2002	4.9		

Table A4-3. Variable group – Employment.

The following course classification of lines of business, according to SE-SIC Swedish Standard Industrial Classification, is used in the table:

1 Agriculture, forestry, hunting, fishing
2 Mining and manufacturing
3 Electricity-, gas- and water supply, plus sewage and refuse disposal
4 Construction
5 Trade and communication
6 Financial intermediates, business activities
7 Education and research
8 Health and social work
9 Personal and cultural activities
10 Public administration etc
11 Unknown activity

Variable	Time series	Data source	Method	Results No.	No. per km²
The total employed night-population (20–64 y)	1997–2002	Statistics Sweden	The latest figure for the total number of employed night population from 2001 Mean value for 1997–2001	1,217 1,220	
The employed night-population by lines of business* (20–64 y)	1997–2002	Statistics Sweden	The distribution over the eleven lines of business was calculated for the year 2001	1 2 3 4 5 6 7 8 9 10 11	4.3% 24.2% 11.7% 7.3% 12.8% 7.7% 5.6% 18.8% 4.2% 2.5% 0.9%
The total employed day-population (20–64 y)	1997–2002	Statistics Sweden	The latest figure over the total number of employed day population from 2001 Mean value for 1997–2001	1,494 1,540	
The employed day-population by lines of business (20–64 y)	1997–2002	Statistics Sweden	The distribution over the eleven lines of business was calculated for the year 2001 *	1 2 3 4 5 6 7 8 9 10 11	3.0% 12.7% 59.9% 1.8% 3.6% 0.7% 4.6% 10.8% 2.5% 0.0% 0.3%
The total number of working sites	1997–2002	Statistics Sweden	The latest figure over the total number of working sites from 2002 Mean value for 1997–2002	263 253	

Working sites by lines of business	2001	Statistics Sweden	The distribution over the eleven lines of business was calculated for the year 2001 *	1 2 3 4 5 6 7 8 9 10 11	39.9% 5.3% 0.0% 4.6% 11.8% 9.1% 1.1% 6.1% 6.1% 0.0% 15.6%
Commuting (20–64 y)	2001	Statistics Sweden	The number of outgoing commuters in 2001 The number of ingoing commuters in 2001 Net commuting calculatec for 2001	538 1,002 464	
The total non-employed population (20–64 y)	1997–2001	Statistics Sweden	The latest figure for the total number of non-employed population from 2001 Mean value for 1997–2001 The percentage non-employed of the total population	306 328 11.0%	
The non employed population by category	1997–2001	Statistics Sweden	The latest figures over the different categories within the non-employed population are from 2001. The number per category was calculated as a percentage of the non-employed		
			Number of students in 2001	44	
			Number of unemployed in 2001	37	
			Number of inhabitants in military service in 2001	0	
			Number of inhabitants with early retirement in 2001	92	
			Number of inhabitants non-employed of other reasons in 2001	132	

Human activities

Table A4-4. Variable group – Forestry.

Variable	Time series	Data source	Method	Results No.	No. per km^2
Wood extraction	1999	Forestry Management Plan, AssiDomän 1999	The amount of wood extracted from the model area during the past 10 years was calculated. Here, the average amount of wood extracted per year is given.	105,340 m^{3}sk/yr	75 m^{3}sk/yr

Table A4-5. Variable group – Agriculture.

Variable	Time series	Data source	Method	Results Total production (kg)	Production kg/km²
Production of Winter Wheat	1990, 1995, 1999	Statistics Sweden	Production is calculated using the crop distribution (hectare winter wheat) multiplied by the standard yield	41,584 89,925 69,133 average 66,881	169.5 (1999)
Production of Spring Wheat	1990, 1995, 1999	Statistics Sweden	Production is calculated using the crop distribution (hectare spring wheat) multiplied by the standard yield	3,291 0 0 average 1,097	0.0 (1999)
Production of Rye	1990, 1995, 1999	Statistics Sweden	Production is calculated using the crop distribution (hectare rye) multiplied by the standard yield	210,379 104,762 79,106 average 131,416	193.9 (1999)
Production of Barley	1990, 1995, 1999	Statistics Sweden	Production is calculated using the crop distribution (hectare barley) multiplied by the standard yield	658,945 575,195 767,485 average 667,208	1,881.6 (1999)
Production of Oats	1990, 1995, 1999	Statistics Sweden	Production is calculated using the crop distribution (hectare oats) multiplied by the standard yield	517,871 240,465 168,674 average 309,003	413.5 (1999)
Production of Mixed Grain	1990, 1995, 1999	Statistics Sweden	Production is calculated using the crop distribution (hectare mixed grain) multiplied by the standard yield	90,990 68,748 90,653 average 83,464	222.2 (1999)
Production of Leguminous Plant	1990, 1995, 1999	Statistics Sweden	Production is calculated using the crop distribution (hectare leguminous plant, peas) multiplied by the standard yield	0 1,866 81,793 average 27,886	200.5 (1999)
Production of Potatoes	1990, 1995, 1999	Statistics Sweden	Production is calculated with the crop distribution (hectare potatoes) multiplied with the standard yield in the appropriate area	111,838 55,919 27,959 average 65,239	68.5 (1999)

Production of Oilseed Crops	1990, 1995, 1999	Statistics Sweden	Production is calculated with the crop distribution (hectare oilseed crops) multiplied with the standard yield in the appropriate area	15,399 0 1,732 average 5,711	4.2 (1999)
Production of Hay, Silage, Green Fodder	1990, 1995, 1999	Statistics Sweden	Production is calculated using the crop distribution (hectare hay, silage, fodder) multiplied by the standard yield	3,916,913 4,029,564 3,996,685 average 3,981,054	10,173.5 (1999)
Veal	1990, 1995, 1999	Statistics Sweden	Production kg/km^2 is calculated using f the number of animals, average slaughter weight and national annual average percentage of slaughtered animals in a herd	51,712 41,861 42,928 average 45,500	105 (1999)
Mutton	1990, 1995, 1999	Statistics Sweden	Production kg/km^2 is calculated using the number of animals, average slaughter weight and national annual average percentage of slaughtered animals in a herd	1,492 2,087 1,397 average 1,659	3.4 (1999)
Pork	1990, 1995, 1999	Statistics Sweden	Production kg/km^2 is calculated using the number of animals, average slaughter weight and national annual average percentage of slaughtered pigs	6,507 29,734 35,994 average 24,078	88.2 (1999)
Chicken	1990, 1995, 1999	Statistics Sweden	Production kg/km^2 is calculated using the number of animals, average slaughter weight and national annual average percentage of slaughtered chickens	4,608 3,480 1,872 average 3,320	4.6 (1999)
Eggs	1990, 1995, 1999	Statistics Sweden	Production is calculated using the number of laying hens and national annual average egg production by hen	2,028 1,531 824 average 1,461	2.02 (1999)
Milk	1990, 1995, 1999	Statistics Sweden	Production is calculated using the number of dairy cows and national annual average milk production by cow	2,905,301 2,216,173 2,310,145 average 2,477,206	5,664 (1999)

Table A4-6. Variable group – Horticulture.

Variable	Time series	Data source	Method	Results No.	No. per km²
Number of horticultural holdings	2003	Statistics Sweden and the publication Fakta om Kalmar län (the County Administrative Board of Kalmar, October 2002)	There were 128 holdings in Kalmar County in 2002. According to the publication Fakta om Kalmar län (Facts about the County of Kalmar), horticultural cultivation is most extensive on the island of Öland. No horticultural holding within Misterhult parish can be found at www.gulasidorna.se. It seams like there is no horticulture within Misterhult parish. This cannot be confirmed without further investigations.	0 (not confirmed, see left)	0
Production of fruit and vegetables	2003	As above	As above		

Table A4-7. Variable group – Aquaculture.

Variable	Time series	Data source	Method	Results No.	No. per km²
Number of enterprises/ production for consumption	2002	The report Aquaculture 2002, Statistics Sweden and Oskarshamn key plan (ÖP 2000)	The number of enterprises in Kalmar County was obtained from Statistics Sweden. The number and location of the enterprises in the municipality was obtained from the key plan for the municipality. There is one aquaculture with crayfish production for recreational fishing within the parish of Misterhult. The amount of crayfish harvested is unknown.	1	

Table A4-8. Variable group – Mineral extraction.

Variable	Time series	Data source	Method	Results No.	No. per km²
Number of mineral extraction leases	2003	Data from the County Administrative Board	Coordinates for the leases acquired from the County Administrative Board was plotted on a GIS-map and compared to the spatial delimitation of the Misterhult parish.	3 (only decoration stone mines)	0.007

Table A4-9. Variable group – Water supply.

Variable	Time series	Data source	Method	Results No.	No. per km²
Water use, by category; house-holds, agriculture, industry and other	1990, 1995 and 2000	Statistics Sweden	The water use by households in 2000 was calculated as the basis of the average use per person according to Statistics Sweden (189 litres/ day) multiplied by the number of inhabitants in the parish.	192,000 m³	
			The water use by holiday houses has been estimated based on average three persons during 60 days per year in each holiday house, according to Statistics Sweden. An average use of 100 litres per person has been presumed (summerwater and private sewage).	13,000 m³	
			The water use within agriculture has been estimated from the average use per farm in the municipality in 1995 (203000 m³ /232 farms) multiplied by the number of farms in the parish (59 in 1999).	52,000 m³	
			The number of working sites within Misterhult parish represented 10,5% of the working sites in Oskarshamn municipality in 2000. To achieve a rough estimate of the water use within industry in Misterhult it is assumed that 10,5% of the water use within that sector in Oskarshamn municipality is used by the industry in Misterhult. The calculated value is summed with the water use within Simpevarp nucelar power plant (approx. 175,000 m³).	240,000 m³	
Water withdrawal subdivided in private and public supply	1990, 1995 and 2000	Statistics Sweden	The same approach has been used to estimate the water use within the category other.	134,000 m³	
			If it is assumed that the allocation between public and private is the same as in the municipality in 1995 (water used in Simpevarp power plant is excluded), a rough figure over the water withdrawal from public water supplies can be estimated.	315,000 m³	
Water withdrawal subdivided in ground water and surface water*	1990, 1995 and 2000	Statistics Sweden	If it is assumed that the allocation between public and private is the same as in the municipality in 1995, a rough figure of water withdrawal from private water supplies canm be estimated. Simpevarp power plant uses a private water supply (Götemar).	317,000 m³	
			If it is assumed that the allocation between groundwater and surface water is the same as in the municipality in 1995, a rough figure of groundwater withdrawal can be estimated.	91,000 m³	
			If it is assumed that the allocation between groundwater and surface water is the same as in the municipality in 1995, a rough figure over the surface water withdrawal can be estimated. Simpevarp power plant uses surface-water (Götemar).	516,000 m³	
			5,4% of the water withdrawal in the municipality in 1995 came from seawater or other unknown sources. The same percentage is assumed for the Misterhult parish.	25,000 m³	

Table A4-10. Variable group – Commercial fishing.

Variable	Time series	Data source	Method	Results No.	No. per km²
Total catch	1995–2002	National Board of Fisheries	When calculating the total catch by the fishermen living in Misterhult parish the average catch per fisherman in Oskarshamn municipality for 2002 has been used.	5,649 kg	14 kg/ km²
			A mean value for 1996 to 2002 was calculated	18,507 kg	45 kg/ km²

Table A4-11. Variable group – Outdoor life.

Variable	Time series	Data source	Method	Results No.			No. per km²
Harvested moose in number	1997–2003	County Administrative Board of Uppsala	The number of harvested moose from the different hunting zones has been summarised for the last hunting season (ended in 2003).	53 (bulls)	37 (cows)	69 (calves)	0.35
Harvested moose in weight	1997–2003	County Administrative Board of Uppsala	Mean values for 1997–2003	66.3 (bulls)	63.6 (cows)	88.7 (calves)	0.49
			According to Swedish Association for Hunting and Wildlife Management the carcass weight is 180–230 kg for a bull, 170–200 kg for a cow and 70 kg for a calf (55% of the living weight). When calculating the weight for the last hunting season (ended in 2003), a carcass weight of 205 kg for a bull, 185 kg for a cow and 70 kg for calves has been used.	22,540 kg			49 kg/km²
Harvested roe deers in number	1997–2001	Swedish Association for Hunting and Wildlife Management	Mean value for 1997–2003	31,559 kg			70 kg/km²
			The latest coarse estimate of the harvested roe deers per km² is from 2001. The actual number of harvested roe deer within the parish was calculated from the number per unit area.	529			1.3
			Mean value for 1997–2001	876			2.15

Harvested roe deers in weight	1997–2001	Swedish Association for Hunting and Wildlife Management	According to Swedish Association for Hunting and Wildlife Management the roe deer weight is 20–30 kg. If it is assumed that the carcass weight is 55% of the living weight, as for the moose, a carcass weight of approximately 14 kg for an adult is obtained.	7,407 kg	18 kg/km^2
			Mean value for 1997–2001	12,262 kg	30 kg/km^2
Picking of wild berries	1997	Statistics Sweden	According to surveys conducted by Statistics Sweden, an approximate average amount of 200–500 g/ha of wild berries is picked in Sweden. This figure was multiplied by the land area of the Misterhult parish.	8,160–20,400 kg	20 –50 kg/ km^2
Picking of fungi	1997	Statistics Sweden	According to surveys conducted by Statistics Sweden, an approximate average amount of 30–100 g/ha of fungi is picked in Sweden. This figure was multiplied by the land area of the Misterhult parish.	1,220–4,080 kg	3–10 kg/ km^2
Number of attractive fishing-waters	2003	The brochure Sportfiske i Oskarshamns kommun (Oskarshamns Turistbyrå, juni 2003)	There is one attractive fishing water within the parish. That is Marströmmen, a river witth running water and small lakes.Fishing licence is required.	1	
Number of sport-fishing clubs	2003	www.sportfiskarna.se Swedish Sport Fishing Association	According to www.sportfiskarna.se there is no sport fishing club in Misterhult parish. (One in the municipality)	0	
Catch by sport fishermen	2002	Report Fiske 2000 – En undersökning om svenskarnas sport- och husbehovsfiske, Fiskeriverket (ISSN 1404-8590)	A theoretical value has been calculated based on the report Fiske 2000. 55% of the inhabitants between 16–64 years catch 18 kg fish per person and year.	16,167 kg	39.6 kg/km^2
Number of golf courses	2003	www.oskarshamn.se	There is one golf course within the parish of Misterhult according to the tourist information at www.oskarshamn.se	1	
Number of jogging tracks	2003	GIS-data from the County Administrative Board of Kalmar and www.oskarshamn.se	There are three jogging tracks within the parish of Misterhult.	3	
Number of areas for country walks	2003	GIS-data from the County Administrative Board of Kalmar and www.h.lst.se.	There are four nature reserves in the parish. These are often attractive areas for out-door life. According to the tourist information at www.h.lst.se there are three hiking trails within the parish.	7	

Number of attractive spots for bird watching	2003	Oskarshamnsbygdens ornithological association http://hem.passagen.se/obfh/.	According to Oskarshamnsbygdens fågelklubb (ornithological association) there are two attractive spots within the parish; Simpevarp and Kråkelund.	2
Number of canoe-routes	2003	www.kanotguiden.com	According to www.kanotguiden.com there is one canoe-route within Misterhult parish. The route is goes between Figeholm and Händelöp.	1
Number of canoe-renters	2003	www.kanotguiden.com	According to www.kanotguiden.com there is one canoe-renter within the parish. That is Figeholm Fritid & konferens.	1
Number of open-air baths	2003	GIS-data from the County Administrative Board of Kalmar	There are two open-air baths at the coastline and four at lakes within the parish.	6
Number of campsites and holiday villages	2003	www.oskarshamn.se www.figeholmsgolf.se/konferens/	Figeholm Fritid och konferens AB is the only camping within the parish. They have 117 cottages and 80 camping sites of which 13 are guest sites.	1
Number of marinas	2003	GIS-data from the County Administrative Board of Kalmar	There are five marinas within the parish of Misterhult.	5
Number of guest harbours	2003	GIS-data from the County Administrative Board of Kalmar	There are two guest harbours within the parish of Misterhult.	2
Number of boat renters	2003	The brochure Sportfiske i Oskarshamns kommun (Oskarshamns Turistbyrå, juni 2003) and www.oskarshamn.se	There are two boat renters within the parish; Figeholm Fritid & konferens AB and Figeholm Marin AB.	2

Appendix 5

Properties of rock domains

RSMA01

Property	Character	Quantitative estimate	Confidence	Basis for interpretation	Comments
Volume (m^3)					
Rock type, dominant	501044		High	See confidence table	
Rock type, subordinate	511058, 501061, 501033, 501058, 505102		High	See confidence table	
Degree of inhomogeneity	Medium		High	See confidence table	
Low temperature alteration	Inhomogeneous hydrothermal alteration (secondary red staining)		High	See confidence table	Confidence based on outcrop database
Low-grade ductile deformation	Isotropic to weakly foliated; scatttered mesoscopic, ductile shear zones		High	See confidence table	

RSMB01

Property	Character	Quantitative estimate	Confidence	Basis for interpretation	Comments
Volume (m^3)					
Rock type, dominant	501030		High	See confidence table	Quantitative estimate based on occurrence in KSH01A
		94.2%			High confidence that this rock type is dominant at the Simpevarp peninsula but lower in the western part of the local scale model area
Rock type, subordinate	501036 511058 501061 505102	3.5% 0.9% 0.8% 0.6%	Medium	See confidence table	Quantitative estimate based on occurrence in KSH01A. (Cf. HSH02 in section 4)
Degree of inhomogeneity	Medium		High	See confidence table	
Low temperature alteration	Inhomogeneous hydrothermal alteration (secondary red staining)		High	See confidence table	Confidence based on KSH01 and outcrop database
Low-grade ductile deformation	Isotropic with scatttered mesoscopic, ductile shear zones		High	See confidence table	Confidence based on KSH01 and outcrop database

RSMB02

Property	Character	Quantitative estimate	Confidence	Basis for interpretation	Comments
Volume (m^3)					
Rock type, dominant	501030		Medium	See confidence table	
Rock type, subordinate	511058, 501061		High	See confidence table	
Degree of inhomogeneity	High		Medium	See confidence table	
Low temperature alteration	Inhomogeneous hydrothermal alteration (secondary red staining)		High	See confidence table	Confidence based on outcrop database
Low-grade ductile deformation	Isotropic with scatttered mesoscopic, ductile shear zones		High	See confidence table	

RSMB03

Property	Character	Quantitative estimate	Confidence	Basis for interpretation	Comments
Volume (m^3)					
Rock type, dominant	501030		High	See confidence table	
Rock type, subordinate	511058, 501061, 501033, 501044		High	See confidence table	
Degree of inhomogeneity	Medium		High	See confidence table	
Low temperature alteration	Inhomogeneous hydrothermal alteration (secondary red staining)		High	See confidence table	Confidence based on outcrop database
Low-grade ductile deformation	Isotropic with scatttered mesoscopic, ductile shear zones		High	See confidence table	

RSMB04

Property	Character	Quantitative estimate	Confidence	Basis for interpretation	Comments
Volume (m^3)					
Rock type, dominant	501030		Medium	See confidence table	Extension at the surface based on /Kornfält and Wikman, 1987/
Rock type, subordinate	511058, 501061,		High	See confidence table	Based on /Kornfält and Wikman, 1987/
Degree of inhomogeneity	Medium		Medium	See confidence table	
Low temperature alteration					No data
Low-grade ductile deformation					No data

RSMC01

Property	Character	Quantitative estimate	Confidence	Basis for interpretation	Comments
Volume (m^3)					
Rock type, dominant	Mixture of 501036 and 501044	51.5% 34,1%	High	See confidence table	Quantitative estimate based on occurrence in KSH01A
Rock type, subordinate	501030 511058 501058 505102 501061 501033	6.5% 4.2% 2.0% 1.2% 0.3% 0.2%	High	See confidence table	Quantitative estimate based on occurrence in KSH01A
Degree of inhomogeneity	High		High	See confidence table	In particular, the degree of inhomogeneity is high in the northeastern part
Low temperature alteration	Inhomogeneous hydrothermal alteration (secondary red staining)		High	See confidence table	Confidence based on KSH01 and outcrop database
Low-grade ductile deformation	Isotropic to weakly foliated; scatttered mesoscopic, ductile shear zones		High	See confidence table	Confidence based on KSH01 and outcrop database

RSMD01

Property	Character	Quantitative estimate	Confidence	Basis for interpretation	Comments
Volume (m^3)					
Rock type, dominant	501036		Medium	See confidence table	
Rock type, subordinate	511058, 501061		Medium	See confidence table	
Degree of inhomogeneity	Medium		Medium	See confidence table	
Low temperature alteration					No data
Low-grade ductile deformation	Isotropic to weakly foliated; scatttered mesoscopic, ductile shear zones		Medium	See confidence table	

RSME01

Property	Character	Quantitative estimate	Confidence	Basis for interpretation	Comments
Volume (m^3)					
Rock type, dominant	501033		Medium	See confidence table	
Rock type, subordinate	511058, 501061, 511044		Medium	See confidence table	
Degree of inhomogeneity	High		Medium	See confidence table	
Low temperature alteration					No data
Low-grade ductile deformation					No data

RSME02

Property	Character	Quantitative estimate	Confidence	Basis for interpretation	Comments
Volume (m^3)					
Rock type, dominant	501033		High	See confidence table	
Rock type, subordinate	511058, 501061		High	See confidence table	
Degree of inhomogeneity	High		Low	See confidence table	
Low temperature alteration					No data
Low-grade ductile deformation					No data

RSME03

Property	Character	Quantitative estimate	Confidence	Basis for interpretation	Comments
Volume (m^3)					
Rock type, dominant	501033		High	See confidence table	
Rock type, subordinate					No data
Degree of inhomogeneity					No data
Low temperature alteration)					No data
Low-grade ductile deformation					No data

RSME04

Property	Character	Quantitative estimate	Confidence	Basis for interpretation	Comments
Volume (m^3)					
Rock type, dominant	501033		High	See confidence table	
Rock type, subordinate	511058, 501061, 501044		High	See confidence table	
Degree of inhomogeneity	Medium		Medium	See confidence table	
Low temperature alteration	Absent or very minor		High	See confidence table	Confidence based on outcrop database
Low grade ductile deformation	Isotropic to weakly foliated		High	See confidence table	

RSME05

Property	Character	Quantitative estimate	Confidence	Basis for interpretation	Comments
Volume (m^3)					
Rock type, dominant	501033		High	See confidence table	
Rock type, subordinate					No data
Degree of inhomogeneity					No data
Low temperature alteration					No data
Low-grade ductile deformation					No data

RSME06

Property	Character	Quantitative estimate	Confidence	Basis for interpretation	Comments
Volume (m^3)					
Rock type, dominant	501033		High	See confidence table	
Rock type, subordinate	511058, 501061		High	See confidence table	
Degree of inhomogeneity	Medium		Medium	See confidence table	
Low temperature alteration	Absent or very minor		High	See confidence table	Confidence based on outcrop database
Low-grade ductile deformation	Isotropic to weakly foliated		Medium	See confidence table	

RSME07

Property	Character	Quantitative estimate	Confidence	Basis for interpretation	Comments
Volume (m^3)					
Rock type, dominant	501033		Medium	See confidence table	
Rock type, subordinate					No data
Degree of inhomogeneity					No data
Low temperature alteration					No data
Low-grade ductile deformation					No data

RSME08

Property	Character	Quantitative estimate	Confidence	Basis for interpretation	Comments
Volume (m^3)					
Rock type, dominant	501033		High	See confidence table	
Rock type, subordinate					
Degree of inhomogeneity	Low		High	See confidence table	
Low temperature alteration	Absent or very minor		High	See confidence table	Confidence based on outcrop database
Low-grade ductile deformation	Isotropic to weakly foliated		High	See confidence table	

RSME09

Property	Character	Quantitative estimate	Confidence	Basis for interpretation	Comments
Volume (m^3)					
Rock type, dominant	501033		High	See confidence table	
Rock type, subordinate	511058, 501061		High	See confidence table	
Degree of inhomogeneity	Medium		Medium	See confidence table	
Low temperature alteration	Absent or very minor		High	See confidence table	Confidence based on outcrop database
Low-grade ductile deformation	Isotropic to weakly foliated		High	See confidence table	

RSME10

Property	Character	Quantitative estimate	Confidence	Basis for interpretation	Comments
Volume (m^3)					
Rock type, dominant	501033		High	See confidence table	
Rock type, subordinate					
Degree of inhomogeneity	Low		High	See confidence table	
Low temperature alteration	Absent or very minor		High	See confidence table	Confidence based on outcrop database
Low-grade ductile deformation	Isotropic to weakly foliated		High	See confidence table	